

**IMPACT OF *LEISHMANIA DONOVANI* INFECTION ON
EARLY EVENTS IN HAEMATOPOIESIS**

Ana Isabel Pinto

Doctor of Philosophy

University of York

Biology

May 2016

ABSTRACT

Visceral leishmaniasis (VL) in humans and in animal models is associated with, among other factors, parasite persistence in the bone marrow (BM) and significant changes in haematological function. However, the mechanisms underlying haematologic dysregulation are largely unknown.

Using a panel of stem cell markers, we characterized murine haematopoietic stem and precursor cells in the BM over the course of *L. donovani*-infection in C57BL/6 (B6) mice. In steady-state, the majority of LT-HSCs (Long-term haematopoietic stem cells) (LSK CD150⁺ CD34⁻ CD48⁻ cells) were found in a quiescent state, representing cells with the highest degree of reconstitution potential. In contrast, during chronic infection, most LT-HSCs were found to have progressed to cell-cycle and this correlated with a reduced potential to engraft into syngeneic recipients. The loss of quiescent LT-HSCs was associated with expansion of cells displaying a phenotype attributed to early, and uncommitted progenitors. However this increase in uncommitted progenitors did not result in an increase in effective haematopoiesis, but rather chronically infected mice displayed signs of anaemia and thrombocytopenia.

The loss of quiescent HSCs and other alterations in the haematopoietic compartment were absent in infected RAG2 KO mice, but adoptive transfer of CD4⁺ T cells restored this phenotype. In subsequent experiments, we transferred IFN γ -deficient CD4⁺ T cells into RAG KO recipients and established that this pro-inflammatory cytokines was pivotal for the depletion of the reservoir of LT-HSCs in quiescence, as well as for the establishment of anaemia and thrombocytopenia.

Subsequently, using mixed BM chimeras, we established that IFN γ signalling and TNF signalling pathways converge to induce an expansion of BM T cells, suggesting that both cytokines are required to drive the development of CD4⁺ T cells with the potential to cause alterations in haematopoiesis and haematological dysfunction in the periphery. These data suggest new avenues for clinical research into the pathogenesis of VL and have relevance for the development of new therapeutic strategies and clinical follow-up.

TABLE OF CONTENTS

ABSTRACT.....	2
TABLE OF CONTENTS	3
LIST OF FIGURES	6
LIST OF TABLES	11
ACKNOWLEDGEMENTS	13
AUTHOR'S DECLARATION	15
CHAPTER 1. GENERAL INTRODUCTION.....	16
1.1 Haematopoiesis in Bone Marrow.....	16
1.1.1 Overview of Haematopoiesis in the Adult	16
1.1.2 Models for haematopoiesis in the adult.....	17
1.1.3 Regulation of haematopoiesis in the adult.....	21
1.1.3.1 The Bone Marrow Microenvironment	22
1.1.3.2 Cytokine Receptors and Haematopoiesis.....	27
1.1.3.3 Transcription Factors in Lineage Commitment	30
1.1.4 Haematopoietic Stem Cells in Adult Mammals.....	32
1.1.4.1 Haematopoietic Stem Cell, Quiescence <i>versus</i> Proliferation.....	33
1.1.4.2 Immunophenotypic evaluation.....	40
1.2 Stress-induced Haematopoiesis	41
1.2.1 Overview of Stress-induced Haematopoiesis.....	41
1.2.2 Inflammatory Modulation of Early Events in Haematopoiesis	42
1.2.2.1 Regulation of stress-induced haematopoiesis by Toll-like receptor signaling....	44
1.2.2.2 Regulation of Stress-induced Haematopoiesis by Cytokine Signalling.....	45
1.3 Visceral Leishmaniasis	53
1.3.1 Overview of Visceral Leishmaniasis.....	53
1.3.2 Immunopathology in VL	54
1.3.3 Haematopoietic alterations during VL in experimental models of disease	55
1.3.4 Haematopoietic alterations during VL in humans	58
1.4 Aims.....	61
CHAPTER 2. MATERIALS AND METHODS.....	62
2.1 Animals.....	62
2.2 Infections.....	62
2.3 Cells isolations.....	63
2.3.1 Bone Marrow cells isolation.....	63
2.3.2 Spleen cells isolation	64
2.4 Flow cytometry and adoptive transfer of sorted cells	64
2.4.1 Staining for surface markers.....	64

2.4.2	Intracellular staining for cytokines	65
2.4.3	Intracellular staining for transcription factors (GATA-3 and β -catenin)	66
2.4.4	Intracellular staining for Annexin-V	66
2.4.5	Intracellular staining for Wnt3a.....	66
2.4.6	Cell sorting of HSCPs cells from bone marrow and adoptive transfer to lethally irradiated recipient mice.....	67
2.4.7	Establishment of BM chimeras B6.c-Myc-eGFP \rightarrow WT B6.CD45.1 and intracellular staining for c-Myc-eGFP	67
2.4.8	Cell sorting of CD4 ⁺ T cells from spleens and adoptive transfer to RAG2 KO mice.....	68
2.4.9	Mixed BM chimeras B6.CD45.1: B6.CD45.2. <i>Ifnγr2^{-/-}</i> (50:50) \rightarrow B6CD45.1 mice... ..	68
2.4.10	Mixed BM chimeras B6.CD45.1:B6.CD45.2. <i>TNF-RdKO</i> (50:50) \rightarrow B6.CD45.1 mice	69
2.4.11	Flow cytometry and sorting of CD4 ⁺ T cells from BM for RNA extraction.....	69
2.4.12	Flow cytometry analysis	70
2.5	Blood collection and hemogram	70
2.6	Total RNA extractions and microarray of BM T cells.....	70
2.6.1	RNA extraction using the miRNeasy Micro Kit	71
2.6.2	RNA extraction using the Direct-zol TM RNA MiniPrep.....	71
2.6.3	Microarray	71
2.7	Reverse transcription reAction and Quantitative real-time polymerase chain reaction of total BM cells	72
2.7.1	Reverse transcription reaction (RT Reaction)	72
2.7.2	Quantitative real-time polymerase chain reaction (qRT-PCR).....	72
2.8	Staining of purified LSK cells for confocal microscopy analysis.....	73
2.9	Statistical analysis	74
CHAPTER 3. ALTERATIONS IN HAEMATOPOIESIS DURING <i>LEISHMANIA DONOVANI</i> INFECTION		77
3.1	Introduction.....	77
3.2	Results.....	80
3.2.1	<i>L. donovani</i> infection was associated with alterations in the number of HSPCs in BM and spleen.....	80
3.2.2	Experimental VL was characterized by increased numbers of primitive haematopoietic progenitors.....	82
3.2.3	Experimental VL is characterized by alterations in blood homeostasis.....	83
3.2.4	<i>L. donovani</i> infection was not associated with increased cell death in BM	84
3.2.5	HSPCs from infected mice showed impaired engraftment in BM and decreased reconstitution of the periphery	84

3.2.6	<i>L. donovani</i> infection stimulates expansion of LSK CD34 ⁻ CD150 ⁺ expressing CD48	85
3.2.7	<i>L. donovani</i> infection was associated with depletion of the reservoir of quiescent LT-HSCs	86
3.2.8	LSK CD34 ⁻ CD150 ⁺ CD48 ⁻ cells were functionally impaired during chronic infection with <i>L. donovani</i>	87
3.2.9	Alteration in expression of transcription factors associated with cell-cycle regulation of HSCs during <i>L. donovani</i> infection	89
3.3	Discussion	93
3.4	Figures	106
CHAPTER 4. CELLULAR AND MOLECULAR DETERMINANTS UNDERLYING ALTERATIONS IN HAEMATOPOIESIS DURING INFECTION WITH <i>L. DONOVANI</i>		139
4.1	Introduction	139
4.2	Results	143
4.2.1	Infection with <i>L. donovani</i> in immunodeficient mice was not associated to the loss of quiescent HSCs in BM	143
4.2.2	Splenectomy did not impact in the increase of intermediary multipotent progenitors nor in the loss of quiescent LT-HSCs during <i>L. donovani</i> infection	143
4.2.3	<i>L. donovani</i> infection was characterized by increased numbers of BM T cells	144
4.2.4	<i>L. donovani</i> infection results in increased numbers of “effector” T cells in BM	145
4.2.5	The number of CD4 ⁺ T cells producing IFN γ and TNF was increased in BM following <i>L. donovani</i> infection	147
4.2.6	Infection-induced loss of quiescent LT-HSCs was mediated by CD4 ⁺ T cells	149
4.2.7	Loss of LT- HSCs in quiescence was mediated by IFN γ	151
4.2.8	Loss of quiescent LT-HSCs was not mediated by intrinsic IFN γ receptor signalling in LT-HSCs	152
4.2.9	The number of LT-HSCs and onward progenitors expressing TNF receptors was increased following infection with <i>L. donovani</i>	157
4.2.10	TNF intrinsic signalling does not regulate loss of LT-HSCs in G0	158
4.2.11	Loss of TNFR signaling prevents expansion of BM CD4 ⁺ T cells with the potential to express IFN γ	162
4.3	Discussion	165
CHAPTER 5. CONCLUDING DISCUSSION		258
5.1	Figures	263
ABBREVIATIONS		267
REFERENCES		279

LIST OF FIGURES

Figure 1.1 - Models for proposed to explain the development of mature haematopoietic.....	19
Figure 1.2 - Haematopoietic stem cell (HSCs) functions are supported by various BM stromal cells, comprising the so-called HSCs niche.	24
Figure 1.3 - Summary of haematopoietic cytokines.....	28
Figure 1.4 - Schematic overview of different HSCs cellular fate choices.....	34
Figure 1.5 - Overview of cell cycle.	35
Figure 1.6- Overview of the “Push and Pull Modell” proposed to frame the alterations observed in haematopoiesis during infection.	43
Figure 3.1 - <i>L. donovani</i> parasites in BM. BM smear from B6 mouse infected for 28 days.....	106
Figure 3.2- Diagram of stepwise differentiation of haematopoietic precursors and panel of associated surface molecular markers commonly used to characterize the different haematopoietic stem and progenitor cells (HSPCs).....	107
Figure 3.3 - Gating strategy for characterizing multipotent progenitors using flow cytometry analysis.....	108
Figure 3.4 - Gating strategy for characterizing BM populations enriched for lineage-committed haematopoietic progenitors using flow cytometry.....	109
Figure 3.5 - Sca1 was expressed in the vast majority of HSPCs in the BM of <i>L. donovani</i> infected mice.....	110
Figure 3.6 - The kinetics of parasite burden in the BM and the spleen of <i>L. donovani</i> infected mice. <i>L. donovani</i> infected B6 mice were examined for parasite burden at times indicated.	111
Figure 3.7 - <i>L. donovani</i> infection affects the BM and the spleen cellularity.	112
Figure 3.8 - <i>L. donovani</i> infection results in changes to the number of HSPCs in BM.	113
Figure 3.9 - <i>L. donovani</i> infection results in changes to the number of HSPCs in the spleen. (a) Relative frequency of Lineage ⁻ cKit ⁺ cells (enriched for HSPCs).	115
Figure 3.10 - <i>L. donovani</i> infection results in increased numbers of multipotent haematopoietic progenitors without a reciprocal increase in lineage-committed progenitors.....	117
Figure 3.11 - <i>L. donovani</i> infection was associated to decreases in mature blood cells in circulation..	118
Figure 3.12 - <i>L. donovani</i> infection was not associated with increased cell death in the bone marrow.....	119
Figure 3.13 - HSPCs from infected mice showed impaired engraftment in BM and decreased reconstitution of the periphery.	120
Figure 3.14 - Increased expression of CD48 on LSK CD150 ⁺ CD34 ⁻ cells (enriched for phenotypic LT-HSCs) following <i>L. donovani</i> infection.....	122
Figure 3.15 - Loss of quiescent LSK CD34 ⁻ CD150 ⁺ CD48 ⁻ cells (enriched for LT-HSCs) following <i>L. donovani</i> infection.....	123

Figure 3.16 - LSK CD150 ⁺ CD34 ⁻ CD48 ⁻ cells (enriched for HSCs) from infected mice were impaired in their efficiency to engraft and poorly reconstituted the periphery. (a	124
Figure 3.17 - LSK CD150 ⁺ CD34 ⁻ CD48 ⁻ cells (enriched for HSCs) from infected mice were impaired in engraftment efficiency in secondary adoptive transfer.	126
Figure 3.18 - LSK CD34 ⁻ CD150 ⁺ CD48 ⁻ cells (enriched for LT-HSCs) accumulate higher levels of β -Catenin.	128
Figure 3.19 - Mature haematopoietic cells in bone marrow of <i>L. donovani</i> infected mice express increased levels of Wnt3a protein.	129
Figure 3.20 - Accumulation of <i>Wnt3a</i> mRNA is reduced in total BM cells from <i>L. donovani</i> infected mice.	130
Figure 3.21 - HSCs in BM expressed increased levels of c-Myc during infection with <i>L. donovani</i> .	131
Figure 3.22 - The expression of CD29 levels in LT-HSCs was unaltered during infection with <i>L. donovani</i> .	132
Figure 3.23 - The frequency of LSK CD150 ⁺ CD48 ⁻ cells (enriched for LT-HSCs) expressing GATA-3 was increased following <i>L. donovani</i> infection.	133
Figure 3.24 - The distribution of LSK CD150 ⁺ CD48 ⁻ cells (enriched for LT-HSCs) segregated according with the expression of GATA-3 and Ki67 is altered following <i>L. donovani</i> infection.	134
Figure 3.25 - Cycling LSK CD150 ⁺ CD48 ⁻ cells (enriched for LT-HSCs) upregulated GATA-3 expression following <i>L. donovani</i> infection.	135
Figure 3.26 - Detection of the subcellular localization of GATA-3 protein by immunofluorescence microscopy analyses in total thymocytes.	136
Figure 3.27 - GATA-3 protein subcellular localization by immunofluorescence microscopy analyses in LSK cells from BM.	137
Figure 3.28 - <i>Leishmania donovani</i> infection resulted in the depletion of the reservoir of quiescent LT-HSCs in BM.	138
Figure 4.1 - RAG2 KO mice do not lose quiescent HSCs following infection with <i>L. donovani</i> .	187
Figure 4.2 - The number of HSPCs was increased in the spleen following infection with <i>L. donovani</i> .	188
Figure 4.3 - The number of HSPCs was increased in spleen following infection with <i>L. donovani</i> .	189
Figure 4.4 - Alterations in BM cellularity occurred independently from the processes taking place in the spleen.	190
Figure 4.5 - <i>L. donovani</i> infection lead to the expansion of T cell compartment in BM.	192
Figure 4.6 - <i>L. donovani</i> infection was associated with the contraction of the B cell compartment in BM, during chronic phase of infection.	193

Figure 4.7 - <i>L. donovani</i> infection was not associated with alterations in the number of total CD11b ⁺ cells in BM.	194
Figure 4.8 - <i>L. donovani</i> infection was associated with alterations in the number of MSCs in BM.	195
Figure 4.9 - <i>L. donovani</i> infection was not associated with alterations in the number of regulatory T cells in BM.	196
Figure 4.10 - The number of T cells CD62L ^{-low} CD44 ^{high} increased in the BM following <i>L. donovani</i> infection.	198
Figure 4.11 - Following infection with <i>L. donovani</i> the number of CD4 ⁺ T cells CD62L ^{-lo} CD44 ^{hi} increased in the spleen.	200
Figure 4.12 - The number “Effector” CD4 ⁺ and CD8 ⁺ T cells increase in BM following <i>L. donovani</i> infection.	201
Figure 4.13 - <i>L. donovani</i> infection was associated with an increase in the number of BM CD4 ⁺ T cells with potential for IFN γ expression.	203
Figure 4.14 - <i>L. donovani</i> infection was associated with increased number of BM CD4 ⁺ T cells with potential for TNF expression.	205
Figure 4.15 - The number of BM CD4 ⁺ T cells with potential for IL-10 expression increased following <i>L. donovani</i> infection.	207
Figure 4.16 - In BM the distribution of cells expressing TNF and/or IL-10 within CD4 ⁺ T cells IFN γ ⁺ was unchanged following <i>L. donovani</i> infection.	209
Figure 4.17 - Proposed mechanism to explain depletion of LT-HSCs in G0 and inefficient haematopoiesis during the chronic infection with <i>L. donovani</i> (1).	210
Figure 4.18 - CD4 ⁺ T cells mediated expansion of intermediary non-committed progenitors onward LT-HSCs in BM following <i>L. donovani</i> infection.	211
Figure 4.19 - CD4 ⁺ T cells mediated the loss of HSCs in G0 in BM, following infection with <i>L. donovani</i> .	213
Figure 4.20 - CD4 ⁺ T cells did mediate alteration in the number of myeloid-committed progenitors, following infection with <i>L. donovani</i> .	216
Figure 4.21 - The transfer of CD4 ⁺ T cells to naive RAG2 KO mice was not associated to alteration in the number of HSPCs in BM.	217
Figure 4.22 - CD4 ⁺ T cells mediate the establishment of mild anaemia and thrombocytopenia following infection with <i>L. donovani</i> .	218
Figure 4.23 - CD4 ⁺ T cells do not induce anaemia and thrombocytopenia in naive RAG2 KO mice.	219
Figure 4.24 - CD4 ⁺ T cells mediated control of parasite burden during chronic infection with <i>L. donovani</i> in immunodeficient mice.	220
Figure 4.25 - Adoptively transferred CD4 ⁺ T cells expand in infected RAG2 recipients and displayed a phenotype similar to BM CD4 ⁺ T cells of infected WT mice.	221

Figure 4.26 - CD4 ⁺ T cells through an IFN γ -dependent mechanism mediated the expansion of intermediary multipotent progenitors following infection with <i>L. donovani</i> .	223
Figure 4.27 - CD4 ⁺ T cells through an IFN γ -dependent mechanism mediated the loss of HSCs in G0 following infection with <i>L. donovani</i> .	224
Figure 4.28 - CD4 ⁺ T cells through an IFN γ -dependent mechanism mediated the establishment of anaemia and thrombocytopenia following infection with <i>L. donovani</i> .	226
Figure 4.29 - CD4 ⁺ T cells through an IFN γ -dependent mechanism mediated decrease in parasites/1000 nuclei in the spleen following infection with <i>L. donovani</i> .	227
Figure 4.30 - Following transfer of CD4 ⁺ T cells to RAG2KO mice infected with <i>L. donovani</i> for 28 days, WT CD4 ⁺ T cells and IFN γ KO CD4 ⁺ T cells expanded at similar extent and displayed an “activated” phenotype.	228
Figure 4.31 - Proposed mechanism to explain depletion of LT-HSCs in G0 and inefficient haematopoiesis during chronic infection with <i>L. donovani</i> (2).	230
Figure 4.32 - Experimental design for competitive mixed bone marrow chimeras using wild-type (WT) and IFN γ R2 knockout (IFN γ R2 KO).	231
Figure 4.33 - The reconstitution potential of WT HSCs and IFN γ R2 ^{-/-} HSCs was similar in infected mixed BM chimeras.	232
Figure 4.34 - The frequency of Lin ⁻ cKit ⁺ Sca1 ⁻ cells was decreased in the WT but not IFN γ R2 ^{-/-} donor cells, following infection with <i>L. donovani</i> .	233
Figure 4.35 - <i>L. donovani</i> infection was associated with an increase in intermediary non-committed progenitors within WT and IFN γ R2 ^{-/-} donor cells.	235
Figure 4.36 -The number of myeloid progenitors in BM was unchanged within WT and IFN γ R2 ^{-/-} donor cells, following <i>L. donovani</i> infection.	236
Figure 4.37 - The absence of direct IFN γ signaling in LT-HSCs did not prevent the depletion of the reservoir of quiescent HSCs, following <i>L. donovani</i> infection.	237
Figure 4.38 - In the absence of intrinsic IFN γ signaling the expansion of T cells was limited in BM of mice infected with <i>L. donovani</i> .	239
Figure 4.39 - The absence of direct IFN γ signaling limited the expansion of macrophages in BM and spleen in mice infected with <i>L. donovani</i> .	241
Figure 4.41 - The number of LT-HSCs and onward multipotent progenitors expressing TNF-R1a increased following <i>L. donovani</i> infection.	242
Figure 4.42 - The number of HSPCs (enriched in Lineage- cKit ⁺ cells) expressing TNF-R1b increased following <i>L. donovani</i> infection.	243
Figure 4.43 - The number of LT-HSCs and onward multipotent progenitors expressing TNF-R1b increased following <i>L. donovani</i> infection.	244
Figure 4.44 - Proposed mechanism to explain depletion of LT-HSCs in G0 and inefficient haematopoiesis during the chronic infection with <i>L. donovani</i> (3).	245

Figure 4.45 - Experimental design for competitive mixed BM chimeras using wild-type (WT) and TNF-R double knockout (TNF-RdKO HSCs) BM cells.....	246
Figure 4.46 - The reconstitution potential of WT HSCs and TNF-RdKO donor cells changed following infection with <i>L. donovani</i>	247
Figure 4.47 - Following infection with <i>L. donovani</i> the frequency of Lin ⁻ cKit ⁺ Sca1 ⁻ cells within WT and TNF-RdKO donor cells decreased in BM.....	248
Figure 4.48 - <i>L. donovani</i> infection was associated with an increase in intermediary non-committed progenitors within WT and TNF-RdKO donor cells in BM.....	249
Figure 4.49 - The absence of intrinsic TNF-RdKO signaling did not prevent the depletion of the reservoir of quiescent HSCs, following <i>L. donovani</i> infection.....	250
Figure 4.50 - Following infection with <i>L. donovani</i> , alterations in the frequency of myeloid progenitors were similar within WT and TNF-dKO donor cells.....	252
Figure 4.51 - The absence of intrinsic TNF receptor signaling prevented the expansion of T cells in the BM of mice infected with <i>L. donovani</i>	253
Figure 4.52 - The absence of intrinsic TNF receptor signaling prevented the expansion of T cells in the spleen, following infection with <i>L. donovani</i>	254
Figure 4.53 - The absence of TNF receptor signaling did not prevent the expansion of the myeloid cells in the spleen, following infection with <i>L. donovani</i>	255
Figure 4.54 - Intrinsic TNF receptor signaling mediated expansion of CD4 ⁺ T cells expressing IFN γ in the BM following infection with <i>L. donovani</i>	256
Figure 4.55 - Proposed mechanism to explain depletion of LT-HSCs in G0 and inefficient haematopoiesis during the chronic infection with <i>L. donovani</i> (4).....	257
Figure 5.1 - Changes in blood parameters after 5-FU treatment.....	263
Figure 5.2 - DE genes in BM CD4 ⁺ T cells of naïve vs. <i>L. donovani</i> infection mapped to IPA canonical pathway of Th cell differentiation.	266

LIST OF TABLES

Table 1.1 - Soluble factors produced by BM cellular niches that participate in the regulation of haematopoiesis	25
Table 1.2 - Summary of relevant genetic mouse models that contributed to the identification of molecular modulators of HSCs cell-cycle	39
Table 1.3 - Summary of most commonly used combinations of cell surface marker used to segregate HSPCs.....	40
Table 2.1 - Surface markers used to characterize HSPCs by flow cytometry analysis	65
Table 2.2 - Monoclonal antibodies used to evaluate expression of surface cell markers, cytokines and transcription factor by flow cytometry analysis.....	75
Table 5.1 - Top ten significantly up-/down-regulated genes in BM CD4 ⁺ T cells from mice infected with <i>L. donovani</i> for 28 days (compared to uninfected controls)	264

“Afinal, a melhor maneira de viajar é sentir.
Sentir tudo de todas as maneiras.
Sentir tudo excessivamente,
Porque todas as coisas são, em verdade, excessivas
E toda a realidade é um excesso, uma violência,
Uma alucinação extraordinariamente nítida
Que vivemos todos em comum com a fúria das almas,
O centro para onde tendem as estranhas forças centrífugas
Que são as psiques humanas no seu acordo de sentidos. (...)”

Álvaro de Campos

ACKNOWLEDGEMENTS

I would like to declare my deepest gratitude to my supervisor Professor Paul M. Kaye for this life changing opportunity, for all his support and mentoring. Under his supervision I have learned how to be a better scientist, but above all, how to be a better professional, and his work ethic will be an example to follow in the future. Finally I would like to thank Prof. Paul Kaye for his generosity in the moments I may have underperformed. I would take this opportunity to acknowledge my training advisory panel members, Dr. Dimitris Lagos and Prof. Betsy Pownall, for their support since the first moment, inestimable comments and advice, not only throughout our meetings but also by making themselves available at all times.

I would like to thank the STROMA ITN program (Marie Curie) for the financial support of my project and fellowship. I would like to make a special mention to Dr. Marianna Ventouratou Morys, who besides being extraordinary in the management of the project was always available to help.

This thesis was possible due to the invaluable collaboration of many colleagues from the Centre of Immunology and Infection (University of York).

I would like to start by thanking all the members of the Prof. Paul Kaye team. Dr. Najmeeyah Brown did much more than helping: she was a true collaborator over the past three years, as a teacher, a co-supervisor and providing technical support. This work would not have been possible without her inestimable participation. Dr. Johannes Doehl provided an enormous help with advice and proofreading over the past two years, and, above all, he was always ready to offer a kind word. I would like to thank Dr. Olivier Preham for always being such a good colleague, always available to help others and me. All the other members were always generous with advice and technical support, namely Dr. Helen Ashwin, Dr. Mohamed Osman, Jonathan Hamp, Dr. John Moore, Dr. Jack Lim, Dr. Eliza Ferreira and Samantha Chan. Finally my deepest acknowledgments to Dr. Jane Dalton and Dr. Lynette Bettie for all their advice, support and motivating words. I would also like to include Dr. Flaviane Pinho for her help with the bone marrow aspirates. I would like to conclude by saying that taking part of a team of such immense generosity, work ethic and commitment to science was more than a pleasure; it was a privilege.

I would like to thank all the academic members that contribute to make the CII such a gratifying place to work and share knowledge. I would like to mention in particular Dr. Marika Kullberg, Dr. Pegine Walrad, Dr. Antal Rot and Dr. Ian Hitchcock, Luis de Pablos Torro, Dr. Tiago Ferreira, Dr. Angela Privat and Stephanie Dyson for always being available to provide advice to my endless questions. I would like to thank Dr. Shraddha Kamdar for her help in so many moments with technical issues and proofreading. I would like to thank Dr. Allison Green for her generosity

providing the conditions to conclude my thesis, whilst working in her team. And last but not least, I need to thank Dr. James Hewitson, who besides being an invaluable source of advice throughout the past two years, contributed by helping with the editing of this thesis. His help was inestimable.

Other members of the CII were extremely generous providing support, guidance and advice over the past three years. The administrative team of the CII was from the first moment restless in providing support for the most various situations; as such I would like to thank Liz Greensted, Rebecca Stokes, Philip Kerrigan and Jenny Purcell. I would like to thank Mr. John for his untouchable good mood in early mornings, and Debbie Pears for her logistic support.

I would like to address a special thanks to all the members of the Biological Services Facility Unit, at the University of York, for their support and flexibility.

I would like to express my immense gratitude to the Technology Facility in particular to Dr. Graeme Park, Dr. Karen Hogg and Dr. Karen Hodgkinson, whom provide me with outstanding support during my analysis with Flow cytometry and cell sorting. I would also like to acknowledge Dr. Sally James for performing the microarray and Dr. Sandy McDonald for his support with the analysis of the microarray data.

This work benefited from the generosity of external collaborators; therefore I would like to acknowledge Dr. John Grainger (The University of Manchester, United Kingdom) and Dr. Dr. Bengt Johansson Lindbom (Lund University, Sweden).

I would like to thank my parents, brothers and grandmother for being on my side in all the moments. Many friends were restless in their encouragement and support, Joao Ventura, Vania Silva, Nuno Barros, Sandra Silva, Virginia Martins, Ana Caldas, Ana Lago, Mafalda Sousela, Dr. Maria Soares, Dr. Iris Caramalho, Dr. Rita Barbosa, Alexandre Salvador, Ana Margarida Gomes and Pedro Machado. Finally I would like to thank my beloved Carlos Oliveira, his unconditional support and encouragement were crucial to overcome many challenges throughout the this PhD.

AUTHOR'S DECLARATION

The findings presented in this thesis are original and resulted from work developed by myself, with the following exception: Figure 5.2, I extracted RNA from sorted BM CD4⁺T cells and Dr. Sally James (Genomics department, Technology Facility, University of York) ran the RNA samples on the RNA microarray, which were analyzed with the help of Dr. Sandy McDonald (Genomics department, Technology Facility, University of York) and my supervisor Prof. Paul M. Kaye.

All sources are acknowledged as References. The work presented in this thesis has not been presented for an award in this, or any other, university.

CHAPTER 1. GENERAL INTRODUCTION

1.1 HAEMATOPOIESIS IN BONE MARROW

1.1.1 Overview of Haematopoiesis in the Adult

The haematopoietic system, comprises blood leucocytes, erythrocytes, platelets and their precursors, therefore this system plays a vital role in immune surveillance, dissemination of essential nutrients, tissue repair and enabling clotting. Almost all organs are circumscribed by anatomical barriers and perform interconnected functions, while the haematopoietic system is poorly delimited and covers a variety of non-related functions (W. C. Aird, 2003).

The haematopoietic system is complex and dynamic. The majority of blood cells are short-lived and it has been estimated that the turnover of cells of the haematopoietic system is 1 trillion cells per day in steady-state, including 400 billion platelets, 200 billion erythrocytes and 70 billion neutrophils (K. S. Fernandez and P. A. de Alarcon, 2013).

The maintenance of the number cellular components of blood in steady-state (steady-state haematopoiesis), as well as in stress situations, such as an infection (demand-adapted haematopoiesis) relies on the continuous and dynamic replacement of haematopoietic cells in a process called haematopoiesis. Haematopoiesis is a strictly regulated process that depends on a very small pool of somatic stem cells, which have self-renewal capacity and potential to originate all mature cells during the lifespan of an individual, the so-called HSCs (M. Kondo *et al.*, 2003a).

As such, the homeostasis of the haematopoietic system depends on the capacity of HSCs to maintain a tight balance between differentiation and self-renewal. The majority of haematopoietic stem cells and progenitors cells reside in the bone marrow, where regulation of their self-renewal and differentiation relies on the intrinsic activation of transcription factors (TFs), in association with extrinsic cytokine signaling that depends not only on signals from their microenvironment (the “niche”), but also on remote signals from the periphery (H. Takizawa *et al.*, 2012).

All the terminally differentiated cells originate from HSCs that differentiate into immature progenitors that are related during development, which we will discuss in further detail later in this chapter. As such, classically based on functional and developmental differences, B cells, T cells and NK cells are referred to as lymphoid cells while, erythrocytes, thrombocytes, granulocytes and macrophages are classified as the myeloid or myeloerythroid cells ((S. Doulatov *et al.*, 2012).

1.1.2 Models for haematopoiesis in the adult

The identification of intermediary haematopoietic progenitor cells is the result of a characterization based on cell surface markers and functional evaluation that has been ongoing for many decades. The process of development from pluripotent progenitors to lineage-committed progenitors and finally to terminally differentiated mature cells has been proposed as a stepwise linear model. Accordingly, in each step of development the progenitor cell becomes more committed and progressively loses the potential to become other cell type. However, some studies suggested that a certain degree of lineage plasticity might be present in late stages of haematopoietic development (M. Kondo *et al.*, 2003b).

According to the classical view of haematopoietic development in mice, the production of all mature haematopoietic cells starts with the long-term haematopoietic stem cells (LT-HSCs) that differentiate into the so-called short-term haematopoietic stem cells (ST-HSCs) still multipotent, but with limited self-renewal capacity. The ST-HSCs proceed to form the heterogeneous group of cells called multipotent progenitors (MPPs) that have lost self-renewal capacity, but conserve a range of multipotency. The MPPs will give rise to a succession of intermediary progenitors that become the common lymphoid progenitors (CLPs) that develop into lymphoid progeny and the common myeloid progenitors (CMPs) with erythromyeloid potential. Further on, CMPs may give rise to both granulocyte/macrophage progenitors (GMPs), which differentiate into the myelomonocytic lineage, and the megakaryocytic/erythrocyte progenitors (MEPs), the precursors of red blood cells and platelets (L. D. Wang and A. J. Wagers, 2011). The combination of haematopoietic stem cells and haematopoietic progenitor cells are commonly designated as HSPCs (haematopoietic stem and progenitor cells) (M. J. Pittet *et al.*, 2014).

The classic model for haematopoiesis was based on *in vitro* assays and on the study of the functions of different HSPCs upon transplantation into irradiated recipients to determine lineage potential and self-renewal properties, but both *ex vivo* culture systems and myeloablative conditions may not be ideal to fully understand HSCP function during homeostatic haematopoiesis (R. A. Nimmo *et al.*, 2015).

According to this model, lineage commitment would take place downstream of HSCs and culminate with the branching into lymphoid and myeloerythroid lineage commitment. Nonetheless, initial gene profiling of highly purified HSCs and ST-HSCs/MPPs demonstrated the promiscuous expression (albeit at low level) of non-haematopoietic, as well as multiple lineage-restricted genes. In contrast, CMPs and CLPs express more lineage-restricted genes. These studies suggested that HSCs maintain a permissive chromatin arrangement allowing a “primed-state” that

works as the foundation for later commitment/differentiation; a phenomenon referred to as multilineage priming (K. Akashi *et al.*, 2003, R. A. Nimmo *et al.*, 2015).

The nature of cell fate decisions in HSPCs is still largely unknown, since studies into cell populations do not distinguish between a phenotypically homogeneous group of cells and a heterogeneous set of cells with a diverse degree of lineage bias and self-renewal potentials. Therefore, to elucidate the molecular basis of cell fate decisions techniques to assess gene expression in individual HSPCs are required (R. A. Nimmo *et al.*, 2015).

Studies coupling clonal functional assays and single cell gene expression analysis have shown that within phenotypically defined HSCs and MPPs, there is a wide range of heterogeneity and confirm simultaneous lineage priming at the individual cell level. The differential potential of HSPCs cannot be fully predicted with currently known markers, albeit inheritable lineage predisposition is found within the so-far defined progenitor cell populations (R. A. Nimmo *et al.*, 2015).

In the light of more recent studies, the classical model of haematopoiesis has been questioned and the assumption that lineage restriction takes place downstream of HSCs in a linear progression coupled to increasing loss of self-renewal potential has been challenged. Two other models of haematopoietic development have been proposed: the “Revised Model” and the “Myeloid Bypass Model” (Figure 1.1) (R. A. Nimmo *et al.*, 2015).

The “Revised Model” for haematopoietic development suggests a very early bifurcation in ontogeny between Megakaryocytes/Erythrocytes (MegE) and lymphomyeloid differentiation capacity. This model was proposed following the description of lymphomyeloid-restricted progenitors in Flt3⁺ (FMS-like tyrosine kinase 3) MPPs, named lymphoid primed multipotent progenitors (LMPPs). LMPPs were found to be the first cells in ontogeny expressing common lymphoid genes, together with myeloid-associated genes, but no longer expressing MegE-associated genes. In contrast, both are expressed at low level in HSCs. More, functional characterization of Flt3⁺ LMPPs showed no potential for producing MegE progeny (R. A. Nimmo *et al.*, 2015).

In support of the “Revised Model”, it was suggested that MegE progenitors separate first and the megakaryocyte lineage begins within the most primitive cells. Using a GFP reporter knocked into the von Willebrand factor (vWF) gene, it was found that vWF⁺ HSCs exhibited clear Megakaryocyte-bias and give rise to myeloid progeny, whereas vWF⁻ HSCs were lymphoid-biased. Both were capable of long-term reconstitution, but only vWF⁺ HSCs could originate vWF⁻ HSCs (R. A. Nimmo *et al.*, 2015).

It is becoming accepted that haematopoietic cell development relies on two distinct steps; (1) first, lineage priming takes place most likely in pluripotent progenitors that become competent to cell specification; (2) lineage priming is then followed by commitment that constrains the primed progenitor to a specific cell type (R. A. Nimmo *et al.*, 2015).

These processes are well represented in B cell differentiation, where it was determined that priming occurs in LMPPs, while commitment takes place in a subpopulation of CLPs. It was shown that Ebf1 (Early B cell factor 1) initiates B cells specification in lymphoid-primed cells, but the accomplishment of mature B cell differentiation requires the co-expression of the deterministic factor for commitment, PAX5 (M. Kondo *et al.*, 2003a).

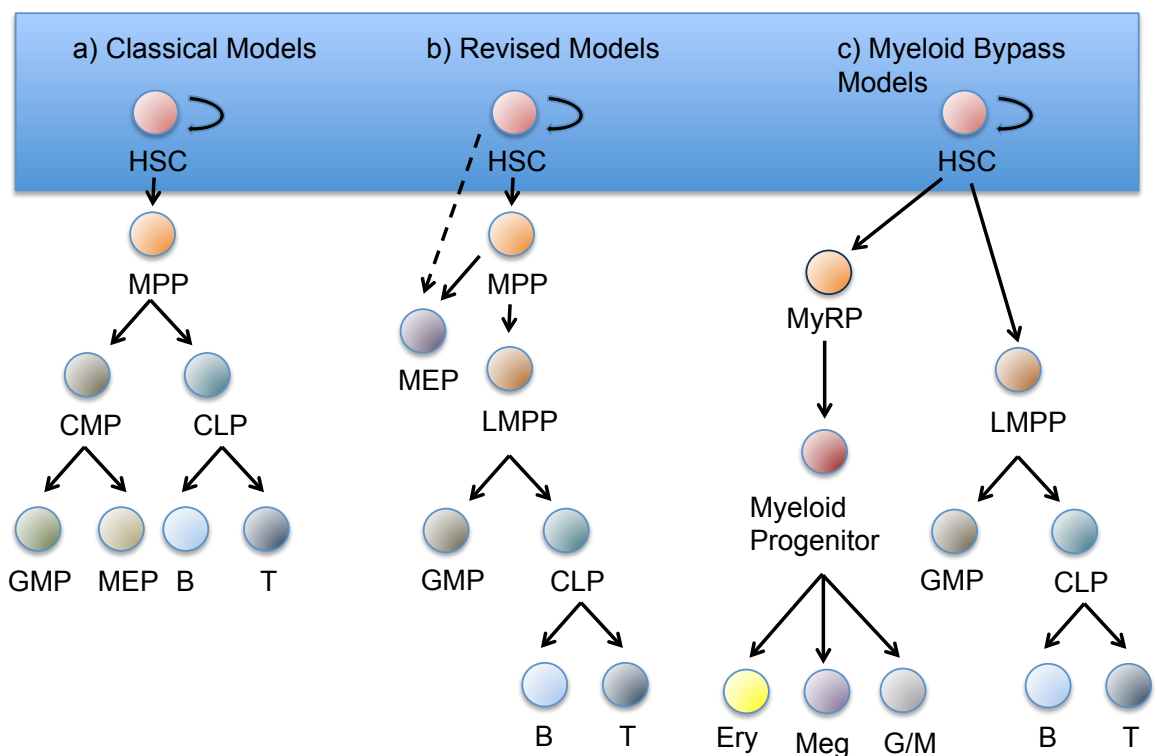


Figure 1.1 - Models for proposed to explain the development of mature haematopoietic.

(A) The classical model purposed that HSCs and non-committed multipotent progenitors differentiate in a stepwise process in lineage restricted myeloid or lymphoid progenitors that no longer display self-renewal capacity. In this model common myeloid progenitors (CMP) and common lymphoid progenitors (CLP) represent the initial step in the lineage commitment. (B) The revised model emerged following the observation that MPPs contain lymphomyeloid-restricted progenitors (LMPPs) that have no longer MegE potential. Additionally, HSCs display MegE potential of differentiation and but no longer lymphoid potential, suggesting that MegE commitment may take place in HSCs, representing a first lineage restriction point. According with the classical model and the revised model, self-renewal capacity and multipotentiality are attributes of HSCs. (C) The myeloid bypass model was proposed as a result of studies performing

multilineage clonal tracking of single HSCs. This model proposed that megakaryocyte- and myeloid-restricted progenitors are already generated in the HSCs compartment, and are capable of long-term self-renewal and reconstitution of restricted myeloid lineages. In contrast to previous models (A, B) this model purposes that self-renewal and multipotentiality can be uncoupled. Abbreviations: c-Kit, c-Kit proto-oncogene; Ery, erythroid;; G/M, granulocyte/monocyte; GMP, granulocyte/monocyte progenitor; HSC, haematopoietic stem cell;; Meg, megakaryocyte; MegE, megakaryocyte/erythroid; MEP, megakaryocyte/erythroid progenitor; MPP, multipotent progenitor; MyRP, myeloid-restricted progenitor; (Adapted from (R. A. Nimmo *et al.*, 2015)).

The alternate “Myeloid Bypass Model” emerged from studies based on single cell transplantation of LT-HSCs, defined as cKit⁺ Sca1⁺ Lineage⁻ (LSK) CD150⁺ CD41⁻ CD34⁻ cells. In recipient mice, it was found that some phenotypic HSCs could be committed to the myeloid lineage, but not give rise to LMPPs, and these were termed myeloid-restricted progenitors (MyRPs). Among these MyRPs, there were progenitor cells with a spectrum of differentiation potential: either restricted to myeloid, megakaryocyte and erythroid lineages (common myeloid repopulating progenitors or megakaryocyte), or restricted to megakaryocytes and erythroid lineages (megakaryocyte-erythroid repopulating progenitors), or restricted to megakaryocyte lineages only (megakaryocyte repopulating progenitors). All these progenitors, although lineage restricted, displayed self-renewal and long-term reconstitution potential (hallmarks of HSCs) in primary and secondary recipient mice (R. Yamamoto *et al.*, 2013).

Further, in studies where paired daughter cell assays were coupled to single cell adoptive transfers, it was shown that MyRP arose directly from HSCs and not from CMPs (R. Yamamoto *et al.*, 2013). In clear opposition to both the classical and the revised models, the myeloid bypass model therefore proposes that the loss of multipotency is not coupled to the loss of self-renewal potential (R. A. Nimmo *et al.*, 2015).

In the light of these findings, the contribution of the different non-restricted and lineage-biased progenitors (long-lived and classically defined) to homeostatic haematopoiesis is not clear. Moreover, when so much is yet to be defined regarding the mechanisms regulating haematopoiesis, the emergent demand to revise the models of blood development point to a far more complex regulation of haematopoiesis than could have been predicted (R. A. Nimmo *et al.*, 2015).

1.1.3 Regulation of haematopoiesis in the adult

Haematopoiesis ensures the production of the required number of each mature cell type in a strictly regulated process that, most likely, results from the cumulative contributions of extrinsic signals and intrinsic/internal processes working in a concerted mode to instruct for lineage choice of HSPCs and subsequent stability of cell identity (M. Endele *et al.*, 2014).

The extrinsic factors comprise local signals provided by the BM niche and systemically produced cytokines. The intrinsic regulation includes different internal processes such as activation of transcription factors, epigenetic and post-translational regulation (M. Endele *et al.*, 2014).

The extent of the contribution of different factors for lineage commitment is technically difficult to demonstrate and therefore still elusive. From longstanding studies to assess the role of cytokines and internal processes in haematopoiesis two general models were proposed: the “Instructive Model” and the “Permissive/stochastic Model” (L. Robb, 2007).

According to the “Instructive Model”, cytokines as well as other molecular signaling mediators can directly instruct lineage decisions in non-committed multipotent progenitors and are fundamental to cell type specification, whilst still recognizing the importance of transcription factors in haematopoiesis (M. Endele *et al.*, 2014).

Initial *in vitro* studies using culture systems showed that some cytokines could specifically favor the development of specific lineages, while others cytokines had a pleiotropic effect in haematopoietic development. Early data supporting the instructive model came from the demonstration that Granulocyte-Macrophage colony forming cells (GM-CFCs) in the presence of Macrophage colony stimulating factor (M-CSF) would differentiate in macrophages, but if the GM-CFCs were cultured in the presence of granulocyte colony stimulating factor (G-CSF), they would instead give rise to granulocytes (L. Robb, 2007).

In support of the “Instructive Model”, a more recent study showed that *in vitro* M-CSF stimulation upregulated PU.1 transcription factor expression (master regulator for myelo-monocytic differentiation) in highly purified HSCs (N. Mossadegh-Keller *et al.*, 2013). In this study from Mossadegh-Keller *et al.*, in adoptive transfer experiments HSCs derived from mice treated with exogenous M-CSF display to an increased myeloid to lymphoid cell ratio in peripheral blood after 4 weeks when transferred to irradiated recipient mice, compared to HSCs derived from untreated controls (N. Mossadegh-Keller *et al.*, 2013). This upregulation of PU.1 by M-CSF on HSCs was critically dependent on the expression of M-CSF receptor (N. Mossadegh-Keller *et al.*, 2013), which is nonetheless most likely regulated by intrinsic processes.

The “Permissive/stochastic Model” suggests that the “decision-making” of a progenitor cell to generate a specific cell type arises from stochastic internal processes promoting the upregulation of cytokine receptors in progenitor cells, which in turn become responsive to cytokine signals (M. Endele *et al.*, 2014). This model is supported by studies showing that among phenotypically defined non-committed progenitor cells, individual cells show a high degree of variability in the promiscuous expression of lineage-specific genes (R. A. Nimmo *et al.*, 2015).

So far gene-targeting studies *in vivo* showed that mice lacking a single cytokine or its receptors are not completely defective in any mature cells, albeit reductions in lineage-specific cells have been observed. Overall these reports suggested that cytokines impact on lineage-primed HSPCs expansion, survival and maturation but are not required for lineage commitment (L. Robb, 2007). It also has to be taken in consideration that compensatory mechanisms can take place *in vivo*, suggesting caution in the interpretation of such loss of function studies (M. Endele *et al.*, 2014).

Most likely lineage priming in HSPCs will allow different receptors to be expressed among phenotypically defined population of progenitors with a variable range of responsiveness to the milieu of signals, preventing exhaustion and simultaneously assuring a degree of lineage plasticity (L. Robb, 2007, R. A. Nimmo *et al.*, 2015).

In the next sections, the internal and external regulatory processes involved in the differentiation of HSCs and lineage commitment of multipotent progenitors will be discussed. The regulation of HSCs quiescence and self-renewal will be discussed in more detail in Section 1.1.4.1.

1.1.3.1 The Bone Marrow Microenvironment

Haematopoiesis takes place in different anatomic sites during mammalian development, first in extra-embryonic tissues and then progressively in the aorta–gonad–mesonephros area, then in the fetal liver and spleen, and postnatally in BM, where most of homeostatic blood cell formation takes place throughout adult life (S. H. Orkin and L. I. Zon, 2008, F. E. Mercier *et al.*, 2012).

The BM is the major haematopoietic organ in adults, but haematopoiesis can also occur in extramedullary sites, such as the spleen and the liver. For example, in mice the spleen is a site of effective haematopoiesis, while in humans it is less defined although stress-induced extramedullary haematopoiesis has been reported (F. E. Mercier *et al.*, 2012).

The initiation and maintenance of haematopoiesis is a complex process that depends on the participation of support cells, which generate the microenvironmental conditions that maintain the size of the stem cell pool and regulate the differentiation of HSCs into the appropriate number of mature blood cells, both under steady-state and during homeostatic imbalance. Therefore, control

of the differentiation of HSPCs is a dynamic process depending on specific direct cell interactions, growth factors, cytokines and components of the extracellular matrix (F. E. Mercier *et al.*, 2012).

This supporting microenvironment is composed of mesenchymal stem and progenitor cells (MSPCs; also called skeletal stem cells), osteoprogenitors, osteoblasts, osteocytes, osteoclasts, fibroblasts and chondrocytes, together forming the so-called BM stroma (P. S. Frenette *et al.*, 2013, B. A. Anthony and D. C. Link, 2014). Other cell populations that reside in BM that may also participate in the regulation of haematopoiesis include neuronal cells, glial cells, leukocytes, macrophages and adipocytes (Figure 1.2) (K. Tokoyoda *et al.*, 2009b, B. A. Anthony and D. C. Link, 2014).

The BM stroma is organized into functional domains, forming specialized niches that regulate the development of HSCs and lineage restricted haematopoietic progenitor cells (F. E. Mercier *et al.*, 2012, B. A. Anthony and D. C. Link, 2014). At different stages of development HSPCs will require different cellular/molecular interactions, some of which were summarize in supplementary Table 1.1 (adapted from (F. E. Mercier *et al.*, 2012)) and reviewed in excellent reviews (F. E. Mercier *et al.*, 2012, L. D. Wang and A. J. Wagers, 2012, B. A. Anthony and D. C. Link, 2014). In this introduction, the focus is on examples of BM components that impact in early events in haematopoiesis.

Within the BM stroma, HSCs localize in haematopoietic stem cells niches, which provide a specialized microenvironment that tightly regulates the balance between self-renewal and differentiation. The identification of cell markers expressed in HSCs allowed the examination of their localization in BM, that were predominantly localized in contact with sinusoidal endothelium and associated with endosteum (M. J. Kiel *et al.*, 2005). These findings were followed by studies showing that most HSCs are found in close association with perivascular C-X-C motif chemokine 12 (CXCL12)-abundant reticular (CAR) cells and nestin-GFP⁺ stromal cells (B. A. Anthony and D. C. Link, 2014).

In the BM, the perivascular spaces are filled with MSPCs in close proximity to HSPCs. MSPCs are a heterogeneous population able to differentiate into osteoblasts, chondrocytes, adipocytes and fibroblasts and participate in BM stroma regeneration (F. E. Mercier *et al.*, 2012, P. S. Frenette *et al.*, 2013).

So far, it is not possible to phenotypically select for single mesenchymal stem cells (MSCs), but by methods to isolate MSCs-enriched cell populations it has been established in mice that ~4% of CD45⁻ lineage⁻ PDGFRa⁺ Sca⁺ cells have CFU (colony forming units)-F (fibroblast) activity and ~1% of nestin-GFP⁺ stromal cells have CFU-F activity, while in humans CD146-expressing

stromal cells characterize a BM cell population enriched for MSCs. Other studies reported that platelet-derived growth factor receptor (PDGFR) and CD51 expression may also select for a cell population that is highly enriched for MSCs and can support HSPCs expansion *in vitro*, both in mice and in humans (B. A. Anthony and D. C. Link, 2014).

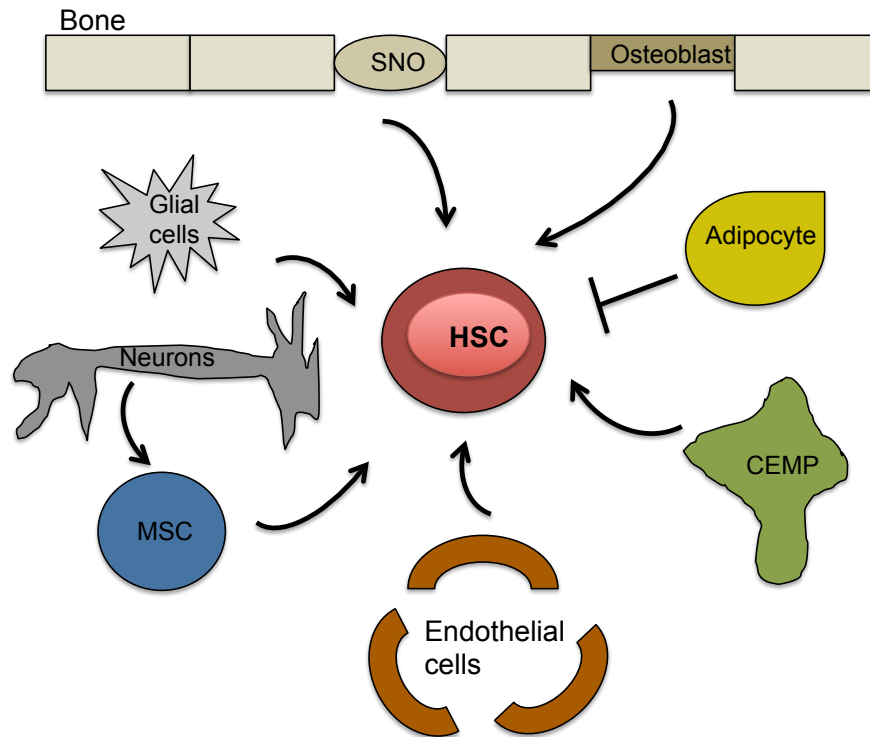


Figure 1.2 - Haematopoietic stem cell (HSCs) functions are supported by various BM stromal cells, comprising the so-called HSCs niche. In BM HSCs are found in close proximity with BM stromal cells: endothelial cells, mesenchymal stem cells (MSCs), which are included in the chemokine CXC ligand (CXCL)12-expressing mesenchymal cells (CEMCs). CEMCs are perivascular stromal cells and express various factors that support HSCs, such as CXCL12, angiopoietin, and stem cell factor (SCF). CEMCs are composed by various cell-types including, CXCL12-abundant reticular (CAR) cells, leptin receptor⁺ stromal (Lepr⁺) cells, and Nestin-GFP⁺ cells. Osteoblasts and spindle-shaped N-cadherin⁺ osteoblast (SNO cells) support HSCs through the expression of thrombopoietin (TPO) and CXCL12. Sympathetic neurons modulate HSCs functions by the induction of CXCL12 expression by other stromal cells. Glial cells, produce transforming growth factor (TGF)- β , and it has been also suggested that might regulate HSCs functions (Adapted from (B. A. Anthony and D. C. Link, 2014)).

Table 1.1 - Soluble factors produced by BM cellular niches that participate in the regulation of haematopoiesis

Soluble factor	Bone marrow source	Effects on HSCs or immune cells
Factors that affect HSCs		
Angiopoietin 1	Osteoblastic cells, nestin-expressing MSCs	Maintenance of long-term repopulating activity and quiescence
CXCL12	CAR cells, nestin-expressing MSCs, endothelial cells, osteoblastic cells,	Homing and retention; maintenance of the HSC pool size
SCF	Endothelial cells, osteoblastic cells, nestin-expressing MSCs	Maintenance of long-term repopulating activity
Notch ligands	Endothelial cells, osteoblastic cells	Increased expression on osteoblastic cells after parathyroid hormone stimulation is associated with increased HSC numbers in the bone marrow; however, loss of this signalling pathway does not impair HSC function in the steady state
Thrombopoietin	Osteoblastic cells	Maintenance of long-term repopulating activity and quiescence
WNT ligands	Osteoblastic cells	Conflicting findings: enhanced self-renewal when used pharmacologically; however, loss of this signalling pathway does not impair HSC function in the steady state; inhibition by osteoblastic cell-specific expression of DKK1 increased HSC cycling and reduced HSC serial transplant capability
Factors that affect immune cells		
APRIL	Granyocytes, lymphocytes, dendritic cells, megakaryocytes	Survival of plasma cell precursors
BAFF	Granulocytes, lymphocytes, dendritic cells	Survival of plasma cell precursors
CXCL12	CAR cells, nestin-expressing MSCs, endothelial cells, osteoblastic cells	Retention of B lymphoid progenitors in the bone marrow; homing and retention of plasma cell precursors; homing and retention of HSCs
IL-6	Endothelial cells, osteoblastic cells, megakaryocytes	Survival of plasma cells; pleiotropic effects on HSCs and myeloid progenitors
IL-7	IL-7-secreting stromal cells	Support of early B cell lymphopoiesis; survival of memory T cells
MIF	Dendritic cells	Survival of plasma cell precursors

APRIL, a proliferation-inducing ligand; BAFF, B cell activating factor; CAR, CXCL12-abundant reticular; CXCL12, CXC-chemokine ligand 12; DKK1, dickkopf-related protein 1; HSC, haematopoietic stem cell; IL, interleukin; MIF, macrophage inhibitory factor; MSC, mesenchymal stromal cell; SCF, stem cell factor

CXCL12-CXCR4 signaling is essential to the maintenance of the HSCs pool. In mice, the administration of CXCR4 antagonist induces increased frequency of HSPCs in circulation and the conditional deletion of CXCR4 was associated with vulnerability to myelosuppressive stress, related to a dramatic decrease in the HSCs pool. Within the BM, CXCL12 is expressed in osteoblasts lining the bone surface and in endothelial cells, but the cells that express the highest levels of this cytokine are chemokine CXC ligand (CXCL)12-expressing mesenchymal cells (CEMCs) present in the perivascular region. CEMCs, include CXCL12-abundant reticular (CAR) cells, leptin receptor⁺ stromal (Lepr⁺) cells, and Nestin-GFP⁺ cells (P. S. Frenette *et al.*, 2013). The CAR cells are also a major source of stem cell factor (SCF) and their localization in close association with HSPCs suggested that CAR cells might be a key component of HSC niches (F. E.

Mercier *et al.*, 2012, P. S. Frenette *et al.*, 2013). Furthermore, short-term ablation of CEMCs cells using a CXCL12-DTR-GFP mice showed a significant decrease in HSCs in the BM (T. Sugiyama *et al.*, 2006).

Endothelial cells were also shown to support the proliferation of HSPCs *in vitro*. For example, deletion of the endothelial specific adhesion molecule, E-selectin, resulted in increased HSCs quiescence, and the deletion of *Kit ligand* (SCF) from endothelial cells resulted in the loss of HSCs. Collectively, these findings suggested that endothelial cells are required for HSCs proliferation regulation and maintenance (B. A. Anthony and D. C. Link, 2014).

Several studies have pointed out an inhibitory role for adipocytes in haematopoiesis. HSCs were decreased in BM areas rich in adipocytes and in mice pharmacological inhibition of adipogenesis was associated with an improved haematopoietic recovery following stem cell transplantation in myeloablated mice (B. A. Anthony and D. C. Link, 2014).

In BM, autonomic nerves have been shown to be in close proximity to HSCs and, recently, several studies have been shown that neurological components may also regulate haematopoiesis. For example, it was reported that pharmacological ablation of adrenergic signaling inhibits G-CSF-induced HSPCs mobilization. G-CSF has been long used in the clinic to mobilizes HSPCs from BM to the periphery through mechanisms that include the induction of proteolytic activity that cleaves CXCL12 (S. Mendez-Ferrer *et al.*, 2008).

In the endosteal niche, osteoblasts interact with HSCs at the interface between the bone and the marrow space. The genetic ablation of osteolineage cells was associated with a dramatic increase in extramedullary haematopoiesis (D. Visnjic *et al.*, 2004) and in a study, where osteoblasts were expanded by enforced expression of parathyroid hormone receptor 1, HSCs were shown to increase in number (B. A. Anthony and D. C. Link, 2014). The BM osteolineage cells secrete cytokines such as M-CSF, GM-CSF, IL (Interleukin)-1, IL-6, IL-7, Thrombopoietin (TPO) and CXCL12, all soluble haematopoietic factors. Moreover, osteoblasts express adhesion molecules such as VCAM1, ICAM1, annexin II, N-cadherin, CD44 and CD164, that may be implicated in cell-cell interactions within the niche (F. E. Mercier *et al.*, 2012).

BM stromal macrophages (distinguished by CD169 expression) are also associated with the endosteal and the vascular niches and may also have a role in the regulation of haematopoietic stem cells niches, through the regulation of the expression of CXCL12 by BM stromal cells (F. E. Mercier *et al.*, 2012, M. Casanova-Acebes *et al.*, 2013). For example, the depletion of CD169⁺ BM macrophages *in vivo* resulted in a higher frequency of LSK cells in circulation. This increased mobilization was associated with a decrease in the levels of CXCL12 expression by Nestin⁺

MSCs, following depletion of BM macrophages *in vivo*. These findings suggested that BM macrophages contributed to the retention of HSCs in the BM by acting on Nestin⁺ MSCs (A. Chow *et al.*, 2011).

T cells are not regarded as “BM stromal cells”, but are present in the BM and they are well known sources of haematopoietic growth factors, such as IL-3 and GM-CSF. Their role in homeostatic haematopoiesis, however, remains unclear (J. P. Monteiro and A. Bonomo, 2005). In athymic BALB/c ^{nu/nu} mice (which lack T cells), it was reported that the accumulation of immature myeloid cells and reduced numbers of granulocytes in peripheral blood could be rescued by the reconstitution with purified CD4⁺ T cells, but not purified CD8⁺ T cells (J. P. Monteiro *et al.*, 2005). T cells are sources of the pro-inflammatory cytokines IFN γ (Interferon-gamma) and TNFs and several reports suggested that both cytokines might impact on the modulation of haematopoiesis in BM (C. Selleri *et al.*, 1995, M. T. Baldrige *et al.*, 2010, C. J. H. Pronk *et al.*, 2011, F.-c. Lin *et al.*, 2014). Collectively, these studies point to a regulatory role for T cells in both homeostatic and stress-induced haematopoiesis.

1.1.3.2 Cytokine Receptors and Haematopoiesis

Haematopoiesis relies on strictly regulated pathways that assure the continuous production of mature cells from HSCs (M. Kondo *et al.*, 2003a). These processes are crucial to survival since the majority of mature haematopoietic cells are short lived and cytokines have been shown to be required to modulate not only steady-state haematopoiesis, but also events that require stress-induced haematopoiesis, such as bleeding and infection (M. Kondo *et al.*, 2003a, J. L. Zhao and D. Baltimore, 2015).

The roles of various cytokines in haematopoiesis are still elusive, therefore in this section we aimed to give some examples of cytokines which role have been well established in lineage commitment, which alongside other relevant cytokines were summarize in Figure 1.3.

c-Kit receptor tyrosine kinase for the stem cell factor (SCF) is expressed in HSCs, MPPs and in early lineage-committed progenitors. SCF seems to act at various levels of ontogeny cooperating with other growth factors in lymphopoiesis, erythropoiesis and megakaryopoiesis (S. D. Lyman and S. E. W. Jacobsen, 1998). For example, the null alleles for c-Kit cause embryonic lethality associated with severe anemia, but viable alleles with impaired c-Kit tyrosine kinase activity have allowed the study of SCF signaling in haematopoiesis. The defective SCF signaling in HSCs was associated to decreased number of HSCs in BM of adult mice and impaired long-term reconstitution potential that could not be rescued by the overexpression of the anti-apoptotic factor BCL2, suggesting that cKit signaling is required to preserve extensive self-renewing divisions and therefore crucial to HSCs function (L. A. Thoren *et al.*, 2008).

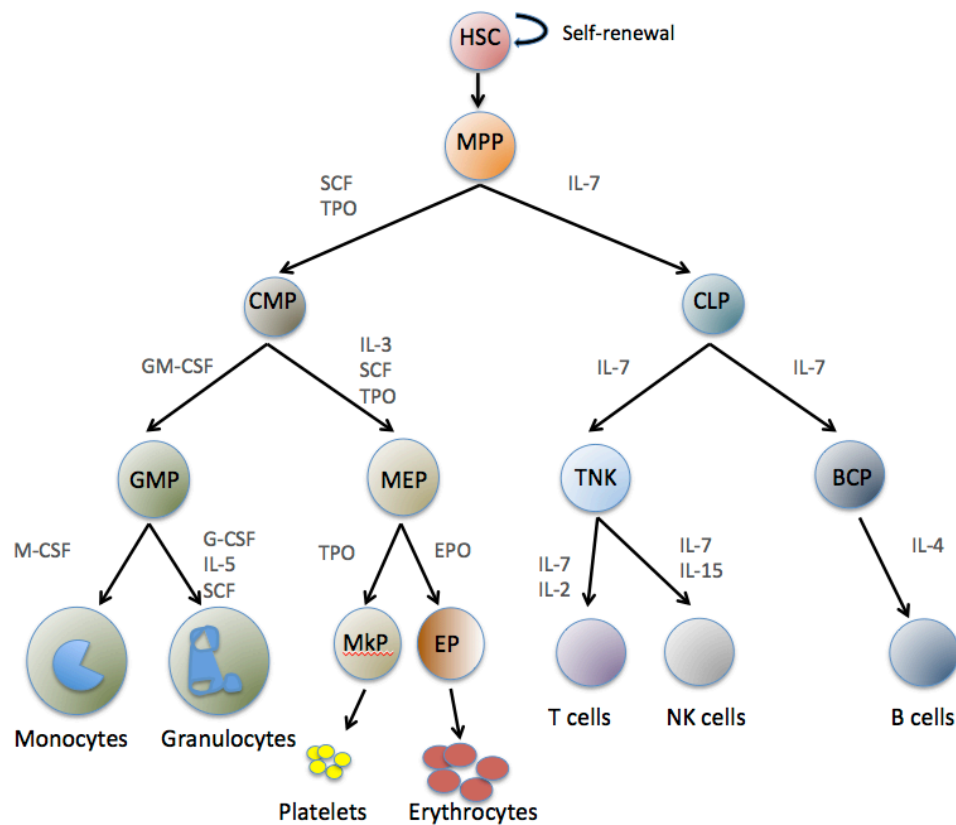


Figure 1.3 - Summary of haematopoietic cytokines. Several cytokines modulate the differentiation of multipotential progenitors and their lineage-committed providing survival, proliferation or instructive signals. BCP, B-cell progenitor; CLP, common lymphoid progenitor; CMP, common myeloid progenitor; EP, erythroid progenitor; HSC, haematopoietic stem cell; GMP, granulocyte-macrophage progenitor; MEP, megakaryocyte erythroid progenitor; Mkp, megakaryocyte progenitor; TNK, T-cell natural killer cell progenitor (Adapted from (L. Robb, 2007)).

The first haematopoietic growth factor identified was later called erythropoietin. The kidney produces the vast majority of erythropoietin, where juxta-tubular interstitial cells are capable of sensing the levels of tissue oxygenation. Erythropoietin blood levels are tuned by the level of oxygenation and according to homeostatic requirements modulate the expansion of erythroid progenitor cells, promoting progression in cell cycle and increased expression of the anti-apoptotic protein BCLXL (K. Kaushansky, 2006).

The growth factors more commonly associated with myeloid lineage cells development were initially identified by their potential to support different myeloid cell colonies when added to

cultures of BM cells in a semisolid medium. These myeloid associated growth factors include the macrophage colony-stimulating factor (M-CSF), granulocyte/macrophage colony-stimulating factor (GM-CSF), the granulocyte colony-stimulating factor (G-CSF) and the multi colony-stimulating factor known as interleukin-3 (multi-CSF or IL-3), and are produced in various organs by several cell types including endothelial cells, fibroblasts, and macrophages (D. R. Barreda *et al.*, 2004).

M-CSF promotes monocyte/macrophage development, while G-CSF has been more associated to granulocyte development and *in vivo* studies using knockout mice identified G-CSF as an essential growth factor for terminal normal maturation of neutrophil progenitors. IL-3 and GM-CSF promote the granulocytic, macrophage and granulocyte-macrophage colony formation and it is believed that these growth factors exert their function in more immature myeloid progenitors. These factors show some level of functional redundancy since *in vivo* defect in one of these growth factors does not lead to a serious impact on homeostasis (D. R. Barreda *et al.*, 2004).

Thrombopoietin (TPO) was identified as the primary regulator of platelet production, supporting the proliferation and survival of megakaryocyte progenitors through the upregulation of the cell-cycle regulator cyclin D and anti-apoptotic molecule BCLXL. In mice deficient for TPO or its receptor the production of megakaryocytes was reduced and platelets production severely impaired. TPO is mostly produced in the liver but kidney and skeletal muscles also produce TPO and the number of platelets in circulation and megakaryocytes in BM regulates its blood levels (K. Kaushansky, 2006). TPO was also shown to be very important for the survival and expansion of HSCs. Donor HSCs from mice deficient for TPO or its receptor (c-mpl) showed impaired capacity to reconstitute recipient mice. Additionally, patient with c-mpl defects present thrombocytopenia and severe anemia due to BM exhaustion (K. Kaushansky, 2006).

Flt3 (fms-like tyrosine kinase 3) receptor tyrosine kinase is expressed in MPPs and early myeloid and lymphoid lineage-committed progenitor cells and binds to FLt3 ligand (FL), which is expressed in various tissues (S. D. Lyman and S. E. W. Jacobsen, 1998). This tyrosine kinase seems to be important in the generation of CLPs since mice deficient in expression of FL showed primarily impairment of lymphopoiesis, although NK and dendritic cells were also reduced (E. Sitnicka *et al.*, 2002).

IL-7 production has been detected in several non-lymphoid cells in lymphoid organs, such as thymus, BM, spleen and kidney. Its importance became evident after the observation that mice deficient for IL-7 were highly lymphopenic. Today is well established that IL-7 is essential to lymphopoiesis both in early and later stages of lymphoid lineage specification, it plays both instructive and permissive functions in lymphoid development such as promotion of survival

signals (e.g. BCL2 expression) and upregulation of lineage transcription factors (e.g. Ebf-1) (U. Vonfreedenjeffry *et al.*, 1995, Q. Jiang *et al.*, 2005, P. Tsapogas *et al.*, 2011).

1.1.3.3 Transcription Factors in Lineage Commitment

The process of differentiation of multipotent cells towards different blood cell lineages depends on the initiation and the sustainment of lineage specific genetic programs. It has been shown that multiple different lineage-restricted genes are expressed in multipotent progenitors and it has been suggested that the processes of lineage commitment require not only the induction/reinforcement of lineage-specific genes but also the repression of genes associated with other lineages (M. A. Rieger and T. Schroeder, 2012). The establishment of stable gene programs depends on transcription networks sustained by transcription factors in association with cofactors, chromatin modifiers, and regulatory RNAs (M. A. Rieger and T. Schroeder, 2012).

The intrinsic molecular networks for lineage differentiation are discussed in excellent reviews (S. I. Kim and E. H. Bresnick, 2007, S. H. Orkin and L. I. Zon, 2008, E. M. Mercer *et al.*, 2011, G. Sashida and A. Iwama, 2012, R. A. Nimmo *et al.*, 2015). In this section, we aimed to at some extent give examples that emphasize the role of transcriptions networks in haematopoiesis.

The requirements for TFs have been temporally defined and vary in different stages of development (S. H. Orkin and L. I. Zon, 2008). For example SCL/*tal1* is essential for the formation of haematopoietic system during embryogenesis. Nonetheless the study of this TF in adult mice using conditional mutants and competitive BM chimeras showed that SCL/*tal1* is not required for HSCs survival and functions (self-renewal and multilineage repopulation of the haematopoietic system) but essential for the terminal differentiation of erythroid and megakaryocytic precursors (H. K. A. Mikkola *et al.*, 2003).

TFs determine lineage specification and commitment, in a context-depend process, (H. Iwasaki *et al.*, 2006, S. H. Orkin and L. I. Zon, 2008) with PU.1 and GATA-1 serving as prototypical examples in haematopoiesis. The co-upregulation of PU.1 and GATA-1 may be one of the earliest steps in lineage commitment of HSCs to CMPs but later in development their expression is segregated. The predominance of GATA1 has been associated to myeloerythroid bias and the predominance of PU.1 to myelolymphoid lineage bias in HSCs (J. Zhu and S. G. Emerson, 2002).

GATA-1 is essential for terminal differentiation of erythroid precursors since it promotes the expression of several erythroid genes. GATA-1 is not appreciably expressed in myeloid cells and induced expression of GATA-1 in the myeloid progenitor line 416B blocked myeloid differentiation and induced erythroid, megakaryocytic, and eosinophilic characteristics in cultured cells (S. H. Orkin, 2000). On the other hand, PU.1 is expressed in myeloid and lymphoid

progenitor cells and in mice deficient for PU.1 gene the development of both lineages was impaired. It was found that this TF is necessary for the transcription regulation of other factors required for lymphoid and myeloid lineage differentiation, such as IL-7 receptor and M-CSF receptor, respectively. It was showed that PU.1 induced expression alone could commit multipotent haematopoietic progenitors to monocytic/granulocytic lineages direction (J. Zhu and S. G. Emerson, 2002).

The potential for inhibitory interactions between transcription factors was implied by the observations that overexpression of GATA-1 or PU.1 blocks myeloid or erythroid differentiation, respectively. It has been proposed that these factors physically interact and antagonize each other's actions, and an extended body of literature supports the proposition that GATA-1 and PU.1 are expressed at low level in undifferentiated stable progenitor that differentiates into to one of the main lineage branches when one of the proteins is expressed at higher levels (S. H. Orkin and L. I. Zon, 2008).

Despite these roles in early commitment of myeloerythroid/myelolymphoid lineages both GATA-1 and PU.1 interact (synergistic or antagonizing interactions) with other TFs across haematopoietic development, emphasizing how fine tuned and complex is the genetic regulation from HSCs to mature blood cells. For examples: GATA-1 and Friend of GATA-1 (FOG-1) are required for in erythroid differentiation; PU.1 and Gfi1 in monocytes and neutrophil cells development, respectively; and in T cell development repression of PU.1 by notch signaling (S. H. Orkin and L. I. Zon, 2008).

One example of the relevance of the order of TFs expression came from Iwasaki H. studies *in vitro* showing that eosinophils and basophils development from purified GMPs requires the both the expression of GATA-2 and CCAAT enhancer-binding protein α (C/EBP α). Importantly it was showed that the differentiation of these two mature cell types critically depended on the order of expression of these two TFs to specifically promote the genetic program for each of these lineages (H. Iwasaki *et al.*, 2006).

The classic representation of haematopoiesis in hierarchic diagrams offer an over simplistic view that although useful does not include the more updated view of the processes of ontogeny. In the light of new findings, haematopoietic populations are best understood as group of cells with different developmental potentials with outcomes that depend on the dynamic crosstalk between intrinsic factors (such as TFs and epigenetic regulation) and signals from their niches. The "lineage priming" phenomenon equipped the HSPCs with flexibility to face the need of blood cells replenishment in homeostasis and injury, but in order to preserve integrity of haematopoietic system the regulation as to be very tight. In this context the further study of TFs is extremely

relevant to determine a clearer picture of haematopoiesis, in the development of cellular therapies and in the study of haematopoietic malignancies where many genes for TFs have been found mutated or translocated (S. H. Orkin and L. I. Zon, 2008, R. A. Nimmo *et al.*, 2015).

1.1.4 Haematopoietic Stem Cells in Adult Mammals

The exposure to radiation during the World War II showed for the first time how ionizing radiation damaged the haematopoietic system (J. Domen *et al.*, 2006). These effects were replicated in mice and it was found that a lethal outcome could be prevented if a bone or the spleen were protected from irradiation, as well as by transplantation of BM cell suspensions (J. Domen *et al.*, 2006).

Seminal experiments from Till and McCulloch found that in mice subjected to heavy doses of radiation, if limiting BM cell suspensions (sub-radioprotective) were transferred between day seven and ten, macroscopic clusters of haematopoietic cells would appear in the spleen. These clusters were composed of dividing haematopoietic cells that could differentiate in erythroid, myeloid and megakaryoid lineages. Furthermore, when a very low number of BM cells displaying an abnormal karyotype (due to exposure to ionizing radiation) were transferred to lethally irradiated mice, it was observed that each cluster in the spleen arose from a single clone; since the daughter cells in each colony presented the same unique alterations in their chromosomes. As such, it was demonstrated that in the BM, cells with the unique ability to perform multilineage haematopoietic reconstitution are present, the so called HSCs (A. J. Becker *et al.*, 1963).

In subsequent experiments it was observed that some of these spleen colonies were constituted by identical daughter cells and could form multilineage colonies in the spleens of secondary irradiated recipients. More, each clonogenic colony contained a variable number of cells and a variable composition of mature and progenitor cells. Collectively these findings suggested that the haematopoietic system would arise from a rare group of BM cells that were characterized by “stemness”, self-renewal capacity, capacity to originate multi haematopoietic lineages and high proliferative potential, the nowadays well established HSCs (A. J. Becker *et al.*, 2014). Further developments in this field came from studies *in vitro* and *in vivo*, all pointed to a hierarchic haematopoietic development from a multipotential progenitor to lineage restricted progenitors (C. J. Eaves, 2015).

Nonetheless, only in 1996 was the proof of principle for an HSC established by Osawa, when the injection of a single lineage negative (negative for a pool of canonical markers for mature haematopoietic cells) CD34^{10/}- c-Kit⁺ Sca-1 (Stem cell antigen)⁺ cell reconstituted the lympho-haematopoietic system of a recipient mouse for more than four months (M. Osawa *et al.*, 1996, C. J. Eaves, 2015).

HSCs have been extensively studied over the past decades because they provide a source of potential stem cell based therapeutic tools in the approach of a wide range of haematopoietic, genetic and immune disorders. HSCs transplantation (enriched from BM cells, mobilized peripheral blood stem cells or umbilical cord blood) is nowadays a well-established procedure that saves thousand of lives every year, but it still relies on the availability of donors with matching human leukocyte antigens (HLA) (M. A. Walasek *et al.*, 2012).

In humans, patient survival upon the HSCs transplantation has been directly associated to the initial amount of stem cells (CD34⁺ cells in humans). To face the scarcity of HSCs obtained by conventional sources, many attempts have been made to establish protocols to expand HSCs *ex vivo* but it was soon found that *in vitro* HSCs readily differentiate and loose self-renewal attributes, becoming therefore inadequate to reconstitute the haematopoietic system when transplanted (M. A. Walasek *et al.*, 2012).

The culture conditions that allow HSCs to undergo *ex vivo* symmetrical self-renewal over unlimited differentiation divisions have not yet be defined. However the intense research over the past decades on the mechanisms regulating of expansion and maintenance of self-renewal of HSCs has disclosed some molecular mechanisms and regulatory networks that modulate HSCs fate (M. A. Walasek *et al.*, 2012, S. Lin *et al.*, 2015).

The lack of a protocol suitable to expand HSCs for clinical purposes, despite its importance in a wide range of disease scenarios, illustrates two important features regarding the study of HSCs in adult mammals: 1) the regulation of HSCs seems to be extremely complex and depend on intricate dynamics between intrinsic and extrinsic factors; 2) the study of HSCs is technically challenging due to their scarcity in the adult and rapid differentiation in *ex vivo* settings.

In the next sections, we will discuss some molecular mechanisms relevant to the regulation of HSCs function.

1.1.4.1 Haematopoietic Stem Cell, Quiescence *versus* Proliferation

The hallmarks of stem cells are their dual capacity to produce more identical stem cells (self-renewal) and to produce cells that ultimately will give rise to mature cells (multipotential of differentiation). One strategy by which HSCs can accomplish these two tasks is either by asymmetric cell division, in which the stem cell divides to generate one daughter with a stem-cell fate (self-renewal) and one daughter that initiate differentiation. Or alternatively, symmetrical divisions may give rise to two identical stem cells (self-renewal) or two lineage-committed daughter cells (differentiation) (Figure 1.4) (A. D. Ho and W. Wagner, 2007).

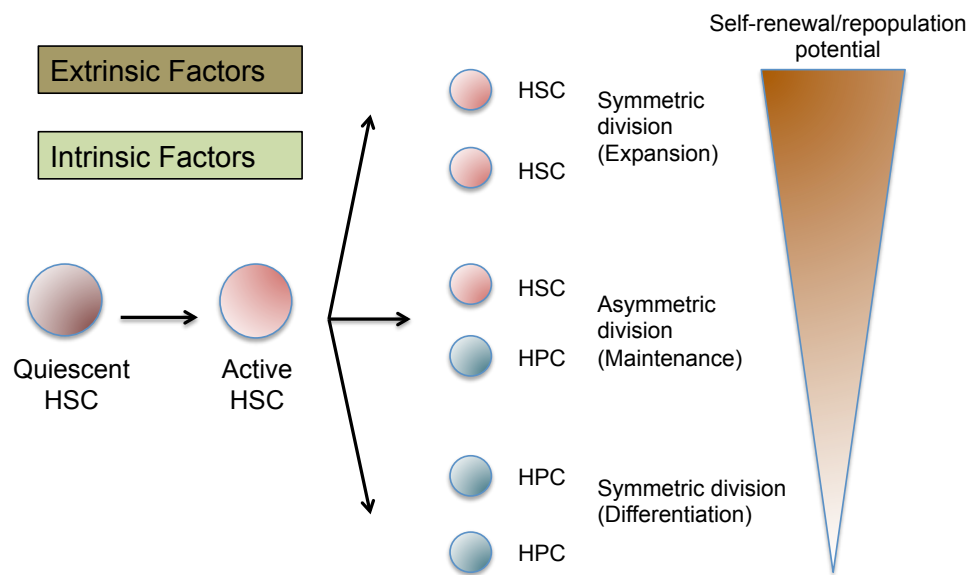


Figure 1.4 - Schematic overview of different HSCs cellular fate choices. Quiescent HSCs (G0) can be activated to enter the cell-cycle (G1/S/G2/M phases) to self-renew and/or differentiate by cell-intrinsic or cell-extrinsic factors, leading to symmetric or asymmetric cell divisions. HPC (hematopoietic progenitor cell) (Adapted from (A. Nakamura-Ishizu et al., 2014)).

In this section, we provide some examples of *in vivo* studies that lead to the characterization of molecular factors relevant in the regulation of HSCs fate. These examples, and others not discussed here, are summarized in Table 1.2 (Adapted from (K. W. Orford and D. T. Scadden, 2008, M. R. Warr et al., 2011, A. Nakamura-Ishizu et al., 2014)).

The quiescent HSCs reside at the top of the haematopoietic hierarchy and fine tuned regulation of their cell cycle, decision to self-renew and/or differentiate is therefore required to maintain the adequate production of blood cells at the expense of minimum stem cell exhaustion. It is accepted that the decision to exit quiescence depends both on cell-intrinsic and -extrinsic factors that induce quiescent HSCs to proliferate and differentiate (A. Nakamura-Ishizu *et al.*, 2014).

Murine embryonic stem cells (mES) can be expanded *in vitro* without compromising their self-renewal potential and this ability has been attributed to their shorter cell cycle. mES have reduced G1 phase because they have constitutive cyclin E-cdk2 activity and express very low levels of the D-type cyclins. In contrast, in adult cells cyclin E-cdk2 activity is transient peaking at the G1 to S transition. Likewise, mES do not display early G1 phase or restriction point of cell cycle (Figure 1.5). In contrast, most somatic cells to progress through the early G1 phase of the cell cycle require

mitogen activated protein kinase (MAPK) signaling, which was shown (particularly prolonged MAPK signaling) to be an inducer of differentiation. Therefore it was suggested that the absence of early G1 in mES cells might allow them to escape the differentiation-inducing effects of certain mitogenic signaling pathways, otherwise active during early G1 in somatic cells. Therefore, it is not surprising that many factors associated with the regulation of HSCs quiescent/self-renewal potential are molecular factors that regulate the cell cycle (K. W. Orford and D. T. Scadden, 2008).

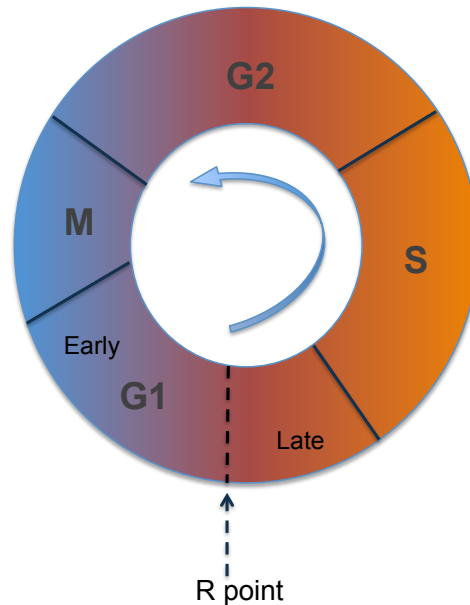


Figure 1.5 - Overview of cell cycle. Cell proliferation occurs through a series of stages that are collectively termed the cell-cycle. Classically, the cell-cycle has been divided into four phases that are organized around the synthesis (S) phase and mitotic segregation (M) phase of the genome with two intervening gap phases (G1 and G2) preceding S and M phases, respectively. Progression through the cell cycle is highly regulated, particularly at the transitions from G1 phase to S phase and from G2 phase to M phase. In addition to other cell-intrinsic checkpoints (for example, the evaluation of the integrity of the genome), combinations of intrinsic and extrinsic signals regulate the passage from early to late G1 phase in somatic cell. This transition is called the restriction (R) point, and divides the G1 phase of the cell cycle into the mitogen-dependent early G1 phase and the mitogen-independent late G1 phase. In general, cells have to be stimulated by mitogenic signals (for example, soluble growth factors) to “cut through” the G1 phase and enter into the cell-cycle. The R point represents the ‘point of no return’ for the cell, after which the cell has committed to enter the cell-cycle and mitogenic stimuli are no longer required. In the absence of mitogenic stimulation, cells can exit from the cell cycle during early G1 phase and enter a dormant, or quiescent, state called the G0 phase that is characterized by small cellular size and low metabolic activity (Adapted from (K. W. Orford and D. T. Scadden, 2008)).

The cyclin-dependent kinase (CDK)-inhibitor p21 seems to be important in DNA damage responses but its role in the steady-state is less clear. Initial studies showed p21^{-/-} lineage negative cells (enriched for HSPCs) were more proliferative and displayed self-renewal defects, characterized by early exhaustion following serial BM transfer and repeated 5-Fluorouracil (FU) treatments (M. R. Warr *et al.*, 2011). Then, an other study using a more purified population enriched for LT-HSCs (LSK CD150⁺ CD48⁻) showed conflicting results. The number of quiescent HSCs was maintained in mice deficient for p21. However, in the absence of this factor, the function of HSCs was impaired compared to wild type (WT) HSCs in BM transplant (BMT) assays, but only if the transplanted BM cells were first treated with 2Gy irradiation. This suggested that p21 was important for DNA repair but not crucial in HSCs function (R. Van Os *et al.*, 2007)

The transcription factor c-Myc has been implicated in the regulation of cell proliferation, differentiation, and apoptosis. c-Myc heterodimerizes with its partner Max induce the expression of genes that promote cell-cycle G1/S transition (including *cyclin D1*, *cyclin D2*, *cyclin E* and *cyclin A*) and represses the expression of cell cycle inhibitors p27 and p21, favoring cell-cycle progression (M. J. Murphy *et al.*, 2005). Conditional deletion of *Myc* in BM was associated to severe anemia and leucopenia and increased number of HSCs (defined as LSK Flt3⁻). *Myc*-deficient HSCs failed to engraft in recipient, suggesting that *Myc*-deficient HSCs were functionally defective, and that in the basis of this impaired haematopoiesis was an intrinsic defect in HSCs function (A. Wilson *et al.*, 2004). Interestingly *p21* a c-Myc target with disputed roles in cell-cycle regulation and in HSCs self-renewal, was found upregulated in HSCs following conditional deletion of c-Myc *in vivo*, and it was proposed that c-Myc may modulate HSCs functions through p21 repression (E. Baena *et al.*, 2007).

An example of the role of extrinsic factors in regulating HSCs function comes from the canonical Wnt signalling cascade, which has been implicated not only in the regulation of HSCs function but also in the development of other haematopoietic progenitors. The specific impact of canonical Wnt signalling in haematopoiesis is still disputed, due to opposing outcomes resulting from various inducible Wnt-signaling loss-of-function and gain-of-function models (T. C. Luis *et al.*, 2010a).

Wnts are secreted glycoproteins that bind to membrane-associated receptors, the Frizzled (FZD) proteins, a family of seven-pass transmembrane receptors. So far, nineteen different Wnt ligands and ten FZD receptors have been identified in humans and mice, and the complexity is further increased because Wnts can use distinct co-receptor proteins that initiate canonical and non-canonical signaling pathways. The activation of canonical Wnt signaling pathway is defined by the translocation of the transcriptional co-activator β -catenin to the nucleus, where together with T-cell factor (TCF) and lymphoid enhancer binding factor (LEF) initiates the transcription of target genes. When Wnt signaling is not activated, β -catenin is associated in the cytoplasm to a protein

complex responsible for the phosphorylation and degradation of β -catenin, preventing its accumulation in the cytoplasm and nuclear translocation. This destruction complex is composed by axis inhibition protein 1 (AXIN1), adenomatous polyposis coli complex (APC), and the serine/threonine glycogen synthase kinase 3 beta (GSK3 β) (C. J. Cain and J. O. Manily, 2013).

The role of canonical Wnt signaling became evident when it was shown that *Wnt3a*-deficient mice die around embryonic day (E) 12.5. HSCs from fetal liver (FL) showed cell intrinsic defects, such as severely reduced reconstitution capacity as measured in transplantation assays into *Wnt3a* competent mice (T. C. Luis *et al.*, 2009).

Nonetheless in adult *Mx-Cre*-mediated β -catenin deficiency, under control of the type I interferon-inducible *Mx* promoter, did not impact in haematopoiesis, although this might be explained by incomplete deletion of Wnt signaling. In contrast, when Wnt signalling was inhibited by ectopically expressing Axin in HSCs, these showed a dramatic impairment in the reconstitution of lethally irradiated mice when compared to control transduced HSCs (T. Reya *et al.*, 2003). To add more confusion, other gain of function assays to determine role of Wnt canonical signaling resulted in conflicting outcomes (T. C. Luis *et al.*, 2010a).

A more recent work, suggested that Wnt signaling during haematopoiesis has to be tightly regulated. This study was performed using mouse models carrying specific hypomorphic mutations at the *Apc* gene resulting in specific Wnt signaling dosage. Mildly increased activation (two fold) of the Wnt signaling pathway in HSCs resulted in increased frequency of repopulating cells compared to control donor HSCs, 12 weeks after transplantation, both in primary and secondary transplantation assays. On the other hand, donor HSCs expressing higher levels of canonical Wnt activation had decreased reconstitution potential in lethally irradiated recipients compared to control donor cells. This suggested that only mildly increased levels of activation enhance long-term repopulation capacity (T. C. Luis *et al.*, 2011).

Another example how the same TFs may play different roles in different stages of haematopoietic development is the role of GATA-3, for long known to be crucial in the development of T cells at multiple stages in the thymus and for Th2 differentiation in the peripheral organs. The TF GATA-3 was found also expressed in various haematopoietic progenitor populations in BM, with HSCs expressing the highest levels of GATA-3 (C.-J. Ku *et al.*, 2012). Recent studies have suggested that GATA-3 is important for the maintenance of a normal number of HSCs and to be required for their entry into the cell cycle, however it was also implicated in loss of self-renewal potential during stress-induced haematopoiesis (C.-J. Ku *et al.*, 2012, C. Frelin *et al.*, 2013).

For example, it was shown that upon poly I:C treatment, proliferating HSCs showed nuclear (i.e. active) GATA-3 and were only capable of short-term multilineage reconstitution. After the proliferative stimulus was removed, GATA-3 re-localized to the cytoplasm and long-term lineage reconstitution was restored. Further, in competitive transplant assays of BM cells from poly I:C treated *GATA-3* cKO and WT mice, GATA-3 deficient donor cells were more efficient in performing haematopoietic reconstitution, upon 32 weeks. These data suggested that GATA-3 might limit long-term self-renewal during proliferation of HSCs. The localization of GATA-3 in the nucleus depended directly on p38 α activation in culture, as shown by *in vitro* pharmacological inhibition (C. Frelin *et al.*, 2013). Additionally, the activation of the p38 MAPK pathway in response to reactive oxygen species has been reported to cause HSC exhaustion, pharmacological inhibition of p38 MAPK maintained stemness of cultured mouse and human HSCs, and *in vitro* studies showed that p38 MAPK modulates the activity of the critical regulator of HSC quiescence p57 (Cdkn1c) (C. Frelin *et al.*, 2013, M. Tesio *et al.*, 2015).

Table 1.2 - Summary of relevant genetic mouse models that contributed to the identification of molecular modulators of HSCs cell-cycle

Cell intrinsic regulators	Gene	Mouse model	HSCs cell cycle activity	Effect on repopulation potential
Cell cycle regulators				
	Cyclin A	Conditional KO	Increased	Decreased
	Rb family (Rb1, Rbl1, Rbl2)	Triple KO (Mx-1-Cre)	Increased	Decreased
	Cdkn2a (p16)	KO (aged mice)	Increased	Increased
	Cdkn1a (p21)	KO	Decreased or Unchanged	Decreased
	Cdkn1c (p57)	Conditional KO (Mx1-Cre)	Decreased	Decreased
	p53 (Trp53)	KO	Increased	Increased
Nuclear regulators				
	Myc/Mycn	Conditional KO (Mx-1-Cre)	Decreased differentiation	Decreased
	Fbxw7	Conditional KO (Mx-1-Cre)	Increased	Decreased
	Runx1	Conditional KO (Mx-1-Cre)	Increased	Decreased
	Gfi1	KO	Increased	Unable to engraft in CRA
	Mef (Elf4)	KO	Increased	Increased
	Foxo1/3/4	KO	Increased	Decreased
	Bmi1	KO	Increased	Decreased
	Foxo1/3/4	KO	Increased	Decreased
	Pten	Conditional KO (Mx-1-Cre)	Increased	Decreased
Epigenetic Regulators				
	Mysm1	KO	Increased	Decreased
	Dnmt3a	Conditional KO	Decreased	Decreased
Environmental factors				
	Tpo	KO	Increased	Decreased
	Ang-1	Retroviral expression	Increased	Decreased
	Kit	Hypomorphic allele	Increased	Decreased
	Cxcr4	Conditional KO	Increased	Decreased

CRA, competitive repopulation assay; HSC, haematopoietic stem cell; KO, knockout, Ang, Angiopoietin; Tpo, Trombopoietin.

1.1.4.2 Immunophenotypic evaluation

The assessment of HSCs function ('stemness') *in vivo* has been possible due to constant technical improvements: *in ex vivo* culture systems, in cell purification strategies through a set of cell-surface markers, in cell-cycle status evaluation and *in vivo* long-term reconstitution assays upon transplantation to conditioned recipients. In spite of decades of research on HSCs, the characterization of markers for isolation is still in flux, with the frequent description of new markers for HSCs purification (Table 1.3). This requires retrospective studies to be evaluated with caution. Another constraint in the study of HSCs function comes from their relative scarcity, which restricts the study of HSCs function to approaches that do not require large amounts of starting material or through inference. More recently, advances in *in vivo* imaging and transcriptomic analysis at the single cell level have started to provide important insights on HSC biology (G. A. Challen *et al.*, 2009, A. Nakamura-Ishizu *et al.*, 2014).

Table 1.3 - Summary of most commonly used combinations of cell surface marker used to segregate HSPCs

Cell type	Phenotype	Ref.
Long-term hematopoietic stem cells (LT-HSCs)	Lineage ^{-low} Sca1 ⁺ cKit ^{hi} FLt3 ⁻ CD34 ⁻	(Kondo et al., 2003)
Short-term hematopoietic stem cell (ST-HSC)	Lineage ^{-low} Sca1 ⁺ cKit ^{hi} FLt3 ⁻ CD34 ⁻	
Multipotent progenitors (MPP)	Lineage ^{-low} Sca1 ⁺ cKit ^{hi} FLt3 ⁺ CD34 ⁻	
Hematopoietic stem cells (HSCs)	Lineage ^{-/low} Sca1 ⁺ cKit ^{hi} CD150 ⁺ CD48 ⁻	(Oguro et al., 2013)
Hematopoietic progenitor cells 1 (HPC-1)	Lineage ^{-/low} Sca1 ⁺ cKit ^{hi} CD150 ⁻ CD48 ⁺	
Hematopoietic progenitor cells 2 (HPC-2)	Lineage ^{-/low} Sca1 ⁺ cKit ^{hi} CD150 ⁺ CD48 ⁺	
Common lymphoid progenitors (CLP)	Lineage ^{-/low} cKit ^{hi} IL-7R α ⁺ CD34 ^{-/low}	(Kondo et al., 2003) (Belyaev et al., 2010)
Common myeloid progenitor (CMP)	Lineage ^{-/low} cKit ^{hi} CD16/32 ^{-/low} IL-7R α ⁻ CD34 ⁺	
Granulocyte-macrophage progenitor (GMP)	Lineage ^{-/low} cKit ^{hi} CD16/32 ⁺ IL-7R α ⁻ CD34 ⁺	
Megakaryocyte-erythrocyte progenitor (MEP)	Lineage ^{-/low} cKit ^{hi} CD16/32 ⁻ IL-7R α ⁻ CD34 ⁻	

The phenotypic identification of haematopoietic progenitor cells relies on the expression (or lack of expression) of a combination of cell surface expressed proteins (markers) on individual cells, since a unique surface-cell marker has yet to be defined to segregate HSCs from onward progenitors. Using flow cytometry became possible to determine which fluorochrome conjugated

monoclonal antibodies binds to each cell, allowing not only the identification of different cell populations but also the isolation of live cells (cell-sort) to use in further functional assays, using the so-called fluorescence activated cell sorting (FACS) technology (G. A. Challen *et al.*, 2009). The vast majority of HSCs isolation approaches include the selection of cells expressing c-Kit (stem cell growth factor receptor/CD117) and Sca-1 and negative selection for markers of mature haematopoietic cell lineages (typically B220, CD4, CD8, Gr-1, Mac-1 and Ter-119), the so-called LSK which are enriched in cells with haematopoietic reconstituting activity, about 10% of LSK cells are bona fide long-term HSCs (G. A. Challen *et al.*, 2009). For the further enrichment in murine HSCs and onward progenitors a variety of combinations of cell-surface marker have been proposed, the most commonly used were resumed in Table 1.3.

1.2 STRESS-INDUCED HAEMATOPOIESIS

1.2.1 Overview of Stress-induced Haematopoiesis

In spite of decades of investigation, much is yet to learn about the regulation of haematopoiesis, and this lack of knowledge becomes further evident regarding the cell fate of HSPCs in non steady-state conditions, such as infection, inflammation or anaemia (J. L. Zhao and D. Baltimore, 2015).

A classic example of stress-induced haematopoiesis is the rapid increased production of myeloid cells in response to acute systemic bacterial infection, often referred to as emergency myelopoiesis. The emergency myelopoiesis is characterized by, leukocytosis, neutrophilia, emergence of immature neutrophils in peripheral blood (PB) and increased production of myelomonocytic cells in BM. The aforementioned phenomenon is an illustrative example of how the haematopoietic system evolved to respond fast and efficiently to the higher demand of innate immune cells to fight an acute infection (H. Takizawa *et al.*, 2012).

Most haematopoietic cells are post mitotic requiring the *de novo* production from BM HSPCs, when they are consumed in response to injury, during an immune response or due to blood loss. Therefore, chronic uncontrolled stimulation may be detrimental to the long-term function of HSCs, on the top of blood cell production. It has been reported that highly proliferative cells (for example, during experimental serial transplantation) showed intrinsic reduced self-renewal activity, suggesting that sustained stress-induced haematopoiesis may result in exhaustion of functional HSCs and increased probability of occurring cumulative genetic alterations (K. Y. King and M. A. Goodell, 2011, H. Takizawa *et al.*, 2012).

In humans it was not yet established if dysregulation of stress-induced haematopoiesis contributes to haematological disorders, such as BM failure or neoplasias, nonetheless epidemiological studies have shown an association between chronic immune stimulation (infections and autoimmune diseases) and increased risk of posterior development of myeloproliferative neoplasms, BM fibrosis and myelodysplastic syndromes (J. L. Zhao and D. Baltimore, 2015).

The adaptation of haematopoiesis to dynamic homeostatic requirements is possible due to the expression of different receptors at each developmental step, which integrate the information provided by different stress mediators.

Haematopoietic progenitors have different mechanism to sense injury that may collaborate to respond to the specific haematopoietic demands: (1) respond to anemia, for example producing more erythrocytes upon sensing increased levels of erythropoietin; (2) respond to inflammatory mediators produced during an immune response to an infection, for example in a mouse model of malaria, $IFN\gamma$ signaling induce the emergency of an $IL-7R^+$ $cKit^{hi}$ myelolymphoid progenitor population that contribute for the increased production myeloid cells beneficial for infection resolution; (3) respond to pathogen-associated molecular patterns (PAMPs) and danger-associated molecular patterns (DAMPs) directly through toll like receptors (TLRs), for example, in mice infected with *Pseudomonas aeruginosa* the expansion of LSK depended on the expression of TLR4, the main receptor for lipopolysaccharide (LPS); (5) respond to signals from the BM mesenchymal stem cell niche, for example mice with infected with *Listeria monocytogenes* have increased serum levels of G-CSF, which was shown to repress the expression of CXCL12 by osteoblasts promoting increased mobilization of HSPCs; (6) so far there are no evidence that HSPCs themselves could be infected by pathogens, nonetheless in theory this may be a further mechanism of haematopoietic regulation (C. Cheers *et al.*, 1988, N. N. Belyaev *et al.*, 2010, K. Y. King and M. A. Goodell, 2011, H. Takizawa *et al.*, 2012, J. L. Zhao and D. Baltimore, 2015).

1.2.2 Inflammatory Modulation of Early Events in Haematopoiesis

The impact of infection on haematopoiesis has been reported in many models, regulated by both, systemic demand for immune cells, and direct sensing of “infection” by haematopoietic precursors, the so-called “Push and Pull Model” (Figure 1.6) (K. Y. King and M. A. Goodell, 2011).

Another common feature associated to haematopoietic alterations during chronic infections is the establishment of extramedullary haematopoiesis that may occurs due to an increased egress of immature haematopoietic cells from the BM to the periphery or *in situ* expansion of circulating

HSPCs (V. M. Peterson *et al.*, 1994, Y. F. Zhan *et al.*, 1998) (A. M. Mirkovich *et al.*, 1986, S. E. J. Cotterell *et al.*, 2000a, T. Junt *et al.*, 2007, S. Massberg *et al.*, 2007).

In steady state, HSCs are mostly found in quiescence and it was formerly believed that HSCs were protected in their niches from infectious challenge. Nowadays, it is well established that HSCs play a central role in the responses to infection (H. Takizawa *et al.*, 2012).

In the following section we will discuss the effects of inflammation on the modulation of haematopoiesis in different models of infection and its functional consequences, focusing on HSCs and immediate early progenitors.

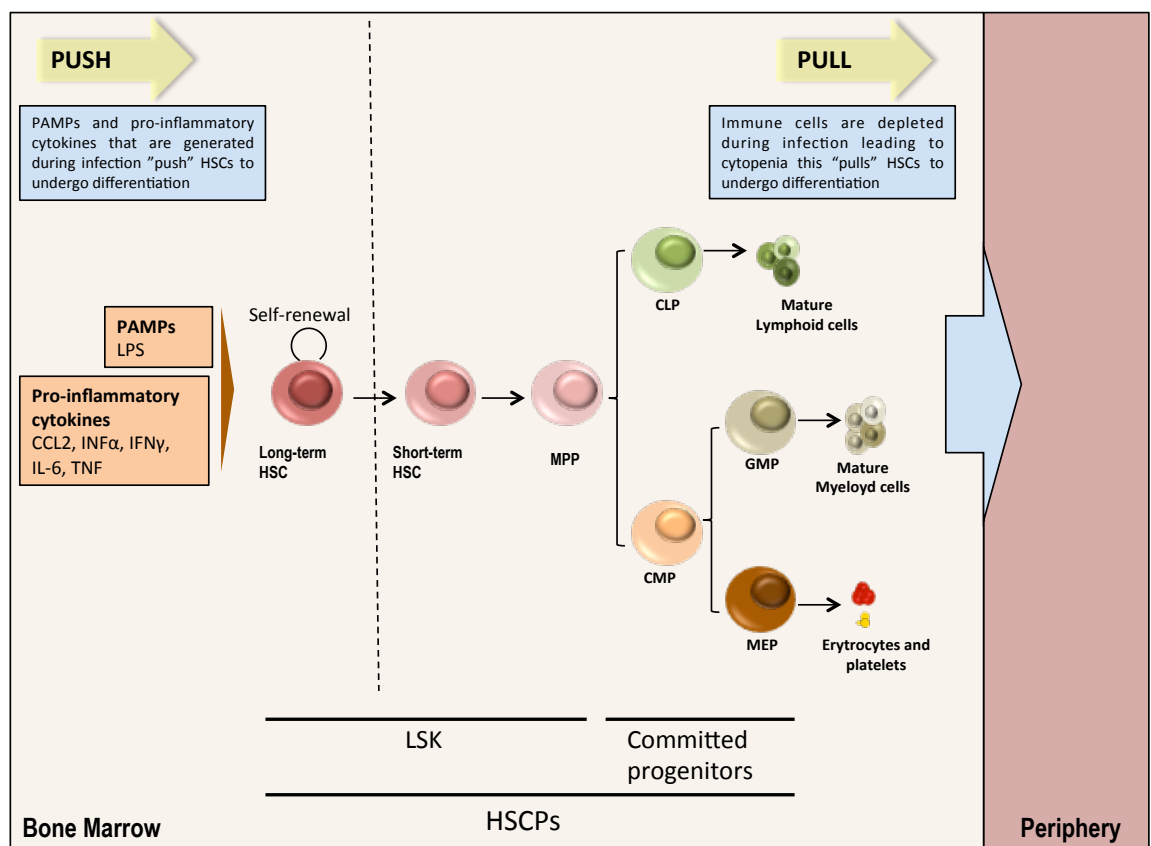


Figure 1.6- Overview of the “Push and Pull Model” proposed to frame the alterations observed in haematopoiesis during infection. All haematopoietic cells originate from a small population of haematopoietic stem cells (HSC), which is separable into at least two subsets: long-term reconstituting HSC (LT-HSC) and short-term reconstituting HSCs (ST-HSC). Differentiation of ST-HSCs generates multipotent progenitors (MPP) and then lineage-committed oligopotent progenitors derived from MPP. These include the common lymphoid progenitor (CLP), common myeloid progenitor (CMP), megakaryocyte-erythrocyte progenitor (MEP) and granulocyte-monocyte progenitor (GMP) populations. To explain demanded- haematopoiesis during infection a model defined as “The push and pull on HSCs” has been proposed; the “push” being associated with the direct response of HSC to stimuli associated with infections (including pathogen-

associated molecular patterns (PAMPs) or in response to pro-inflammatory cytokines; and the “pull” associated with the HSCs proliferation due to the depletion of committed progenitor populations from the bone marrow. CCL2, CC-chemokine ligand 2; CLP,; IFN, interferon; IL-6, interleukin-6; LPS, lipopolysaccharide; MEP, megakaryocyte and erythrocyte progenitor; MPP, multipotent progenitor; NK, natural killer; TNF, tumor necrosis factor (Adapted from (K. Y. King and M. A. Goodell, 2011, L. D. Wang and A. J. Wagers, 2011)).

1.2.2.1 Regulation of stress-induced haematopoiesis by Toll-like receptor signaling

Pathogen-associated molecular patterns (PAMPs), including lipids, lipoproteins, proteins and nucleic acids, can be recognized by germline-encoded pattern-recognition receptors (PRRs), including Toll-like receptors (TLRs), C-type lectin receptors and NOD-like receptors, amongst others expressed in immune cells. For example, TLRs recognized PAMPs derived from various pathogens and initiate MyD88-dependent or TIR-domain-containing adapter-inducing interferon beta (TRIF)-dependent signaling pathways, leading to the activation of IRF3 and/or late-phase nuclear factor kappa light chain enhancer of activated B cells (NF- κ B) TF (T. Kawai and S. Akira, 2010).

HSPCs have high expression and respond to engagement of TLR2 and TLR4 with entry into cell cycle and selective myeloid lineage differentiation *in vitro* (Y. Nagai *et al.*, 2006a) and *in vivo* (J. Megias *et al.*, 2012).

For example, during sepsis using an established murine model by inoculation of the virulent strain of *P. aeruginosa* UCBPP-PA14 or *P. aeruginosa* LPS it was observed a significant increase in LSK cells, but BM cellularity was reduced, as well as BM Gr1⁺Mac1⁺ population, which includes maturing myeloid cells, monocytes, and neutrophils, suggesting a block in myeloid differentiation. In competitive BMT assays, BM donor cells pre-challenged with *P. aeruginosa* LPS showed low engraftment potential, both in the long and short term periods, and defective ability to generate myeloid progenitors, in comparison to control BM donor cells. TLR4 expression was upregulated in LSK by LPS, and in mutant mice deficient for TLR4 the phenotype upon LPS challenge observed in WT mice was at great extent prevented, LSK cells were not significantly increased, and the number of myeloid cells preserved, suggesting that TLR4 signaling could modulate HSCs functions (long-term self-renewal and multilineage differentiation) (S. Rodriguez *et al.*, 2009).

Staphylococcus aureus infection was also associated to an expansion of HSCs and multipotent progenitors. However, in mice MyD88^{-/-} TRIF^{-/-} (dKO) mice, which lack all TLR signaling the

expansion of HSPCs was comparable to infected WT mice, suggesting that TLR signaling is not required for HSPCs activation during *S. aureus* infection (P. O. Scumpia *et al.*, 2010).

It was also proposed that the modulation of HSPCs function may also be mediated by TLR signaling in non-haematopoietic cells that compose their microenvironment. In this study using BM mixed chimeric challenged with *Escherlichia coli*, it was established that endothelial cells produce increased level of G-CSF production in a MyD88-dependent mechanism, which results in emergency myelopoiesis and reduced BM cellularity in this model of infection (S. Boettcher *et al.*, 2014).

Stress-induced haematopoiesis complex and dynamic processes integrate signals from the pathogen, HSPCs, BM stromal cells, and non-haematopoietic tissues. The aforementioned studies discussed in this section suggested that the TLR signaling impact in stress-induced haematopoiesis is pathogen-specific, can be deleterious or advantages and most likely characterized by redundancy with other mechanisms coping in each infectious context (J. L. Zhao and D. Baltimore, 2015).

1.2.2.2 Regulation of Stress-induced Haematopoiesis by Cytokine Signalling

In response to an infection a wide range of soluble factors are released locally, and as soon as its levels increase in serum they become available to impact in the BM niches for haematopoiesis. The soluble factors, as referred above, include PAMPs but also cytokines (colony-stimulating factors, interleukins and interferons) and chemokines, for which HSPCs express cognate receptors (H. Takizawa *et al.*, 2012).

Initial studies on the impact of infection in haematopoietic development focused in immune effector cells and committed progenitors, and the alterations were described as an homeostatic reaction to the increased demand of immune effector cells described as “emergency myelopoiesis/granulopoiesis” and “emergency lymphopoesis”. In order to maintain a reservoir of HSCs for the lifetime of an organism, these rare cells are in either a dormant or homeostatic proliferative state, but in the light of recent findings HSCs have assumed a preeminent role in the response to infection, because alterations in its function have been described in a wide range of acute and chronic infection models (M. T. Baldrige *et al.*, 2011, K. Y. King and M. A. Goodell, 2011).

Many growth factors required for steady-state haematopoiesis may be present the serum in increased levels in inflammatory contexts such as, G-CSF, M-CSF, GM-CSF, IL-3, IL-6, and Flt3 ligand, with the potential to modulate cell fate “decisions” both in non-committed and lineage-committed precursors (H. Takizawa *et al.*, 2012). Beside the release of haematopoietic growth

factors, during infection may occur the release of pro-inflammatory cytokines such as interferon (IFN) α/β , IFN γ and tumor necrosis factor (TNF), which have been implicated in the direct modulation of HSCs function in various pathogen-specific contexts (M. T. Baldrige *et al.*, 2011).

M-CSF, traditionally viewed as a lineage-specific cytokine, provides an example for the potential impact of a growth factor in increased availability in the HSCs cell-fate decisions, promoting higher availability of innate immune cells in response to an infection. M-CSF is strongly induced during infection and it was shown that high systemic levels of M-CSF could act on M-CSF receptor expressed on HSCs and induce the expression of the transcription factor PU.1, a key regulator of haematopoietic differentiation. *In vivo* experiments showed the induction of PU.1 expression in HSCs after transfer to LPS-challenged hosts or after injection of recombinant M-CSF. The adoptive transfer of *in vivo* M-CSF primed HSCs to non-stimulated recipients showed an increase in the GMPs:MEPs progenitors ratio in the spleen and an increased myeloid to lymphoid cell ratio in circulation, the ratios returned to baseline upon six weeks and long-term multi-lineage contribution of M-CSF-primed HSCs was not compromised (N. Mossadegh-Keller *et al.*, 2013).

Another example illustrating that alterations in haematopoiesis due to infection can impact positively in the immune response came from experimental model for malaria. In this model IFN γ signalling led to the emergence of a Lin⁻ IL-7R⁺ cKit^{hi} progenitor with myelolymphoid potential of differentiation that *in vivo* generated mainly myeloid cells. This alteration in haematopoiesis seemed to be advantageous in response to infection since when infection-induced atypical progenitors from infected mice were transplanted into non-irradiated mice infected prior to *P. chabaudi* infection, the recipient mice showed significantly lower parasitemia compared to untransplanted infected controls (N. N. Belyaev *et al.*, 2010).

The rapid activation of HSCs to proliferate and differentiate, often along the myeloid lineage, during infection in response to pro-inflammatory cytokines may be required, because enhanced haematopoiesis dependent solely on onwards progenitors could not be equipped to sustain the demand of effector cells required to resolve infection, and prevents the accumulation differentiation-ready progenitor cells in steady-state. If in acute conditions HSCs activation may assist in host defense, the continuous activation of HSCs during chronic inflammation or infection may be detrimental for HSCs function, impairing their ability to cope with future demands (proliferation-associated functional exhaustion) or increasing the rate of genetic mutation accumulation (neoplastic syndromes) (K. W. Orford and D. T. Scadden, 2008, C. Mirantes *et al.*, 2014). In humans several haematological disorders have been associated to the overproduction of proinflammatory cytokines and therefore increasing efforts have been made to clarify the impact

of these immunomodulators on HSCs function, with the aim to improve treatment of chronic inflammation and blood disorders (C. Mirantes *et al.*, 2014, J. L. Zhao and D. Baltimore, 2015).

Several studies have suggested that chronic IFN stimulation might lead HSCs to functional exhaustion that in long run might result in anergy or increased death susceptibility (M. T. Baldrige *et al.*, 2011, C. Mirantes *et al.*, 2014).

Interferons are produced by immune cells in response to intracellular pathogens, such as viruses and bacteria, but also tumor cells. In steady-state IFNs are constitutively produced, albeit at very low levels. The Type I IFNs contain multiple IFN α species and a single IFN β , which are expressed by many cell types. The type II IFNs are comprised solely by IFN γ , mainly produced by NK (Natural Killer) and T cells. The IFNs are important in the limitation of replication of virus through innate mechanisms (induction of anti-proliferative state and pro-apoptotic “antiviral state”), and in the generation of adaptive immune responses, in collaboration with other immune cells, to resolve infections and produce immunological memory to prevent reinfection (A. M. Prendergast and M. A. G. Essers, 2014).

The Type I IFNs, IFN α and IFN β/α signal through the IFN α/β receptor (IFNAR), and their potent expression can be induced by the viral RNA, which can be mimicked by the double-stranded RNA mimetic polyinosinic-polycytidylic acid (poly(I:C)). The type I IFN-inducible Mx1-Cre allele has been commonly used in mouse lines to eliminate genes flanked by loxP sites (floxed) in HSCs and other haematopoietic cells. In these mutant mice the expression of the Cre recombinase is controlled by the Mx1 promoter, since the expression of MX1 gene in haematopoietic cells is induced by interferon α or β and by pI-pC (an interferon inducer), this system allows gene targeting in hematopoietic cells (R. Kuhn *et al.*, 1995). It was first observed that poly(I:C) treatment induced the proliferation of HSCs both in mice containing or lacking the Mx1-Cre or floxed genes. Then, in WT mice poly(I:C)-mediated proliferation of homeostatic HSCs and also dormant HSCs (BrdU long-retainer cells), but this effect was prevented in mice deficient for IFNAR. These findings suggested that IFN α signalling induced HSCs proliferation *in vivo*, which was quite a surprise at the data since it had been extensively showed *in vitro* that IFN α act as an inhibitor of cellular proliferation for multiple other cells types, including haematopoietic progenitors. These findings also should be considered in the interpretation of other studies using this conditional loss-of-function approach to study the biology of HSCs (M. A. G. Essers *et al.*, 2009).

The functional relevance of chronic IFNAR signaling was demonstrated *in vivo* BM transplant (BMT) competitive assays. In mixed BM chimeric mice 50:50% wild type:Ifnar^{-/-} upon eight challenges with poly(I:C) (every second day) and eight day of recovery, HSCs from WT donors

could not be detected and all the HSCs in BM, as well as the vast majority of mature cells derived from *Ifnar*^{-/-} donor. These findings strongly suggested that chronic activation of IFN- α signaling significantly impairs HSCs function (M. A. G. Essers *et al.*, 2009).

A mechanism to explain the impact of type I interferon was proposed in a study by Pitetras *et al.* In this work, it was showed that IFN- α induced HSC proliferation by 12 h, with BrdU incorporation peaking after 1–3 days of poly I:C treatment, while upon 5-30 days of continuous administration of poly I:C the incorporation of BrdU in HSCs was at basal levels, suggesting that IFN- α challenge induces a rapid and transitory proliferation in HSCs, which rapidly return to a quiescent state during chronic exposure (E. M. Pietras *et al.*, 2014).

In subsequent experiments it was showed that HSCs chronically exposed IFN- α were functionally impaired compared to “intact” HSCs, in despite of returning to quiescence. IFN-Is have been shown to be pro-apoptotic in multiple cell types, therefore in subsequent experiments the expression of pro-apoptotic and pro-survival was assessed in HSCs challenged *in vivo* with poly I:C for either three (cycling) or seven (quiescent) days directly *ex vivo* and upon forced to proliferation in *in vitro* culture, transplantation, or 5-FU-mediated myeloablation. These experiments lead to the proposal of the following model: in steady-state HSCs are largely found in quiescence and protected from pro-apoptotic signals, upon IFN- α exposition HSCs enter in cell-cycle due to transitory down regulation of quiescence-enforcing mechanisms and are therefore vulnerable to pro-apoptotic signals, if IFN α levels remain elevated the HSCs return to quiescence to prevent IFN- α induced apoptosis, nonetheless if due to other stimuli they are forced to enter in cell-cycle p53-dependent proapoptotic gene program may be activated rendering HSCs highly susceptible to cell-death (E. M. Pietras *et al.*, 2014).

In humans there are studies establishing an association between inflammatory contexts and alterations in BM functions, therefore indicating that inflammatory stimuli have the potential to modulate humans HSCs functions. Across the few studies performed in human the pro-inflammatory cytokines that are more prevalent were IFN γ and TNF, which expression was increased in BM of patients with myelodysplastic syndrome (MDS), idiopathic aplastic anemia and Fanconi Anemia (FA) (M. Kitagawa *et al.*, 1997, L. G. Schuettpelz and D. C. Link, 2013). Additionally, alterations in haematopoiesis have been often reported among patient in anti-TNF- α agents and interferon therapeutic regimes (L. G. Schuettpelz and D. C. Link, 2013). For example, in BM samples from MDS patient it was found the expression of TNF and IFN γ mRNA, otherwise not detected in control samples and these results were then confirmed by immunohistochemical staining in BM sections (M. Kitagawa *et al.*, 1997).

Aplastic anaemia (AA) is a clinical syndrome characterized by hypocellular BM and pancytopenia, which in the most severe presentations results in BM failure (BMF). There are inherited and acquired forms of AA: inherited forms have been associated to genetic defects, including DNA repair defects (Fanconi anemia, FA), abnormal telomere physiology (dyskeratosis congenita,) or abnormalities of ribosomal biogenesis (Shwachman-Diamond syndrome); it has been suggested that acquired forms of AA, are in most of the cases idiopathic and may result from the autoimmune response of cytotoxic T cells targeting HSPCs inducing apoptosis and BMF (A. E. DeZern and E. C. Guinan, 2014).

In patients with idiopathic AA it was initially found that IFN γ concentration was increased in the supernatants of PB mononuclear cells (PBMNCs), as well as in the supernatant of stimulated BM T-lymphocytes, compared to healthy controls. Following these experiments, IFN γ and TNF mRNA expression was detected in the BM of newly diagnosed patients, but not in the BM of healthy controls or AA patients treated with immunosuppressive drugs. Furthermore, it was found that AA patients bear in their BM more CD4⁺ and CD8⁺ T cells compared to healthy controls, and these lymphocytes have an increased potential to produce IFN γ and TNF upon stimulation. Interestingly, it was found that in PB the fraction of T cells producing IFN γ and TNF was comparable among AA patients and controls, suggesting that “reactive” T cells may localize preferentially in BM where they exert their deleterious effects upon HSPCs (C. Dufour *et al.*, 2001). More recently it was determined that an individual homozygous for a single mutation (in intron 1 at position -874, T \rightarrow A) that results in increased levels of IFN γ expression was associated to a higher predisposition to AA (B. Serio *et al.*, 2011).

According with the aforementioned findings it was proposed a model to explain the pathogenesis of AA: lymphocytes T are activated by an unknown antigen become autorreactive and sustain the anomalous secretion of pro-inflammatory mediators such as IFN γ and TNF, which by not yet completely defined mechanisms may impair effective haematopoiesis (C. Dufour *et al.*, 2001). This proposed immunopathogenic model has been supported by several studies performed in experimental models of disease (F.-c. Lin *et al.*, 2014, C. Arieta Kuksin *et al.*, 2015).

More recently it has been shown that CD4⁺ T cells play an important role in alterations observed at the haematopoietic progenitors during infection, using experimental models of disease for AA and human monocytic ehrlichiosis (HME) (Y. Zhang *et al.*, 2013, F.-c. Lin *et al.*, 2014, C. Arieta Kuksin *et al.*, 2015).

For example, it was shown using mutant mice (IFN γ ARE-del mice), in which IFN γ is constantly expressed in T cells and NK cells that this is sufficient to promote AA phenotype (BM hypocellularity and pancytopenia). In the BM of IFN γ ARE-del mice it was determined that HSCs

(LSK CD34⁻ Flt3⁻ CD150⁺ cells) numbers were increase, MPPs were maintained and all the lineage-committed progenitors decreased. The functions of CMPs, GMPs, and MEPs were analyzed *in vitro* using colony-forming assay, in IFN γ ARE-del mice their ability to form colonies was significantly decreased, suggesting quantitative and qualitatively impairment. The functional impairment in differentiation was further evidenced by the accumulation in immature erythrocytes and a two-fold decrease in the mature erythrocytes, disruption in early B-cell differentiation and decreased potential of proliferation among lineage-committed progenitors. Using BM chimeras it was shown that it was a cell intrinsic defect, ARE-del \rightarrow WT chimeras showed clinical signs of AA while WT \rightarrow ARE-del chimeras presented haematological parameters within the normal range. As such, this study suggested that abnormal expression of IFN γ have the potential to establish AA in mice, as shown by the capacity of its chronic expression to suppress efficient haematopoiesis in a cell-intrinsic manner (F.-c. Lin *et al.*, 2014).

In steady-state mature CD4⁺ T cells and CD8⁺ T cells reside in BM in low numbers, where priming of antigen-specific T cells can take place, and BM was found to be a privileged site for homing of memory T cells (F. Di Rosa and R. Pabst, 2005).

During homeostatic traffic T cells migrate to the BM in response to chemokines, such as stromal-cell derived factor-1a (SDF-1a or CXCL12), the ligand for the chemokine receptor CXCR4 expressed in CD4⁺ T cells. Recently, it was shown that CXCR4 mediates migration of pathogenic T cells to the BM in an experimental model for lethal AA, characterized by pancytopenia, increased levels of IFN γ and TNF, all features found in patients with AA. In this study, it was reported that expression of CXCR4 was increased in T cells isolated the BM of AA mice and when the SDF-1a–CXCR4 interactions were pharmacologically prevented there was a significant reduction in BM T cells infiltration in AA mice compared to controls. Because it was showed in breast cancer models that NF-kB signaling modulates CXCR4 expression, the authors pharmacologically inhibited NF-kB signaling in AA mice. Blocking NF-kB signaling in AA mice prevented BM hypocellularity, BM T cell infiltration, pancytopenia and increased concentration of TNF and IFN γ in PB. Overall this study suggested that anomalous expression of CXCR4 dependent on NF-kB-signaling may be one of the mechanisms underlying AA progression (C. Arieta Kuksin *et al.*, 2015).

The regulation of stress-induced haematopoiesis by infection is poorly understood, however studies using a wide range of infection models have been showing that activated immune cells act upon haematopoietic BM compartment. Also in the models of infections where alterations were reported, those were commonly associated to the increased expression of TNF and IFN γ (S. E. J. Cotterell *et al.*, 2000a, L. G. Schuettepelz and D. C. Link, 2013, A. M. de Bruin *et al.*, 2014), and

IFN γ has been appointed as a major regulator of functional activation of HSCs during infection (M. T. Baldrige *et al.*, 2010, Y. Zhang *et al.*, 2013).

Initial studies performed *in vitro* showed that IFN γ decreased CFU activity of BM cells, as well as their long-term repopulating activity upon *in vivo* transfer. On the other hand, *in vivo* studies showed that upon immune challenge, IFN γ induced expansion of LSKs and impaired HSCs long-term functions (M. T. Baldrige *et al.*, 2010, A. M. de Bruin *et al.*, 2014).

The mouse model of *M. avium* infection allowed the study of the impact of infection on HSCs function in a chronic non-cytopenic systemic infection. In BM it was reported an increase in the proportion of cycling of LT-HSCs (LSK CD34⁻ Flt3⁻ or LSK CD150⁺, or LSK Side Population) and an increase in the absolute number of ST-HSCs (LSK CD34⁺ Flt3⁻) and MPPs (LSK CD34⁺ Flt3⁻), while the number of myeloid lineage committed precursors was decreased. The increased proliferation of HSCs accounted for functional impairment, in BMT assays LT-HSCs recovered from *M. avium*-infected mice showed impaired engraftment in comparison to LT-HSCs derived from not infected mice. *In vitro*, HSCs proliferated when challenged with purified mouse recombinant IFN γ (rIFN γ), and no increase in apoptosis was reported. In addition, *in vivo* challenge with rIFN γ induced a significant increase in the fraction of HSCs in cell division. The alterations in haematopoietic progenitors during *M. avium* infection were abrogated in mice lacking IFN γ receptor 1 (Ifngr1) or the Stat1, encoding the downstream signal transducer for IFN γ receptor subunit 1. This set of experiments suggested that the increase in proliferating HSCs and subsequent functional impairment during *M. avium* infection could be mediate solely by IFN γ (K. Y. King *et al.*, 2010).

Other example, come from mouse model for HME which is an infectious disease caused by the obligate intracellular pathogen *Ehrlichia chaffeensis*, characterized by anemia and thrombocytopenia. In mice, *Ehrlichia muris* infection was used as experimental model of HME and it was found that the infection was associated to the expansion of LSK cells in BM dependent of IFN γ R signalling. In WT mice at day 8 post-infection (p.i.) were reported alterations in PB, decrease in hemoglobin, platelets, lymphocytes and increase in monocytes concentrations, and all these manifestation of disease were much less expressive in IFN γ R deficient mice (K. C. MacNamara *et al.*, 2011b). In following studies using this same experimental model it was determined that in BM of infected mice CD4⁺ T cells mice play a non-redundant role in LSK expansion being the main source of IFN γ (Y. Zhang *et al.*, 2013).

Fanconi anemia (FA) is a rare genetic disease characterized by BMF and susceptibility to cancer, most often acute myelogenous leukemia. Most genetic alteration described so far were in genes implicated in DNA repair. In a clinical study, it was showed that the frequency of BM cells from

FA patients expressing TNF and IFN γ was very increased compared to BM cells from controls. Interestingly, using colony-forming assays it was reported that in FA patients the number of CFU-E was lower compared to the controls, but upon addition of anti-TNF fusion protein the number of CFU-E resulting from BM cells derived from FA patients increased significantly, while in control BM cells the addition of anti-TNF had no impact. These findings suggested that TNF may participate in the development of erythropoietic failure in FA patients, and it is reasoned to speculate that this might also be true regarding other haematopoietic lineages not assessed in this clinical study (C. Dufour *et al.*, 2003). The increased production of TNF in FA was confirmed by other studies in humans and in experimental models of the disease (W. Du *et al.*, 2014).

TNF anomalous expression is commonly associated to a wide range of haematopoietic alterations, nonetheless the mechanisms by which this pro-inflammatory regulates stress-induced haematopoiesis remain unresolved. Different *in vitro* studies suggested adverse and beneficial impact of TNF in HSPCs growth and development (T. Tian *et al.*, 2014). More recently, a study *in vivo* reported that BM cells from TNF receptor deficient mice showed competitive advantage over WT BM cells in their ability to long-term reconstitute myeloid and lymphoid cell lineages in myeloablated recipients. In addition, administration of TNF results in reduced BM cellularity, that is further evident in mice treated with 5-FU, suggesting that *in vivo* TNF signaling may be detrimental for HSCs functions (C. J. H. Pronk *et al.*, 2011).

The sum of the studies reported in this section pointed out for a beneficial role of stress-induced haematopoiesis in acute infection, favoring the formation of immune cells in enough number to mount an effective response against a pathogen in detriment of erythropoiesis, which transient suppression might be tolerated and leaves more growth factors and space available in the BM to assist emergency myelopoiesis. Nonetheless if the pro-inflammatory stimuli are chronically sustained it might lead in first instance to anemia and thrombocytopenia, since erythrocytes and platelets are required in very higher number and have a small life span, and in more severe cases it may underlie the establishment of pancytopenia due to exhaustion of HSCs function rendering the individual more vulnerable to subsequent infections or BMF.

The impact of cytokines in the regulation of HSCs function is far from fully clarified, therefore more studies are required to understand the modulation of HSCs responses to infection and injury, to improve diagnostic, prophylactic and therapeutic approaches to the immense range of debilitating haematological alterations that afflict patients suffering from autoimmune disorders and chronic infections.

1.3 VISCERAL LEISHMANIASIS

1.3.1 Overview of Visceral Leishmaniasis

Visceral leishmaniasis (VL) is an intracellular infection caused by the protozoan *Leishmania donovani* and *L. infantum* in vertebrate hosts, including humans. The main targets of parasitism in mammalian hosts are the liver, the spleen and the BM, where the parasites may establish a chronic infection (P. Kaye and P. Scott, 2011).

Leishmaniasis is a vector-borne parasitic disease caused by protozoan of the genus *Leishmania*, consisting of trypanosomatid protozoans belonging to the order Kinetoplastida. There are approximately twenty species identified and different species types have been characterized among different endemic areas. *Leishmania* is found in the Old World (Europe, Asia and Africa) and in the New World (Central and South America), where female sandflies, belonging to the genera *Phlebotomus* in the Old World and *Lutzomyia* in the New World, are the vectors for Leishmaniasis transmission (D. Pace, 2014).

The propagation of leishmaniasis relies on the accomplished transmission between the sandfly vector and a mammalian reservoir. *Leishmania* parasites have a complex life-cycle: 1) in the sandfly parasites reside in the gut where they multiply as free flagellated promastigotes, 2) then the parasites differentiate into non-dividing 'metacyclic' promastigotes transmitted in the course of a sandfly blood meal, 3) finally within the mammal host through additional morphological changes, parasites differentiate into non-flagellated amastigotes that multiply as obligatory intracellular parasites mostly in mononuclear phagocytes, eventually parasites are released to infect other cells when an infected host cell bursts, 4) if an infected individual is again bitten the cycle of transmission resumes (P. Kaye and P. Scott, 2011).

VL is still a neglected tropical infection and responsible for significant morbidity and mortality in the developing world, particularly in India, Sudan, Nepal, Bangladesh, and Brazil. The epidemiological impact of this disease can only be estimated, due to insufficient epidemiological supervision and lack of appropriate diagnostic "tools" in endemic areas. The most recent estimates indicated that the number of new VL cases ranges between 0.2 to 0.4 million and 20,000 to 40,000 leishmaniasis deaths per year (D. Pace, 2014).

The main groups of individuals infected with VL vary on endemic geographic areas, for example in Europe, North Africa and West and Central Asia, children between one and four years old are the most affected group, while in East Africa VL occurs more frequently in adults. Upon infection the emergence of clinical symptomatology can take ten days to over one year, and the main

manifestations include fever, anorexia, weight loss, abdominal distension due to splenomegaly and hepatomegaly, hyperglobulonemia and disturbances in the haematopoietic homeostasis, including anemia, leucopenia and thrombocytopenia (D. Pace, 2014).

Post-kala-azar dermal leishmaniasis (PKDL) may occur as a complication of VL, months to years after treatment of VL. It takes place mainly in India, Kenya, and Sudan in 20-50% of treated patient. In PKDL patients present with macules, papules, or nodules in the skin as a result of dermal parasitic persistence, which constitutes an important reservoir for transmission (A. Ismail *et al.*, 2006).

VL is fatal if left untreated and due to lack of investment an effective vaccine is not yet available (A. Maroof *et al.*, 2012). The most commonly drugs used to treat infected people are pentavalent antimony and amphotericin B (and its liposomal derivatives), which have been associated with parasite resistance and increased drug toxicity, caused by the need for long periods of treatment. The pharmacological treatment is highly effective however the frequency of relapses within six to twelve months is significant, and even with treatment patients may succumb to VL-associated pathology or increased vulnerability to opportunistic infections. In the absence of treatment, VL patients may develop anaemia, haemorrhagic bleeding secondary to low platelets, secondary infections and death within two to three years (D. Pace, 2014).

1.3.2 Immunopathology in VL

In order to develop new effective prophylactic or therapeutic approaches intrusive techniques would be required to analyze responses in VL patients, therefore our current understanding of the host immune response during VL largely derives from studies performed in mice (P. M. Kaye *et al.*, 2004).

In mice, it was found that parasites establish chronic infection in the spleen and BM (S. E. J. Cotterell *et al.*, 2000b), whilst the infection in the liver was self-resolving within 6–8 weeks and relies on the development of a Th1-dominated granulomatous response. In the liver parasites are mostly found in Kupffer cells (KCs) the most prevalent population of hepatic resident macrophages, that upon infection release chemokines including CCL3 (MIP-1a), CCL2 (MCP-1) and CXCL10 (gIP-10), which results in the rapid increase of monocytes, neutrophils and T cells. Activated T cells are responsible for the secretion of Th1 cytokines such as IL-12, IFN γ , TNF, lymphotoxin- α (LT), GM-CSF and IL-2. These cytokines are required for the activation of KCs and other macrophage to produce leishmanicidal molecules such as reactive oxygen intermediates (ROI) and reactive nitrogen intermediates (RNI) and the establishment of granulomas (A. C. Stanley and C. R. Engwerda, 2007).

In the spleen, IFN γ -producing Th1 responses are not able to control parasite replication, although why this happens is unclear, various mechanisms have been proposed. The presence of high levels of TNF, which is a key cytokine for parasite clearance in the liver, promotes the disruption of the splenic marginal zone micro-architecture, impeding the migration of DCs and naive T cells to the T-cell area. Furthermore, the presence of suppressive CD4⁺T cells secreting IL-10 and IFN γ was reported, and these cells have also been observed in VL patients (S. Staeger *et al.*, 2010). More recently, it was shown that at 28 days p.i. with *L. donovani* there was an increase in the frequency of DCs CD11c^{lo} CD45RB⁺ in the spleen and *in vitro* cells with this same phenotype after lipopolysaccharide (LPS) stimulation produced large amounts immunoregulatory cytokine IL-10 (A. Wakkach *et al.*, 2003).

BM has long been recognized as a site of infection in mice (V. Leclercq *et al.*, 1996) but much less is known about the relationship between parasite dynamics in this organ, changes in cytokine and chemokine expression, and local haematopoietic activity. Nevertheless, a striking correlation between increased haematopoietic activity and parasite growth in both the spleen and BM has been noted previously (S. E. J. Cotterell *et al.*, 2000a).

1.3.3 Haematopoietic alterations during VL in experimental models of disease

Inbred mice have been widely used to study the VL immunology due to the genetic homogeneity among strains and the great availability of “tools” for immunological assessment. Nonetheless the course of infection varies considerably between mice and human, for instance in mice VL is not fatal, the infections becomes chronic in the spleen but it is self-resolving in the liver with the Th1-dependent formation of granulomas (P. M. Kaye *et al.*, 2004).

Another experimental model widely used to study VL is the Syrian golden hamster (*Mesocricetus auratus*), despite of limited availability of immunological reagents and more genetic variability. Syrian golden hamsters are very susceptible to *L. donovani* infection requiring a much smaller inoculum of parasites and the progression of disease during the course of infection is much closer to humans; persistence of parasites in the BM, spleen, and liver, hepatosplenomegaly, anaemia, leucopenia and death by 9–10 weeks after infection (J. M. Requena *et al.*, 2000). In hamsters it was shown that regardless of the infection-driven high expression of Th1 cytokines in the liver, spleen, and BM, macrophages were able to induce Nitric oxide synthase 2 (NOS2) activity, which is an essential antileishmanial effector mechanism in mice. The expression of IL-10 and TGF- β was significantly increased in infected hamsters, and both cytokines are known inhibit macrophage activation and NOS2 expression (P. C. Melby *et al.*, 2001).

The establishment of anemia in the Syrian golden hamster during the course of infection is well-characterized, initial studies reported drop a in haemoglobin levels followed by a significant increase in the reticulocyte in circulation and suggested that osmotic fragility was on the basis of anaemia (T. Biswas *et al.*, 1992).

More recently an extensive study focusing on the impact of *L.donovani* infection on erythropoiesis in the spleen and BM of infected Syrian hamsters was performed. In this study it was described that in infected hamster the number of erythrocytes and leukocytes were decreased. Using colony-forming assays, it was determined that the frequency of erythroid progenitors was increased both in BM and spleen, indicating that disruption of erythropoiesis might occur in later stages of differentiation and not due to lack of progenitors. Subsequent experiments showed that the expression of erythroid differentiation genes (alpha-globin, beta-globin, and ALAS2) was decreased in BM while increased in the spleen of infected hamster compared to the controls. The expression of mRNA for IL-10, TGF- β , and IFN γ mRNA was highly increased in BM and the spleen of infected mice and all these cytokines have been showed to be able to inhibit erythropoiesis. Furthermore, the fraction of apoptotic erythroblasts was higher in infected hamsters than control hamsters. According to these findings it was suggested that the occurrence of anemia could be due to an impairment of terminal differentiation of erythrocytes and/or increased apoptosis of erythroblasts that resulted in the establishment of emergency extramedullary erythropoiesis in the spleen (W. P. Lafuse *et al.*, 2013).

In mice experimental model of VL, chronic infection has been associated with alteration in the haematopoietic progenitors and in the stroma of haematopoietic sites. During the course of *L. donovani* infection, it was observed that the increase in parasite burden in the BM and spleen was associated with a gain in HSPCs numbers at both haematopoietic sites. Using colony-forming precursors assays it was found that in the BM there was an increase in colony forming unit-granulocyte, erythrocyte, monocyte, megakaryocyte (GEMM-CFU), CFU-granulocyte, monocyte (GM-CFU) and burst forming unit-erythrocyte (BFU-E), while in the spleen there was a specific increase in GM-CFU. These findings suggested that the infection could induce an increase in the egress of haematopoietic precursors and/or in the rates of haematopoiesis in extramedullary sites (S. E. J. Cotterell *et al.*, 2000a).

In the same study, it was shown that the frequency of cycling progenitors in the spleen of *scid* mice was not increased following infection, while in the BM the frequency of cells in proliferation increased about 1.5 fold in both the infected *scid* mice (lacking functional T and B lymphocytes) and infected BALB/C mice. In addition, it was determined that there were higher levels of mRNA for the growth factors G-CSF, M-CSF and GM-CSF in the BM and spleen from infected *scid* mice and infected BALB/C, during chronic phase of infection. This upregulation of the colony

stimulating factors was observed in the BM of infected BALB/C *and scid* mice but not in the spleen of the latter. Taken together the findings suggested the modulation of haematopoiesis might rely that different cellular and molecular signaling pathways at these two distinct sites during chronic infection with *L. donovani* (S. E. J. Cotterell *et al.*, 2000a).

Studies have shown that BM macrophages could become infected with *L. donovani* both *in vivo* and *in vitro*, but there were no indication that a significant number of progenitors harbored parasites. Infected BM derived macrophages showed an increased efficiency to support the formation of GM-CFU *in vitro*. When BM or spleen cells were plated in methylcellulose in the absence of exogenous growth factors, the addition of 14M1.4 (BM derived macrophage-like cells line) promoted formation of CFU-GM, BFU-E, and additionally in BM, CFU-GEMM. Furthermore, the addition of *L. donovani*-infected 14M1.4 cells instead to these assays was associated to a specific increase in CFU-GM formation. The infected macrophages express more GM-CSF and TNF, and the addition of neutralizing antibodies to the cultures caused a reduction in the formation of GM-CSF. These *in vitro* experiments suggested that *L. donovani* infection has the potential to selectively enhance myelopoiesis, acting upon the stromal macrophages (S. C. Smelt *et al.*, 2000).

In vitro splenic stromal cells from mice infected with *L. donovani* had an enhanced capacity to direct haematopoietic progenitors (BM Lineage⁻ cells) toward a regulatory dendritic cells (rDCs) phenotype *in vitro*, CD11c^{low} CD45RB⁺, while DCs derived from co-cultures of BM Lineage⁻ cells with naive stroma cells or GM-CSF protocol were CD11c^{hi}. These *in vitro* generated rDCs expressed higher levels of IL-10 compared to the controls (GM-CSF derived DCs) and using co-cultures with primed rDCs and it was showed that these could induce CD4⁺ T cells to produce immunosuppressor IL-10, while primed GM-CSF derived DCs induced CD4⁺ T cells to secrete pro-inflammatory IFN- γ , under the same experimental conditions (M. Svensson *et al.*, 2004).

Following *in vitro* studies, using transwell co-cultures suggested that the infection of the MBA-1 cell line (BM derived stromal cell line) with *L. donovani* could promote the differentiation of haematopoietic precursors (BM Lin⁻ cKit⁺) towards immunosuppressor DCs *in vitro*. When CD4⁺ T cells were stimulated either with GM-CSF-LPS-stimulated DCs alone, or in the presence of CD11c⁺ DCs differentiated in co-culture with control MBA-1 cells, or CD11c⁺ cells differentiated in co-culture with infected MBA-1 cells, it was observed that DCs generated in the presence of MBA-1 infected cells could prevent T cells proliferation, suggesting that they were functionally immunosuppressor. It was determined that in the spleen of infected mice the mRNA expression of CCL8 and CXCL12 was increased. Taking advantage of the transwell co-culture system and using neutralizing Abs for CXCL12 and CCL8 it was determined that these two chemokines collaborate in the recruitment of HSPCs induced by MBA-1 cell line *in vitro*. All these finding suggested that

infected splenic stromal cells could induce the increase seeding of HSPCs and modulate their differentiation favoring the generation of rDC, during *L. donovani* infection (A. T. Nguyen Hoang *et al.*, 2010).

Taken together the aforementioned studies suggest that the *L. donovani* infection might regulate haematopoiesis by modulating the function of cells that compose the haematopoietic supporting stroma.

Recently our laboratory reported that alterations in peripheral blood (PB) also take place in mice chronically infected with *L. donovani* (28 days post-infection), such as a significant decrease in the number of erythrocytes (normocytic anemia), leukocytes (leucopenia) and platelets (thrombocytopenia) which dropped 36.7%, 43% and 88%, respectively in infected mice compared to controls. Within the leukocytes compartment, it was also noticed that there is an inversion in the T cell:B cell relation, in healthy animals there are more B cells than T cells but upon infection the number of T cells in circulation was almost twice that of the B cells (F. A. d. Pinho, 2015).

The histopathologic evaluation of the BM from mice chronically infected with *L. donovani* revealed significant alterations in the myeloid/erythroid ratio, with infected mice bearing more myeloid lineage cells and less mature erythrocytes. Other morphological alterations were also reported, such as asynchronous nuclear-cytoplasmic maturation (reflecting delayed or incomplete nuclear maturation relative to cytoplasmic development), presence of megalocytes and binucleated erythroid cells, among other atypical cells. Additionally, profound alterations were described in BM architecture, in infected mice there was significant increase in cells expressing the macrophage specific marker F4/80, and in further characterization a significant alteration in the distribution of different mature myeloid cell populations within the BM of infected mice was noticed (F. A. d. Pinho, 2015). These findings suggested that haematopoietic alterations in BM during VL are clinically relevant being expressed in significant decrease of haematopoietic components of PB, and indicate that impaired haematopoiesis could be one of the mechanisms underlying cytopenias in chronic VL. Nonetheless the mechanisms underlying the impact of infection on haematopoiesis and its consequences to the immune responses to VL are yet to be determined.

1.3.4 Haematopoietic alterations during VL in humans

In humans, a wide range of alteration to the haematopoietic system following *L. donovani* infection have been described, which are reflected in the haematopoietic composition of PB and BM cellularity. The alterations in PB are very common but the degree of alteration varies considerably in terms of severity (N. Varma and S. Naseem, 2010).

Normochromic normocytic anemia was described as a common finding among VL patients in several clinical reports, both in adults and children. The presentation of anaemia is quite variable amongst patients, accounting for mild to severe anaemia with haemoglobin values ranging from 2.4 to 8.3 g/dl, compared to 11.5 to 18g/dl normal reference values (G. E. Cartwright *et al.*, 1948, N. Marwaha *et al.*, 1991, N. A. M. Aljurayyan *et al.*, 1995). Various mechanisms have been proposed to explain the onset of anemia in VL patients: haemolysis in spleen and liver, haemodilution due to expansion of the plasma volume, inhibition of erythrocyte enzymes, and immune mechanisms of haemolysis such as increased vulnerability to complement and presence of anti-erythrocyte antibodies (N. Varma and S. Naseem, 2010).

According with several clinical reports, leucopenia was reported in over 60% of VL patients and it was characterized by low number of neutrophils and eosinophils in circulation and mild lymphocytosis (G. E. Cartwright *et al.*, 1948, N. Marwaha *et al.*, 1991, N. Varma and S. Naseem, 2010, Y. Agrawal *et al.*, 2013).

Thrombocytopenia has been reported as a later occurrence in the course of infection. The values for platelets number varied considerably among patients ranging from 4-633 x 10⁹/l, and over 50%-85% of patients were thrombocytopenic according to different clinical reports, both in adults and children. Antibodies against platelets have not yet been reported in VL patients and the most consensual explanation for thrombocytopenia have been the splenic sequestration and progressive loss of hepatic function, the main responsible for thrombopoietin production in adult (G. E. Cartwright *et al.*, 1948, N. Marwaha *et al.*, 1991, N. A. M. Aljurayyan *et al.*, 1995, G. A. Hamid and G. A. Gobah, 2009).

Splenic sequestration has been appointed as the main cause behind peripheral cytopenias in VL patients but cannot account for the emergence of BM alterations. The alterations most commonly described in BM aspirates included erythroid hyperplasia, increased frequency of plasma cells, increased frequency of granulocytic and megakaryocyte immature forms, dyserythropoiesis, bi and multinuclearity in the erythroid series and histiocytic hyperplasia, suggesting that alterations in haematopoiesis could contribute to pancytopenia (K. K. Dhingra *et al.*, 2010, N. Varma and S. Naseem, 2010). However the degree of BM alterations was not correlated to the level of BM parasitemia (N. Varma and S. Naseem, 2010). Furthermore, several clinical reports described pancytopenia in VL patients followed by BM multilineage myelodysplasia reminiscent of true myelodysplastic syndrome (MDS), which could not be explained by the presence of hypersplenism, suggesting the presence of ineffective haematopoiesis (N. Yarali *et al.*, 2002, P. Kopterides *et al.*, 2003, G. M. de Vasconcelos *et al.*, 2014).

The onset of pancytopenia extensively contributes to the morbidity and mortality following *L. donovani* infection; therefore more efforts should be made to elucidate the impact of infection in haematopoiesis. Understand the mechanism underlying the establishment of haematopoietic dysfunction in VL patients would contribute to the development of better clinical approaches and prevent fatal outcomes due to massive bleeding or increased vulnerability to secondary infections.

1.4 AIMS

It is well established that haematopoietic dysfunction (notably various forms of cytopenias) is associated with human VL, and may contribute to the disease outcome. However the mechanisms underlying the impairment of haematopoietic function are poorly defined (G. E. Cartwright *et al.*, 1948, N. Varma and S. Naseem, 2010). The aim of this thesis was to characterize the alterations in BM haematopoiesis during experimental infection with *L. donovani* and establish whether there is a correlation with the establishment haematopoietic dysfunction in the periphery. The specific aims were as follows:

Chapter 3

- To characterized alterations in BM haematopoiesis;
- To examine phenotypic alterations of LT-HSCs;
- To examine functional alterations of LT-HSCs;
- To relate the alteration in the proliferative status of LT-HSCs with changes in the expression of selected transcription factors.

Chapter 4

- To examine alterations in cellular components of the BM microenvironment;
- To establish whether there was a correlation between changes in cellular components of BM and alterations in haematopoiesis;
- To characterize phenotypic and functional changes in BM T cells and assess the role of CD4⁺ T cells in regulating changes in haematopoiesis;
- To examine the specific contributions of IFN γ and TNF signalling in haematopoietic dysfunction.

CHAPTER 2. MATERIALS AND METHODS

2.1 ANIMALS

Mouse lines C57/BL6 (Black 6 (B6)), (B6).CD45.1, B6.CD45.2, B6.CD45.1xCD45.2 and B6.Rag2KO.CD45.1Cg (Z. Y. Hao and K. Rajewsky, 2001) used in this study, were bred and maintained under SPF conditions at the Biological Services Facility (BSF) within the University of York.

B6.Myc-eGFP were originally developed by Dr. Ching-Yu Huang (Department of Pathology and Immunology, Washington University School of Medicine, St. Louis, USA) (C.-Y. Huang *et al.*, 2008). Both B6.Myc-EGFP mice and derived BM cells were kindly provided by Dr. Dinis Pedro Calado (Cancer Research UK, The Francis Crick Institute London, United Kingdom). BM cells from mice lacking the *ifngr2* gene (IFN γ -R2 KO) on B6 background were generously provided by Dr. John Grainger (Faculty of Life Sciences, University of Manchester, United Kingdom) (B. F. Lu *et al.*, 1998). Tnfrsf1-dKO B6.129S mice (TNF receptor double KO) were originally obtained from the Jackson Laboratory (stock no. 003243) followed by subsequent backcrossing for at least ten generations to C57BL/6 mice at the Lund University animal facility. Tnfrsf1-dKO mice were originally generated through the interbreeding of mice deficient for Tnfrsf1a (or Tnfr-p55, generated on a C57BL/6 background) with mice deficient for Tnfrsf1b (or Tnfr-p75, generated on a 129 background) (J. J. Peschon *et al.*, 1998). Dr. Bengt Johansson Lindbom (Division of Immunology, Faculty of Medicine Lund University, Sweden) generously provided BM cells from TNF receptor double KO mice. IFN γ -KO (B6.129S7-Ifng^{tm1Ts}/J, stock no. 002287) mice, in B6 background, were obtained from the Jackson Laboratory (D. K. Dalton *et al.*, 1993).

All mice were females between 5-8 weeks of age at the start of experimental work, except for the experiment with B6.Rag2KO.CD45.1Cg that included in the naive controls male mice. All experiments in this thesis were carried out with the approval of the UK home office (United Kingdom Home Office Project License PPL 60/4377) and under ARRIVE guidelines.

2.2 INFECTIONS

Mice were infected via the lateral tail vein with 3×10^7 amastigotes of the Ethiopian strain of *Leishmania donovani* (LV9), maintained by passage in B6.Rag2KO.CD45.1Cg and B6. EYFPKI. Rag1KO immunodeficient mice. Amastigotes were isolated from infected spleens. The infected spleens were removed following CO₂ euthanasia and dislocation of the neck. The spleen was homogenized in RPMI 1640 medium (Gibco, Paisley, UK) in a glass homogenizer (Fisher Scientific, UK), the resulting suspension was transferred to 50 milliliters (ml) Falcon tube

(Sarstedt AG & Co, Germany) and centrifuged at 137 G for 5 minutes at room temperature (RT) in a Heareus Multifuge 3S-R (DJB labcare, UK). The supernatant was retained and transferred to a 50ml Falcon tube coated with 25mg saponin (BDH, Leicestershire, UK) per 20ml supernatant, for 5 minutes at RT to lyse erythrocytes. The suspension was washed with in RPMI 1640 medium at 2063 G at 37°C for 10 minutes three times. Finally, the pellet was suspended in RPMI 1640 medium and passed through a 26-gauge needle (BD Biosciences, USA) 2-3 times to break up clumps of parasites using a 10 ml syringe (BD Biosciences, USA). Parasites were counted using a Thomas bacteriological counting chamber (Weber Scientific International, Middlesex, UK).

Spleen parasite burden was determined from impression smears following methanol fixation and Giemsa staining. Parasite burden was expressed as Leishmania-Donovani units (LDU), where LDU was equal to the number of parasites per 1,000 host nuclei times the organ weight in milligrams or, alternatively, it was expressed as number of parasites per 1,000 host nuclei. BM aspirates from the iliac crest were removed with the aid of a 23G needle and a 5ml syringe, placed onto a slide (Thermo Scientific) and squashed between two slides (“squash” technique). Dr. Flaviane Pinho performed this procedure. Smears were then fixed with methanol and stained with Hemacolor Rapid staining of blood smears (Merck, Germany). The parasite burden was determined microscopically as the number of parasites per 1,000 host nuclei.

2.3 CELL ISOLATIONS

2.3.1 Bone Marrow cells isolation

Mice were sacrificed by CO₂ euthanasia and followed by dislocation of the neck. The tibiae and fibulae were removed and placed into a petri dish containing Dulbecco's Modified Eagle Medium (DMEM) (Gibco, Paisley, UK). All the fat and muscles were removed from the bones using a scalpel (Swann-Morton, Sheffield, UK) and the very edges of the bones were cut. Each bone was flushed with 10 ml of phosphate buffered saline (PBS) 1x with 2% HyClone foetal calf serum (FCS) (purchased from Thermo Fisher Scientific (Loughborough, UK) and heat inactivated by incubating in a 56°C water bath for 30 minutes) and forced through a 70µm strainer (Scientific Laboratory Supplies (SLS), East Riding of Yorkshire, UK) into a 50 ml Falcon tube. The cell suspensions were centrifuge for 7 minutes at 309 G at 4°C, and the resulting pellets were suspended in 1ml of ACK Lysing Buffer (Gibco, Paisley, UK) for 2 minutes at RT to lyse the erythrocytes. After adding 18 ml of 1x PBS with 2% FCS, the cell suspensions were centrifuged at 309 G for 10 minutes at 4°C and the resulting pellets suspended in 10 ml of complete DMEM (DMEM containing 10% of FCS, 100 U/ml penicillin (Sigma-Aldrich, Dorset, UK) and 100 µg (milligrams)/ml streptomycin (Sigma-Aldrich, Dorset, UK). The cell viability and concentrations were assessed manually by dye exclusion with Trypan Blue (Sigma-Aldrich, Dorset, UK) and

counted on an Improved Neubauer haemocytometer (Weber Scientific International, Middlesex, UK) or using the Vi-CELL Cell Viability Analyzer (Beckman Coulter, HighWycombe, UK) (adapted from (S. E. J. Cotterell *et al.*, 2000a)).

2.3.2 Spleen cells isolation

Spleens were removed from sacrificed animals and placed in a petri dish containing RPMI-1640, and all the fat and muscle were removed using a scalpel. The tissue was forced through a 70 µm (micrometers) strainer using the back of a 10 ml syringe into a 50ml Falcon. Cell suspensions were centrifuged at 309 G for 7 minutes at 4°C, the resulting pellets were suspended in ACK lysing Buffer for 5 minutes to lyse erythrocytes. After adding 18 ml of 1x PBS with 2% FCS, the cell suspensions were centrifuged at 309 G for 10 minutes at 4°C and the resulting pellets were resuspended in 10 ml complete DMEM. The cell viability and concentration were assessed manually by dye exclusion with Trypan Blue and counted on an Improved Neubauer haemocytometer or using the Vi-CELL Cell Viability Analyser (adapted from (S. E. J. Cotterell *et al.*, 2000a)).

2.4 FLOW CYTOMETRY AND BM TRANSFER ASSAYS

2.4.1 Staining for surface markers

HSPCs were assessed according with the phenotype for expression of surface markers displayed in supplementary Table 2.1. Cell suspensions were diluted to a concentration of 20-30 x 10⁶ cells/ml, and then 200 µl (microliters) were transferred to individual wells on a 96 round bottom well plate (Sarstedt AG & Co, Germany). The cell suspensions were incubated for 20 min at 4°C with 0.125µg/100 µl fragment crystallizable region receptor (FcR block) (CD16 (Fc gamma III Receptor) and CD32 (Fc gamma II Receptor); eBioscience) and then centrifuged for 7 min at 309 G at 4°C. The supernatants were discarded and the pellet was suspended in optimized concentration of surface antibodies (Table 2.2) and fixable live-dead dye (Invitrogen, Paisley, UK) diluted in 1x PBS 1% FCS and left at 4°C for 30 minutes in the dark. Plates were centrifuged for 7 min at 309 G at 4°C, supernatants were discarded and the cells were washed twice in 1x PBS 1 % FCS by centrifugation at 309 G for 7 min at 4°C. When only surface staining was performed, cells were fixed post-washing in 200 µl 2% formaldehyde (PFA) (Sigma-Aldrich) for 20 min at 4°C in the dark, followed by two washes with 1x PBS 1% FCS by centrifuging at 309 G for 7 min at 4°C. Finally, cells were suspended in 400 µl of 1x PBS 1% FCS and stored protected from light at 4°C until acquisition on either the BD LSR Fortessa X-20 (BD Biosciences, Oxford, UK) or the CyAn ADP analyzer (Beckman Coulter, High Wycombe, UK).

Table 2.1 - Surface markers used to characterize HSPCs by flow cytometry analysis

Cell type	Phenotype	Ref.
Long-term hematopoietic stem cells (LT-HSCs)	Lineage ^{-low} Sca1 ⁺ cKit ^{hi} FLt3 ⁻ CD34 ⁻	(Kondo et al., 2003)
Short-term hematopoietic stem cell (ST-HSC)	Lineage ^{-low} Sca1 ⁺ cKithi FLt3 ⁻ CD34 ⁻	
Multipotent progenitors (MPP)	Lineage ^{-low} Sca1 ⁺ cKit ^{hi} FLt3 ⁺ CD34 ⁻	
Hematopoietic stem cells (HSCs)	Lineage ^{-/low} Sca1 ⁺ cKit ^{hi} CD150 ⁺ CD48 ⁻	(Oguro et al., 2013)
Hematopoietic progenitor cells 1 (HPC-1)	Lineage ^{-low} Sca1 ⁺ cKit ^{hi} CD150 ⁻ CD48 ⁺	
Hematopoietic progenitor cells 2 (HPC-2)	Lineage ^{-low} Sca1 ⁺ cKit ^{hi} CD150 ⁺ CD48 ⁺	
Common lymphoid progenitors (CLP)	Lineage ^{-low} cKit ^{hi} IL-7R α ⁺ CD34 ^{-low}	(Kondo et al., 2003) (Belyaev et al., 2010)
Common myeloid progenitor (CMP)	Lineage ^{-low} cKit ^{hi} CD16/32 ^{-low} IL-7R α ⁻ CD34 ⁺	
Granulocyte-macrophage progenitor (GMP)	Lineage ^{-low} cKit ^{hi} CD16/32 ⁺ IL-7R α ⁻ CD34 ⁺	
Megakaryocyte-erythrocyte progenitor (MEP)	Lineage ^{-low} cKit ^{hi} CD16/32 ⁻ IL-7R α ⁻ CD34 ⁻	

2.4.2 Intracellular staining for cytokines

Cell suspensions were diluted to 3×10^7 cells/ml in complete DMEM and 200 μ l were transferred to individual wells on round bottom 96 well plates. Unstimulated cells were used as controls. For stimulation, required volumes of Phorbol-12-myristate-13-acetate (PMA) (Sigma-Aldrich) and ionomycin (Sigma-Aldrich) were added to final concentrations of 10 ng/ml of PMA and 1 μ g/ml of ionomycin to the cells. Cells were then incubated at 37°C in 5% CO₂ for 2 hours. Brefeldin A (Sigma-Aldrich) was then added to each well at a final concentration of 10 μ g/ml and the cells incubated for a further 3 hours at 37 °C in 5% CO₂. The plates were centrifuged at 309 G for 7 minutes at 4°C, the resulting pellets suspended in complete DMEM and then stained as described in section 2.4.1. Following surface staining the cells were fixed in 2% PFA and washed twice with 1x PBS 1% FCS by centrifuging at 309 G for 7 minutes at 4°C, and suspended in 200 μ l of permeabilisation buffer (1x PBS, 1% FCS, 0.2% saponin and 0.5 % bovin serum albumin (BSA) (Sigma-Aldrich, Dorset, UK)). The cells were centrifuged at 309 G for 7 minutes at 4°C and the pellets suspended in optimized concentrations of intracellular antibodies diluted in permeabilization buffer (Table 2.2) and left at 4°C for 30 minutes in the dark. Then, the cell suspensions were washed twice by centrifugation at 309 G for 7 minutes at 4°C in permeabilization buffer, and washed further twice in 1x PBS 1% FCS by centrifugation at 309 G for 7 minutes at 4°C. Finally, the pellets were suspended in 400 μ l of 1x PBS 1% FCS and stored protected from light at 4°C until acquisition on either the BD LSR Fortessa X-20 (BD Biosciences, Oxford, UK) or the CyAn ADP analyzer (Beckman Coulter, High Wycombe, UK). (Adapted from (T. Jung *et al.*, 1993)) .

2.4.3 Intracellular staining for transcription factors (GATA-3 and β -catenin)

Following surface staining the cells were centrifuged at 309 G for 7 min at 4°C and suspended in ice-cold fixation-permeabilisation buffer (eBioscience, Hatfield, UK) for 2-16 hours at 4°C in the dark. Cells were washed by centrifugation at 309 G for 7 min once in permeabilization buffer (eBioscience, Hatfield, UK), suspended in optimized concentrations of intracellular antibodies diluted in permeabilization buffer (Table 2), and left at 4°C for 60 min in the dark. Cells were washed twice by centrifugation at 309 G for 7 minutes in permeabilization buffer and then washed further twice by centrifugation at 309 G for 7 min in PBS1x 1% FCS. Finally, the pellets were suspended in 400 μ l of 1x PBS 1% FCS and stored protected from light at 4°C until acquisition on either the BD LSR Fortessa X-20 (BD Biosciences, Oxford, UK) or the CyAn ADP analyzer (Beckman Coulter, High Wycombe, UK).

2.4.4 Intracellular staining for Annexin-V

BM cells were isolated as described in section 2.3.1. Cell suspensions were diluted to a concentration of 20-30 x 10⁶ cells/ml and 200ul of cell suspensions were transferred to individual wells on a 96 round bottom well plate. The cells suspensions were incubated for 20 minutes at 4°C with 0.125 μ g/100 μ l FcR block and then centrifuged for 7 minutes at 309 G at 4°C. Supernatants were discarded and the pellets were suspended in optimized concentration of surface antibodies CD45, Lineage cocktail, Sca1, cKit, CD150, CD48, CD34 and (Table 2.2) and fixable live-dead dye (Invitrogen, Paisley, UK) diluted in 1x PBS 1% FCS and left at 4°C for 30 min in the dark. The plate was centrifuged for 7 minutes at 309 G at 4°C, the supernatant was discarded and the cells were washed in 1x PBS 1 % FCS by centrifugation at 309 G for 7 minutes twice. Following the second wash, cell pellets were suspended in 250 μ l of 1x Binding Buffer (Annexin-V: PE apoptosis detection kit, BD Biosciences, Oxford, UK) and 12.5 μ l of Annexin V-PE was added. The cells were gently vortexed and incubated for 15 minutes at RT in the dark. Then cells were washed in Binding Buffer by centrifugation at 309 G for 7 minutes twice, and fixed in 2 % PFA diluted in Binding Buffer for 20 min at 4°C. Finally, the cells were washed in Binding Buffer by centrifugation at 309 G for 7 minutes twice and suspended in 400 μ l of Binding Buffer and stored protected from light at 4°C until acquisition on either the BD LSR Fortessa X-20 (BD Biosciences, Oxford, UK) or the CyAn ADP analyzer (Beckman Coulter, High Wycombe, UK).

2.4.5 Intracellular staining for Wnt3a

BM cells were isolated as described in section 2.3.1 and suspended in complete DMEM. Brefeldin A was then added to each well at a final concentration of 10 μ g/ml and the cells were incubated for 2 hours at 37°C in 5% CO₂ incubator. The cells were stained for Sca1, cKit, CD150,

CD48, CD34 and Live-dead staining as described in section 2.4.1. Following surface staining cells were stained for Wnt3a in the presence of Rat serum (1:500) as described in section 2.4.2. All buffers were kept ice-cold.

2.4.6 Cell sorting of HSCPs cells from bone marrow and adoptive transfer to lethally irradiated recipient mice.

BM cells were isolated from naive and 28 days infected mice as described in section 2.3.1. Cell suspensions were diluted to a final concentration of 30×10^6 cells/ml and transferred to a sterile 5 ml BD Falcon Round Bottom Polystyrene capped tube. The cells were labeled with in optimized concentration of CD45.2, Lineage cocktail, Sca1, cKit, CD150, CD48 and CD34 (Table 2.2) diluted in 1x PBS 1% FCS and left at 4°C for 30 minutes in the dark. Then 2 ml 1x PBS 1% FCS were added and the cells were centrifuged for 10 minutes at 309 G. The resulting pellets were washed with a further 4 ml of PBS. The samples were then suspended in 1x PBS 5% FCS and filtered through a 70 μ m and a 40 μ m strainers. Cells were sort purified according with the following phenotype: CD45⁺ Lin⁻ Sca1⁺ cKit⁺ CD150⁺ CD48⁻ CD34⁻ cells (HSCs); CD45⁺ Lin⁻ cells (enriched for HSCPs), CD45⁺ Lin⁻ Sca1⁻ cKit⁻ cells (LSK^{neg}) and CD45⁺ Lin⁻ Sca1⁺ cKit⁺ cells (LSK). Cells were sorted into pre-coated 50 ml Falcon tubes containing complete DMEM. Following the cell-sort in the MoFlo Astrios (Beckman Coulter, High Wycombe, UK), the purities of the various selected cell populations were assessed to attest that purity of sorted cells were > 95%. Sorted cells were centrifuged at 4°C for 15 minutes at 309 G, suspended in RPMI-1640 and then 200 μ l were transplanted into recipient mice via the lateral tail vein post-irradiation treatment. Recipient mice were placed with water acidified with hydrochloric acid (pH 2.5) for five days, then irradiated with 550 rad / 5 minutes on two consecutive days and they were kept in Baytril (Bayer) for seven day upon first irradiation treatment. In competitive adoptive transfer experiments infected and naive donor cells were mixed at 50:50 ratio, in non-competitive adoptive transfer experiments a minimum of 3.5×10^5 radio protective total bone marrow cells were transferred together with the sorted donor cells.

2.4.7 Establishment of BM chimeras B6.c-Myc-eGFP → WT B6.CD45.1 and intracellular staining for c-Myc-eGFP

BM cells from B6.CD45.1 donor mice were isolated as described in section 2.3.1. Vials containing frozen BM cells from B6.Myc-EGFP (CD45.2) were placed in on water bath pre-heated to 37°C for 1-2 minutes to thaw (defrost). Cell suspensions were transferred to a 50 ml Falcon tubes and topped up with warmed complete DMEM, centrifuged at 309 G for 5 minutes, the resulting pellets were suspended and the cells counted. Each recipient B6.CD45.1 received a 2×10^6 BM cells from B6.Myc-EGFP cell (CD45.2) donors post-irradiation treatment. Recipient

mice were placed with water acidified with hydrochloric acid (pH 2.5) for three days, then irradiated with 550 rad/5 minutes on two consecutive days and then they were kept in Baytril (Bayer) for seven day upon first irradiation treatment. Following a period of 10 weeks, recipient mice were infected with LV9 for 28 days.

Mice were sacrificed by CO₂ euthanization and followed by dislocation of the neck. BM cells from recipient mice were isolated as described in section 2.3.1. Cells were labeled for CD45.2, Lineage cocktail, Sca1, cKit, CD150, CD48, CD34 and Live-dead staining, as described in section 2.4.1. Following surface staining the cells were centrifuged at 309 G for 7 minutes at 4°C and suspended in cold 2% PFA for 60 minutes on ice protected from light. Cells were washed by centrifugation at 309 G for 7 minutes once in permeabilization buffer (eBioscience, Hatfield, UK), suspended in permeabilization buffer and left at 4°C for 60 min in the dark. The cells were washed twice by centrifugation at 309 G for 7 minutes in permeabilization buffer and then washed further twice by centrifugation at 309 G for 7 minutes in 1x PBS 1% FCS. Finally, the pellets were suspended in 400 µl of 1x PBS 1% FCS and stored protected from light at 4°C until acquisition on BD LSR Fortessa X-20 (BD Biosciences, Oxford, UK).

2.4.8 Cell sorting of CD4⁺ T cells from spleens and adoptive transfer to RAG2 KO mice.

Splenocytes were isolated from naive and infected mice as described in section 2.3.2. Cell suspensions were diluted to a concentration of 30 x 10⁶ cells/ml and transferred to a sterile 5 ml BD Falcon Round Bottom Polystyrene capped tube. The cells were labeled with in optimized concentration of CD45, CD4, CD8, B220, TCRγδ, CD49b and CD3 antibodies (Table 2.2) diluted in 1x PBS 1% FCS and left at 4°C for 30 minutes in the dark. Then 2 ml 1x PBS 1% FCS were added and the cells were centrifuged for 10 minutes at 309 G. The resulting pellets were washed with a further 4 ml of 1x PBS 1% FCS. The samples were then suspended in 1x PBS 5% FCS and filtered through 70 µm and 40 µm strainers. CD45⁺ CD4⁺ CD3⁺ CD8⁻ B220⁻ TCRγδ⁻ CD49b⁻ cells were sort-purified using the MoFlo Astrios (Beckman Coulter, High Wycombe, UK). Cells were sorted into pre-coated 50 ml Falcon tubes containing complete DMEM. Following the cell-sort, the purities of the cell populations were assessed to attest that purity of sorted cells were > 95%. Sorted cells were centrifuged at 4°C for 15 minutes at 309 G, resuspended in RPMI-1640 at 3x10⁶ cells/ml, then 200µl were transplanted into B6.Rag2KO.CD45.1Cg recipient mice via the lateral tail vein. In the following day recipient mice and controls were infected with LV9 as described in section 2.2.

2.4.9 Mixed BM chimeras B6.CD45.1: B6.CD45.2.*Ifnγ*2^{-/-} (50:50) → B6CD45.1 mice

BM cells from WT B6.CD45.1 and B6.IFN γ -R2KO donor mice were isolated as described in section 2.3.1. Each recipient B6.CD45.1 received 1×10^6 BM cells from WT B6.CD45.1 donor mice and 1×10^6 BM cells from B6.IFN γ -R2KO donor mice post-irradiation treatment. Recipient mice were previously placed with water acidified with hydrochloric acid (pH 2.5) for three days, then irradiated with 550rad /5 minutes on two consecutive days and then they were kept in Baytril (Bayer) for seven day upon first irradiation treatment. Recipient mice were infected with LV9 for 28 days, following nine weeks from the adoptive transfer.

2.4.10 Mixed BM chimeras B6.CD45.1:B6.CD45.2.TNF-RdKO (50:50) \rightarrow B6.CD45.1 mice

BM cells from WT B6.CD45.1 donor mice were isolated as described in section 2.3.1. Vials containing frozen BM cells from mice deficient for both Tnfrsf1a (TNF-R1a, p55) and Tnfrsf1b (TNF-R1b, p75) receptors, hereafter called TNF-RdKO (CD45.2), were placed in on water bath pre-heated to 37 $^{\circ}$ C for 1-2 minutes to thaw (defrost). Cell suspensions were transferred to a 50 ml Falcon tube, topped up with pre-warmed complete DMEM and centrifuged at 309 G for 5 minutes. The resulting pellets were suspended and the cells counted. Each recipient B6.CD45.1 received a 2×10^6 BM cells from each donor post-irradiation treatment. Recipient mice were previously placed with water acidified with hydrochloric acid (pH 2.5) for three days, then irradiated with 550rad /5 minutes on two consecutive days and then they were kept in Baytril (Bayer) for seven day upon first irradiation treatment. Recipient mice were infected with LV9 for 28 days, following nine weeks from the adoptive transfer.

2.4.11 Flow cytometry and sorting of CD4 $^{+}$ T cells from BM for RNA extraction

BM cells were isolated from naive and infected mice as described in section 2.3.1. Cell suspensions were diluted to a concentration of 30×10^6 cells/ml and transferred to a sterile 5 ml BD Falcon Round Bottom Polystyrene capped tube. The cells were labeled with in optimized concentration of CD45, CD4, CD8, TCR $\gamma\delta$, B220 (CD45R), DX5 (CD49d) and CD3 antibodies (Table 2.2) diluted in 1x PBS 1% FCS and left at 4 $^{\circ}$ C for 30 min in the dark. Then 2 ml 1x PBS 1% FCS were added and the cells were centrifuged for 10 minutes at 309 G, the resulting pellets were washed with a further 4 ml of PBS. The samples were then suspended in 1x PBS 5% FCS and filtered through 70 μ m and 40 μ m strainers. CD45 $^{+}$ CD4 $^{+}$ CD3 $^{+}$ CD8 $^{-}$ B220 $^{-}$ DX5 $^{-}$ cells (CD4 $^{+}$ T cells) and CD45 $^{+}$ CD4 $^{-}$ CD3 $^{+}$ CD8 $^{+}$ B220 $^{-}$ DX5 $^{-}$ cells were sort-purified using the MoFlo Astrios cell sorter (Beckman Coulter, High Wycombe, UK). Cells were sorted into pre-coated 50 ml Falcon tubes (Sigma-Aldrich, Dorset, UK) containing complete DMEM. Following the sort, cell purities were assessed to ascertain > 95% purity. Sorted cells were centrifuged at 4 $^{\circ}$ C for 15 minutes at 309 G, the supernatant was discarded, the pellets were suspended in DMEM and transferred to an RNase free 1.5 ml Eppendorf, cells were centrifuged at 4 $^{\circ}$ C for 10 minutes at

425 G in a Accuspin Micro centrifuge (Fisher Scientific, Pittsburg, USA). The supernatant was carefully removed and cell pellet suspended in 700 µl of Qiazol (Qiagen, UK), vortexed for 1 minute and then placed on dry ice before storing the samples at -80°C.

2.4.12 Flow cytometry analysis

For phenotypic analysis and cell sorting, cell suspensions were stained with monoclonal antibodies as described in Supplementary Table 2.2. Negative controls were stained with matched-isotype controls. Dead cells were excluded by Fixable Viability Dye eFluor780 (eBioscience) or LIVE/DEAD Fixable Aqua Cell Stain (ThermoFisher) and cellular aggregates were electronically excluded in all experiments. A Fortessa II (Becton Dickinson) or CyAn (Dako-Beckman) were used for analytical flow cytometry, and data were analyzed with FlowJo software (TreeStar).

The measurements derived from flow cytometric analysis were presented in relative and absolute quantifications. The frequencies of various cell populations although important to determined the relative proportion of each cell type within the tissue may be vary due to egress or ingress of cells, and therefore not reflect a true alteration in the number of cells in the organ.

2.5 BLOOD COLLECTION AND HEMOGRAM

Mice were anesthetized by inhalation (dispensed by Apollo TEC3 Isoflurane Vaporise, Sound Veterinary Equipment) of Isoflurane (Baxter)(2-chloro-2-(difluoromethoxy)-1,1,1-trifluoro-ethane) and blood was then collected through heart puncture into 1.5 ml Eppendorfs coated with heparine (Sigma-Aldrich) or Microtainer Blood Collection Tubes with K2EDTA (Becton, Dickinson and Company). Hemavet (Drew Scientific) and Vet abc Plus+ (Horiba Medical) were used to determine blood parameters.

2.6 TOTAL RNA EXTRACTIONS AND MICROARRAY OF BM T CELLS

Sorted BM CD8⁺ T cells (section 2.4.11) were stored at -80°C in 700 µl of Qiazol (Qiagen, Manchester, UK) and used to test the miRNeasy Micro Kit (Qiagen, Manchester, UK) and the Directzol kit (Zymo Research Corporation, Irvine, USA). Extracted RNA was kindly assessed by Dr. Sally James (Genomics, Technology facility, York, UK) for yield and quantity, using the Agilent RNA 6000 Pico Kit (Agilent Technologies, USA), according to the manufacturer's instructions. The Directzol kit showed best results with limiting number of sorted cells and, therefore, was selected to perform the RNA extraction on our samples (BM CD4⁺ T cells).

2.6.1 RNA extraction using the miRNeasy Micro Kit

Sorted T cells were stored at -80°C in 700 µl of Qiazol. Samples were allowed to thaw and RNA extracted by carrying out a Qiazol/chloroform phase extraction. Once the samples had thawed, 200 µl of chloroform were added and the tubes shaken vigorously by hand for 2 minutes. The samples were allowed to stand at room temperature for 5 minutes and then spun down at 13,000 x g for 15 minutes in a microcentrifuge (Microcentrifuge 5424R, Eppendorf) at 4°C. The aqueous phase was carefully pipetted out and transferred to a fresh Eppendorf tube. 1.5 volumes of 100% ethanol were added, the samples thoroughly mixed and subsequently the extractions were carried out using the miRNeasy micro kits (Qiagen, Manchester, UK), according to the manufacturer's instructions. On-column DNase digestion was carried out to remove any contaminating genomic DNA using the RNase-free DNase set (Qiagen, Manchester, UK) according to the manufacturer's instructions. RNA quality and quantity was assessed by measuring the absorbance at 230, 260 and 280 nm with a NanoDrop 2000 spectrophotometer (Thermo Fisher Scientific, Loughborough, UK) and by Sally James using the Agilent RNA 6000 Pico Kit according to the manufacturer's instructions (Genomics, Technology facility, York, UK). All samples were then stored at -80 °C.

2.6.2 RNA extraction using the Direct-zol™ RNA MiniPrep

One volume ethanol (100%) was added directly to one volume sample homogenate (1:1) in Qiazol and mixed well by vortexing. The mixture was loaded into a Zymo-Spin™ IIC Column in a Collection Tube and centrifuge for 30 seconds. The column was transferred into a new collection tube. At this point, on-column DNase digestion was carried out to remove any contaminating genomic according to the manufacturer's instructions (Direct-zol™ RNA MiniPrep). 400 µl Direct-zol™ RNA PreWash was added to the column and centrifuge for 30 seconds and the flow-through discarded, this step was then repeated. 700 µl RNA Wash Buffer was added to the column and centrifuged for 2 minutes to ensure complete removal of the wash buffer. The column was transferred carefully into an RNase free Eppendorf tube. 25 µl of DNase/RNase-Free Water were pipetted directly onto the column matrix and centrifuge for 30 seconds. RNA quality and quantity was assessed by measuring the absorbance at 230, 260 and 280 nm in a NanoDrop 2000 spectrophotometer (Thermo Fisher Scientific, Loughborough, UK) and by Sally James using the Agilent RNA 6000 Pico Kit according to the manufacturer's instructions (Genomics, Technology facility, York, UK). All samples were then stored at -80 °C.

2.6.3 Microarray

The microarray was performed using the microarray slide SurePrint G3 Mouse Gene Expression 8 x 60K Microarray (Agilent Technologies, Stockport, UK), composed by eight arrays and

representing a complete coverage of known coding transcripts (59308 transcripts). Dr. Sally James conducted the microarray according to the manufacturer's instructions (Genomics, Technology facility, York, UK). The resulting data was analyzed by Dr. Sandy McDonald (Genomics, Technology facility, York, UK) using GeneSpring GX Software (Agilent Technologies, Stockport, UK).

2.7 REVERSE TRANSCRIPTION REACTION AND QUANTITATIVE REAL-TIME POLYMERASE CHAIN REACTION OF TOTAL BM CELLS

BM cell suspensions were obtained as described in section 2.3.1, and then centrifuged at 4 °C for 15 minutes at 309 G. The supernatants were discarded; the pellets suspended in DMEM and transferred to RNase free 1.5 ml Eppendorf tubes. Cells were centrifuged at for 10 minutes at 425 G in Accuspin Micro centrifuge (Fisher Scientific, Pittsburg, USA). The supernatants were carefully removed, cell pellets suspended in 700 µl of Qiazol (Qiagen, UK), vortexed for 1 minutes and then placed on dry ice before storing the samples at -80°C. Total RNA was extracted as previously described in section 2.6.2.

2.7.1 Reverse transcription reaction (RT Reaction)

The cDNA syntheses were performed with the Superscript II reverse transcriptase system (Invitrogen), according to manufacture's instructions. Previously, RNA purity was assessed in the device a NanoDrop 2000 spectrophotometer (Thermo Fisher Scientific, Loughborough, UK). About 1 µl Oligo (dT)₁₂₋₁₈ (0,5µg/µl), 1µl dNTPs [10mM] and appropriate volume of nuclease free water (Qiagen, UK) to complete a final volume of 13 µl were added to 500 ng of total RNA. This mixture was heated for 5 minutes at 65°C and then placed immediately in ice. Then the cDNA synthesis master mix (4 µl of 5x Reverse Transcription Buffer, 1 µl DTT (0.1 M; dithiothreitol), 1 µl RNase Out (40U/µl) and 1 µl Superscript Reverse Transcriptase II (200 U/ul)) was prepared, mixed thoroughly and spun down at 10000 G for 5 seconds. 8 µl of master mix were added to 12 µl of RNA/ Oligo (dT)₁₂₋₁₈ to complete a final volume of 20 µl per reaction. cDNA synthesis reaction mixtures were incubated for 60 minutes at 50°C, and then for 5 minutes at 70°C and finally placed on ice. The newly generated cDNA was stored at -20 °C.

2.7.2 Quantitative real-time polymerase chain reaction (qRT-PCR)

The qRT-PCR of Wnt3a mRNA expression in total BM was performed with the SYBR-green qPCR Kit (Applied Biosystems, Warrington, UK) in StepOnePlus Real Time PCR detection system (Applied Biosystems), accordingly to manufacturers' instructions. The reactions were

performed in MicroAmp Optical 96-well reaction plates (Applied Biosystems) in ice-cold conditions. Reactions contained 10 µl Fast SYBR Green Mix (2x), 0.8 µl of cDNA, 8.2 µl of nuclease free water (Qiagen, UK) and 0.5 µl of mix of primers pair (10 µM of each primer) (FORWARD: tactacgaggcctcacccaa; REVERSE: acccatctatgccatgag). The plates were sealed and centrifuged to assure all liquid was at the bottom of the well. Then qRT-PCRs were performed under the following cycling conditions: 95°C for 20 seconds followed by 40 cycles of 95°C for 1 second and 60°C for 20 seconds. Data were analysed using the StepOne Software version 2.2.2 (Applied Biosystems, Warrington, UK). mRNA expression levels were normalized to HPRT1 housekeeping gene using $\Delta\Delta C_t$ calculations. Mean relative microRNA expression levels between control and experimental groups were calculated using the $2^{-\Delta\Delta C_t}$ calculations.

2.8 STAINING OF PURIFIED LSK CELLS FOR CONFOCAL MICROSCOPY ANALYSIS

BM cell suspensions were obtained as described in section 2.3.1, and following cell-surface staining (described in section 2.4.1), were sort-purified in the MoFlo Astrios (Beckman Coulter). Sort-purified LSK cells were centrifuged for 7 minutes at 309 G at 4°C, the supernatant was discarded and the cells were fixed of 2% PFA (Sigma-Aldrich) for 20 minutes at 4°C in the dark. Cells were washed twice with 1x PBS 1% FCS by centrifugation at 309 G for 7 minutes and suspended in 1x PBS 1% FCS. Following the slides preparation, chamber and blotter were placed carefully in the Cytospin™ 4 Cyto centrifuge (Thermo Scientific). Then, 100 µl of cell suspensions were placed into the slide chamber and spun down at 137 G for 5 minutes. Slides were carefully removed from the cytopsin-centrifuge and left to dry, prior to staining. The areas containing the samples on the slides were delimited with an ImmEdge pen (Vector Laboratories, USA). The slides were washed in PBS 0.05% Bovine Serum Albumin (BSA) (Sigma-Aldrich), hereafter called wash buffer, then blocked by the addition of 10% Goat serum (Sigma-Aldrich) and 0.001mg of Fc block diluted in wash buffer for 20 minutes at RT. Excess wash buffer was removed and the cells were permeabilized by addition of PBS + 0.2% Triton X-100 (Sigma-Aldrich) for 5-10 minutes at RT. The slides were washed by incubation with wash buffer for 5 minutes, then anti-GATA-3 (HG3-31, Santa Cruz Inc.) (1:500) or Isotype control (anti-IgG1 mouse, eBioscience) were added diluted in PBS containing 10% Goat serum and 0.001 mg of Fc block. Slides were incubated overnight at 4°C. The slides were washed three times in wash buffer the following day. Then secondary antibody IgG goat anti-mouse Alexa 594 (Invitrogen) (1:400) was added diluted in PBS containing 10% Goat serum and 0.001 mg of Fc block and the slides were incubated for 30 minutes at RT. The slides were wash three times in wash buffer and then once in PBS. 1µg/ml DAPI (4',6-diamidino-2-phenylindole) (Sigma-Aldrich) diluted in PBS was added to the slides, incubated for 5 minutes and then washed twice in PBS. Excess PBS was removed and a small amount of ProlongGold (Invitrogen) was applied in each sample to mount

by the placement coverslips over the samples. Slides were kept protected from light overnight at 4°C, and were then sealed with nail varnish. Slides were stored protected from light at 4°C until analysis in confocal microscope (Zeiss LSM 710, Zeiss).

2.9 STATISTICAL ANALYSIS

In most experiments the statistical analyses were performed by parametric or non-parametric tests, selected according to the distribution of the raw data. The comparisons between experimental groups were performed using student Unpaired t test, Mann-Whitney and one-way ANNOVA. The analysis of population distribution was performed using Chi-square test. The statistical analyses fold changes were performed using Wilcoxon signed-rank test. All analyses were conducted using GraphPad InStat (versions 5 and 6) software (GraphPad software, San Diego, California, US).

Table 2.2 - Monoclonal antibodies used to evaluate expression of surface cell markers, cytokines and transcription factor by flow cytometry analysis

Antigen	Clone	Fluorochrome	Supplier
β -Catenin	15B8	PE	eBioscience
Wnt3a	217804	APC	R&D Systems
TNF	MP6-XT22	PE	eBioscience
Ter-119	TER-119	PE-Cy7	eBioscience
TCR $\gamma\delta$	eBioGL3 (GL-3, GL3)	PE	eBioscience
Mouse Lineage Antibody Cocktail (CD3e, Ly-6G and Ly-6C, TER-119, CD45R, CD11b)	145-2C11, RB6-8C5, TER-119, RA3-6B2, M1/70	PerCPCy5.5	Becton Dickinson (BD) Bioscience
MHC II	M5/114.15.2	APC	eBioscience
MHC II	M5/114.15.2	PerCP-Cy5.5	Biologend
MHC II	M5/114.15.2	eF450	eBioscience
Ly6C	AL-21	FITC	Becton Dickinson (BD) Bioscience
Ly6A/E (Sca1)	D7	BV510	Becton Dickinson (BD) Bioscience
Ly6A/E (Sca1)	D7	APC	eBioscience
Ly6A/E (Sca1)	D7	V500	Becton Dickinson (BD) Bioscience
Ki67	MOPC-21	PE	Becton Dickinson (BD) Bioscience
IL-10	JES5-16E3	APC	eBioscience
IFN γ	XMG1.2	APC	eBioscience
IFN γ	XMG1.2	eF450	eBioscience
GR1	RB6-8C5	PE-Cy7	eBioscience
GATA3	16E10A23	BV421	Biologend
FOXP3	FJK-165	APC	eBioscience
F4/80	BM8	FITC	eBioscience
F4/80	BM8	BV421	Biologend
CD8 α	53-6.7	APC	Becton Dickinson (BD) Bioscience
CD8 α	53-6.7	PE	eBioscience
CD8	H35-17.2	PerCP-eF710	eBioscience
CD62L	MEL-14	PE	eBioscience
CD51	RMV-7	PE	eBioscience
CD49b	DX5	PE	eBioscience
CD48	HM48-1	Pe-Cy7	eBioscience
CD45R (B220)	RA3-6B2	Alexa 647	eBioscience
CD45R (B220)	RA3-6B2	PE	eBioscience
CD45R (B220)	RB6-8C5	PE	Biologend
CD45.2	104	APC-eFluor 780	eBioscience
CD45.2	104	FITC	eBioscience
CD45.2	104	Alexa 700	eBioscience

Table 2.2 (cont.) - Monoclonal antibodies used to evaluate expression of surface cell markers, cytokines and transcription factor by flow cytometry analysis

Antigen	Clone	Fluorochrome	Supplier
CD45.1	A20	FITC	Becton Dickinson (BD) Bioscience
CD45.1	A20	BV650	Biologend
CD45.1	A20	PE	Becton Dickinson (BD) Bioscience
CD45	30-F11	Alexa 700	eBioscience
CD45	30-F11	APC	eBioscience
CD44	IM7	Alexa647	Biologend
CD4	4SM95	ef660	eBioscience
CD4	GK1.5	APC	eBioscience
CD4	RM4-5	Briliant Violet 650	Biologend
CD4	RM4-5	FITC	Biologend
CD34	RAM34	FITC	Becton Dickinson (BD) Bioscience
CD31	390	FITC	eBioscience
CD3	145-2C11	FITC	eBioscience
CD3	145-2C11	Pe-Cy7	Biologend
CD3	MEC14.7	BV421	Biologend
CD29 (Integrin beta 1)	eBioHMb1-1 (HMb1-1)	PE	eBioscience
CD25	PC61	Pe-Cy7	Biologend
CD16/32	93	PE-Cy7	eBioscience
CD150	TC15-12F12.2	Briliant Violet 421	Biologend
CD150	TC15-12F12.3	Briliant Violet 650	Biologend
CD135 (Flt3)	A2F10	Biotin	eBioscience
CD127	A7R34	Briliant Violet 421	Biologend
CD127	A7R34	ef450	eBioscience
CD127	A7R34	PE-Cy5	eBioscience
CD120b (TNF R Type II/p75)	55R-286	PE	Biologend
CD120a (TNF R Type I/p55)	TR75-89	PE	Biologend
CD11c	N418	PE	Biologend
CD11b	M1/70	Alexa 488	eBioscience
CD11b	M1/70	BV510	Biologend
CD11b	M1/70	APC	eBioscience
CD117 (cKit)	2B8	PE	Becton Dickinson (BD) Bioscience
CD117 (cKit)	2B8	Briliant Violet 421	Biologend
CD117 (cKit)	2B8	FITC	Biologend
B220 (CD45R)	RA3-6B2	Alexa 647	Biologend
B220 (CD45R)	RA3-6B2	PE	eBioscience
Streptavidin		PE-Cy7	Becton Dickinson (BD) Bioscience

CHAPTER 3. ALTERATIONS IN HAEMATOPOIESIS DURING *LEISHMANIA DONOVANI* INFECTION

3.1 INTRODUCTION

VL is a vector-borne disease caused by the intracellular protozoa *Leishmania donovani* and *L. infantum*. In vertebrate hosts, including humans, parasites reside mainly in mononuclear phagocytes where they multiply as obligatory intracellular amastigotes. *L. donovani* amastigotes are detected primarily in the spleen, lymph nodes, BM and liver, and their persistence contributes to chronic infection (E. Handman, 2000).

In humans, VL is characterized by hypergammaglobulinaemia, hepato-splenomegaly and disturbances in blood homeostasis, including anemia, thrombocytopenia, leucopenia and neutropenia. Unfortunately, an effective vaccine has not yet been produced and the therapeutic drugs available have been associated with increased parasite resistance and toxicity (C. R. Davies *et al.*, 2003, C. R. Engwerda *et al.*, 2004a). It has been estimated that 500,000 new cases of VL occur annually. The infection is fatal without drug treatment and even treated patients may die from the pathology, bleeding or opportunistic bacterial infections (M. A. Santos *et al.*, 2002, V. E. Miranda de Araujo *et al.*, 2012).

In humans, splenic sequestration and ineffective haematopoiesis have been suggested as possible causes to explain peripheral cytopenia. In addition to alterations in the blood, VL has been associated with the alterations in the BM, including erythroid hyperplasia, increased plasma cells, increased frequency of granulocytic and megakaryocyte immature forms, and histiocytic hyperplasia (N. Varma and S. Naseem, 2010). Furthermore, several clinical reports described pancytopenia in VL patients followed by BM multilineage myelodysplasia reminiscent of true myelodysplastic syndrome (MDS), suggesting the presence of ineffective haematopoiesis (N. Yarali *et al.*, 2002, P. Kopterides *et al.*, 2003, G. M. de Vasconcelos *et al.*, 2014).

Experimental mouse models have been extensively used to study the immunopathology of VL, and these have reported alterations in haematopoietic function. For example, in the spleen, a secondary site of haematopoiesis in adult mice, higher frequencies of macrophages and dendritic cells (DCs) were described in chronic infection (J. E. Dalton *et al.*, 2010). DCs that produce low levels of the proinflammatory cytokine IL-12 and high levels of the immunoregulatory cytokine IL-10 were found in the spleen of infected mice, and it was shown that these impact negatively on parasite clearance (B. M. J. Owens and P. M. Kaye, 2012). Splenic stromal cells isolated from *L. donovani* infected mice showed an enhanced capacity *in vitro* to direct haematopoietic progenitors

toward a regulatory dendritic cell (rDC) phenotype (M. Svensson *et al.*, 2004), suggesting that *L. donovani* infection is able to modulate haematopoiesis and alters the function of immune effector cells towards immunosuppression in the spleen. Alterations in spleen function in experimental VL are further described in Chapter 4.

In experimental VL, amastigotes also persist during chronic infection in the BM (S. E. J. Cotterell *et al.*, 2000a, S. E. J. Cotterell *et al.*, 2000b) (Figure 3.1), though the impact of infection at this site is less well studied. During the course of *L. donovani* infection in BALB/c mice, increased BM parasite burden was associated with increased numbers of all haematopoietic precursor cells, as assessed by the number of colony-forming units in culture (S. E. J. Cotterell *et al.*, 2000a). These studies showed that BM macrophages (including stromal macrophages defined by CD169 expression) could become infected with *L. donovani* both *in vivo* and *in vitro*, but there were no indications that a significant number of haematopoietic progenitor cells harbored parasites (S. E. J. Cotterell *et al.*, 2000b). Infected BM-derived macrophages showed an increased efficiency to support the formation of GM-CFU *in vitro*, and this effect was partially mediated by higher expression of GM-CSF and TNF by infected macrophages (S. C. Smelt *et al.*, 2000). Furthermore, infection of a fibroblast-like BM stromal cell line (MBA-1) with *L. donovani* directed differentiation of haematopoietic precursors into “regulatory DCs”, and this is thought to be due to an infection-dependent increase in the levels of CCL8 expression (A. T. N. Hoang *et al.*, 2010). Taken together these findings indicated that VL has the potential to alter haematopoiesis. This could be due to the modulation of haematopoiesis-supporting stromal cells, or through the systemic action of cytokines or other mediators. Hence, the mechanisms underlying the impact of infection on haematopoiesis and its consequences on immune responses during VL remain unclear.

During infection, the systemic release of pro-inflammatory mediators induces changes in BM populations, either directly or through alteration in their microenvironment, which may impact on their rates of proliferation, lineage fates or mobilization (K. Y. King and M. A. Goodell, 2011). Therefore, an impact of infection on haematopoiesis has been reported in association with many infections, although with variable pathogen-specific outcomes. An increase in haematopoietic stem and progenitor cells (HSPCs) has been reported to occur in response to the increased demand for immune cells and/or in direct response to pathogen associated molecular patterns (PAMPs) and pro-inflammatory cytokines, recognized respectively by the pattern recognition receptors and cytokines receptors expressed by HSPCs (K. Y. King and M. A. Goodell, 2011). Within several infectious contexts, HSCs have in recent years emerged as central players in the development of immune responses, nonetheless in some models, infection-induced haematopoiesis was reported to negatively impact on HSCs function (M. T. Baldrige *et al.*, 2011).

Haematopoiesis is a strictly regulated process that depends on a very small pool of long-term haematopoietic stem cells (LT-HSCs), which have self-renewal capacity and the potential to give rise to all mature blood cells during the lifespan of an individual. According to the classical pathway of haematopoiesis, LT-HSCs differentiate into short-term haematopoietic stem cells (ST-HSCs) that then give rise to a heterogeneous group of multipotent progenitors (MPPs). LT-HSCs, ST-HSCs and MPPs are contained within the LSK population, so called for their lack of expression of mature blood cell-associated markers (Lineage negative) and their expression of Sca1 (Stem cells antigen 1) and cKit (Stem cell factor receptor). MPPs give rise to a succession of intermediary progenitors, the common lymphoid progenitors (CLPs) and the common myeloid progenitors (CMPs). CMPs may then give rise to both granulocyte/macrophage progenitors (GMPs), and the megakaryocytic/erythrocyte progenitors (MEPs). The lineage-committed precursors, CMPs, CLPs, GMPs and MEPs are all contained in the Lineage negative, Sca1 negative and cKit positive cell population (cKit^{hi}) [24]. Herein, we use the term HSPCs to collectively include all Lineage negative cKit⁺ cells (multipotent progenitors and lineage-committed progenitors), each defined by their pattern of surface molecular markers, as highlighted in Figure 3.2 (M. Kondo *et al.*, 2003a).

In this chapter, we aimed to characterize HSPCs during experimental *L. donovani* infection in order to establish whether infection affects their function and / or survival. This is the first study evaluating HSPCs in the BM directly *ex vivo* in experimental VL. Using a panel of stem cell markers, we characterized HSPCs over the course of *L. donovani*-infection in C57BL/6 (B6) mice. Chronically infected mice showed a significant increase in intermediary non-committed multipotent haematopoietic precursors (Lineage⁻ Sca1⁺ cKit⁺ (LSK), CD150⁺ CD48⁺ cells) without reciprocal increases in either lineage-committed precursors or mature cells in circulation. In steady state, the majority of LT-HSCs (LSK CD150⁺ CD48⁻ CD34⁻ cells) were found in a quiescent state, representing cells with the highest degree of reconstitution potential. In contrast, during chronic infection most were found to have progressed to cell-cycle and this correlated with a reduced potential to engraft into syngeneic recipients. These finding suggested that *L. donovani* infection have the potential to impair haematopoietic development through the “functional exhaustion” of HSCs.

3.2 RESULTS

3.2.1 *L. donovani* infection was associated with alterations in the number of HSPCs in BM and spleen

Alterations in the number of haematopoietic progenitors, both in BM and spleen during *L. donovani* infection have been previously described during the course of infection in BALB/c mice using colony-forming assays (S. E. J. Cotterell *et al.*, 2000a). To confirm the previously reported increase in haematopoietic progenitors during the course of infection, we quantified HSPCs (including LT-HSCs, ST-HSCs, MPPs, CMPs, GMPs, MEPs and GMPs) in the BM and in the spleen of B6 mice infected with *L. donovani* over a period 64 days, using a flow cytometric rather than functional approaches.

Haematopoietic progenitors were defined using a panel of cellular markers as previously described (M. Kondo *et al.*, 2003a) (Figure 3.3; Figure 3.4). In several models of infection, it has been reported that Sca1 expression was upregulated in all progenitors upon infection (N. N. Belyaev *et al.*, 2010, K. Y. King and M. A. Goodell, 2011, K. C. MacNamara *et al.*, 2011b, J. L. Granick *et al.*, 2012). We observed the same phenomenon in mice chronically infected with *L. donovani* (Figure 3.5). Therefore, we included all Lineage⁻ cKit⁺ cells even those expressing Sca1 to quantify lineage-committed precursors in all the experiments where a group of infected mice was included.

During the course of *L. donovani* infection, the parasite burden in the spleen increased from day 3 to day 28, with a degree of resolution by d64 p.i. (Figure 3.6a). Nevertheless, splenomegaly and increased number of splenocytes were maintained in infected mice at day 64 (Figure 3.6c; Figure 3.7b), which suggested that in spite of the decline in parasite burden the inflammation persisted. Parasite burden in BM followed a similar trend (Figure 3.6b). In contrast, the number of cells in BM was decreased at later time points (Figure 3.7a).

The relative frequency of HSPCs in BM within Lineage⁻ cKit⁺ cells was increased on day 7 (1.434 ± 0.064 , $\bar{x} \pm \text{SEM}$). On days 16 and 28 p.i. with *L. donovani*, the frequencies of HSPCs were comparable to naive mice. However by day 64 p.i., their frequency was increased 2.039 ± 0.232 fold compared to naive controls (Figure 3.8a). A similar biphasic response was observed when evaluating the absolute number of HSPCs (Figure 3.8b). In the spleen, the relative frequencies of HSPCs in BM were increased compared to control uninfected mice from day 16, peaked at day 28 and declined at day 64 p.i. (Figure 3.9a), again with a similar trend observed in terms of absolute

numbers (reflecting fourteen times more HSPCs in the spleen of infected mice compared to the controls at later time points; Figure 3.9b).

The increase in the frequency of multipotent progenitors was an early event following infection in BM, with the maximum fold increase taking place at day 28 p.i.. The frequency of CD150⁺ Flt3⁻ CD34⁻ (LT-HSCs) cells was increased 117.750 ± 32.684 fold and the frequency of CD150⁺ Flt3⁻ CD34⁺ cells (ST-HSCs) was increased 22.175 ± 6.974 fold at 28 days p.i.. At later time points, the frequencies of LSK CD150⁺ Flt3⁻ CD34⁻ cells and LSK CD150⁺ Flt3⁻ CD34⁺ cells remained high in infected mice compared to control mice (Figure 3.8c). Changes in LSK CD150⁻ Flt3⁺ CD34⁺ cell (MPPs) frequencies during the course of infection were relatively mild compared to earlier progenitors (of LSK CD150⁺ Flt3⁻ CD34⁻ cells and LSK CD150⁺ Flt3⁻ CD34⁺ cells). On day 28 p.i., there was a 18.750 ± 7.091 fold increase in MPPs frequency in infected mice, but this normalized by day 64 p.i. (Figure 3.8c). Changes in the absolute number of LSK CD150⁺ Flt3⁻ CD34⁻ cells, LSK CD150⁺ Flt3⁻ CD34⁺ cells and LSK CD150⁻ Flt3⁺ CD34⁺ cells followed the same trend (Figure 3.8d).

The frequency of lineage-committed precursors during the course of infection was also assessed in BM. By day 7 p.i., the frequency of GMPs increased 1.584 ± 0.245 fold, but was comparable to naive at other time points. The frequency of CMPs increased 2.079 ± 0.333 fold at day 28 p.i., returning to normal by d64 p.i.. MEPs frequency remained relatively unchanged during the course of infection, with only a 2.814 ± 1.747 fold increase at d64 p.i. (Figure 3.8e). In term of absolute numbers, CLPs were significantly increased only at day 7 p.i. (1.88 ± 0.29 fold). At latest time point, MEPs were found 2.386 ± 0.829 fold increased at day 64 p.i.. The absolute number of CMPs and GMPs did not alter as a result of infection (Figure 3.8f).

In the infected spleen, there was an increase in multipotent progenitors, with the peak fold increase at day 28 p.i., following the same pattern observed in BM (Figure 3.9c; Figure 3.9d). At day 28 p.i., the frequency of LSK CD150⁺ Flt3⁻ CD34⁻ cells was 1051.128 ± 228.787 fold and LSK CD150⁺ Flt3⁻ CD34⁺ cells was 46.470 ± 8.165 fold increased in infected mice, their frequencies remained high at the latest time point (Figure 3.9c). In early time points, we could not detect LSK CD150⁻ Flt3⁺ CD34⁺ cells in the spleen of infected or naive mice, but at day 28 p.i. the frequency of LSK CD150⁻ Flt3⁺ CD34⁺ cells was increased 11.777 ± 3.863 fold, while at day 64 p.i. it was comparable to naive controls (Figure 3.9c). This pattern was repeated in terms of absolute numbers for multipotent progenitors in the spleen (Figure 3.9d). For lineage-committed precursors in the spleen, MEPs increased 16.353 ± 4.63 fold at day 28 p.i., remaining high at day 64 p.i.. The frequency of CMPs in infected mice was not significantly different at any evaluated time point. The frequency of GMPs increased 3.451 ± 0.188 fold on day 64 p.i., while CLPs were reduced (0.455 ± 0.080 fold) at this time point (Figure 3.9e). Absolute cell numbers showed a

similar trend for GMPs and MEPs. However, the number of CMPs was 5.105 ± 1.814 and 7.216 ± 1.533 fold increased in infected, at days 28 and 64, respectively. The number of CLPs was not significantly changed in the spleen of infected mice at all time points (Figure 3.9f).

In spite of the significant changes in the number of multipotent progenitors, the overall number of total cells in BM remained relatively unchanged in mice infected with *L. donovani* over a period 64 days (Figure 3.7a). In contrast, the increased number of HSPCs in the spleen coincided with increased cellularity over time (Figure 3.7b).

Overall, these data showed a significant increase in the number of multipotent precursors both in BM and spleen, during the course of infection that was most evident at day 28, overlapping with the peak of parasite burden both in the spleen and in the BM. At day 28, the extent of increase in non-committed progenitors was not reproduced in the degree of alterations in the lineage-committed progenitors both in BM and in the spleen. This suggested the possibility of inhibition in HSPCs differentiation and that the expansion/accumulation of multipotent progenitors might not be underlying an increase in effective haematopoiesis, during the chronic phase of infection, previously defined as the stage of infection when pathological remodeling of lymphoid tissue becomes prominent i.e. post d21 (C. R. Engwerda *et al.*, 2004a) (28 and 64 days p.i.).

In further analysis, we focused on day 28 p.i., where both the parasite burden and altered cellularity were most striking.

3.2.2 Experimental VL was characterized by increased numbers of primitive haematopoietic progenitors

To confirm changes in BM HSPCs at day 28 p.i., further independent experiments were conducted. In the BM of the infected mice the frequency of LSK cells increased approx. 10-fold and the absolute number increased approx. 8 fold compared to naive mice (Figure 3.10a).

Next we focused in the most immature haematopoietic progenitors, which are contained within the LSK population. The frequency and number of LSK Flt3⁻ CD150⁺ CD34⁻ cells was significantly increased in the mice infected with *L. donovani* (Figure 3.10a; Figure 3.10b).

LSK Flt3⁻ CD150⁺ CD34⁺ cells and LSK Flt3⁺ CD150⁻ CD34⁺ cells were also increased in both frequency and number in infected mice (Figure 3.10a; Figure 3.10b). These results also indicate that among early progenitors considered in these analyses, LSK Flt3⁻ CD150⁺ CD34⁻ cells were the largest contributor to the observed increase in total LSK cells.

For Lineage⁻ cKit⁺ cells, which are enriched for all HSPCs, there was a significant though modest increase in frequency ($3.35\% \pm 0.52$ vs. $2.30\% \pm 0.53$ in day 28 infected and control mice respectively) (Figure 3.10c) although absolute number was unchanged (Figure 3.10d). The frequency and absolute number of CMPs, GMPs and MEPs in the BM of infected mice were not significantly different from naive controls. CLPs frequency was found slightly increased in infected mice, but the absolute cell number was not significantly change upon infection (Figure 3.10c; Figure 3.10d).

In summary, these independent experiments confirmed our initial observations (Figure 3.8) pointing to significant differences in BM cellularity at 28 day of *L. donovani* infection. These alterations were characterized by a large increase in the number of early multipotent progenitors, suggesting that haematopoiesis was significantly modulated at the peak of *L. donovani* infection.

3.2.3 Experimental VL is characterized by alterations in blood homeostasis

In order to determine if the aforementioned alterations in the BM (section 3.2.2) were accompanied by alterations in the blood, we performed a completed blood count, hemogram, as a broad screening test to assess for haematological disorders at day 28 p.i.

In infected mice we found that the number of erythrocytes (red blood cells) were significantly decreased, 5.84×10^6 (M)/ $\mu\text{l} \pm 0.61$ ($\bar{x} \pm \text{SD}$), compared to the basal values obtained in naive controls, $7.69 \text{ K}/\mu\text{l} \pm 0.85$ (Figure 3.11a). Haematocrit, which indicates the percentage of volume occupied by red blood cells in a given volume of whole blood, was also significantly lower in infected mice ($31.46\% \pm 3.11$) in comparison to naive controls ($40.20\% \pm 4.86$) (Figure 3.11b). The other parameter assessed was the concentration of hemoglobin in PB, which in line with the others parameters was also found decreased in infected mice ($6.93 \text{ g/dl} \pm 0.77$) compared to the values determined for controls ($8.50 \text{ g/dl} \pm 1.31$) (Figure 3.11c).

The number of platelets in circulation in infected mice was also significantly lower in infected mice ($246.1\text{K}/\mu\text{l} \pm 61.87$) when compared to the number of platelets found in healthy controls ($435.6 \text{ K}/\mu\text{l} \pm 187.7$) (Figure 3.11d). The number of total leukocytes (or white blood cells) in PB in infected mice and controls was comparable. However, when we analyzed the number of leukocytes segregated into different cell types we found significant differences between infected and non-infected mice. In infected mice the number of neutrophils was increased, while the number of basophils and eosinophils contracted (Figure 3.11e).

In summary, these analyses indicate that anaemia, thrombocytopenia, coupled with mild neutrophilia and basopenia / eosinopenia, emerge in B6 mice as a consequence of *L. donovani* infection.

3.2.4 *L. donovani* infection was not associated with increased cell death in BM

Pro-inflammatory cytokines commonly released in response to infection have the potential to induce increased cell-death in BM (C. Selleri *et al.*, 1995, K. Y. King and M. A. Goodell, 2011). We observed that during the peak of infection with *L. donovani* there was a specific increase in early non-committed progenitors, however infected mice displayed anaemia and thrombocytopenia. It was conceivable that an increase susceptibility to cell death of haematopoietic progenitors was on the basis these alterations; as such, the proportion of live/viable cells, excluding both dead and apoptotic cells was assessed, in BM cells from mice infected with *L. donovani* for 28 days (Figure 3.12a).

The analysis performed in BM to determine the proportion of live cells among stromal cells (CD45⁻ Lineage⁻ cells) and mature haematopoietic cells (CD45⁺ Lineage⁺ cells) revealed that there were no differences between infected and healthy controls (Figure 3.12b). Surprisingly across all the populations of HSPCs assessed, we found that infected mice showed a significant increase in the fraction of live cells (i.e. neither dead nor apoptotic) (Figure 3.12b).

Hence, increased cell death and apoptosis in BM could be excluded as a mechanism underlying the establishment of impaired haematopoietic function in PB. Collectively, these findings raised the possibility that infection could induce changes in haematopoietic differentiation prior to lineage commitment. Therefore, we decided to study in further detail the phenotypic and functional alterations in early haematopoietic progenitors.

3.2.5 HSPCs from infected mice showed impaired engraftment in BM and decreased reconstitution of the periphery

To evaluate whether *L. donovani* infection affected the function of HSPCs, we used a competitive adoptive transfer model. BM lineage negative cells (enriched for HSPCs) from day 28 infected B6.CD45.2 mice and from uninfected B6.CD45.1 mice were mixed 50:50 and transferred into non-infected x-irradiated (B6.CD45.1 x B6.CD45.2)F₁ recipients. By using donor cells expressing distinct CD45 isoforms, we could follow the fate of the transferred cells in recipient mice and separate these from any cells not eliminated by irradiation (which co-express CD45.1 and CD45.2). Analyses were performed seven weeks after adoptive transfer (Figure 3.13a).

The contribution to haematopoiesis was significantly different between the donor populations, with infected donor-derived cells accounting for $21.81\% \pm 11.27$ in comparison to $78.19\% \pm 11.27$ of naive donor-derived cells amongst total donor cells in the BM of recipient mice (Figure 3.13b). In the spleen, the results followed the same trend, with infected donor cells contributing for $24.76\% \pm 2.43$ of total splenocytes while naive donor cells comprised $75.24\% \pm 2.43$ of total donor-derived splenocytes (Figure 3.13b).

To assess whether *L. donovani* infection could impact on the differentiation potential of HSPCs, the frequencies of terminally differentiated blood cells were determined in the spleen (here representing the periphery). There were no significant differences found in the frequencies of B cells, T cells and CD11b⁺ cells (Myeloid cells) arising from infected and naive donor cells (Figure 3.13c). In the BM of recipient mice, we assessed the frequency of the multipotent progenitors, LSK CD150⁺ Flt3⁻ CD34⁻ cells, LSK CD150⁺ Flt3⁻ CD34⁺ cells and LSK CD150⁻ Flt3⁺ CD34⁺ cells (Figure 3.13d) and the lineage committed precursors, CMPs, GMPs, MEPs and CLPs (Figure 3.13e), within the two groups of donor cells. No significant differences were determined in their frequencies between infected and naive derived donor cells.

Collectively, these data suggested that infection is impacting negatively on the reconstitution potential of HSPCs, both in BM and spleen, where the frequency of infected donor cells, in both sites, was significantly lower compare to naive donor cells. Despite the overall lower frequency of infected donor cells, the infection did not promote alterations in cell fate, since no changes were detected in the relative proportion of different progeny when transferred to a healthy recipient. Hence, infection may result in cell intrinsic functional impairment of HSCs prior to lineage commitment.

3.2.6 *L. donovani* infection stimulates expansion of LSK CD150⁺ CD34⁻ expressing CD48

CD48 is a GPI-linked member of the signaling lymphocyte activation molecule (SLAM) family broadly expressed on haematopoietic cells except for LT-HSCs (M. J. Kiel *et al.*, 2005). It acts as ligand for 2B4 receptor expressed in T and NK cells and has been implicated in cell activation, proliferation and differentiation (M. Elishmereni and F. Levi-Schaffer, 2011).

The frequency and the number LSK CD150⁺ CD34⁻ cells (enriched for LT-HSCs) not expressing CD48 were unchanged upon infection with *L. donovani* (Figure 3.14a; Figure 3.14b). In contrast, the frequency and absolute number of LSK CD150⁺ CD34⁻ CD48⁺ cells were significantly increased in the BM of infected mice compared to the controls (Figure 3.14a; Figure 3.14b).

Whereas at steady-state the vast majority of LT-HSCs, as defined so far (LSK CD150⁺ CD34⁻ cells) lacked CD48, upon infection less than 5% of phenotypic LT-HSCs were CD48 negative (Figure 3.14c; Figure 3.14d). Hence, these data suggested that during infection phenotypic LT-HSCs population have progressed further in their differentiation, since CD48 expression is associated to a loss of stemness (M. J. Kiel *et al.*, 2005, M. J. Nemeth and D. M. Bodine, 2007).

3.2.7 *L. donovani* infection was associated with depletion of the reservoir of quiescent LT-HSCs

LT-HSCs are largely in G0 or G1 and it has been shown that the quiescent state is functionally important. Studies in experimental models characterized by increased proliferation of multipotent progenitors reported loss of LT-HSCs and increased susceptibility to stress-induced haematopoietic exhaustion (K. W. Orford and D. T. Scadden, 2008). In order to shed some light into the mechanisms responsible for the increase in the most immature haematopoietic precursors and loss of reconstitution potential, we determined the frequency and number of HSCs in G0, by staining for Ki67, an antigen expressed in all phases of the cell-cycle, but absent in quiescent or resting cells (J. Gerdes *et al.*, 1984).

Within the population of LSK CD150⁺ CD34⁻ CD48⁻ cells (enriched for LT-HSCs) approximately half were quiescent (43.05 ± 0.017 expressing Ki67) in steady-state. At day 28 p.i., the frequency of cells that progressed into cell-cycle was significantly increased ($96.52\% \pm 3.19$ of total LSK CD150⁺ CD34⁻ CD48⁻ cells). On the other hand, onward populations of multipotent progenitors, namely LSK CD150⁺ CD34⁻ CD48⁺ cells and LSK CD150⁺ CD34⁺ cells were highly proliferative both in steady-state and upon infection, with more than 90% expressing Ki67 (Figure 3.15a).

The absolute number of cells in proliferation showed that the overall increase of multipotent progenitors was due to the increase in the number of LSK CD150⁺ CD34⁻ CD48⁺ Ki67⁺ cells and LSK CD150⁺ CD34⁺ Ki67⁺ cells in infected mice (90 fold and 4.8 fold, respectively, increased compared to naive mice) (Figure 3.15b). The number of LSK CD150⁺ CD34⁻ CD48⁻ Ki67⁺ cells (enriched for LT-HSCs) although significantly altered in infected compared to naive mice, was increased to a lesser extent in comparison with the other populations assessed (1.5 fold increased in infected mice; Figure 3.15b).

These results showed that the upregulation of CD48 in HSCs (see section 3.2.6, above) was associated with the progression into active cell-cycle, with almost all the CD48 positive cells also expressing Ki67, both in non-infected and infected mice. Furthermore, the loss of LSK CD150⁺ CD34⁻ CD48⁻ Ki67⁻ cells (enriched for quiescent LT-HSCs) during infection represents a 24 fold decrease in the number (from 831 ± 0.017 to only 34.62 ± 31.93 cells in total BM) of this already

very rare cell population (Figure 3.15c; Figure 3.15d). This alteration may account for the loss of reconstitution efficiency of HSPCs in adoptive transfer, suggesting that proliferation may be depleting the reservoir of HSCs with long-term reconstitute potential.

3.2.8 LSK CD34⁻ CD150⁺ CD48⁻ cells were functionally impaired during chronic infection with *L. donovani*

Mice chronically infected with *L. donovani* showed alterations in HSCs proliferative status that may reflect impairment in the mechanisms regulating proliferation. It has been shown that quiescence is inherently related to the ability of HSCs to achieve long-term reconstitution of the haematopoietic system in lethally irradiated recipient mice (A. Nakamura-Ishizu *et al.*, 2014). Therefore loss of quiescence during *L. donovani* infection may account for loss of HSCs function (i.e. long-term multilineage reconstitution and self-renewal).

To test this hypothesis, we performed long-term non-competitive adoptive transfer of LSK CD150⁺ CD34⁻ CD48⁻ cells (enriched for LT-HSCs) from CD45.2 naive or infected mice into naive CD45.1 recipients (Figure 3.16a). Donor mice belonged to a congenic mouse strain expressing the same allelic variant of CD45 (CD45.2), excluding the impact of subtle functional differences of CD45.1 and CD45.2 in their efficiency to reconstitute the haematopoietic system following transplant into lethally irradiated recipients (S. Basu *et al.*, 2013).

LSK CD150⁺ CD34⁻ CD48⁻ cells (enriched for LT-HSCs) from infected mice in comparison to naive donor cells were less efficient in their ability to reconstitute the haematopoietic system of lethally irradiated recipient mice. The contribution of donor HSCs from infected mice showed a trend towards being lower both in BM (51.60% ± 22.95 vs. 21.17% ± 27.68, for naive and infected mice, respectively) and in the spleen (32.30% ± 16.76 vs. 10.81% ± 18.75, for naive and infected mice, respectively). However, the large variation within groups prevented this being significantly different (Figure 3.16b).

The number of BM cells derived from naive mice ($2.72 \times 10^7 \pm 1.41 \times 10^7$) was significantly greater than those derived from infected donor cells ($6.95 \times 10^6 \pm 7.89 \times 10^6$). In the spleen, one sample could not be used to perform absolute quantification due to technical problems. In the spleen the number of cells derived from infected donor was on average 3.4 fold decreased compared to the number of cells recovered from naive donor in the recipient mice (Figure 3.16c).

In infected mice, the frequencies of HSPCs derived from naive and infected mice donor cells were comparable in the BM of recipient mice, except for LSK CD150⁺ FLT3⁻ CD34⁻ cells (enriched for

LT-HSCs). The frequency of these most immature progenitors was significantly higher within naive donor cells suggesting that HSCs from infected mice were less efficient in their ability to reconstitute the rare pool of HSCs (i.e. loss of self-renewal potential; Figure 3.16d).

In spleen, here representing the periphery, we could not detect any alteration in the distribution mature cells derived from infected compared to naive donor cells; we detected an overall decrease in all populations in mice receiving HSCs from infected mice, but not a lineage bias toward any cell population (Figure 3.16e).

To further investigate the long-term reconstituting potential and to more accurately evaluate the reduction in functional capacity of HSCs from infected mice, we transferred a reduced number of LSK CD150⁺ CD34⁻ CD48⁻ cells (enriched for LT-HSCs) that were isolated from the primary adoptive transfer recipients into secondary recipients. Once again, we used different CD45 isoforms expressed in donor and recipient cells to track the progeny of transferred cells (Figure 3.17a).

Unfortunately one of the mixed BM chimeric died leaving us with small number of samples in the group receiving cells primarily derived from infected donors, further the variation within groups was very high. Nevertheless the results were suggestive of further functional impairment in HSCs primarily derived from infected donors, in the secondary adoptive transfers. Regarding cells derived from infected mice, we could detect infected donor cells in the BM of two out of three recipients, and in the spleen of one out of three recipients, whereas donor cells derived from HSCs isolated from naive mice were detected in the BM and spleen of 4/4 recipients of HSCs from naive mice (Figure 3.17b).

Furthermore, in one of the recipient mice receiving HSCs isolated from infected donor we were unable to detect any LSK cells, and in the remaining two recipients the numbers of total progenitors was on average less than 30 cells (Figure 3.17c). Furthermore, in only one recipient receiving cells derived from infected donors, were Lin⁻ cKit^{hi} cells (enriched for lineage-committed progenitors) detected in BM (Figure 3.17d). However, in all secondary recipient mice transplanted with HSCs isolated from non-infected mice we could detect donor HSPCs for the three lineages in BM of recipient mice (Figure 3.17c; Figure 3.17d).

In summary, these data show that following an overall period of 40 weeks of transfer into healthy recipients, LSK CD150⁺ CD34⁻ CD48⁻ cells derived from naive donors were capable of self-renewal and of giving rise to all lineages (hallmarks of stemness). In secondary recipient mice, 2316 ± 3472 LSK CD150⁺ CD34⁻ CD48⁻ cells derived from the original naive donor were present in total BM. In contrast, in the only secondary recipient where LSK CD150⁺ CD34⁻ CD48⁻ cells

could be found that originated from HSCs derived from infected mice, only 16 LSK CD150⁺ CD34⁻ CD48⁻ cells were present (Figure 3.17c). Similarly, in all recipient mice transplanted with HSCs originating from non-infected mice we could consistently detect mature progeny in both the lymphoid and myeloid lineages, whereas among recipient receiving HSCs originating from infected mice we could only detect very low numbers of mature cells in the spleen of one out of three recipient mice (Figure 3.17e). Collectively, these data suggested that HSCs from infected mice show intrinsic long-term functional impairment, linked to alterations in cell-cycle regulation.

3.2.9 Alteration in expression of transcription factors associated with cell-cycle regulation of HSCs during *L. donovani* infection

3.2.9.1 LSK CD150⁺ CD34⁻ CD48⁻ cells (enriched for LT-HSCs) in infected mice expressed of β -catenin at increased levels

It has been showed that wingless and int (Wnt) signaling is required for the adequate function of HSCs using several gain and loss-of-functions approaches. However the results from different studies aimed at clarifying its role in HSCs self-renewal were conflicting (P. Kirstetter *et al.*, 2006, T. C. Luis *et al.*, 2010a, C. J. Cain and J. O. Manilay, 2013). More recently experiments using different combinations of APC (Adenomatous polyposis coli gene) mutants have shown that mild increases (about 2 fold) in Wnt signaling enhanced HSC function, while impaired HSC repopulation capacity was associated with intermediate and higher levels of activation of the Wnt signaling pathway (T. C. Luis *et al.*, 2011).

In order to assess if a higher degree of activation of Wnt canonical signal was associated with the alterations observed in HSCs during infection with *L. donovani*, we used intracellular flow cytometry to assess the relative accumulation of β -catenin in multipotent progenitors in naive and day 28 infected mice. The relative amount of β -catenin protein in multipotent progenitors was determined by the fold change in Mean Intensity Fluorescence (MFI), since we found β -catenin to be expressed in all multipotent progenitors (Figure 3.18a). We observed a significant increase in β -catenin protein detected in LSK CD150⁺ CD34⁻ CD48⁻ cells (enriched for LT-HSCs), LSK CD150⁺ CD34⁻ CD48⁺ cells and LSK CD150⁺ CD34⁺ cells in the BM of infected mice (1.41 ± 0.39 fold, $1.49 \text{ fold} \pm 0.45$ and 1.33 ± 0.24 fold, respectively in infected compared to naive mice; Figure 3.18b).

Wnt3a, the prototypical Wnt ligand for the canonical pathway, has been suggested to play an important role in activation of HSCs that express its cognate receptors (R. Sugimura *et al.*, 2012). Therefore, we next assessed expression of Wnt3a, using flow cytometry to detect intracellular

expression in cells treated with brefeldin A prior to staining, to promote Wnt3a intracellular accumulation.

Across all the populations assessed in BM, we could not detect a significant increase in the frequency of cells expressing Wnt3a during infection (Figure 3.19a; Figure 3.19d). However, when we evaluated the amount of Wnt3a expressed in each cell population significant alterations were detected. In infected mice, mature haematopoietic cells (CD45⁺ Lin⁺ cells) expressed higher levels of Wnt3a as assessed by the MFI, than naive mice (Figure 3.19b; Figure 3.19c). A significant increase in Wnt3a expression, following *L. donovani* infection, was also determined in LSK CD150⁺ CD48⁻ cells (enriched for LT-HSCs) displaying a 1.5 fold increase in Wnt3a expression (Figure 3.19b; Figure 3.19c).

Thus, we assessed if *Wnt3a* mRNA accumulation was altered in total BM in infected mice compared to naive mice. Contrary to protein expression, the Wnt3a mRNA accumulation was decreased in total BM cells from infected mice (Figure 3.20), suggesting that level of Wnt3a could be controlled by post-transcriptional mechanisms.

Overall these findings suggested that alterations in BM during infection with *L. donovani* were associated with enhanced activation of Wnt canonical pathway in haematopoietic progenitors that may be supported by an increase availability of Wnt3a in BM stem cells niche, as well as by increased autocrine Wnt3a signaling in LT-HSCs.

3.2.9.2 LSK CD150⁺ CD34⁻ CD48⁻ cells (LT-HSCs) in infected mice have increased expression of the transcription factor c-Myc

The *Myc* proto-oncogene has been described as a central transcription factor in haematopoiesis, and is expressed in all haematopoietic progenitors. Mice deficient for *Myc* die before birth and it is believed that defects in the haematopoietic system development are the basis of embryonic lethality (M. D. Delgado and J. Leon, 2010). This hypothesis was confirmed by observing the marked haematological changes associated with conditional *Myc* deletion, in MxCre;*c-myc*^{fllox/fllox} mice (A. Wilson *et al.*, 2004). These studies also suggested that *Myc* participates in the regulation of HSCs self-renewal and differentiation through the regulation of adhesion molecules expression, notably CD29 (A. Wilson *et al.*, 2004).

The HSCs phenotype we observed during *L. donovani* infection shared many features that have been reported in mice following conditional ablation of *Myc* (A. Wilson *et al.*, 2004). Therefore, we next assessed the expression of c-Myc in HSCs. c-Myc protein is difficult to detect by direct antibody staining. Therefore we transferred total BM cells from *c-Myc-Egfp* mice, expressing

EGFP under the control of the *c-Myc* endogenous promoter, into lethally irradiated recipients. After a period of ten weeks, these mice were infected with *L. donovani* and HSPCs phenotype examined at day 28 p.i., using intracellular flow cytometry to detect the EGFP tag. In infected mice, LSK CD150⁺ CD48⁻ cells (enriched for LT-HSCs) expressed more c-Myc compared to naive mice, and the same trend was observed in LSK CD150⁺ CD48⁺ cell (Figure 3.21). We also assessed the level of CD29 protein expression in haematopoietic multipotent progenitors including HSCs, but we could not determine any significant differences between naive controls and mice infected mice (Figure 3.22). In summary, although we identified an increase in the expression c-Myc in LT-HSCs isolated from *L. donovani* infected mice, this was not coupled to a detectable change in expression of the adhesion molecule CD29.

3.2.9.3 LSK CD150⁺ CD48⁻ cells (enriched for LT-HSCs) in infected mice have increased expression of the transcription factor GATA-3

The transcription factor GATA-3 is expressed in various haematopoietic progenitor populations in BM, with HSCs expressing the highest levels of GATA-3 (C.-J. Ku *et al.*, 2012). Recent studies have suggested that GATA-3 is important in the regulation of HSCs proliferative status and self-renewal potential during stress-induced haematopoiesis (C.-J. Ku *et al.*, 2012, C. Frelin *et al.*, 2013). For example, in GATA-3 KO mice the deleterious impact of Poly:IC challenge on HSCs function could be prevented (C.-J. Ku *et al.*, 2012, C. Frelin *et al.*, 2013). We observed that during *L. donovani* infection the number of HSCs in active cell-cycle increased with concomitant loss of quiescent cells, suggesting an alteration in the regulation of cell-cycle, which prompted us to investigate intracellular expression of GATA-3 in HSPCs.

We first observed that neither the frequency of mature haematopoietic cells nor the frequency of total HSPCs (enriched in Lin⁻ cKit⁺ cells) expressing GATA-3 was altered by the infection (Figure 3.23a). Upregulation of GATA-3 expression in BM was restricted to the most immature cells contained in the LSK CD150⁺ cells compartment (Figure 3.23a; Figure 3.23c). The frequency LSK CD150⁺ CD48⁻ cells (enriched for LT-HSCs) expressing GATA-3 was 48.93% ± 21.11 in infected mice compared to 21.31% ± 13.61 in naive controls (Figure 3.23a). Within LSK CD150⁺ CD48⁺ cells (other multipotent progenitors) the increase in cells expressing this transcription factor was also significant in BM of infected mice compared to naive mice (54.82% ± 27.80 vs. 79.15% ± 9.47) (Figure 3.23a; Figure 3.23c). This increase in very immature cells expressing GATA-3 was concomitant with a 1.22 ± 0.19 fold increase in the amount of GATA-3 expressed in LSK CD150⁺ CD48⁻ GATA-3⁺ cells, and a 1.29 ± 0.16 increase in LSK CD150⁺ CD48⁺ GATA-3⁺ cells in infected compared to naive controls, as assessed by the fold change in MFI (Figure 3.23b).

We next sought to determine whether the expression of GATA-3 could be related to the proliferative state of LSK CD150⁺ CD48⁻ cells (enriched LT-HSCs). In infected mice, a significant alteration in the distribution of LSK CD150⁺ CD48⁻ cells segregated according with the expression of GATA-3 and Ki67 was observed (Figure 3.24).

In fact, we observed that the expression of this transcriptional factor was almost absent in cells in G0 (Ki67⁻ cells). In naive mice, 43.24% ± 5.69 of LSK CD150⁺ CD48⁻ cells were Ki67⁻ GATA-3⁻, but following infection there was a significant decrease in cells falling in this group (5.20% ± 5.31). Also, concomitant with chronic infection, we observed a significant increase in LSK CD150⁺ CD48⁻ cells expressing Ki67 and GATA-3 (17.64 ± 11.23 vs. 46.68 ± 21.66, in naive and infected, respectively), while in steady-state the majority of LSK CD150⁺ CD48⁻ cells in cycle were GATA-3 negative (Figure 3.25).

These data demonstrate that GATA-3 expression was up-regulated in LSK CD150⁺ CD48⁻ cells (enriched LT-HSCs) during induced haematopoiesis following *L. donovani* infection. As such, GATA-3 over expression due to inflammation may represent a mechanism for impaired maintenance of homeostatic numbers of LT-HSCs in quiescence, during *L. donovani* chronic infection.

It is known that upon poly I:C treatment, GATA-3 re-locates to the nucleus in proliferating HSCs and restricts these cells to short-term multilineage reconstitution, however after the removal of proliferative stimulus, GATA-3 returns to the cytoplasm and long-term lineage reconstitution is restored (C. Frelin *et al.*, 2013). We therefore attempted to determine the subcellular localization of GATA-3 in HSCs in infected vs. naive mice. We optimized protocols for sort purification of HSCs and for imaging GATA-3 expression by confocal microscopy, using thymocytes in suspension as a positive control (Figure 3.26). Despite our efforts in sorted LSK we were unable to obtain a reliable staining (Figure 3.27).

3.3 DISCUSSION

VL in humans and animal models is associated with significant changes in haematological function, and parasite persistence in BM is well characterized (G. E. Cartwright *et al.*, 1948, S. E. J. Cotterell *et al.*, 2000a, N. Varma and S. Naseem, 2010, W. P. Lafuse *et al.*, 2013, F. A. d. Pinho, 2015). However, very little is known about the impact of *L. donovani* infection on upstream processes underlying haematopoiesis.

In this chapter, we showed that *L. donovani* infection impacts on BM haematopoiesis. Using a panel of stem cell markers, we characterized murine HSPCs in the BM over the course of *L. donovani*-infection in B6 mice. At the peak of infection, mice showed a significant increase in intermediary non-committed multipotent haematopoietic precursors (LSK CD150⁺ CD34⁻ CD48⁺ cells and LSK CD150⁺ CD34⁺ cells) without reciprocal increases in either lineage-committed precursors or mature cells in circulation. In the steady-state, the majority of LT-HSCs (LSK CD150⁺ CD34⁻ CD48⁻ cells) were quiescent, representing cells with the highest degree of reconstitution potential. In contrast, during infection most were found to have progressed to cell-cycle and this correlated with a reduced potential to engraft into syngeneic recipients. The functional alterations in proliferative LT-HSCs were associated with the upregulation of the co-activator surface molecule CD48 and the transcription factors GATA-3 and β -catenin.

In the only work that previously characterized the alteration in haematopoiesis in experimental VL, it was shown that following infection with *L. donovani* myelopoiesis was increased, both in BM and in the spleen. This study by Cotterell and colleagues used an assay of colony-forming precursors and progenitors to determine the association between *L. donovani* parasite burdens and changes in haematopoietic activity. They showed that the frequency of all progenitor cells from the BM increased during the course of *L. donovani* infection; while in the spleen there was a specific increase in GM-CFU. These correlate with the increase in parasite burden both in the BM and the spleen. Furthermore, the proportion of progenitors in S phase in both the spleen and BM increased, indicating a higher level of proliferation, during chronic infection. Additionally, it was found that there is greater accumulation of mRNA for the growth factors G-CSF, M-CSF, and GM-CSF in the BM during chronic phase of infection (S. E. J. Cotterell *et al.*, 2000a).

This study was performed in BALB/c while our model of experimental VL was established in B6 mice. The outcome of *L. donovani* infection varies considerably among mouse strains, for example BALB/c genetic background was associated to an impaired clearance of parasites from the liver compared to B6 mice (M. Lipoldova and P. Demant, 2006). Therefore, we decided to characterize the kinetics of alterations in HSPCs and parasite burden during the course of infection in B6 mice.

Instead of CFU assays, we chose to characterize HSPCs (LT-HSCs, ST-HSCs, MPPs, CMPs, GMPs, MEPs and CLPs), as defined previously (M. Kondo *et al.*, 2003a, J. L. Granick *et al.*, 2012) according with their pattern of surface markers expression using flow cytometry, directly *ex vivo*. More, although short-term cultures are very useful to study lineage-committed progenitor cells that differentiate in less than 3 weeks, they are unable to quantify more primitive progenitors that require longer culture periods to produce mature cells (L. Coulombel, 2004). On the other hand, the usage of long-term cultures could overcome this limitation, but the growth factors required for HSCs and immediate progeny culture are not well established and may, therefore, impact in the differentiation process (L. Coulombel, 2004).

In steady-state, the LSK cell population contains the most immature non-committed progenitors, conventionally called haematopoietic progenitor cells (HPCs) (K. Y. King and M. A. Goodell, 2011), whereas lineage-committed progenitors are contained in the Lineage⁻ Sca1⁻ cKit⁺ cells (cKit^{hi} cells; Figure 3.2) (M. Kondo *et al.*, 2003a). In adults, Sca1 expression is mainly restricted to non-committed progenitors but its expression may be induced in other cells by Interferon Type I and II, TNF and IL-1, commonly found present at increased levels at sites of infections (A. Sinclair *et al.*, 1996, S. Maltby *et al.*, 2014). It has also been shown in a wide range of infection models that Sca1 expression is upregulated in all HSPCs. Likewise upon an infection; the immune-phenotypically defined LSK fraction may contain functional lineage-committed progenitors (N. N. Belyaev *et al.*, 2010, M. B. Buechler *et al.*, 2013, E. M. Pietras *et al.*, 2014). During the course of infection we observed the expansion of the LSK compartment concomitant with the contraction in Lineage⁻ Sca1⁻ cKit⁺ cell number. Taking in account the above findings, we included Lineage⁻ cKit⁺ Sca1^{+/-} cells in the process of selecting for lineage-committed progenitors in addition to the other defined cell surface markers.

In B6 mice, contrary to BALB/c mice, the peak parasite burden was reached at day 28 p.i. and by day 64 the number of parasites in the BM and spleen were very low, although the splenomegaly was maintained indicating that inflammation persisted. Another difference related to the number of myeloid progenitors in BM that, except for MEPs, were not significantly increased (S. E. J. Cotterell *et al.*, 2000a). Over 64 days following infection the number multipotent progenitors, namely LSK CD150⁺ Flt3⁻ CD34⁻ cells and LSK CD150⁺ Flt3⁻ CD34⁺ cells increased steadily, and their number remained high even at the latest time point, when the parasite burden was minimal in BM and in the spleen. The number of multipotent progenitors was increased in the spleen at later time points, as well as, CMPs and MEPs.

The detection of HSPCs in increased number in the spleen has been described in other models of infection (K. C. MacNamara *et al.*, 2009, M. T. Baldrige *et al.*, 2010). HSCs survey the periphery and have the potential to seed and originate myeloid immune cells in extramedullary

tissues. It was suggested that during infection migratory HSCs may function as a prompt provider of progenitors that expand *in situ* and give rise to myeloid effector cells (S. Massberg *et al.*, 2007). In the spleen of mice infected with *L. donovani* the frequencies of macrophages and dendritic cells (DCs) are found increased (J. E. Dalton *et al.*, 2010). Most likely, the increase in HSPCs that occurs during infection may result from non-exclusive phenomena such as alteration in the egress of HSCs from BM, splenic sequestration and subsequent expansion and differentiation *in loco*.

Dramatic increases in LSK CD150⁺ Flt3⁻ CD34⁻ cells and LSK CD150⁺ Flt3⁻ CD34⁺ cells in BM were observed at day 28 p.i. that was highly consistent across multiple experiments. Yet the number of lineage-committed progenitors remained at basal values, providing the first evidence for a block in HSPCs progression.

The expansion of HSCs and/or onward multipotent progenitors has been described in a wide range of experimental models of infections (S. Rodriguez *et al.*, 2009, M. T. Baldrige *et al.*, 2010, K. C. MacNamara *et al.*, 2011a, S. Maltby *et al.*, 2014). The acute model of respiratory infection (pneumonia virus of mice) provides an example of the impact of a localized infection on alterations in haematopoiesis. In mice infected with pneumonia virus of mice (PMV), the fraction of LSK cells and LT-HSCs (LSK CD150⁺ CD48⁻ cells) expanded in BM, while the number of granulocytes was found greatly increased in peripheral blood (S. Maltby *et al.*, 2014). In the present study, we observed expansion of LT-HSCs (LSK CD150⁺ Flt3⁻ CD34⁻ cells) in BM of *L. donovani* infected mice, but only a modest neutrophilia was observed.

In a model of sepsis, an increase in the number of LSK cells, as well as LT-HSCs (LSK Flt3⁻ CD34⁻ cells) and MPPs (LSK Flt3⁺CD34⁺ cells) was observed following inoculation with a virulent *Pseudomonas aeruginosa* strain. These mice displayed severe neutropenia that was partially explained by a block in differentiation of MPPs to myeloid lineage-committed progenitors. CMPs and GMPs were found at very decreased number in BM and expressed less lysozyme compared to controls, an indication of delayed maturation (S. Rodriguez *et al.*, 2009).

The accumulation of immunophenotypic LT-HSCs (characterized as LSK CD150⁺ Flt3⁻ cells) was reported in the BM in other models of acute infection (P. O. Scumpia *et al.*, 2010, K. C. MacNamara *et al.*, 2011a). In mice inoculated with *Ehrlichia muris*, it was reported that an accumulation of LT-HSCs and loss of functional myeloid committed progenitors occurred in BM (K. C. MacNamara *et al.*, 2011a). Furthermore, similarly to our model, mice infected with *E. muris* displayed splenomegaly, thrombocytopenia and anaemia, features common to human monocytic ehrlichiosis (K. C. MacNamara *et al.*, 2009). Interestingly, in mice infected with *Ehrlichia muris* erythroid progenitors also expand in great number (defined by the expression of

CD71 and Ter119) (K. C. MacNamara *et al.*, 2009). Data from our laboratory showed that in spleens of mice infected with *L. donovani*, the number of erythroid progenitors is also greatly increased (O. Preham unpublished data). The data provided here on the number of MEPs in the spleen support the proposition that during infection the spleen becomes a site of extramedullary erythropoiesis.

Activation of multipotent progenitors toward expansion is not restricted to models of acute infection, for instance in mice, chronic systemic infection with *Mycobacterium avium* resulted in enlarged spleens, thrombocytopenia, the accumulation of immunophenotypic ST-HSC (defined as LSK Flt3⁻ CD34⁺ cells) and marginal increase in the number of LT-HSC (defined as LSK Flt3⁻ CD34⁻ cells) and MPPs (defined as LSK Flt3⁺ CD34⁺ cells) in the BM. In the spleen, the number of LT-HSCs (defined as LSK CD150⁺ cells) was also very increased in mice chronically infected, suggesting that the infection may result in the mobilization of progenitors to the periphery (M. T. Baldridge *et al.*, 2010). These findings resemble the phenotype we described in mice infected with *L. donovani* for 28 days.

The clinical symptoms vary considerably among VL patients, ranging from asymptomatic to very severe clinical symptoms, including fever, splenomegaly and hepatomegaly, cachexia, pancytopenia and hypergammaglobinemia. Anaemia is often described in association with *L. donovani* chronic infection, but there are many reports showing that other haematological alterations may emerge such as, leucopenia, thrombocytopenia, pancytopenia, haemophagocytosis and coagulation abnormalities (G. E. Cartwright *et al.*, 1948, N. Varma and S. Naseem, 2010). In addition to alterations in peripheral blood, several clinical reports describe alteration in BM cellularity; these alterations include histiocytic hyperplasia, erythroid hyperplasia, increase in the number immature forms of granulocyte and megakaryocyte (N. Yarali *et al.*, 2002, N. Varma and S. Naseem, 2010). These haematological alterations have been mainly attributed to spleen sequestration of circulating cells and ineffective haematopoiesis (G. E. Cartwright *et al.*, 1948, N. Yarali *et al.*, 2002, N. Varma and S. Naseem, 2010).

In the present study, we found that mice infected with *L. donovani* show signs of impairment of haematopoietic function, such as anaemia and thrombocytopenia.

In the experimental model of VL using Syrian golden hamsters infected with *L. donovani*, an experimental model that more resembles end stage human VL, it has been shown that chronic infection is associated with anaemia and leucopenia and increased number of erythroid progenitors both in BM and in the spleen. In hamsters, the increase in erythroid progenitors and the emergence of stress-induced erythropoiesis in the spleen was associated to the elevation in the concentration of erythropoietin in circulation, as a response to the increase cells death of BM

erythroblasts (W. P. Lafuse *et al.*, 2013). Dogs bearing natural *L. donovani* infection have also been described to have significant haematological alterations, including anaemia, thrombocytopenia and leucopenia, alongside with alteration in BM cellularity (F. A. d. Pinho, 2015).

In contrast to human disease, and that in hamsters and dogs, experimental VL in mice is not fatal and although parasites number increase in spleen and liver following infection, in the latter the infection is self-resolving with the formation of granulomas (P. M. Kaye *et al.*, 2004). Nevertheless, more recently it was reported that B6 mice chronically infected with *L. donovani* display mild pancytopenia (anemia, leucopenia and thrombocytopenia) (F. A. d. Pinho, 2015). These findings were obtained through the analysis of PB using flow cytometric approaches, and agree with results we obtained using automated method to perform PB hemogram at same time point of infection. Furthermore, in B6 mice were also described morphological alterations in BM, such as asynchronous nuclear-cytoplasmic maturation, presence of megalocytes and binucleated erythroid cells (F. A. d. Pinho, 2015). Overall these findings suggested that stress induce haematopoiesis during chronic infection with *L. donovani* may induce ineffective haematopoiesis and contribute to the (most likely multifactorial) establishment of cytopenias, in spite of the increased haematopoietic activity in BM.

In malaria infection, anaemia is a common finding and contributes very significantly to the morbidity and mortality of this parasitic infection. Its thought that on the basis of anaemia is the destruction of infected erythrocytes and changes in erythropoiesis (J. Pablo Quintero *et al.*, 2011). Alteration in haematopoietic function were also described in experimental models of disease, in which besides the establishment of anaemia were described alterations of haematopoiesis such as decreased clonogenic activity of BM cells in colony-forming assays and decreased number of phenotypic myeloid-committed progenitors in BM (N. N. Belyaev *et al.*, 2010, N. N. Belyaev *et al.*, 2013).

Expansion of the LSK compartment in the BM may be required to respond to the increase demand of immune cells during the response to an acute infection. For example, the infection with *Plasmodium chabaudi* results in the IFN γ -dependent emergence of a LSK IL7-R α ⁺ progenitor cell otherwise absent in steady-state, with the potential to produce myeloid cells that contributed to the parasite clearance (N. N. Belyaev *et al.*, 2010). In response to acute *pneumovirus* infection the expansion of LSK in BM is concomitant with the increase of functional myeloid progenitors, as determined by CFU in BM cells. In this model of infection the increase in myeloid-committed progenitors is TNF- and IFN γ -dependent, since administration of anti-TNF or anti-IFN γ prevented the increase in myeloid progenitors and lead to an increased the virus load in the lung in comparison to the controls (S. Maltby *et al.*, 2014).

However in several models of disease it was showed that the sustainment of the stress-induced haematopoiesis such as during a chronic infection might result in the functional exhaustion of HSCs (K. Y. King and M. A. Goodell, 2011, C. Mirantes *et al.*, 2014). For instance in humans, anaemia, leucopenia, or pancytopenia have been commonly described in association with chronic infectious diseases, such as HIV, atypical mycobacterial infection and viral hepatitis (A. Jain and M. Naniwadekar, 2013).

In fact, it was shown in various models of infection or following poly:IC stimulation (inducer of Interferons Type I release) that HSCs perform poorly reconstitution of the haematopoietic system when transplanted to lethally irradiated syngeneic mice (S. Rodriguez *et al.*, 2009, K. C. MacNamara *et al.*, 2011a, A. M. de Bruin *et al.*, 2013, C. Frelin *et al.*, 2013, K. A. Matatall *et al.*, 2014). As so, we hypothesized that infection with *L. donovani* resulted in the activation of HSCs followed by their functional compromise.

To evaluate if the expansion of LSK compartment accounted for functional alterations early in haematopoiesis or down the line in lineage-committed progenitors we established competitive radiation BM chimeras with equal numbers of BM Lineage⁻ cells (enriched for all HSPCs) sort-purified from naive and infected mice. In recipient mice, donor cells derived from infected mice were much less efficient in their ability to engraft in BM and reconstitute the periphery. However, in spite of the overall lower number of infected donor mice we failed to determined any lineage bias. These findings suggested that *L. donovani* infection was impacting early in haematopoiesis prior to lineage-commitment, and the increase in HSCs cell number was not associated with an increase in stem cell activity, but resulting from cell-intrinsic functional impairment of multipotent progenitors, as observed previously in several models of infection (S. Rodriguez *et al.*, 2009, K. C. MacNamara *et al.*, 2011a, A. M. de Bruin *et al.*, 2013, C. Frelin *et al.*, 2013, K. A. Matatall *et al.*, 2014).

HSCs are far from being fully characterized. The most common markers to select HSCs are LSK cells, CD34 negative/low and Flt3 negative and more recently LSK CD150 positive and CD48 negative, and it was shown that the self-renewal and reconstituting potentials of HSCs decrease as CD150 expression levels decline (G. A. Challen *et al.*, 2009). Nevertheless, the alterations in the phenotype of HSCs and MPPs in proinflammatory conditions are yet to be fully resolved (J. L. Granick *et al.*, 2012).

In the present study, the magnitude of the increase in the number of phenotypic LT-HSCs induced following *L. donovani* infection was such that it raised the possibility that LSK CD150⁺ FLt3⁻ CD34⁻ cells could no longer be true LT-HSCs. As such, we have included CD48 as an extra surface marker to select for true LT-HSCs.

CD48 expression was shown to be transiently upregulated when HSCs were stimulated to cycle by systemic administration of 5-fluorouracil (5-FU) (which promotes cell death in dividing cells), and using BMT assays it was found that the majority of HSCs with long-term potential of reconstitution were contained in the CD48 negative compartment. Furthermore, in CD48-deficient mice it was described that HSCs are more quiescent both in steady-state and upon 5-FU administration, suggesting that the repression of CD48 expression may be required to preserve the pool of LT-HSCs in G0 (M. J. Kiel *et al.*, 2005, N. C. Boles *et al.*, 2011).

In steady-state, we found that CD48 was not expressed in the vast majority of LSK CD150⁺ Flt3⁻ CD34⁻ cells but was up-regulated upon infection with *L. donovani* in the majority of phenotypic LT-HSCs. Therefore, in subsequent experiments LT-HSCs were defined as LSK CD150⁺ CD48⁻ CD34⁻ cells. In fact, when CD48 was used as an additional maker of haematopoietic differentiation, we found that the number of LT-HSCs (LSK CD150⁺ CD48⁻ CD34⁻ cells) was conserved in the BM, but this was followed by a significant increase in intermediary non-committed precursors. Similarly, in mice infected with *E. muris*, it was reported that while in steady-state the LSK CD150⁺ Flt3⁻ cells express low levels of CD48, upon infection it is almost evenly expressed at high levels in LSK CD150⁺ Flt3⁻ cells (K. C. MacNamara *et al.*, 2011a).

In the adult, LT-HSCs are mainly found in a quiescent state and the regulation of HSC quiescence/proliferation relies on cell-intrinsic and -extrinsic factors, which availability may vary considerably between homeostatic haematopoiesis and infection-induced haematopoiesis (K. Y. King and M. A. Goodell, 2011, C. Mirantes *et al.*, 2014, A. Nakamura-Ishizu *et al.*, 2014). The proliferative status of HSCs has been assessed in various models of infection. For instance, in mice infected with *Ehrlichia muris*, the number of dividing phenotypic HSCs increase almost two fold following infection (K. C. MacNamara *et al.*, 2011a). Identical alterations in HSCs cell-cycle activation were made in mice challenged with Poly:IC (C. Frelin *et al.*, 2013, D. Walter *et al.*, 2015), mice infected with *Mycobacterium avium* (M. T. Baldrige *et al.*, 2010) and mice infected with LCMV (K. A. Matatall *et al.*, 2014). In all these studies the increase in proliferative activity in HSCs correlated with loss of long-term reconstitution potential upon transplant into lethally irradiated recipients, suggesting that proliferation of HSCs under infection-induced conditions may result in cell-intrinsic functional impairment.

In line with the above studies, we also found that in steady state the majority of LSK CD150⁺ CD34⁻ CD48⁻ cells (LT- HSCs) were quiescent. However, during *L. donovani* infection the vast majority progressed into active cell-cycle, resulting in a dramatic depletion in the reservoir of quiescent LT-HSCs. On the contrary, the other populations of multipotent progenitors characterized, namely LSK CD150⁺ CD34⁺ CD48⁺ cells and LSK CD150⁺ CD34⁺, were highly proliferative both in steady-state and upon infection.

Decision making for HSC progression to active cell-cycle and subsequent decision to self-renew and/or differentiate (symmetric versus asymmetric division) is far from fully understood. However in the past decade many progresses were made to address these questions (K. W. Orford and D. T. Scadden, 2008). It is known that signaling by morphogens, such as Wnt, Notch and Hedgehog pathways have the potential to regulate entry to the G1 phase of the cell-cycle, and the presence of these morphogens was reported in stem cell niches raising the possibility that morphogen signaling prevents HSCs differentiation. In very simple lines, it was proposed that the decision towards self-renewal and/or differentiation depends on the different balances established by the availability of mitogens inducing differentiation (such as cytokines and growth factor inducing MAPK signaling) and the availability of morphogens promoting self-renewal (K. W. Orford and D. T. Scadden, 2008). Hence, it would be possible that during infection the relative abundance of pro-inflammatory mediators and growth factors could promote an “excess” of stem cell commitment that was not compensated by the mechanisms regulating quiescence and self-renewal, increasing the chances of HSCs functional exhaustion in the long-term.

It has long been postulated that the maintenance of adults stem cell quiescence is an evolutionary advantage, protecting them from genomic instability and therefore, preventing accumulation of mutations that could be perpetuated in their progeny (A. Trumpp *et al.*, 2010). Nevertheless, only recently a direct correlation was established between stress-induced haematopoiesis and the deterioration of HSCs function. In mice stimulated with Poly:IC, there is an immediate activation of LT-HSCs (LSK CD150⁺ CD34⁻ CD48⁻ cells) into active cell-cycle, and this is concomitant with the accumulation DNA double-strand breaks and single-strand breaks. Moreover, these same effects were replicated in mice stimulated with IFN- α , G-CSF, TPO or by serial bleeding, suggesting that the emergence of damages in DNA is a common result of stress-induced HSCs proliferation and may therefore, be present during infection-induced haematopoiesis (D. Walter *et al.*, 2015). The functional consequences of the accumulation of DNA damage in LT-HSCs became evident through the observation that in competitive BM transfer donor cells derived from mice subjected to extended poly:IC treatment had a two fold decrease in their repopulating activity compared to controls, 24 weeks upon transplant (D. Walter *et al.*, 2015). This work, for the first time established a direct evidence that increased proliferation of HSCs may account for accumulation of defects, that if sustained beyond the limit of repair may result in BM failure, but also provides a plausible explanation to the increased frequency of haematopoietic dysplastic cells observed in chronic VL (N. Yarali *et al.*, 2002, N. Varma and S. Naseem, 2010, G. M. de Vasconcelos *et al.*, 2014, F. A. d. Pinho, 2015).

Nowadays, it is indisputable that infection has the potential to drive proliferation with outcomes that vary considerably from pathogen to pathogen (K. Y. King and M. A. Goodell, 2011, C. Mirantes *et al.*, 2014, A. M. Prendergast and M. A. G. Essers, 2014). In our model of

experimental VL, we determined that the fraction of proliferative LT-HSCs was increased and this related to loss of potential to perform long-term haematopoietic reconstitution in healthy recipients, indicating that *L. donovani* infection led to cell-intrinsic functional impairment. Aiming to determine potential molecular targets underlying these alteration, we then evaluated the expression of several transcription factors previously determined to play important roles regulating of LT-HSCs proliferation including, β -catenin (T. C. Luis *et al.*, 2011), GATA-3 (C.-J. Ku *et al.*, 2012, C. Frelin *et al.*, 2013), and c-Myc (A. Wilson *et al.*, 2004).

Canonical Wnt signaling pathway is very important mediator of HSCs functions (T. C. Luis *et al.*, 2011, W. Lento *et al.*, 2013). For example, it was shown that Wnt3a deficient mice die around embryonic day (E) 12.5, and HSCs from fetal livers showed cell intrinsic defects, such as severely reduced reconstitutive activity (T. C. Luis *et al.*, 2009). Furthermore, in adult mice its activity seems to be very fine-tuned. Using mutant displaying Wnt signaling pathway at different levels of activation, it was shown that mild increase in Wnt signaling activation enhances HSCs function, nevertheless higher levels of activation of the Wnt signaling pathway impair HSCs repopulation capacity (T. C. Luis *et al.*, 2011).

Wnt canonical signaling is initiated when Wnt ligands engage their cognate receptor complex in the membrane of the target cell, which ultimately results in the translocation of β -catenin, a transcriptional coactivator, to the nucleus, where it binds to the classical canonical Wnt transcription factors, T-cell factor (TCF) and lymphoid enhancer binding factor (LEF) to initiate transcription of target genes. When Wnt receptors are not engaged, β -catenin is localized to the cytoplasm, and in association a destruction complex, which target β -catenin for proteasomal degradation (T. Reya and H. Clevers, 2005, C. J. Cain and J. O. Manilay, 2013). In mice expressing a stable form of β -catenin under the control of *Mx-cre*, resulting in higher expression of Wnt target genes in BM cells, signs of pancytopenia and an accumulation of granulocytic cells and immature erythroid cells in the BM were reported. Underlying these alterations was the establishment of a block in differentiation of all three lineages, expansion of LSK cells, accumulation of multipotent progenitors (LSK Flt-3⁻ CD34⁺ cells), decreased number of lineage-committed progenitors, and finally functional decline of LT-HSCs (LSK Flt-3⁻ CD34⁻ cells) which were unable to perform reconstitution in competitive adoptive transplant assays (P. Kirstetter *et al.*, 2006). Mice expressing a stable form of β -catenin display a severe form of the haematopoietic alterations, resembling the phenotype we observed in mice infected with *L. donovani*, including pancytopenia, accumulation of intermediary multipotent progenitors and impairment of LT-HSCs function. Therefore, we evaluated the relative accumulation β -catenin in LT-HSCs, and found this to be increased following infection, suggestive of increased activation of Wnt signaling pathway in LT-HSCs. Future experiments should seek to evaluate β -catenin subcellular localization.

Wnt- β -catenin signaling canonical pathway is activated following binding of Wnt1, Wnt3a, or Wnt8 to its receptor the seven-transmembrane domain receptor Frizzled (Fzd) and co-receptor, the single-membrane-spanning low-density receptor-related protein 5/6 (LRP5/6), expressed in target cell (L. Grumolato *et al.*, 2010). Wnt3a was the first Wnt protein purified and it has been described as the prototypical Wnt ligand for the canonical pathway. Wnt3a homozygous mutants die early during embryonic development, and it was showed using a Wnt reporter that Wnt3a is unique in its ability to activate canonical Wnt signaling in the HSCs in fetal livers (T. C. Luis *et al.*, 2009, T. C. Luis *et al.*, 2010b). Studies *in vitro* showed that adult HSCs stimulated with purified Wnt3a had an improved capacity to reconstitute the haematopoietic system of conditioned mice *in vivo* (T. Reya and H. Clevers, 2005). These studies suggested that Wnt3a may play an important role in activation of HSCs that express its cognate receptors (R. Sugimura *et al.*, 2012). Therefore, we assessed expression of Wnt3a on BM cells in mice infected with *L. donovani*.

In the BM of infected mice we found that of Wnt3a was expressed at increased levels by mature haematopoietic cells (CD45⁺ Lineage⁺ cells), suggesting increased availability of Wnt3a in the BM microenvironment during infection might drive an enhanced activation of Wnt canonical pathway within LT-HSCs. LT-HSCs did also expressed increased levels of Wnt3a following infection with *L. donovani*. Interestingly, it was previously described that HSCs display an increased potential to produce Wnt3a, and therefore mediate autocrine induction of canonical Wnt signaling, as a compensatory mechanism in the absence of Wnt expression by osteoblasts (C. Schaniel *et al.*, 2011).

We failed to determine an increase in the *Wnt3a* mRNA expression in total BM cells from infected, suggesting that protein levels may depend of post-transcriptional regulation.

c-Myc was identified as a Wnt/ β -catenin target gene in colorectal cancer cell lines characterized by the accumulation of β -catenin and the activation of Wnt target genes including *c-Myc* (M. D. Delgado and J. Leon, 2010). This transcription factor is implicated in the regulation of a wide range of gene groups including, apoptosis, cell-cycle regulation and metabolism. However, c-Myc may play as a transcriptional repressor of genes regulating cell adhesion and quiescence, for example the cyclin-dependent kinase inhibitors p21^{CIP1} and p15^{INK4B} (J. A. Wilkins and O. J. Sansom, 2008).

Alterations in c-Myc expression have been also reported in various haematological malignancies, and c-Myc seems to act as an important regulator of haematopoiesis, for instance mice deficient for *c-Myc* die before birth, mostly due to defective haematopoiesis (M. D. Delgado and J. Leon, 2010).

In the adult, the function of c-Myc in haematopoiesis was evaluated using *c-Myc* conditional KO mice under the control of MX-cre transgene (MxCre;*c-myc*^{flox/flox} mice). In these mice observed the following was observed: an accumulation of non-committed multipotent progenitors (LSK Flt3⁻ cells) in BM, severe pancytopenia, and HSPCs were very impaired in their ability to reconstitute conditioned recipient mice, which was associated to the inability of HSCs to proliferate (A. Wilson *et al.*, 2004). On the other hand, over expression of c-Myc lead to loss of HSCs, and in mixed BM chimeric mice donor cells overexpressing c-Myc although capable of homing in BM and perform multilineage reconstitution in the short-term, in the long-term they nearly disappear, and it was proposed that enforced expression of c-Myc may result in HSCs premature functional exhaustion due to premature differentiation (A. Wilson *et al.*, 2004, M. J. Murphy *et al.*, 2005). These studies revealed that the fine-tuning of c-Myc expression in HSCs might be very important in the modulation of cell self-renewal and differentiation (A. Wilson *et al.*, 2004). In the present study, we found the expression of c-Myc increased in LT-HSC following infection, suggesting that c-Myc upregulation may contribute to the impairment of HSCs function under pro-inflammatory conditions established by *L. donovani* infection.

c-Myc deficiency in HSCs is not associated with significant alterations in differentiation *in vitro*, therefore is thought that the alterations observed *in vivo* may be partially explained by changes HSCs-BM stroma signals crosstalk (M. J. Murphy *et al.*, 2005). In MxCre;*c-myc*^{flox/flox} mice there were alterations in the expression of several adhesion molecules in LSK cells, including the increased expression of CD29 (β 1-integrin), and it was suggested that c-Myc conditional deletion resulted in accumulation of HSCs and impaired differentiation due to withholding of HSCs in the BM niche (A. Wilson *et al.*, 2004). In mice chronically infected with *L. donovani* we failed to determine any alteration in the expression of CD29. Overall, these finding suggested that *L. donovani* infection prompted the up-regulation of c-Myc in HSCs, but there was no indication that this was associated with impaired HSC-niche adhesion, at least mediated by CD29.

The transcription factor GATA-3 is expressed in various HSPCs in BM, with LT-HSCs expressing the highest levels of GATA-3. In competitive transfer assays, *GATA-3*-null haematopoietic donor cells are less efficient to engraft, even though the fraction HSCs in quiescence is higher compared to WT mice. Furthermore, upon myelosuppression LT-HSCs from *GATA-3* deficient mutants fail to enter into active cell-cycle, suggesting that GATA-3 is required for HSCs proliferation under conditions of stress-induce haematopoiesis (C.-J. Ku *et al.*, 2012). More recently it was shown that upon poly I:C treatment proliferating HSCs display nuclear GATA-3 (active form), and although capable of performing short-term multilineage reconstitution are no longer efficient in long-term multilineage reconstitution of lethally irradiated recipients. However, if the proliferative stimulus is removed, GATA-3 re-localizes to the cytoplasm and the long-term lineage reconstitution is restored. Additionally, in competitive

transplant assays of BM cell from poly I:C treated *GATA-3*-deficient and WT mice, *GATA-3* deficient cells are much more efficient performing haematopoietic reconstitution. These data suggested that *GATA-3* might limit self-renewal during proliferation of HSCs (C. Frelin *et al.*, 2013).

Despite the conflicting data from the above cited studies, both pointed out that *GATA-3* has a role in cell-cycle entry regulation in LT-HSCs during stress induced haematopoiesis (T. Yoshida and K. Georgopoulos, 2013). In mice infected with *L. donovani*, we determined that *GATA-3* expression was up-regulated in LT-HSCs. However, its expression was mainly restricted to LT-HSCs in active cell-cycle. In fact, LT-HSCs in active cell-cycle expressing *GATA-3* were the population that mostly contributed to the overall increase of LT-HSCs in proliferation, since the fraction of proliferating LT-HSCs not expressing *GATA-3* remain unchanged following infection. The specific increase of *GATA-3* in proliferative HSCs but not HSCs in G0 following *L. donovani*, and its limited contribution to the fraction of HSCs in homeostatic proliferation, suggested *GATA-3* over expression due to inflammation was associated with an impaired maintenance of homeostatic numbers of LT-HSCs in quiescence, during *L. donovani* chronic infection. Therefore, *GATA-3* and upstream regulators should be considered as potential targets for therapeutic intervention in the prevention of HSCs impairment during stress-induced haematopoiesis.

In vitro studies suggested that nuclear localization of *GATA-3* depends directly on p38 MAPK activation, as shown by pharmacological inhibition (C. Frelin *et al.*, 2013). More recently, it was shown that the (deubiquitinase cylindromatosis) CYLD - (tumor necrosis factor-associated factor 2) TRAF2 pathway is very important for the regulation of LT-HSCs quiescence through the repression of p38MAPK activity (M. Tesio *et al.*, 2015). In *Mx1-Cre* conditional KO for functional CYLD (CYLD^{Δ932Mx}) mice, the majority of LT-HSCs are found in active proliferation and in BMT assays BM cells from CYLD^{Δ932Mx} mice perform very poor reconstitution of all lineages in blood and HSCs in BM. TRAF2 is a CYLD substrate and using mutant mice displaying hyper-ubiquitinated TRAF2, it was observed loss of quiescent LT-HSCs was similar to that seen in CYLD^{Δ932Mx} mice. TRAF2 controls the activation of p38 MAPK, and it was shown that therapeutic inhibition (using two different specific inhibitors) *in vivo* of p38 activation could restore the frequency of quiescent LT-HSCs to baseline levels both, in mutant mice displaying hyperubiquitinated TRAF2 and in CYLD^{Δ932Mx} mice, suggesting that CYLD-TRAF2 pathway regulates HSCs passage to active cell-cycle preventing p38MAPK activity (M. Tesio *et al.*, 2015). However, in these experiments p38 activity was inhibited in all cells, as such to isolate the impact of p38 in HSCs, those cells from mice treated with the pharmacological inhibitors should have been transfer to conditioned recipients. These studies emphasize the pertinence of the further

investigation focusing in the role of p38MAPK and GATA-3 in loss of HSCs function in the context of chronic infection.

Alterations in haematopoietic function have been commonly found in patients suffering from chronic infections. VL is a pernicious chronic infection that has been associated with the establishment of haematopoietic alterations and increased vulnerability to secondary infections or bleeding (P. M. Kaye *et al.*, 2004). Nevertheless, very few systematic reports have addressed the underlying mechanisms responsible for these haematological alterations or their association with the stage of disease, geographic area, response to treatment and relapse, among others (G. E. Cartwright *et al.*, 1948, N. Varma and S. Naseem, 2010). The research discussed in this Chapter provides a first step in readdressing this deficiency in knowledge on the impact of *L. donovani* in the haematopoietic function. We have shown that following *L. donovani* infection in mice, expansion of multipotent progenitors occurs at the expense of quiescent LT-HSCs, which resulted in intrinsic impairment of HSCs function (Figure 3.28). We were able to relate the alteration in the proliferative status of LT-HSCs and consequent functional decline with the upregulation of the co-activator CD48, and transcription factors β -catenin, c-Myc and GATA-3. These findings support the hypothesis that during *L. donovani* chronic infection, sustained infection-induced immune responses compromise HSCs function and in the long-term the sustainability of the haematopoietic compartment. Furthermore, we identified potential molecular targets that, although requiring further investigation, could be in the basis of novel therapeutic approaches to address haematological impairment in VL patients, and other chronic inflammatory conditions.

3.4 FIGURES

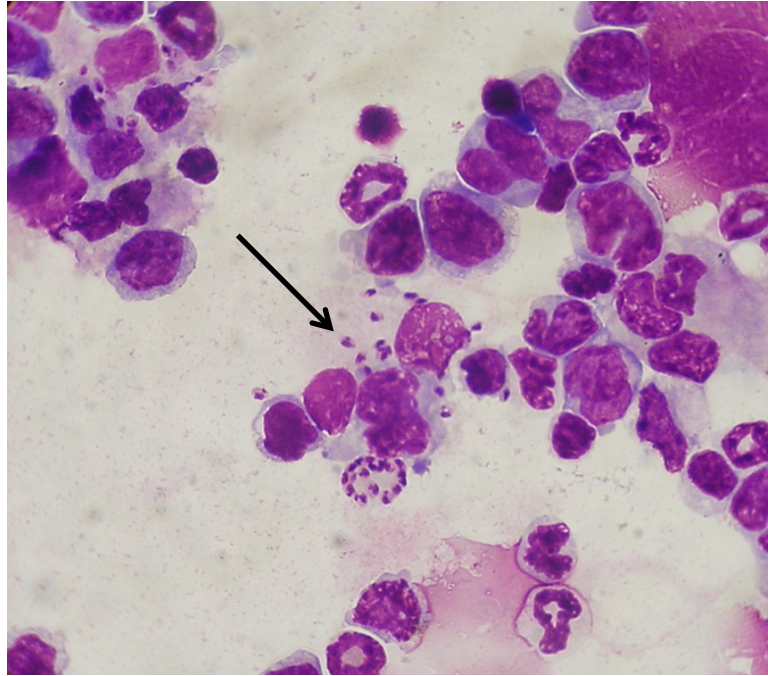


Figure 3.1 - *L. donovani* parasites in BM. BM smear from B6 mouse infected for 28 days. Parasite indicated by arrow. Giemsa staining 63x. Source: Pinho F. and Pinto A.I. (Unpublished).

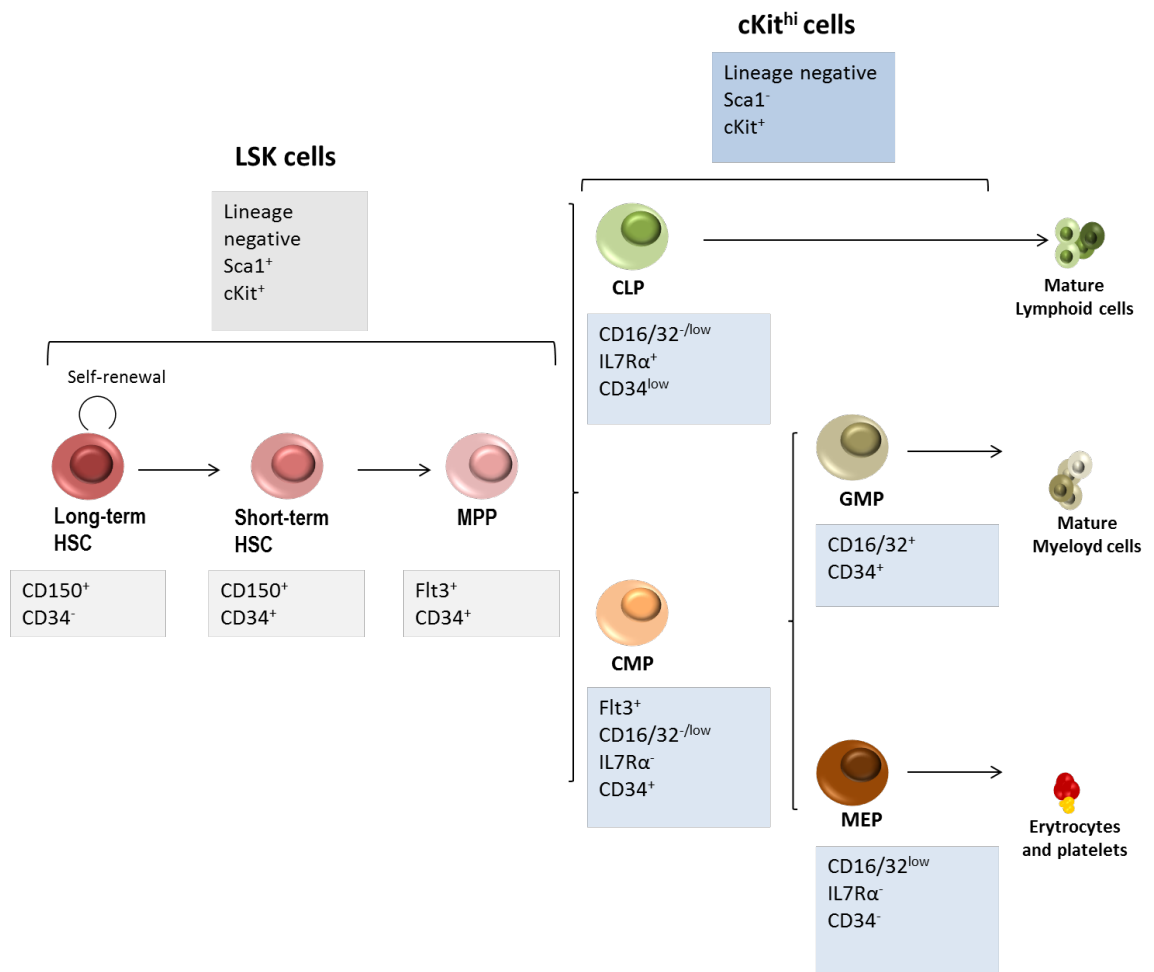


Figure 3.2- Diagram of stepwise differentiation of haematopoietic precursors and panel of associated surface molecular markers commonly used to characterize the different haematopoietic stem and progenitor cells (HSPCs). According with the “Classical Model” of haematopoiesis, all haematopoietic cells originate from a small population of haematopoietic stem cells (HSCs), which can be subdivided into at least two subsets based on the period of maintenance of self-renewal potential following transfer to lethally irradiated recipient mice: long-term reconstituting HSC (LT-HSCs) and short-term reconstituting HSCs (ST-HSCs). Differentiation of ST-HSCs generates multipotent progenitors (MPPs) and then lineage-committed oligopotent progenitors derived from MPPs. These include the common lymphoid progenitor (CLPs), common myeloid progenitor (CMPs), megakaryocyte-erythrocyte progenitor (MEP) and granulocyte-monocyte progenitor (GMP) populations (Adapted from (M. J. Nemeth and D. M. Bodine, 2007)).

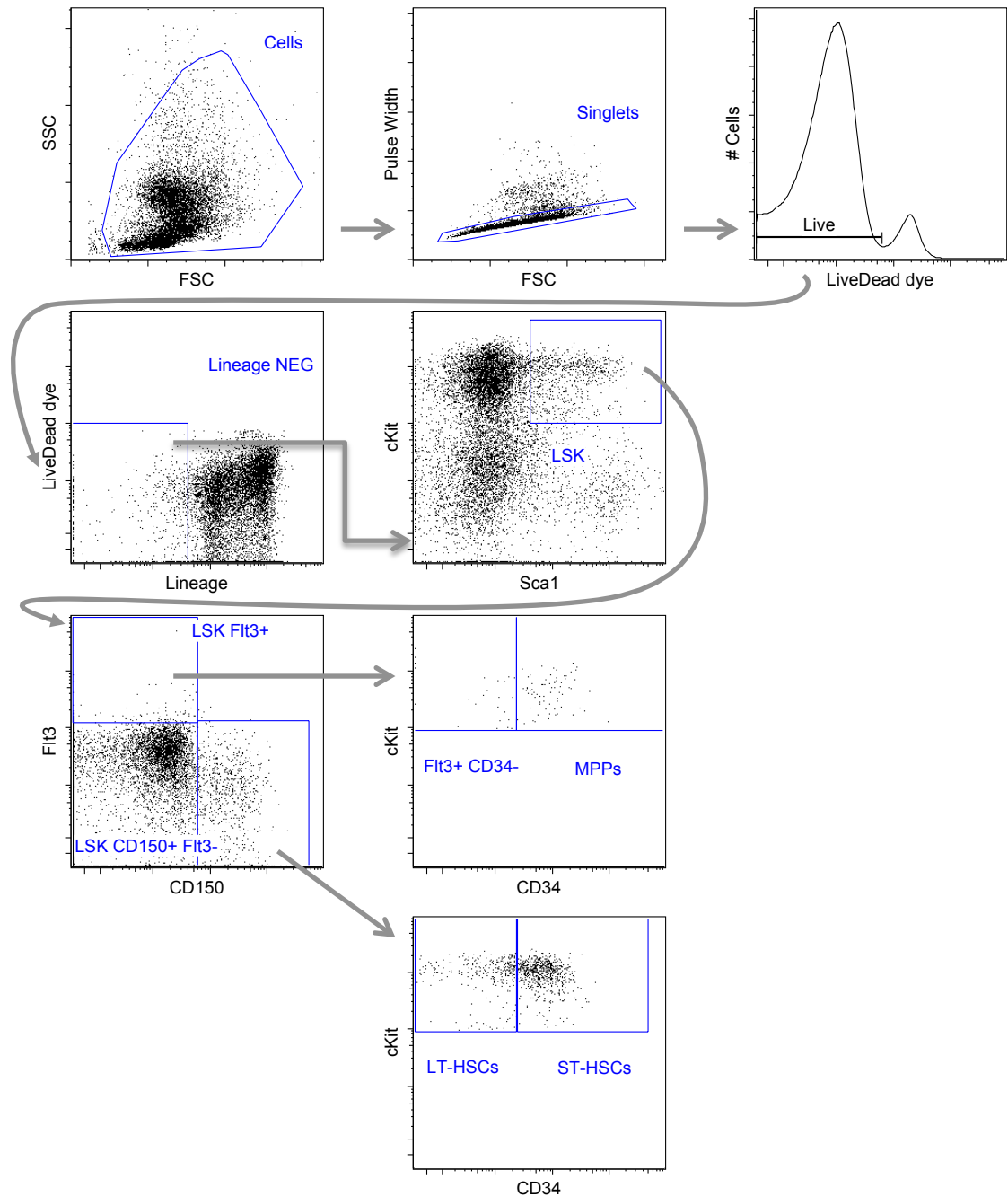


Figure 3.3 - Gating strategy for characterizing multipotent progenitors using flow cytometry analysis. Representative dot plots from BM cells from a naive B6 mouse. LSK CD150⁺ Flt3⁻ CD34⁻ cells (enriched for phenotypic LT-HSCs), LSK CD150⁺ Flt3⁻ CD34⁺ cells (enriched for phenotypic ST-HSCs) and LSK CD150⁻ Flt3⁺ CD34⁺ cells (enriched for phenotypic MPPs). LSK stands for Lineage^{neg} (CD3e⁻ CD45R/B220⁻ TER-119⁻ Ly-6G⁻ Ly-6C⁻ cells) Sca1^{hi} cKit^{hi} cells.

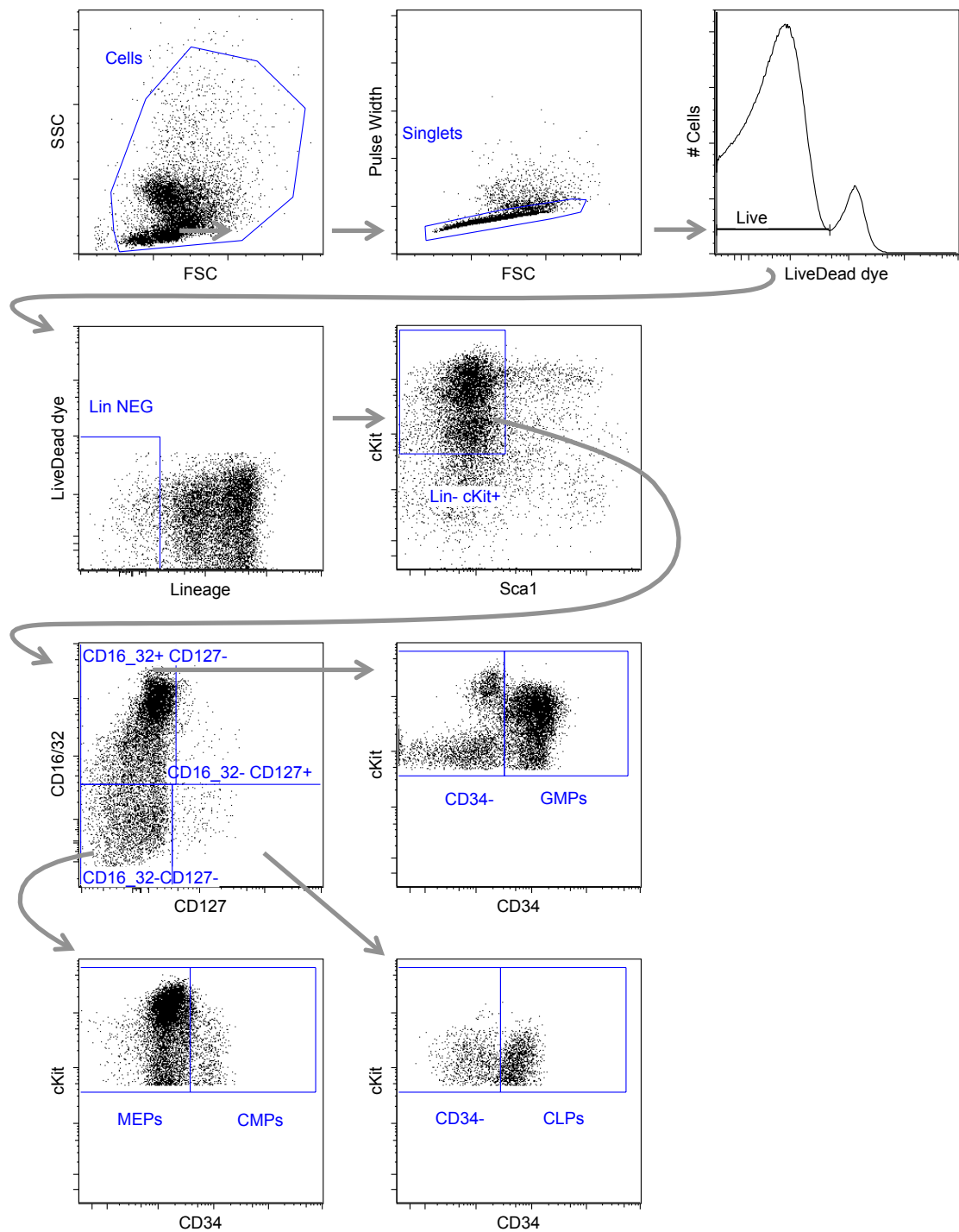


Figure 3.4 - Gating strategy for characterizing BM populations enriched for lineage-committed haematopoietic progenitors using flow cytometry. Representative dot plots of characterization of lineage-committed progenitor cells in the BM of a naive B6 mouse. CMPs (common myeloid progenitor cells), GMPs (granulocyte-monocyte progenitor cells), MEPs (megakaryocyte-erythrocyte progenitor cells) and CLPs (common lymphocyte progenitor cells).

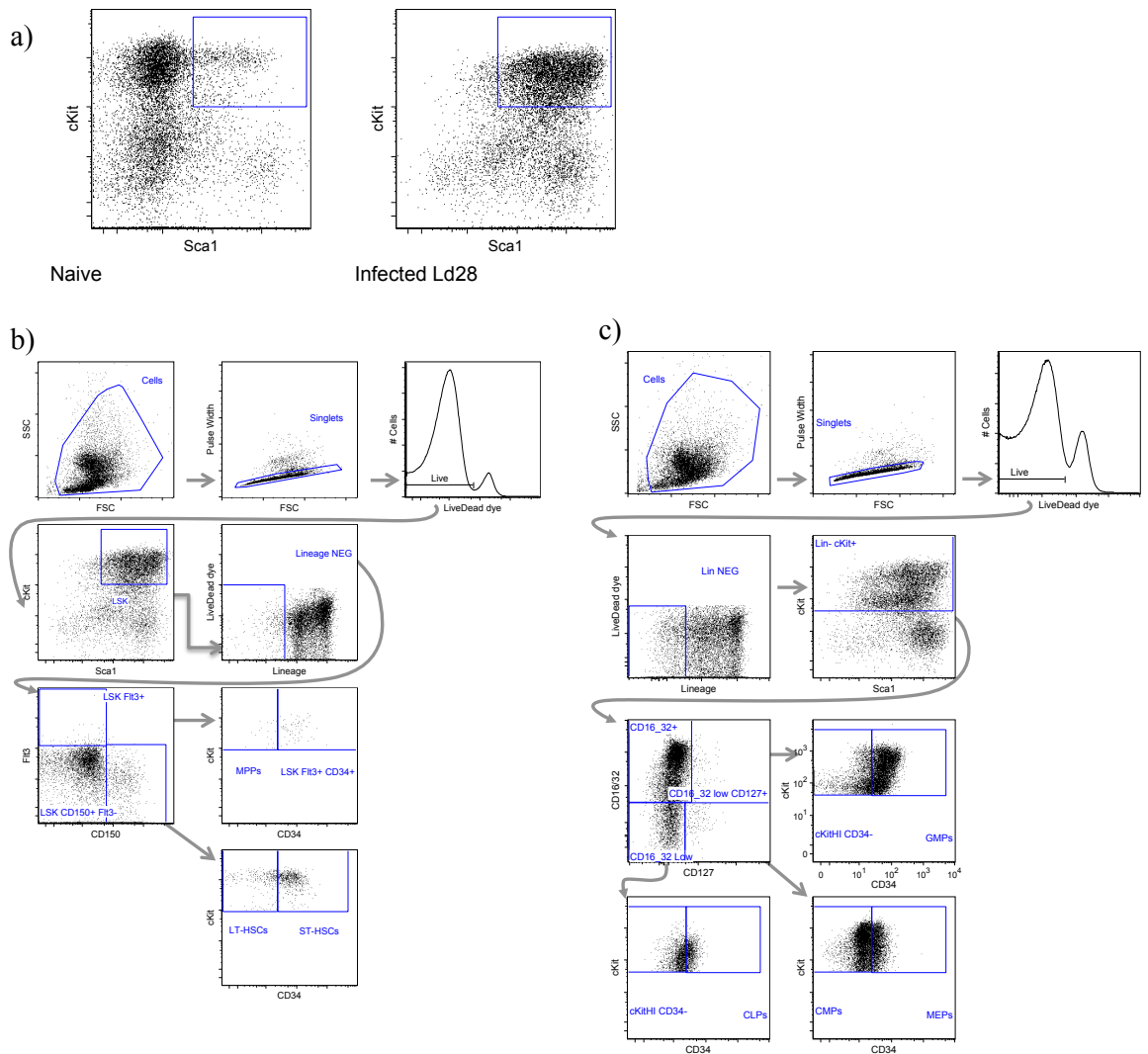


Figure 3.5 - Sca1 was expressed in the vast majority of HSPCs in the BM of *L. donovani* infected mice. Representative dot plots of expression of Sca1 within lineage negative cells in the BM of a naive (left) and day 28 - infected mice (right). b) Representative dot plots from BM cells from a B6 mouse infected for 28 days with *L. donovani*. LSK CD150⁺ Fli3⁻ CD34⁻ cells (enriched for phenotypic LT-HSCs), LSK CD150⁺ Fli3⁻ CD34⁺ cells (enriched for phenotypic ST-HSCs) and LSK CD150⁻ Fli3⁺ CD34⁺ cells (enriched for phenotypic MPPs). LSK stands for Lineage^{neg} (CD3^{e-} CD45R/B220⁻ TER-119⁻ Ly-6G⁻ Ly-6C⁻ cells) Sca1^{hi} cKit^{hi} cells. c) Representative dot plots of characterization of lineage-committed progenitor cells in the BM of B6 mouse infected for 28 days with *L. donovani*. CMPs (common myeloid progenitor cells), GMPs (granulocyte-monocyte progenitor cells), MEPs (megakaryocyte-erythrocyte progenitor cells) and CLPs (common lymphocyte progenitor cells).

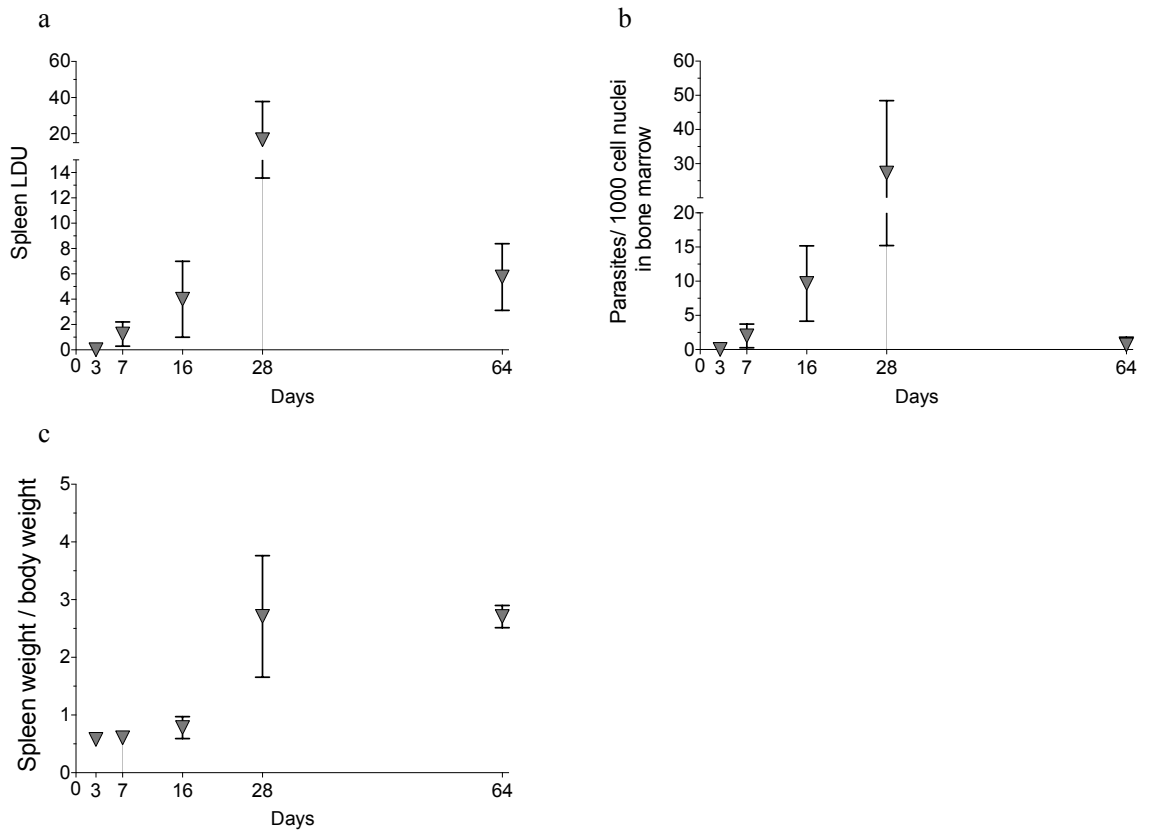


Figure 3.6 - The kinetics of parasite burden in the BM and the spleen of *L. donovani* infected mice. *L. donovani* infected B6 mice were examined for parasite burden at times indicated. (a) Spleen parasite burden determined from Giemsa stained impression smears and expressed as Leishman Donovan Units (LDU). (b) BM parasite burden determined from BM aspirates smears stained with eosin and azur staining and expressed as number of amastigotes per 1,000 host cells. (c) Degree of splenomegaly, expressed as spleen / body weight ratio. Data from one experiment represented as Mean \pm SD (n=3-4 mice per time point).

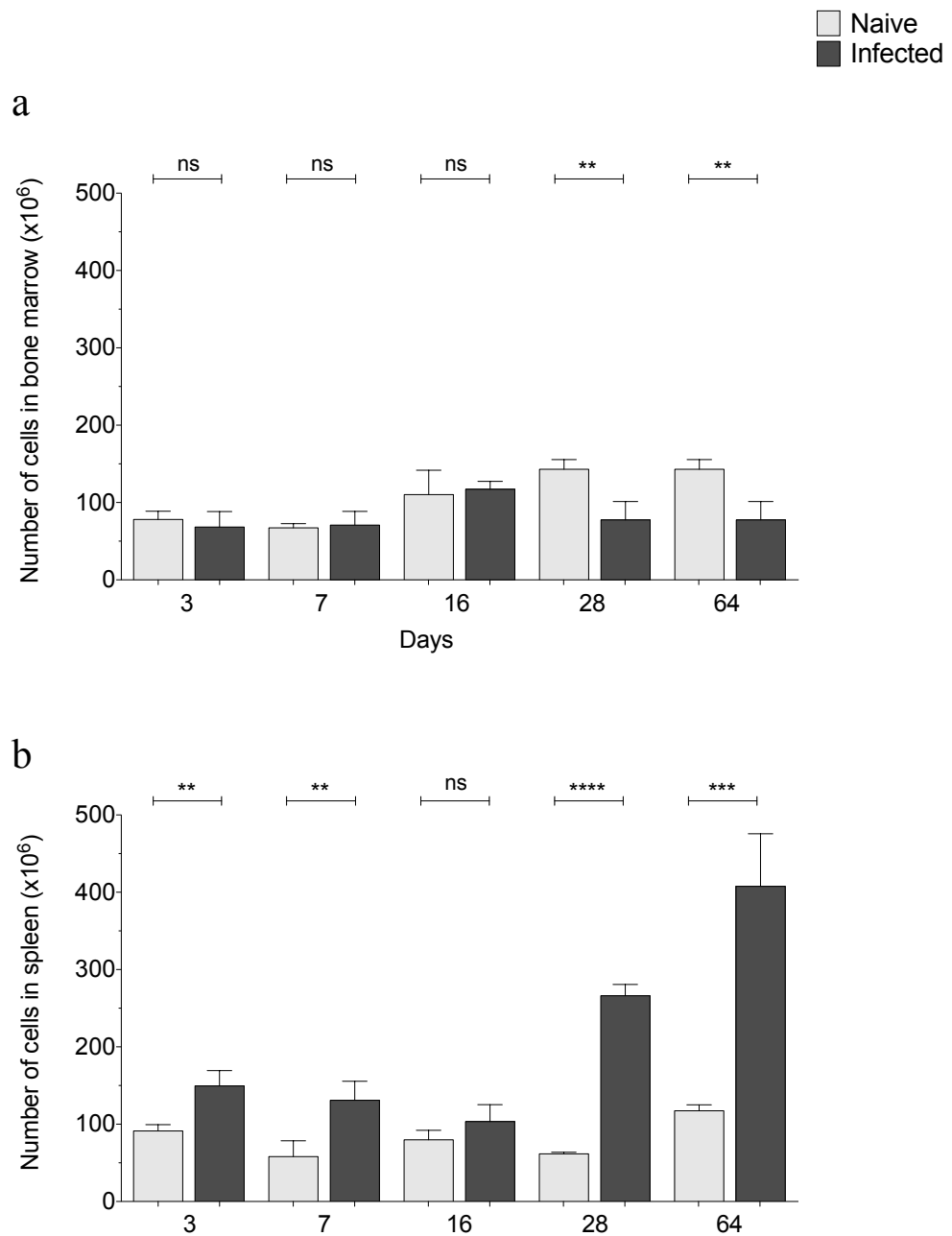


Figure 3.7 - *L. donovani* infection affects the BM and the spleen cellularity. (a) Absolute cells number of BM cells per two legs for each sample at indicated times post infection with *L. donovani*. (b) Absolute cells number of splenocytes. Data presented as Mean \pm SD for (n=4 mice per group per time point). Data from one experiment was presented as Mean \pm SD, p values were determined using unpaired t test: *p \leq 0.05, **p \leq 0.01, ***p \leq 0.001, ****p \leq 0.0001.

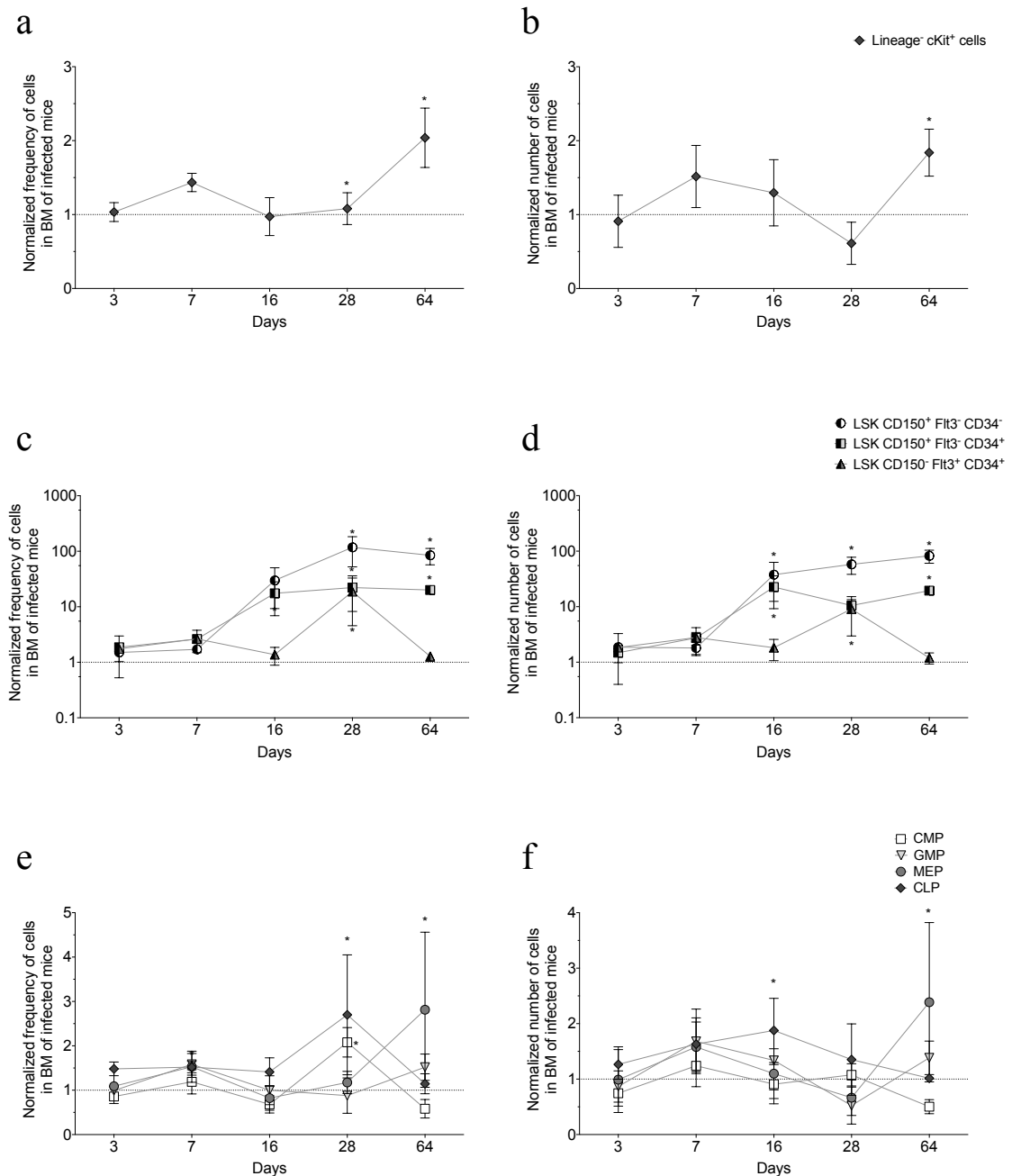


Figure 3.8 - *L. donovani* infection results in changes to the number of HSPCs in BM. (a) Relative frequency of Lineage⁻cKit⁺ cells (enriched for HSPCs). (b) Relative number of Lineage⁻cKit⁺ cells (enriched for HSPCs). (c) Relative frequency of LSK CD150⁺ Flt3⁻ CD34⁻ cells (enriched for phenotypic LT-HSCs), LSK CD150⁺ Flt3⁻ CD34⁺ cells (enriched for phenotypic ST-HSCs), and LSK CD150⁻ Flt3⁺ CD34⁺ cells (enriched for phenotypic MPPs). (d) Relative number of LSK CD150⁺ Flt3⁻ CD34⁻ cells, LSK CD150⁺ Flt3⁻ CD34⁺ cells and LSK CD150⁻ Flt3⁺ CD34⁺ cells. (f) Relative frequency of CMPs, GMPs, MEPs and CLPs. (f) Relative number of CMPs, GMPs, MEPs and CLPs. Data from one experiment was presented as Mean \pm SD of normalized values for each infected mice (n=4) with the mean of values determined in naive mice (n=4), for each time point. Measurements were performed at 3 (n=4), 16 (n=4), 28 (n=4) and 64 (n=3) days post-infection with *L. donovani* in the BM (two femurs and two tibias *per* mice). Significant

differences with control (* $p < 0.05$) were determined by one-way ANOVA followed by post-hoc analysis using Dunnett's Multiple Comparison Test.

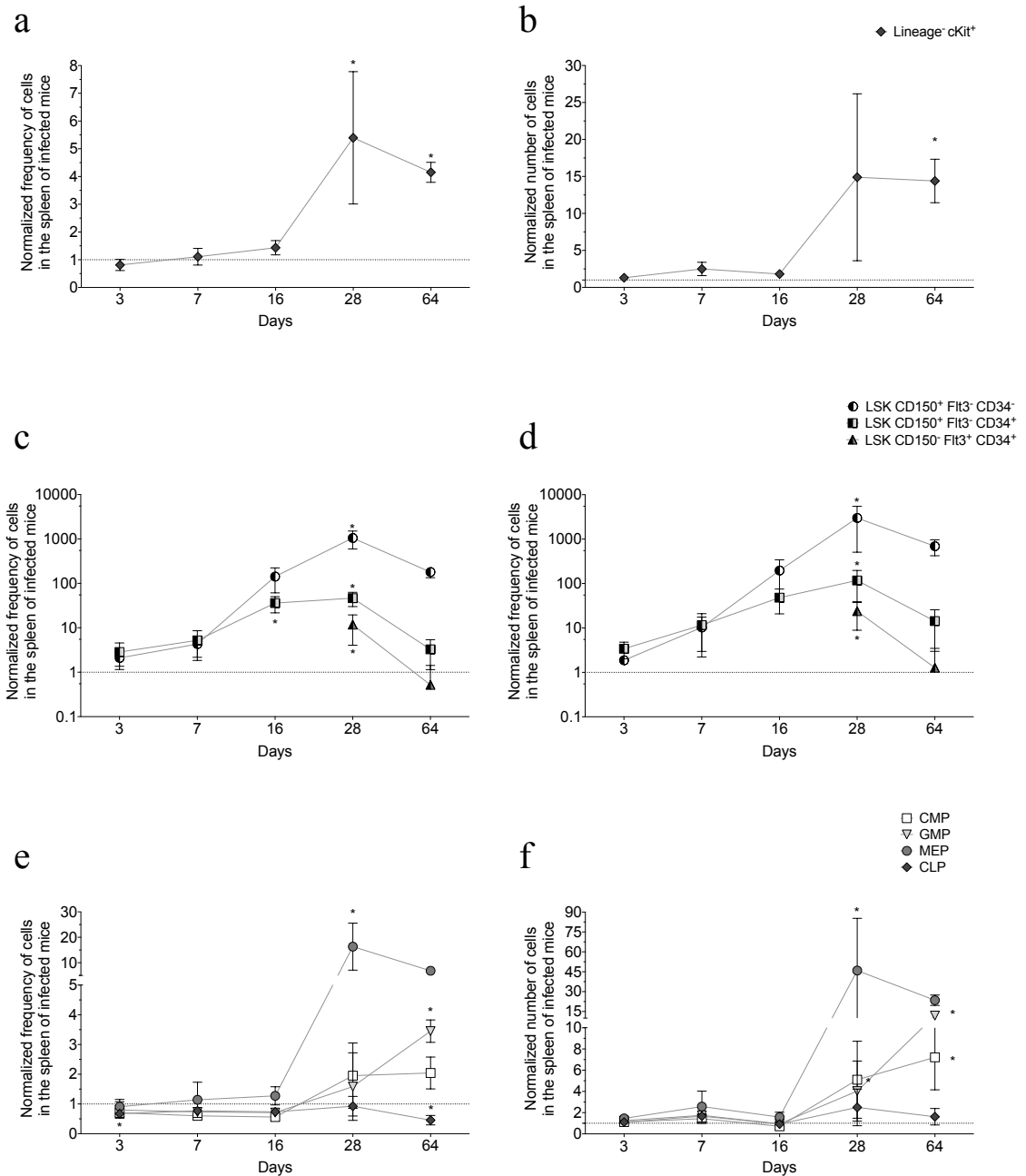


Figure 3.9 - *L. donovani* infection results in changes to the number of HSPCs in the spleen. (a) Relative frequency of Lineage⁻ cKit⁺ cells (enriched for HSPCs). (b) Relative number of Lineage⁻ cKit⁺ cells (enriched for HSPCs). (c) Relative frequency of LSK CD150⁺ Flt3⁻ CD34⁻ cells (enriched for phenotypic LT-HSCs), LSK CD150⁺ Flt3⁻ CD34⁺ cells (enriched for phenotypic ST-HSCs), and LSK CD150⁻ Flt3⁺ CD34⁺ cells (enriched for phenotypic MPPs). (d) Relative number of LSK CD150⁺ Flt3⁻ CD34⁻ cells, LSK CD150⁺ Flt3⁻ CD34⁺ cells and LSK CD150⁻ Flt3⁺ CD34⁺ cells. (e) Relative frequency of CMPs, GMPs, MEPs and CLPs. (f) Relative number of CMPs, GMPs, MEPs and CLPs. Data from one experiment was presented as Mean \pm Standard Error Mean (SD) of normalized values for each infected mice (n=4) against the mean of values determined in naive mice (n=4), for each time point. Measurements were performed at 3 (n=4), 16 (n=4), 28 (n=4) and 64 (n=3) days post-infection with *L. donovani* in the spleen.

Significant differences with control (* $p < 0.05$) were determined by one-way ANOVA followed by post-hoc analysis using Dunnett's Multiple Comparison Test.

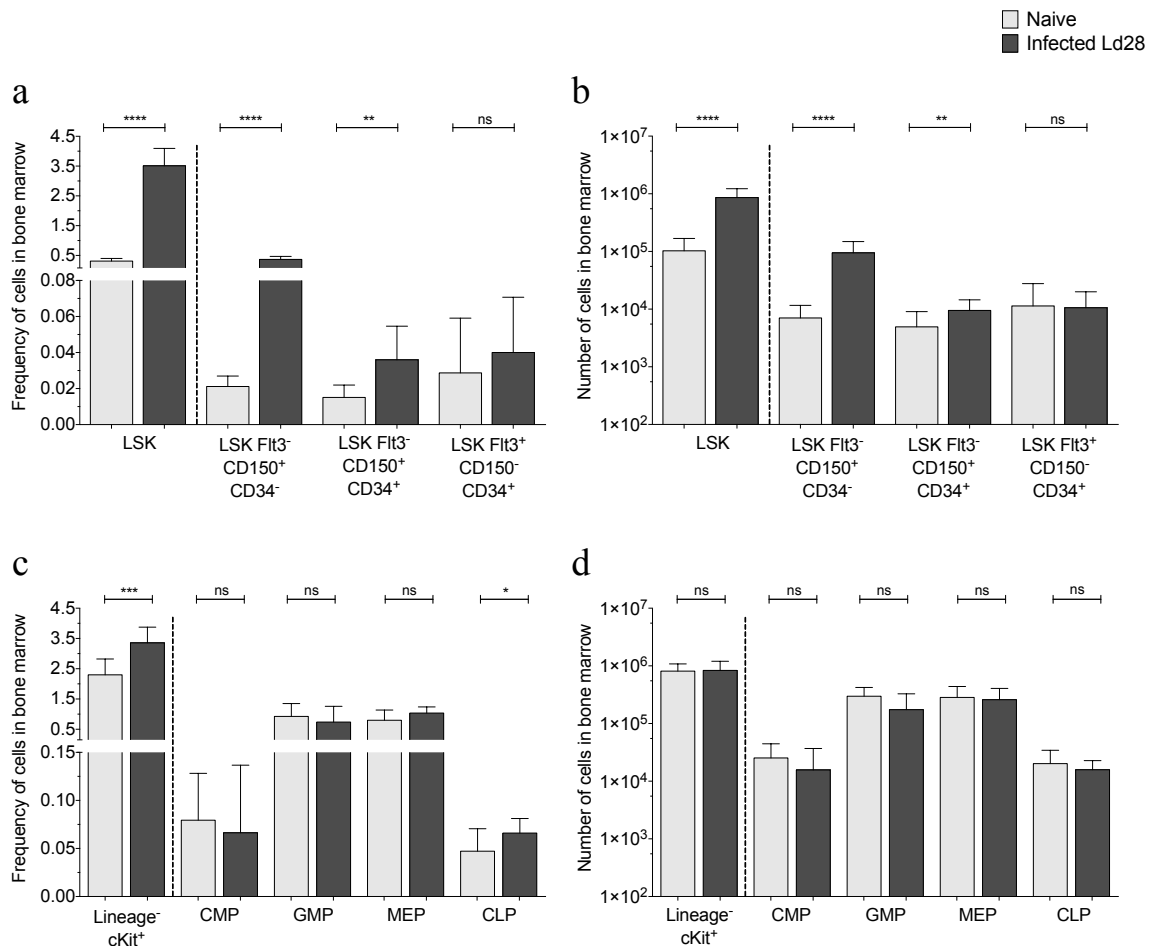


Figure 3.10 - *L. donovani* infection results in increased numbers of multipotent haematopoietic progenitors without a reciprocal increase in lineage-committed progenitors. (a) Frequency of Lineage⁻ Sca1⁺ cKit⁺ cells (LSK), enriched for multipotent progenitors, LSK CD150⁺ Flt3⁻ CD34⁻ cells (enriched for phenotypic LT-HSCs), LSK CD150⁺ Flt3⁻ CD34⁺ cells (enriched for phenotypic ST-HSCs) and LSK CD150⁻ Flt3⁺ CD34⁺ cells (enriched for phenotypic MPPs). (b) Number of LSKs, LSK CD150⁺ Flt3⁻ CD34⁻ cells, LSK CD150⁺ Flt3⁻ CD34⁺ cells and LSK CD150⁻ Flt3⁺ CD34⁺ cell. (c) Frequency of CMPs, GMPs, MEPs and CLPs. (d) Number of CMPs, GMPs, MEPs and CLPs. Measurements were performed at 28 post-infection with *L. donovani* (Ld28) in BM. Absolute number calculated from two femurs and two tibias for each mouse. Comparisons were made between naive (n=12) and infected mice (n=8) in three independent experiments. Data presented as Mean ± SD, p values were determined using unpaired t test: *p ≤ 0.05, **p ≤ 0.01, ***p ≤ 0.001, ****p ≤ 0.0001.

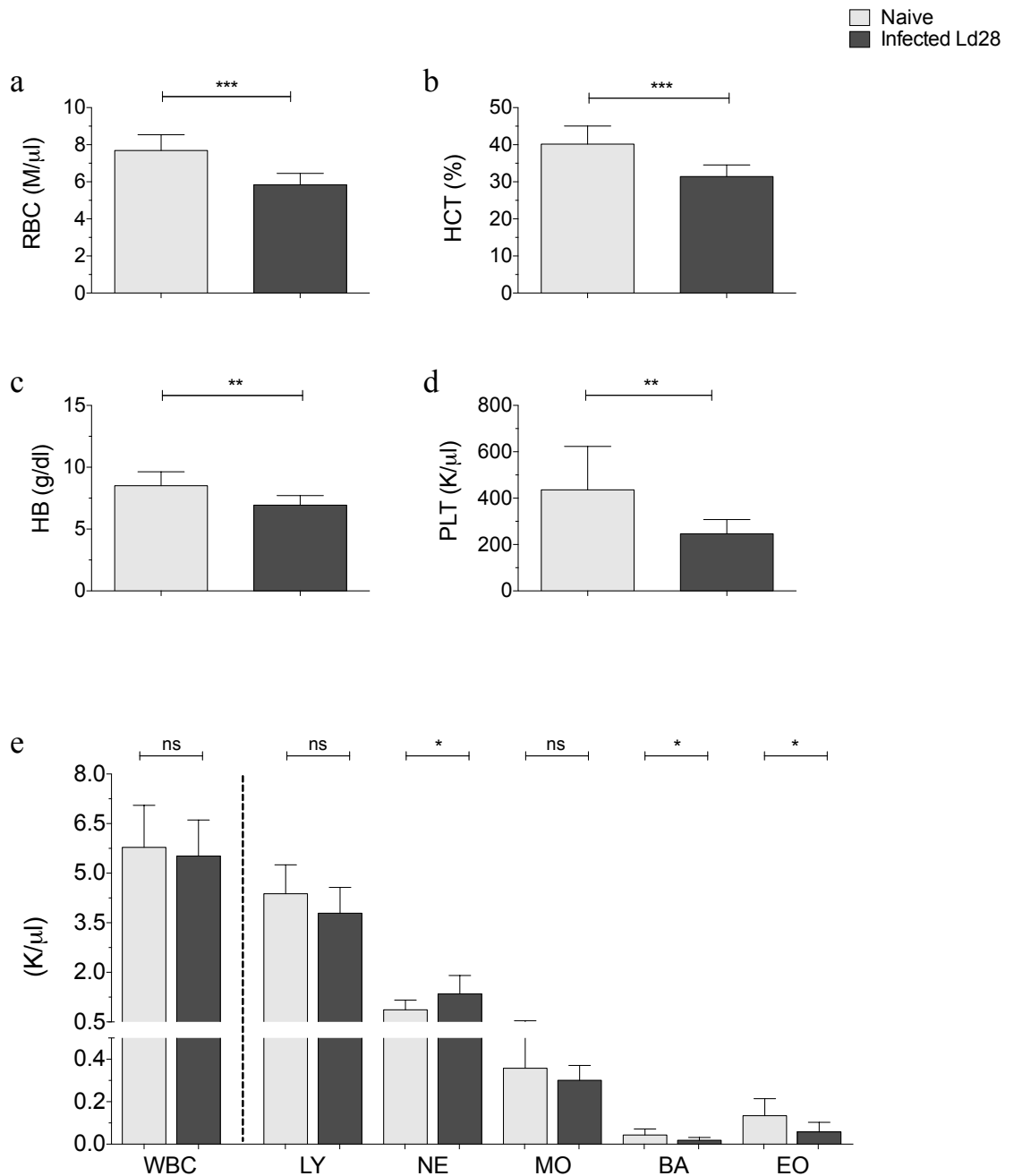


Figure 3.11 - *L. donovani* infection was associated to decreases in mature blood cells in circulation. (a) Concentration of red blood cells (RBC) in peripheral blood (PB). (b) PB hematocrit (HCT). (c) Concentration of hemoglobin (Hb) in PB. (d) Concentration of platelets (PLT) in PB. (e) Concentrations of total white blood cells (WBC), lymphocytes (LY), neutrophil (NE), monocytes (MO), basophils (BA) and eosinophils (EO) in PB. Values were determined in whole blood collected in heparin using an automated system for blood cell counting (Hemavet). Comparisons were made between mice at day 28 p.i. (Ld28) (n=9) and naive mice (n=9). Data from two independent experiments is presented as Mean ± SD, p values were determined using unpaired t test: not significant (ns), * $p \leq 0.05$, ** $p \leq 0.01$, *** $p \leq 0.001$, **** $p \leq 0.0001$.

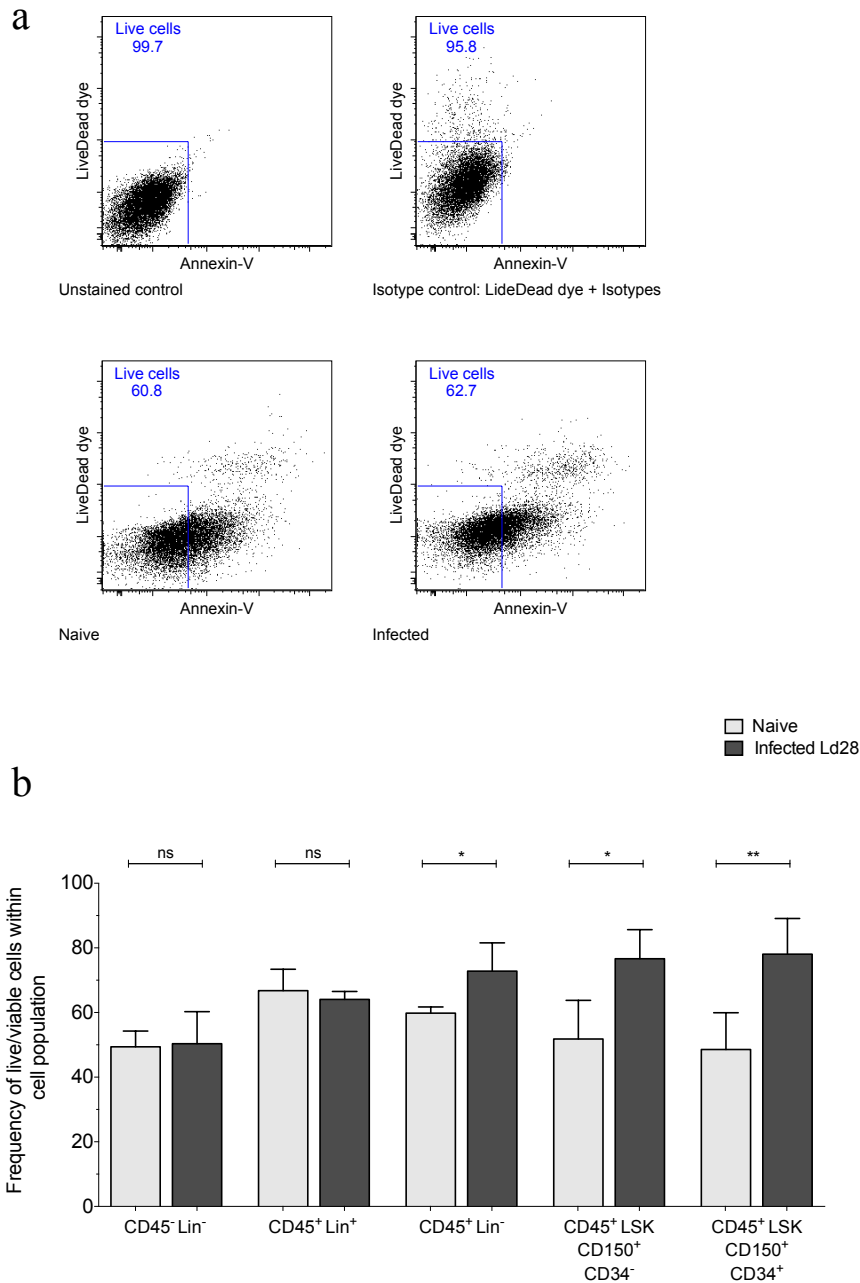


Figure 3.12 - *L. donovani* infection was not associated with increased cell death in the bone marrow. The frequency of live/viable cells was determined within mature cells and HSPCs in bone marrow through the exclusion of cells permeable to the live dead dye (dead) and/or positive to annexin-v (apoptotic). (a) Representative dot plots of gating applied to select live/dead cells. (b) Frequency of live/viable cells within CD45⁻ Lin⁻ cells (stromal cells), CD45⁺ Lin⁺ cells (mature haematopoietic cells), CD45⁺ Lin⁻ (enriched for haematopoietic progenitor cells), CD45⁺ LSK CD150⁺ CD34⁻ cells (enriched for LT-HSCs) and CD45⁺ LSK CD150⁺ CD34⁺ (enriched for ST-HSCs). Comparisons were made between mice infected with *L. donovani* for 28 days (Ld28) (n=4) and naive mice (n=4). Data from one experiments is presented as Mean ± SD, p values were determined using unpaired t test: not significant (ns), *p ≤ 0.05, **p ≤ 0.01, ***p ≤ 0.001, ****p ≤ 0.0001.

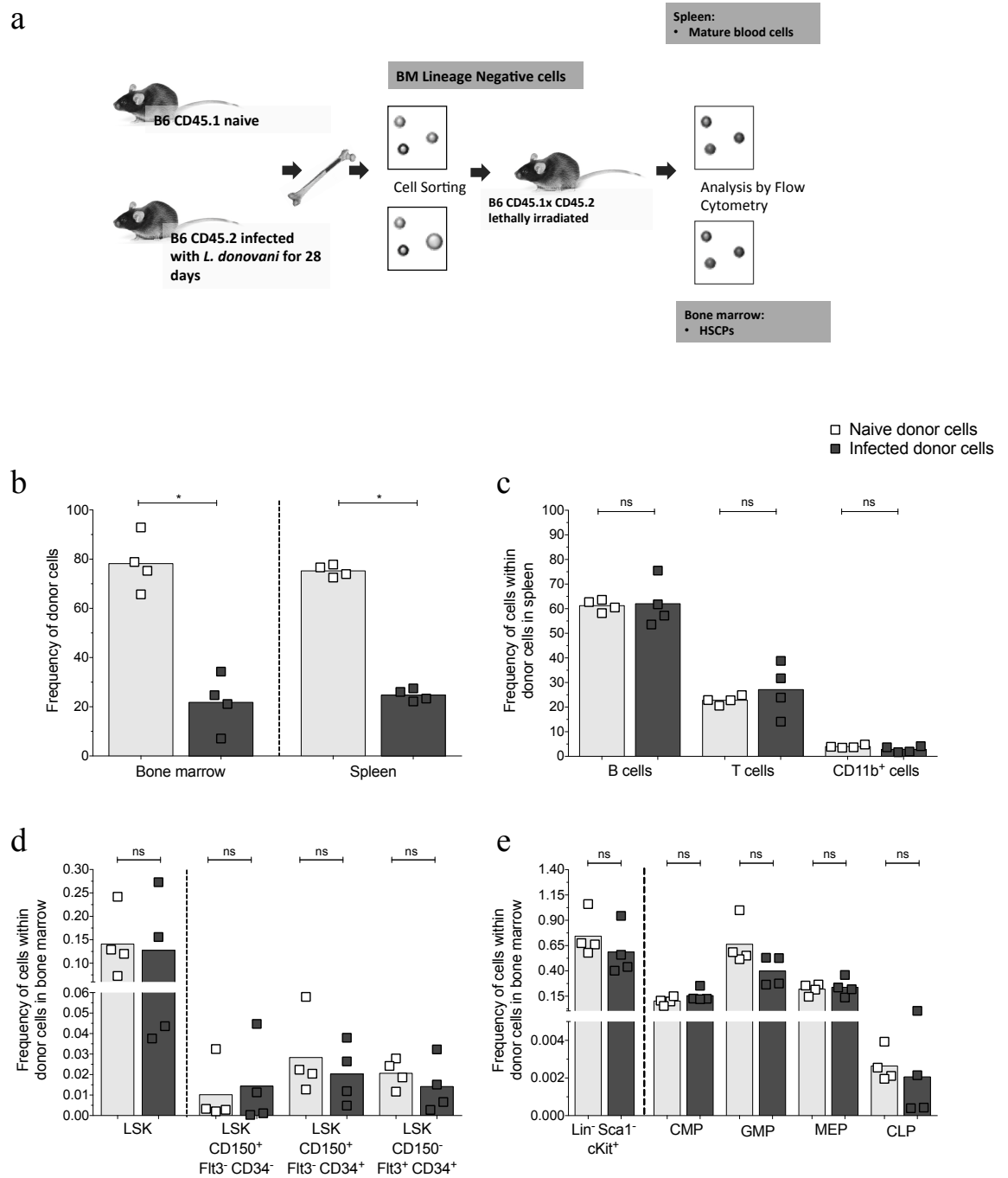


Figure 3.13 - HSCPs from infected mice showed impaired engraftment in BM and decreased reconstitution of the periphery. (a) Diagram of experimental design: non-infected B6.CD45.1 x CD45.2 (n=4) lethally irradiated recipient mice received BM Lineage negative cells from B6.CD45.2 mice infected for 28 days with *L. donovani* and B6.CD45.1 naive mice (50:50 mixed BM chimera). After seven weeks, the contribution of each group of donor cells to the reconstitution of the haematopoietic system was assessed in the BM and spleen of recipient mice, by gating on single CD45.1 or CD45.2 cells. (b) Frequency of donor haematopoietic cells in BM and spleen of recipient mice. (c) Frequencies of T cells, B cells and myeloid cells (CD11b⁺) within donor compartment in the spleen of non-infected recipient mice. (d) Frequencies LSKs, LSK CD150⁺ Fli3⁻ CD34⁻ cells, LSK CD150⁺ Fli3⁻ CD34⁺ cells and LSK CD150⁻ Fli3⁺ CD34⁺ cell

within each donor compartment in the BM of non-infected recipient mice. (e) Frequency of CMPs, GMPs, MEPs and CLPs within each donor compartment in the BM of non-infected recipient mice. Data presented as Mean and Scatter plot. Comparisons made between infected donor cells and naive donor cells. p value were determined using Mann Whitney test: not significant (ns), * $p \leq 0.05$, ** $p \leq 0.01$, **** $p \leq 0.001$.

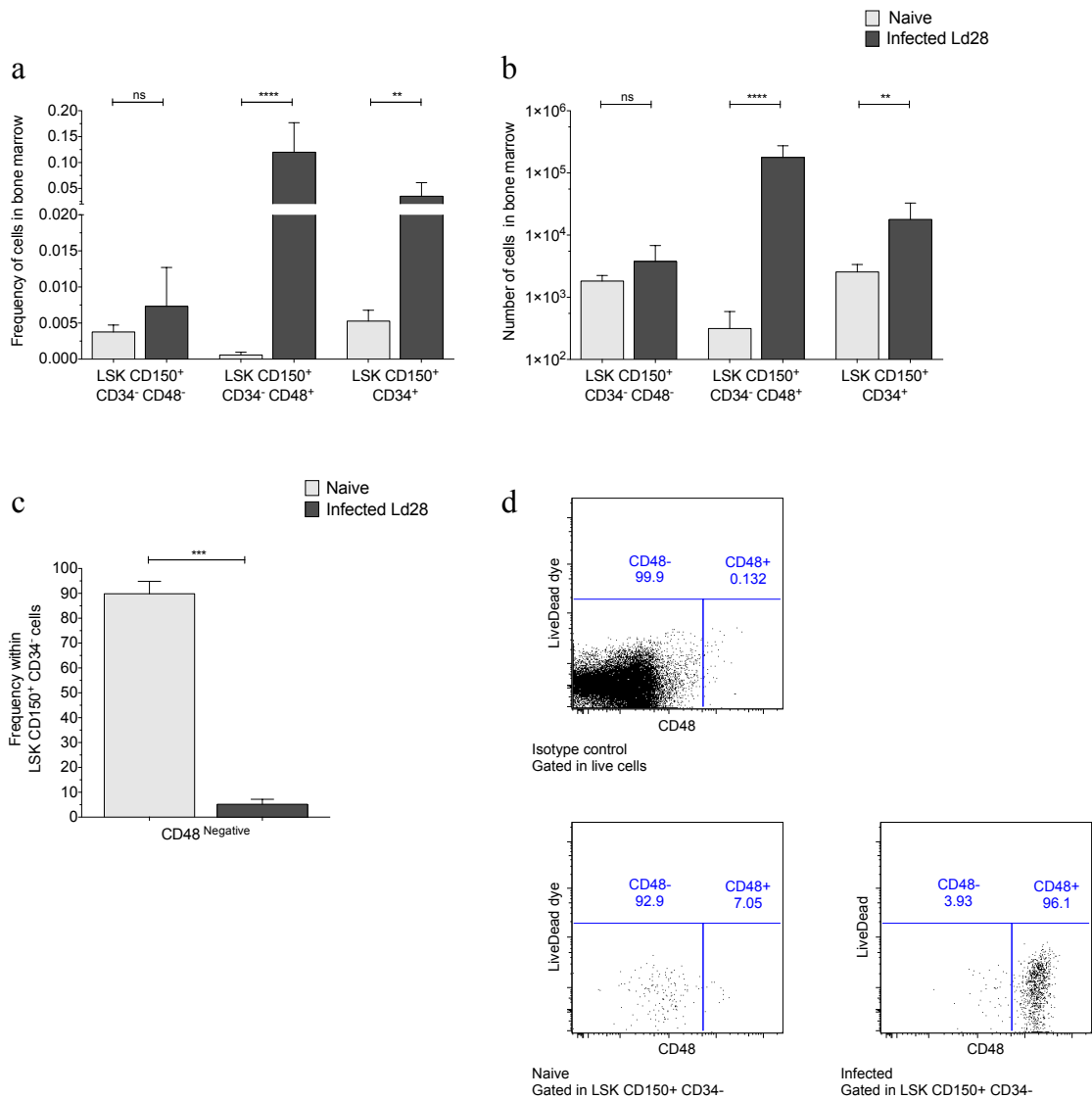


Figure 3.14 - Increased expression of CD48 on LSK CD150⁺ CD34⁻ cells (enriched for phenotypic LT-HSCs) following *L. donovani* infection. (a) Frequency of LSK CD150⁺ CD34⁻ CD48⁻ cells, LSK CD150⁺ CD34⁻ CD48⁺ cells and LSK CD150⁺ CD34⁺ cells in BM of B6 mice non-infected and infected mice. (b) Number of LSK CD150⁺ CD34⁻ CD48⁻ cells, LSK CD150⁺ CD34⁻ CD48⁺ cells and LSK CD150⁺ CD34⁺ cells in BM of B6 mice non-infected and infected mice. (c) Frequency of cells not expressing CD48 within LSK CD150⁺ CD34⁻ cell in BM of B6 mice non-infected and infected mice. (d) Representative dot plots of gating strategy applied to define CD48 positive expression according with the isotype control background (top left), dot plots displaying frequency of CD48⁺ and CD48⁻ cells within LSK CD150⁺ CD34⁻ population in a naive (bottom left) and in a infected mouse (bottom right). Comparisons were always made with BM cells recovered from non-infected mice and mice infected with *L. donovani* for 28 days (Ld28). Absolute numbers were calculated from two femurs and two tibias for each mouse. Comparisons were made between naive (n=12) and infected mice (n=12), from three independent experiments. Data was presented as Mean ± SD, p values were determined using unpaired t test: not significant, *p ≤ 0.05, **p ≤ 0.01, ***p ≤ 0.001, ****p ≤ 0.0001.

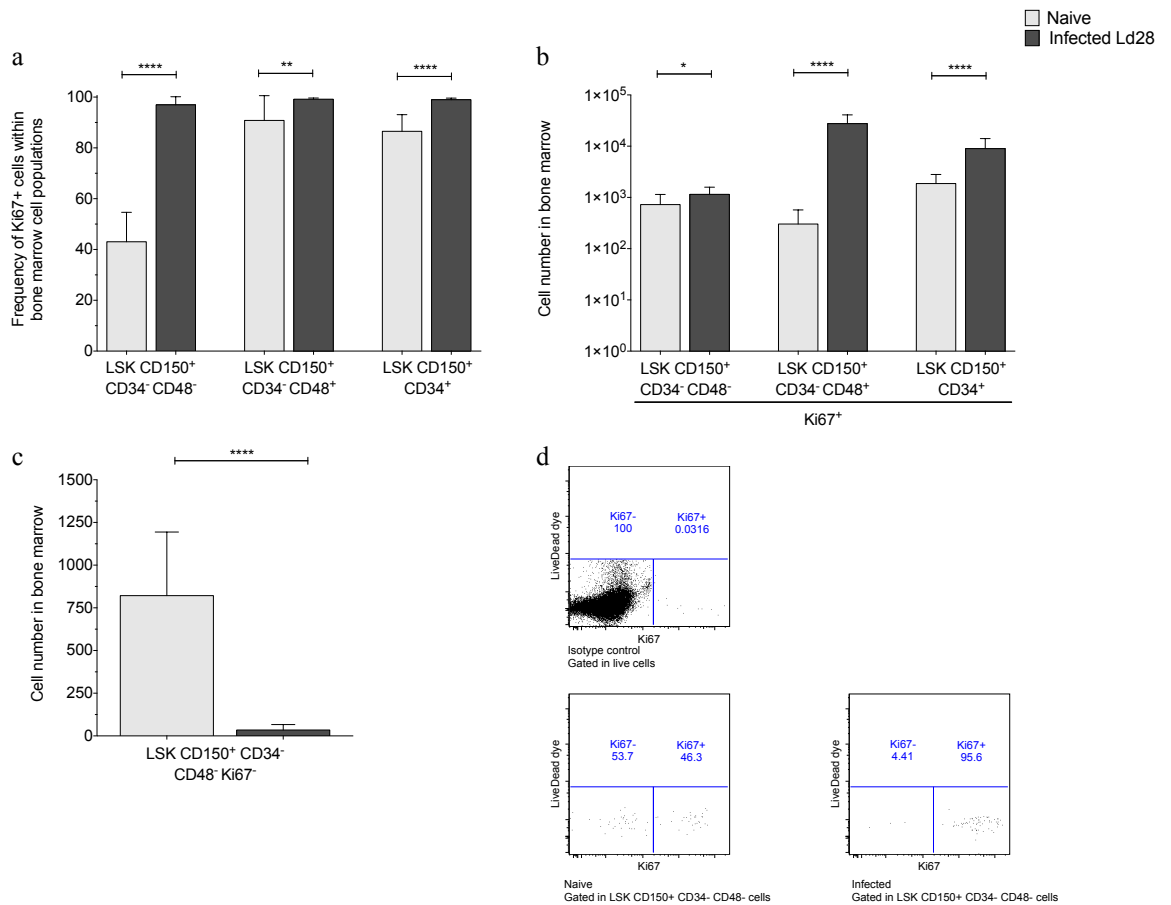


Figure 3.15 - Loss of quiescent LSK CD34⁻ CD150⁺ CD48⁻ cells (enriched for LT-HSCs) following *L. donovani* infection. (a) Frequency of Ki67⁺ within LSK CD150⁺ CD34⁻ CD48⁻ cells, LSK CD150⁺ CD34⁺ CD48⁺ cells and LSK CD150⁺ CD34⁺ cells in BM of B6 mice non-infected and infected mice. (b) Number of LSK CD150⁺ CD34⁻ CD48⁻ cells, LSK CD150⁺ CD34⁺ CD48⁺ cells and LSK CD150⁺ CD34⁺ in active cell-cycle (expressing Ki67) in BM of B6 mice non-infected and infected mice. (c) Number of LSK CD150⁺ CD34⁻ CD48⁻ cells in G0 (not expressing Ki67) in BM of B6 mice non-infected and infected with LV9 for 28 days. (d) Representative dot plots of gating strategy applied to define Ki67 expression according with the isotype control background (top left), dot plots displaying frequency of Ki67⁺ and Ki67⁻ cells within LSK CD150⁺ CD34⁻ CD48⁻ population in a naive (bottom left) and in a infected mouse (bottom right). Comparisons were always made with cells recovered from the BM of non-infected mice (n=10) and mice infected with *L. donovani* for 28 days (Ld28), (n=11). Absolute numbers were calculated from two femurs and two tibias for each mouse. Data presented from three independent experiments was presented as Mean ± SD, p values were determined using unpaired t test: not significant (ns), *p ≤ 0.05, **p ≤ 0.01, ***p ≤ 0.001, ****p ≤ 0.0001.

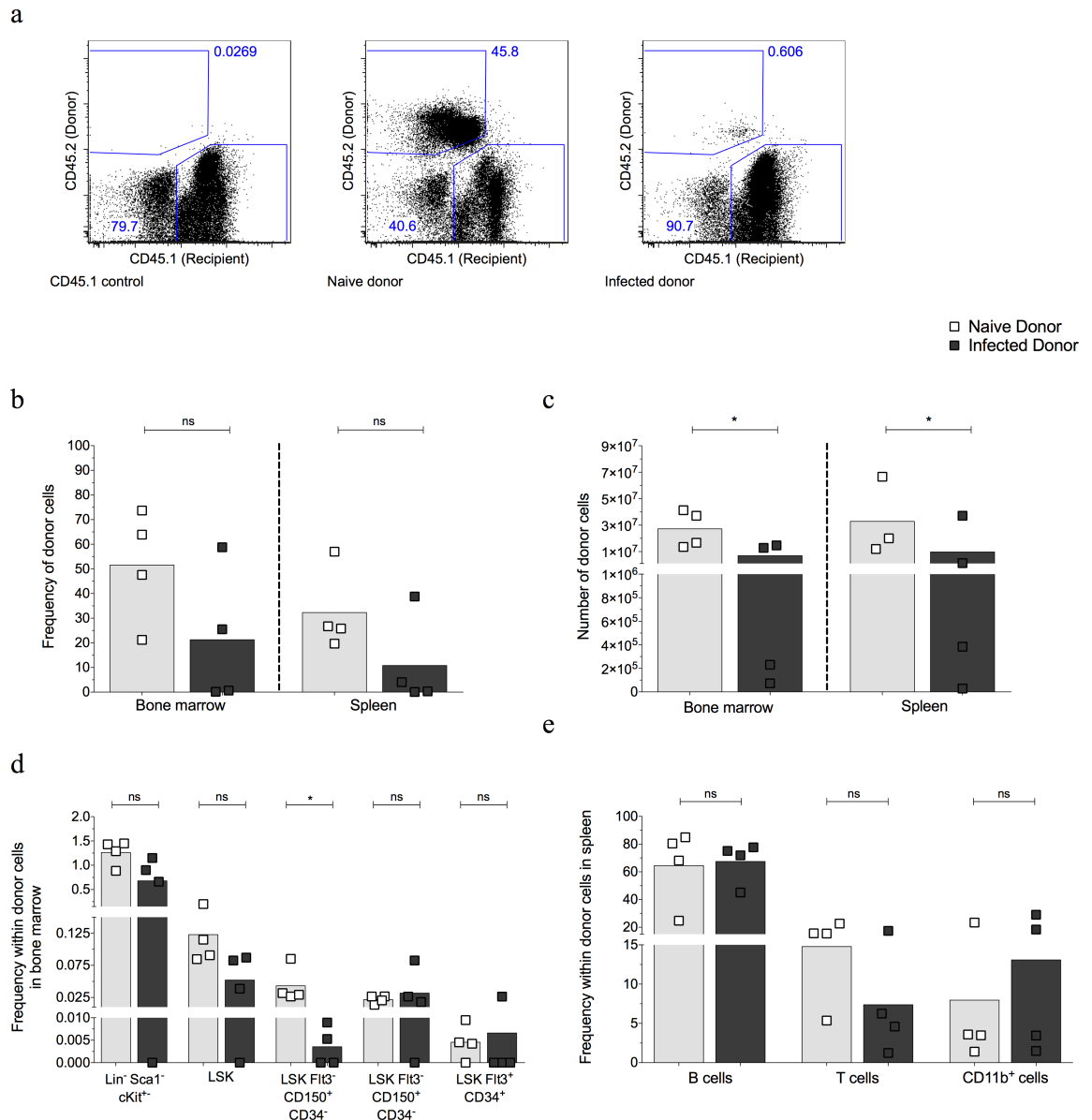


Figure 3.16 - LSK CD150⁺ CD34⁻ CD48⁻ cells (enriched for HSCs) from infected mice were impaired in their efficiency to engraft and poorly reconstituted the periphery. (a) Representative dot plots of gating strategy used to segregate between recipient (CD45.1) and donor cells (CD45.2) within live cells, displaying frequency for each population in BM: naive B6 CD45.1 control (left), recipient transplanted HSCs derived from naive donor (center) and recipient transplanted with HSCs derived from infected donor (right). (b) Frequency of donor haematopoietic cells in the BM and in the spleen of recipient mice. (c) Number of donor haematopoietic cells in the BM and in the spleen of recipient mice. (d) Frequency of donor haematopoietic progenitors cells: Lin⁻ Sca1⁻ cKit⁺ cells (enriched for lineage-committed progenitors), LSK cells (enriched for non-committed progenitors), LSK CD150⁺ FLT3⁻ CD34⁻ cells, LSK CD150⁺ FLT3⁻ CD34⁺ cells, LSK CD150⁺ FLT3⁺ CD34⁺ cells within donor cells in BM of recipient mice. (e) Frequency of mature haematopoietic cells: B cells, T cells and CD11b⁺ cells (myeloid cells) within donor cells in the spleen of recipient mice. Analysis were performed 16 weeks after transplant of CD45.2 HSCs (160 cells) sort purified from mice naive or day 28

infected mice along with a radiation protective dose of 3.5×10^5 CD45.1 total BM cells to lethally irradiated CD45.1 recipients. Absolute numbers were calculated from two femurs and two tibias for each mouse. Data shown as scatter plot and mean bar. Comparisons were made between naive donor cells (n=4) and infected donor cells (n=4 or n=3). p values were determined using unpaired t test: not significant (ns), *p \leq 0.05, **p \leq 0.01, ****p \leq 0.001.

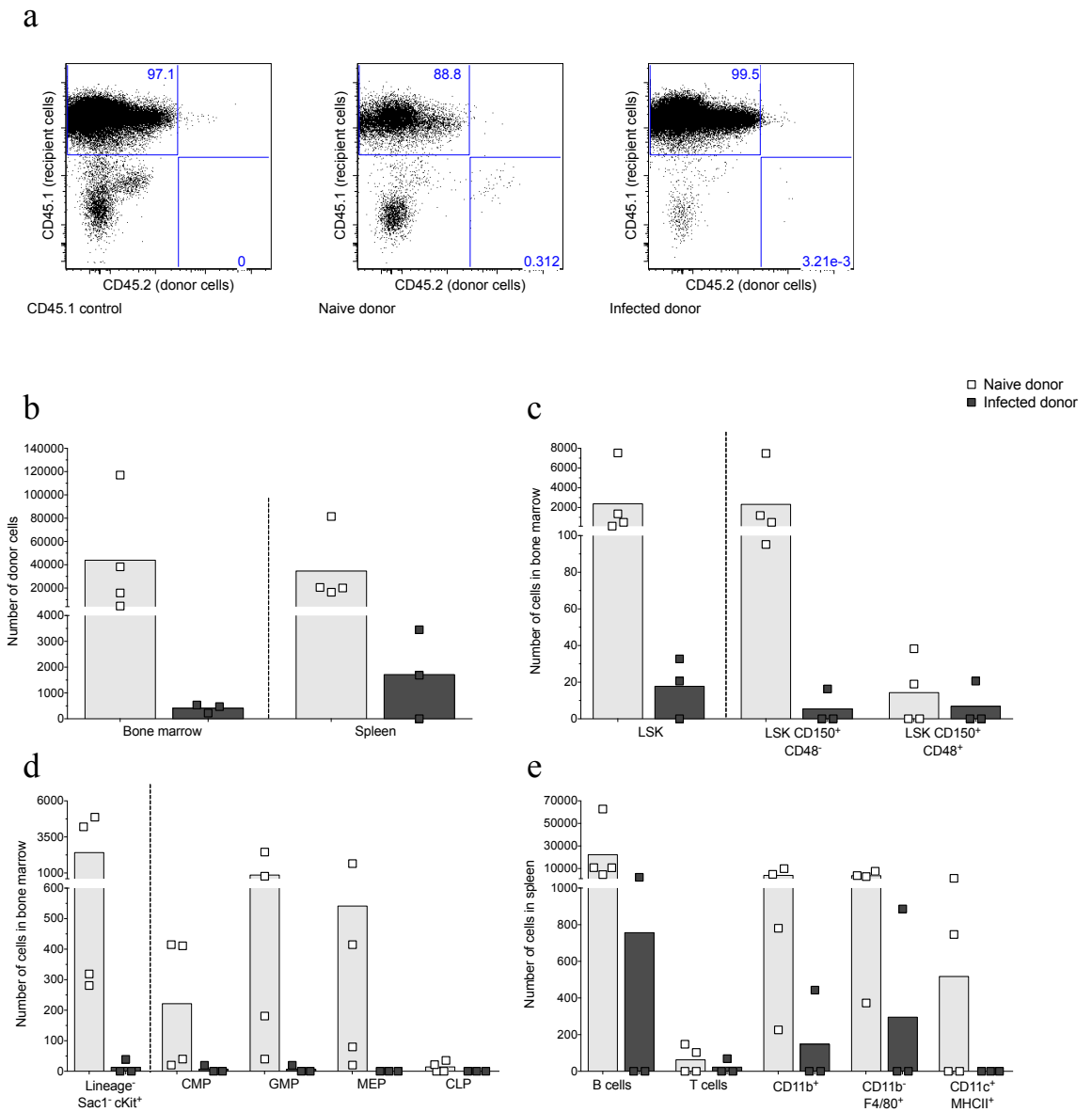


Figure 3.17 - LSK CD150⁺ CD34⁻ CD48⁻ cells (enriched for HSCs) from infected mice were impaired in engraftment efficiency in secondary adoptive transfer. (a) Representative dot plots of gating strategy used to segregate between recipient (CD45.1) and donor cells (CD45.2) within live cells, displaying frequency for each population in BM: naive B6 CD45.1 control (left), recipient transplanted HSCs derived from naive donor (center) and recipient transplanted with HSCs derived from infected donor (right). (b) Number of donor haematopoietic cells in the BM and in the spleen. (c) Number of LSK cells (enriched for non-committed progenitors), LSK CD150⁺ CD48⁻ cells and LSK CD150⁺ CD48⁺ cells derived from donor cells, in BM. (d) Number of lineage-committed progenitors (enriched among Lin⁻ Sca1⁻ cKit^{hi} cells), CMPs, GMPs, MEPs and CLPs derived from donor cells in the BM. (e) Number of mature haematopoietic cells derived from donor cells in the spleen of recipient mice: B cells, T cells and CD11b⁺ cells, CD11b⁻ F4/80⁺ cells, CD11c⁺ MHC II⁺ cells. Analysis performed 24 weeks after transplant into B6 CD45.1 lethally irradiated mice of radiation protective total BM cells (3.5×10^5) and 50 CD45.2 HSCs

(LSK CD150⁺ CD34⁻ CD48⁻ cells) sort purified from CD45.1 recipient mice previously that were previously adoptively transferred with CD45.2 HSCs from mice naive or day 28 infected mice, alongside a radiation protective dose of total BM cells, to lethally irradiated CD45.1 recipient mice for 16 weeks. Absolute numbers were calculated from two femurs and two tibias for each mouse. Data was presented as scatter plot and mean bar.

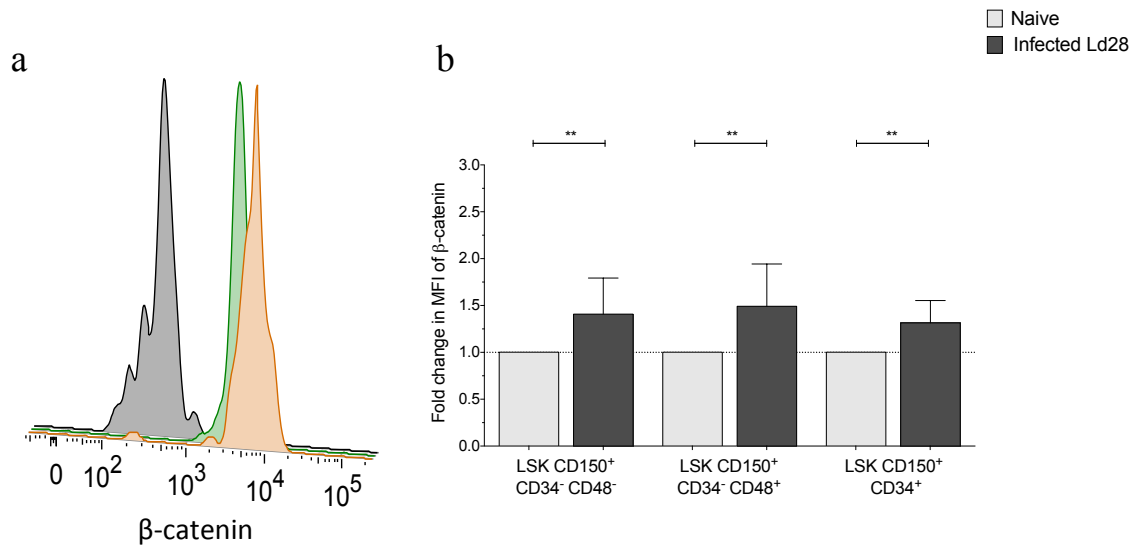


Figure 3.18 - LSK CD34⁻ CD150⁺ CD48⁻ cells (enriched for LT-HSCs) accumulate higher levels of β -Catenin. (a) Representative histogram overlay of β -catenin expression in LSK CD34⁻ CD150⁺ CD48⁻ cells (enriched for LT-HSCs): isotype control (grey), naive mouse (green) and infected mouse (orange). (b) Fold change in mean intensity fluorescence (MFI) of β -catenin in LSK CD150⁺ CD34⁻ CD48⁻ cells (enriched for LT-HSCs), LSK CD150⁺ CD34⁻ CD48⁺ cells and LSK CD150⁺ CD34⁺ cells infected mice, in each experiment the MFI calculated for infected mice was divided by the average MFI calculated for naive controls in each experiment. Comparisons were always made with cells recovered from the BM of non-infected mice (n=13) and mice infected with *L. donovani* for 28 days (Ld28), (n=13). Data presented from three independent experiments was presented as Mean \pm SD, p values were determined using Wilcoxon signed-rank test: not significant (ns), *p \leq 0.05, **p \leq 0.01, ***p \leq 0.001, ****p \leq 0.0001.

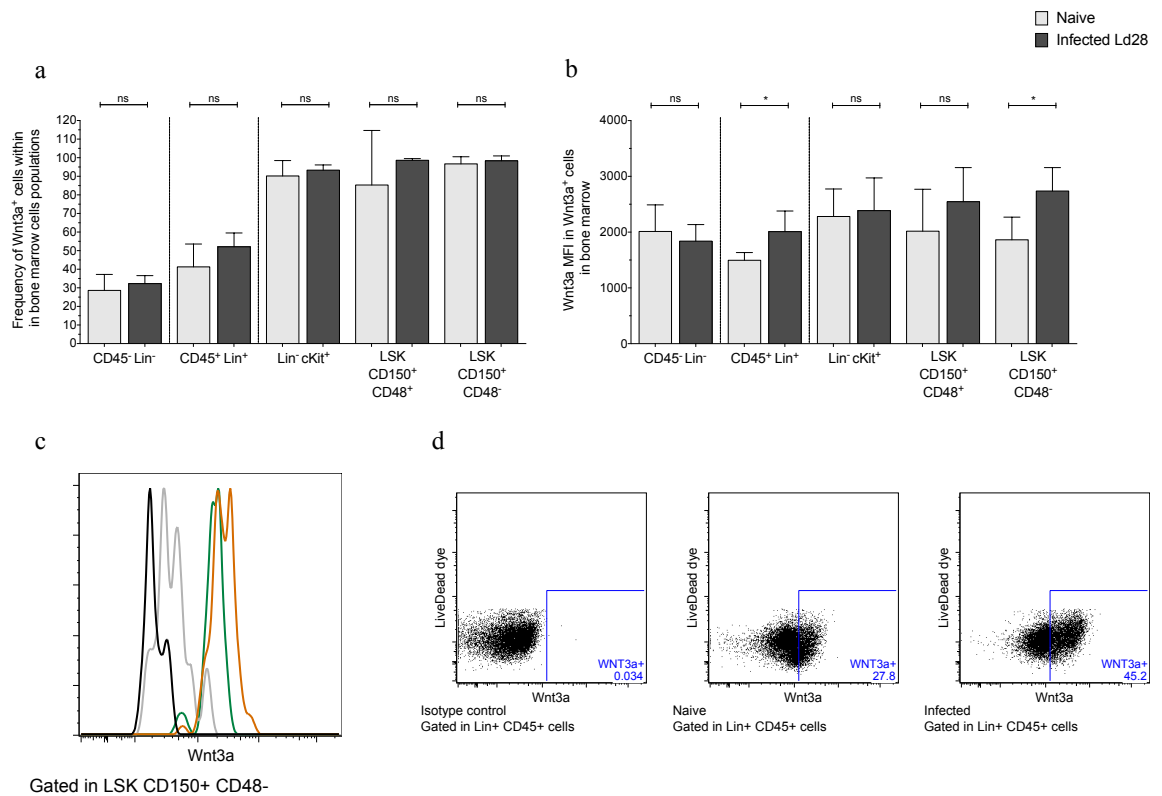


Figure 3.19 - Mature haematopoietic cells in bone marrow of *L. donovani* infected mice express increased levels of Wnt3a protein. (a) The frequency of cells Wnt3a⁺ was determined within CD45⁻ Lin⁻ cells (stromal cells), CD45⁺ Lin⁺ cells (mature haematopoietic cells), CD45⁺ Lin⁻ cells (enriched for haematopoietic progenitor cells), CD45⁺ LSK CD150⁺ CD48⁺ cells and CD45⁺ LSK CD150⁺ CD48⁻ cells. (b) Mean intensity fluorescence (MFI) of Wnt3a in LSK CD150⁺ CD48⁻ cells (enriched for LT-HSCs) and LSK CD150⁺ CD48⁺ cells expressing Wnt3a in BM of naive and infected mice. (c) Representative histogram overlay of Wnt3a expression in LSK CD150⁺ CD48⁻ cells (enriched for LT-HSCs): naive isotype control (dark grey), infected isotype control (light grey), naive mouse (green) and infected mouse (orange). (d) Representative dot plots of gating applied to select Wnt3a positive cells in CD45⁺ Lin⁺ cells. Comparisons were always made with cells recovered from the BM of non-infected mice (n=4) and mice infected with *L. donovani* for 28 days (Ld28), (n=4). Data from one experiment was presented as Mean ± SD, p values were determined using unpaired t test: not significant (ns), *p ≤ 0.05, **p ≤ 0.01, ***p ≤ 0.001, ****p ≤ 0.0001.

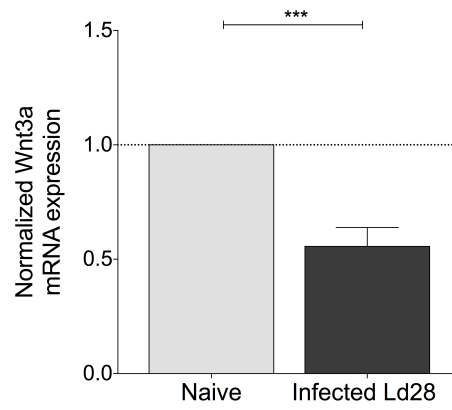


Figure 3.20 - Accumulation of *Wnt3a* mRNA is reduced in total BM cells from *L. donovani* infected mice. Quantitative PCR (qPCR) analysis of *Wnt3a* mRNA accumulation in total bone marrow cells. Results are presented in-terms of a fold change after normalizing with HPRT1 mRNA. Comparisons were made with cells recovered from the BM of non-infected mice (n=3) and mice infected with *L. donovani* for 28 days (Ld28), (n=3). Data from one experiment was presented as Mean \pm SD, p values were determined using unpaired t test: not significant (ns), *p \leq 0.05, **p \leq 0.01, ***p \leq 0.001, ****p \leq 0.0001.

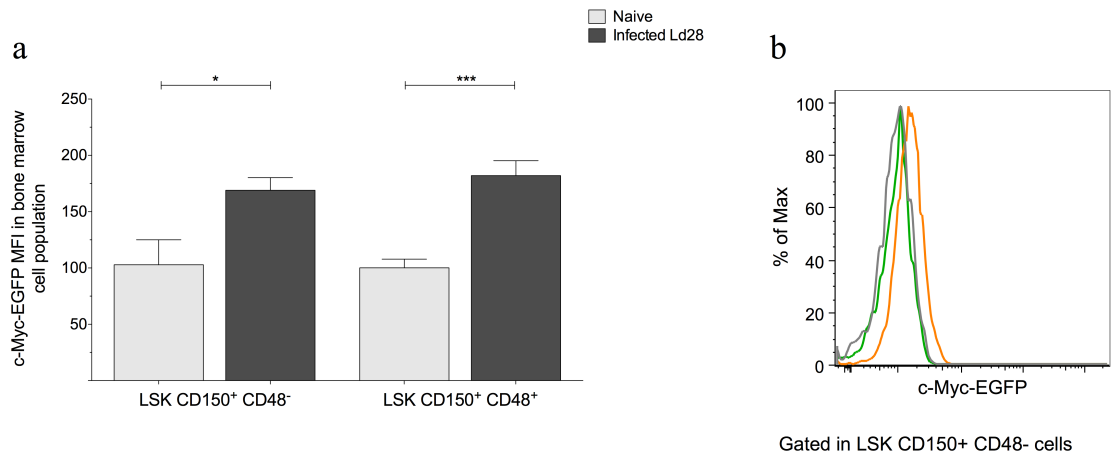


Figure 3.21 - HSCs in BM expressed increased levels of c-Myc during infection with *L. donovani*. (a) Mean intensity fluorescence (MFI) of cMyc-EGFP in LSK CD150⁺ CD48⁻ cells (enriched for LT-HSCs) and LSK CD150⁺ CD48⁺ cells in BM of naive and infected mice. (b) Representative histogram overlay of c-Myc-EGFP expression in LSK CD150⁺ CD48⁻ cells (enriched for LT-HSCs): WT control (grey), naive mouse (green) and infected mouse (orange). Comparisons were always made with cells recovered from the BM of non-infected mice (n=3) and mice infected with *L. donovani* for 28 days (Ld28), (n=3). Data from one experiment was presented as Mean \pm SD, p values were determined using unpaired t test: not significant (ns), *p \leq 0.05, **p \leq 0.01, ***p \leq 0.001, ****p \leq 0.0001.

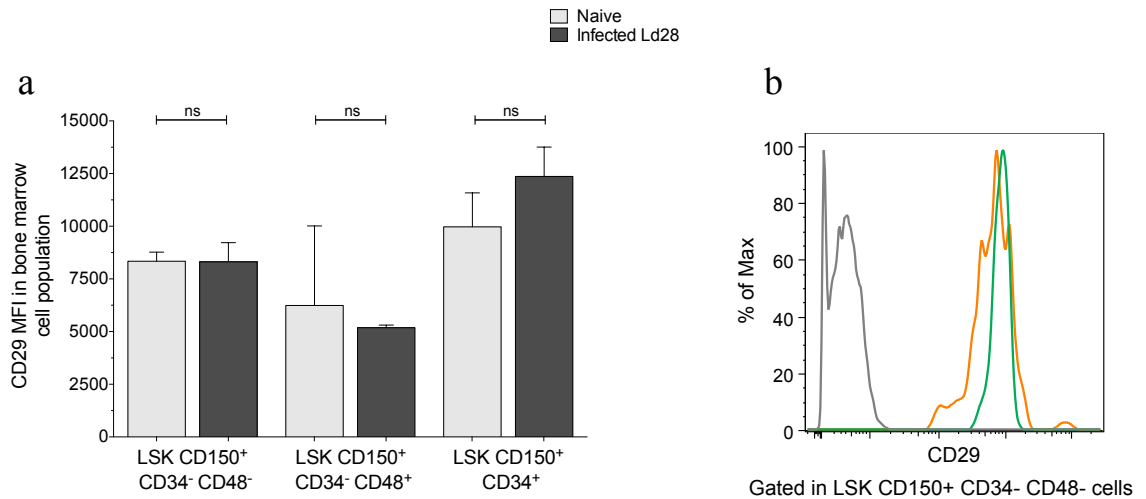


Figure 3.22 - The expression of CD29 levels in LT-HSCs was unaltered during infection with *L. donovani*. (a) Mean intensity fluorescence (MFI) of CD29 in LSK CD150⁺ CD34⁻ CD48⁻ cells (enriched for LT-HSCs) LSK CD150⁺ CD34⁻ CD48⁺ cells and LSK CD150⁺ CD34⁺ cells in BM of naive and infected mice. (b) Representative histogram overlay of CD29 expression in LSK CD150⁺ CD34⁻ CD48⁻ cells (enriched for LT-HSCs): WT control (grey), naive mouse (green) and infected mouse (orange). Comparisons were always made with cells recovered from the BM of non-infected mice (n=3) and mice infected with *L. donovani* for 28 days (Ld28), (n=3). Data from one experiment was presented as Mean \pm SD, p values were determined using unpaired t test: not significant (ns), *p \leq 0.05, **p \leq 0.01, ***p \leq 0.001, ****p \leq 0.0001.

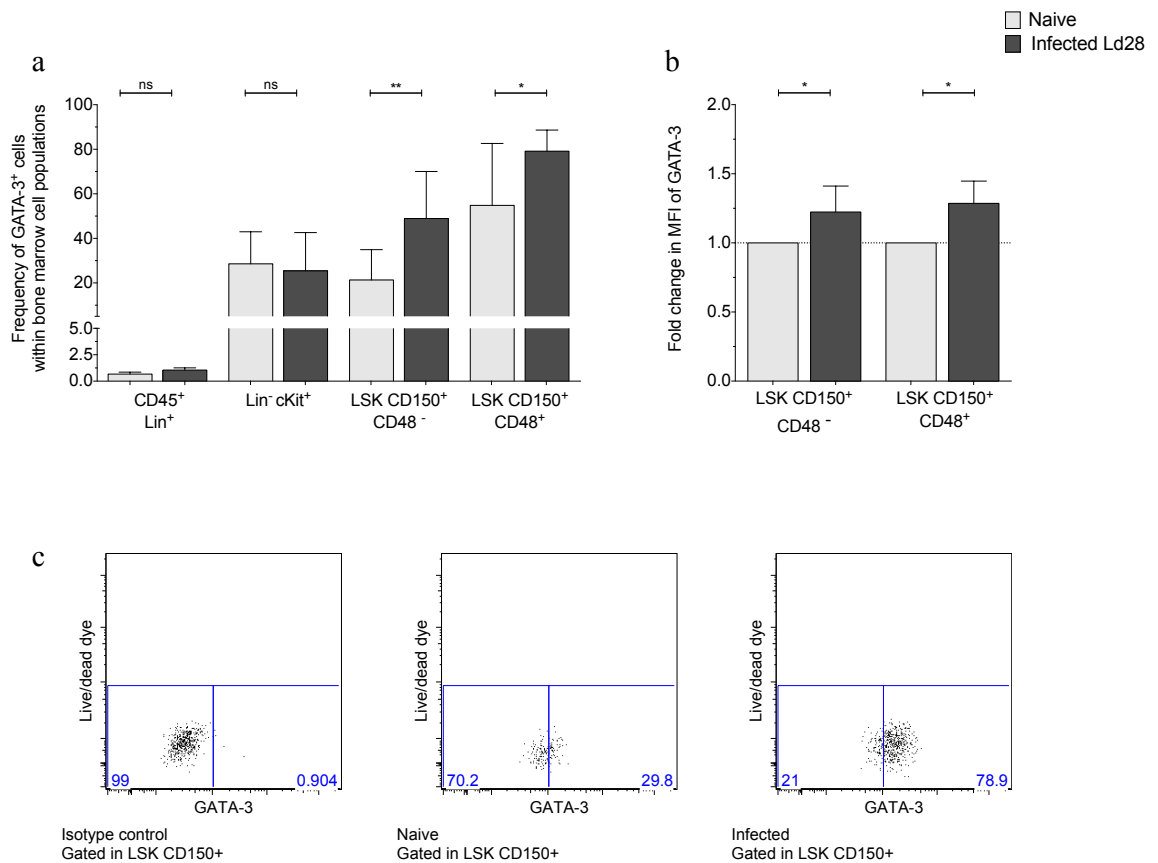


Figure 3.23 - The frequency of LSK CD150⁺ CD48⁻ cells (enriched for LT-HSCs) expressing GATA-3 was increased following *L. donovani* infection. (a) The frequency of GATA-3⁺ cells was determined within CD45⁺ Lin⁺ cells (mature haematopoietic cells), CD45⁺ Lin⁻ cKit⁺ cells (enriched for haematopoietic progenitor cells), CD45⁺ LSK CD150⁺ CD48⁺ (other multipotent progenitors) cells and CD45⁺ LSK CD150⁺ CD48⁻ cells (enriched for LT-HSCs). Data from two independent experiment was presented as Mean \pm SD, p values were determined using unpaired t test: not significant (ns), *p \leq 0.05, **p \leq 0.01, ***p \leq 0.001, ****p \leq 0.0001. (b) Fold change in mean intensity fluorescence (MFI) of GATA-3 in LSK CD150⁺ CD48⁻ cells and LSK CD150⁺ CD48⁺ cells expressing GATA-3 in BM of infected mice calculated using the average MFI determined in naive mice for each experiment. Data from two independent experiment was presented as Mean \pm SD, p values were determined using Wilcoxon signed-rank test: not significant (ns), *p \leq 0.05, **p \leq 0.01, ***p \leq 0.001, ****p \leq 0.0001. Comparisons were always made with cells recovered from the BM of non-infected mice (n=8) and mice infected with *L. donovani* for 28 days (Ld28), (n=8). (c) Representative dot plots of gating applied to select GATA-3 positive cells in LSK CD150⁺ cells.

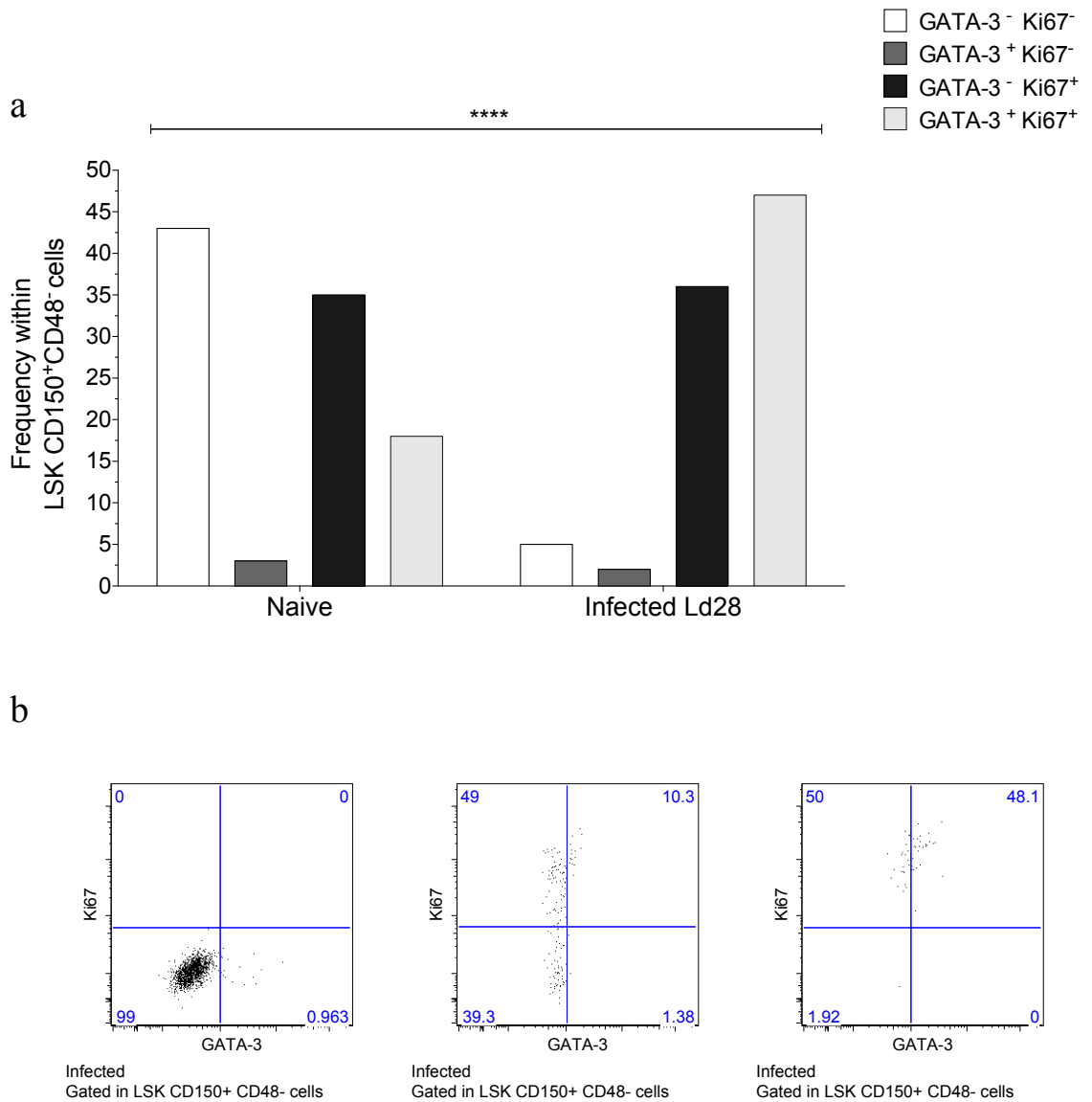


Figure 3.24 - The distribution of LSK CD150⁺ CD48⁻ cells (enriched for LT-HSCs) segregated according with the expression of GATA-3 and Ki67 is altered following *L. donovani* infection. (a) Distribution of cells according with Ki67 and GATA-3 expression within LSK CD150⁺ CD48⁻ cells. Comparisons were always made with cells recovered from the BM of non-infected mice (n=8) and mice infected with *L. donovani* for 28 days (Ld28), (n=8). Data presented from two independent experiment is presented as Mean, p value was determined using Chi-square test: not significant (ns), *p ≤ 0.05, **p ≤ 0.01, ***p ≤ 0.001, ****p ≤ 0.0001. (b) Representative dot plots of Ki67 and GATA-3 expression within LSK CD150⁺ CD48⁻ cells.

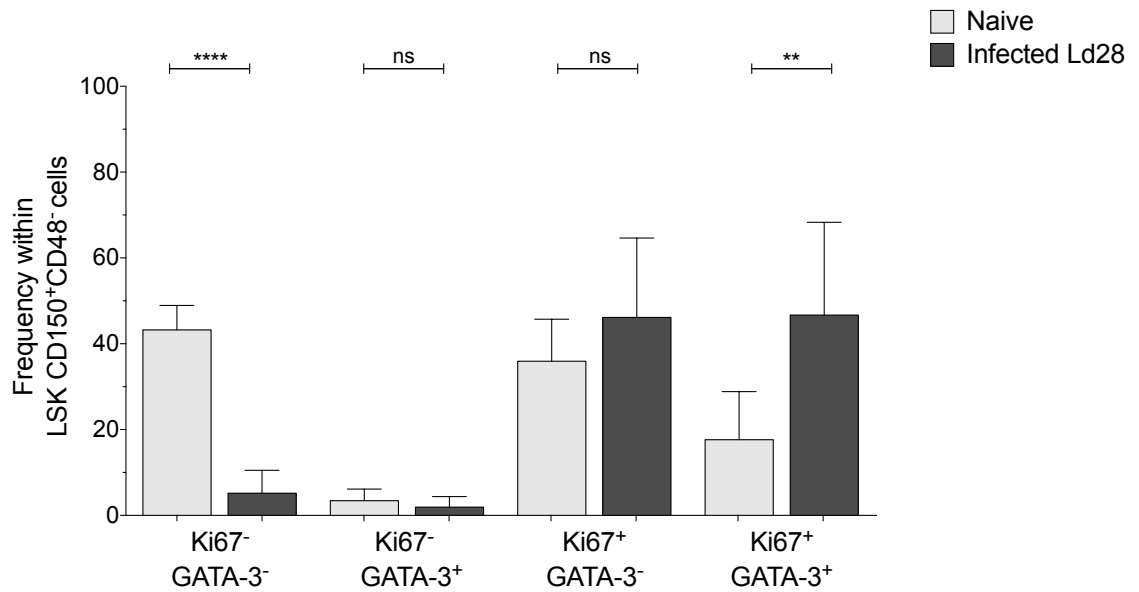


Figure 3.25 - Cycling LSK CD150⁺ CD48⁻ cells (enriched for LT-HSCs) upregulated GATA-3 expression following *L. donovani* infection. Frequency of cells expressing Ki67 and GATA-3 within LSK CD150⁺ CD48⁻ cells, in BM of naive and infected mice. Comparisons were always made with cells recovered from the BM of naive mice (n=8) and mice infected with *L. donovani* for 28 days (Ld28), (n=8). Data from two independent experiment was presented as Mean \pm SD, p values were determined using unpaired t test: not significant (ns), *p \leq 0.05, **p \leq 0.01, ***p \leq 0.001, ****p \leq 0.0001.

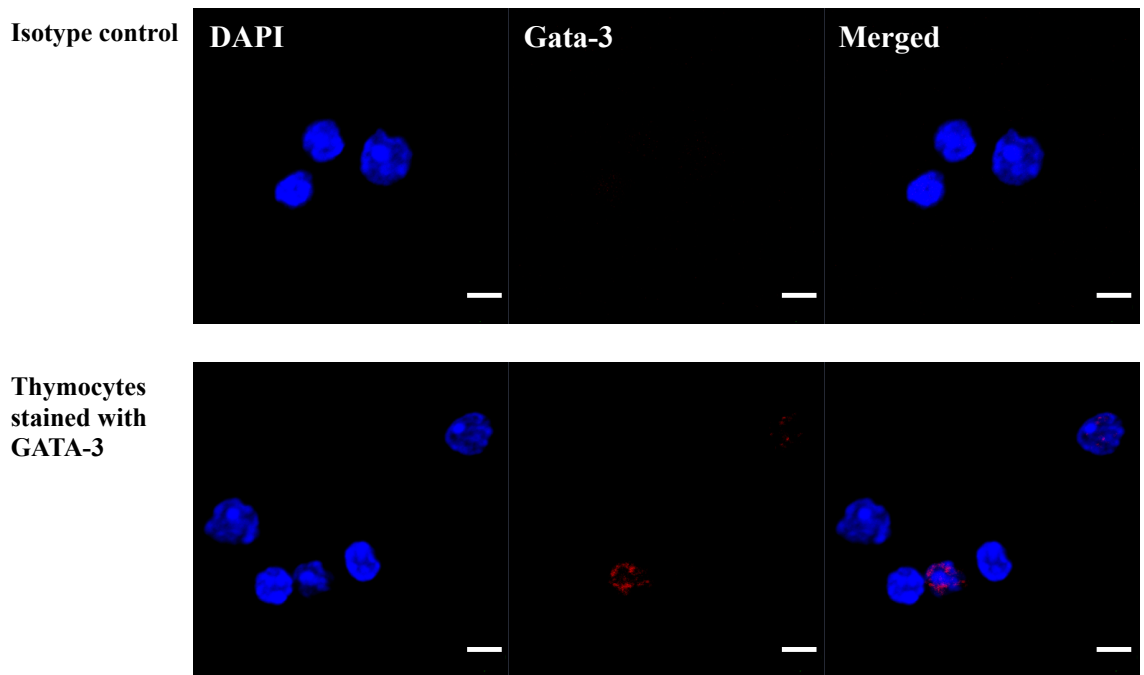


Figure 3.26 - Detection of the subcellular localization of GATA-3 protein by immunofluorescence microscopy analyses in total thymocytes. Representative confocal immunofluorescence microscopy images of thymocytes of mice infected with *L. donovani* for 28 days were fixed, permeabilized, and examined for GATA-3 (red) and the DNA-intercalating dye DAPI (blue) expression. Confocal fluorescent images were obtained with a objective Plan-Apochromat 63x. Bar, 5 μ m

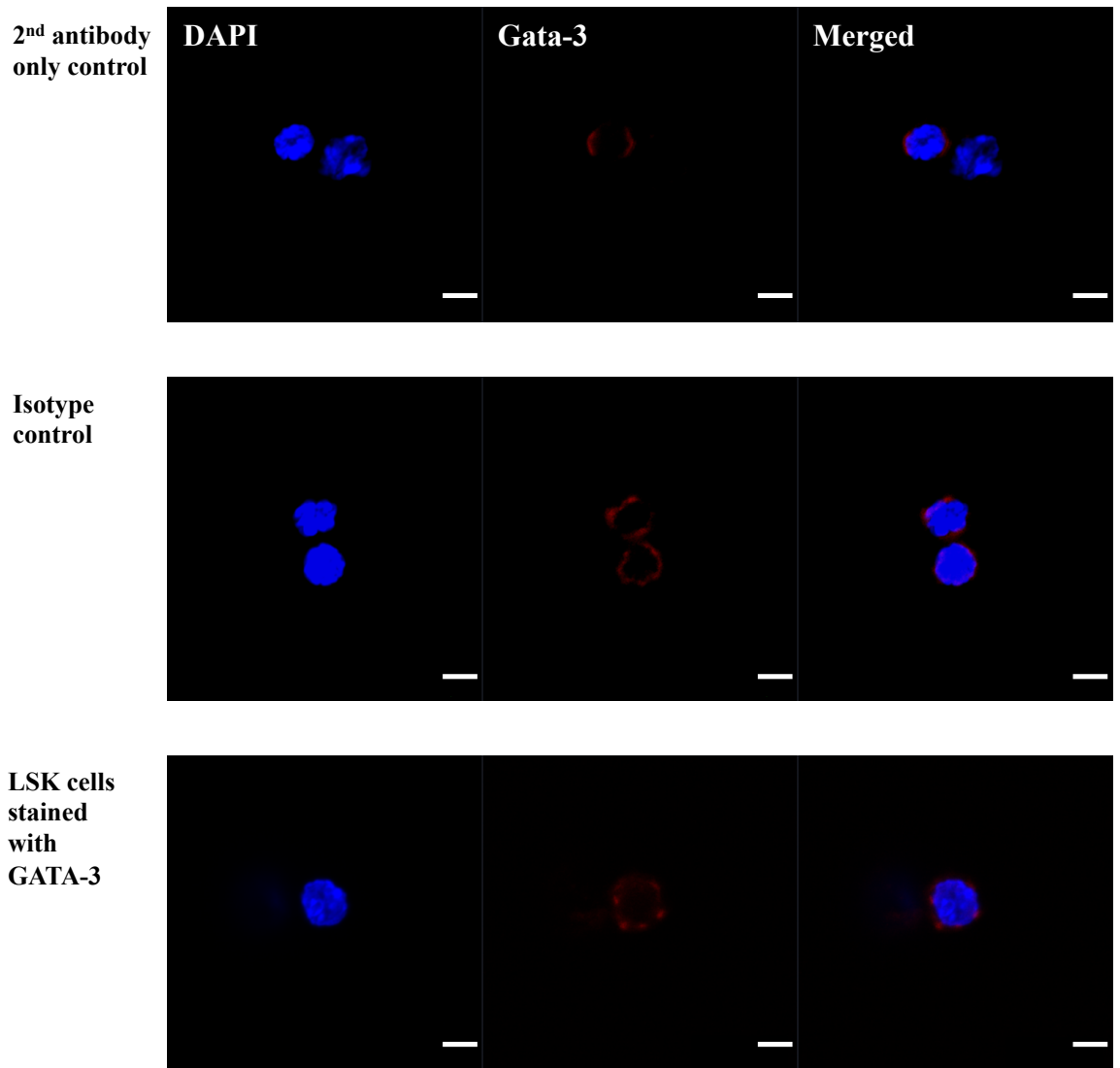


Figure 3.27 - GATA-3 protein subcellular localization by immunofluorescence microscopy analyses in LSK cells from BM. Representative confocal immunofluorescence microscopy images of sorted LSK cells from the BM of mice infected with *L. donovani* for 28 days, which were fixed, permeabilized, and examined for GATA-3 (red) and the DNA-intercalating dye DAPI (blue) expression. Confocal fluorescent images were obtained with objective Plan-Apochromat 63x. Bar, 5 μ m.

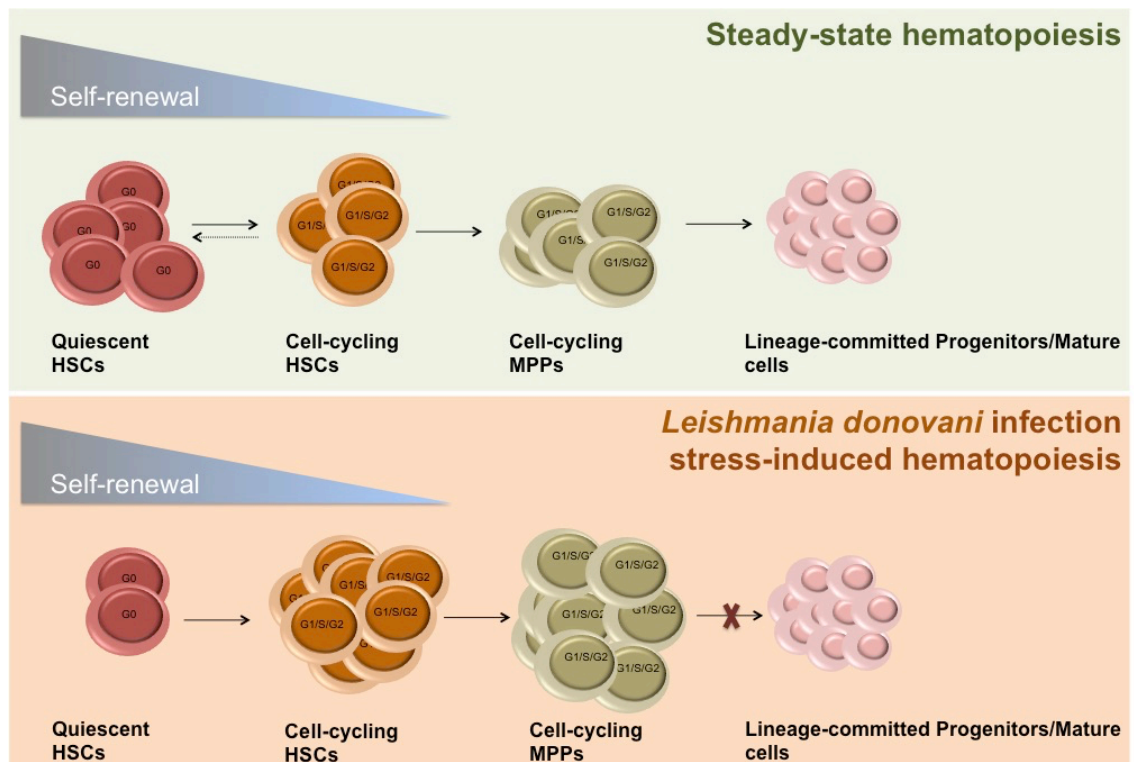


Figure 3.28 - *Leishmania donovani* infection resulted in the depletion of the reservoir of quiescent LT-HSCs in BM. Following *L. donovani* infection LT-HSCs and onward multipotent progenitors expand greatly at the expense of LT-HSCs in G0. The accumulation of intermediary multipotent progenitors is not associated to an increase in effective haematopoietic activity since the numbers of effector haematopoietic cells are unchanged or even reduced in circulation.

CHAPTER 4. CELLULAR AND MOLECULAR DETERMINANTS UNDERLYING ALTERATIONS IN HAEMATOPOIESIS DURING INFECTION WITH *L. DONOVANI*

4.1 INTRODUCTION

VL is still one of the most neglected tropical diseases despite its dramatic impact in morbidity and mortality in endemic areas. This infection is fatal if left untreated and a prophylactic vaccine is not yet available. In very severe cases, patients may die due to increased vulnerability to secondary infection or due to coagulopathies (M. A. Santos *et al.*, 2002, V. E. Miranda de Araujo *et al.*, 2012). In humans, the clinical manifestations of disease vary considerably from sub-clinical to severe and include, hepatosplenomegaly, fever, weight loss and pancytopenia (P. M. Kaye *et al.*, 2004).

Alterations in the haematological system are common in chronic VL, not only in humans and dogs, natural reservoirs for *L. donovani* (N. Varma and S. Naseem, 2010, F. A. d. Pinho, 2015), but also in experimental models of disease such as mice and hamsters (W. P. Lafuse *et al.*, 2013, F. A. d. Pinho, 2015). The impairment of the haematological system includes changes not only in peripheral blood, such as anaemia, thrombocytopenia and leucopenia, but also alterations in BM such as erythroid hypoplasia, dysplasia of myeloid cells, accumulation of blasts and histiocytic hyperplasia (N. Varma and S. Naseem, 2010, F. A. d. Pinho, 2015). Nevertheless, the mechanisms by which VL modulates alterations in the haematological system remain elusive.

The induction of stress-induced haematopoiesis during infection have been long described as means to replace the large numbers of immune effector cells consumed fighting invading pathogens, for example emergency myelopoiesis in septicemia. In recent years, it has been shown that HSPCs, besides responding to the increased demand for immune cells, can be directly activated by pathogen-associated patterns and pro-inflammatory cytokines, recognized respectively by pattern recognition receptors and cytokines receptors, expressed on their surface. Furthermore, the impact of infection is not restricted to lineage-committed progenitors, but includes more immature cells such as LT-HSCs (K. Y. King and M. A. Goodell, 2011).

The regulation of LT-HSCs numbers is a strictly regulated process aiming to maintain the homeostatic levels of blood cells and simultaneously prevent LT-HSCs exhaustion (C. Mirantes *et al.*, 2014). Under homeostatic condition most LT-HSCs are in quiescence, which have been

correlated to the maintenance of long-term self-renewal potential and multipotency, and protects these cells from cytotoxicity and mutagenesis (M. R. Warr *et al.*, 2011). Nevertheless, LT-HSCs can be very quickly pushed into active cell-cycle by a multiplicity of stimuli, including TLR-signalling, pro-inflammatory cytokines and growth factors (K. Y. King and M. A. Goodell, 2011).

Haematopoietic progenitors possess the machinery to directly sense infectious particles, such as TLRs, and high expression of TLR2, TLR4, and MD-2 mRNA was observed in HSCs (Y. Nagai *et al.*, 2006b). *In vitro* cultures of purified LSK cells (a population highly enriched in HSCs) showed that these primitive cells respond to LPS, a TLR4 ligand, or Pam3CSK4, a ligand for TLR2, increasing the expression of markers associated with myeloid lineage commitment. The stimulation of TLR2 and TLR4 was also associated with increased proportions of cells in cell-cycle within HSCs (LSK Flt3⁻ cells), as assessed by BrdU labelling experiments (Y. Nagai *et al.*, 2006a). In mice infected with *Pseudomonas aeruginosa*, a model for severe sepsis, intact TLR4 signalling was required to activate LSK cells into proliferation in response to the infection (S. Rodriguez *et al.*, 2009).

It was proposed that during infection, high systemic levels of M-CSF may act on M-CSF receptor expressed on LT-HSCs and induce the expression of the transcription factor PU.1, driving HSCs differentiation toward the myelomonocytic lineage (N. Mossadegh-Keller *et al.*, 2013). *In vivo* experiments showed the induction of PU.1 expression in LT-HSCs in LPS-challenged hosts or after injection of recombinant M-CSF, and this was correlated to an increase in myeloid progenitors in BM and myeloid effector cells in the spleen (N. Mossadegh-Keller *et al.*, 2013).

The mouse model of *M. avium* infection allowed the study of HSC in a chronic non-cytopenic systemic infection, characterized by the maintenance of the absolute number of mature cells in circulation. During infection an increase in the proliferation and mobilization of LT-HSCs was observed, and these displayed decreased repopulation capacity in secondary recipients. These features were abrogated in mice lacking IFN γ receptor 1 (*Ifngr1*) or *Stat1*, encoding the downstream signal transducer for IFN γ receptor subunit 1 (M. T. Baldrige *et al.*, 2010).

In addition to systemic factors, signals provided by the BM microenvironment including osteoblasts, osteoclasts, endothelial cells, adipocytes and mesenchymal stem and progenitor cells, the so-called BM stroma (F. E. Mercier *et al.*, 2012), regulate the functions of HSCs and other haematopoietic progenitors. Several studies have suggested that the BM stroma can respond to infection through the expression and secretion of immunomodulatory molecules, which can then modulate the haematopoiesis (F. E. Mercier *et al.*, 2012). For example, it has been showed that following LPS administration, MSCs express CCL2, and this was also reported in mice infected with *Listeria monocytogenes*. The deletion of CCL2 in MSCs (Nestin⁺ cells) was associated with

impaired monocyte emigration from the BM resulting in increased susceptibility to *L. monocytogenes* infection (C. Shi *et al.*, 2011). Furthermore, exogenous administration of G-CSF, which is released during inflammation, was associated with a decrease in CXCL12 production by osteoblasts that resulted in increased mobilization of HSCs (M. J. Christopher *et al.*, 2009).

More recently, it was shown that in mice infected with LCMV, a model of acute viral infection, CD8⁺ T cells expressing IFN γ favor myelopoiesis indirectly through the induction of IL-6 secretion by BM stromal cells (C. M. Schuerch *et al.*, 2014), suggesting that BM T cells may have an important role in mediating changes in haematopoiesis during infection.

T cells reside in BM, composing 4-8% of total BM cells. The function of the T cell compartment in BM has, however, seldom been investigated. Recent studies positioned BM as a preferential site for homing and persistence of memory T cells with high proliferative potential to a second encounter with a cognate antigen (F. Di Rosa and R. Pabst, 2005, K. Tokoyoda *et al.*, 2009b, K. Tokoyoda *et al.*, 2010). Furthermore, alterations in BM T cells have been reported in patients suffering from BMF syndromes (C. Dufour *et al.*, 2003) and in experimental models for aplastic anaemia (AA) (F.-c. Lin *et al.*, 2014, C. Arieta Kuksin *et al.*, 2015).

The association between alterations in haematopoietic function and changes in BM T cells were also described in mice infected with *Ehrlichia muris*, displaying severe haematopoietic impairment (K. C. MacNamara *et al.*, 2011b, Y. Zhang *et al.*, 2013). In infected mice, LSK cells were found to be proliferating, which was mediated by IFN γ acting directly on LT-HSCs, with BM CD4⁺ T cells defined as the main source of IFN γ (Y. Zhang *et al.*, 2013).

The integration of systemic and local signals by HSCs and other haematopoietic progenitors may be a mechanism to allow these cells to respond to the presence of invading pathogens, and guide progenitors to supply the haematopoietic systems with adequate cell types and amounts of effector cells required to mount an efficient immune response (C. Mirantes *et al.*, 2014). On the other hand, prolonged activation of HSCs into active proliferation has been associated with functional exhaustion in several infection models (S. Rodriguez *et al.*, 2009, M. T. Baldrige *et al.*, 2010, Y. Zhang *et al.*, 2013, K. A. Matatall *et al.*, 2014), and may underlie the association between chronic infection and hematological dysfunction, commonly described in humans (A. Jain and M. Naniwadekar, 2013).

Very recently it was shown that in mice challenged with Poly (I:C) (TLR3 ligand), which mimics the conditions for infection-induced haematopoiesis, HSCs are “pushed” to active cell-cycle and this was associated with the acquisition of DNA-damage and severe functional impairment in long-term BMT assays (D. Walter *et al.*, 2015). As such, study of the mechanisms

underlying haematological dysfunctions, frequently emerging as a consequence of an infection, are fundamental in the process of developing improved therapeutic approaches for the prevention of BMF syndromes.

In Chapter 3, we established that *L. donovani* chronic infection induced the activation of LT-HSCs into active proliferation at the expense of cells in quiescence, and this was related to the functional impairment of LT-HSCs following transfer to lethally irradiated mice. Both in humans and in experimental models of disease, the basis for the establishment of haematological alterations during chronic infection with *L. donovani* remain elusive. As such, in this chapter we aimed to study the molecular and cellular determinants underlying the impairment haematological function during experimental chronic VL.

4.2 RESULTS

4.2.1 Infection with *L. donovani* in immunodeficient mice was not associated to the loss of quiescent HSCs in BM.

Our initial characterization of *L. donovani* infection kinetics showed an overlap between the major alterations in the number of HSPCs and the peak of infection at 28 days p.i., both in BM and the spleen. In BM, there was a significant expansion of non-committed progenitors at the expense of LT-HSCs in G0 (Chapter 3). To determine whether these alterations were a function of parasite load per se, we infected immunodeficient Recombination activating gene 2 knockout (RAG2 KO) mice, establishing the conditions for a super-infection. We could not detect any differences in the number of multipotent haematopoietic progenitors onward from LT-HSCs in day 28 infected mice vs. non-infected mice (Figure 4.1a). Furthermore RAG2 KO mice were not depleted in the reservoir of quiescent HSCs upon infection (Figure 4.1b). As expected, extensive differences in parasite burden were found between RAG2 KO and wild-type (WT) mice (Figure 4.1c) and splenomegaly was absent (Figure 4.1d). These data indicated that the alterations in LT-HSCs and onward progenitors were not directly induced by parasite-derived molecules or through stimulus of innate immune response, but rather suggested a central role for the adaptive immune system as a driver of the haematopoietic alterations observed in WT mice.

4.2.2 Splenectomy did not impact in the increase of intermediary multipotent progenitors nor in the loss of quiescent LT-HSCs during *L. donovani* infection

In experimental VL, previous work using BALB/c mice suggested that the number of myeloid progenitors was increased in the spleen of infected mice based on the observation that the development of GM-CFU derived from infected mice splenocytes was enhanced *in vitro* assays (S. E. J. Cotterell *et al.*, 2000a). To confirm these findings in B6 mice we evaluated the number of haematopoietic progenitors in the spleen of mice chronically infected with *L. donovani* directly *ex vivo* using flow cytometry. In the spleens of B6 we found significant increases in the frequency and number of HSPCs during chronic phase of infection (Figure 4.2a; Figure 4.2b). There were also significant alterations in lineage-committed cell compartment both in relative and absolute numbers. (Figure 4.3a; Figure 4.3b). These findings confirmed that experimental chronic VL is characterized by a noticeable increase in haematopoietic progenitors in the spleen, and therefore the establishment of extramedullary haematopoiesis.

To determine the impact of the spleen in the alterations seen in the BM, we assessed the effect of splenectomy on BM cellularity in mice infected for 28 days with *L. donovani*. Our data showed that splenectomy did not impact on changes in BM cellularity during chronic phase of *L. donovani* infection. Splenectomized mice and “sham” infected mice showed the same degree of losses in the reservoir of quiescent HSCs (Figure 4.4a; Figure 4.4b), as well as, similar increases in multipotent precursors (Figure 4.4c; Figure 4.4d). We also could not determine any differences between splenectomized and “sham” infected mice regarding alteration neither in the frequency of lineage-committed progenitors (Figure 4.4e; Figure 4.4f), nor in the frequency of mature haematopoietic cells in BM (Figure 4.4g; Figure 4.4h).

Hence, we could conclude that the alterations in the spleen and BM haematopoietic compartment during chronic infection with *L. donovani* were independent processes, and that the presence of splenomegaly was not impacting directly in the haematopoiesis in BM during chronic infection.

If extramedullary haematopoiesis is taking place in the spleen its efficiency should be very limited since its abolishment did not account for further impairment in the haematopoietic system, such as further loss of HSCs in G0 or further alterations in lineage-committed progenitors and mature cells. Furthermore, recent findings from our laboratory determined that in B6 mice chronically infected with *L. donovani* splenectomy prior to the establishment of infection could not prevent the onset of anaemia, but limited thrombocytopenia (Preham O., unpublished data). Nevertheless, it is conceivable that compensatory mechanisms of extramedullary haematopoiesis take place in other organs following infection.

4.2.3 *L. donovani* infection was characterized by increased numbers of BM T cells

In the steady state CD4⁺ T cells represented 0.64 % ± 0.19 of total BM cells, or $2.26 \times 10^5 \pm 7.49 \times 10^4$ cells / femur-tibia pair. CD4⁺ T cells increased 24-fold ($4.42 \times 10^6 \pm 2.92 \times 10^6$) during *L. donovani* infection, composing now 8.71% ± 2.83 of total BM cells (Figure 4.5a; Figure 4.5b). The frequency of CD8⁺ T cells in BM was also increased in infected compared to naive mice (2.74 % ± 0.98 vs 1.43 % ± 0.45, respectively), mirrored by an ~2-fold increase in the CD8⁺ T cell number ($1.10 \times 10^6 \pm 7.99 \times 10^5$ vs. $5.07 \times 10^5 \pm 1.17 \times 10^5$) (Figure 4.5a; Figure 4.5b). CD3⁺ CD4⁻ CD8⁻ (double negative (DN)) T cells comprised 0.94 % ± 0.41 of BM cells in healthy controls, but their frequency dropped to 0.56 % ± 0.43 in the BM of chronically infected mice, however in absolute number no changes were observed following *L. donovani* infection (Figure 4.5a; Figure 4.5b). The extent of the CD4⁺ T cell increase in BM was much more evident compared to the other lymphocytes evaluated, and accounted for an inversion in the proportion of CD4⁺ / CD8⁺ T cells in BM of mice chronically infected with *L. donovani* (Figure 4.5c).

The B cell compartment also presented significant changes during infection. The frequency of B cells was 3 fold decreased in the BM of infected mice (Figure 4.6a), consistent with a reduction in absolute number from $4.72 \times 10^6 \pm 2.32 \times 10^6$ in naive to $1.24 \times 10^6 \pm 3.50 \times 10^6$ cells in infected mice (Figure 4.6b). We also assessed the frequency and number of overall myeloid cells (CD11b⁺ cells) in non-infected and infected mice. Despite the modest increase in the frequency of CD11b⁺ we did not find any significant alterations in cell number after 28 days of *L. donovani* infection (Figure 4.7a; Figure 4.7b).

We then assessed if the stromal compartment presented alterations during infection. As there are not yet definitive cell markers to select for stromal cells in BM, we selected for cell populations enriched for MSCs (CD45⁻ Ter119⁻ CD31⁻ Sca1⁺ CD51⁺ cells), osteoblastic lineage cells (CD45⁻ Ter119⁻ CD31⁻ Sca1⁻ CD51⁺ cells), and endothelial cells (CD45⁻ Ter119⁻ CD31⁺ cells), using parameters defined by others previously (I. G. Winkler *et al.*, 2010, D. Fonseca-Pereira *et al.*, 2014) (Figure 4.8a). The overall stromal compartment (CD45⁻ Ter119⁻ cells) did not show significant differences during infection, either in frequency and absolute cell number (Figure 4.8b; Figure 4.8c). However a small but significant increase in MSCs was observed in infected mice (Figure 4.8d; Figure 4.8e).

The analysis of cell distribution and counts revealed that the infection was modulating BM cellularity during chronic infection with *L. donovani*, of which amplification of the BM T cell pool was the most substantive.

4.2.4 *L. donovani* infection results in increased numbers of “effector” T cells in BM

Given the increase in number and frequency of BM CD4⁺ T cells during infection, these were further characterized for phenotype and function. CD4⁺ T regulatory cells (Tregs), defined as CD45⁺ CD3⁺ B220⁻ CD4⁺ CD25^{hi} FOXP3⁺ cells, were not contributing to the increase in total CD4⁺ T cell number (Figure 4.9a; Figure 4.9b). In contrast, Treg numbers did increase in the spleen (Figure 4.9c; Figure 4.9d).

Next, we used CD62L (L-selectin) and CD44 to discriminate naive (CD62L^{high} CD44^{-/low}), effector memory (CD62L^{-/low} CD44^{high}) and central memory (CD62L^{high} CD44^{high}) CD4⁺ T cells (J. Hu and A. August, 2008, T. Lucas *et al.*, 2010). In the BM of mice infected mice, CD62L^{-/low} CD44^{high} effector T cells appeared to contribute most to the changes in overall CD4⁺ T cell frequency and number in BM (Figure 4.10a; Figure 4.10b).

Within the CD8⁺ T cell compartment, “central memory” and “effector memory” CD8⁺ T cells also increased in frequency and number (Figure 4.10c; Figure 4.10d).

When we analyzed the distribution of each subset within the total CD4⁺ T cell compartment, it was clear that the majority of CD4⁺ T cells were CD62L^{-/low} CD44^{high} in the BM of infected mice (91.66 % ± 2.17 vs. 58.09% ± 8.36 in infected vs. naive respectively) (Figure 4.10e; Figure 4.10g). The proportion of CD62L^{-/low} CD44^{high} CD8⁺ T cells within the CD8⁺ T cell compartment also increased significantly at the expense of CD62L^{high} CD44^{-/low} cells (Figure 4.10f).

It was reported by others that the distribution of T cells populations differs considerably between the BM and the spleen (P. W. Price and J. Cerny, 1999). Therefore these analyses were also performed on splenic T cells (Figure 4.11). The increase of CD4⁺ T cells in the spleen of infected mice appeared mainly due to CD62L^{-/low} CD44^{high} CD4⁺ T cells (Figure 4.11a; Figure 4.11b). Similarly, analysis of the frequencies of CD62L^{-/low} CD44^{-/low} and CD62L^{high} CD44^{high} CD8⁺ T cells in total splenocytes showed no differences in infected mice compared to healthy controls (Figure 4.11c), although both populations increased in absolute cell number in infected mice (Figure 4.11d).

In comparison to BM, CD4⁺ and CD8⁺ T cell subsets were more heterogeneous in spleen. Over half of CD4⁺ T cells were CD62L^{-/low} CD44^{high} in the BM of infected mice (26.93 % ± 3.58 vs 60.28 % ± 7.27, naive vs infected), while CD62L^{hi} CD44^{low} the most representative population in naive mice was decreased in chronically infected mice (47.21 % ± 7.85 vs. 23.76 % ± 8.71, naive vs. infected) (Figure 4.11e; Figure 4.11g). The proportion of CD62L^{-/low} CD44^{high} CD8⁺ T cells also increased significantly at the expense of CD62L^{high} CD44^{-/low} cells (Figure 4.11f).

To determine if BM T cells were phenotypically similar to the recently described BM resident effector cells, we examined the expression of CD127 and Ly6C (F. Di Rosa and R. Pabst, 2005, K. Tokoyoda *et al.*, 2010). In the BM of infected mice the total number of “activated cells” (defined by the high expression of CD44) was 12 fold increased compared to that in naive mice (Figure 4.13a). The CD4⁺ T cells CD44^{high} Ly6C^{-/low} CD127^{-/low} (“effector T cells”) was the population with the maximum increase in absolute cell number (4.47 x 10⁴ ± 3.46 x 10⁴ vs. 1.26 x 10⁶ ± 3.21 x 10⁵, naive vs infected). The number of CD4⁺ T cells CD44^{high} Ly6C^{high} CD127^{high} (“memory T cells”) was also increased in the BM of infected mice (6.15 x 10³ ± 5.04 x 10³ vs. 2.42 x 10⁴ ± 9.56 x 10³, naive vs. infected), but their contribution to the overall increase in CD4⁺ T cell CD44^{high} was limited compared to those from CD4⁺ T cells CD44^{high} Ly6C^{-/low} CD127^{-/low}. Additionally, the number of CD4⁺ T cells CD44^{high} Ly6C^{-/low} CD127^{high} and CD4⁺ T cells CD44^{high} Ly6C^{high} CD127^{-/low} were also increased in the BM of infected mice compared to healthy controls (Figure 4.12a).

We also analysed of the frequencies of CD44^{high} CD4⁺ T cells segregated according to the expression of Ly6C and CD127 within total CD4⁺ T cells. In the BM we found that the majority

of CD4⁺ T cells were CD44^{high} cells, increasing from 72.22 % ± 8.67 of total CD4⁺ T cells in naive mice to 93.56 % ± 1.39 in infected mice, and the most abundant population of CD4⁺ T cells was CD44^{high} Ly6C^{-/low} CD127^{-/low} (“effector T cells”) (Figure 4.12b; Figure 4.12e).

The number of CD44^{high} CD8⁺ T cells was 5 fold increased in the BM of infected mice compared to naive mice (Fig. 4.13c), due largely to increases in the CD44^{high} Ly6C^{-/low} CD127^{-/low} CD8⁺ T cells and CD44^{high} Ly6C^{high} CD127^{-/low} populations (Figure 4.12d; Figure 4.12e).

Together, these data shows that the increase in T cells in the BM of infected mice was due to expansion and/or accumulation of activated CD4⁺ T cells, the majority of which were phenotypically characterized as CD44^{high} Ly6C^{-/low} CD127^{-/low} “effector” T cells, consistent with the accumulation of BM resident effector CD4⁺ T cell during chronic infection with *L. donovani*.

4.2.5 The number of CD4⁺ T cells producing IFN γ and TNF was increased in BM following *L. donovani* infection

Pro-inflammatory cytokines including IFN γ and TNF are important in the immunopathology of *L. donovani* infection. In mice, hepatic infection is self-resolving through the Th1-dominated formation of granulomas. On the other hand, in the spleen where parasites remain persistent, TNF is responsible for the disruption of the microarchitecture that is associated with impaired immunity (S. Staeger *et al.*, 2010). Several reports suggested that both cytokines might impact negatively on the modulation of haematopoiesis in the BM (M. T. Baldrige *et al.*, 2010, C. J. H. Pronk *et al.*, 2011, C. Mirantes *et al.*, 2014).

To characterize the potential for cytokine production by BM T cells, we used *ex vivo* stimulation of cells with Phorbol Myristate Acetate (PMA) and ionomycin stimulation followed by flow cytometry. The frequency of CD4⁺ T cells capable of producing IFN γ within the total BM was very low (0.10% ± 0.05) in naive mice, but increased substantially following infection (7.64% ± 3.57 of total BM cells). The percentage of CD8⁺ T cells with the potential to produce IFN γ also increased in the BM of infected mice (0.24% ± 0.14 vs 1.16% ± 1.03, naive vs. infected) (Figure 4.13a).

The absolute number of CD4⁺ T cells capable of producing IFN γ ⁺ in naive mice increased >40 fold in infected compared to naive mice. In contrast, we did not detect a significant change in the absolute numbers of CD8⁺ T cell able to produce IFN γ (Figure 4.13b). Within the CD4⁺ T cell population, 82.06% ± 14.23 had the potential to produce IFN γ in infected BM, compared to 17.33% ± 8.95 in naive controls (Figure 4.13c; Figure 4.13f). Similarly, the percentage of IFN γ ⁺ CD8⁺ T cells within total BM CD8⁺ T cells also significantly increased in infected mice (Figure

4.13c). Analysis of the MFI for IFN γ ⁺ within CD4⁺ T cells also demonstrated an increase in cytokine production on a per cell basis, compared to CD4⁺ T cells from naive mice, and this was also observed with CD8⁺ T cells (Figure 4.13d).

Next, we assessed cytokine production by cells from naive and infected mice directly *ex vivo* as a better measure of ongoing function. Less than 1% of steady-state CD4⁺ T cells expressed IFN γ (0.33% \pm 0.39), while in infected mice 9.29% \pm 3.22 were IFN γ positive (Figure 4.13e; Figure 4.13f). Surprisingly the fraction of CD8⁺ T cells producing IFN γ recovered from the BM of infected mice was very low (< 1%) and was comparable to naive controls (Figure 4.13e).

We then examined BM T cells for TNF production. After PMA and ionomycin stimulation the frequency of CD4⁺ T cells but not CD8⁺ T cells in total BM producing TNF was increased (Figure 4.14a). The number of CD4⁺ T cells with the potential to produce TNF was increased almost 17 fold in infected compared to naive mice (Figure 4.14b). Within total BM CD4⁺ T cells and CD8⁺ T cells, the fraction of cells producing TNF was unchanged following infection, suggesting that the increase in TNF⁺ CD4⁺ T cells resulted from the overall expansion of CD4⁺ T cell compartment in the BM of infected mice (Figure 4.14c; Figure 4.14f). However, it was also found that the amount of TNF expressed by stimulated CD4⁺ T cells (as judge by MFI) was enhanced in infected mice compared to naive controls (Figure 4.14d). Increased levels of TNF expression were also seen in TNF⁺ CD8⁺ T cells (Figure 4.14d). Direct *ex vivo* analysis showed that in steady state less than 0.42% \pm 0.35 of CD4⁺ T cells expressed TNF, while in infected mice 1.54% \pm 0.91 were TNF⁺ (Figure 4.14e; Figure 4.14f). Similarly, the fraction of BM CD8⁺ T cells spontaneously producing TNF increased following infection, to a lesser extent than observed in BM CD4⁺ T cells (Figure 4.14e).

IL-10 is generally considered an immunosuppressive cytokine, since *in vitro* studies showed that IL-10 limits the production of pro-inflammatory cytokines such as TNF, IL-1a, IL-1b and IL-6 by activated immune cells (W. Ouyang *et al.*, 2011). IL-10 is known to play a central role in the immune response to *L. donovani* infection, as blockade of IL-10 signalling blockade caused rapid clearance of the parasite, whilst mice over expressing IL-10 were unable to control the parasite burden (H. W. Murray *et al.*, 2002). In the spleen of chronically infected mice, CD4⁺ T cells co-expressing IL-10 and IFN γ have been described (S. Stager *et al.*, 2006). However, no published study has determined whether BM T cells produce IL-10 following *L. donovani* infection.

Following stimulation with PMA/Ionomycin, the frequency of BM CD4⁺ T cells from infected mice that were IL-10⁺ was increased compared to naive controls, but nevertheless comprised a small fraction of total BM. The frequency of BM CD8⁺ T cells with the potential to produce IL-10 was unchanged (Figure 4.15a). Similar trends were determined for the absolute numbers of BM T

cells expressing IL-10 (Figure 4.15b). The fraction of CD4⁺ T cells expressing IL-10 cells was unchanged in infected mice compared to naive, whilst the fraction of CD8⁺ T cells IL-10⁺ in total BM CD8⁺ T was only slightly increased (Figure 4.15c; Figure 4.15f). Additionally, the analysis of the IL-10 MFI within CD4⁺ T cells IL-10⁺ and CD8⁺ T cells IL-10⁺ showed no significant alteration upon infection (Figure 4.15d).

Directly *ex vivo*, the fraction of IL-10⁺ cells within CD4⁺ T cells was comparable between naive and infected mice, whereas, the fraction of CD8⁺ T cells producing IL-10 increased from 0.30% ± 0.32 in naive mice to 0.75% ± 0.35 in infected mice (Figure 4.15e). Within the BM CD4⁺ T cells IFN γ ⁺ population the proportion of cells that expressed either or both TNF and IL-10 was unchanged following infection (Figure 4.16a; Figure 4.16c), and the same was observed for CD8⁺ T IFN γ ⁺ cells (Figure 4.16b). As such, the increase of total CD4⁺ T cells observed in BM of chronically infected mice was mainly due to the accumulation of IFN γ ⁺ or IFN γ ⁺ TNF⁺ CD4⁺ T cells (Figure 4.16a; Figure 4.16c).

Overall these data show that *L. donovani* promoted alterations in the cytokine milieu in BM. This was mainly due to the increased production of cytokines by CD4⁺ T cells with the potential to promote inflammation in the BM through the expression of Th1 cytokines.

4.2.6 Infection-induced loss of quiescent LT-HSCs was mediated by CD4⁺ T cells

Based on the data presented above, we hypothesized that CD4⁺ T cells might act as drivers of the alterations observed in the haematopoietic compartment during chronic infection (Figure 4.17). To assess whether this was the case, RAG2 KO mice were adoptively transferred with sorted CD4⁺ T cells from naive mice, and then infected in the following day with *L. donovani*. At day 28 p.i., we analysed the distribution of haematopoietic progenitors in the BM, compared to WT infected mice and infected RAG2 KO mice that did not receive adoptively transferred CD4⁺ T cells. Analyses of cell frequencies were performed gating on Lineage negative cells, to avoid biases due to the lack of lymphocytes in RAG2 KO mice. The transfer of CD4⁺ T cells to infected RAG2 KO mice was associated with a recovery of the phenotype observed in WT infected mice (Figure 4.18; Figure 4.19; Figure 4.20; Figure 4.21). Adoptive transfer of CD4⁺ T cells prior to infection significantly increased the frequency and the number of LSK cells and intermediary non-committed progenitors (LSK CD150⁺ CD34⁻ CD48⁺ cells and LSK CD150⁺ CD34⁺ cells) to a similar extent as observed in infected WT mice (Figure 4.18a-h). More importantly, infected RAG2 KO mice preserved their reservoir of quiescent HSCs, whereas these were significantly depleted in RAG2 KO mice given CD4⁺ T cells, (Figure 4.19a; Figure 4.19b). In RAG2 KO

infected mice, $42.85\% \pm 21.69$ of LT-HSC were in G0, but this was reduced to $8.82\% \pm 3.27$ in mice that received CD4⁺ T cells prior to the infection (Figure 4.19c; Figure 4.19d).

CD4⁺ T cell transfer was not associated with alteration in the frequencies of CMPs or GMPs, and only minor changes in absolute number of CMPs were observed, among lineage-committed progenitors (Figure 4.20). CLPs were decreased irrespective of the presence of CD4⁺ T cells, which may be due to their inherent inability to produce *de novo* T and B cells (Figure 4.20f; Figure 4.20j). The frequency of MEPs was increased in BM of infected RAG2 KO mice adoptively transferred with CD4⁺ T cells in comparison to naive RAG2 KO mice, a trend observed in infected WT mice compared to naive WT. However, in absolute number, there were no differences amongst all the experimental groups (Figure 4.20e; Figure 4.20i).

To exclude that these alterations were the result of homeostatic proliferation of T cells in the RAG host, HSPC populations and the proliferative status of LT-HSCs were assessed in adoptively transferred RAG2 mice that were not subsequently infected (Figure 4.21). These control mice were unaltered compared to naive RAG2 KO mice with regards the number of the HSPCs (Figure 4.21a; Figure 4.21c) and the frequency of LT-HSCs in G0 (Figure 4.21b). As such, the expansion of multipotent progenitors and subsequent loss of LT-HSCs in G0 following T cell transfer requires T cell activation as a consequence of infection.

In infected WT mice, we observed signs of mild anaemia and thrombocytopenia, features absent in infected RAG2 KO mice. On the other hand, infected RAG2 KO mice adoptively transferred with CD4⁺ T cells showed a significant loss of RBCs (Figure 4.22a), lower concentration of haemoglobin (Figure 4.22c) and reduced platelet counts (Figure 4.22b). These haematological alterations were absent in RAG2 KO mice adoptively transferred with CD4⁺ T cells but not infected (Figure 4.23a-d). These findings suggested that alterations in CD4⁺ T cell compartment were sufficient to mediate the onset of anaemia and thrombocytopenia in experimental VL.

CD4⁺ T cells are crucial for the control of parasite burden. In WT mice the number of parasites per 1000 nuclei in the spleen was on average 31.25 ± 28.49 . This value increase to 1469 ± 1334 parasites/1000 nuclei in infected RAG2 KO. However in RAG2 KO mice given CD4⁺ T cells prior to infection the parasite counts dropped to 64.89 ± 68.92 parasites/1000 nuclei (Figure 4.24a). Moreover, in RAG2 KO mice given CD4⁺ T cells following infection developed splenomegaly, as observed in WT mice (Figure 4.24b), suggesting that CD4⁺ T cells were required to drive inflammation in the spleen.

CD4⁺ T cells expanded greatly in the BM of RAG2 KO mice following infection, with associated signs of activation (Figure 4.25a). In WT infected mice, the number of CD44^{high} Ly6C^{-/low} CD127⁻

$^{/low}$ CD4⁺ T cells was on average 13 fold increased compare to naive mice, and the number CD4⁺ T cells CD44^{high} Ly6C^{high} CD127^{-/low} about 19 fold (Figure 4.25b). In adoptively transferred RAG2 KO mice, the number of CD44^{high} Ly6C^{-/low} CD127^{-/low} CD4⁺ T cells was on average 72 fold, and the number CD44^{high} Ly6C^{high} CD127^{-/low} CD4⁺ T cells about 174 fold, greater in infected mice compared to naive mice where only homeostatic proliferation of T cells occurred (Figure 4.25b). The analysis of the distribution of cells within CD4⁺ T cells showed that in uninfected RAG2 KO mice most cells displayed an phenotype CD44^{high} Ly6C^{high} CD127^{high} attributed to “memory T cells”, while in RAG2 KO infected mice CD4⁺ T cells were mainly CD44^{high} Ly6C^{high} CD127^{-/low} or CD44^{high} Ly6C^{-/low} CD127^{-/low} (phenotype attributed to “BM effector T cells”), as observed in WT infected mice (Figure 4.25c).

In summary, CD4⁺ T cells transferred to RAGKO mice and examined 28 days after *L. donovani* infection displayed immunophenotype alterations that resemble those found in similarly infected WT mice.

4.2.7 Loss of LT- HSCs in quiescence was mediated by IFN γ

About 90% of total BM CD4⁺ T cells were primed to produce IFN γ , and even in the absence of *in vitro* stimulation a significant fraction was found actively producing this pro-inflammatory cytokine following infection (section 4.2.6). We also showed that CD4⁺ T cells, which were found in expanded numbers and were the major producer of IFN γ in BM following *L. donovani* infection, could mediate the loss of HSCs in G0 (section 4.2.8). As such, we assessed whether IFN γ KO CD4⁺ T cells were also able to affect BM function.

As previously shown in Figure 4.21, the transfer of WT CD4⁺ T cells to RAG2 KO mice prior to infection with *L. donovani* resulted in the increased frequency of LSK cells, LSK CD150⁺ CD34⁻ CD48⁺ cells and LSK CD150⁺ CD34⁺ cells, within Lineage negative population. However, CD4⁺ T cells derived from IFN γ KO mice were unable to mediate these effects (Figure 4.26a). Instead, in RAG2 KO mice that received IFN γ KO CD4⁺ T cells, there was a significant increase in the frequency of CMPs and GMPs in comparison to infected RAG2 KO and RAG2 KO transplanted with WT CD4⁺ T cells, and we did not observed significant differences in MEPs and CLPs in comparison with infected RAG2 KO (Figure 4.26b).

Likewise, whereas transfer of WT CD4⁺ T cells to RAG2 KO mice resulted in a significant decrease in the frequency and number of LT-HSCs in G0, this did not occur following transfer of IFN γ KO CD4⁺ T cells (Figure 4.27a; Figure 4.27b). As with infected RAG2 KO mice, infected mice given IFN γ KO CD4⁺ T cells had approximately half their LT-HSC population in quiescence ($48.40\% \pm 11.30$), whereas this was significantly reduced in infected RAG2 KO given

WT CD4⁺ T cells mice (8.82% ± 3.27) (Figure 4.27c Figure 4.27d). These findings suggested that IFN γ production by CD4⁺ T cells underlies the depletion in the reservoir of quiescent LT-HSCs, as well as, the expansion of intermediate multipotent progenitors in BM during infection with *L. donovani*.

Infected RAG2 KO mice given WT CD4⁺ T cells developed anaemia and thrombocytopenia, but this did not occur in RAG2 KO mice given IFN γ KO CD4⁺ T cells prior to infection (Figure 4.28a-d). As such, IFN γ production by CD4⁺ T cells also underlies impaired haematological function.

Not surprisingly, IFN γ produced by CD4⁺ T cells was important to limit the number of parasites/1000 nuclei in the spleen, as RAG2 KO given IFN γ KO CD4⁺ T cells had comparable numbers of parasites / 1000 host cell nuclei in the spleen (1267 ± 342) to RAG2 KO infected mice (1996 ± 802), whereas this was reduced in mice receiving WT CD4⁺ T cell (257 ± 129, parasites/1000 nuclei) (Figure 4.29a). Additionally, whereas WT CD4⁺ T cells transfer induced splenomegaly following infection, this did not occur following IFN γ KO CD4⁺ T cells transfer (Figure 4.29b), suggesting that CD4⁺ T cells IFN γ ⁺ are required to drive inflammation in the spleen.

Finally, it was found that both WT and IFN γ KO CD4⁺ T cells expanded to similar numbers in the BM of RAG2 KO recipient mice, which in both cases was due to high number of cell with an activated CD44^{hi} phenotype (Figure 4.30a). The number of CD4⁺ T cells expressing either or both Ly6C or CD127 was comparable between WT CD4⁺ T cells and IFN γ KO CD4⁺ T cells (Figure 4.30b). Nevertheless, significant changes were observed in the percentages of cells within the CD4⁺ T cell compartment; 82.85% ± 3.22 of WT CD4⁺ T cells were CD44^{high} Ly6C^{-/low} CD127^{/low} compared to 66.62% ± 9.53 of IFN γ KO CD4⁺ T cells, whilst the frequency of CD44^{high} Ly6C^{high} CD127^{-/low} was increased within of IFN γ KO CD4⁺ T cells (25.98% ± 10.62) compared to WT CD4⁺ T cells (5.68% ± 1.05) (Figure 4.30c). These findings show that IFN γ is dispensable for the expansion of CD4⁺ T cells (at least in a non-competitive environment). In contrast, CD4⁺ IFN γ ⁺ T cells contributed to the immunophenotypic changes observed during the immune response to *L. donovani* infection.

4.2.8 Loss of quiescent LT-HSCs was not mediated by intrinsic IFN γ receptor signalling in LT-HSCs

HSCs express receptors for IFN γ , which have been directly associated with LSK expansion and impaired engraftment in X-irradiated hosts (K. Y. King *et al.*, 2010, A. M. de Bruin *et al.*, 2013, Y. Zhang *et al.*, 2013). As such, we hypothesized that IFN γ signaling would be responsible for the

depletion of LT-HSCs in G0 during chronic infection with *L. donovani* (Figure 4.31). To test this hypothesis, we generated 50:50 mixed BM chimeras using cells derived from both WT and IFN γ R2^{-/-} mice. We assessed donor cells chimerism and alterations in progeny in response to subsequent infection with *L. donovani* (Figure 4.32).

Twelve weeks after transplantation, in infected chimeric mice, the frequency of IFN γ R2^{-/-} cells was higher in the BM (60.18% \pm 15.20) compared to naive mice (39.82% \pm 15.20) but not statistically different, and in absolute cell number we found no significant differences. Furthermore, the frequency and number of WT or IFN γ R2^{-/-} donor cells did not change in BM following *L. donovani* infection (Figure 4.33a; Figure 4.33b).

In the spleen, the percentage of cells derived from IFN γ R2^{-/-} donor cells was increased both in non-infected mice and infected mice (Figure 4.33c; Figure 4.33e), with similar data for absolute cell numbers (Figure 4.33d). This suggested that IFN γ signalling impacts on haematopoietic function both in steady-state and inflammatory conditions. The frequency of WT or IFN γ R2^{-/-} donor cells in the spleen was similar following *L. donovani* infection (Figure 4.33c). However, the absolute number of IFN γ R2^{-/-} donor cells was increased compared to WT (Figure 4.33d), suggesting that in the periphery IFN γ R2^{-/-} donor cells had a competitive advantage over WT cells in inflammatory conditions.

In the BM of non-infected mice, the frequency and the number of LSK cells (enriched in multipotent progenitors) and Lin⁻ Sca1⁻ cKit⁺ cells (enriched in lineage-committed progenitors) was comparable between WT and IFN γ R2^{-/-} donor cells, suggesting that IFN γ signaling was not required for the maintenance of HSPCs under homeostatic conditions (Figure 4.34a; Figure 4.34b; Figure 4.349e).

Following infection, the number of BM LSK cells derived from WT and IFN γ R2^{-/-} donor cells was increased compared to respective WT and IFN γ R2^{-/-} donor cell numbers found in non-infected recipients (Figure 4.34b), and the same changes were observed in regard to their frequency within donor compartment cells (Figure 4.34a). However, the magnitude of the increase in number of LSK cells in infected mice was greater for WT donor cells (6 fold) compared to IFN γ R2^{-/-} derived LSK cells (2.6 fold) (Figure 4.34b).

In the BM of infected mice, the increase in the frequency of WT LSK cells was concomitant with the contraction in the percentage Lin⁻ Sca1⁻ cKit⁺ cells (0.66% \pm 0.32 vs 0.07 % \pm 0.07, naive *versus* infected), while the increase in IFN γ R2^{-/-} LSK cells was not followed by alterations in Lin⁻ Sca1⁻ cKit⁺ cells frequency or absolute cell numbers (Figure 4.34a; Figure 4.34b; Figure 4.34e).

These alterations suggested that the up-regulation of Sca1 in HSPCs during *L. donovani* infection in WT B6 was directly mediated by IFN γ signaling.

In the spleen of non-infected mice, we found comparable numbers and frequencies of LSK cells and Lin⁻ Sca1⁻ cKit⁺ cells derived from WT and IFN γ R2^{-/-} donor cells (Figure 4.34c; Figure 4.34d). In infected mice the frequency and the cell numbers of WT LSK cells and IFN γ R2^{-/-} LSK cells were both increased in infected mice, compared to their respective cell numbers in non-infected recipients (Figure 4.34d). In the spleen, we did not observe any differences in WT Lin⁻ Sca1⁻ cKit⁺ cells, but found the number of Lin⁻ Sca1⁻ cKit⁺ cells derived from IFN γ R2^{-/-} donor cells was increased following infection compared to WT cells (Figure 4.34c; Figure 4.34d). In summary, these findings suggested that IFN γ signaling acting directly upon HSPCs was not required to drive the increase in HSPCs in the spleen during chronic infection with *L. donovani*.

We found no significant differences in the frequency of LSK CD150⁺ CD48⁻ cells (enriched for LT-HSCs) and LSK CD150⁺ CD48⁺ cells (enriched for other multipotent progenitors) derived from WT donor cells and IFN γ R2^{-/-} donor cells, both in BM (Figure 4.35a) and in the spleen (Figure 4.35c). This was true in absolute cell number (Figure 4.35b; Figure 4.35d), suggesting that IFN γ signaling was dispensable in the steady-state to regulate the number of multipotent progenitors.

In infected recipient mice, the frequency of WT LSK CD150⁺ CD48⁻ cells and IFN- γ R2^{-/-} LSK CD150⁺ CD48⁻ cells in the BM was unchanged (Figure 4.35a), and the same was observed in regard to their cell number (Figure 4.35b). Among IFN γ R2^{-/-} donor cells only in the spleen, there was a significant increase in the frequency and in the number of LSK CD150⁺ CD48⁻ cells, while the frequency and the number of WT LSK CD150⁺ CD48⁻ cells were not impacted by the infection (Figure 4.35c; Figure 4.35d). Finally, in infected mice, both in BM and in the spleen, an increase in LSK CD150⁺ CD48⁺ cells derived from WT donor cells and IFN γ R2^{-/-} donor cells was observed both in frequency and absolute cell number (Figure 4.35a-d). Overall, these results suggested that direct IFN γ signaling was not mediating the expansion of multipotent progenitors onward from LT-HSCs during infection with *L. donovani*.

In the BM of naive chimeric mice, the study of lineage-committed progenitors showed that the frequencies and the absolute cell numbers of all the populations assessed were comparable between WT donor cells and IFN- γ R2^{-/-} donor cells (Figure 4.36a; Figure 4.36b). Following infection, the frequency of IFN γ R2^{-/-} GMPs was increased, while within WT donor cells the populations increased were the MEPs and CLPs, in comparison to respective populations in naive recipient mice (Figure 4.36a). However, we did not observe any significant changes in absolute cell number following infection in all the other populations assessed. As such, it appears that

IFN γ signalling in lineage-committed progenitors was not required to sustain cell numbers under homeostatic conditions or in inflammatory conditions.

In the spleen of non-infected recipient mice, there were no differences either in frequency or absolute number of all the lineage-committed progenitors evaluated (Figure 4.36c; Figure 4.36d). During infection, the alterations in WT and IFN- γ R2^{-/-} derived CLPs followed the same trends, i.e. in both compartments there was a significant decrease in their frequency compared to naive recipients, but in absolute cell numbers we did not observe any differences (Figure 4.36c; Figure 4.36d). On the other hand, the frequencies and number of IFN- γ R2^{-/-} CMPs and GMPs were increased, whilst WT CMPs and WT GMPs were unchanged compared to respective naive populations (Figure 4.36c; Figure 4.36d). Finally, we observed that the number of MEPs derived either from donor WT or IFN- γ R2^{-/-} donor cells was increased following infection. These findings suggested that IFN γ signaling in lineage-committed progenitors was not necessary to sustain their number neither under homeostatic conditions nor for the expansion of CMPs, GMPs and MEPs in the spleen that followed infection.

Under homeostatic conditions, the frequency and the number of BM LT-HSCs in G0 were comparable between WT and IFN- γ R2^{-/-} derived cells (Figure 4.37a; Figure 4.37b). Most importantly, there were no differences in the frequency or number of quiescent HSCs following infection between WT and IFN- γ R2^{-/-} derived cells, both decreasing compared to naive controls (Figure 4.37a-c). Overall, these findings led us to reject the hypothesis that cell intrinsic IFN γ signalling was responsible for the reductions in frequency and number of HSCs in G0 in VL.

As previous experiments had shown IFN γ derived from CD4⁺ T cells was responsible for enhanced LT-HSCs proliferation (section 4.2.9), yet this was not due to IFN γ intrinsic signalling, these data suggested that IFN γ could indirectly regulate HSCs proliferation, during chronic infection with *L. donovani*.

IFN γ is important in Th1 differentiation, but its role in T cells proliferation is unresolved due to opposing findings attributed to different models of infection (J. K. Whitmire *et al.*, 2005, J. S. Haring and J. T. Harty, 2006, X. Li *et al.*, 2007, O. Sercan *et al.*, 2010). As such, we evaluated the alterations in T cell compartment in (B6.CD45.1 + B6.CD45.2.*Ifn γ r2^{-/-}*) \rightarrow B6.CD45.1 chimeric mice following *L. donovani* infection. We also assessed whether IFN γ signalling was responsible for the alterations in other effector cells during infection and analyzed the B cell and myeloid compartments. In BM and spleen of non-infected recipient mice, the frequency and absolute number of T cells was comparable between WT and IFN- γ R2 KO donor cells, (Figure 4.38a-d), indicating that IFN γ signalling in T cells was not required for their development or homeostatic

maintenance. In contrast, IFN- γ R2 KO T cells in BM did not increase following infection, unlike their WT counterparts (Figure 4.38a; Figure 4.38b).

In summary, in uninfected mice WT and IFN- γ R2 KO donor cells made approximately equal contributions to the BM and splenic T cell populations, while during chronic infection IFN γ responsive (WT) T cells were significantly enriched at both sites, suggesting that IFN γ signalling in T cells conferred a competitive advantage under inflammatory conditions. As such, intrinsic IFN γ signalling confers a proliferative or survival advantage during *L. donovani* induced inflammation, but not in homeostatic conditions.

In naive recipient mice, the analysis of the B cell compartment showed an increase in the frequency in BM B cells derived from IFN γ R2 KO donor cells compared to BM WT B cells in non-infected mice (Figure 4.38a). Nevertheless, we did not detect differences in their absolute cell numbers (Figure 4.38b). Similarly, WT and IFN γ R2 KO donor cells contributed at similar extent to the splenic B cell compartment in steady-state (Figure 4.38c; Figure 4.38d). Overall, these findings suggested that IFN γ signalling is not critical to sustain the number of B cell numbers under non-inflammatory conditions.

In infected mice, there was a significant decrease in the frequency and number of WT BM B cells and IFN γ R2 KO BM B cells, but no differences were observed in their absolute cell number, compared to uninfected mice (Figure 4.38a; Figure 4.38b). Following infection, in the spleen the percentages of WT B cells and IFN γ R2 KO B cells were unchanged, nevertheless the absolute number of B cells derived from IFN γ R2 KO donor cells was increased, in comparison to respective populations in naive recipients (Figure 4.38c; Figure 4.38d). As such, there was no indication that IFN γ signalling played a major role regulating the B cell compartment in BM and in the spleen.

BM from non-infected mice displayed comparable frequencies and number of most myeloid populations derived from WT and IFN γ R2 KO donor cells, except that CD11b⁺ F4/80⁻ cells from IFN γ R2 KO donor cells were reduced in frequency compared to WT, and the number CD11b^{hi} F4/80^{hi} cells and CD11b⁻ F4/80^{hi} cells from IFN γ R2 KO donor were also decreased compared to WT (Figure 4.39a; Figure 4.39b). In the BM of infected mice the number of IFN γ R2 KO CD11b⁺ F4/80^{hi} cells was decreased (Figure 4.39b). In contrast, the number WT CD11b⁺ F4/80^{hi} cells increased ~ 2 fold following infection (Figure 4.39b). The number of CD11c^{hi} MHC II^{hi} cells (DCs) and CD11b⁻ F4/80^{hi} cells derived from WT were increased compared IFN γ R2 KO donor cells in BM following infection (Figure 4.39a; Figure 4.39b).

In the spleens of non-infected mice, all populations of myeloid cells derived from IFN- γ R2 KO donor cells were decreased compared to WT donor cells, both in frequency and cell number (Figure 4.39c; Figure 4.39d). Following infection, with the exception of IFN- γ R2 KO CD11b⁺ F4/80⁻ cells, all other myeloid populations derived from IFN- γ R2 KO donor cells failed to expand (Figure 4.39c; Figure 4.39d). In contrast, the number of CD11c^{hi} MHCII^{hi} cells and CD11b⁺ F4/80⁻ cells, derived from WT donor cells increased following infection (Figure 4.39d). To the quantitative differences in myeloid cells may have contributed cells derived from the recipient mice, since it was reported that macrophage resident cells are more resistant to x-irradiation (D. Hashimoto *et al.*, 2013).

In summary, with these findings we could exclude IFN γ signaling as a direct mediator of loss of LT-HSCs in G0 during experimental VL. Nevertheless, our results support a role for T cell intrinsic IFN γ signaling leading to expansion of T cell number in BM and the spleen during chronic VL.

4.2.9 The number of LT-HSCs and onward progenitors expressing TNF receptors was increased following infection with *L. donovani*

TNF has been proposed to play an important role in directly modulating HSCs function and may cooperate with other mechanisms in driving stress-induced haematopoiesis and mediating haematopoietic dysfunction (C. J. H. Pronk *et al.*, 2011), and we have shown above that the number of T cells producing TNF was greatly enhanced in the BM during infection. We therefore tested an alternate hypothesis, namely that TNF may mediate changes in the BM HSPCs population.

We first assessed the expression of the two functional receptors for TNF, TNFR1a (or TNFR-p55), and TNFR1b (TNFR-p75), the latter normally restricted to haematopoietic cells and upregulated in inflammatory conditions (N. Askenasy, 2015).

The majority of mature BM haematopoietic cells expressed TNFR1a in steady-state, and this increased following infections (60.98% \pm 5.02 *vs* 75.70% \pm 5.02, naive *vs* infected), whilst the absolute number of TNFR1a⁺ cells remained unchanged (Figure 4.40a; Figure 4.40b). We also found that the frequency and number of TNFR1a expressing Lineage⁻ cKit⁺ cells (enriched for all HSPCs) were increased in chronically infected mice (Figure 4.40a; Figure 4.40b).

Next we focused on the most primitive progenitors. Most LT-HSCs (enriched in LSK CD150⁺ CD34⁻ CD48⁻ cells) expressed TNFR1a under homeostatic conditions (Figure 4.41a), nevertheless their number increased following infection (Figure 4.41b), and TNFR1a was expressed at

increased levels following infection (Figure 4.41c; Figure 4.41d). These alterations were replicated in the onward multipotent progenitors (Figure 4.41a; Figure 4.41b; Figure 4.41c).

The percentage of mature haematopoietic cells expressing TNFR1b increased significantly upon infection ($27.74\% \pm 8.42$ vs $59.98\% \pm 18.37$, naive vs infected), but this did not result in significant alterations in absolute cell number in BM (Figure 4.42a; Figure 4.42b). The frequency of Lineage⁻ cKit⁺ TNFR1b⁺ cells increased from $36.52\% \pm 12.67$ in naive mice to $71.60\% \pm 15.64$ in infected mice, and this was reflected by an increase in absolute cell numbers (Figure 4.42a; Figure 4.42b). The frequency and number of LT-HSCs expressing TNFR1b increased in infected mice (Figure 4.43a; Figure 4.43b), and LT-HSCs in infected mice also expressed TNFR1b at elevated levels, as judged by MFI (Figure 4.43c; Figure 4.43d). Similar results were seen for onward multipotent progenitors (Figure 4.43a-c), suggesting a potential role for TNF signalling in the mediation of changes in HSPCs function.

4.2.10 TNF intrinsic signalling does not regulate loss of LT-HSCs in G0

To formally test whether direct cell intrinsic TNF signalling plays a role in driving LT-HSCs into active cell-cycle and subsequent depletion of the reservoir of quiescent LT-HSCs we generated further mixed chimeras (Figure 4.44). We transferred equal numbers of BM WT donor cells and BM donor cells devoid for both TNF receptors (TNFR-dKO) into lethally irradiated recipients (Figure 4.45). After thirteen weeks, it was expected that most of the haematopoietic cells found in the recipient would be derived from donor LT-HSCs, since most haematopoietic cells have a relatively short life (R. Duran-Struuck and R. C. Dysko, 2009).

Under homeostatic conditions, WT donor cells constituted $28.88\% \pm 9.17$ of total BM donor cells compared to $68.51\% \pm 7.58$ TNFR-dKO cells (Figure 4.46a; Figure 4.46c). In absolute cells number TNFR-dKO donor cells were also dominant (Figure 4.46a). The competitive advantage of donor cell devoid in TNFR signaling over WT donor cells was also observed in the spleen of non-infected recipient mice, in which the frequency and number of TNFR-dKO cells were also increased compared to WT donor cells (Figure 4.46a; Figure 4.46b), suggesting that TNF signalling may modulate on haematopoietic function in homeostasis.

Following infection, the frequency of WT cells in BM was increased ~10% but their cell number remained comparable to those found non-infected recipients. In contrast, in infected mice the frequency of donor TNFR-dKO cells was not significantly changed (Figure 4.46a; Figure 4.46c), but their numbers decreased from $2.19 \times 10^7 \pm 4.22 \times 10^6$ cells in non-infected recipients to $1.17 \times 10^7 \pm 3.17 \times 10^6$ cells in the BM of infected recipients (Figure 4.46b). The cell numbers of WT and TNFR-dKO donor cells in BM were comparable in mice chronically infected with *L.*

donovani (Figure 4.46b). The frequency of WT donor cells expanded in the spleen of infected mice, but their absolute cell numbers seemed to follow this trend, although these changes were not statistically significant (Figure 4.46a; Figure 4.46b). In contrast, the percentage of engraftment of TNFR-dKO donor cells contracted following infection, whilst their absolute cell numbers were unchanged (Figure 4.46a; Figure 4.46b)

In the BM of non-infected mice the frequency and the number of LSK cells (enriched in multipotent progenitors) and Lin⁻ Sca1⁻ cKit⁺ cells (enriched in lineage-committed progenitors) was comparable between TNFRdKO donor cells and WT donor cells, implying that TNF signaling was dispensable to sustain HSPCs number under homeostatic conditions (Figure 4.47a; Figure 4.47a). The expansion of both WT LSK cells and TNFR-dKO LSK cells was made at the expense of the contraction in the Lin⁻ Sca1⁻ cKit⁺ cells compartment, suggesting that TNF signaling was not implicated in the up-regulation of Sca1 in most HSPCs during *L. donovani* infection (Figure 4.47c).

In line with findings described above, in non-infected mice we could not find significant differences in the frequency of LSK CD150⁺ CD48⁻ cells (enriched for LT-HSCs) and LSK CD150⁺ CD48⁺ cells (enriched for other multipotent progenitors) derived from WT donor cells and TNFR-dKO donor cells in the BM of non-infected recipients (Figure 4.48a) although in the latter, the absolute cell number of both cell populations was increased (Figure 4.48b). Following infection, the frequencies of WT LSK CD150⁺ CD48⁻ cells and TNFR-dKO LSK CD150⁺ CD48⁻ cells in the BM were unchanged (Figure 4.48a), but the number of TNFR-dKO LSK CD150⁺ CD48⁻ cells was about two fold decreased in infected mice (Figure 4.48b), which can partially be explained by the contraction on BM cellularity (Figure 4.46b). In infected mice, we found that LSK CD150⁺ CD48⁺ cells were greatly increased both in percentage within WT donor cells and TNFRdKO donor cells (Figure 4.48a), and the same was observed in absolute terms (Figure 4.48b). In summary, these findings argued against the possibility that TNF signaling was intrinsically mediating the expansion of multipotent progenitors onward from LT-HSCs during infection with *L. donovani*.

In recipient mice under homeostatic conditions, the frequency of LT-HSCs in G0 was comparable between WT and TNFR-dKO donor derived cells (Figure 4.49a), but the number TNFR-dKO LT-HSCs in G0 was 2.5 fold the number of WT HSCs in quiescence (Figure 4.49b). Of relevance, following infection, we observed no significant differences either in the percentage LT-HSCs in quiescence between donor cells or in their absolute cell number (Figure 4.49a; Figure 4.49b).

Lastly, we determined that LT-HSCs lacking TNF functional signaling receptors were as with WT LT-HSCs, driven into active cell-cycle as a consequence of infection (Figure 4.49c; Figure

4.49d). Hence, TNF acting directly on LT-HSCs was not the underlying mechanisms responsible for the alteration in LT-HSCs proliferative status, and subsequent loss of the reservoir of LT-HSCs in G0.

TNF has been suggested to have direct effects on lineage-committed progenitors (C. J. H. Pronk *et al.*, 2011). As such, we examined the frequency and number of mature haematopoietic cells in BM and spleen in the mixed chimeras described above. In BM, lineage-committed progenitors in non-infected mice were comparable between WT donor cells and TNFR-dKO donor cells (Figure 4.50a). Most likely due to an overall competitive advantage of TNFR-dKO donor cells, the number of all considered cell populations of TNFR-dKO lineage-committed cells were increased compared to WT (Figure 4.50b). Following infection, the frequency of WT lineage-committed progenitors was unchanged or minimally reduced, and cell numbers were unchanged relative to TNFR-dKO donor derived cells (Figure 4.50a; Figure 4.50b). Reflecting an overall decrease in total BM cells derived from TNFR-dKO donor cells in infected recipient mice, the number of CMPs, GMPs and CLPs were decreased following infection (Figure 4.50b). These results suggested that TNF signaling neither was required nor deleterious to sustain the number of lineage-committed progenitors under homeostatic conditions, but may contribute to the decrease in myeloid-committed progenitors in BM that followed infection.

In non-infected chimeras, we failed to find significant differences either in the frequencies or in the cell number of total T cells and CD4⁺ T cell derived from WT in comparison to TNFR-dKO donor cells (Figure 4.51a; Figure 4.51b). In contrast following infection, differences in T cells derived from WT and TNFRdKO donor cells became evident in the BM (Figure 4.51a). The frequency of T cells within WT donor cells expanded from 9.43% ± 2.76 to 37.29% ± 11.32 following infection, while the percentage of T cells derived from TNFRdKO donor cells was unchanged. These patterns of alterations were replicated in the alterations in absolute cell numbers (Figure 4.51b).

Next focusing on WT BM CD4⁺ T cells, we observed an expansion in their frequency (2.17% ± 0.82 vs. 27.70% ± 6.92, “WT naive” vs. “WT infected”) (Figure 4.51a) and number (~13 fold) in infected recipient mice (Figure 4.51b). In contrast, BM CD4⁺ T cells lacking TNF signaling failed to expand significantly following infection (0.5% ± 0.19 vs. 0.85% ± 0.28, “TNFR-dKO naive” vs. “TNFR-dKO infected”) (Figure 4.51a), and their cell number remain at basal levels (Figure 4.51b). These findings did not suggest that intrinsic TNF signalling provided T cells with a competitive advantage to expand or seed in the BM under homeostatic conditions. Moreover, following infection, it appeared that TNF receptor signalling was critical to the expansion of the BM T cell compartment, and of CD4⁺ T cells in particular.

The frequency of BM TNFR-dKO B cells within donor was increased compared to WT donor cells in steady-state, but comparable following infection (Figure 4.51a). In the BM of infected recipient mice the percentage of WT B cells decreased about 2.4 fold compared to non-infected mice, while TNFR-dKO B had a less expressive 2 fold decrease following infection (Figure 4.51a), and similar reductions were determined in B cell numbers (Figure 4.51b).

In BM, the frequency of CD11b⁺ cells within WT and TNFR-dKO donor cells was comparable in steady-state (Figure 4.51a), however the number of CD11b⁺ cells TNFRdKO was found to be increased (Figure 4.51b). Following infection, the frequency of WT CD11b⁺ cells decreased while the frequency of TNFR-dKO CD11b⁺ cells was unchanged compared to non-infected mice (Figure 4.51a), but in absolute cell number there were no alteration in WT donor cells and TNFR-dKO CD11b⁺ cells decreased (Figure 4.51b).

According with these findings, intrinsic TNF signalling was dispensable to establishment of B cell and CD11b⁺ cell compartments in BM in steady-state. Following infection, in the absence of TNF signaling the alterations in these populations in BM resembled those observed in WT donor cells. In contrast, in BM the T cell compartment diverged considerably between WT and TNFR-dKO donor cells. The lack of intrinsic TNF signaling was not associated to an impairment of T cell reconstitution in BM, under homeostatic conditions, indicating that TNF signaling is not essential to the maintenance of BM T cells number in homeostasis. However, following infection, the lack of TNF signaling receptors completely abolished the expansion of T cells observed in WT T cells, which was mainly sustained by CD4⁺ T cells.

In the spleen under homeostatic conditions, the percentage of total T cells and CD4⁺ T cells was decreased within TNFR-dKO donor cells compared to WT donor cells (Figure 4.52a). Nevertheless, in absolute cell number they were comparable (Figure 4.52b), suggesting that TNF signaling was not critical to T cell development nor conferred T cells with a competitive reconstitution advantage in steady-state. Following infection, WT T cells were increased in frequency and cell number (Figure 4.52a; Figure 4.52b). On the contrary, the percentage and the number of T cells within TNFRdKO donor cells were unchanged following infection (Figure 4.52a; Figure 4.52b). The increase in total WT T cells observed during chronic infection in the spleen, was mainly sustained by the increase in WT CD4⁺ T cells, which percentage varied from 31.00% ± 3.56 in non-infected mice to 46.19% ± 4.03 in infected mice (Figure 4.52a) and their cell number increased ~ 3.55 fold (Figure 4.52b). In TNF-RdKO CD4⁺ T cells we failed to find any alteration both in percentage and cell number following infection (Figure 4.52a; Figure 4.52b). Thus, TNF acting directly in CD4⁺ T cells mediated the expansion of CD4⁺ T cells compartment in the spleen following infection with *L. donovani*.

In the spleen, we also assessed the distribution of myeloid cells characterized according with the expression of CD11c, CD11b, MHC-II and F4/80 (Figure 4.53a). In steady-state, the percentages and the cell numbers of the myeloid populations assessed within donor cells were comparable between WT and TNF-RdKO cells, suggesting that TNF intrinsic signalling was unnecessary to the development and maintenance of homeostatic numbers of myeloid cells in the spleen. Following infection, the alterations in myeloid cells were characterized by an increase the frequencies of in CD11b⁺ F4/80⁻ cells and CD11c^{hi} MHC-II^{hi} cells derived from TNF-RdKO donor cells, whilst in WT cells only the frequency of CD11b⁻ F4/80^{hi} cells was increased, compared to naive recipients (Figure 4.53a). In absolute cell number, only TNF-RdKO CD11b⁻ F4/80⁺ cells were increased in comparison to naive recipients (Figure 4.53b). Finally, the comparison between WT and TNF-RdKO donor cells showed that following infection all myeloid cells displayed similar cell number, except TNF-RdKO CD11b⁺ F4/80⁻ cells, which were found increased in comparison to WT donor cells in infected recipients. These findings suggested that TNF signaling intrinsic signalling in these myeloid populations was dispensable for their expansion following infection with *L. donovani*.

According with our findings TNF signaling was not a direct mediator of loss of LT-HSCs in G0 during experimental VL. Of relevance, the results suggested that TNF acting directly on T cells underlined the huge enhancement in BM T cells that characterized infection with *L. donovani*, by means that remain to be established. TNF signaling may be required to recruitment, survival or proliferation of BM and splenic T cells during experimental VL.

4.2.11 Loss of TNFR signaling prevents expansion of BM CD4⁺ T cells with the potential to express IFN γ

In previous experiments, we established that CD4⁺ T cells could solely mediate the loss of LT-HSC in G0 in BM and impairment of haematological function (anaemia and thrombocytopenia) in the periphery (section 4.2.8). The potential of CD4⁺ T cells to mediate these alterations *during L. donovani* infection critically relied on the expression of IFN γ (section 4.2.9). The expansion of T cells following infection was prevented in cells lacking TNF signaling receptors, as such it was conceivable that this could also impact in their function. Therefore, we decided to assess if T cells devoid of TNF signaling were impaired in their efficiency to produce IFN γ .

The requirement of TNF intrinsic signaling in T cells to express IFN γ during infection with *L. donovani* was evaluated in mixed BM chimeras WT:TNF-RdKO established as described in previous section. In our analysis we included B cells as a potential source of IFN γ that was not evaluated in previous analysis (Figure 4.54a; Figure 4.54b). The number of WT and TNF-RdKO

B cells expressing IFN γ in BM following infection was very low, excluding B cells as a relevant producer of IFN γ (Figure 4.54b). In total BM cells from infected mice upon *in vitro* stimulation, CD4⁺ T cells expressing IFN γ comprised 21.41% \pm 4.83 within WT donor cells compartment, but less than 1% (0.6% \pm 0.19) of TNF-RdKO donor cells (Figure 4.54a). This disparity in WT and TNF-RdKO donor CD4⁺T cells contribution to the overall expression IFN γ in BM, following infection was manifest in absolute cell number. The number of WT CD4⁺ T cells IFN γ ⁺ increased about 100 fold upon infection, while the number of TNF-RdKO CD4⁺ T cells IFN γ ⁺ was unchanged, following infection with *L. donovani* (Figure 4.54b).

CD8⁺ T cells also contributed to the overexpression of IFN γ during chronic infection although to a limited extent in comparison to CD4⁺ T cells (Figure 4.54a; Figure 4.54b). The number of WT CD8⁺ T cells expressing IFN γ increased 2.5 fold in infected compared to non-infected recipient mice, while the number TNF-RdKO CD8⁺ T IFN γ ⁺ remain at levels found under homeostatic conditions (Figure 4.54b). The frequency and the cell number of CD3⁺ CD4⁻ CD8⁻ T cells expressing IFN γ derived from both, WT and TNF-RdKO donor cells was very low under homeostatic conditions and remained unaltered following infection (Figure 4.54a; Figure 4.54b).

These findings confirmed CD4⁺ T cells as the main source of IFN γ in BM of mice infected with *L. donovani*. Noteworthy, in the absence of TNF intrinsic signaling the number of CD4⁺ T cells expressing IFN γ was unchanged, suggesting that TNF may play a pivotal role in the expansion of CD4⁺ T cells mediating the loss of HSCs in G0 during experimental chronic VL. Arguing in favor of a central role for TNF in the mediation of IFN γ overexpression in BM of infected mice, was the observation that beside impairing the expansion of CD4⁺ T cell compartment in BM, TNF intrinsic signaling impacted on their efficiency to express IFN γ (Figure 4.54c; Figure 4.54d). In BM cells from infected recipient mice stimulated *in vitro*, 90.95% \pm 3.43 of WT CD4⁺ T cell expressed IFN γ , but this dropped to 70.48% \pm 6.66 in TNF-RdKO CD4⁺ T cells (Figure 4.54c; Figure 4.54d). Following infection, directly *ex vivo* we detected IFN γ in 12.05% \pm 1.19 of WT CD4⁺ T cell, while within TNF-RdKO CD4⁺ T cells this frequency was limited to 4.47% \pm 1.02 (Figure 4.54c; Figure 4.54d).

In summary, these findings suggested that TNF acting directly on CD4⁺ T cells was required to the accumulation of CD4⁺ T cells expressing IFN γ in BM of mice infected with *L. donovani*, at least in this competitive chimeric setting. In previous experiments, we determined that lack of IFN γ signaling in T cells also prevented their accumulation in BM during infection. Further experiments would be required to definitely determine the role of IFN γ and TNF intrinsic signaling in the alteration of BM CD4⁺ T cells in mice infected with *L. donovani* and, how these alterations relate to the loss of HSCs in G0. Nevertheless, in the light of the set of experiments its conceivable that following infection, (1) IFN γ and TNF signaling produced as part of immune

response co-operate to mediate the CD4⁺ T cells accumulation in BM; (2) in these cells, TNF signaling in association with other mediators drive the expression of IFN γ that by indirect mechanisms stimulate LT-HSCs to enter in active-cell cycle; (3) the “perpetuation” of LT-HSCs stimulation results in the depletion of HSCs in quiescence with consequent loss of function, and the accumulation of intermediary progenitors that are less efficient to produce effector mature progeny, resulting in the establishment of anaemia (Figure 4.55).

4.3 DISCUSSION

The collection of findings presented in this chapter revealed that alongside the depletion of LT-HSCs in G0 and subsequent loss of function associated to anaemia and thrombocytopenia (Chapter 3) induced by infection with *L. donovani*, there was the establishment of evident alterations in the composition of T cells residing in the BM. Following infection, there was a dramatic increase in the frequency and number of T cells, mainly sustained by the expansion of CD4⁺ T cells displaying an “effector” phenotype and releasing IFN γ at increased levels. The production of IFN γ by CD4⁺ T cells was sufficient to drive the depletion in LT-HSCs in G0 in addition to anaemia, defining this pro-inflammatory cytokine as a key modulator of haematopoiesis during infection with *L. donovani*. The absence of TNF signaling in CD4⁺ T cells prevented their expansion in the BM of infected mice, and limited their potential to produce IFN γ , suggesting that TNF plays a central role in regulating the alterations in the T-cell compartment of the BM, and therefore indirectly contributing to the impairment of haematopoietic function during chronic infection with *L. donovani*.

To assess the direct impact of the parasite burden in haematopoiesis we established the condition for a “super-infection” in immunodeficient RAG2 KO mice, lacking functional T and B cells. In the current study, despite the increase of parasites/1000 nuclei in the spleen of immunodeficient mice compared to WT mice, RAG2 KO mice did not display any alterations in the number of HSPCs following infection. Additionally, the depletion of the reservoir of quiescent LT-HSCs in the BM was prevented in the absence of functional T and B cells in infected hosts. These findings suggested that in B6 mice, the alterations in haematopoiesis were not directly induced by pathogen-associated molecular patterns from *L. donovani* parasites, but dependent on mechanisms associated with the adaptive immune system.

However, in previous studies carried out in BALB/c mice infected with *L. donovani*, in which CFU assays were used to quantify haematopoietic progenitors in the BM and spleen, it was shown that the magnitude of parasite burden was directly associated to the extent of increase in the number of haematopoietic progenitors found at both sites (S. E. J. Cotterell *et al.*, 2000a). This trend was also observed in SCID (severe combined immunodeficiency) mice, suggesting that innate immune mechanisms contribute to the expansion of haematopoietic progenitors (S. E. J. Cotterell *et al.*, 2000a).

Different antigens from *Leishmania* species induce alterations in TLR signaling, and TLR4 specifically seems to be required to control parasite burdens by acting as an inducer of nitric oxide synthase (iNOS), which is a crucial mechanism for parasites killing (R. K. Singh *et al.*, 2012). LT-HSCs and other early haematopoietic progenitors express TLRs, and *in vitro* stimulation of

LSK cells with TLR ligands is sufficient to induce proliferation and myelopoiesis *in vitro* (Y. Nagai *et al.*, 2006a). Similar results were described in mice challenged with TLR2, TLR4 and TLR9 agonists (J. Megias *et al.*, 2012).

Another example regarding the potential of TLRs to activate HSCs came from mice infected with *Pseudomonas aeruginosa*, model for sepsis, characterized by severe neutropenia due to block in myelopoiesis and expansion of HSCs associated with functional impairment in long-term repopulating capacity. Interestingly, in mice deficient for TLR4 signalling, the neutropenia was prevented and the expansion of LSK cells limited, suggesting that TLR-signalling although advantageous to induce replenishment of post-mitotic short-lived myeloid cells during infection, may also be associated with the emergence of dysfunctional haematopoiesis (S. Rodriguez *et al.*, 2009).

In contrast, it was reported that expansion of LSK cells during *Staphylococcus aureus* infection is independent of TLR signaling. The expansion of LSK cell following infection is not prevented in *S. aureus*-infected RAGKO mice (P. O. Scumpia *et al.*, 2010), emphasizing the variability of mechanisms mediating alterations in haematopoiesis in response to different microbe insults. Another study showed that the loss of myeloid-committed progenitors in the BM during acute phase of infection in WT mice infected with the parasite *Plasmodium chabaudi* (malaria) is not prevented in mice deficient for MyD88 and TRIF, adaptor molecules that are required for TLR-signalling (N. N. Belyaev *et al.*, 2013).

As previously described in BALB/c (S. E. J. Cotterell *et al.*, 2000a), in the present study we also found the number of myeloid-committed progenitors increased in the spleen of mice chronically infected with *L. donovani*, in addition to increased frequency and number of non-committed progenitors. Signs of extramedullary myelopoiesis were also described in other models of parasitic infection such as malaria (N. N. Belyaev *et al.*, 2013).

In adult mammals, most of haematopoiesis takes place in the BM. The regulation of the dynamic process of retention and egress of haematopoietic progenitors is poorly understood, however, the current understanding is that various cell types composing the BM stroma such as, osteoblasts, CXC chemokine ligand 12 (CXCL12)-expressing reticular cells, and vascular endothelium cells contribute to these complex processes (C. H. Kim, 2010).

However, during the response to an infection extramedullary haematopoiesis may be established in the spleen and liver as a consequence of increased haematopoietic activity in the BM, mobilization of haematopoietic progenitors and release of chemokines and growth factors, (J. L. Johns and M. M. Christopher, 2012). For example, the trafficking of LSK cells (with

reconstitution potential following transplant into x-irradiated recipients), between the BM and the periphery has been established in steady-state, however it was reported that pro-inflammatory conditions established by the administration of LPS, correlated to increased number of HSCs seeding into peripheral organs (S. Massberg *et al.*, 2007).

In humans and in animal models of disease, infection with *L. donovani* has been associated with the advents of BM alterations and cytopenias at various degrees of severity (N. Varma and S. Naseem, 2010, F. A. d. Pinho, 2015). The basis for these alterations are poorly defined, however splenic sequestration of blood cells and ineffective haematopoiesis have been appointed as the principal factors underlying the emergency of haematopoietic alterations both in the BM and in the periphery (N. Varma and S. Naseem, 2010). For instance, spleen removal has been for long defined as a therapeutic intervention when pharmacological approaches fail, which results in the recovery of blood cells in circulation to normal values (G. E. Cartwright *et al.*, 1948). The clinical improvement upon splenectomy is not well defined, and some authors suggest that may be due to removal of a large amount of parasites (the spleen being a major reservoir), increased chemotherapeutic drugs available upon removal of hyperplastic spleen, and/or due to increased haemophagocytic activities of the enlarged spleen (G. E. Cartwright *et al.*, 1948, R. A. Dutra *et al.*, 2012).

To assess the contribution of the spleen to the establishment of inflammation-induced haematopoiesis in the BM of mice infected for 28 days with *L. donovani*, the impact of spleen removal in BM cellularity was determined in the current study. During chronic infection with *L. donovani*, we failed to determine any differences either in frequencies of quiescent LT-HSCs, HSPCs (LSK CD150⁺ CD34⁻ CD48⁻ cells, LSK CD150⁺ CD34⁻ CD48⁻ cells, LSK CD150⁺ CD34⁻ CD48⁻ cells, CMPs, GMPs, MEPs and CLPs) or mature cells in the BM between splenectomized mice and “sham” infected mice, suggesting that for the alteration in BM cellularity do not contribute the alteration in the spleen, either by increased sequestering of haematopoietic effector cells or by its establishment as a site for extramedullary haematopoiesis. Nevertheless, it is conceivable that following spleen removal, extramedullary haematopoiesis could be established elsewhere, like the liver.

Importantly, in previous work from P. T Bunn *et al.* it was reported that long-lasting immune response against *L. donovani* can be established in B6 mice lacking secondary lymphoid tissues and spleen, and that antigen-specific CD4⁺ T cells critical to control parasite growth can be generated in the liver (P. T. Bunn *et al.*, 2014).

We determined that alterations in haematopoiesis during infection with *L. donovani* were absent in mice lacking functional T and B cells, which suggested that adaptive immunity might play a

pivotal role in the regulation of haematopoietic function. In fact, the analysis of BM cellularity revealed profound alterations in the frequency and in the number of haematopoietic effector cells in BM. Amongst these alterations, the most compelling were the expansion of the T cell compartment followed by the contraction of the B cell compartment. However, the degree of the expansion of T cells, mainly sustained by CD4⁺ T cells, was far more extensive than the contraction of B cells. Furthermore, T cells in the BM are found in close proximity to IL-7 producing stromal cells, which are required for maturation of B cells (F. E. Mercier *et al.*, 2012). Most likely B cells are found in decreased numbers because they have to compete with T cells for the same niches in the BM, whose cell numbers are hugely increased during infection.

In mice infected with *L. donovani* for 28 days we found the number of BM CD4⁺ T cells was increased ~20 fold compared to naive mice, and spleen removal did not limit the expansion of the CD4⁺ T cell compartment in BM. However, previous work carried out in mice infected with OVA-transgenic *L. donovani* parasites reported that 5 days following infection the number of proliferating Ag-specific CD4⁺ T cells in BM was unchanged compared to control (P. T. Bunn *et al.*, 2014). In addition, treatment with FTY720 which causes S1P1R internalization preventing lymphocytes trafficking lead to a significant decrease in the number of Ag-specific CD4⁺ T cells in BM (P. T. Bunn *et al.*, 2014). These finding suggested that is not BM a privileged site for T cell priming during *L. donovani* infection. As such in future experiment it would be pertinent to access using an OVA-Leish system the proportion of CD4⁺ T cells Ag-specific in BM, as well as, determined the contribution of ingress of Ag-specific T cells into BM, at various time points following infection.

In steady-state mature CD4⁺ T cells and CD8⁺ T cells reside in BM in low numbers (K. Tokoyoda *et al.*, 2009b, Y. Zhang *et al.*, 2013), where priming of antigen-specific T cells can take place (M. Feuerer *et al.*, 2003). The proof that BM T cells are fully functional came from the onset of graft *versus* host disease in allogeneic host receiving total BM cells transplants (F. Di Rosa and R. Pabst, 2005). Furthermore BM has been described as a privileged site for homing of memory T cells (C. Arieta Kuksin *et al.*, 2015).

It has been shown that CD4⁺ T cells play an important role in the regulation of normal haematopoiesis (J. P. Monteiro *et al.*, 2005). Furthermore, changes in T cells in BM have been described in association with haematological alterations in experimental models of BMF syndromes and human monocytic ehrlichiosis (HME) (Y. Zhang *et al.*, 2013, F.-c. Lin *et al.*, 2014, C. Arieta Kuksin *et al.*, 2015). As such, there is an emerging demand to better understand the role of BM resident T cells in the immune response and in the regulation of haematopoiesis.

The association between alteration in T cells and haematopoietic activity has been formerly established in aplastic anaemia (AA) (C. Dufour *et al.*, 2001, C. Dufour *et al.*, 2003, N. S. Young *et al.*, 2008). In humans, AA is characterized by the expansion of T cells displaying Th1 phenotype that release IFN γ at increased levels. It was proposed that on the basis of AA pathophysiology is the increased cell death of HSPCs mediated by these expanded T cells, that ultimately results in BM failure (C. Dufour *et al.*, 2001). Using experimental models for AA, it has been also suggested that T cells are key mediators of haematopoietic dysfunction and ultimately result in BM failure (F.-c. Lin *et al.*, 2014, C. Arieta Kuksin *et al.*, 2015). T cells migrate to the BM in response to chemokines, such as stromal-cell derived factor-1 (SDF-1, also known as CXCL12), the ligand for the chemokine receptor CXCR4 expressed in CD4⁺ T cells (C. Arieta Kuksin *et al.*, 2015). Using an experimental model for lethal AA it was shown that the number of BM-infiltrating T cells was increased, in which the CXCR4 expression was aberrantly up-regulated, however, when the interaction of CXCR4-SDF1 was blocked this resulted in reduced accumulation of pathogenic T cells and sick mice were rescued from lethal BMF (N. S. Young *et al.*, 2008, C. Arieta Kuksin *et al.*, 2015).

In other study, using mutant mice where IFN γ is constitutively expressed at low levels in T cells and Natural Killer cells (NK cells), it was reported that this is sufficient to promote AA phenotype (F.-c. Lin *et al.*, 2014). Furthermore, in this experimental model of disease, as a result of the persistent exposure to low levels of IFN γ , the number of phenotypic HSCs (Lin⁻ cKit⁺ Sca1^{hi} CD34⁻ Flt3⁻ CD150⁺ cells) is increased and the differentiation of MPPs to myeloid progenitors, erythrocytes and B cells is defective, suggesting that the emergence of ineffective haematopoiesis contributes to AA (F.-c. Lin *et al.*, 2014).

Alterations in T cells in association with haematopoietic impairment are not restricted to BMF syndromes. For example, in experimental model of human monocytic ehrlichiosis (HME), infected mice, similarly to infected humans, display anaemia and thrombocytopenia (Y. Zhang *et al.*, 2013). The establishment of infection correlated with the expansion of LSK cells in BM, which was dependent of IFN γ R signalling in mice infected with *Ehrlichia chaffeensis* (experimental model of the disease), and then it was determined that during infection the main source of IFN γ were CD4⁺ T cells (Y. Zhang *et al.*, 2013).

A recent review compiled the most relevant studies performed on the characterization of T cells in BM using experimental models of disease. In an attempt to shed some light on the classification of activated T cells in the BM, it proposed the following: “effector” BM T cells are enriched in the CD44^{high} CD127 (IL-7R α)^{-low} Ly6C^{-low} population and “memory” BM T cells are enriched in CD44^{high} CD127^{high} Ly6C^{high} population (K. Tokoyoda *et al.*, 2010).

Based on the above studies reporting that T cells have the potential to impair haematopoietic function in periphery and induce the activation of HSCs into active cell-cycle in BM, we decided to characterize BM T cells in further detail. In the current study, the phenotypic and functional characterization of BM T cells revealed that following infection with *L. donovani* the vast majority (about 90%) of CD4⁺ T cells were CD44^{hi} CD127^{-/low} Ly6C^{-/low} cells, a phenotype previously attributed to BM “effector-T cell” (K. Tokoyoda *et al.*, 2010). Additionally, we found that both in steady-state percentage of BM CD4⁺ T cells CD44^{hi} was higher in the spleen compared to BM, and this become further evident following infection.

The observation of a higher proportion of T cells with an “activated” phenotype reside in BM in steady-state compared with the spleen has been made previously by others. These differences in the distribution of T cells population in BM are followed by other important phenotypic and functional differences in T cells between BM and the spleen (F. Di Rosa and R. Pabst, 2005).

For example, it was reported that in mice, BM T cells express higher level of CD44 compared to other sites, as studies in LCMV models of infection demonstrated that CD8⁺ T cells CD44^{hi} are more activated in BM compared to those found in the spleen. Antigen-specific CD8⁺ T cells persist for much longer periods of time in BM compared to other extra-lymphoid following infection resolution, while retaining their ability to perform an efficient secondary immune response when transferred to an immunodeficient infected host (F. Di Rosa and R. Pabst, 2005). In more recent study using LCMV model of infection these same features were also attributed to BM CD4⁺ T cells (K. Tokoyoda *et al.*, 2009b).

Activated T cells have been classically segregated in short-lived “effector” T cells and long-lived “memory”. “Memory” T cells are then classified into “central memory” that are in permanent circulation between the blood and secondary lymphoid organs and have a higher potential of expansion compared to the “effector memory” T cells, which survey extra-lymphoid organs providing a quick response to invading pathogens (F. Di Rosa and R. Pabst, 2005). The classification into the above mentioned categories has been a matter of debate for a long time due to differences in the expression of surface markers among T cells from different tissues, and due to the plasticity of “memory” and “effector” cells. In chronic infection where residual pathogens persist over time the distinction becomes even harder as effector T cells may be present for extended periods of time (F. Di Rosa and R. Pabst, 2005, K. Tokoyoda *et al.*, 2010).

The distinction between central memory and effector memory has been usually made on the assumption that “central memory” T cells express CCR7 and have a more proliferative compared to “effector memory” T cells that do not express CCR7 (F. Di Rosa and R. Pabst, 2005). To add more complexity to this subject it was reported that BM memory T cells may not express CCR7

or CD62L but the majority express Ly6C, rarely found expressed in memory T cells in other sites (K. Tokoyoda *et al.*, 2009a, K. Tokoyoda *et al.*, 2009b). Furthermore, memory T cells in BM rapidly expand extensively upon challenge, displaying simultaneously functional features classically associated to the so-called “central memory” (i.e. rapid extensive proliferation) and “effector memory” T cells (i.e. residing in BM) (F. Di Rosa and R. Pabst, 2005, K. Tokoyoda *et al.*, 2009b).

Further experiments would be required to functionally define the CD4⁺ T cells found in BM as “effector” or “memory” cells. A “memory” T cells is defined as a antigen-specific cells that persist after antigen removal and is capable to expand following a second encounter with cognate antigen (F. Di Rosa and R. Pabst, 2005). For example, experiments could be developed using transgenic mice bearing CD4⁺ T cells expressing a TCR specific for a defined antigen, in immunized mice following the removal of the cognate-antigen, the persistence and the phenotype of CD4⁺ T could be assessed, as well as their kinetics of expansion in a subsequent stimulation with target antigen, for example using an OVA-Leish OT II system. In addition, different populations Ag-specific BM CD4⁺ T cells (based on the differential expression of CD44, CD127 and Ly6C) could be transferred to RAG2 KO recipients and their localization, phenotype and response to secondary *L. donovani* infection in comparison to naive BM CD4⁺ T cells isolated from naive mice.

In the present study, we found that ~ 90% of BM CD4⁺ T cells, besides displaying an “effector” phenotype (CD44^{hi} CD127^{-low} Ly6C^{-low} cells), were primed to express IFN γ at increased levels. A substantial proportion of CD4⁺ T cells were actively expressing IFN γ and TNF in the BM of infected mice, suggesting though not proving a degree of antigen specificity to the response.

In hamsters infected with *L. donovani*, characterized by severe anaemia and leucopenia, it was reported that mRNA levels of IFN γ and TNF-related apoptosis-inducing ligand (TRAIL) are significantly increase both in BM and the spleen, and this is coincident with an increase in apoptotic erythroblasts in BM, collectively suggesting that in the hamster, anaemia is mediated by cytokine-induced increased apoptosis of erythroid progenitors (W. P. Lafuse *et al.*, 2013).

Additionally, previous studies reported that both IFN γ and TNF are found expressed increased in the BM of patients suffering from BMF syndromes, suggesting that increased levels of expression of these cytokines may contribute to the decline of a haematopoietic function (C. Dufour *et al.*, 2001, C. Dufour *et al.*, 2003).

Initial studies *in vitro* suggested that IFN γ has an inhibitory impact in haematopoiesis, through the inhibition of proliferation and induction of apoptosis (A. M. de Bruin *et al.*, 2014). However, *in*

in vivo studies in different models of infections have been less consensual regarding the impact of IFN γ in the modulation of inflammation-induced haematopoiesis, and respective mechanisms of action (A. M. de Bruin *et al.*, 2014). For example, in mice infected with *Mycobacterium avium*, it was proposed that IFN γ acting directly on LT-HSCs through the activation of the transcription factor STAT1 (Signal transducer and activator of transcription 1) induced proliferation with significant decrease of cells in quiescence, accumulation of early committed progenitors and loss of myeloid-committed progenitor in the BM (M. T. Baldrige *et al.*, 2010). In this study from Baldrige *et al.*, it was reported that in BMT competitive assays, BM cells derived from donors treated with IFN γ performed poorly in the reconstitution of haematopoietic system following transplantation in lethally x-irradiated recipients, compared to PBS treated controls. The cell numbers for LT-HSCs in the donors were very similar irrespective of IFN γ treatment, suggesting that the competitive disadvantage of “IFN γ -activated” LT-HSCs results from their lower degree of quiescence, a property intrinsically related to engraftment potential (M. T. Baldrige *et al.*, 2010).

The experimental model for HME provided another example supporting a role for IFN γ as a key mediator of haematopoietic dysfunction, established not only in the periphery but coincident with increased proliferation of HSCs and consequent loss of engraftment potential in long-term BMT assays (K. C. MacNamara *et al.*, 2011a, K. C. MacNamara *et al.*, 2011b). Mice infected with *Ehrlichia muris* are characterized by the emergence of anaemia, thrombocytopenia and BM cells show decreased colony forming activity *in vitro*, however all these features were prevented in infected mice deficient for IFN γ signalling. Importantly, infected mice lacking receptor for IFN γ only in the stromal compartment display similar alterations in haematopoiesis, including the expansion of LSK cells compartment in BM, compared to the IFN γ R competent control (K. C. MacNamara *et al.*, 2011b). Overall, these findings suggested that IFN γ signalling in haematopoietic cells is required to induce haematopoietic impairment during infection with *E. muris* (K. C. MacNamara *et al.*, 2011b). In a following study, it was reported that infection with *E. muris* leads to the activation of HSCs (LSK CD150⁺ Flt3⁻ cells) into active cell-cycle and this correlated with poor reconstitution upon transfer to non-infected recipient mice. In competitive BMT experiments, LSK cells derived from infected IFN γ R deficient mice showed competitive advantage over LSK cells derived from infected WT mice. And so, it was proposed that IFN γ directly mediates HSCs loss of function through the induction of increased proliferation during infection with *E. muris*, however proliferative state of IFN γ R KO HSCs in chimeric mice was not assessed (K. C. MacNamara *et al.*, 2011a).

On the contrary, in LCMV infected mice, a model for acute viral infection, it was proposed that IFN γ acting directly on LT-HSCs (LSK CD150⁺ CD48⁻ cells) inhibits proliferation and reduces self-renewal divisions (A. M. de Bruin *et al.*, 2013). Mice infected with Armstrong strain of

LCMV display BM hypocellularity, low number of LT-HSCs and leucopenia. In this study from de Bruin *et al.*, it was reported that *in vitro* stimulation of LT-HSCs with IFN γ results in a lower division index. However, the infection of IFN γ -deficient mice or mixed BM-chimeric mice reconstituted with BM cells from IFN γ -deficient mice and WT mice, resulted in both scenarios in a faster recovery of HSCs number from IFN γ -signalling deficient cells during the course of infection. *In vitro* stimulation of LT-HSCs with IFN γ impaired TPO-mediated phosphorylation of STAT5 by the induction of SOCS1 (inhibitor of STAT5 activation) and abrogated TPO-mediated proliferation of LT-HSCs, then it was determined that IFN γ limit the downregulation of the cell-cycle inhibitor p57 induced by TPO in LT-HSCs. Finally, it was reported that WT HSCs from LCMV mice upregulate the expression of mRNA for p57 but this was prevented in HSCs deficient for IFN γ R (A. M. de Bruin *et al.*, 2013). As such, IFN γ in the context of LCMV infection seems to limit LT-HSCs function through the downregulation of the expression of genes involved in the regulation of cell-cycle progression (A. M. de Bruin *et al.*, 2013).

On the other hand, in a study designed to study the impact of CD8⁺ T cells in haematopoiesis in mice infected with WE strain LCMV, it was proposed that IFN γ mediates increased myelopoiesis not acting directly on HSPCs but instead mediating the release of IL-6 by BM stromal cells (C. M. Schuerch *et al.*, 2014). In this study, to isolate the impact of CD8⁺ T cells, cells from TCR-gp33 epitope of LCMV transgenic mice (p14 CD8⁺ T cells) were transferred for mice expressing gp33 in all cells (H8 mice). In H8 mice, the transfer of p14 CD8⁺ T cells was related to the expansion of Lin⁻ cKit⁺ cells, maintenance of LT-HSCs number followed by the expansion of all the other HSPCs, increase colony-forming activity biased toward myeloid differentiation *in vitro* and increased number of Ly6C⁺Ly6G⁻SSC^{lo} inflammatory monocyte in circulation. These alterations were prevented in both H8 mice receiving IFN γ -deficient p14 CD8⁺ T cells and in IFN γ R-deficient H8 mice receiving WT p14 CD8⁺ T cell. Subsequently, using mixed BM chimeras, it was demonstrated that in this system IFN γ released by CD8⁺ T cells acts directly on BM stromal cells to induce IL-6 release, which then mediates the downregulation of *Runx-1* and *Cebpa* in Lin⁻ cKit⁺ cells thus favoring myeloid differentiation (C. M. Schuerch *et al.*, 2014).

A different role for IFN γ in the modulation of alterations in the haematopoietic system was proposed following experiments in an experimental model for Malaria. Mice infected with *Plasmodium chabaudi* are characterized by the loss of myeloid-committed progenitors in BM, and it was proposed that this is mediated by IFN γ signalling acting directly on the stromal compartment, and increased systemic levels of CCL2, therefore promoting the conditions for increased mobilization of myeloid-committed progenitors to the periphery via CCR2 expressed on these progenitors (N. N. Belyaev *et al.*, 2013).

These above given examples illustrate the requirement of studies on the impact of IFN γ in the infection-induced haematopoiesis in the pathogen-specific contexts, additionally emphasise the limitation associated to the so far proposed general mechanisms concerning the regulation of haematopoiesis in the face of stress or injury.

In the present study, to dissect the role of CD4⁺ T cells in the changes in haematopoiesis in BM and haematopoietic dysfunction in periphery, purified CD4⁺ T cells from naive B6 mice were transplanted to RAG2 KO mice, subsequently infected with *L. donovani*. In line with previous experiments, in mice lacking functional T and B cells, the infection with *L. donovani* parasites did not result in significant changes in the number of HSPCs nor in the number of LT-HSCs in G0. On the contrary, RAG2 KO mice that received CD4⁺ T cells displayed profound alterations in the haematopoietic compartment, such as the expansion of early progenitors and the depletion in the reservoir of quiescent LT-HSCs, resembling the phenotype observed in WT infected mice.

Furthermore, we determined that the establishment of anaemia and thrombocytopenia in WT mice chronically infected with *L. donovani* were absent in immunodeficient RAG2 KO mice, however those haematological anomalies in the periphery emerged in RAG2 KO mice transplanted with CD4⁺ T cells following infection. These findings demonstrated that CD4⁺ T cells could solely mediate the alteration in haematopoiesis in BM and in haematopoietic function in the periphery during infection with *L. donovani*. CD4⁺ T cells showed a much higher degree of alteration compared to CD8⁺ T in the BM of infected mice. Nevertheless, it is conceivable that CD8⁺ T cells could also play an important role in the haematological changes resulting from infection.

The phenotypic alteration of transplanted CD4⁺ T cells replicated those from BM CD4⁺ T cells found in WT infected mice i.e. massive expansion and skewing towards “effector” BM T cells (CD44^{hi} LyC6^{-/lo} CD127^{-/lo} T cells). Interestingly, in naive RAG2 KO mice, the vast majority of transplanted CD4⁺ T cells had a “memory” phenotype (CD44^{hi} LyC6^{hi} CD127^{hi} T cells), which argues in favor of the phenotype proposed for memory T cells in the BM (K. Tokoyoda *et al.*, 2010).

Given the central role of IFN γ in the mediation of haematological dysfunction in other models of infection (M. T. Baldrige *et al.*, 2010, K. C. MacNamara *et al.*, 2011a, K. C. MacNamara *et al.*, 2011b, A. M. de Bruin *et al.*, 2013) in the present study, we assessed whether CD4⁺ T cells modulated stress-induced haematopoiesis during infection with *L. donovani* through the release of IFN γ , expressed at increased levels in the BM in chronically infected mice. This hypothesis was further supported by the report that expansion of LSK cells compartment of mice infected with *E. muris* depended of IFN γ derived from CD4⁺ T cells (Y. Zhang *et al.*, 2013).

In clear opposition to the results obtained by the transfer of WT CD4⁺ T cells, the phenotype of infected RAG2 KO transferred with CD4⁺ T cells lacking IFN γ was identical to infected RAG2 KO mice not subjected to any cell transfer, namely in the number of HSPCs in BM, number of quiescent LT-HSCs and maintenance of blood parameters (RBC and platelets) at basal levels. The number CD4⁺ T cells in IFN γ KO and WT mice were identical in the BM of infected RAG2 KO, suggesting that CD4⁺ T cells lacking IFN γ were competent to expand in response to infection in non-competitive experimental settings. As such, in our model of experimental VL, we defined CD4⁺ T cells expressing IFN γ as key modulators for the depletion of quiescent LT-HSCs driven by the massive expansion early progenitors and ineffective haematopoiesis reflected in the establishment of anaemia. Additionally, in the sequence of these set of experiments we also resolved that CD4⁺ T cells expressing IFN γ were required to the clearance of parasites and the onset of splenomegaly in immunodeficient mice, which is strongly suggestive of a central role of these cells underlying these same manifestations in WT infected mice.

These findings conform to previous reports establishing IFN γ as a mediator of disease progression in VL (A. P. Taylor and H. W. Murray, 1997, R. Kumar *et al.*, 2014). In culture of splenic aspirates from VL patients with clinical symptoms of Kala-azar, the addition of blocking antibodies against IFN γ correlated with increased parasite load, suggesting that IFN γ is important to control the parasite growth in humans (R. Kumar *et al.*, 2014). Interestingly, in this same study CD4⁺ T cells were defined as the main source of IFN γ in PB blood of VL patients (R. Kumar *et al.*, 2014). Furthermore, it was formerly reported in experimental VL using BALB/c mice infected with *L. donovani* that the absence of IFN γ signalling resulted in uncontrolled parasite burdens in the liver, which is controlled in IFN γ competent littermates (A. P. Taylor and H. W. Murray, 1997).

Increased proliferation of LT-HSCs into active cell-cycle and impaired repopulating activity, as a consequence of stress-induced haematopoiesis has been attributed to IFN γ signalling acting directly on these cells in other models of infection (M. T. Baldrige *et al.*, 2010, K. C. MacNamara *et al.*, 2011a, K. A. Matatall *et al.*, 2014). To test the hypothesis that IFN γ signalling in LT-HSCs were driving increased proliferation during chronic infection with *L. donovani*, we established BM mixed chimeras with equal number of total BM cells derived from WT and IFN γ R2KO (WT: IFN- γ R2KO \rightarrow WT). This approach allowed the experimental evaluation of the impact of IFN γ R signalling in LT-HSCs, whilst excluded confounding findings resulting from a global loss of IFN γ signalling. In agreement with previous findings from Bruin and MacNamara, we determined that donor cells lacking IFN γ signalling displayed higher repopulating potential in lethally irradiated recipients, following the establishment of infection (K. C. MacNamara *et al.*, 2011a, A. M. de Bruin *et al.*, 2013). Nonetheless, an increased repopulation activity of IFN γ R2 KO was already prevalent in uninfected recipient mice, and this was not significantly changed

following infection with *L. donovani*. These findings suggested that basal levels of IFN γ regulate haematopoietic activity, as formerly reported by others (A. M. de Bruin *et al.*, 2013). Nevertheless in the current study, under conditions established by infection with *L. donovani*, the lack of IFN γ signalling did not constitute a further competitive advantage.

In our study, the lack of intrinsic IFN γ signalling did not prevent the expansion of LSK cells compartment in BM of mice chronically infected with *L. donovani*. However, in the BM of chronically infected recipient mice, we found that within the WT compartment, the increase in the frequency of LSK cells was coincident with a dramatic contraction of Lin $^-$ cKit $^+$ cells, whilst within IFN γ R2 KO donor cells those remain unaltered. As such, to the increase in WT LSK cells may contribute to the upregulation of Sca1 in functional lineage-committed progenitors classically included Lin $^-$ cKit $^+$ cells mediated by intrinsic IFN γ signalling. This phenomenon has been formerly reported in other models of infection (N. N. Belyaev *et al.*, 2010, N. N. Belyaev *et al.*, 2013) and following IFN γ stimulation haematopoietic cells *in vivo* and *in vitro* (T. R. Malek *et al.*, 1989, A. Sinclair *et al.*, 1996, A. M. de Bruin *et al.*, 2013).

In the absence of intrinsic IFN γ signalling, we found that early committed progenitors expanded extensively follow infection, and noticeably LT-HSCs were driven to an active proliferative status at a similar extent as WT LT-HSCs. Therefore, in mice infected with *L. donovani* we could exclude IFN γ as a direct mediator of LT-HSCs loss of quiescence, and subsequent functional impairment (Chapter 3). As a consequence of these findings, it would be important to establish BM chimeras in which the receptor for IFN γ is expressed in LT-HSCs but not in radio-resistant BM stromal cells, to determine whether the deleterious effect of IFN γ impact in haematopoietic function could be mediated by the IFN γ signalling acting directly on BM stromal cells. In fact, this mechanism has been proposed previously to explain increased myelopoiesis in mice infected with LCMV strain WE (C. M. Schuerch *et al.*, 2014).

Former studies proposed that IFN γ R expressed in HSPCs was directly implicated in activation of “dormant” LT-HSCs and/or haematopoietic dysfunctions, which was attributed to the lack of increased proliferation in LT-HSCs and/or alteration in other progenitors and mature effector cells in IFN γ RKO mice, (M. T. Baldrige *et al.*, 2010, K. C. MacNamara *et al.*, 2011a, K. C. MacNamara *et al.*, 2011b, Y. Zhang *et al.*, 2013). Under those conditions, infections were established in an “all system” deficient for IFN γ signalling, which could explain the conflicting results obtained in our model of chronic infection. On the other hand, in mixed BM chimeric mice with WT and IFN γ R2 KO donor cells, following LCMV strain Armstrong infection the proportion of LT-HSCs in active cell-cycle was comparable between WT and IFN γ R2KO donor cells at various time points, as such it was proposed that IFN γ -signalling in HSCs to be not

responsible the activation of quiescent LT-HSCs into an active proliferative status (A. M. de Bruin *et al.*, 2013).

In the current study, we established that in steady-state IFN γ was not required to T cell development; on the contrary, lack of intrinsic IFN γ signalling clearly limited the expansion of these cells following infection with *L. donovani*. This competitive advantage based on IFN γ R-signalling on T cells, was further evident in BM, suggesting that IFN γ contributes to the dramatic increase in the T cell compartment during experimental VL. On the other hand, in non-competitive settings, as a consequence of transfer into RAG2 KO recipients, IFN γ KO T cells were able to expand in the BM at a similar rate to WT T cells. These findings are difficult to reconcile and pointed to various conceivable scenarios; it is plausible that in immunodeficient mice compensatory mechanisms are in place and IFN γ from other sources (i.e. NK cells) may be sufficient to drive the increase in T cells in the BM, yet below a threshold required to propel haematopoietic dysfunction.

Another hypothesis would be that IFN γ R-signalling equipped T cells with an increased capacity to expand and the endogenous expression of IFN γ intrinsically related to other functions, such as additional expression of growth factor or anti-apoptotic mediators, features not assessed in this experiment. For instance, it is well established that IFN γ is important for the differentiation of CD4⁺ T cells into Th1 cells in detriment of Th2 cells (V. Lazarevic *et al.*, 2013). It was proposed that IFN γ receptor and TCR signalling induce the expression of T-bet, the master regulator of Th1 cell differentiation, the expression of T-bet promotes the expression of IFN γ , which in an autocrine manner regulates further expression of T-bet and therefore the stabilization of Th1 phenotype, and consequent acquisition of functional and migratory features (V. Lazarevic *et al.*, 2013). As such, it would be important to determine in further experiments if IFN γ signalling in CD4⁺ T cells is required to the upregulation of T-bet during chronic infection with *L. donovani*.

In other models of infection there is evidence that direct IFN γ signalling modulates T cells either by enhancing or suppressing their responses to infection (J. K. Whitmire *et al.*, 2005, J. S. Haring and J. T. Harty, 2006). For example, in mice immunized with LCMV, using competitive transfer assays it was shown that antigen-specific CD4⁺ T cells expand at a much higher rate compared to antigen-specific CD4⁺ T cells lacking IFN γ signalling. The expression of IFN γ receptor correlated with higher efficiency of IFN γ production, suggesting that direct IFN γ signalling enhance CD4⁺ T cells functions (J. K. Whitmire *et al.*, 2005). On the contrary, in an experimental model for *Listeria monocytogenes* infection, it was observed that a higher percentage of antigen-specific CD4⁺ T cells expressed IFN γ and IL-12 in IFN γ R KO mice compared to WT mice, their frequency in IFN γ R KO mice remained increased at later time points while in WT mice it steadily decreased over a period from 7 to 150 days post-infection. As such, it was proposed that IFN γ

signalling is not required for the differentiation of effector Th1 cells but important for the contraction of CD4⁺ T cell compartment upon LCMV infection resolution (J. S. Haring and J. T. Harty, 2006). These two examples frame the relevance of determining the role of IFN γ signalling in the regulation of T cells functions in the context of specific microbe insults.

In the current study, we demonstrated that CD4⁺ T cells competent to produce IFN γ mediate haematopoietic impairment during chronic infection with *L. donovani*. To definitely establish the role of IFN γ R-signalling on these cells, it would be important to determine whether the transfer of CD4⁺ T cell devoid IFN γ R to RAG2 KO mice prevents the onset of haematopoietic alterations, otherwise present following transfer of WT CD4⁺ T cells, and subsequently determine how the lack of IFN γ R-signalling relates to the proficiency to express IFN γ in our model of chronic infection.

In BM mixed chimeric mice WT: IFN- γ R2KO \rightarrow WT, we also determined noteworthy alterations in the myeloid cell compartment. Following infection with *L. donovani*, within the IFN γ R KO donor progeny there was a contraction in the frequency of CD11b⁺ F4/80⁺ myeloid cells (phenotype associated to macrophages in most tissues (X. Zhang *et al.*, 2008)) in the BM of infected recipient, in an opposite trend to the increase observed among WT derived CD11b⁺ F4/80⁺ myeloid cells. In steady-state, the frequency of CD11b⁺ F4/80⁺ myeloid cells lacking intrinsic IFN γ signalling was already decreased compared to those from derived WT donor cells, both in BM and in the spleen, suggesting that basal IFN γ levels contribute to their development and/or survival. The differences in the frequency of CD11b⁺ F4/80⁺ myeloid cells and other myeloid populations became further evident in chronically infected mice, both in the BM and spleen, suggesting that in the conditions established by the infection with *L. donovani*, intrinsic IFN γ signalling provides a competitive advantage to myeloid cells. These findings raised non-exclusive hypothesis: that IFN γ -signalling may “equip” infected myeloid cells to kill the parasites more effectively and avoid cell-death (A. C. Stanley and C. R. Engwerda, 2007); IFN γ signalling could induce myeloid biased differentiation of haematopoietic progenitors, which was proposed in other models of infection (K. C. MacNamara *et al.*, 2011b, A. M. de Bruin *et al.*, 2012, K. A. Matatall *et al.*, 2014).

BM macrophages mediate the development of erythrocytes and the retention of HSCs in the BM, this was established in CD169-DTR mice expressing diphtheria toxin receptor (DTR) knocked in downstream of the endogenous CD169 promoter, which allowed to examine the specific role of BM macrophages in haematopoiesis, since CD169 in BM is specifically expressed in macrophages, but not in other myeloid cells. (A. Chow *et al.*, 2011, A. Chow *et al.*, 2013). In mice, the depletion of BM CD169⁺ macrophages leads to a substantial increase in the number of LSK Flt3⁻ cells (enriched in HSCs) in circulation, and this enhanced mobilization of HSCs driven

by the deletion of BM CD169⁺ macrophages correlated with the down-regulation in the gene expression of molecular mediators associated to HSCs retention within mesenchymal stromal cells (A. Chow *et al.*, 2011). Moreover, the maturation of erythroid progenitors in BM takes place in special niches, the so-called erythroblastic islands, in which erythroblasts at various stages of development are found in close association with BM macrophages. In transgenic mice the deletion of BM CD169⁺ macrophages correlates with a dramatic reduction in the numbers of both F4/80⁺/Ter119⁺ islands, and erythroblasts in the BM, in addition to increased mobilization of erythroblasts to the circulation and the spleen (A. Chow *et al.*, 2013). Given the important role of BM macrophages in haematopoiesis exemplified above, the alterations we observed in the myeloid compartment in the BM of chimeric mice WT:IFN- γ RKO following *L. donovani* infection, it would be important to further assess the identity of BM myeloid cells (and expression of CD169), dissect their role in the establishment of haematopoietic dysfunction, and finally explore the significance of IFN γ signalling in these cells in the context of the alterations of haematopoiesis characterizing mice chronically infected with *L. donovani*. Moreover, it was recently reported in our laboratory that the frequency of myeloid cells CD169^{hi} is decreased in the BM of B6 mice following *L. donovani* infection (O. Preham unpublished data).

In the current study, we found that in mice chronically infected with *L. donovani* there was a significant increase in the level of TNF receptors (TNF-R1a or p55 and TNF-R1b or p75) expression in early haematopoietic progenitors including LT-HSCs, suggesting that these immature cells were responsive to the increase in pro-inflammatory cytokine availability in BM. These findings agree with previous studies reporting that TNF receptors expression is up-regulated under conditions of stress-induced haematopoiesis, such as following transplantation (K. Mizrahi and N. Askenasy, 2014).

In addition to IFN γ , changes in TNF levels of expression, both in BM and systemically have been reported in patients suffering from BMF syndromes (C. Dufour *et al.*, 2001, C. Dufour *et al.*, 2003, W. Du *et al.*, 2014). An important role for TNF mediating the establishment of haematopoietic dysfunction in patients suffering from Fanconi anaemia was proposed following the observation that the addition of anti-TNF fusion protein to cultures of BM cells from these patients was associated with an improvement in their potential to originate erythroid colonies *in vitro* (C. Dufour *et al.*, 2003). Other *in vitro* studies, using human cells, defined TNF as a suppressor of haematopoiesis, for example the addition of TNF or IFN γ to total BM cultures results in a significant reduction of colony formation both from myeloid and erythroid lineages, however this inhibition was further increased by the combination of both cytokines, suggesting that TNF and IFN γ signalling may cooperate in the impairment of haematopoietic function (C. Selleri *et al.*, 1995). Similar findings, reporting TNF as an inhibitor of haematopoiesis, were

produced in *in vitro* experiments conducted with murine cells (Y. Zhang *et al.*, 1995, D. Bryder *et al.*, 2001, C. J. H. Pronk *et al.*, 2011).

Nevertheless, other studies performed *in vitro* suggested that under specific contexts TNF might induce HSCs activation (H. W. Snoeck *et al.*, 1996, M. T. Baldrige *et al.*, 2011). For example, TNF in combination with IL-3 induced increased colony-formation activity of human BM CD34⁺ CD38⁻ cells (enriched for HSCs), which was nearly absent in cultures supplemented with IL-3 alone (H. W. Snoeck *et al.*, 1996). In addition, it was reported that TNF acts synergistically with IL-3 and GM-CSF in the formation of colonies *in vitro* when added to the culture system in low concentration, but it had an antagonistic impact at high concentrations, suggesting that TNF impact in haematopoietic activity may be dosage-dependent (L. S. Rusten *et al.*, 1994).

Additionally, it was observed that the transfer of LSK cells pre-stimulated *in vitro* with TNF to lethally irradiated recipients correlated with impaired HSCs activity, since after a period of 14-18 weeks, the level of reconstitution of these cells was very poor compared to control LSK cells culture in the same conditions without TNF, and the same was observed with donor cells deficient for Fas, suggesting that this cytokine has the potential to limit HSCs self-renewal activity independently of Fas pathway (D. Bryder *et al.*, 2001). However, in another study carried out in a co-culture system, it was proposed that CD8⁺ cells through the release of TNF induce LSK expansion, and that these cells contribute to long-term engraftment (F. Rezzoug *et al.*, 2008).

Increased release of TNF was also described in mice infected with *Ehrlichia muris* (Y. Zhang *et al.*, 2013) and in mice stimulated with Poly:IC (E. M. Pietras *et al.*, 2014). Both of these inflammatory models display extensive expansion of LSK cells in BM.

TNF plays a very important role in the establishment of an effective immune response to a wide variety of pathogens (J. J. Peschon *et al.*, 1998, T. Ellerin *et al.*, 2003), including *L. donovani* (C. R. Engwerda *et al.*, 2004b). Despite the controversy regarding the role of TNF, either as inducer or inhibitor of haematopoietic activity, the present body of literature agrees that alterations of TNF expression impact haematopoietic function and in HSCs activity, and that the regulation of haematopoiesis by TNF should be a complex and context-dependent process (M. T. Baldrige *et al.*, 2011, K. Mizrahi and N. Askenasy, 2014, N. Askenasy, 2015).

In mice infected with *L. donovani* we found that the frequency of CD4⁺ T cells expressing TNF at increased levels was significantly expanded in the BM. Additionally, the expression of TNF can be also upregulated by myeloid population in pro-inflammatory condition (K. Matsui *et al.*, 2013). As such, we hypothesized that TNF could be acting directly on HSCs during experimental VL as a mediator of the activation of HSCs into active cell-cycle, and subsequent functional

impairment. Aiming to dissect the role of TNF receptor signalling during chronic VL, BM mixed chimeras were established with equal number of total BM cells derived from WT and TNF-RdKO (doubly deficient cells for TNF-R1a and TNF-R1b) into WT recipients (B6.CD45.1 : B6.CD45.2TNF-RdKO → B6.CD45.1), and therefore avoid confounding results due to the absence of TNF signalling in other cell populations.

Similar to a previous study carried out by Pronk et al (C. J. H. Pronk *et al.*, 2011), we demonstrated that lack of TNF receptor signalling constitutes a competitive advantage in the reconstitution of lethally irradiated recipients, which was reflected in a higher proportion of TNFR-dKO donor cells compared to WT donor cells, both in the BM and spleen of recipient mice. These analyses were performed after a period of 13 weeks, and at this time point it is expected that the vast majority of mature cells to be derived from donor HSCs.

On the other hand, these findings contradict a study that proposed that intrinsic TNF signalling is required for long-term engraftment of BM donor cells into WT lethally irradiated recipients (M. Pearl-Yafe *et al.*, 2010). In the study by Pearl-Yafe et al, the transplantation experiments were not performed in a competition with WT donor cells and it is therefore conceivable that TNF signalling in other cells beside HSCs is required to efficiently reconstitute the haematopoietic system (M. Pearl-Yafe *et al.*, 2010).

Importantly, we observed that following chronic infection with *L. donovani* the frequency of TNF-RdKO donor cells decreased in BM and in the spleen, in an opposite trend to the proportional increase observed the WT donor cells at both sites. This finding suggested that under the conditions established by infection with *L. donovani*, TNF signalling might contribute to the maintenance of the number of cells, both in the BM and spleen.

In infected mice, we reported an expansion of the LSK cell compartment at the expense of a contraction Lin⁻ cKit⁺ Sca⁻ cells, both in WT and TNF-RdKO donor cells, suggesting that TNF receptor signalling is not required to the up-regulation of Sca1 in lineage-committed progenitors. Furthermore, the lack of TNF intrinsic signalling could not prevent the expansion of LSK CD150⁺ CD48⁺ cells (cell population onward LT-HSCs enriched in multipotent progenitors). Most importantly, there were no evidence that TNF acting directly of LT-HSCs was mediating the depletion of the reservoir of quiescent LT-HSCs, since a decline in the number of these cells were comparable between WT and TNF-RdKO donor cells in the BM of recipient mice during infection.

As such, our findings excluded TNF as a direct mediator of loss of HSCs in G0. The higher proportion of donor cells deficient for TNF signalling, both in steady-state or following infection,

may be partially explained by the susceptibility of WT donor cells progeny to activation-induced cell death mediated by TNF signalling on competent donor cells (N. Askenasy, 2015), otherwise absent in TNF-RdKO donor cells. In agreement with this hypothesis, is the report that stimulation of LSK cells in culture with TNF leads to up-regulation of Fas in differentiated progeny, suggesting that differentiation leaves cells more vulnerable to apoptosis (D. Bryder *et al.*, 2001).

Our findings contrast with a study from Pronk *et al.*, in which it was proposed that TNF signalling could directly mediate the loss of HSCs self-renewal *in vivo* under conditions of stress-induced haematopoiesis (C. J. H. Pronk *et al.*, 2011). In this study, the potential of long-term reconstitution of HSCs lacking either one of the TNF receptors was enhanced compared to WT cells, and this was further enhanced when both TNF receptors were defective. Additionally, donor cells from mice subjected to myeloablation (induced by 5-Fluororacil administration) and then treated with TNF showed impaired ability to reconstitute the haematopoietic system following transfer to lethally irradiated recipients, in comparison to donor cells from myeloablated mice treated with PBS. These findings suggested that TNF acting upon both TNF receptors expressed on HSCs significantly impairs the maintenance of self-renewal potential (C. J. H. Pronk *et al.*, 2011).

However, in a former study it was proposed that TNF-R1a is required to maintain HSCs self-renewal potential following the observation that donor cells from older mice (>6 months) deficient for TNF-R1a display decreased reconstitution activity in comparison to those from age-matched WT or TNF-R1b^{-/-} donor mice (V. I. Rebel *et al.*, 1999). The discrepancies between the above-cited works may be attributed to the age of the mice, suggesting that the impact of TNF signalling may suffer alterations across the lifetime of an individual. Nonetheless, despite the somewhat conflicting conclusion, these two studies performed *in vivo* agree that TNF is an important regulator of HSCs function in stress-induced conditions.

In WT:TNF-RdKO mixed BM chimeric mice, we also evaluated the impact TNF signalling in the differentiation, of lineage-committed progenitors and mature cells. In the steady-state, WT and TNF-RdKO mice progeny displayed comparable frequencies for all the lineage-committed progenitors assessed. Additionally, mice chronically infected displayed similar pattern of alterations between the two groups of donor cells. No major differences were found in the percentage of myeloid effector cells present in the spleen of recipient mice, segregated according with the expression of CD11c, CD11b and F4/80, both in steady-state or following infection. Moreover the lack of striking changes either in the percentages of myeloid progenitors or mature myeloid cells in mice infected with *L. donovani* suggested that in our model of infection, intrinsic TNF signalling is dispensable for the expansion of myeloid effector cells.

Consistently with previous characterization of TNF-RdKO mice (J. J. Peschon *et al.*, 1998), we found no indication that intrinsic TNF signalling was required for the development or sustenance of effector myeloid cells in basal conditions. Previous characterization of the mice lacking both receptors for TNF reported no signs that in steady-state TNF signalling was required to the development of T and B cells, which was assessed by flow cytometry in the thymus, spleen and mesenteric lymph node. Regarding others populations of leucocytes, the evaluation in histologic sections of spleen, mesenteric and inguinal lymph nodes did not reveal significant changes between WT and mutant mice (J. J. Peschon *et al.*, 1998). Following infection with the bacteria *Micropolyspora faeni*, responsible for pulmonary infection characterized by high levels of TNF in the lungs, the frequency of lymphocytes and monocytes in the lung was comparable between WT mice, p55^{-/-} mice, p75^{-/-} and p55^{-/-} p75^{-/-} mice (J. J. Peschon *et al.*, 1998).

Nonetheless, in a model for acute infection using mice infected with pneumonia virus of mice (PVM), characterized by a specific increase in myeloid cells both in the BM and systemically, as well as an increase in myeloid progenitors in the BM, these features were prevented by the administration of anti-TNF mAbs, suggesting that in this model of infection TNF induces myelopoiesis under pro-inflammatory conditions (S. Maltby *et al.*, 2014).

In the current study the frequencies of overall T cells and CD4⁺ T cells deficient for TNF signalling were comparable in the BM, while in the spleen were decreased compared to those derived from WT donor cells, nonetheless their cell numbers were comparable at both sites in steady-state. These findings suggested that TNF receptor signalling did not provide a competitive advantage of WT T cells over TNF-RdKO T cells, arguing against impairment in the development or survival of T cells lacking TNF signalling. However, following infection with *L. donovani*, the deficiency in TNF signalling in T cells abolished their ability to expand in number in response to the presence of parasites, both in BM and in the spleen of recipient mice, otherwise greatly expanded within WT compartment. According to these findings, TNF acting directly on T cells and CD4⁺ T cells seems crucial to mediate their expansion and/or migration in mice infected with *L. donovani*.

Rheumatoid arthritis (RA) is an autoimmune disease that ultimately results in the wastage of bone and cartilage. This affliction is driven by the production of autoantibodies in addition to the persistent inflammation of the synovial tissues. The chronic synovial inflammation is sustained by the presence of large infiltrates of leucocytes, amongst those CD4⁺ T cells were shown to be required to the establishment of disease (M. Mellado *et al.*, 2015). TNF is crucial in RA, as proven by the effectiveness of TNF-signalling blocking agents in clinical contexts. It was reported that CD4⁺ T cells from RA patients; in transwell experiments migrate toward a TNF gradient, which was not observed in CD4⁺ T cells from controls. Subsequent experiments using blocking

antibodies demonstrated that the “migratory” potential of CD4⁺ T cells from RA patients depends on the expression of TNF-R1a, and this correlated to increased levels of intercellular adhesion molecule-1(ICAM-1) (M. Rossol *et al.*, 2013). In mice, following LPS challenge in the absence of TNF-R1a mediated signalling there was a significant reduction in the number of lymphocytes found in the lungs airway (M. K. Oyoshi *et al.*, 2007). These collection of findings suggested that TNF signalling is pivotal for the recruitment of T cells to sites of inflammation not only in autoimmune context but also under condition established by infection, and as such it is conceivable that in *L. donovani* chronic infection, TNF acting directly on T cells induces their recruitment to the BM, where through indirect mechanism they mediate alteration in haematopoiesis. Therefore, in future experiments it would be recommended to assess the expression of TNF receptors in T cells recovered from mice infected with *L. donovani*, and *in vivo* and *in vitro* to determine if they display aberrant migratory patterns.

In addition to its role in the recruitment of cells to sites of inflammation, intrinsic TNF signalling has been implicated in the regulation of T cell development and survival during the course of the establishment of the immune response in experimental models of infection (A. Zganiacz *et al.*, 2004, E. Y. Kim *et al.*, 2006). For example, in a study carried out to dissect the role of CD4⁺ and CD8⁺ T cell immune responses during *Listeria monocytogenes* infection, taking advantage of the availability well-characterized specific TCR transgenic systems for either MHC class I or MHC class II, it was reported that TNF receptor signalling plays a central role in T cell functions in mice infected with *L. monocytogenes*, a model widely used to study immune responses mediated by T cells following infection with intracellular bacteria (E. Y. Kim *et al.*, 2006). The lack of TNF-R1b nearly abolish the expansion of CD4⁺ and CD8⁺ T cells in response to low concentrations of specific antigens, and even at high concentrations they expanded poorly compared to WT T cells, which was associated with a lower expression of anti-apoptotic mediators. Furthermore the absence of TNF-R1b signaling in CD4⁺ and CD8⁺ T cells extensively compromised the ability of T cells to express IFN γ following challenge with cognate antigen *in vivo* (E. Y. Kim *et al.*, 2006). These findings suggested that TNF signalling under conditions established by infection with intracellular pathogens might be required to the development, expansion and survival of effector T cells.

In contrast, other studies suggested that TNF was either not required or act as a suppressor in the expansion of T cells during the immune response to intracellular pathogens (M. I. Kafrouni *et al.*, 2003, A. Zganiacz *et al.*, 2004). For example, the study of the role of TNF signalling in the development of T cell immune response during antiviral-immune responses in mice challenged with a replication-deficient β -galactosidase encoding recombinant adenovirus (AdCMV-lacZ), suggested that TNF signalling was dispensable to the expansion of CD8⁺ IFN γ ⁺ T cells in mice deficient for the TNF receptors p55 or p75 (M. I. Kafrouni *et al.*, 2003). This could be explained

by TNF receptor redundancy, since in TNF KO mice the expansion of these cells was limited compared to WT mice following infection (M. I. Kafrouni *et al.*, 2003). Additionally, in TNF-deficient mice infected with *Mycobacterium bovis*, it was reported that there is uncontrolled expansion of antigen-specific T cells expressing IFN γ , which depended on the expression of both TNF receptors to prevent the development of fatal immunopathology (A. Zganiacz *et al.*, 2004). These above-mentioned examples embody the complexity of TNF signaling during immune response putting forward the requirement for studies in pathogen specific contexts and the risks associated anti-TNF therapies (T. Ellerin *et al.*, 2003, X. Chen and J. J. Oppenheim, 2011).

As such, we evaluated the impact of intrinsic TNF signaling in BM T cells potential to express IFN γ , during *L. donovani* infection. The lack of intrinsic TNF signalling limited over 30 times the expansion in BM CD4⁺ cells expressing IFN γ in chronically infected mice, and completely abrogated the expansion of BM CD8⁺ IFN γ ⁺ T cells. The lack of CD4⁺ IFN γ ⁺ T cells development from TNF-RdKO donor cells was evident not only in terms of the overall decrease in their cell numbers, but also their impaired efficiency to express IFN γ . Therefore, in our model of infection, TNF seems to be a crucial mediator in the development of functional T cells in the BM. However, to determine if TNF receptor signalling plays a pivotal role in the establishment of haematological dysfunction, it would be necessary to transfer CD4⁺ T cells TNF-RdKO to immunodeficient recipient mice and evaluate the alteration in haematopoietic progenitors within BM and haematological parameters in circulation, following the establishment of chronic infection with *L. donovani*.

To our knowledge, this is the first study focusing on the factors modulating the alterations in BM haematopoiesis in experimental VL in B6 mice *in vivo*. In our model, we established that IFN γ produced by CD4⁺ T cells was sufficient to drive haematopoietic dysfunction, which was mirrored by the expansion of multipotent progenitors at the expense of quiescent LT-HSCs and the establishment of anaemia and thrombocytopenia. In addition, we determined that intrinsic IFN γ and TNF receptors signalling mediate the massive expansion of CD4⁺ T cells in BM of mice chronically infected with *L. donovani*. Furthermore, intrinsic TNF signalling in BM CD4⁺ T cells modulate their potential to produce IFN γ during chronic infection. As such, the collection of our findings suggested that TNF and IFN γ signalling pathway converge to induce the onset of impairment of haematopoietic function, during experimental VL.

The pro-inflammatory mediators, IFN γ and TNF, are central players in the resolution of *L. donovani* infection, according to extensive studies carried in experimental models of disease (A. P. Taylor and H. W. Murray, 1997, P. M. Kaye *et al.*, 2004). Therefore, directly targeting these molecules to prevent the establishment of dysfunctional haematopoiesis in the context of experimental VL would not be a viable option. However, we believe this study has paved new

avenues for future studies aimed at isolating potential targets to prevent the onset of haematopoietic functional impairment, and consequent impact on morbidity, without compromising the parasite clearance following infection with *L. donovani*.

4.3 FIGURES

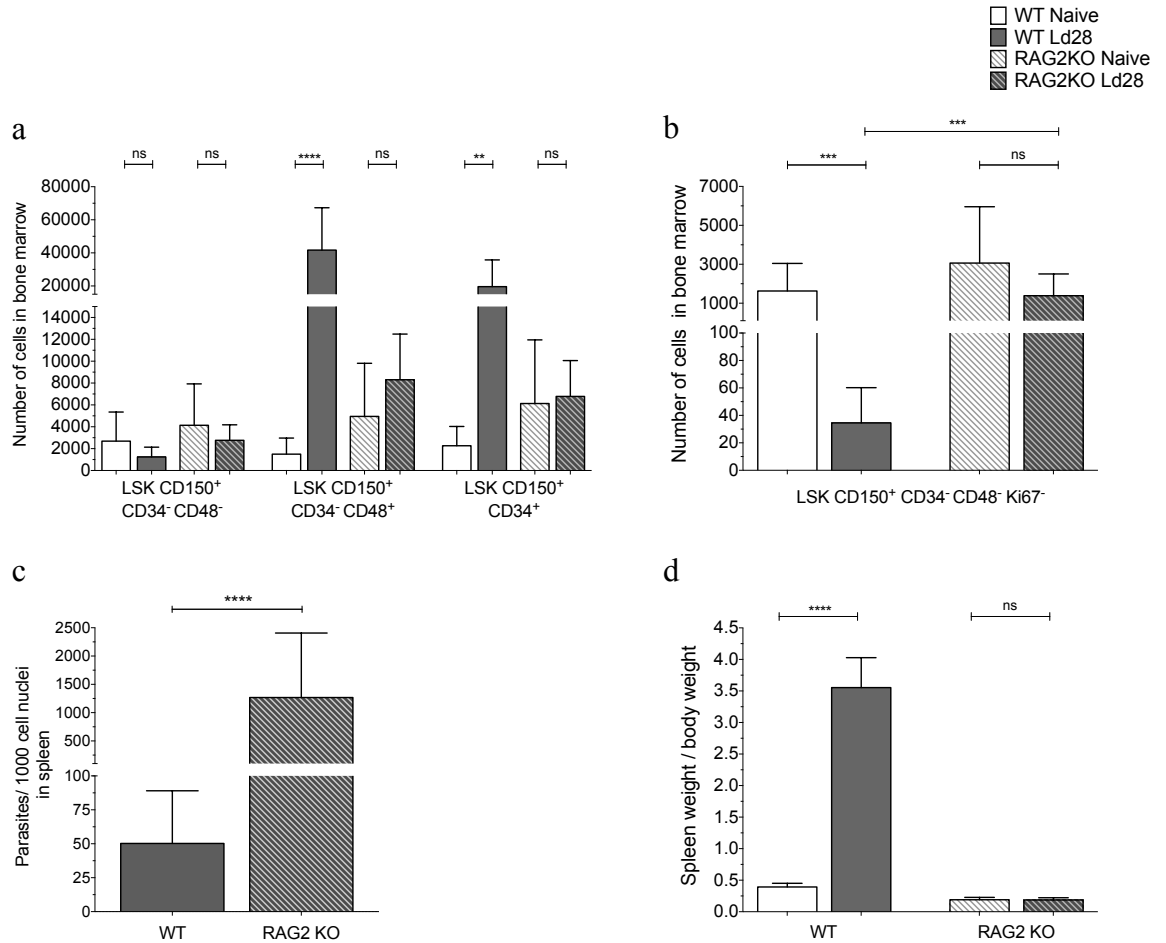


Figure 4.1 - RAG2 KO mice do not lose quiescent HSCs following infection with *L. donovani*. (a) Number of LSK CD150⁺ CD34⁻ CD48⁻ cells (enriched for LT-HSCs), LSK CD150⁺ CD34⁻ CD48⁺ cells and LSK CD150⁺ CD34⁺ cells in bone marrow (BM). (b) Number of LSK CD150⁺ CD34⁻ CD48⁻ cells in G0 (Ki67⁻) in BM. (c) Spleen parasite burden presented as number of parasites per 1000 nuclei. (d) Spleen weight as percentage of body weight. Comparisons made between BM cells of wild-type (WT) B6 mice non-infected (n=12) and WT B6 mice infected (n=12) with *L. donovani* for 28 days or B6 RAG2 KO mice non-infected (n=9) and B6 RAG2 KO mice infected (n=13) with *L. donovani* for 28 days. Two femur and two tibias were used from each animal. Data from three independent experiments was presented as Mean \pm SD; *p* values were determined using unpaired t test: not significant (ns), **p* \leq 0.05, ***p* \leq 0.01, ****p* \leq 0.001 and *****p* \leq 0.0001.

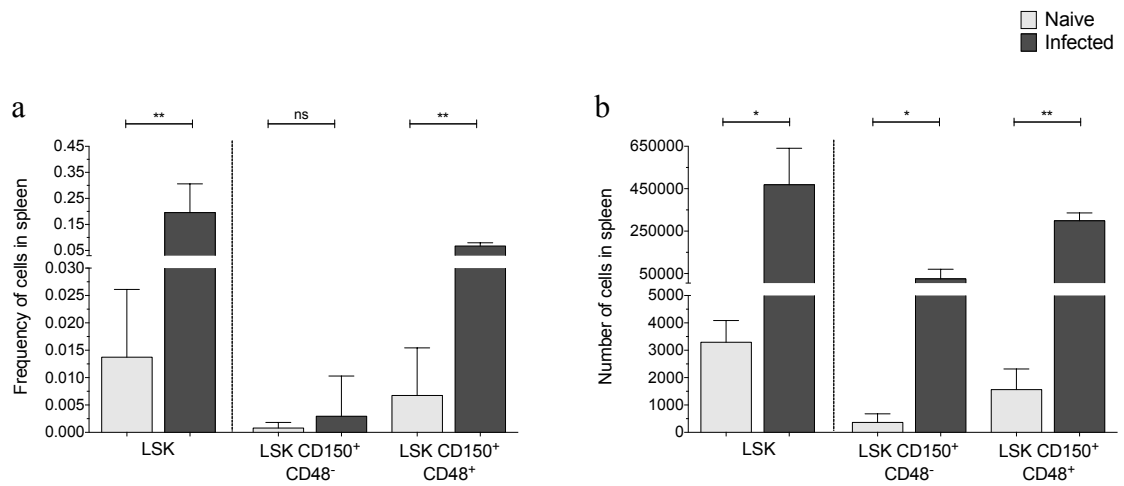


Figure 4.2 - The number of HSPCs was increased in the spleen following infection with *L. donovani*. (a) Frequency of LSK, LSK CD150⁺ CD48⁻ cells (enriched for LT-HSCs) and LSK CD150⁺ CD48⁺ cells in the spleen of naive mice (n=5) and infected mice (n=8), in two independent experiments. (b) Number of LSK, LSK CD150⁺ CD48⁻ cells (enriched for LT-HSCs) and LSK CD150⁺ CD48⁺ cells in the spleen of naive mice (n=4) and infected mice (n=4), in one experiment. Comparisons were made between naive B6 mice and B6 mice infected with *L. donovani* for 28-35 days. Two femur and two tibias were used from each animal. Data was presented as Mean ± SD, p values were determined using unpaired t test: not significant (ns), *p ≤ 0.05 and **p ≤ 0.01.

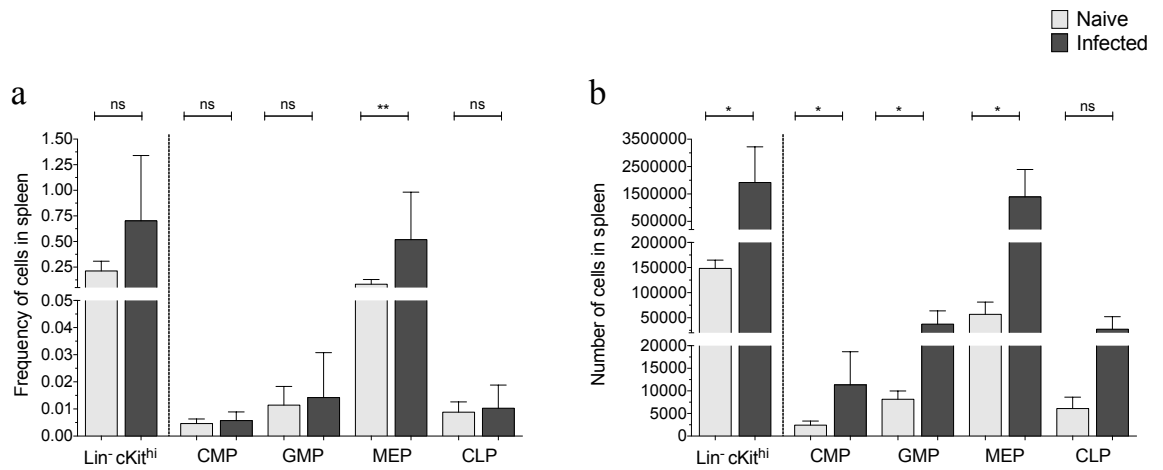


Figure 4.3 - The number of HSPCs was increased in spleen following infection with *L. donovani*. (a) Frequency of Lin⁻ cKit^{hi} cells (enriched for haematopoietic progenitors), CMPs, GMPs, MEPs and CLPs cells in spleen of naive (n=5) and infected mice (n=8), determined in two independent experiments. (b) Number of Lin⁻ cKit^{hi} cells, CMPs, GMPs, MEPs and CLPs cells in spleen of naive (n=4) and infected mice infected (n=4), determine in one experiment. Comparisons always made between naive mice and mice infected with *L. donovani* for 28-35 days. Two femur and two tibias were used from each animal. Data was presented as Mean ± SD, p values were determined using unpaired t test: not significant (ns), *p ≤ 0.05, **p ≤ 0.01, ***p ≤ 0.001 and ****p ≤ 0.0001.

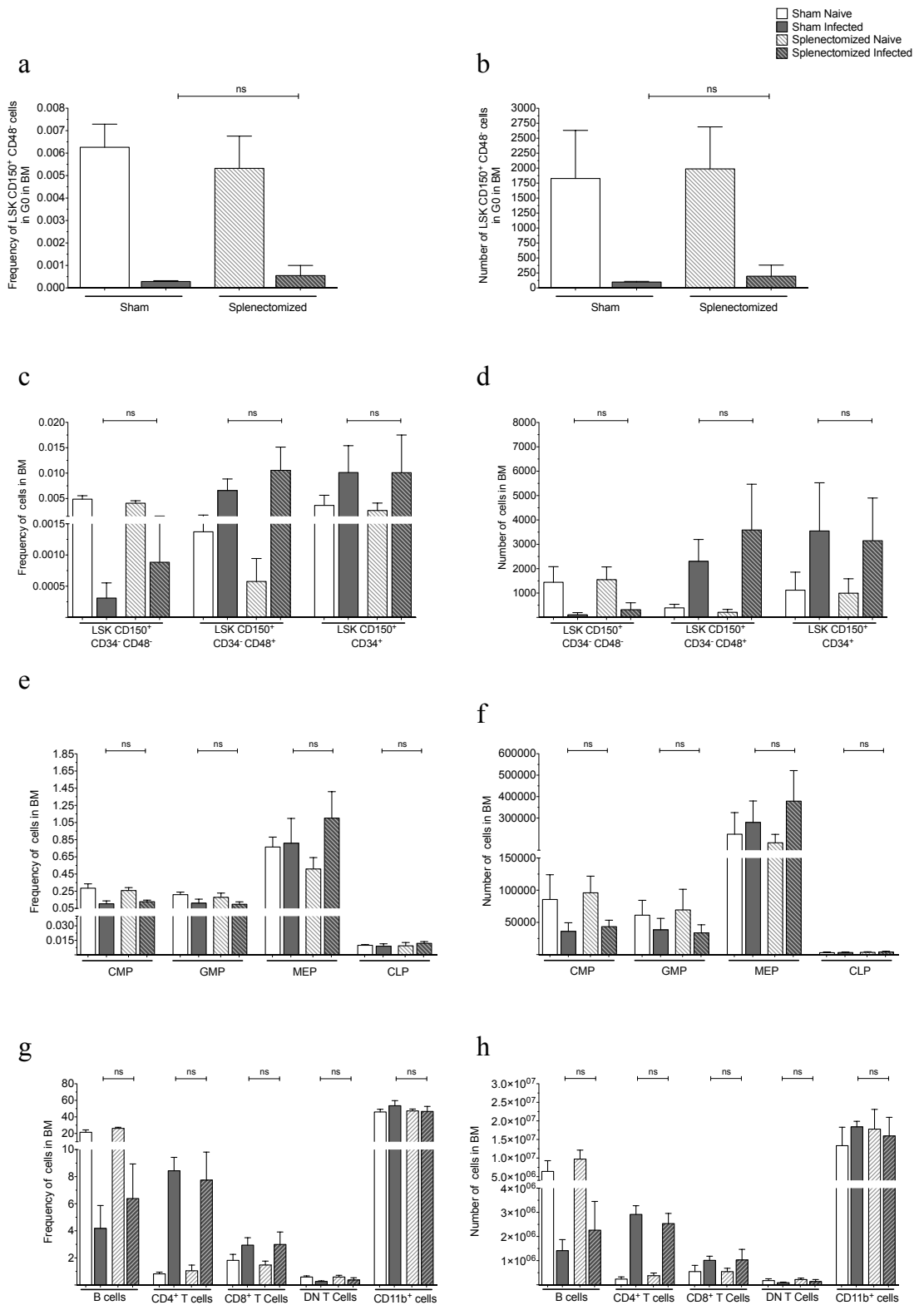


Figure 4.4 - Alterations in BM cellularity occurred independently from the processes taking place in the spleen. (a and b) Frequency and number LSK CD150⁺ CD48⁻ CD34⁻ cells (enriched for LT-HSCs) in G0 (Ki67-) in BM. (c and d) Frequency and number of non-committed progenitors (LSK CD150⁺ CD34⁻ CD48⁻ (enriched for LT-HSCs), LSK CD150⁺ CD34⁻ CD48⁺ and LSK CD150⁺ CD34⁺ cells) in BM. (e and f) Frequency and number of lineage-committed

progenitor cells (CMPs, GMPs, MEPs and CLPs) in BM. (g and h) Frequency and number of mature haematopoietic cells B cells, CD4⁺ T cells, CD8⁺ T cells, CD4⁻ CD8⁻ CD3⁺ cells (DN T cells) and myeloid cells (CD11b⁺ cells) in BM. Comparisons were made between splenectomized (n=5) and “sham” (n=5) mice infected for 28 days with *L. donovani*. Data from one experiment was presented as Mean ± SD, p values were determined using Mann-Whitney: not significant (ns), *p ≤ 0.05, **p ≤ 0.01, ***p ≤ 0.001 and ****p ≤ 0.0001.

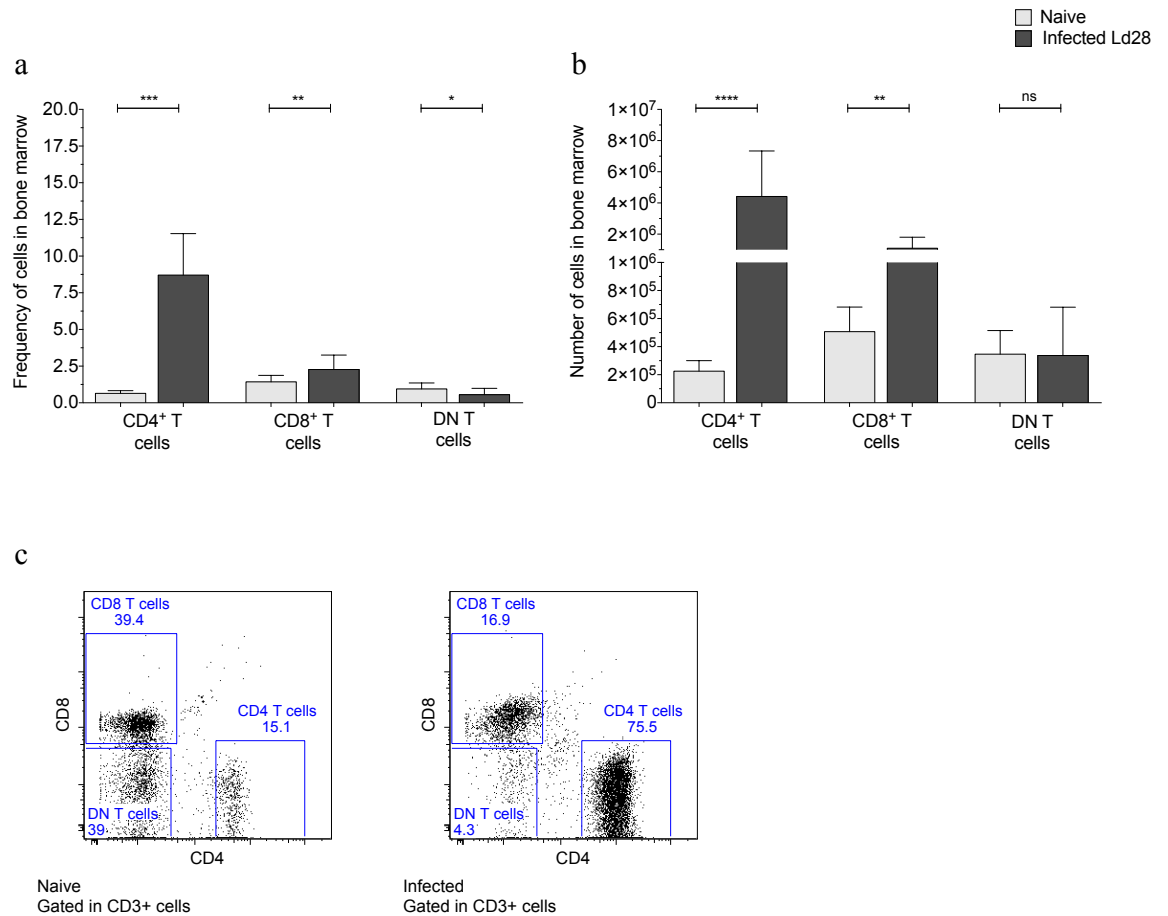


Figure 4.5 - *L. donovani* infection lead to the expansion of T cell compartment in BM. (a) Frequency of CD4⁺ T cells, CD8⁺ T cells and CD4⁻ CD8⁻ T (double negative (DN) T cells in bone marrow of naive mice and infected mice. (b) Number of CD4⁺ T cells, CD8⁺ T cells and DN T cells in bone marrow of non-infected mice and infected mice. (c) Representative dot plots of distribution of CD4⁺ T cells, CD8⁺ T cells and DN T cells within CD45⁺ CD3⁺ cells in bone marrow. Comparisons were made between naive mice (n=14) and mice infected (n=14) for 28 days with *L. donovani* (Ld28). Two femur and two tibias were taken per animal. Data from four independent experiments was presented as Mean ± SD, p values were determined using unpaired t test: not significant (ns), *p ≤ 0.05, **p ≤ 0.01, ***p ≤ 0.001 and ****p ≤ 0.0001.

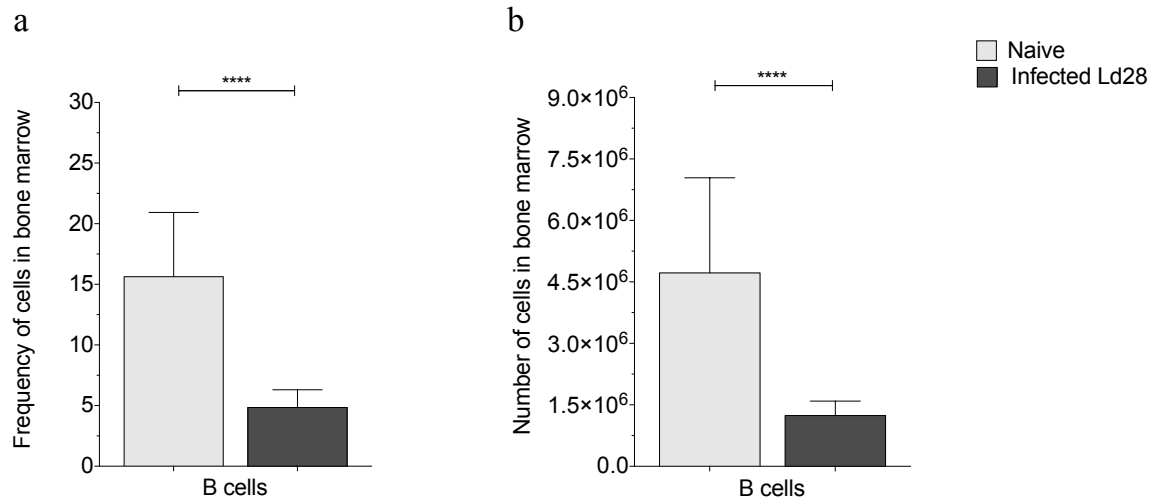


Figure 4.6 - *L. donovani* infection was associated with the contraction of the B cell compartment in BM, during chronic phase of infection. (a) Frequency of B cells (CD45⁺ CD3⁻ B220⁺ cells) in BM of non-infected mice and infected mice. (b) Number of B cells in BM of non-infected mice and infected mice. Comparisons were made between naive mice (n=14) and mice infected (n=13) for 28 days with *L. donovani* (Ld28). Two femur and two tibias were taken per animal. Data from three independent experiments was presented as Mean ± SD, p values were determined using unpaired t test: not significant (ns), *p ≤ 0.05, **p ≤ 0.01, ***p ≤ 0.001 and ****p ≤ 0.0001

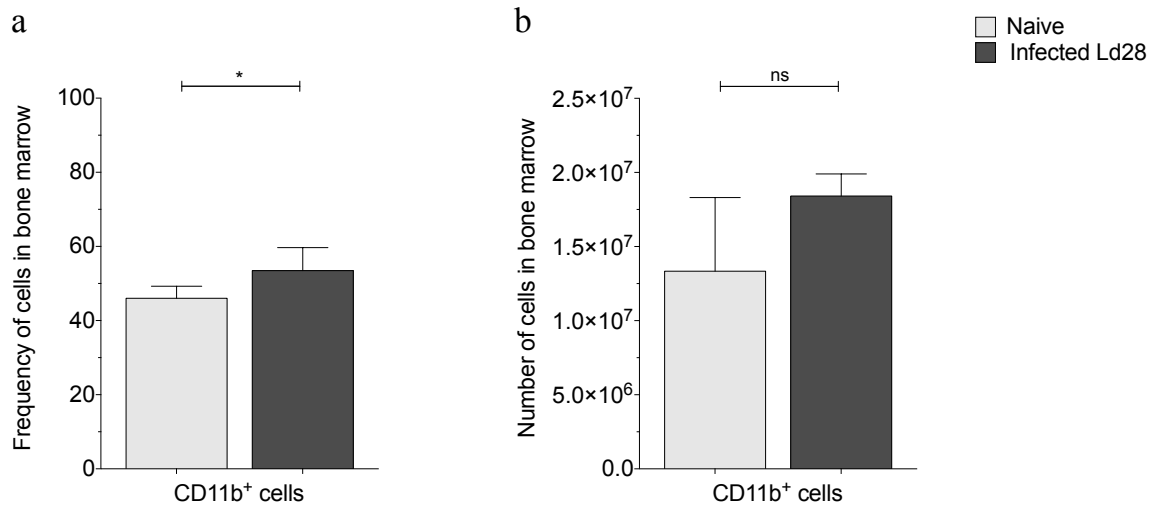


Figure 4.7 - *L. donovani* infection was not associated with alterations in the number of total CD11b⁺ cells in BM. (a) Frequency of myeloid cells (CD45⁺ CD3⁻ B220⁻ CD11b⁺ cells) in BM of naive and infected mice. (b) Number of myeloid cells in BM of naive and infected mice. Comparisons were made between naive mice (n=5) and mice infected (n=5) for 28 days with *L. donovani* (Ld28). Two femur and two tibias were used from each animal. Data from one experiment was presented as Mean ±SD, p values were determined using unpaired t test: not significant (ns), *p ≤ 0.05, **p ≤ 0.01, ***p ≤ 0.001 and ****p ≤ 0.0001.

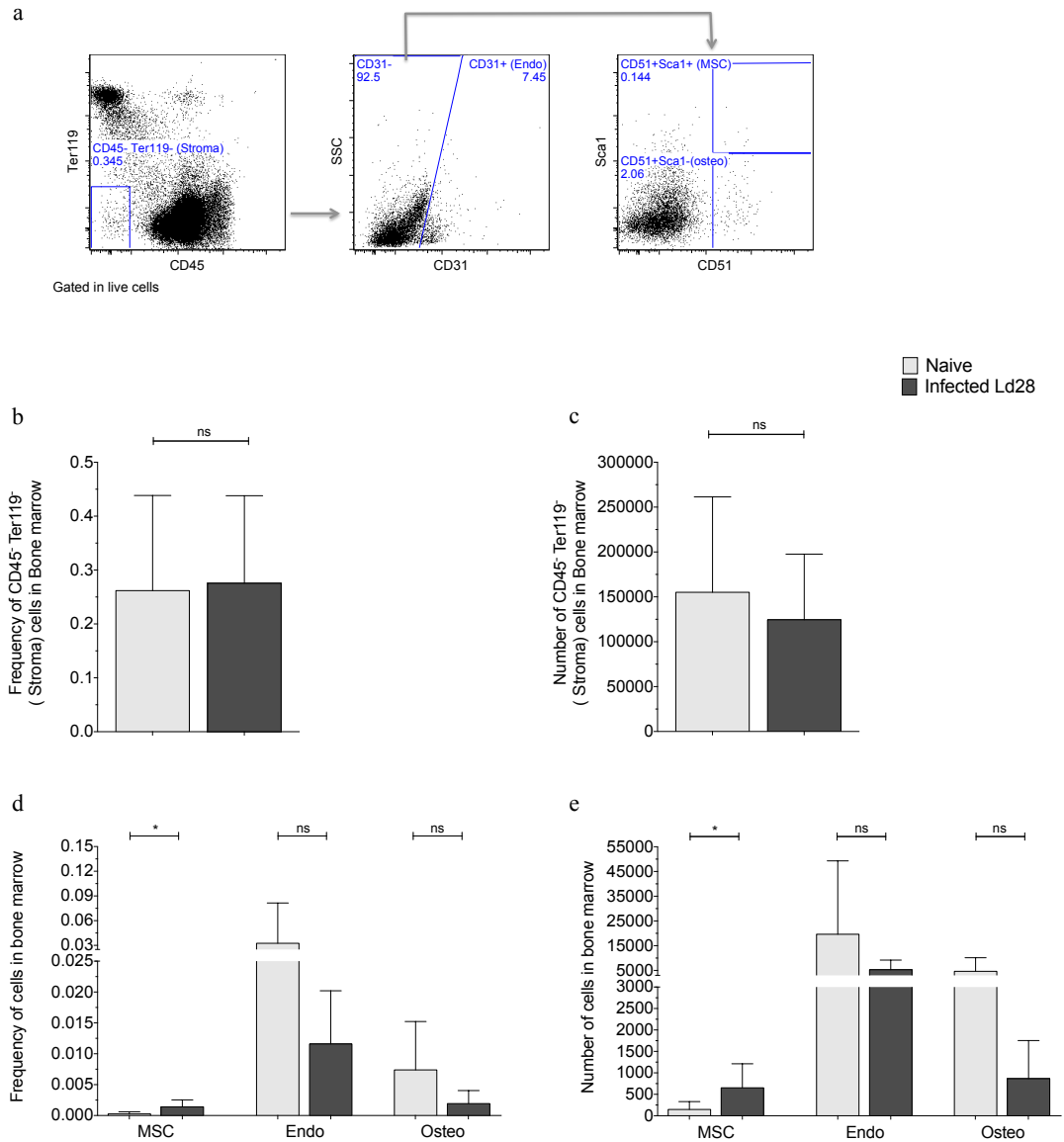


Figure 4.8 - *L. donovani* infection was associated with alterations in the number of MSCs in BM. (a) Diagram of gating strategy applied to select for stromal cells populations in BM. (b) Frequency of stromal cells (CD45⁻ Ter119⁻ cells), MSCs (CD45⁻ Ter119⁻ CD31⁻ Sca1⁺ CD51⁺ cells), endothelial cells (CD45⁻ Ter119⁻ CD31⁺ cells) and osteoblastic lineage cells (CD45⁻ Ter119⁻ CD31⁻ Sca1⁻ CD51⁺ cells) in BM of naive and infected mice. (c) Number of stromal cells, MSCs, endothelial cells and osteoblastic lineage cells in BM of naive mice and infected mice. Comparisons were made between naive mice (n=8) and mice infected (n=6) for 28 days with *L. donovani* (Ld28). Two femur and two tibias were taken per animal. Data from two independent experiments was presented as Mean ± SD, p values were determined using unpaired t test: not significant (ns), *p ≤ 0.05, **p ≤ 0.01, ***p ≤ 0.001 and ****p ≤ 0.0001. MSCs (mesenchymal stem cells), Endo (endothelial cells), Osteo (osteolineage cells), SSC (Side Scatter).

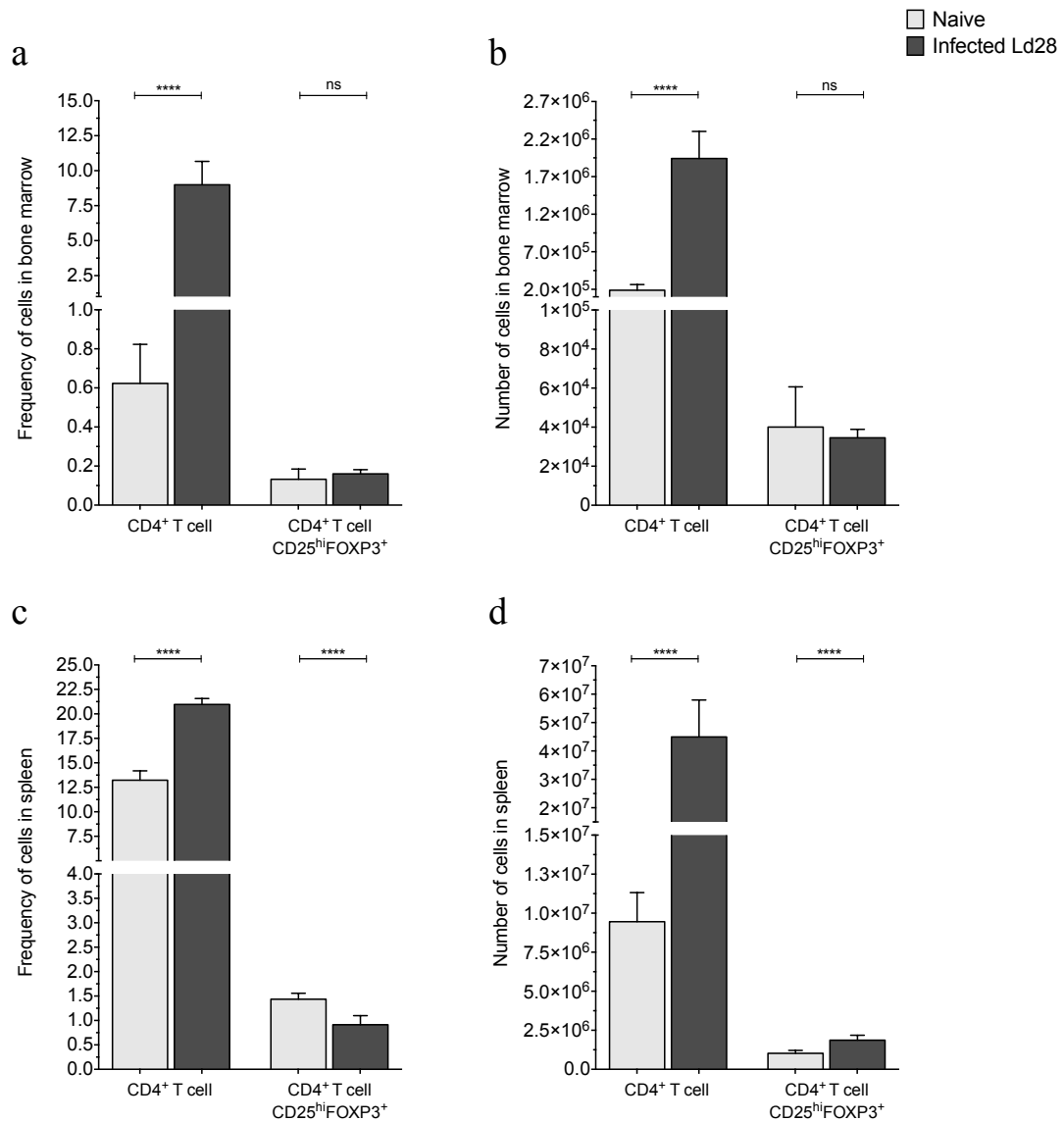


Figure 4.9 - *L. donovani* infection was not associated with alterations in the number of regulatory T cells in BM. (a) Frequency of CD4⁺ T cells and regulatory T cells (CD3⁺ CD4⁺ CD25^{hi} FOXP3⁺ cells) in BM. (b) Number of CD4⁺ T cells and regulatory T cells in BM. (c) Frequency of CD4⁺ T cells and regulatory T cells in the spleen. (d) Number of CD4⁺ T cells and regulatory T cells in the spleen. Comparisons were made between naive mice (n=9) and mice infected (n=8) for 28 days with *L. donovani* (Ld28). Two femur and two tibias were used from each animal. Data from two independent experiments was presented as Mean ± SD, p values were determined using unpaired t test: not significant (ns), *p ≤ 0.05, **p ≤ 0.01, ***p ≤ 0.001 and ****p ≤ 0.0001.

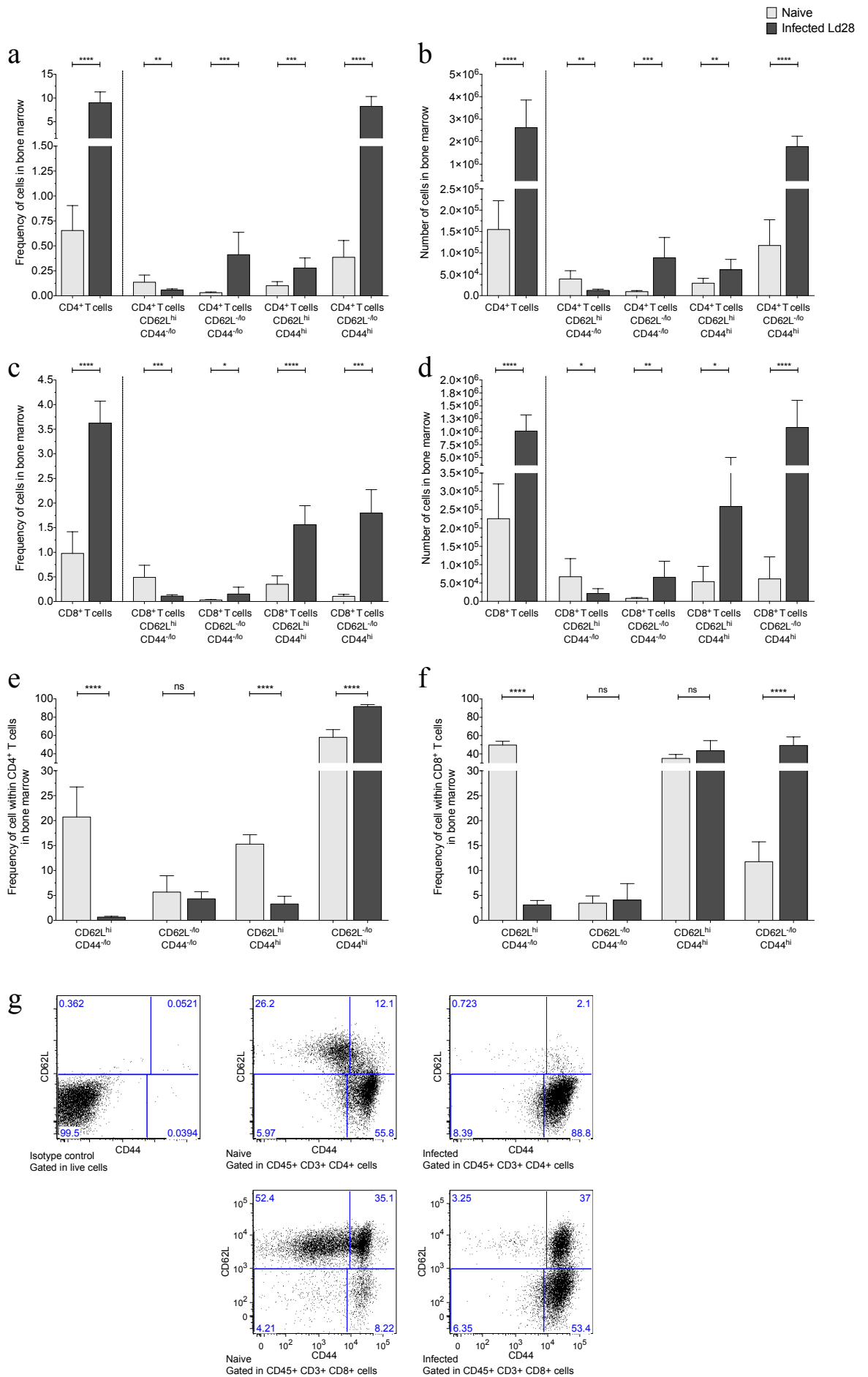


Figure 4.10 - The number of T cells CD62L^{-low} CD44^{high} increased in the BM following *L. donovani* infection. (a) Frequency of total CD4⁺ T cells, and CD62L^{hi} CD44^{-lo} (naive), CD62L^{-lo} CD44^{-lo} (“effector”), CD62L^{hi} CD44^{hi} (“central-memory”) and CD62L^{-lo} CD44^{hi} (“effector-memory”) CD4⁺ T cells in BM. (b) Number of total and CD4⁺ T cell subsets in BM. (c) Frequency of total CD8⁺ T cells, and CD62L^{hi} CD44^{-lo} (naive), CD62L^{-lo} CD44^{-lo} (“effector”), CD62L^{hi} CD44^{hi} (“central-memory”) and CD62L^{-lo} CD44^{hi} (“effector-memory”) CD8⁺ T cells in BM. (d) Number of total and CD8⁺ T cell subsets in BM. (e) Distribution of CD62L^{hi} CD44^{-lo}, CD62L^{-lo} CD44^{-lo}, CD62L^{hi} CD44^{hi} and CD62L^{-lo} CD44^{hi} cells within CD4⁺ T cells in the BM. (f) Distribution of CD62L^{hi} CD44^{-lo}, CD62L^{-lo} CD44^{-lo}, CD62L^{hi} CD44^{hi} and CD62L^{-lo} CD44^{hi} cells within CD8⁺ T cells in BM. (g) Representative dot plots of the expression of CD44 and CD62L in CD45⁺ CD3⁺ CD4⁺ cells in BM, from left to right: isotype control, naive mouse and infected mouse. Comparisons were made between naive mice (n=9) and mice infected (n=8) for 28 days with *L. donovani* (Ld28). Two femur and two tibias were taken per animal. Data from two independent experiments was presented as Mean ± SD, p values were determined using unpaired t test: not significant (ns), *p ≤ 0.05, **p ≤ 0.01, ***p ≤ 0.001 and ****p ≤ 0.0001. hi, high; lo, low.

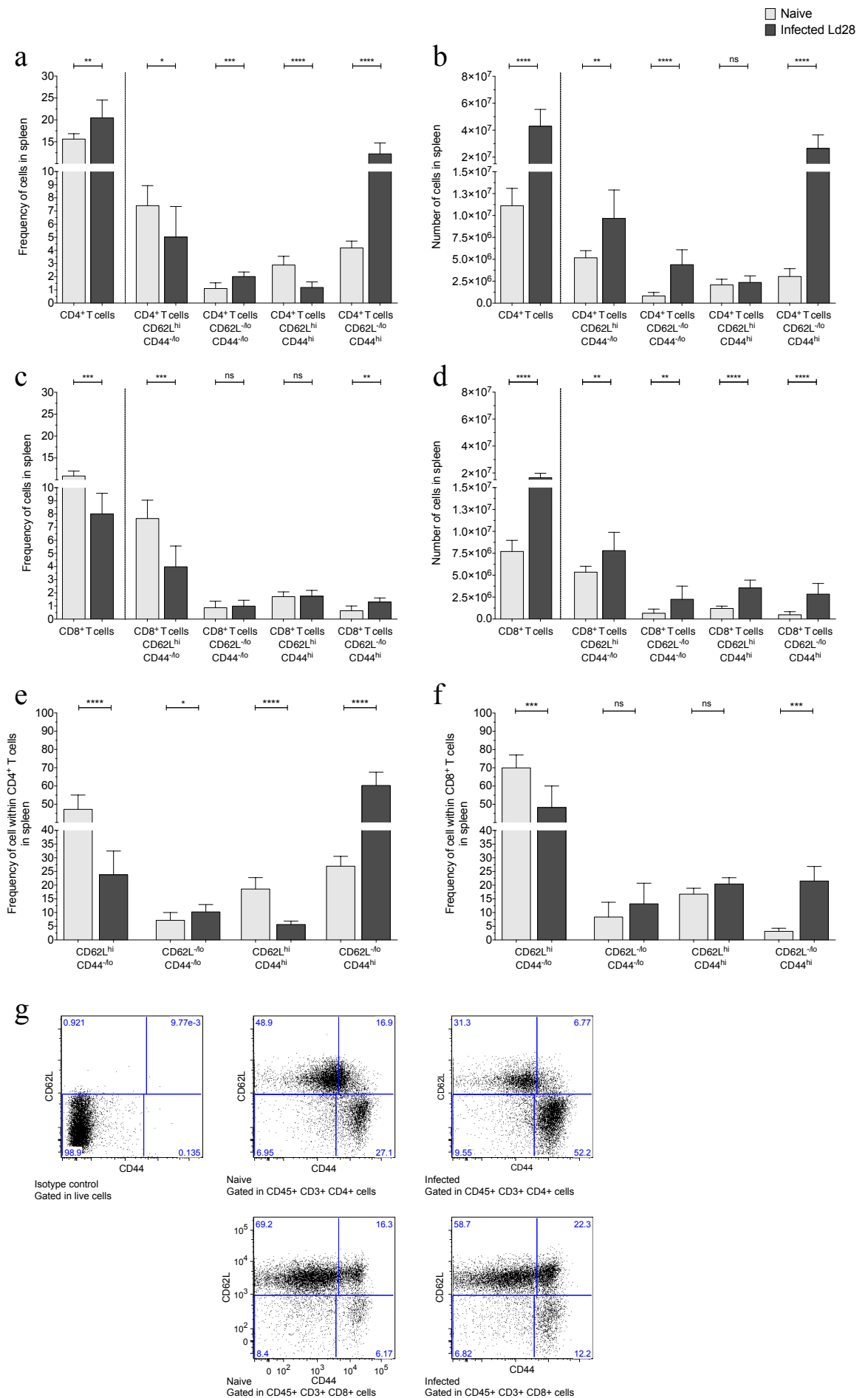


Figure 4.11 - Following infection with *L. donovani* the number of CD4⁺ T cells CD62L^{-/lo} CD44^{hi} increased in the spleen. (a) Frequency of total CD4⁺ T cells, and CD62L^{hi} CD44^{-/lo} (naive), CD62L^{-/lo} CD44^{-/lo} (“effector”), CD62L^{hi} CD44^{hi} (“central-memory”) and CD62L^{-/lo} CD44^{hi} (“effector-memory”) CD4⁺ T cells in spleen. (b) Number of total and CD4⁺ T cell subsets in the spleen. (c) Frequency of total CD8⁺ T cells, and CD62L^{hi} CD44^{-/lo} (naive), CD62L^{-/lo} CD44^{-/lo}, CD62L^{hi} CD44^{hi} (“central-memory”) and CD62L^{-/lo} CD44^{hi} (“effector-memory”) CD8⁺ T cells in spleen. (d) Number of total and CD8⁺ T cell subsets in spleen. (e) Distribution of CD62L^{hi} CD44^{-/lo}, CD62L^{-/lo} CD44^{-/lo}, CD62L^{hi} CD44^{hi} and CD62L^{-/lo} CD44^{hi} cells within CD4⁺ T cells in the spleen. (f) Distribution of CD62L^{hi} CD44^{-/lo}, CD62L^{-/lo} CD44^{-/lo}, CD62L^{hi} CD44^{hi} and CD62L^{-/lo} CD44^{hi} cells within CD8⁺ T cells in spleen. (g) Representative dot plots of the expression of CD44 and CD62L in CD45⁺ CD3⁺ CD4⁺ cells in spleen, from left to right: isotype control, naive mouse and infected mouse. Comparisons were made between naive mice (n=9) and mice infected (n=8) for 28 days with *L. donovani* (Ld28). Data from two independent experiments was presented as Mean ± SD, p values were determined using unpaired t test: not significant (ns), *p ≤ 0.05, **p ≤ 0.01, ***p ≤ 0.001 and ****p ≤ 0.0001. hi, high; lo, low.

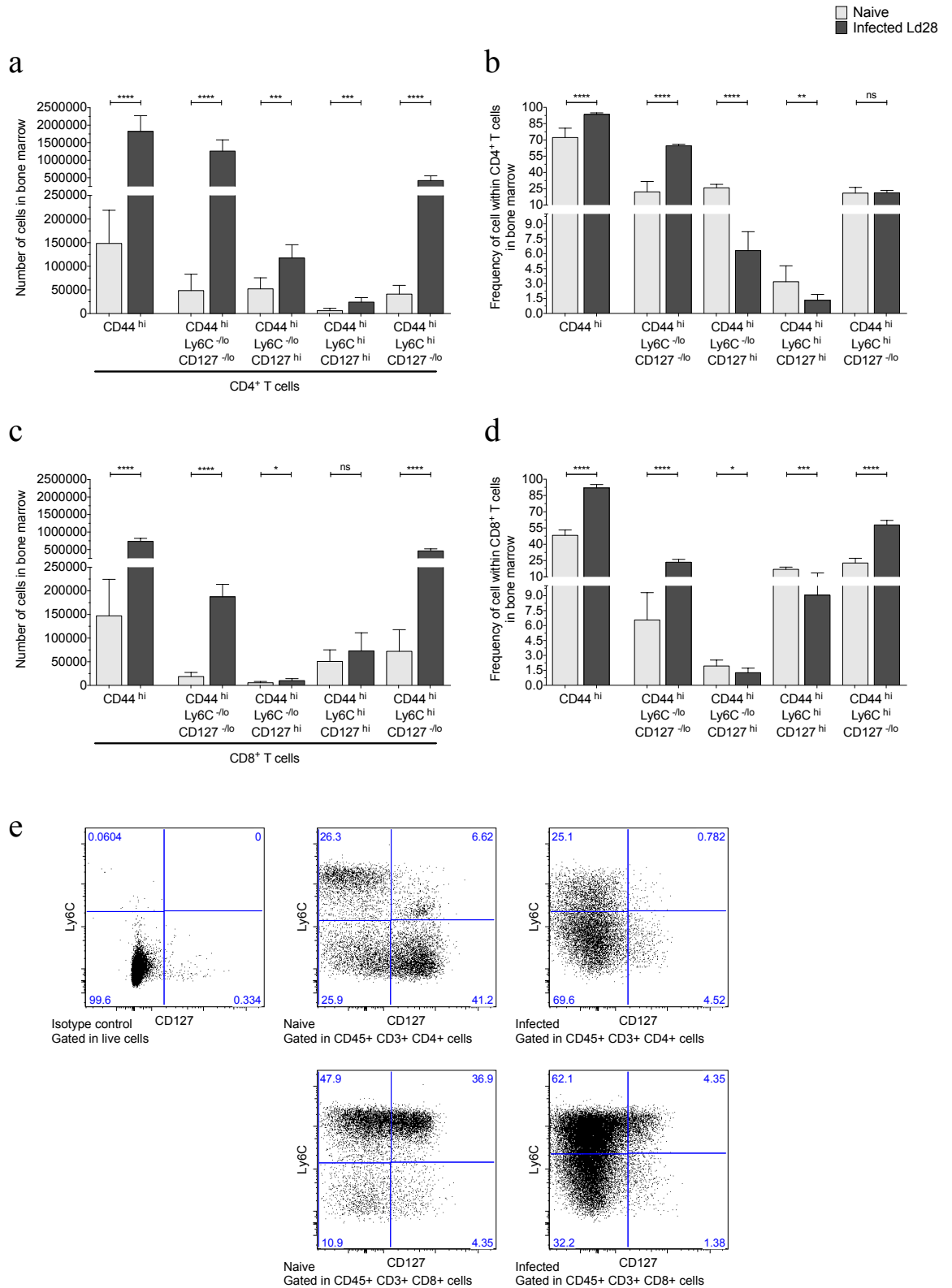


Figure 4.12 - The number “Effector” CD4⁺ and CD8⁺ T cells increase in BM following *L. donovani* infection. (a) Number of total CD4⁺ CD44^{hi} T cells, and CD44^{hi} Ly6C^{-/lo} CD127^{-/lo} (“effector”), CD44^{hi} Ly6C^{-/lo} CD127^{hi}, CD44^{hi} Ly6C^{hi} CD127^{hi} T cells (“memory”) and CD44^{hi} Ly6C^{hi} CD127^{-/lo} CD4⁺ T cell subsets in the BM. (b) Frequency within of total CD4⁺ T cells of CD44^{hi} T cells, and CD44^{hi} Ly6C^{-/lo} CD127^{-/lo} (“effector”), CD44^{hi} Ly6C^{-/lo} CD127^{hi}, CD44^{hi} Ly6C^{hi} CD127^{hi} (“memory”) and CD44^{hi} Ly6C^{hi} CD127^{-/lo} CD4⁺ T cell subsets in the BM. (c)

Number of CD8⁺ CD44^{hi} T cells, CD44^{hi} LyC6^{-/lo} CD127^{-/lo} (“effector”), CD44^{hi} LyC6^{-/lo} CD127^{hi}, CD44^{hi} LyC6^{hi} CD127^{hi} T cells (“memory”) and CD44^{hi} LyC6^{hi} CD127^{-/lo} CD8⁺ T cell subsets in the BM. (d) Frequency within of total CD8⁺ T cells of CD44^{hi} T cells, CD44^{hi} LyC6^{-/lo} CD127^{-/lo} (“effector”), CD44^{hi} LyC6^{-/lo} CD127^{hi}, CD44^{hi} LyC6^{hi} CD127^{hi} T cells (“memory”) and CD44^{hi} LyC6^{hi} CD127^{-/lo} CD8⁺ T cell subsets in the BM. (e) Representative dot plots of the expression of Ly6C and CD127 in CD45⁺ CD3⁺ CD4⁺ CD44⁺ cells and CD45⁺ CD3⁺ CD8⁺ CD44⁺ cells in BM: (middle left) isotype control, (top left) naive and (top right) infected gated in CD45⁺ CD3⁺ CD4⁺ CD44⁺ cells, (bottom left) naive mouse and (bottom right) infected mouse gated in CD45⁺ CD3⁺ CD8⁺ CD44⁺ cells. Comparisons were made between naive mice (n=9) and mice infected (n=8) for 28 days with *L. donovani* (Ld28). Data from two independent experiments was presented as Mean ± SD, p values were determined using unpaired t test: not significant (ns), *p ≤ 0.05, **p ≤ 0.01, ***p ≤ 0.001 and ****p ≤ 0.0001. Two femur and two tibias were used from each animal. hi (high); lo (low).

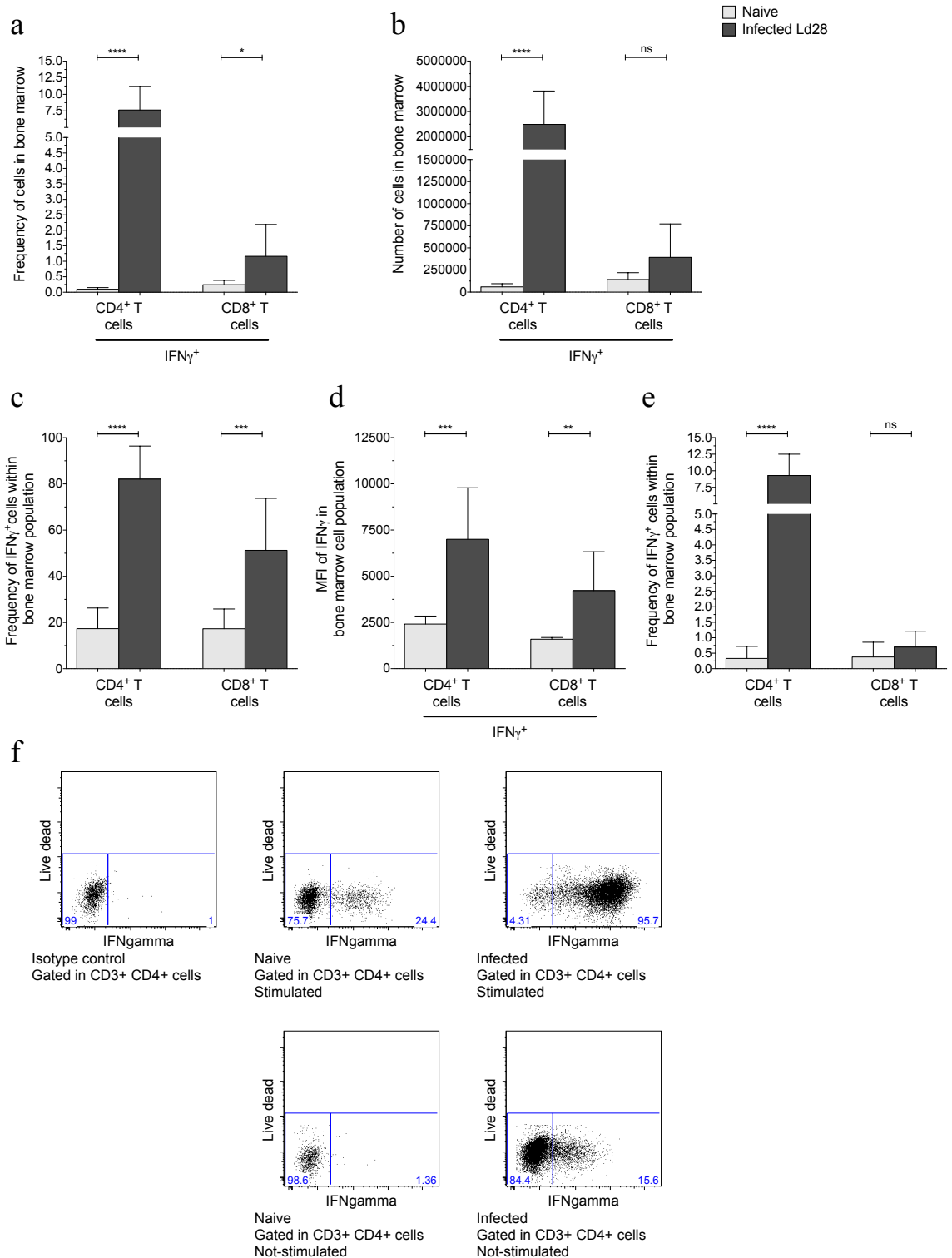


Figure 4.13 - *L. donovani* infection was associated with an increase in the number of BM CD4⁺ T cells with potential for IFN γ expression. (a) Frequency of CD4⁺ T cells IFN γ ⁺ and CD8⁺ T cells IFN γ ⁺ in total BM upon *in vitro* stimulation. (b) Number of CD4⁺ T cells IFN γ ⁺ and CD8⁺ T cells IFN γ ⁺ upon *in vitro* stimulation. (c) Frequency of IFN γ ⁺ cells within CD4⁺ T cells and CD8⁺ T cells following *in vitro* stimulation. (d) Mean of Fluorescence Intensity (MFI) of IFN γ in CD4⁺ T cells IFN γ ⁺ and CD8⁺ T cells IFN γ ⁺ following *in vitro* stimulation. (e) Frequency of IFN γ ⁺ within CD4⁺ T cells and CD8⁺ T cells in *ex vivo* BM cells (not stimulated). (f)

Representative dot plots displaying frequencies of IFN γ expression within in CD45⁺ CD3⁺ CD4⁺ cells in BM: (top left) isotype control for IFN γ staining, (top center) naive mouse and (top right) infected upon *in vitro* stimulation with PMA/ionomycin, (bottom left) CD4⁺ T cells from (bottom right) naive and infected mice analyzed directly *ex vivo*. Comparisons were made between naive mice (n=9) and mice infected (n=9) for 28 days with *L. donovani* (Ld28). Two femur and two tibias were taken per animal. Data from three independent was presented as Mean \pm SD, p values were determined using unpaired t test: not significant (ns), *p \leq 0.05, **p \leq 0.01, ***p \leq 0.001 and ****p \leq 0.0001.

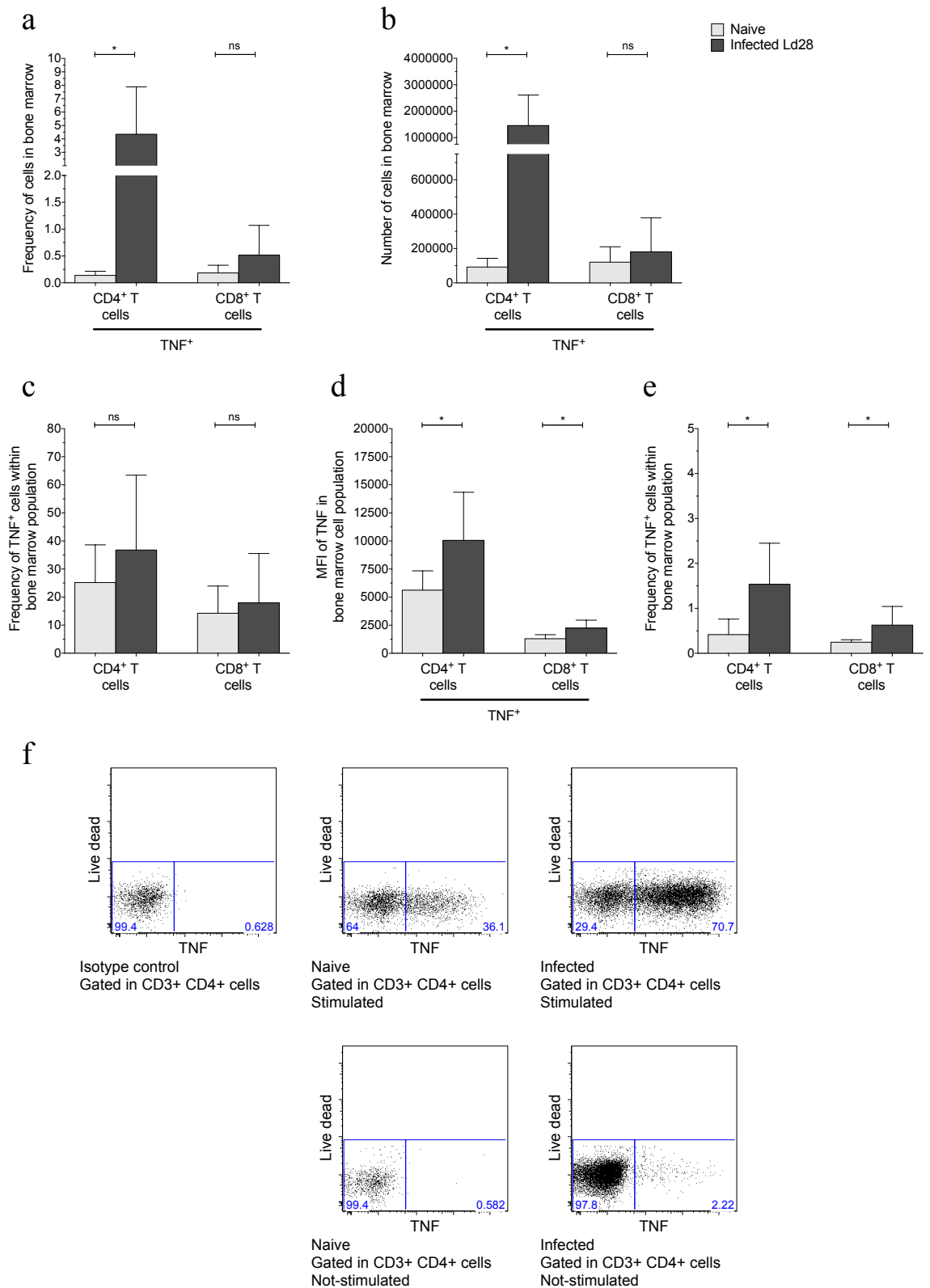


Figure 4.14 - *L. donovani* infection was associated with increased number of BM CD4⁺ T cells with potential for TNF expression. (a) Frequency of CD4⁺ T cells TNF⁺ and CD8⁺ T cells TNF⁺ in total bone marrow following *in vitro* stimulation. (b) Number of CD4⁺ T TNF⁺ and CD8⁺ T TNF⁺ in total BM following *in vitro* stimulation. (c) Frequency of TNF⁺ cells within CD4⁺ T cells and CD8⁺ T cells following *in vitro* stimulation. (d) MFI of TNF in CD4⁺ T cells TNF⁺ and

CD8⁺ T cells TNF⁺ following *in vitro* stimulation. (e) Frequency of TNF⁺ cells within CD4⁺ T cells and CD8⁺ T cells determined in the absence of exogenous stimulation in BM. (f) Representative dot plots displaying frequencies TNF expression within in CD45⁺ CD3⁺ CD4⁺ cells in BM: (top left) isotype control for TNF staining, gated in CD4⁺ T cells from (top center) naive mouse and (top right) infected mouse upon *in vitro* stimulation, gated in CD4⁺ T cells from (bottom left) naive and infected analyzed in BM cells directly *ex vivo* Comparisons were made between naive mice (n=6) and mice infected (n=6) for 28 days with *L. donovani* (Ld28). Two femur and two tibias were taken per animal. Data from two independent was presented as Mean ± SD, p values were determined using unpaired t test: not significant (ns), *p ≤ 0.05, **p ≤ 0.01, ***p ≤ 0.001 and ****p ≤ 0.0001.

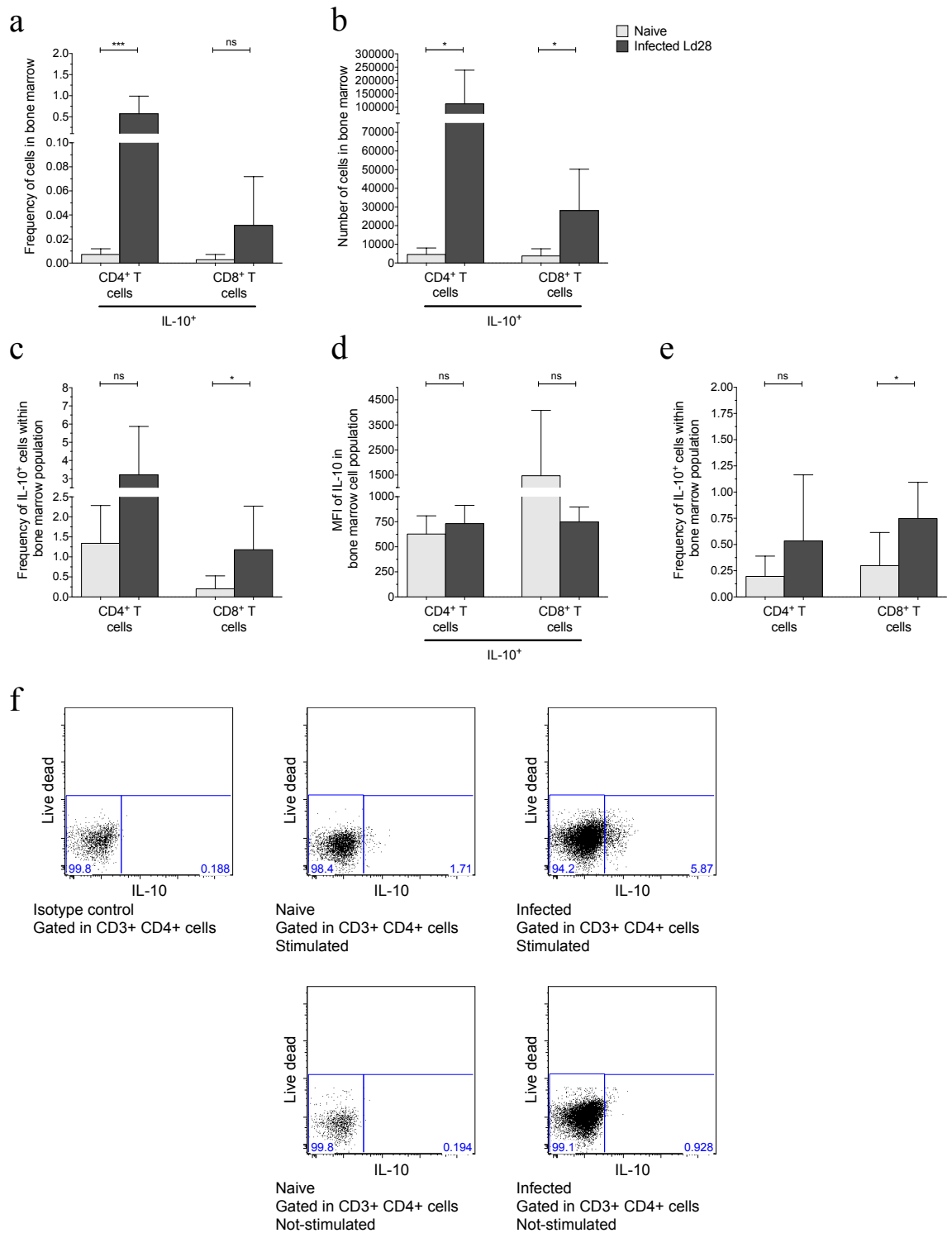


Figure 4.15 - The number of BM CD4⁺ T cells with potential for IL-10 expression increased following *L. donovani* infection. (a) Frequency of CD4⁺ T cells IL-10⁺ and CD8⁺ T cells IL-10⁺ in total BM following *in vitro* stimulation. (b) Number of CD4⁺ T IL-10⁺ and CD8⁺ IL-10⁺ in BM following *in vitro* stimulation. (c) Frequency of IL-10⁺ cells within CD4⁺ T cells and CD8⁺ T cells following *in vitro* stimulation. (d) Mean of Fluorescence Intensity (MFI) of IL-10 in CD4⁺ T cells IL-10⁺ and CD8⁺ T cells IL-10⁺ following *in vitro* stimulation. (e) Frequency of IL-10⁺ cells within CD4⁺ T cells and CD8⁺ T cells in *ex vivo* bone marrow. (f) Representative dot plots

displaying frequencies of IL-10 expression within in CD45⁺ CD3⁺ CD4⁺ cells in BM: (top left) isotype control for IL-10 staining, gated in CD4⁺ T cells from (top center) naive mouse and (top center) infected mouse analyzed in BM cells upon *in vitro* stimulation, gated in CD4⁺ T cells from (bottom left) naive mouse and infected mouse analyzed in BM cells directly *ex vivo*. Comparisons were made between naive mice (n=9) and mice infected (n=9) for 28 days with *L. donovani* (Ld28). Two femur and two tibias were taken per animal. Data from three independent was presented as Mean ± SD, p values were determined using unpaired t test: not significant (ns), *p ≤ 0.05, **p ≤ 0.01, ***p ≤ 0.001 and ****p ≤ 0.0001.

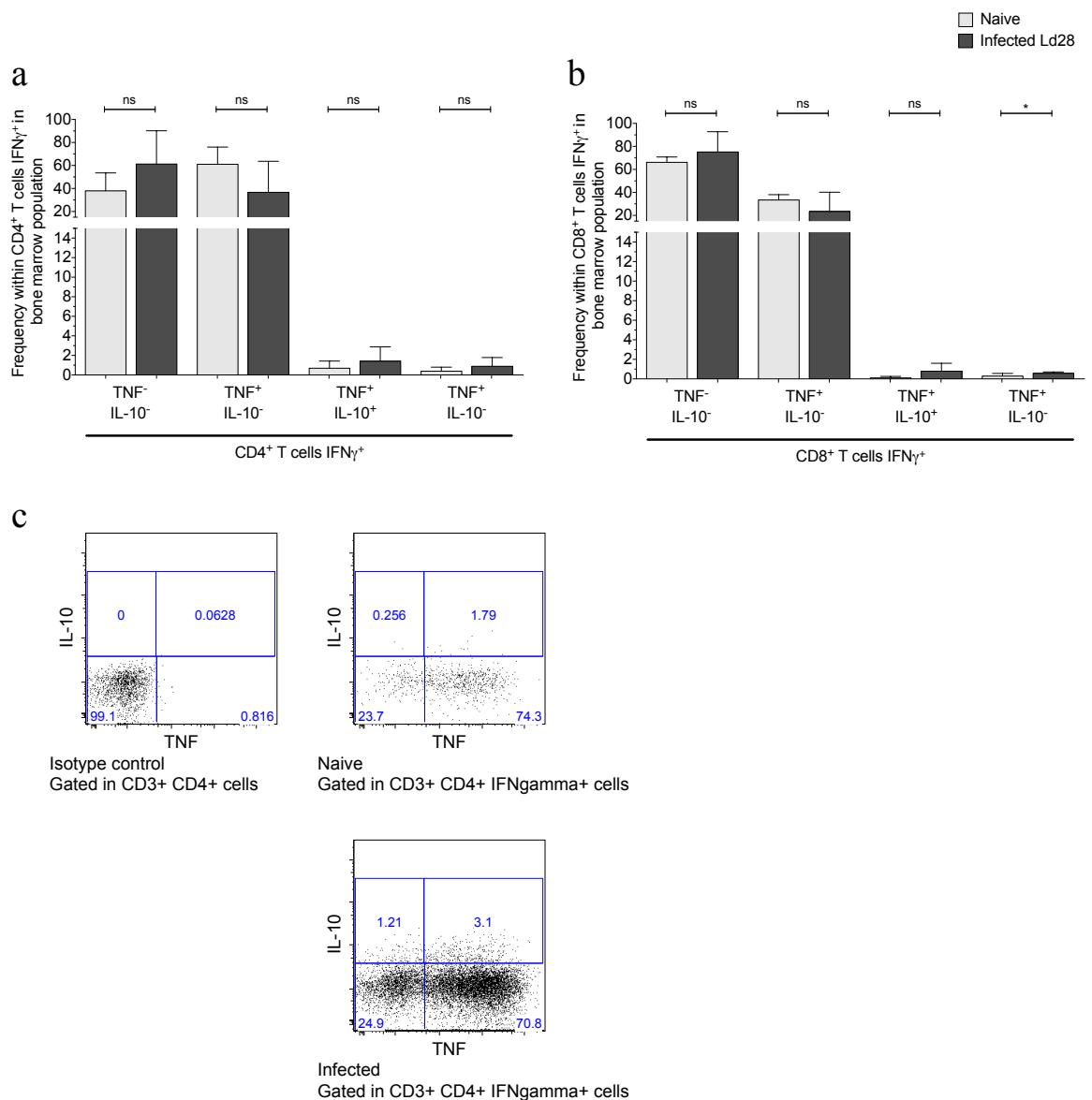


Figure 4.16 - In BM the distribution of cells expressing TNF and/or IL-10 within CD4⁺ T cells IFN γ ⁺ was unchanged following *L. donovani* infection. (a) Frequency of CD4⁺ T cells IFN γ ⁺ expressing IL-10 and/or TNF following *in vitro* stimulation. (b) Frequency of CD8⁺ T cells IFN γ ⁺ expressing IL-10 and/or TNF following *in vitro* stimulation. (f) Representative dot plots displaying frequencies of IL-10 and TNF expression within in CD4⁺ CD3⁺ CD4⁺ IFN γ ⁺ cells in BM: (top left) Isotype control for TNF and IL-10 staining, gated in CD4⁺ T cells IFN γ ⁺ from (top right) naive mouse and (bottom) infected mouse, analysis performed in BM upon *in vitro* stimulation. Comparisons were made between naive mice (n=6) and mice infected (n=6) for 28 days with *L. donovani* (Ld28). Two femur and two tibias were taken per animal. Data from two independent was presented as Mean \pm SD, p values were determined using unpaired t test: not significant (ns), *p \leq 0.05, **p \leq 0.01, ***p \leq 0.001 and ****p \leq 0.0001.

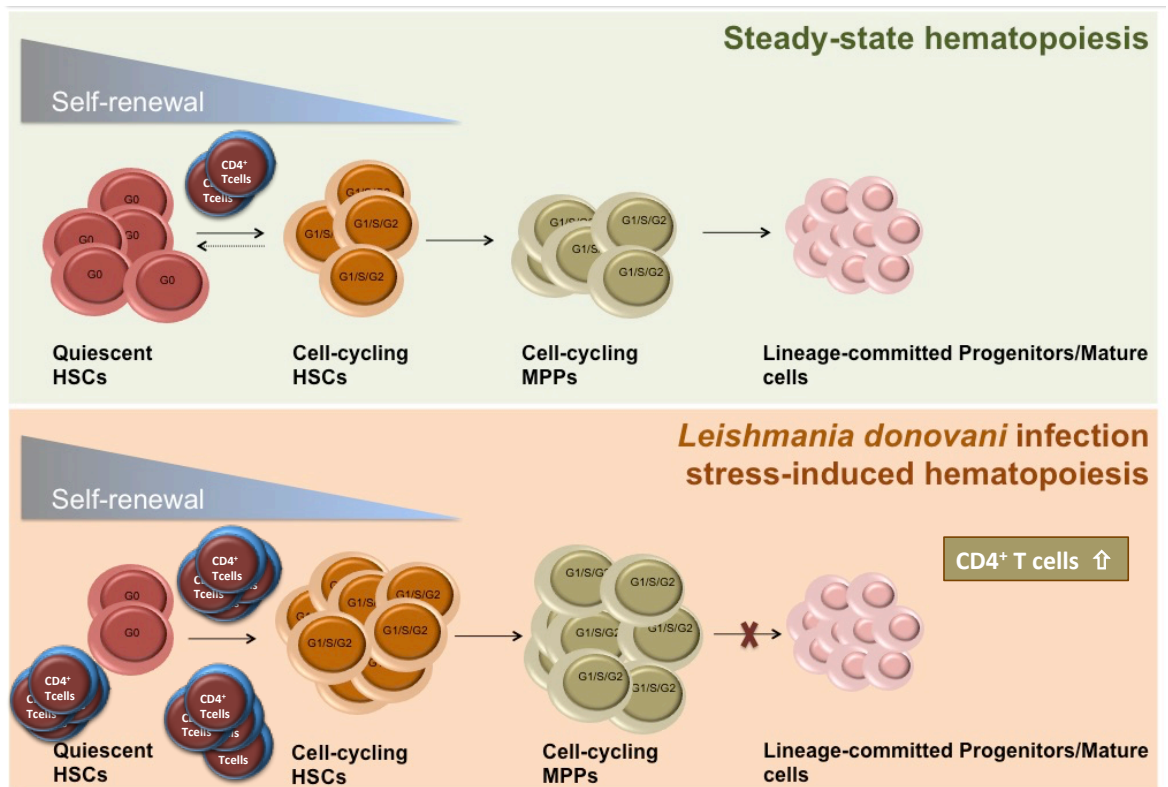


Figure 4.17 - Proposed mechanism to explain depletion of LT-HSCs in G0 and inefficient haematopoiesis during the chronic infection with *L. donovani* (1). Following *L. donovani* infection, proliferating LT-HSCs and onward multipotent progenitors expand greatly at the expense of LT-HSCs in G0. The accumulation of intermediary multipotent progenitors was not associated with an increase in effective haematopoietic activity, since the numbers of effector haematopoietic cells were found either decreased or unchanged in PB. BM CD4⁺ T cells numbers greatly increase following infection and displayed immunophenotypic and functional alterations, suggesting that BM CD4⁺ T cell may act underlie haematological impairment.

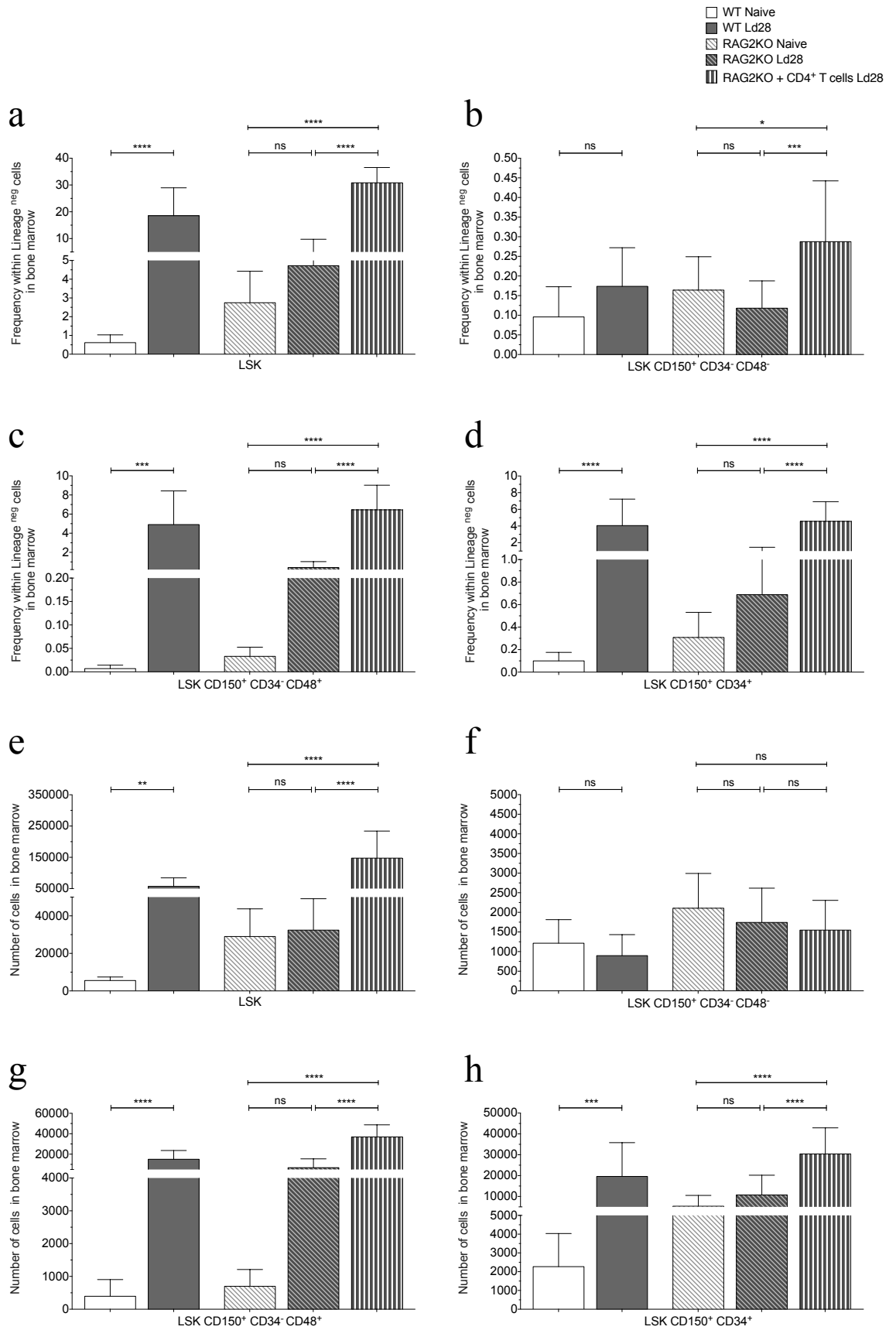


Figure 4.18 - CD4⁺ T cells mediated expansion of intermediary non-committed progenitors onward LT-HSCs in BM following *L. donovani* infection. Frequency in Lineage^{negative} cells of

(a) LSK cells, (b) LSK CD150⁺ CD34⁻ CD48⁻ cells (enriched for LT-HSCs), (c) LSK CD150⁺ CD34⁻ CD48⁺ cells and (d) LSK CD150⁺ CD34⁺ cells. Number of (e) LSK cells, (f) LSK CD150⁺ CD34⁻ CD48⁻ cells (enriched for LT-HSCs), (g) LSK CD150⁺ CD34⁻ CD48⁺ cells and (h) LSK CD150⁺ CD34⁺ cells. Comparisons were made with BM cells recovered from B6 wild-type (WT) (n=12), B6 WT infected with LV9 for 28 days (Ld28) (n=12), B6 RAG2 knockout (KO)(lacking B and T cells) naive (n=12), RAG2KO B6 infected (n=17) and RAG2KO B6 infected inoculated with CD4⁺ T cells purified from spleen of naive WT mice (n=13). Two femur and two tibias were taken per animal. In each bar, data from at least three independent experiments was presented as Mean \pm SD, p values were determined using One-way Anova followed by Tukey's multiple comparisons test: not significant (ns), *p \leq 0.05, **p \leq 0.01, ***p \leq 0.001 and ****p \leq 0.0001.

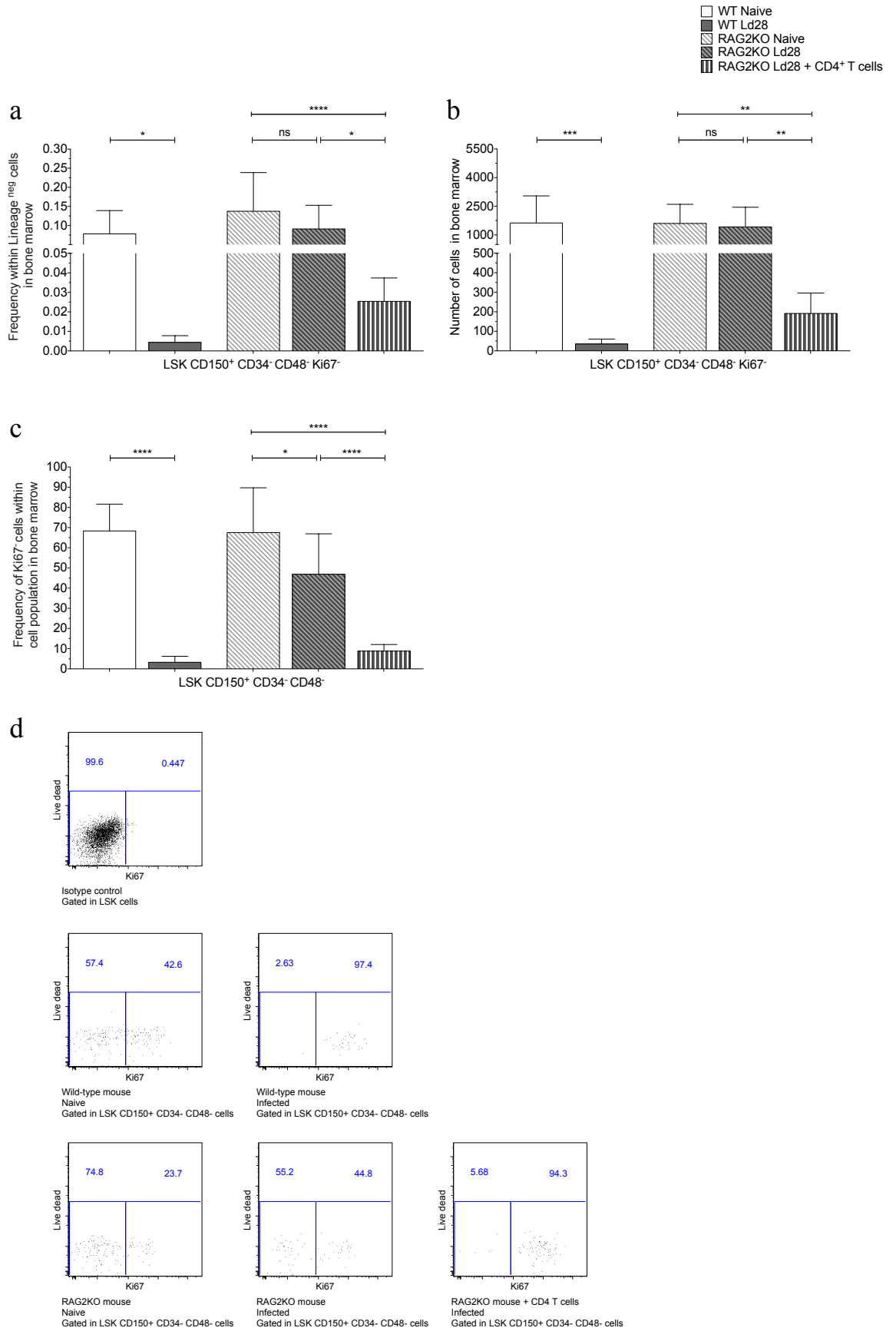


Figure 4.19 - CD4⁺ T cells mediated the loss of HSCs in G0 in BM, following infection with *L. donovani*. (a) Frequency within Lineage^{negative} cells of LSK CD150⁺ CD34⁻ CD48⁻ Ki67 cells (enriched for LT-HSCs in G0). (b) Number of LSK CD150⁺ CD34⁻ CD48⁻ Ki67 cells. (c)

Frequency of Ki67⁺ cells within LSK CD150⁺ CD34⁻ CD48⁻ cells. (d) Representative dot plots of Ki67 expression within LSK CD150⁺ CD34⁻ CD48⁻ cells: (top left) isotype control for Ki67 staining gated in LSK cells, (middle left) WT naive mouse, (middle right) WT infected mouse, (bottom left) RAG2 KO naive mouse, (bottom) centre RAG2 KO infected mouse and (bottom right) RAG2 KO mouse transplanted with CD4⁺ T cells prior to infected. Comparisons were made with BM cells recovered from B6 WT mice (n=12), B6 WT mice infected with *L. donovani* for 28 days (Ld28) (n=12), B6 RAG2KO mice naive (lacking B and T cells) (n=9), RAG2KO B6 infected mice (n=14) and RAG2KO B6 infected mice inoculated with CD4⁺ T cells purified from spleen of naive WT mice (n=13). Two femur and two tibias were taken per animal. In each bar, data from three independent experiments was presented as Mean \pm SD, p values were determined using One-way Anova followed by Tukey's multiple comparisons test: not significant (ns), *p \leq 0.05, **p \leq 0.01, ***p \leq 0.001 and ****p \leq 0.0001.

□ WT Naive
 ■ WT Infected Ld28
 ▨ RAG2KO Naive
 ▩ RAG2KO Ld28
 ▤ RAG2KO + CD4⁺ T cells Ld28

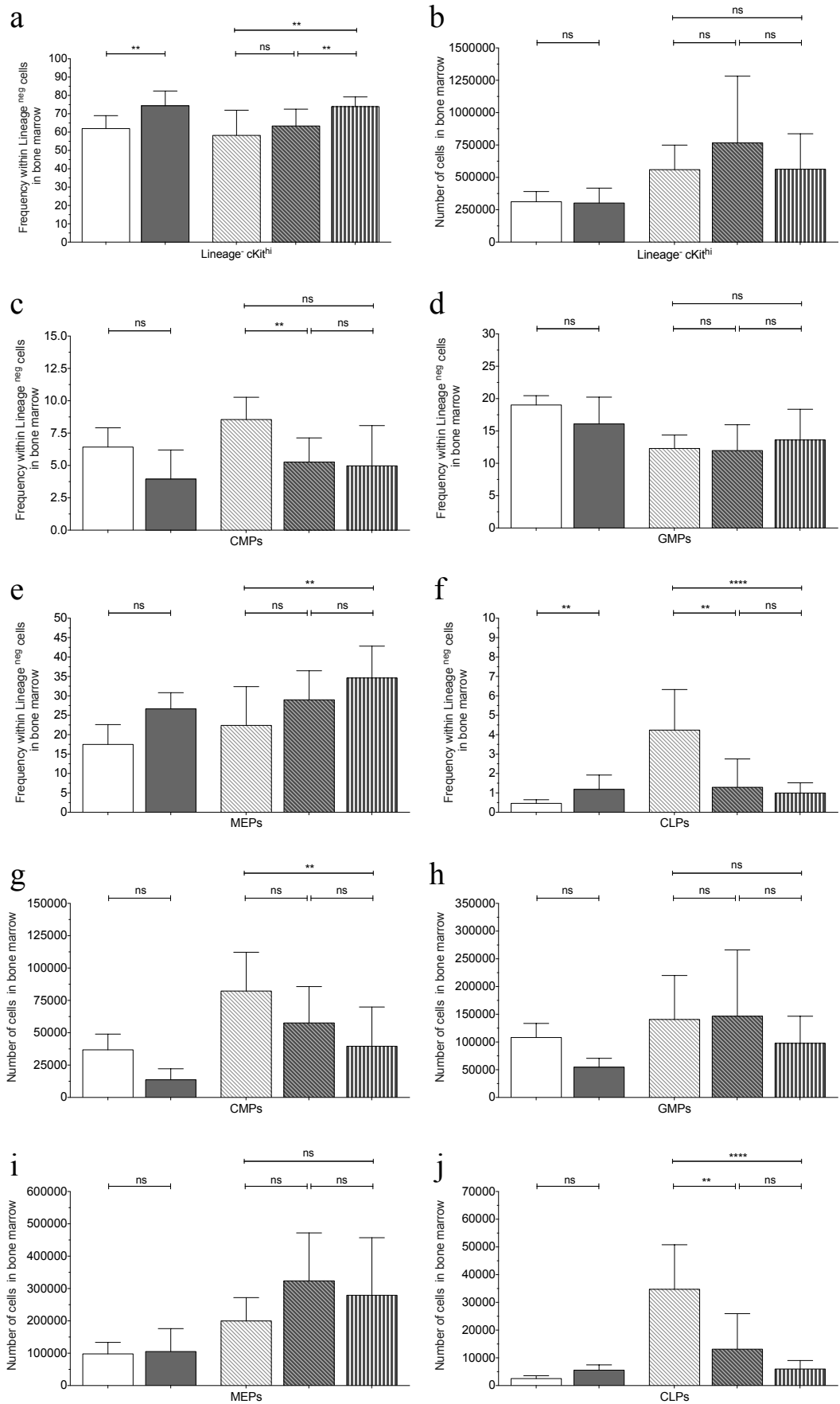


Figure 4.20 - CD4⁺ T cells did mediate alteration in the number of myeloid-committed progenitors, following infection with *L. donovani*. (a) Frequency of Lineage^{negative} cells (enriched for all HSPCs). (b) Frequency in Lineage^{negative} cells. Frequency within Lineage^{negative} cells of (c) CMPs, (d) GMPs, (e) MEPs and (f) CLPs. Number of (g) CMPs, (h) GMPs, (i) MEPs and (j) CLPs. Comparisons were made with BM cells recovered from B6 Wild Type (WT) (n=8), B6 WT mice infected with *L. donovani* for 28 days (Ld28) (n=8), B6 RAG2KO mice naive (lacking B and T cells) (n=7), RAG2KO B6 infected mice (n=12) and RAG2KO B6 infected mice inoculated with CD4⁺ T cells purified from spleen of naive WT mice (n=13). Two femur and two tibias were taken per animal. In each bar, data from at least two independent experiments was presented as Mean ± SD, p values were determined using One-way Anova followed by Tukey's multiple comparisons test: not significant (ns), *p ≤ 0.05, **p ≤ 0.01, ***p ≤ 0.001 and ****p ≤ 0.0001. Common-myeloid progenitors (CMPs); Granulocyte-macrophage progenitors (GMPs); Megakaryocyte-erythrocyte progenitors (MEPs); Common lymphocyte progenitors (CLPs).

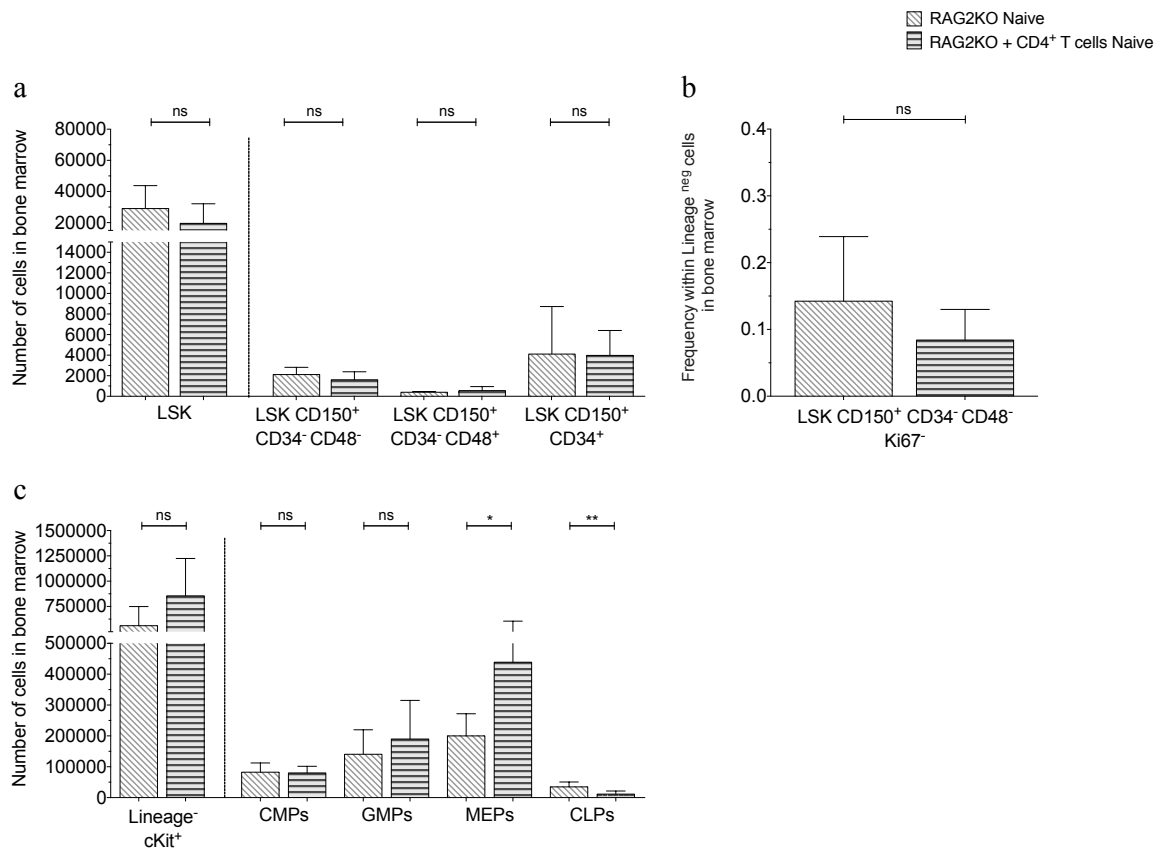


Figure 4.21 - The transfer of CD4⁺ T cells to naive RAG2 KO mice was not associated to alteration in the number of HSPCs in BM. (a) Number of LSK cell, LSK CD150⁺ CD34⁻ CD48⁻ cells (enriched for LT-HSCs), LSK CD150⁺ CD34⁻ CD48⁺ cells and LSK CD150⁺ CD34⁺ cells. (b) Frequency within Lineage^{neg} cells of LSK CD150⁺ CD34⁻ CD48⁻ Ki67⁻ cells. (c) Number of CMPs, GMPs, MEPs and CLPs. Comparisons were made with BM cells recovered from naive B6 RAG2KO mice (n=5), and naive B6 RAG2KO mice infected inoculated with CD4⁺ T cells purified from spleen of naive WT mice (n=5). Two femur and two tibias were taken per animal. Data from one experiment was presented as Mean ± SD, p values were determined using unpaired t test: not significant (ns), *p ≤ 0.05, **p ≤ 0.01, ***p ≤ 0.001 and ****p ≤ 0.0001.

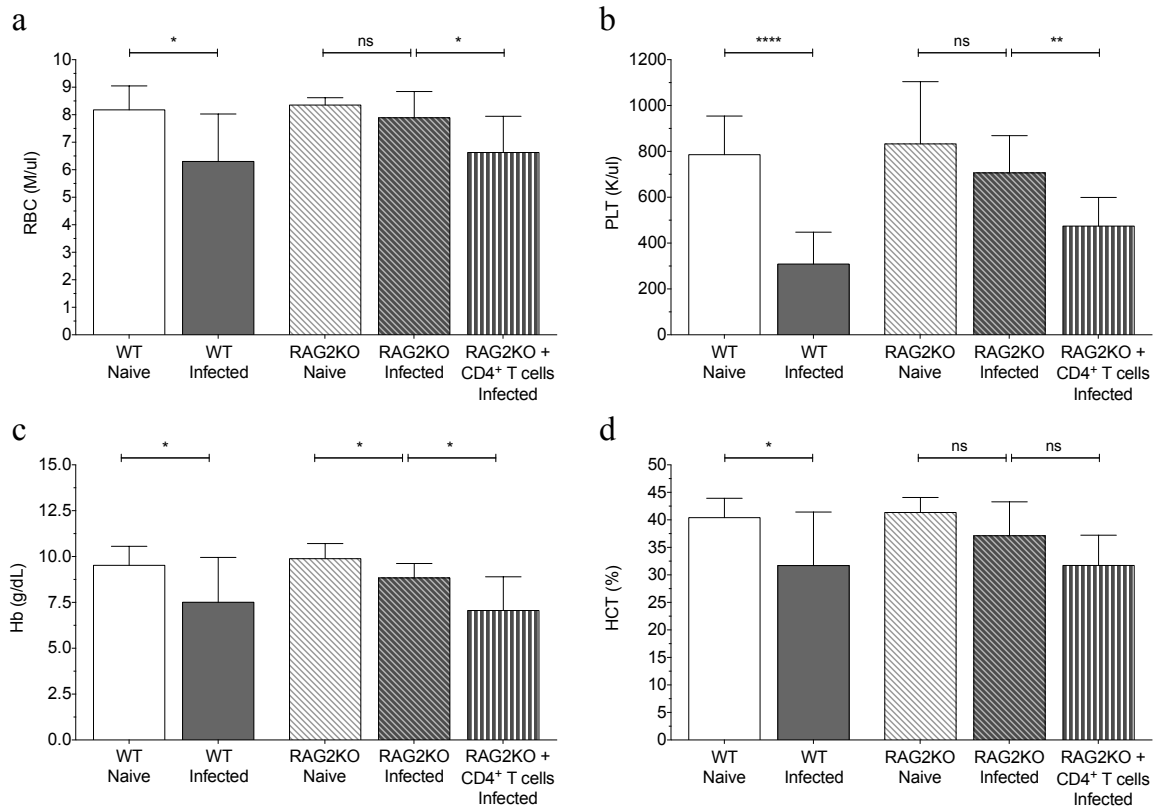


Figure 4.22 - CD4⁺ T cells mediate the establishment of mild anaemia and thrombocytopenia following infection with *L. donovani*. (a) Concentration of red blood cells (RBC) in peripheral blood (PB). (b) Concentration of platelets (PLT) in PB. (c) PB hematocrit (HCT). (d) Concentration of haemoglobin (Hb) in PB. Values were determined in whole blood collected in EDTA using an automated system for blood cell counting (Hemavet). Comparisons were made with PB recovered from B6 Wild Type (WT) (n=8), B6 WT infected with LV9 for 28 days (Ld28) (n=8), B6 RAG2KO (n=6), RAG2KO B6 infected (n=9) and RAG2KO B6 infected inoculated with CD4⁺ T cells purified from spleen of naive WT mice (n=8). Two femur and two tibias were taken per animal. Data from two independent experiments was presented as Mean \pm SD, p values were determined using unpaired t test: not significant (ns), *p \leq 0.05, **p \leq 0.01, ***p \leq 0.001 and ****p \leq 0.0001.

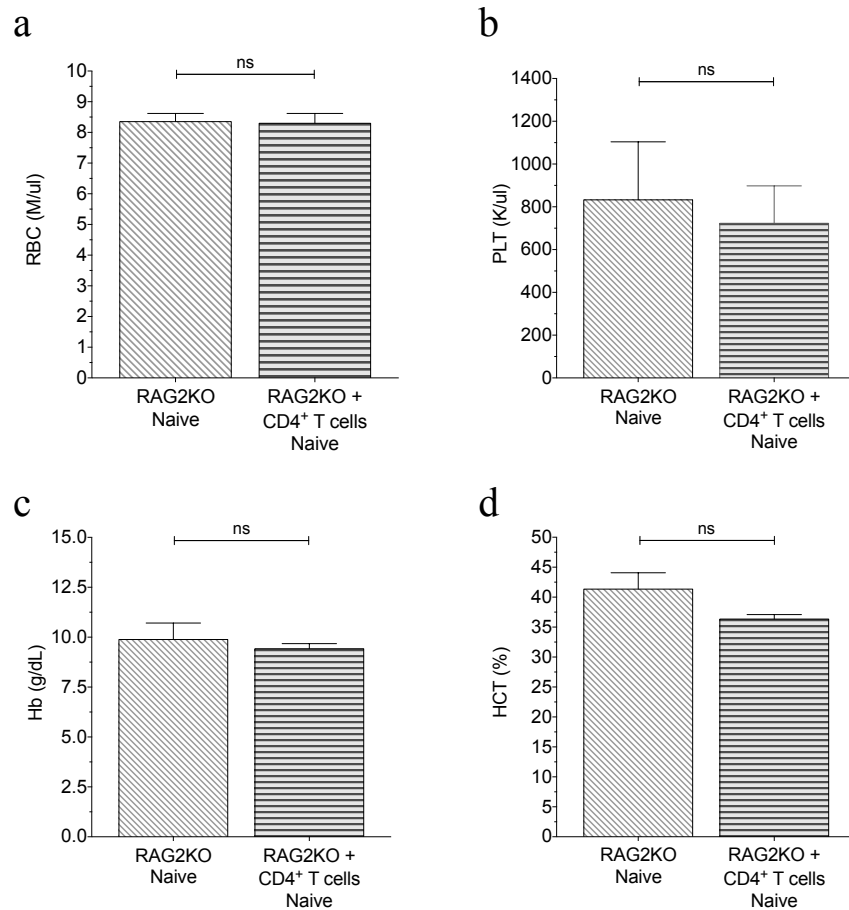


Figure 4.23 - CD4⁺ T cells do not induce anaemia and thrombocytopenia in naive RAG2 KO mice. (a) Concentration of red blood cells (RBC) in peripheral blood (PB). (b) Concentration of platelets (PLT) in PB. (c) Concentration of haemoglobin (Hb) in PB. (d) PB hematocrit (HCT). Values were determined in whole blood collected in EDTA, using an automated system for blood cell counting (Hemavet). Comparisons were made with PB recovered naive B6 RAG2KO mice (n=5) and naive B6 RAG2KO mice inoculated with CD4⁺ T cells purified from spleen of naive WT mice for 28 days (n=5). Data from one experiment was presented as Mean \pm SD, p values were determined using unpaired t test: not significant (ns), *p \leq 0.05, **p \leq 0.01, ***p \leq 0.001 and ****p \leq 0.0001.

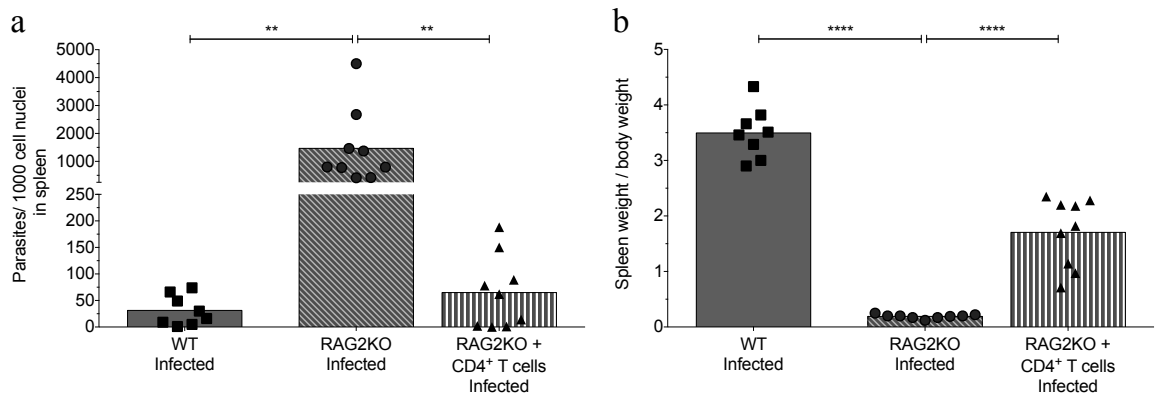


Figure 4.24 - CD4⁺ T cells mediated control of parasite burden during chronic infection with *L. donovani* in immunodeficient mice. (a) Parasites *per* 1000 nuclei in the spleen. (b) Spleen weight as percentage of body weight. Comparisons were made between B6 WT mice (n=8) and infected B6 RAG2KO mice (n=9), or between B6 RAG2KO infected mice and RAG2KO B6 infected mice inoculated with CD4⁺ T cells purified from spleen of naive WT mice (n=9). All mice were infected with *L. donovani* for 28 days. Data from two independent experiments was presented as Mean ± SD, p values were determined using unpaired t test: not significant (ns), *p ≤ 0.05, **p ≤ 0.01, ***p ≤ 0.001 and ****p ≤ 0.0001.

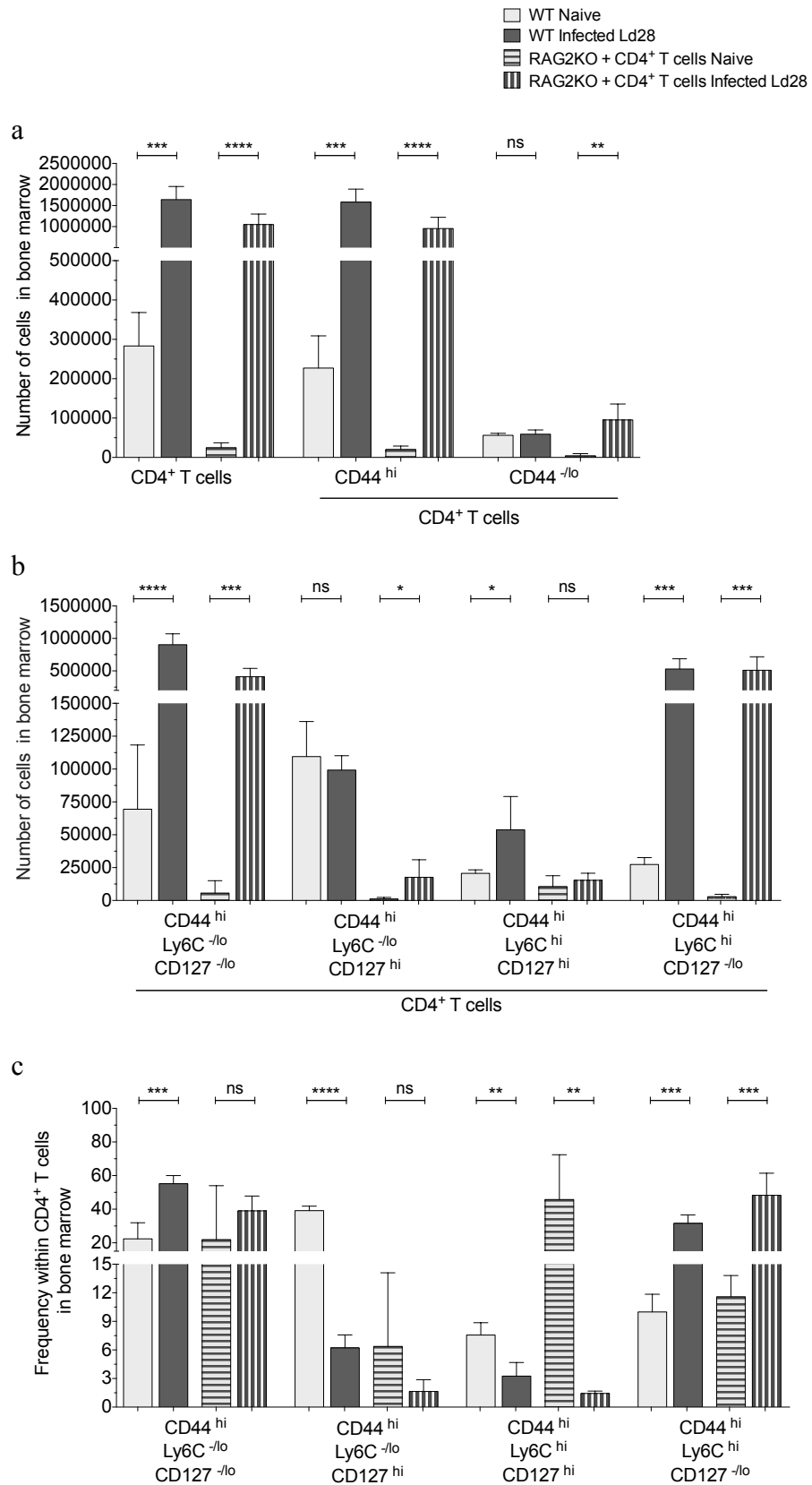


Figure 4.25 - Adoptively transferred CD4⁺ T cells expand in infected RAG2 recipients and displayed a phenotype similar to BM CD4⁺ T cells of infected WT mice. (a) Number of CD4⁺ T cells, CD4⁺ T cells CD44^{hi} and CD4⁺ T cells CD44^{lo} cells. (b) Number of CD4⁺ CD44^{hi} Ly6C^{-/-} CD127^{-/-} T cells (“effector” T cells), CD4⁺ CD44^{hi} Ly6C^{-/-} CD127^{hi} T cells, CD4⁺ CD44^{hi} Ly6C^{hi} CD127^{hi} T cells, CD4⁺ CD44^{hi} Ly6C^{hi} CD127^{-/-} T cells (“effector” T cells), CD4⁺ CD44^{hi} Ly6C^{-/-} CD127^{hi} T cells, CD4⁺ CD44^{hi} Ly6C^{hi} CD127^{hi} T cells, CD4⁺ CD44^{hi} Ly6C^{hi} CD127^{-/-} T cells (“effector” T cells).

CD127^{hi} T cells (“memory” T cells) and CD4⁺ CD44^{hi} LyC6^{hi} CD127^{-/lo} T cells in the bone marrow of naive and infected mice. (c) Frequency within of total CD4⁺ T cells of CD44^{hi}, CD44^{hi} LyC6^{-/lo} CD127^{-/lo} T cells (“effector” T cells), CD44^{hi} LyC6^{-/lo} CD127^{hi} T cells, CD44^{hi} LyC6^{hi} CD127^{hi} T cells (“memory” T cells) and CD44^{hi} LyC6^{hi} CD127^{-/lo} CD4⁺ T cells. Comparisons were made between naive B6 WT mice (n=4) and infected B6 WT mice, or between naive RAG2KO inoculated with CD4⁺ T cells purified from spleen of naive WT mice (n=5) and infected RAG2KO inoculated with CD4⁺ T cells purified from spleen of naive WT mice (n=5). Mice were infected with *L. donovani* for 28 days (Ld28). Two femur and two tibias were taken per animal. Data from one experiments was presented as Mean ± SD, p values were determined using unpaired t test: not significant (ns), *p ≤ 0.05, **p ≤ 0.01, ***p ≤ 0.001 and ****p ≤ 0.0001.

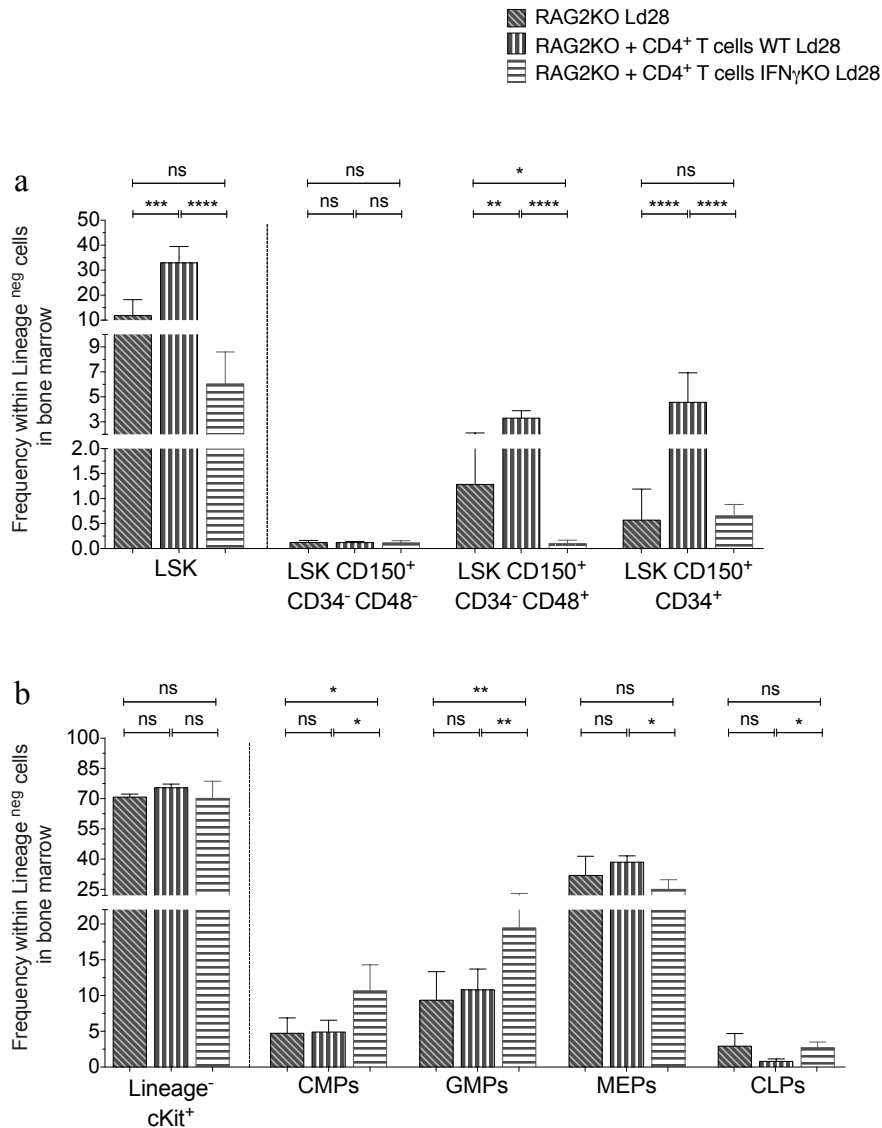


Figure 4.26 - CD4⁺ T cells through an IFN γ -dependent mechanism mediated the expansion of intermediary multipotent progenitors following infection with *L. donovani*. (a) Frequency in Lineage⁻ cells of LSK cells, LSK CD150⁺ CD34⁻ CD48⁻ cells (enriched for LT-HSCs), LSK CD150⁺ CD34⁻ CD48⁺ cells and LSK CD150⁺ CD34⁺ cells. (b) Frequency within Lineage⁻ cells of Lineage^{negative} cKit⁺ cells, CMPs, GMPs, MEPs and CLPs. Comparisons were made between, B6 RAG2KO infected mice (n=4), B6 RAG2KO infected mice inoculated with CD4⁺ T cells purified from spleen of naive WT mice (n=4), and B6 RAG2KO infected mice inoculated with CD4⁺ T cells purified from spleen of naive IFN γ KO mice (n=5), all mice were infected with *L. donovani* for 28 days (Ld28). Data from one experiment was presented as Mean \pm SD, p values were determined using One-way Anova followed by Tukey's multiple comparisons test: not significant (ns), *p \leq 0.05, **p \leq 0.01, ***p \leq 0.001 and ****p \leq 0.0001.

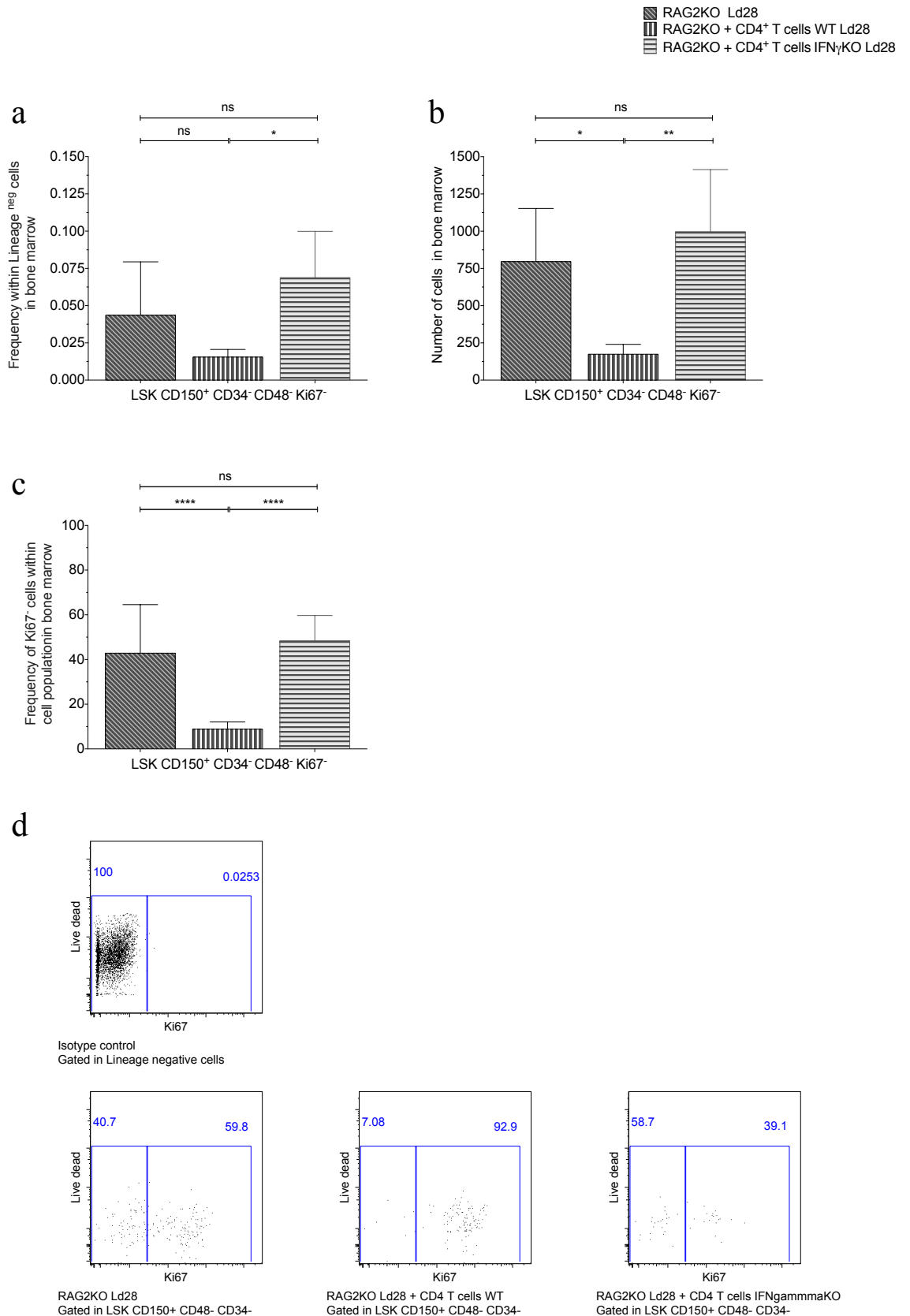


Figure 4.27 - CD4⁺ T cells through an IFN γ -dependent mechanism mediated the loss of HSCs in G0 following infection with *L. donovani*. (a) Frequency within Lineage^{negative} cells of LSK CD150⁺ CD34⁻ CD48⁻ Ki67 cells (enriched for LT-HSCs in G0). (b) Number of LSK

CD150⁺ CD34⁻ CD48⁻ Ki67⁻ cells. (c) Frequency of Ki67⁻ cells within LSK CD150⁺ CD34⁻ CD48⁻ cells. (d) Representative dot plots of Ki67 expression within LSK CD150⁺ CD34⁻ CD48⁻ cells: (top left) isotype control for Ki67 staining gated in Lineage^{negative} cells, (bottom left) RAG2KO mouse infected, (bottom centre) RAG2KO mouse infected transplanted with WT CD4⁺ T cells, (bottom) right RAG2KO mouse infected transplanted with IFN γ KO CD4⁺ T cells. Comparisons were made between, RAG2KO mice infected (n=3), RAG2KO mice infected inoculated with CD4⁺ T cells purified from spleen of naive WT mice (n=4), and RAG2KO mice infected inoculated with CD4⁺ T cells purified from spleen of naive IFN γ KO mice (n=5), all mice were infected with *L. donovani* for 28 days (Ld28). Two femur and two tibias were taken per animal. Data from one experiment was presented as Mean \pm SD, p values were determined using unpaired t test: not significant (ns), *p \leq 0.05, **p \leq 0.01, ***p \leq 0.001 and ****p \leq 0.0001.

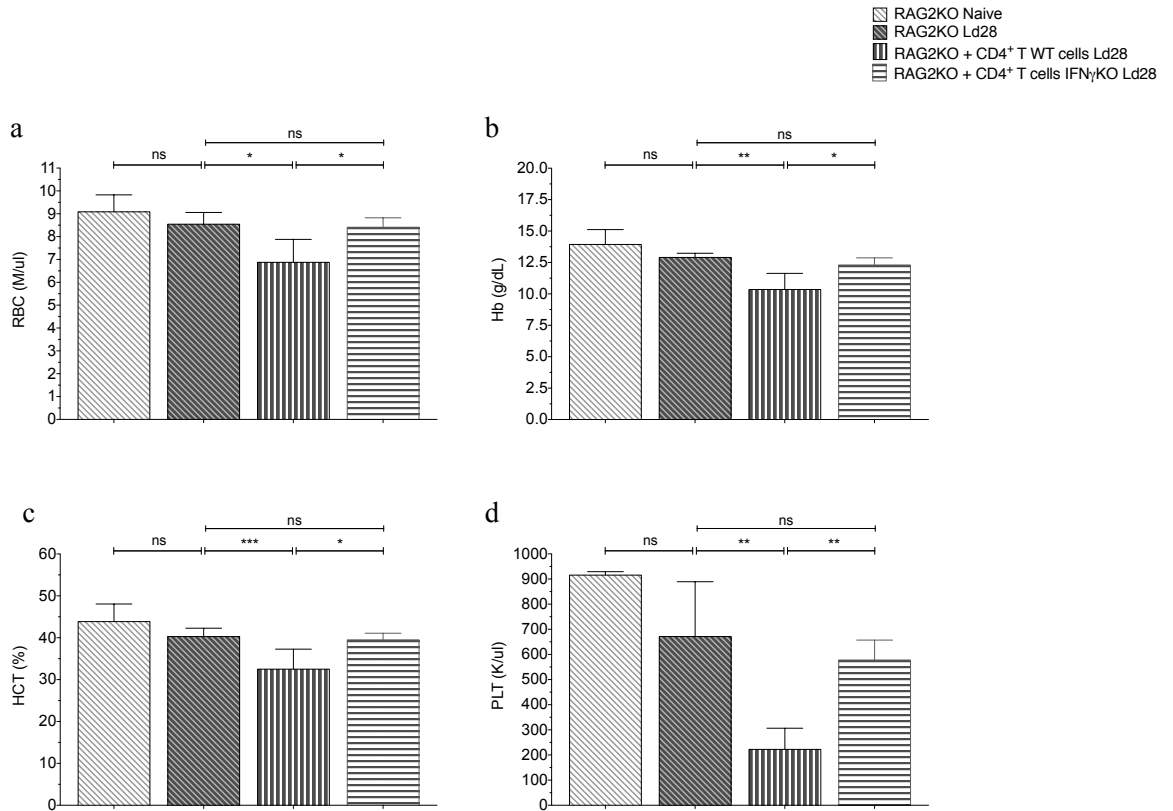


Figure 4.28 - CD4⁺ T cells through an IFN γ -dependent mechanism mediated the establishment of anaemia and thrombocytopenia following infection with *L. donovani*. (a) Concentration of red blood cells (RBC) in peripheral blood (PB). (b) Concentration of haemoglobin (Hb) in PB. (c) Hematocrit (HCT) in PB. (d) Concentration of platelets (PLT) in PB. Values were determined in whole blood collected in EDTA, using an automated system for blood cell counting (Vet abc Plus+). Comparisons were made between, RAG2KO infected mice (n=3), RAG2KO infected mice inoculated with CD4⁺ T cells purified from the spleen of naive WT mice (n=4), and RAG2KO mice infected inoculated with CD4⁺ T cells purified from the spleen of naive IFN γ KO mice (n=5), mice were infected with *L. donovani* for 28 days (Ld28). Data from one experiment presented as Mean \pm SD, p values were determined using One-way Anova followed by Tukey's multiple comparisons test: not significant (ns), *p \leq 0.05, **p \leq 0.01, ***p \leq 0.001 and ****p \leq 0.0001

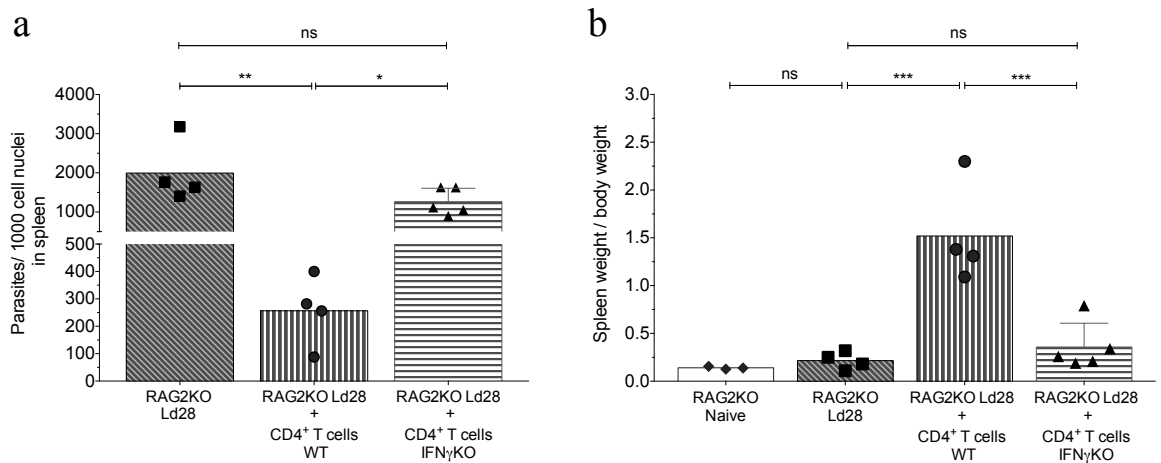


Figure 4.29 - CD4⁺ T cells through an IFN γ -dependent mechanism mediated decrease in parasites/1000 nuclei in the spleen following infection with *L. donovani*. (a) Parasites per 1000 nuclei in the spleen. (b) Spleen weight as percentage of body weight. Comparisons were made between, RAG2KO mice infected (n=3), RAG2KO mice infected inoculated with CD4⁺ T cells purified from the spleen of naive WT mice (n=4), and RAG2KO mice infected inoculated with CD4⁺ T cells purified from the spleen of naive IFN γ KO mice (n=5), mice were infected with *L. donovani* for 28 days (Ld28). Data from one experiment presented as Mean \pm SD, p values were determined using One-way Anova followed by Tukey's multiple comparisons test: not significant (ns), *p \leq 0.05, **p \leq 0.01, ***p \leq 0.001 and ****p \leq 0.0001.

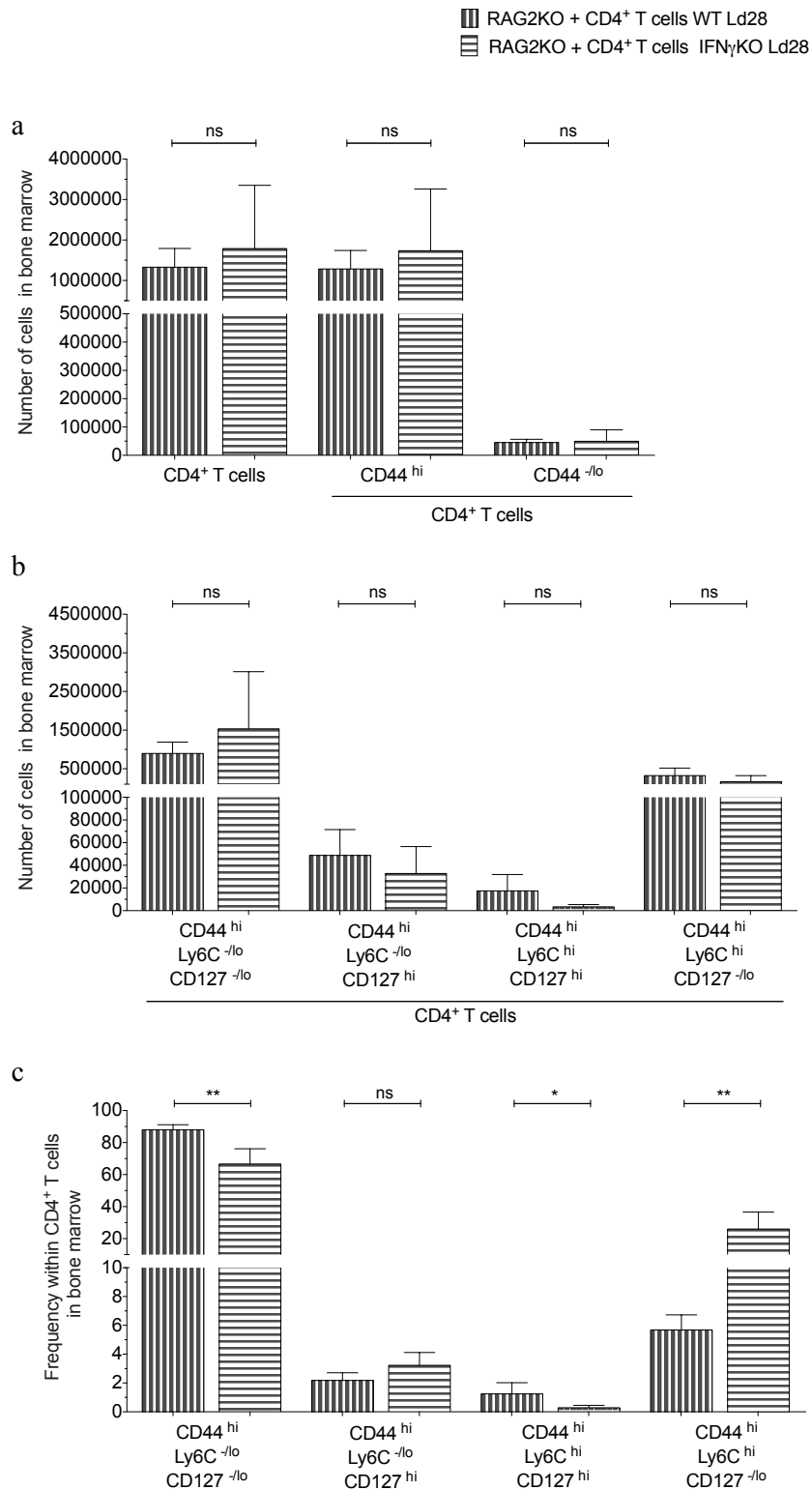


Figure 4.30 - Following transfer of CD4⁺ T cells to RAG2KO mice infected with *L. donovani* for 28 days, WT CD4⁺ T cells and IFN γ KO CD4⁺ T cells expanded at similar extent and displayed an “activated” phenotype. (a) Number of CD4⁺ T cells, CD4⁺ T cells CD44^{hi} and CD4⁺ T cells CD44^{lo} cells. (b) Number of CD4⁺ T CD44^{hi} Ly6C^{-/-lo} CD127^{-/-lo} (“effector” T cells), CD4⁺ T CD44^{hi} Ly6C^{-/-lo} CD127^{hi}, CD4⁺ T CD44^{hi} Ly6C^{hi} CD127^{hi} (“memory” T cells) and CD4⁺ T CD44^{hi} Ly6C^{hi} CD127^{-/-lo} in BM. (c) Frequency within of Total CD4⁺ T cells of CD44^{hi} cells,

CD44^{hi} LyC6^{-/lo} CD127^{-/lo}, CD44^{hi} LyC6^{-/lo} CD127^{hi}, CD44^{hi} LyC6^{hi} CD127^{hi} and CD44^{hi} LyC6^{hi} CD127^{-/lo} cells CD4⁺ T cells. Comparisons were made between, RAG2KO mice infected (n=3), RAG2KO mice infected inoculated with CD4⁺ T cells purified from the spleen of naive WT mice (n=4), and RAG2KO mice infected inoculated with CD4⁺ T cells purified from the spleen of naive IFN γ KO mice (n=5), mice were infected with *L. donovani* for 28 days (Ld28). Two femur and two tibias were taken per animal. Data from one experiment presented as Mean \pm SD, p values were determined using unpaired t test: not significant (ns), *p \leq 0.05, **p \leq 0.01 and ***p \leq 0.001.

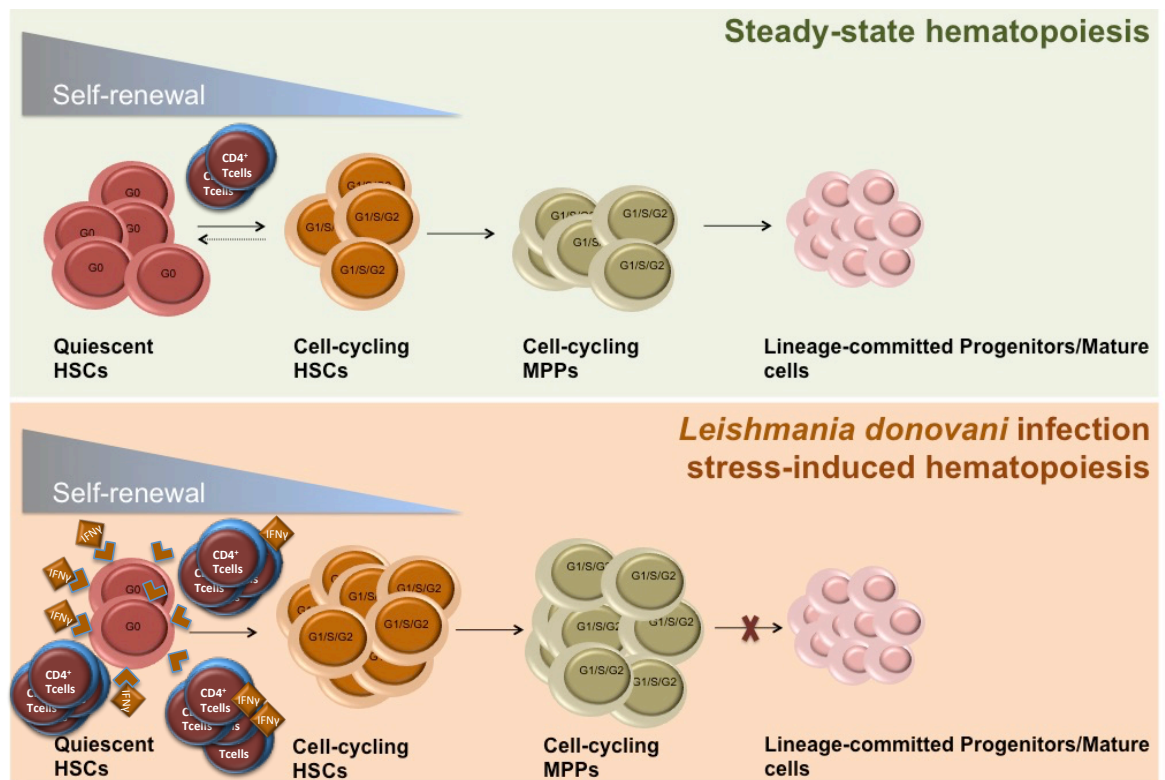


Figure 4.31 - Proposed mechanism to explain depletion of LT-HSCs in G0 and inefficient haematopoiesis during chronic infection with *L. donovani* (2). Following *L. donovani* infection LT-HSCs and onward multipotent progenitors expand greatly at the expense of LT-HSCs in G0. The accumulation of intermediary multipotent progenitors was not associated to an increase in effective haematopoietic activity, since the numbers of effector haematopoietic cells were found either decreased or unchanged in circulation. These alterations could be solely mediated by the transfer CD4⁺ T cells IFN γ ⁺, but not by CD4⁺ T cells deficient for IFN γ expression, following transfer to *L. donovani*-infected immunodeficient mice, which are otherwise protected from impairment of haematological function. As such, IFN γ was defined as a critical modulator of haematopoiesis during chronic infection with *L. donovani*. As LT-HSCs express receptors for this pro-inflammatory cytokine, we hypothesized that IFN γ could act directly on the activation of LT-HSCs into active cell-cycle, following infection.

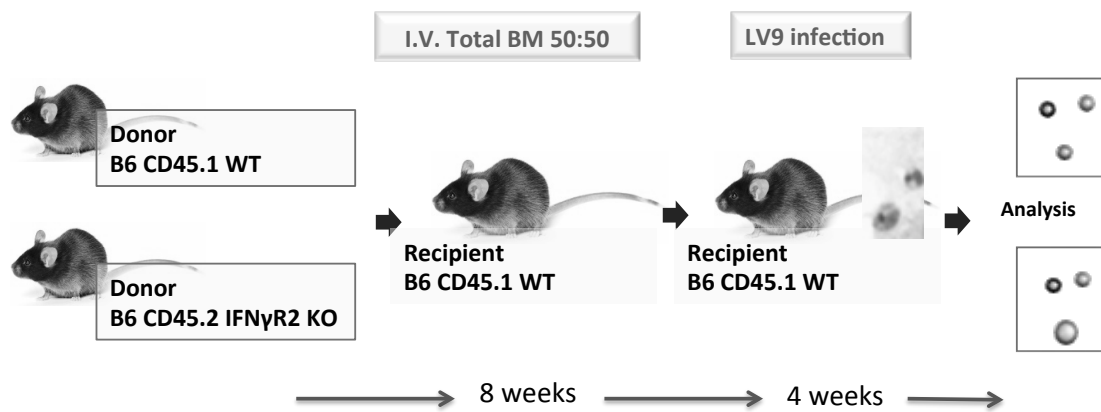


Figure 4.32 - Experimental design for competitive mixed bone marrow chimeras using wild-type (WT) and IFN γ R2 knockout (IFN γ R2 KO). Total unfractionated BM cells from WT (CD45.1) and IFN γ R2 KO (CD45.2) mice were transferred in equal number into lethally irradiated recipients (CD45.1). Following eight weeks recipient mice were infected for 28 days with *L. donovani*, and haematopoietic reconstitution activity was assessed both in BM and in the spleen.

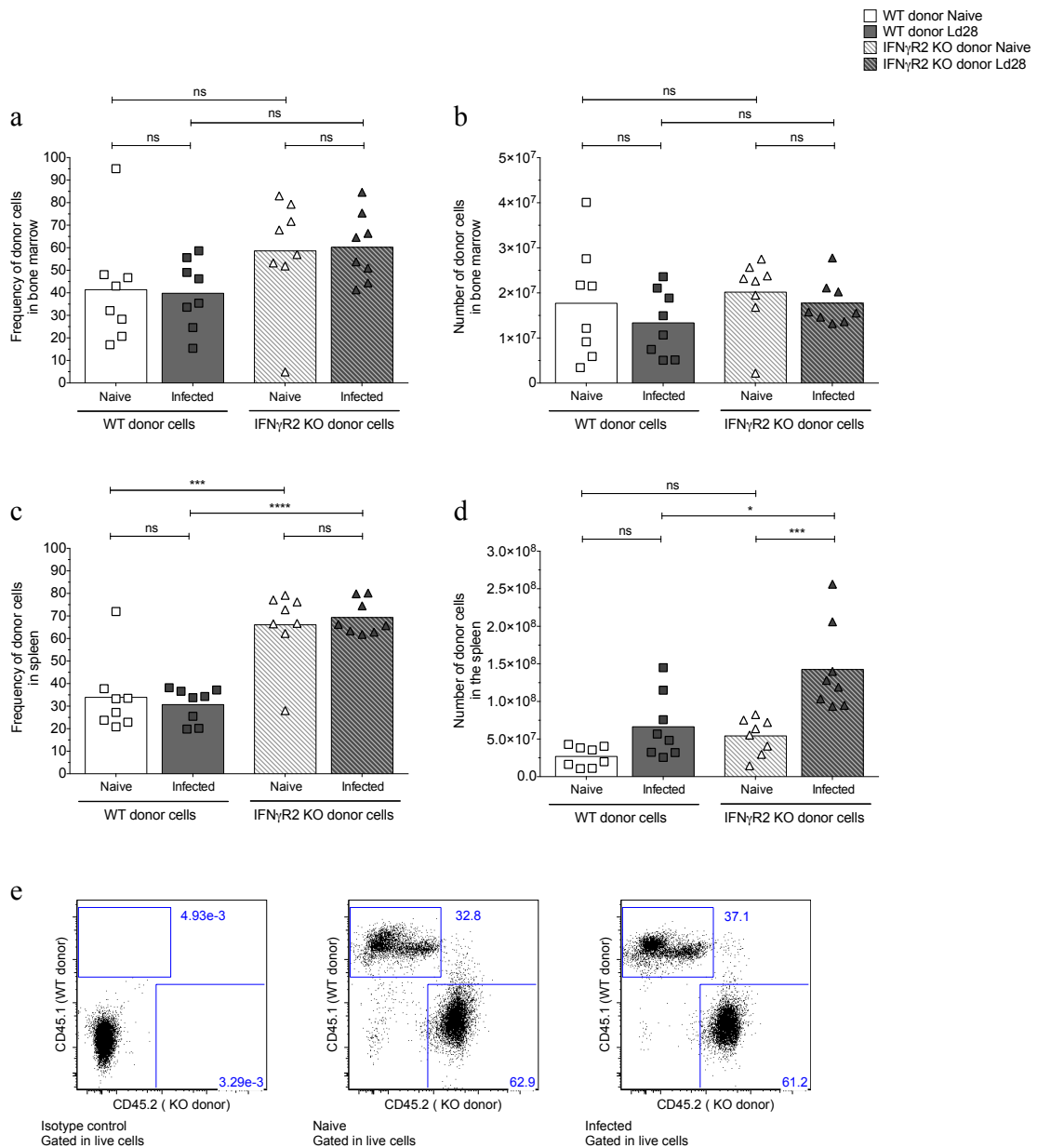


Figure 4.33 - The reconstitution potential of WT HSCs and IFN γ R2^{-/-} HSCs was similar in infected mixed BM chimeras. (a) Frequency of donor cells in BM. (b) Number of donor cells in BM. (c) Frequency of donor cells in spleen. (d) Number of donor cells in spleen. (e) Representative dot plots of frequency of donor cells in BM live cells; (left) isotype control, (centre) naive recipient and (right) infected recipient. Analyses were performed 12 weeks after transplant of total BM cells from CD45.2 IFN γ R2^{-/-} mice and CD45.1 WT mice (50:50) to lethally irradiated CD45.1 recipient mice. Comparisons were made within donor compartment between non-infected recipients (n=8) and recipient mice infected with *L. donovani* for 28 days (Ld28) (n=8). Two femur and two tibias were taken per animal. Data from two independent experiments was presented as scatter plot and mean bar. p values were determined using One-way Anova followed by Tukey's multiple comparisons test: not significant (ns), *p \leq 0.05, **p \leq 0.01, ***p \leq 0.001 and ****p \leq 0.0001.

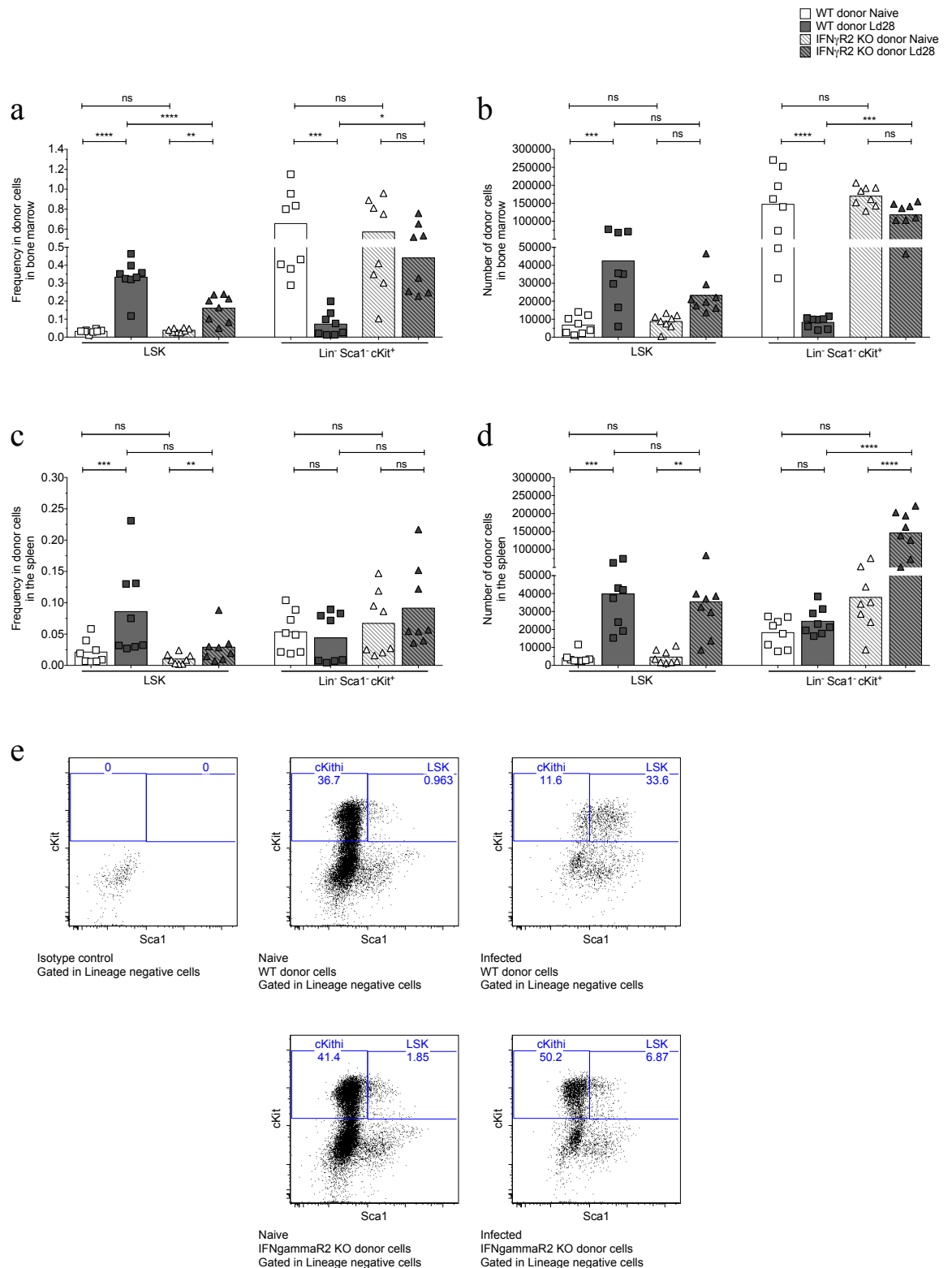


Figure 4.34 - The frequency of Lin⁻ cKit⁺ Sca1⁻ cells was decreased in the WT but not IFN γ R2^{-/-} donor cells, following infection with *L. donovani*. (a) Frequency of LSK cells and Lin⁻ cKit⁺ Sca1⁻ cells within donor cells in BM. (b) Number of LSK cells and Lin⁻ cKit⁺ Sca1⁻ cells within donor cells in BM. (c) Frequency of LSK cells and Lin⁻ cKit⁺ Sca1⁻ cells within donor cells in the spleen. (d) LSK cells and Lin⁻ cKit⁺ Sca1⁻ cells within donor cells in the spleen. (e) Representative dot plots of the frequency of LSK cells and Lin⁻ cKit⁺ Sca1⁻ cells within donor Lin⁻

cells in BM; (top left) isotype control gated in Lin⁻ cells, (top centre) naive recipient gated in WT donor Lin⁻ cells, (top right) infected recipient gated in WT donor Lin⁻ cells, (bottom left) naive recipient gated in IFN γ R2^{-/-} Lin⁻ donor cells, (bottom right) infected recipient gated in IFN γ R2^{-/-} Lin⁻ donor cells. Analysis performed 12 weeks after transplant of total BM cells from CD45.2 IFN γ R2^{-/-} mice and CD45.1 WT mice (50:50) to lethally irradiated CD45.1 recipient mice. Comparisons were made within donor compartment between non-infected recipients (n=8) and recipient mice infected with *L. donovani* for 28 days (Ld28) (n=8). Two femur and two tibias were taken per animal. Data from two independent experiments was presented as scatter plot and mean bar, p values were determined using One-way Anova followed by Tukey's multiple comparisons test: not significant (ns), *p \leq 0.05, **p \leq 0.01, ***p \leq 0.001 and ****p \leq 0.0001.

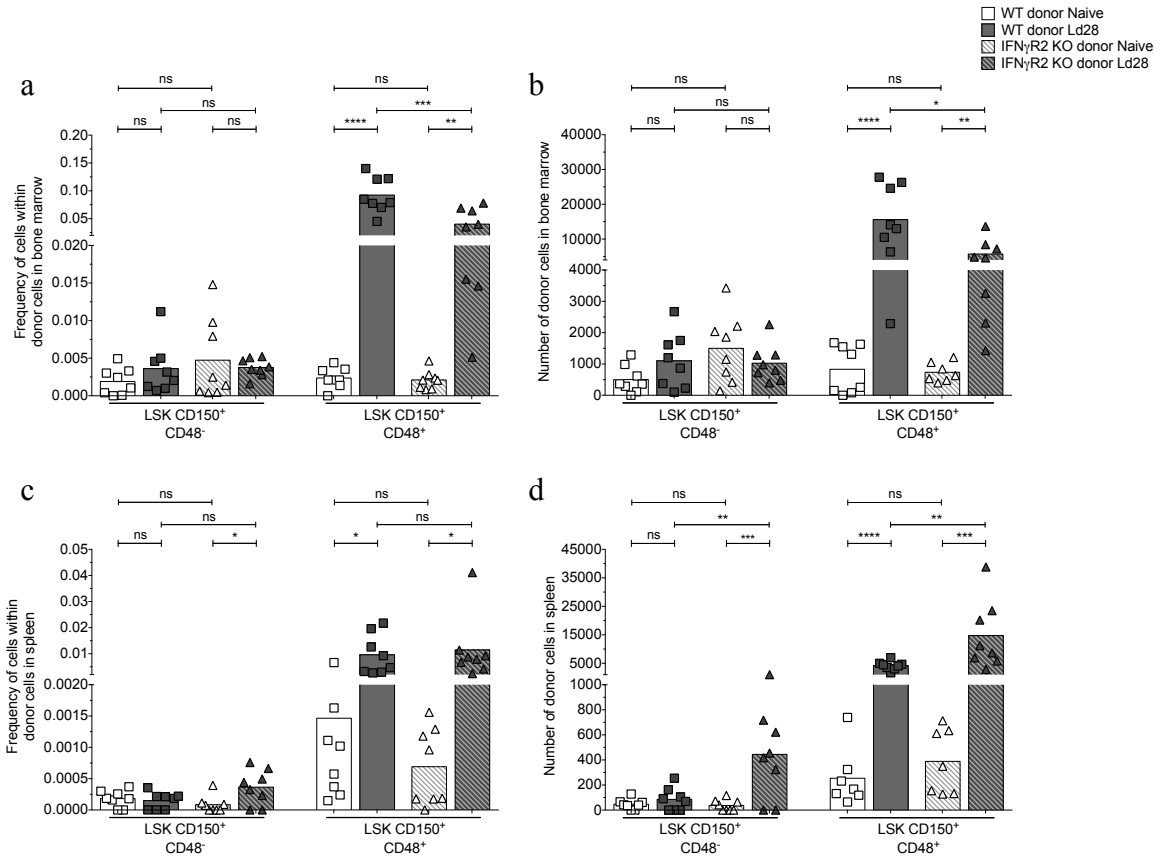


Figure 4.35 - *L. donovani* infection was associated with an increase in intermediary non-committed progenitors within WT and $IFN\gamma R2^{-/-}$ donor cells. (a) Frequency of LSK CD150⁺ CD48⁻ cells (enriched for LT-HSCs) and LSK CD150⁺ CD48⁺ cells within donor cells in BM. (b) Number of LSK CD150⁺ CD48⁻ cells and LSK CD150⁺ CD48⁺ cells in BM. (c) Frequency of LSK CD150⁺ CD48⁻ cells (enriched for LT-HSCs) and LSK CD150⁺ CD48⁺ cells within donor cells in spleen. (d) Number of LSK CD150⁺ CD48⁻ cells and LSK CD150⁺ CD48⁺ cells within donor cells in spleen. Analyses were performed 12 weeks after transplant of total BM cells from CD45.2 $IFN\gamma R2^{-/-}$ mice and CD45.1 WT mice (50:50) to lethally irradiated CD45.1 recipient mice. Comparisons were made within donor compartment between non-infected recipients (n=8) and recipient mice infected with *L. donovani* for 28 days (Ld28) (n=8). Two femur and two tibias were taken per animal. Data from two independent experiments was presented as scatter plot and mean bar, p values were determined using One-way Anova followed by Tukey's multiple comparisons test: not significant (ns), *p ≤ 0.05, **p ≤ 0.01, ***p ≤ 0.001 and ****p ≤ 0.0001.

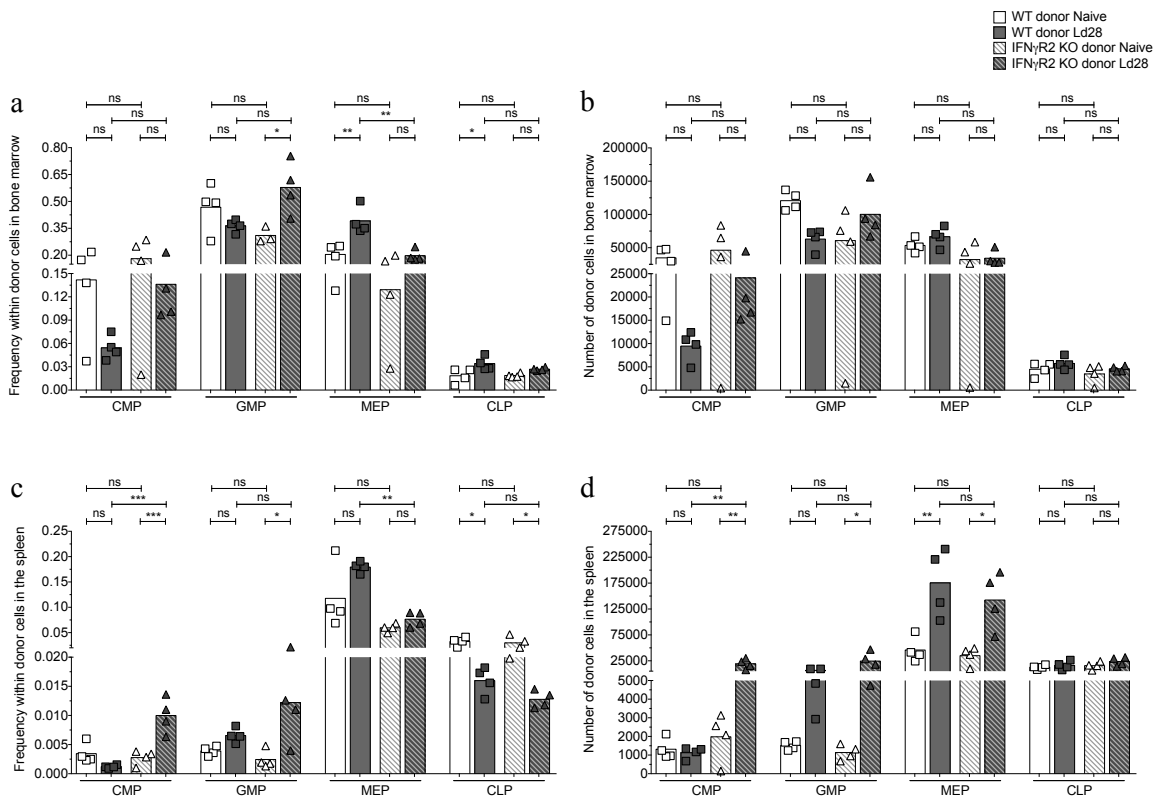


Figure 4.36 –The number of myeloid progenitors in BM was unchanged within WT and IFN γ R2^{-/-} donor cells, following *L. donovani* infection. (a) Frequency of lineage-committed progenitor cells (CMPs, GMPs, MEPs and CLPs) in BM. (b) Number of lineage-committed progenitor cells (CMPs, GMPs, MEPs and CLPs) in BM. (c) Frequency of lineage-committed progenitor cells (CMPs, GMPs, MEPs and CLPs) in the spleen. (d) Number of lineage-committed progenitor cells (CMPs, GMPs, MEPs and CLPs) in the spleen. Analyses were performed 12 weeks after transplant of total BM cells from CD45.2 IFN γ R2^{-/-} mice and CD45.1 WT mice (50:50) to lethally irradiated CD45.1 recipient mice. Comparisons were made within donor compartment between non-infected recipients (n=4) and recipient mice infected with *L. donovani* for 28 days (Ld28) (n=4). Two femur and two tibias were taken per animal. Data from two independent experiments was presented as scatter plot and mean bar, p values were determined using One-way Anova followed by Tukey's multiple comparisons test: not significant (ns), *p ≤ 0.05, **p ≤ 0.01, ***p ≤ 0.001 and ****p ≤ 0.0001.

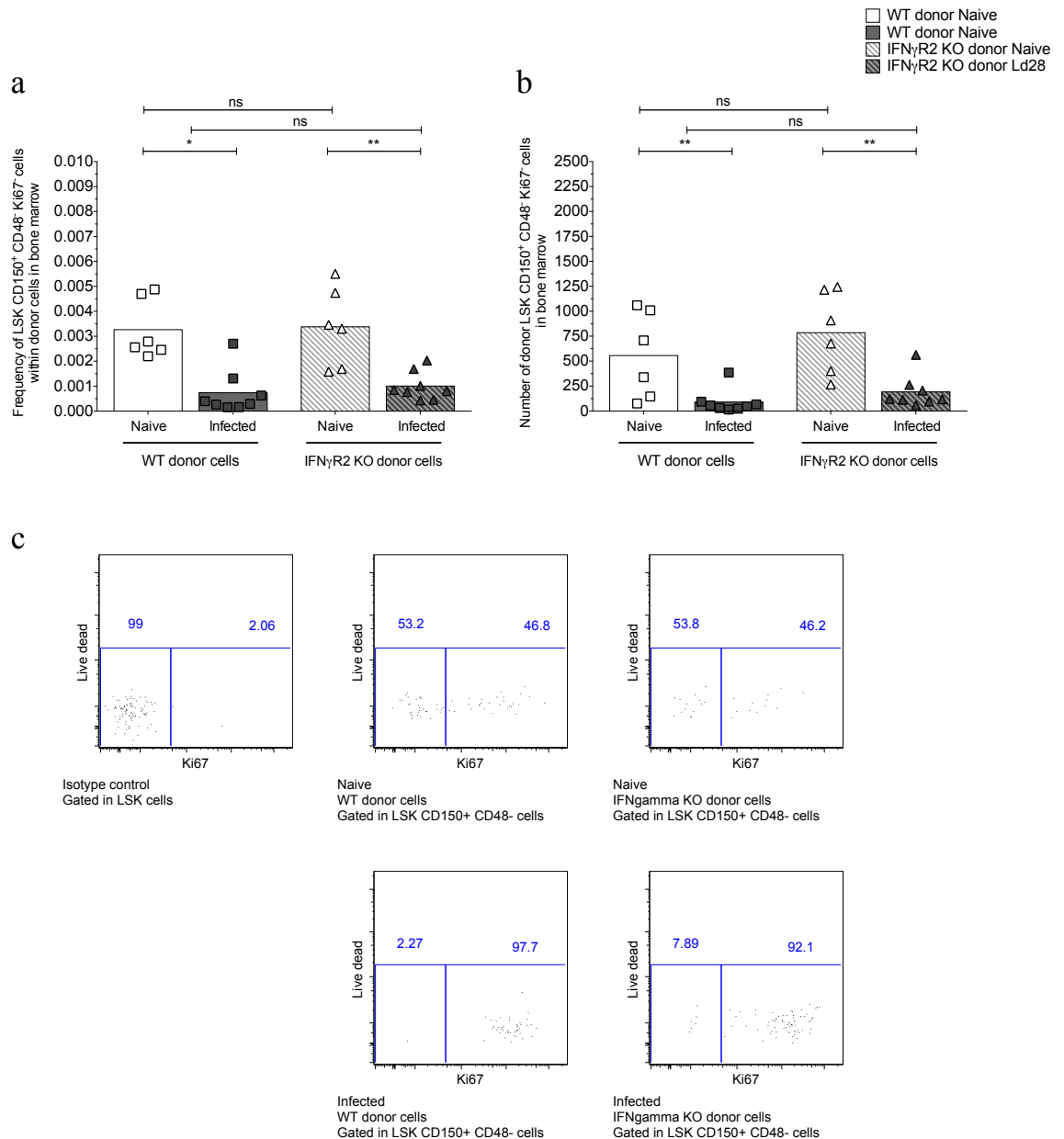


Figure 4.37 - The absence of direct IFN γ signaling in LT-HSCs did not prevent the depletion of the reservoir of quiescent HSCs, following *L. donovani* infection. (a) Frequency of LSK CD150⁺ CD48⁻ cells (enriched for LT-HSCs) in G0 (Ki67⁺) within donor cells in BM. (b) Number of LSK CD150⁺ CD48⁻ cells in G0 (Ki67⁺) in BM. (c) Representative dot plots of Ki67 expression; (top left) isotype control gated in LSK cells, (top centre) naive recipient gated in WT donor LSK CD150⁺ CD48⁻ cells, (top right) naive recipient gated in IFN γ R2^{-/-} donor LSK CD150⁺ CD48⁻ cells, (bottom left) infected recipient gated in WT donor LSK CD150⁺ CD48⁻ cells, (bottom right) infected recipient gated in IFN γ R2^{-/-} donor LSK CD150⁺ CD48⁻ cells. Analyses were performed 12 weeks after transplant of total BM cells from CD45.2 IFN γ R2^{-/-} mice and CD45.1 WT mice (50:50) to lethally irradiated CD45.1 recipient mice. Comparisons were made within donor compartment between non-infected recipients (n=6) and recipient mice infected with *L. donovani* for 28 days (Ld28) (n=6). Two femur and two tibias were taken per

animal. Data from two independent experiments was presented as scatter plot and mean bar, p values were determined using One-way Anova followed by Tukey's multiple comparisons test: not significant (ns), * $p \leq 0.05$, ** $p \leq 0.01$, *** $p \leq 0.001$ and **** $p \leq 0.0001$.

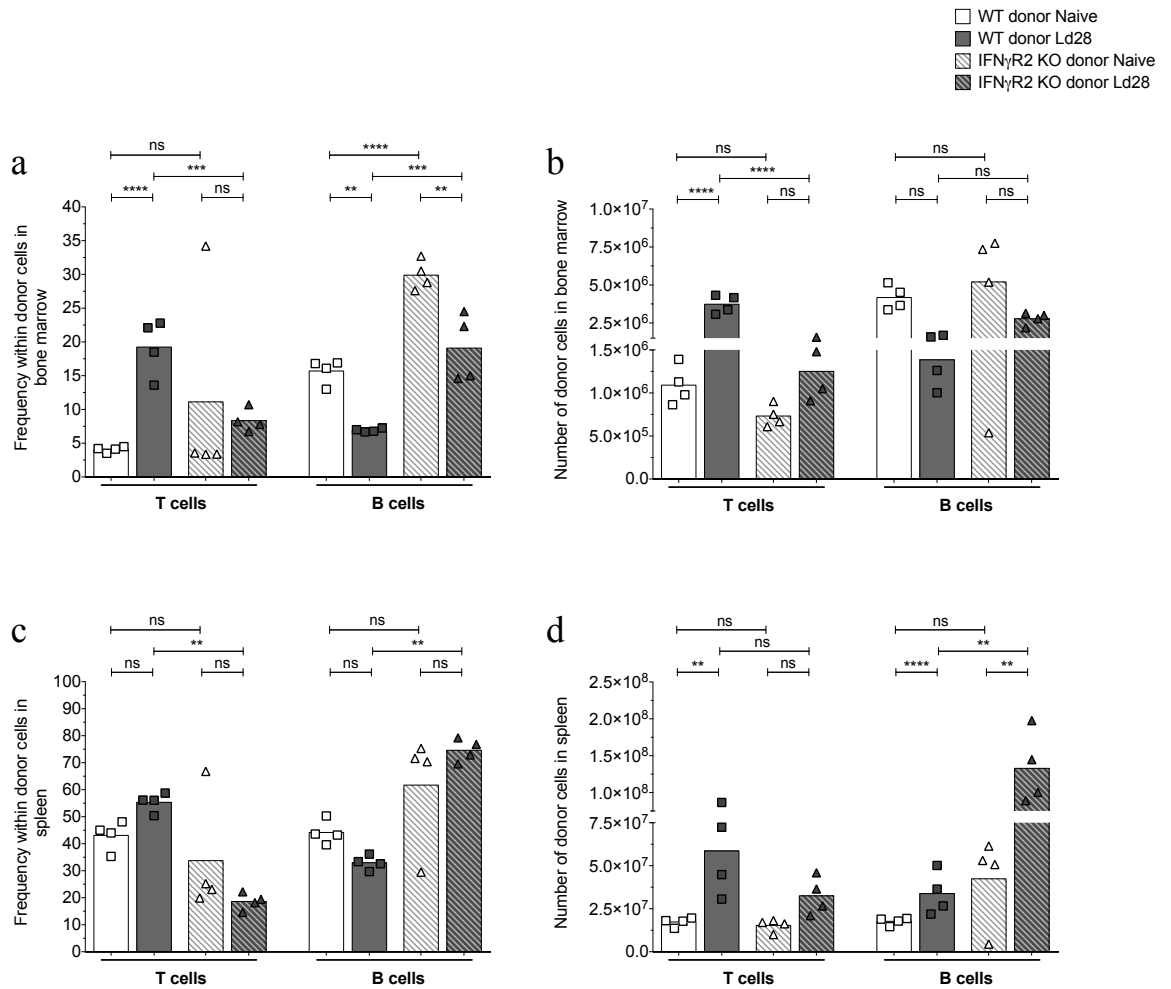


Figure 4.38 - In the absence of intrinsic IFN γ signaling the expansion of T cells was limited in BM of mice infected with *L. donovani*. (a) Frequency of T cells and B cells within donor cells in BM. (b) Number of donor T cells and B cells in BM. (c) Frequency of T cells and B cells within donor cells in the spleen. (d) Number of donor T cell and B cells in the spleen. Analyses were performed 12 weeks after transplant of total BM cells from CD45.2 IFN γ R2^{-/-} mice and CD45.1 WT mice (50:50) to lethally irradiated CD45.1 recipient mice. Comparisons were made between non-infected recipients (n=4) and recipient mice infected with *L. donovani* for 28 days (Ld28) (n=4). Two femur and two tibias were taken per animal. Data from one experiment was presented as scatter plot and mean bar, p values were determined using One-way Anova followed by Tukey's multiple comparisons test: not significant (ns), *p \leq 0.05, **p \leq 0.01, ***p \leq 0.001 and ****p \leq 0.0001.

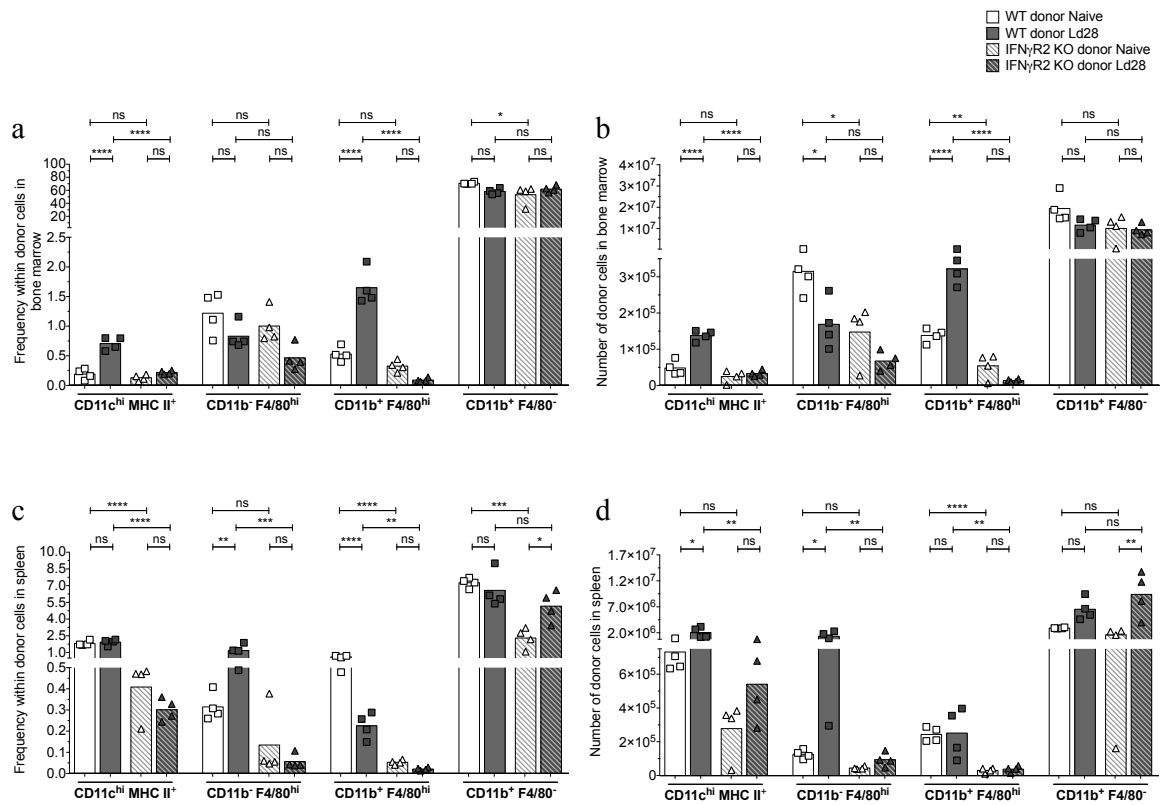


Figure 4.39 - The absence of direct IFN γ signaling limited the expansion of macrophages in BM and spleen in mice infected with *L. donovani*. (a) Frequency of CD11c^{hi} MHC-II^{hi} cells, CD11b⁻ F4/80^{hi} cells, CD11b⁺ F4/80^{hi} cells and CD11b⁺ F4/80⁻ cells within donor cells in BM. (b) Number of donor CD11c^{hi} MHC-II^{hi} cells, CD11b⁻ F4/80^{hi} cells, CD11b⁺ F4/80^{hi} cells and CD11b⁺ F4/80⁻ cells in BM. (c) Frequency of CD11c^{hi} MHC-II^{hi} cells, CD11b⁻ F4/80^{hi} cells, CD11b⁺ F4/80^{hi} cells and CD11b⁺ F4/80⁻ cells within donor cells in the spleen. (d) Number of donor CD11c^{hi} MHC-II^{hi} cells, CD11b⁻ F4/80⁺ cells, CD11b⁺ F4/80⁺ cells and CD11b⁺ F4/80⁻ cells in the spleen. Analyses were performed 12 weeks after transplant of total BM cells from CD45.2 IFN γ R2^{-/-} mice and CD45.1 WT mice (50:50) to lethally irradiated CD45.1 recipient mice. Comparisons were made within donor compartment between non-infected recipients (n=4) and recipient mice infected with *L. donovani* for 28 days (Ld28) (n=4). Two femur and two tibias were taken per animal. Data from one experiment was presented as scatter plot and mean bar, p values were determined using One-way Anova followed by Tukey's multiple comparisons test: not significant (ns), *p \leq 0.05, **p \leq 0.01, ***p \leq 0.001 and ****p \leq 0.0001.

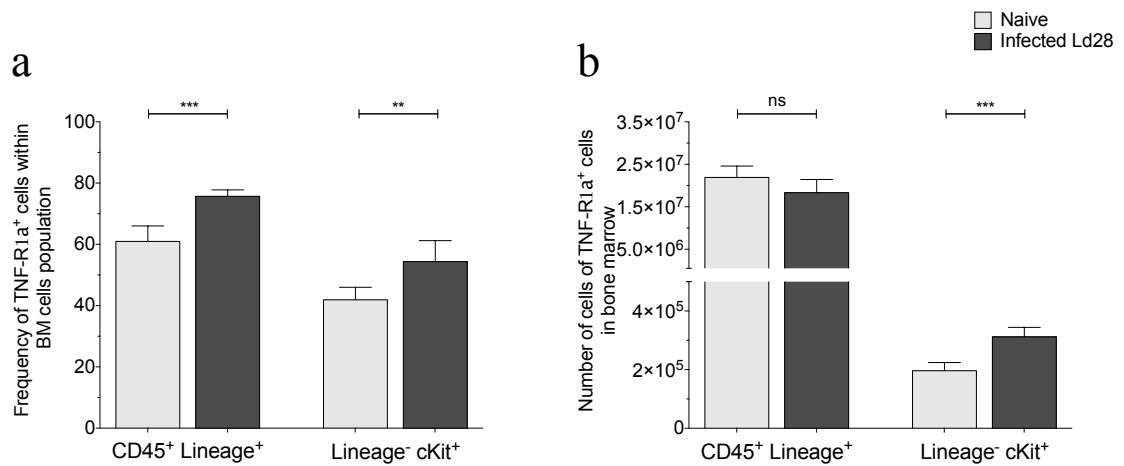


Figure 4.40 - The number of HSPCs (enriched in Lineage⁻ cKit⁺ cells) expressing TNF-R1a in BM increased *L. donovani* following infection. (a) Frequency of CD45⁺ Lineage⁺ cells (mature haematopoietic cells) TNF-R1a⁺ and Lineage⁻ cKit⁺ cells (enriched for all HSPCs) TNF-R1a⁺ in total BM cells. (b) Number of CD45⁺ Lineage⁺ TNF-R1a⁺ cells and Lineage⁻ cKit⁺ TNF-R1a⁺ cells. Comparisons were made between naive mice (n=5) and mice for 28 days with *L. donovani* (n=5). Two femur and two tibias were taken per animal. Data from one experiment was presented as Mean ± SD, p values were determined using unpaired t test: not significant (ns), *p ≤ 0.05, **p ≤ 0.01, ***p ≤ 0.001 and ****p ≤ 0.0001.

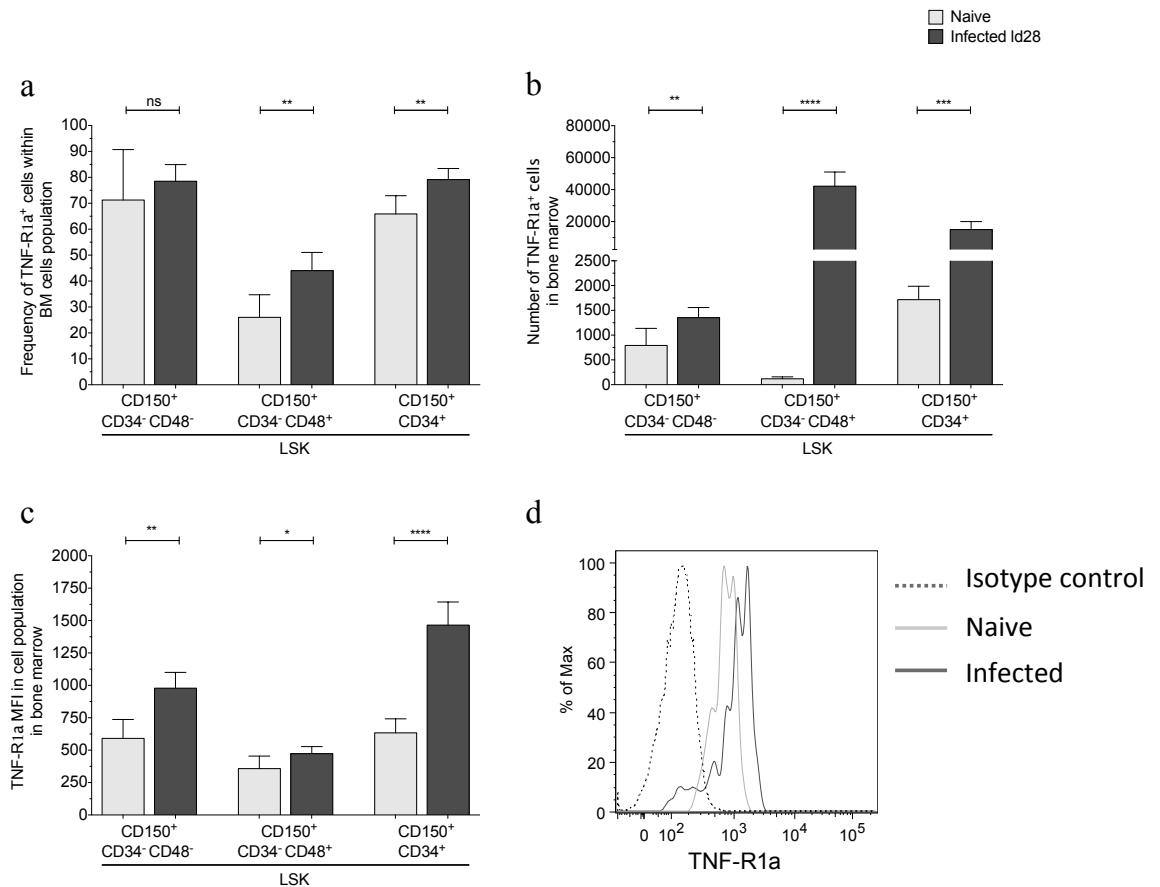


Figure 4.41 - The number of LT-HSCs and onward multipotent progenitors expressing TNF-R1a increased following *L. donovani* infection. (a) Frequency of LSK CD150⁺ CD34⁻ CD48⁻ cells (enriched for LT-HSCs), LSK CD150⁺ CD34⁻ CD48⁺ cells and LSK CD150⁺ CD34⁺ cells expressing TNF-R1a in total BM cells. (b) Number of LSK CD150⁺ CD34⁻ CD48⁻ cells, LSK CD150⁺ CD34⁻ CD48⁺ cells and LSK CD150⁺ CD34⁺ cells expressing TNF-R1a. (c) Mean intensity fluorescence (MFI) of TNF-R1a in LSK CD150⁺ CD34⁻ CD48⁻ cells (enriched for LT-HSCs), LSK CD150⁺ CD34⁻ CD48⁺ cells and LSK CD150⁺ CD34⁺ cells expressing TNF-R1. (d) Representative histogram of TNF-R1a expression on LSK CD150⁺ cells. Comparisons were made between naive mice (n=5) and mice for 28 days with *L. donovani* (n=5). Two femur and two tibias were taken per animal. Data from one experiment was presented as Mean ± SD, p values were determined using unpaired t test: not significant (ns), *p ≤ 0.05, **p ≤ 0.01, ***p ≤ 0.001 and ****p ≤ 0.0001.

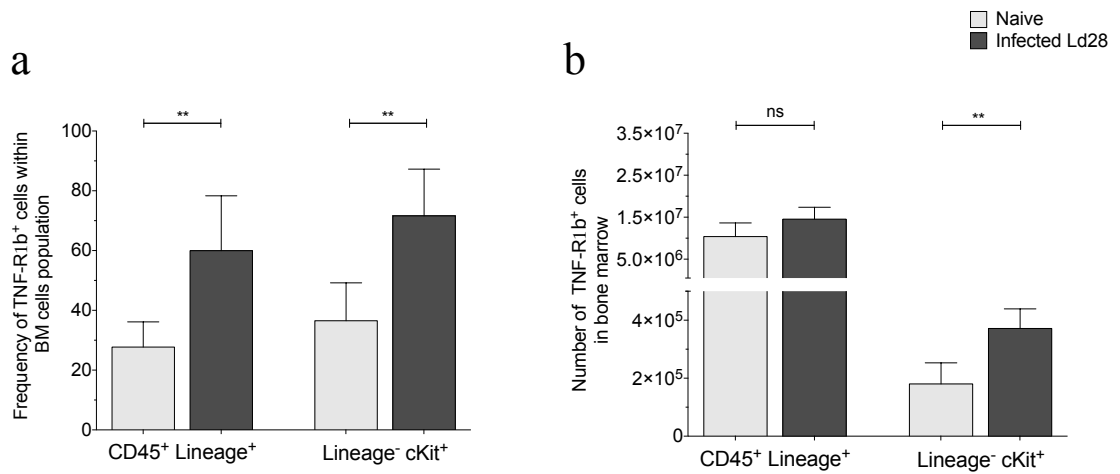


Figure 4.42 - The number of HSPCs (enriched in Lineage⁻ cKit⁺ cells) expressing TNF-R1b increased following *L. donovani* infection. (a) Frequency of CD45⁺ Lineage⁺ cells TNF-R1b⁺ (mature haematopoietic cells) and Lineage⁻ cKit⁺ cells (enriched for all HSPCs) TNF-R1b⁺ in total BM cells. (b) Number of CD45⁺ Lineage⁺ TNF-R1b⁺ cells and Lineage⁻ cKit⁺ TNF-R1b⁺ cells. Comparisons were made between naive mice (n=5) and mice for 28 days with *L. donovani* (n=5). Two femur and two tibias were taken per animal. Data from one experiment was presented as Mean ± SD, p values were determined using unpaired t test: not significant (ns), *p ≤ 0.05, **p ≤ 0.01, ***p ≤ 0.001 and ****p ≤ 0.0001.

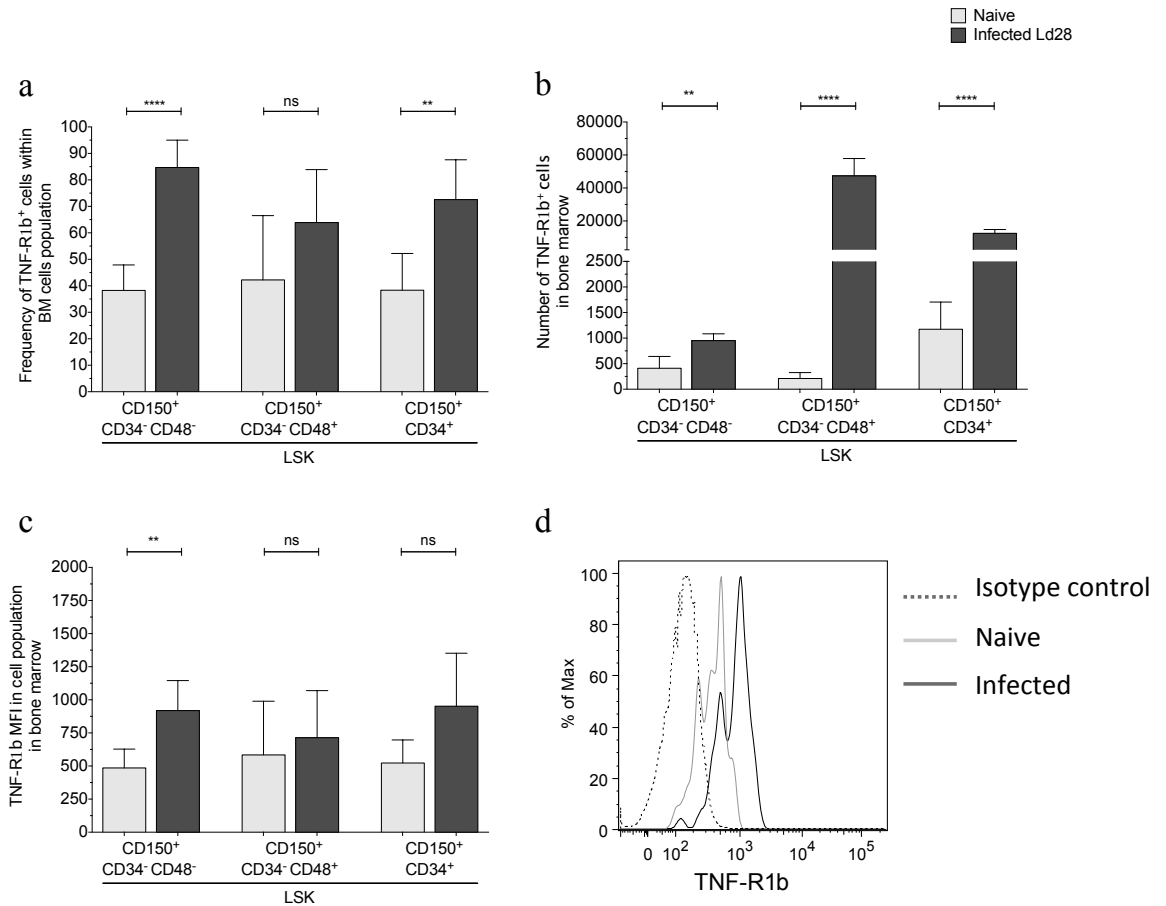


Figure 4.43 - The number of LT-HSCs and onward multipotent progenitors expressing TNF-R1b increased following *L. donovani* infection. (a) Frequency of LSK CD150⁺ CD34⁻ CD48⁻ cells (enriched for LT-HSCs), LSK CD150⁺ CD34⁻ CD48⁺ cells and LSK CD150⁺ CD34⁺ cells expressing TNF-R1b in total BM cells. (b) Number of LSK CD150⁺ CD34⁻ CD48⁻ cells (enriched for LT-HSCs), LSK CD150⁺ CD34⁻ CD48⁺ cells and LSK CD150⁺ CD34⁺ cells expressing TNF-R1b. (c) Mean intensity fluorescence (MFI) of TNF-R1b expression on LSK CD150⁺ CD34⁻ CD48⁻ cells (enriched for LT-HSCs), LSK CD150⁺ CD34⁻ CD48⁺ cells and LSK CD150⁺ CD34⁺ cells expressing TNF-R1b. (d) Representative histogram of TNF-R1b expression on LSK CD150⁺ cells. Comparisons were made between naive mice (n=5) and mice for 28 days with *L. donovani* (n=5). Two femur and two tibias were taken per animal. Data from one experiment was presented as Mean ± SD, p values were determined using unpaired t test: not significant (ns), *p ≤ 0.05, **p ≤ 0.01, ***p ≤ 0.001 and ****p ≤ 0.0001.

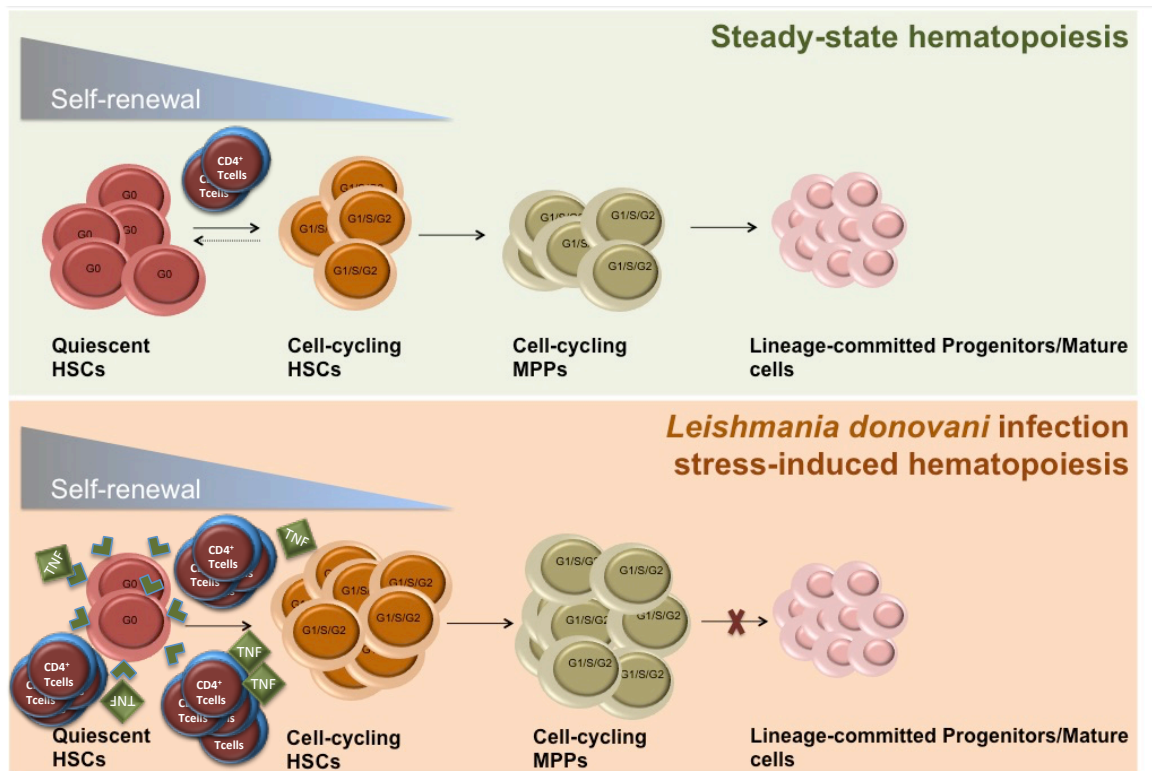


Figure 4.44 - Proposed mechanism to explain depletion of LT-HSCs in G0 and inefficient haematopoiesis during the chronic infection with *L. donovani* (3). Following *L. donovani* infection proliferating LT-HSCs and onward multipotent progenitors expand greatly at the expense of LT-HSCs in G0. The accumulation of intermediary multipotent progenitors was not associated with an increase in effective haematopoietic activity, since the numbers of effector haematopoietic cells were found either decreased or unchanged in PB. CD4⁺ T cells could solely mediate these alterations through an IFN γ -dependent mechanism following transfer to *L. donovani* infected immunodeficient mice, otherwise protected from impairment of haematological function. The impact of IFN γ was not directly mediated through IFN γ receptor signalling in LT-HSCs. In the BM of chronically infected mice, CD4⁺ T cells expressed increased levels of TNF, and LT-HSCs expressed increased levels of TNF receptors, being therefore conceivable that TNF could act directly modulating LT-HSCs proliferative status in mice chronically infected with *L. donovani*.

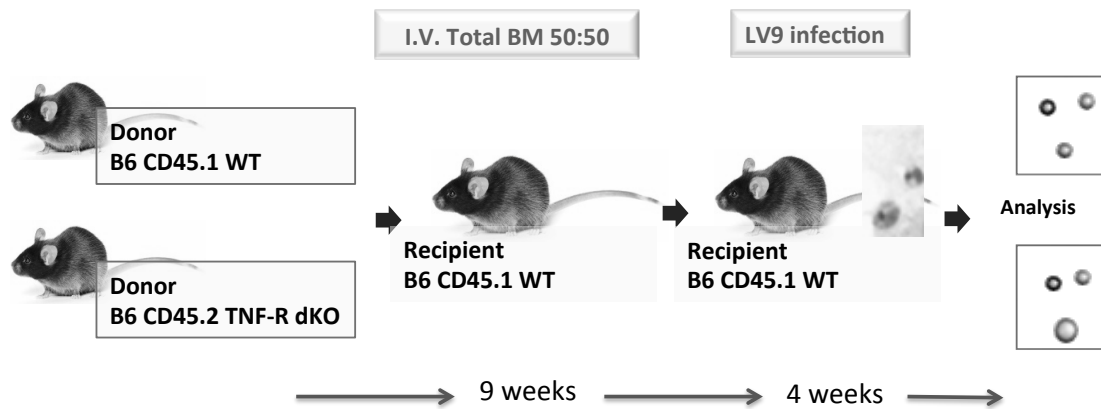


Figure 4.45 - Experimental design for competitive mixed BM chimeras using wild-type (WT) and TNF-R double knockout (TNF-RdKO HSCs) BM cells. Total unfractionated BM cells from WT (CD45.1) and TNF-RdKO (CD45.2) mice were transferred in equal number into lethally irradiated recipients (CD45.1). Following nine weeks recipient mice were infected for 28 days with *L. donovani*, and haematopoietic reconstitution activity was assessed both in BM and in the spleen.

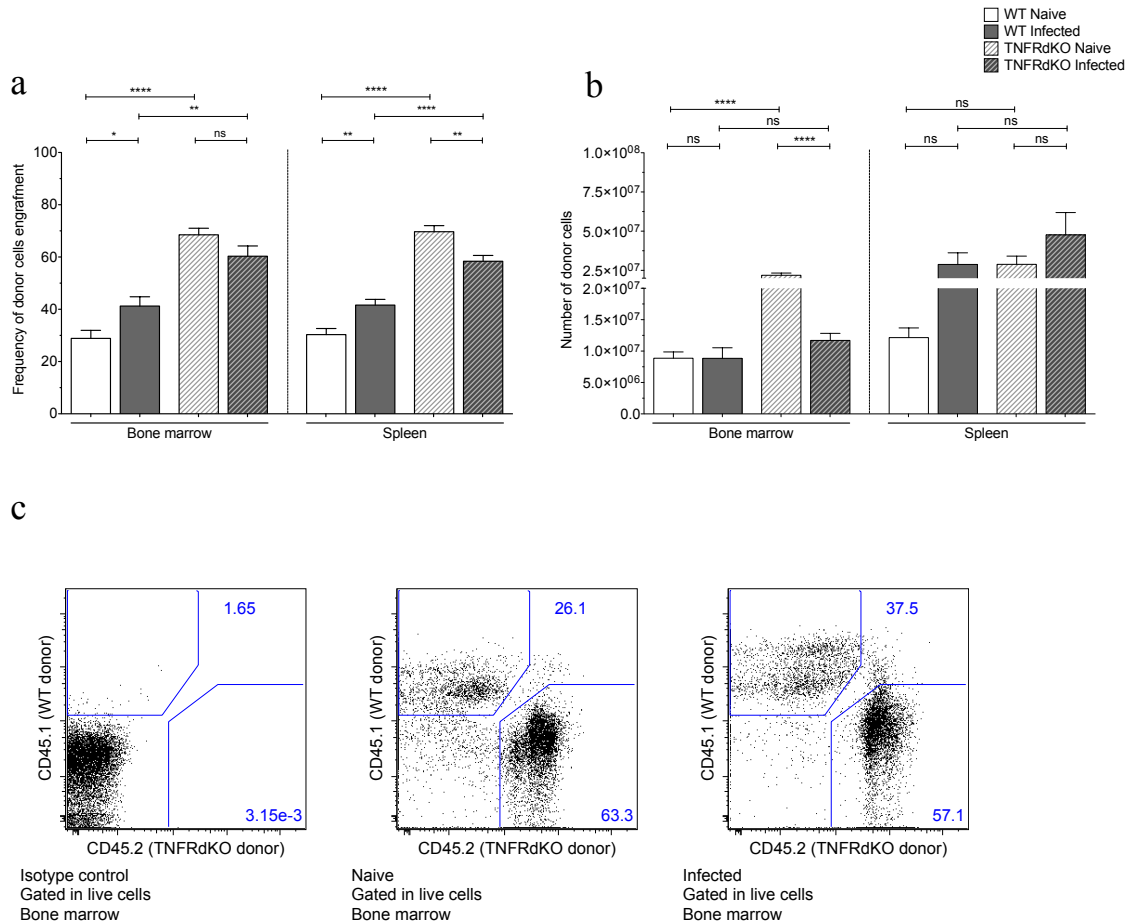


Figure 4.46 - The reconstitution potential of WT HSCs and TNF-RdKO donor cells changed following infection with *L. donovani*. (a) Frequency of donor cells in BM and in the spleen. (b) Number of donor cells in BM and in the spleen. (c) Representative dot plots of frequency of donor cells in gated BM live cells; (left) isotype control, (centre) naive recipient and (right) infected recipient. Analysis performed 13 weeks after transplant of total BM cells from CD45.2 TNFRdKO mice and CD45.1 WT mice (50:50) to lethally irradiated CD45.1 recipient mice. Comparisons were made within donor compartment between naive recipients (n=9) and recipient mice infected with *L. donovani* for 28 days (Ld28) (n=8). Two femur and two tibias were taken per animal. Data from two independent experiments was presented as Mean ± SD, p values were determined using One-way Anova followed by Tukey's multiple comparisons test: not significant (ns), *p ≤ 0.05, **p ≤ 0.01, ***p ≤ 0.001 and ****p ≤ 0.0001.

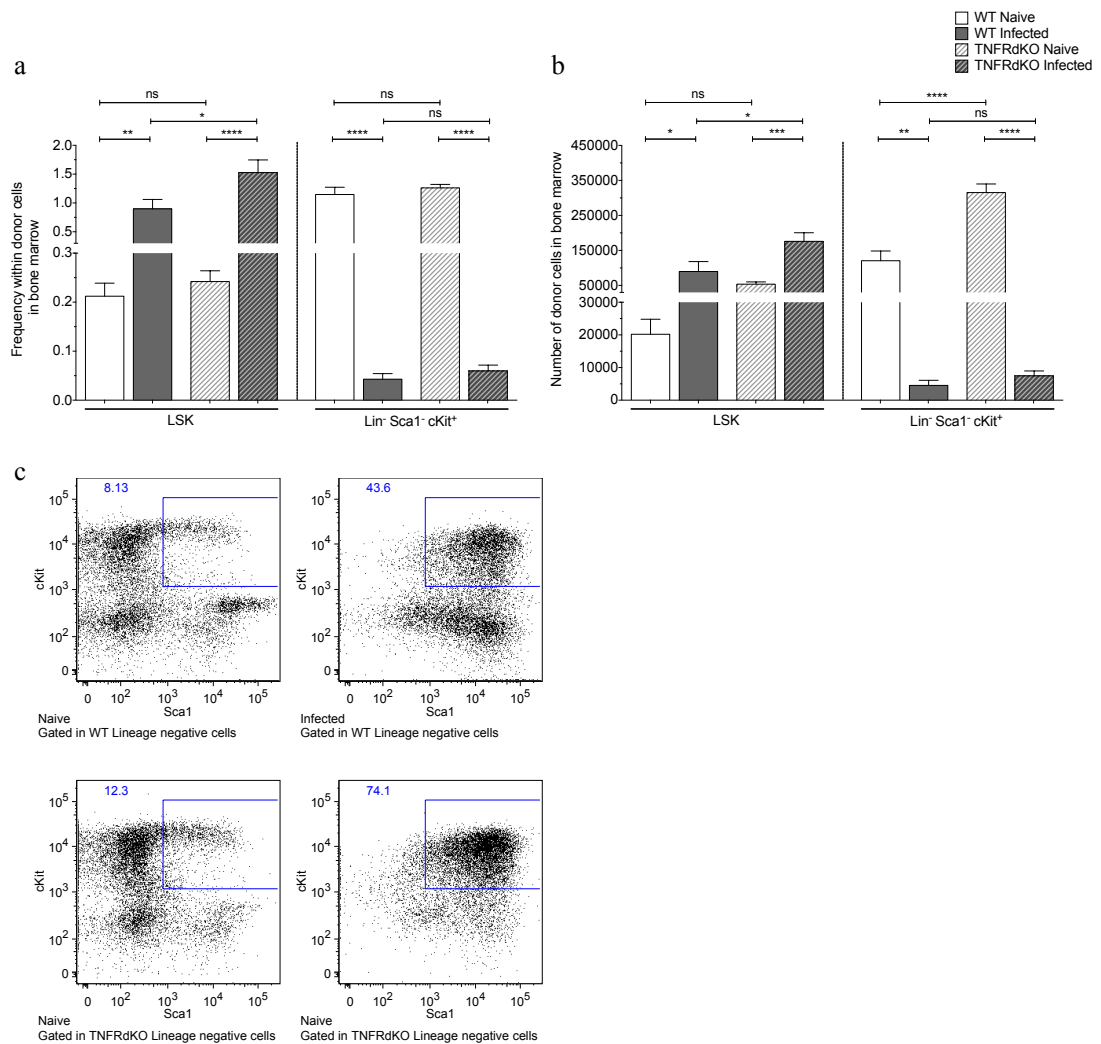


Figure 4.47 - Following infection with *L. donovani* the frequency of Lin⁻ cKit⁺ Sca1⁻ cells within WT and TNF-RdKO donor cells decreased in BM. (a) Frequency of LSK cells and Lin⁻ cKit⁺ Sca1⁻ cells within donor cells in BM. (b) Number of LSK cells and Lin⁻ cKit⁺ Sca1⁻ cells within donor cells in BM. (c) Representative dot plots of frequency of LSK cells and Lin⁻ cKit⁺ Sca1⁻ cells within donor Lin⁻ cells in BM; (top left) naive recipient gated in WT donor Lin⁻ cells, (top right) infected recipient gated in WT donor Lin⁻ cells, (bottom left) naive recipient gated in TNF-RdKO donor Lin⁻ donor cells, (bottom right) infected recipient gated in TNF-RdKO donor Lin⁻ donor cells. Analysis performed 13 weeks after transplant of total BM cells from CD45.2 TNF-RdKO donor mice and CD45.1 WT mice (50:50) to lethally irradiated CD45.1 recipient mice. Comparisons were made within donor compartment between non-infected recipients (n=9) and recipient mice infected with *L. donovani* for 28 days (Ld28) (n=8). Two femur and two tibias were taken per animal. Data from two independent experiments was presented as Mean \pm SD, p values were determined using One-way Anova followed by Tukey's multiple comparisons test: not significant (ns), *p \leq 0.05, **p \leq 0.01, ***p \leq 0.001 and ****p \leq 0.0001.

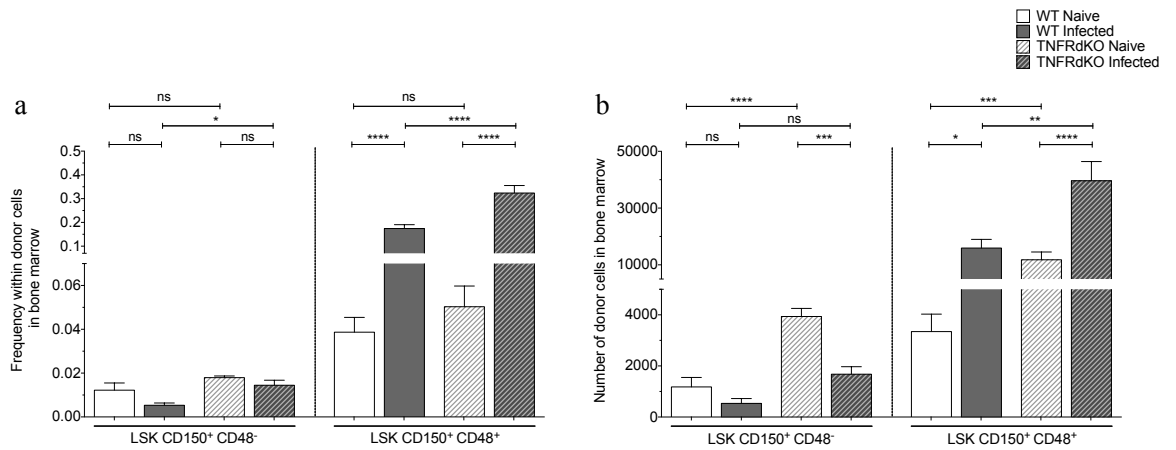


Figure 4.48 - *L. donovani* infection was associated with an increase in intermediary non-committed progenitors within WT and TNF-RdKO donor cells in BM. (a) Frequency of LSK CD150⁺ CD48⁻ cells (enriched for HSCs) and LSK CD150⁺ CD48⁺ cells within donor cells in BM. (b) Number of LSK CD150⁺ CD48⁻ cells (enriched for HSCs) and LSK CD150⁺ CD48⁺ cells. Analyses were performed 13 weeks after transplant of total BM cells from CD45.2 TNF-RdKO mice and CD45.1 WT mice (50:50) to lethally irradiated CD45.1 recipient mice. Comparisons were made within donor compartment between non-infected recipients (n=9) and recipient mice infected with *L. donovani* for 28 days (Ld28) (n=8). Two femur and two tibias were taken per animal. Data from two independent experiments was presented as Mean ± SD, p values were determined using One-way Anova followed by Tukey's multiple comparisons test: not significant (ns), *p ≤ 0.05, **p ≤ 0.01, ***p ≤ 0.001 and ****p ≤ 0.0001.

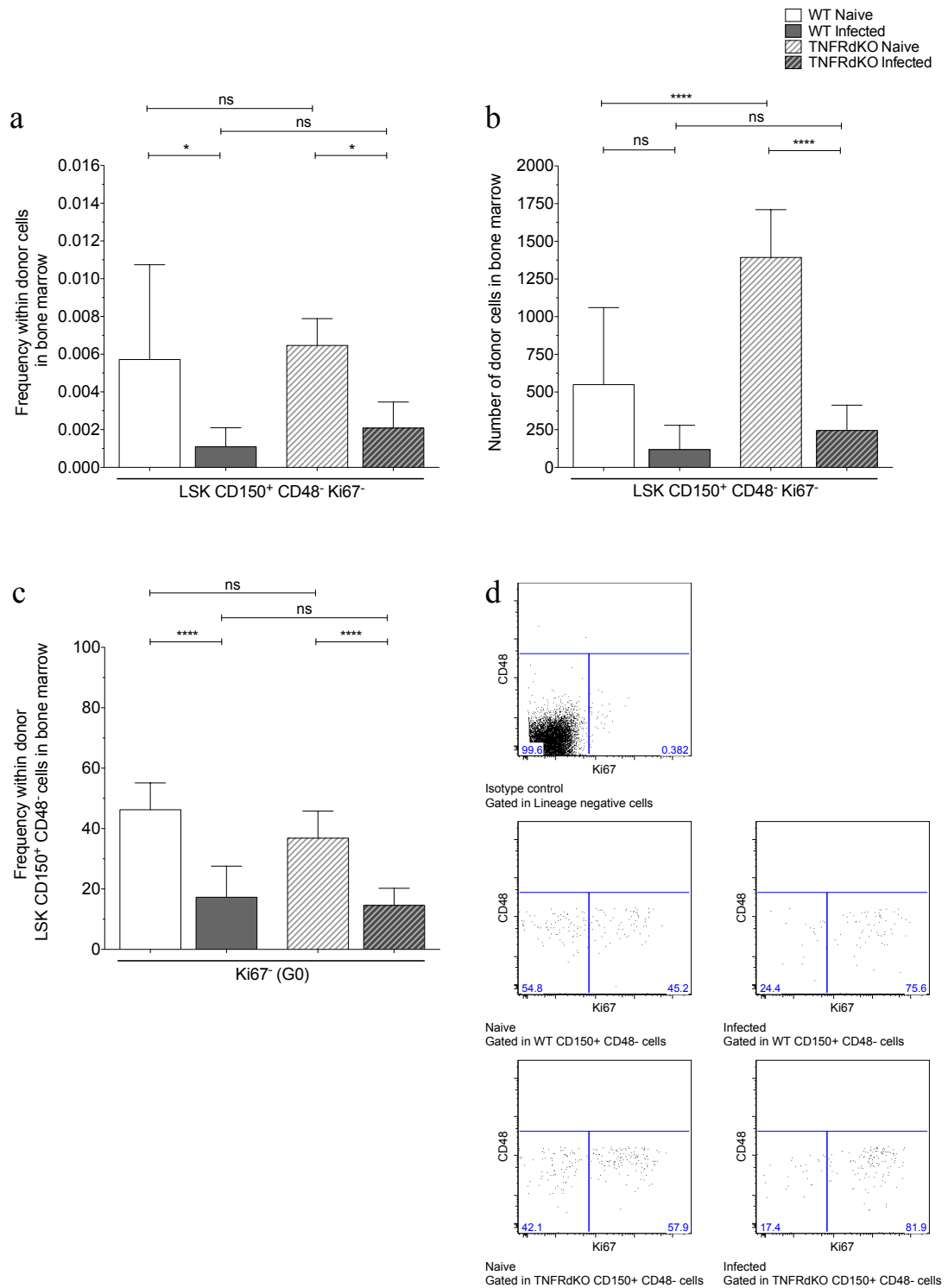


Figure 4.49 - The absence of intrinsic TNF-RdKO signaling did not prevent the depletion of the reservoir of quiescent HSCs, following *L. donovani* infection. (a) Frequency of LSK CD150⁺ CD48⁻ cells (enriched for HSCs) in G0 (Ki67⁻) within donor cells in BM. (b) Number of LSK CD150⁺ CD48⁻ cells (enriched for HSCs) in G0 (Ki67⁻). (c) Frequency of LSK CD150⁺ CD48⁻ cells in G0. (d) Representative dot plots of Ki67 expression; (top left) Isotype control gated in Lineage^{negative}, (middle left) naive recipient gated in WT donor LSK CD150⁺ CD48⁻ cells, (middle right) naive recipient gated in TNF-RdKO donor LSK CD150⁺ CD48⁻ cells, (bottom left) naive recipient gated in WT donor LSK CD150⁺ CD48⁻ cells, (bottom right) naive recipient gated in TNFRdKO donor LSK CD150⁺ CD48⁻ cells.

infected recipient gated in WT donor LSK CD150⁺ CD48⁻ cells, (bottom right) infected recipient gated in TNF-RdKO donor LSK CD150⁺ CD48⁻ cells. Analyses were performed 13 weeks after transplant of total BM cells from CD45.2 TNF-RdKO mice and CD45.1 WT mice (50:50) to lethally irradiated CD45.1 recipient mice. Comparisons were made within donor compartment between non-infected recipients (n=9) and recipient mice infected with *L. donovani* for 28 days (Ld28) (n=8). Two femur and two tibias were taken per animal. Data from two independent experiments was presented as Mean \pm SD, p values were determined using One-way Anova followed by Tukey's multiple comparisons test: not significant (ns), *p \leq 0.05, **p \leq 0.01, ***p \leq 0.001 and ****p \leq 0.0001.

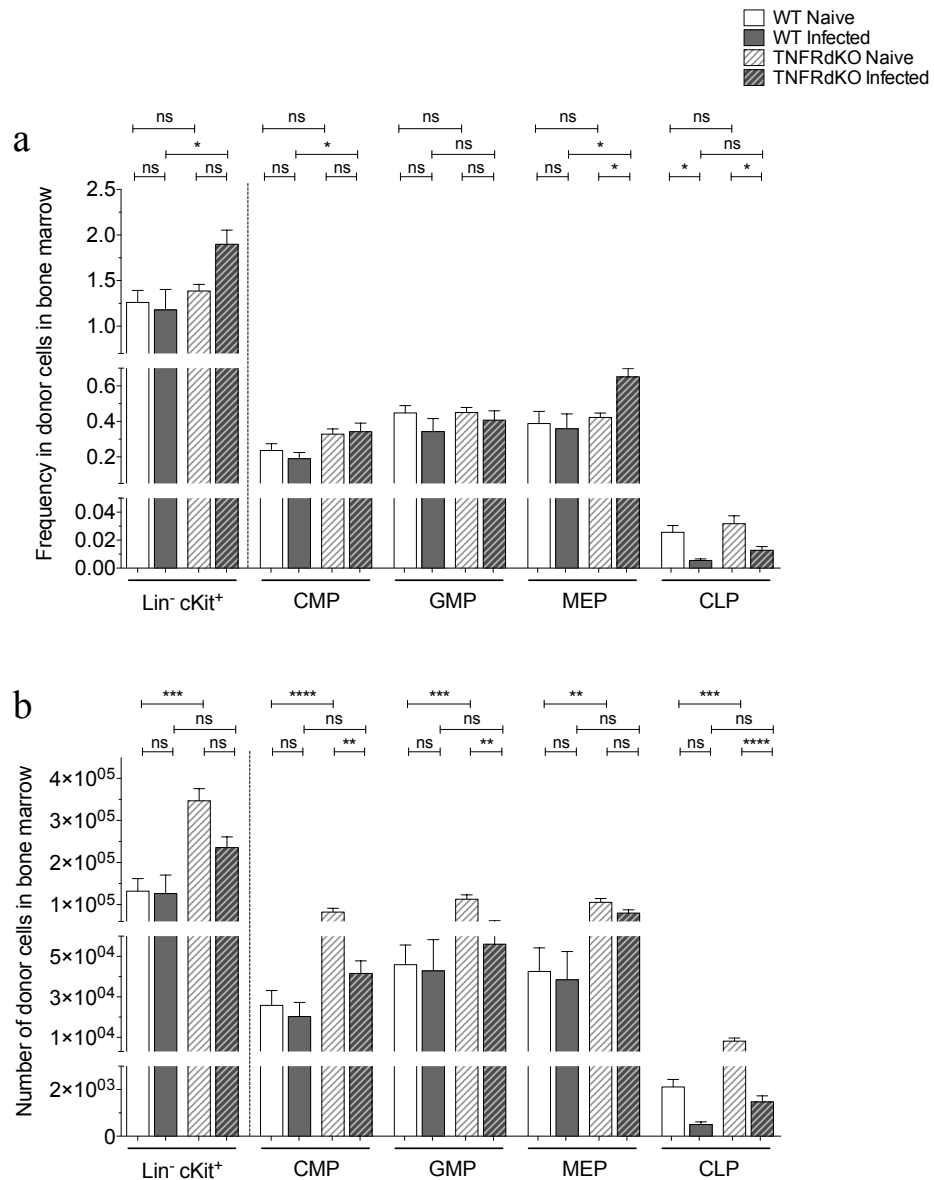


Figure 4.50 - Following infection with *L. donovani*, alterations in the frequency of myeloid progenitors were similar within WT and TNF-dKO donor cells. (a) Frequency of lineage-committed progenitor cells (CMPs, GMPs, MEPs and CLPs) in BM. (b) Number of lineage-committed progenitor cells (CMPs, GMPs, MEPs and CLPs) in BM. Analyses were performed 13 weeks after transplant of total BM cells from CD45.2 TNF-RdKO mice and CD45.1 WT mice (50:50) to lethally irradiated CD45.1 recipient mice. Comparisons were made within donor compartment between non-infected recipients (n=9) and recipient mice infected with *L. donovani* for 28 days (Ld28) (n=8). Two femur and two tibias were taken per animal. Data from two independent experiments was presented as Mean \pm SD, p values were determined using One-way Anova followed by Tukey's multiple comparisons test: not significant (ns), *p \leq 0.05, **p \leq 0.01, ***p \leq 0.001 and ****p \leq 0.0001.

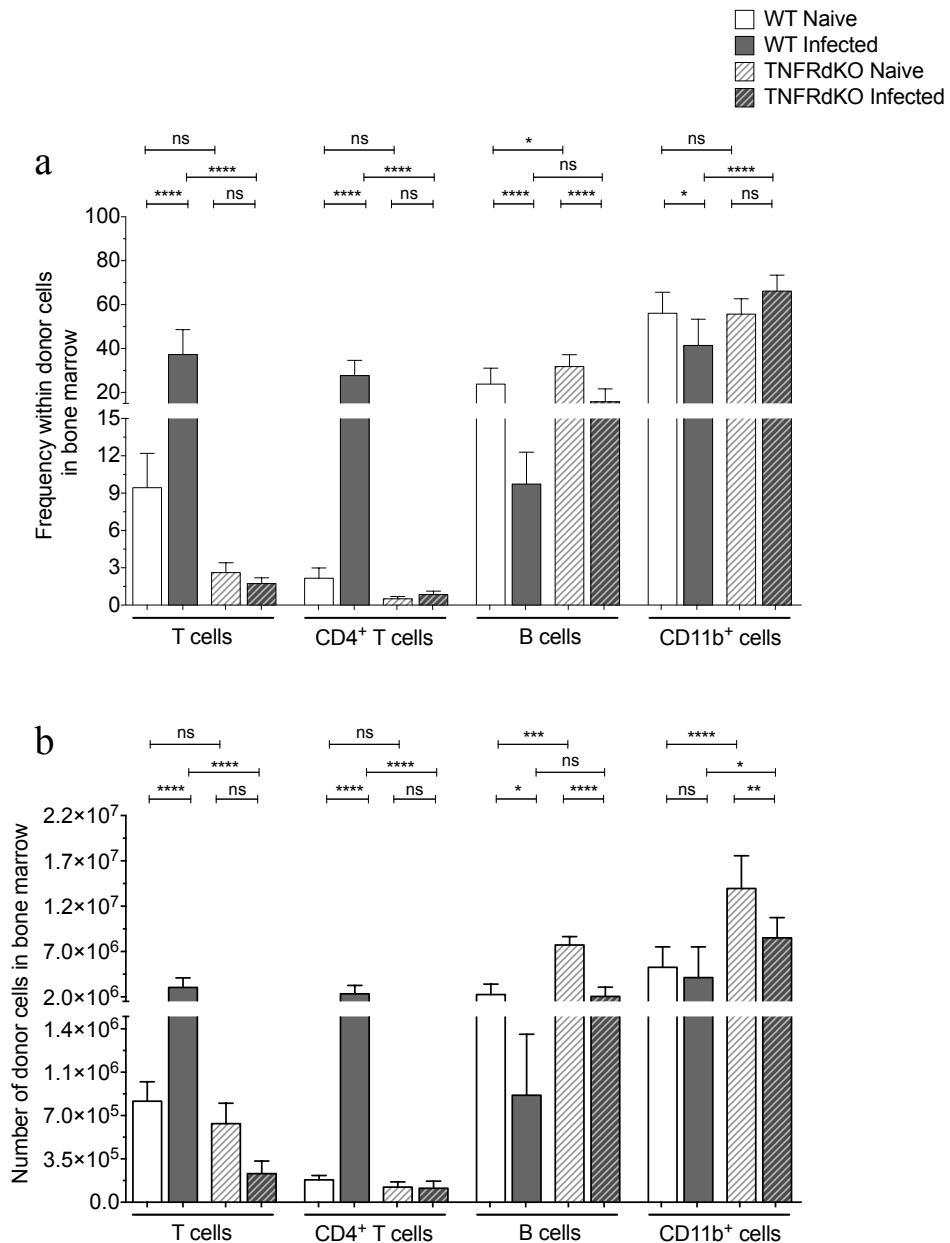


Figure 4.51 - The absence of intrinsic TNF receptor signaling prevented the expansion of T cells in the BM of mice infected with *L. donovani*. (a) Frequency of T cell, B cells and CD11b⁺ cells within donor cells in BM. (b) Number of donor of T cell, B cells and CD11b⁺ cells in BM. Analyses were performed 13 weeks after transplant of total BM cells from CD45.2 TNF-RdKO mice and CD45.1 WT mice (50:50) to lethally irradiated CD45.1 recipient mice. Comparisons were made within donor compartment between non-infected recipients (n=9) and recipient mice infected with *L. donovani* for 28 days (Ld28) (n=8). Two femur and two tibias were taken per animal. Data from two independent experiments was presented as Mean ± SD, p values were determined using One-way Anova followed by Tukey's multiple comparisons test: not significant (ns), *p ≤ 0.05, **p ≤ 0.01, ***p ≤ 0.001 and ****p ≤ 0.0001.

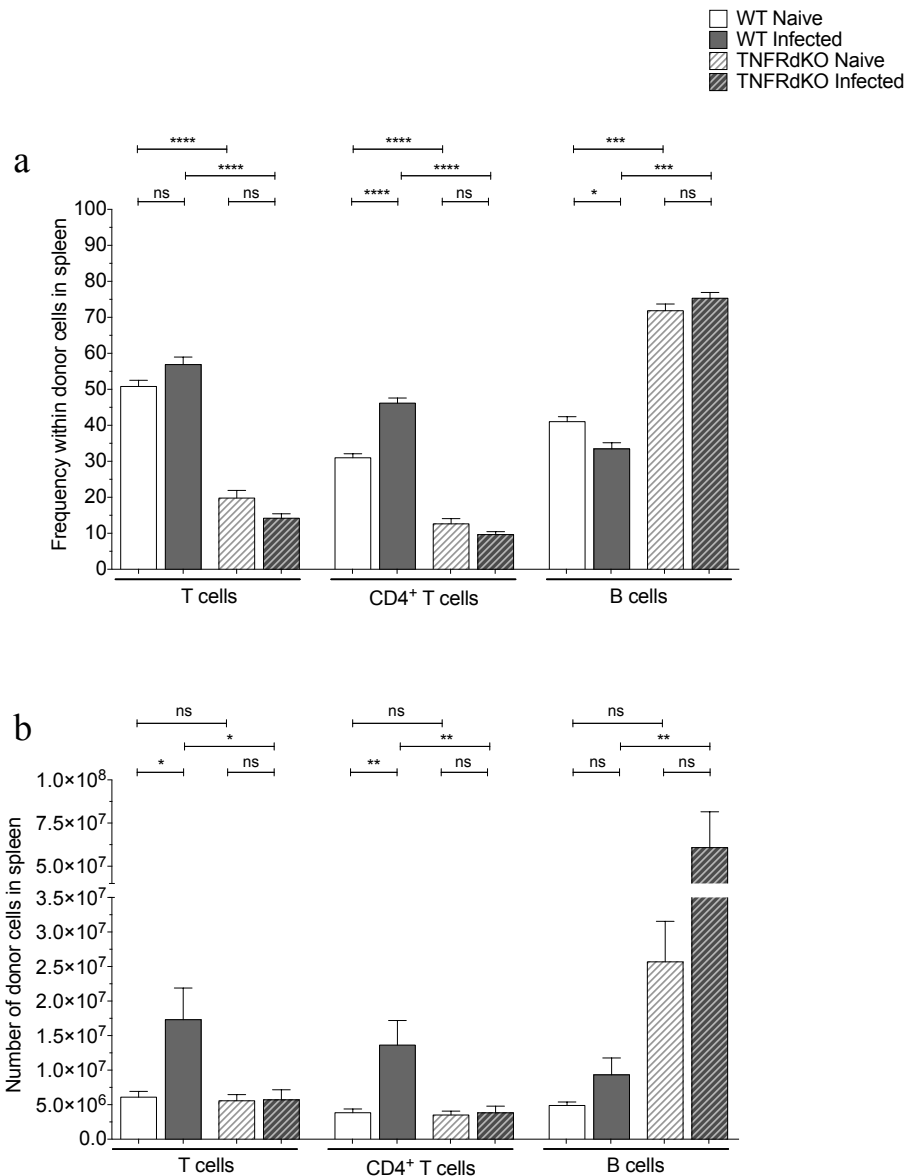


Figure 4.52 - The absence of intrinsic TNF receptor signaling prevented the expansion of T cells in the spleen, following infection with *L. donovani*. (a) Frequency of T cell, CD4⁺ T cells and B cells within donor cells in the spleen. (b) Number of donor of T cell, CD4⁺ T cells and B cells in the spleen. Analyses were performed 13 weeks after transplant of total BM cells from CD45.2 TNF-RdKO mice and CD45.1 WT mice (50:50) to lethally irradiated CD45.1 recipient mice. Comparisons were made within donor compartment between non-infected recipients (n=9) and recipient mice infected with *L. donovani* for 28 days (Ld28) (n=8). Data from two independent experiments was presented as Mean ± SD, p values were determined using One-way Anova followed by Tukey's multiple comparisons test: not significant (ns), *p ≤ 0.05, **p ≤ 0.01, ***p ≤ 0.001 and ****p ≤ 0.0001.

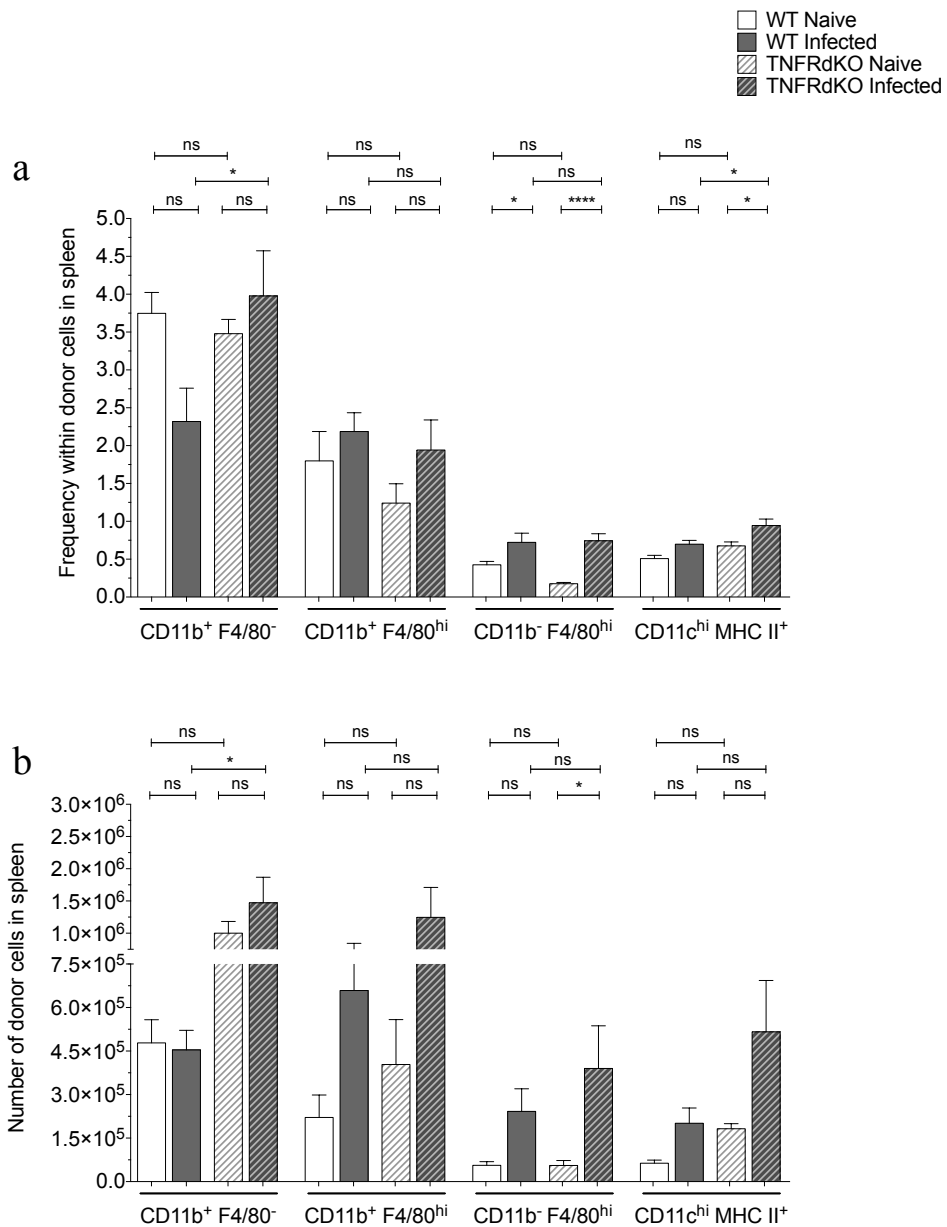


Figure 4.53 - The absence of TNF receptor signaling did not prevent the expansion of the myeloid cells in the spleen, following infection with *L. donovani*. (a) Frequency of CD11b⁺ F4/80⁻ cells, CD11b⁺ F4/80^{hi} cells, CD11b⁻ F4/80^{hi} cells and CD11c^{hi} MHC-II^{hi} cells within donor cells in the spleen. (b) Number of donor CD11b⁺ F4/80⁻ cells, CD11b⁺ F4/80^{hi} cells, CD11b⁻ F4/80^{hi} cells and CD11c^{hi} MHC-II^{hi} cells in the spleen. Analyses were performed 13 weeks after transplant of total BM cells from CD45.2 TNF-RdKO mice and CD45.1 WT mice (50:50) to lethally irradiated CD45.1 recipient mice. Comparisons were made within donor compartment between non-infected recipients (n=9) and recipient mice infected with *L. donovani* for 28 days (Ld28) (n=8). Data from two independent experiments was presented as Mean ± SD, p values were determined using One-way Anova followed by Tukey's multiple comparisons test: not significant (ns), *p ≤ 0.05, **p ≤ 0.01, ***p ≤ 0.001 and ****p ≤ 0.0001.

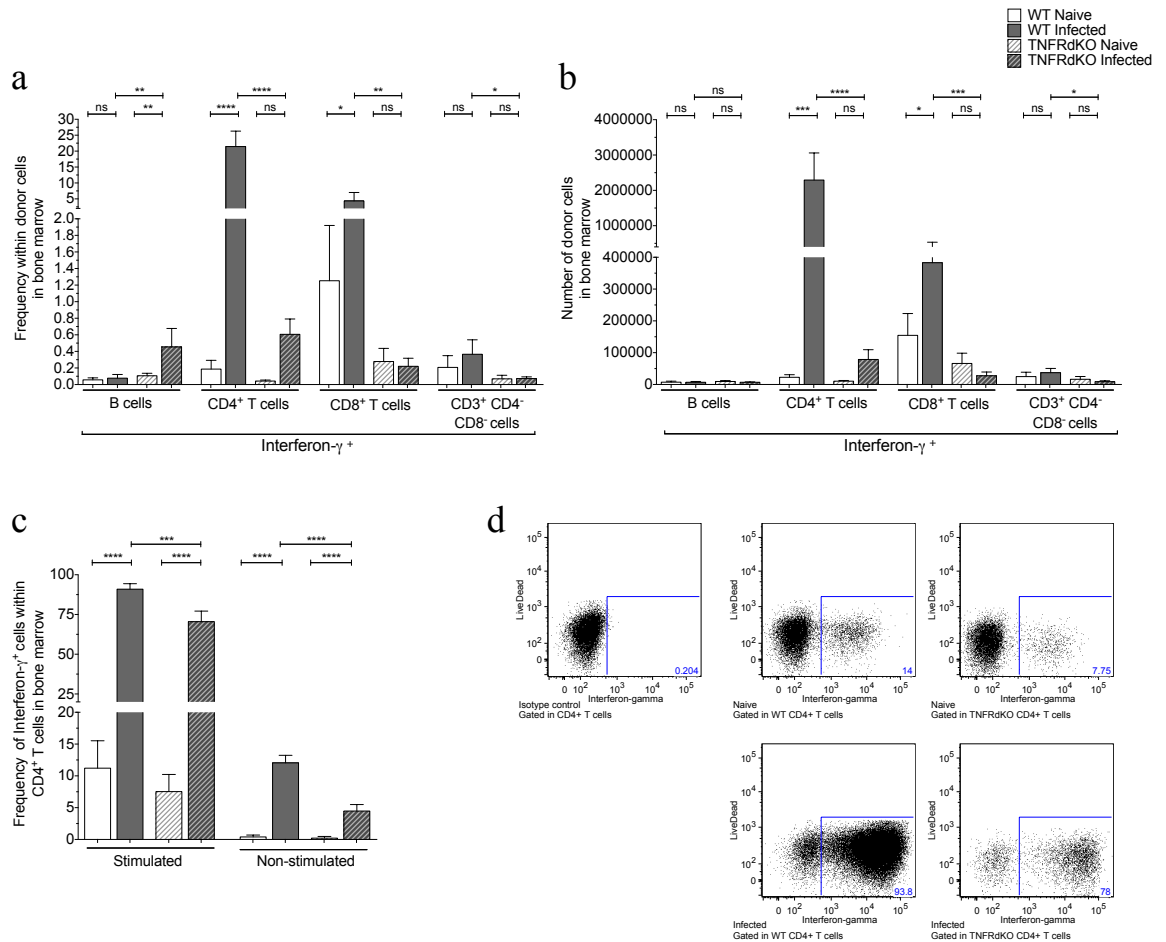


Figure 4.54 - Intrinsic TNF receptor signaling mediated expansion of CD4⁺ T cells expressing IFN γ in the BM following infection with *L. donovani*. (a) Frequency of B cells, CD4⁺ T cells, CD8⁺ T cells and CD3⁺ CD4⁻ CD8⁻ cells expressing IFN γ , following *in vitro* stimulation with PMA/ionomycin, within donor cells in BM. (b) Number of B cells, CD4⁺ T cells, CD8⁺ T cells and CD3⁺ CD4⁻ CD8⁻ cells expressing IFN γ following *in vitro* stimulation in BM. (c) Frequency of IFN γ ⁺ cells within donor CD4⁺ T cells following *in vitro* stimulation and without exogenous stimulation. (d) Representative dot plots displaying frequencies of IFN γ expression gated in CD4⁺ T cells in BM; (top left) isotype control, (top centre) naive recipient gated in WT donor CD4⁺ T cells, (top right) naive recipient gated in TNF-RdKO donor CD4⁺ T cells, (bottom left) infected recipient gated in WT donor CD4⁺ T cells cells, (bottom right) infected recipient gated in TNF-RdKO donor CD4⁺ T cells. Analyses were performed 13 weeks after transplant of total BM cells from CD45.2 TNF-RdKO mice and CD45.1 WT mice (50:50) to lethally irradiated CD45.1 recipient mice. Comparisons were made within donor compartment between non-infected recipients (n=4) and recipient mice infected with *L. donovani* for 28 days (Ld28) (n=4). Two femur and two tibias were taken per animal. Data from two independent experiments was presented as Mean \pm SD, p values were determined using One-way Anova followed by Tukey's multiple comparisons test: not significant (ns), *p \leq 0.05, **p \leq 0.01, ***p \leq 0.001 and ****p \leq 0.0001.

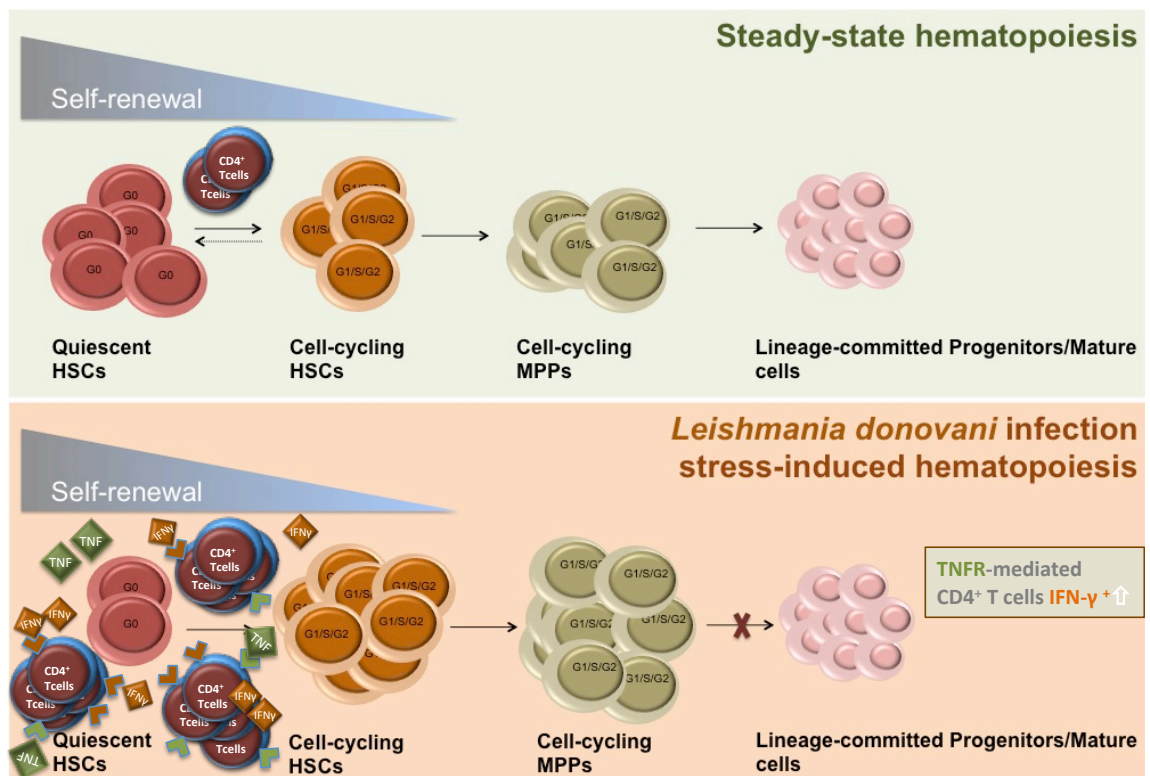


Figure 4.55 - Proposed mechanism to explain depletion of LT-HSCs in G0 and inefficient haematopoiesis during the chronic infection with *L. donovani* (4). Following *L. donovani* infection proliferating LT-HSCs and onward multipotent progenitors expand greatly at the expense of LT-HSCs in G0. The accumulation of intermediary multipotent progenitors was not associated with an increase in effective haematopoietic activity, since the numbers of effector haematopoietic cells were found either decreased or unchanged in PB. CD4⁺ T cells could solely mediate these alterations, through an IFN γ -dependent mechanism following transfer to *L. donovani* infected immunodeficient mice, otherwise protected from impairment of haematological function. The expansion CD4⁺ T cells IFN γ ⁺ was limited by the absence of intrinsic TNF receptor signaling, suggesting that TNF indirectly modulate LT-HSCs proliferative status through the induction of expansion of CD4⁺ T cell compartment, the main source of IFN γ in BM, during chronic infection in *L. donovani*.

CHAPTER 5. CONCLUDING DISCUSSION

Although it is well established that impairment of haematological function occurs during human VL, the underlying mechanisms are poorly understood. In the current study, we sought to clarify these mechanisms by characterizing alterations in cellular components of BM and, through functional assays, to identify molecular mediators modulating haematopoietic activity.

To our knowledge, this work represents the first detailed report characterizing the alterations in haematopoietic progenitors *ex vivo* during chronic experimental infection with *L. donovani* in mice. We identified accumulation of phenotypically defined non-committed early haematopoietic progenitors, without reciprocal increase in lineage-committed progenitors as a major change compared to steady state haematopoiesis, and this correlated with the establishment of anaemia and thrombocytopenia. The accumulation of early haematopoietic progenitors was driven by an increase in active proliferation at the expense of the reservoir of quiescent LT-HSCs, and resulted in loss of function, as determined by the impairment of long-term reconstitution potential in lethally irradiated syngeneic recipients. These findings are in agreement with studies reporting alterations in the proliferative status of LT-HSCs under pro-inflammatory conditions (M. T. Baldridge *et al.*, 2010, K. C. MacNamara *et al.*, 2011a, A. M. de Bruin *et al.*, 2013, C. Frelin *et al.*, 2013, K. A. Matatall *et al.*, 2014, D. Walter *et al.*, 2015). Recently, *in vivo* stress-induced haematopoiesis, including that promoted by chronic pro-inflammatory conditions, was shown to drive HSCs into active cell-cycle, and result in DNA damage (D. Walter *et al.*, 2015), suggesting that single and double-strand breaks might also be found in LT-HSCs from *L. donovani*-infected mice.

Alterations in haematopoiesis have been described in many models of infection. In some, it has been proposed that this promotes the differentiation of important effector cells (N. N. Belyaev *et al.*, 2010, N. Mossadegh-Keller *et al.*, 2013). In others, it has been suggested that inflammation-induced haematopoiesis could result in impairment of haematopoietic function (K. C. MacNamara *et al.*, 2009, S. Rodriguez *et al.*, 2009), as suggested here. VL patients may die due to increased vulnerability to secondary infections or bleeding (F. Chappuis *et al.*, 2007, V. E. Miranda de Araujo *et al.*, 2012). The results reported here suggest that chronic infection with *L. donovani* may lead to deterioration of HSCs function and the ability of haematopoiesis to respond to an increase demand of cells in a subsequent infection/injury. As such, further studies might profitably focus on examining how the haematopoietic system from mice chronically infected with *L. donovani* (or in resolution) copes with a secondary infection/injury.

To begin to answer this important question we performed a pilot study in which mice infected with *L. donovani* for a period of seven weeks were treated with a single dose of 5-Fluorouracil (5-

FU), a cytotoxic drug that eliminates haematopoietic progenitors in active proliferation and leads to the activation of quiescent HSCs into active proliferation (Figure 5.1). There was a significant decrease in the number of LT-HSCs in infected compared to naïve mice, and this difference became further evident after seven days. At both time points, the loss of HSCs in infected mice correlated with a decrease in the number of cells in circulation, that was far more deleterious in infected compared to naïve mice. This preliminary data suggested that following *L. donovani* infection, the haematopoietic system is functionally impaired to produce effector haematopoietic cells under severe stress conditions.

In the current study the alteration in the proliferative status of LT-HSCs was associated with the upregulation of the expression of transcription factors GATA-3 and β -catenin. Alterations in the expression of these transcription factors have been previously associated with losses in the reconstitution potential of HSCs in BMT assays (T. C. Luis *et al.*, 2011, T. Yoshida and K. Georgopoulos, 2013). These findings indicated that *L. donovani* infection has the potential to induce deleterious alterations in the mechanism regulating HSCs quiescence. In order to clarify the signaling networks inducing alterations in expression of GATA-3 and β -catenin, examination of the transcriptional profile of these cells, ideally using single cells analysis would be highly informative.

The loss of quiescent LT-HSCs and expansion of early non-committed progenitors was not observed in chronically infected RAG2 KO mice, and these mice did not display alteration in PB. Together, these findings indicated that the presence of the parasite by itself was not responsible for the alterations in BM and PB cellularity, and pointed to a critical role for adaptive immunity in driving the haematopoietic dysfunction. We characterized for the first time a significant expansion of CD4⁺ T cells expressing IFN γ in the BM of chronically infected mice. Then, using adoptive transfer of WT and IFN γ KO CD4⁺ T, we established that CD4⁺ T cells mediate depletion of the reservoir of quiescent HSCs and the establishment of anaemia through an IFN γ -dependent-mechanism.

The vast majority of BM CD4⁺ T cells in infected mice were CD44⁺ Ly6C⁻ CD127⁻, an immunophenotype associated with activated effector T cells in BM (K. Tokoyoda *et al.*, 2010). These could be further characterized, for example, by determining the expression of T-bet (master regulator of Th1 differentiation), their persistence after spontaneous or drug induced disease resolution, and for their role in the control of parasite burden and the development of immunopathology. The application of MHC II tetramers would allow such analyses to be conducted on a defined antigen-specific population.

Finally, by using BM mixed chimeras we established that during *L. donovani* infection, intrinsic IFN γ and TNF receptor signaling did not directly mediate the loss of quiescent LT-HSCs. These results were unexpected since a wide body of literature suggested that IFN γ has the potential to directly mediate the activation of HSCs into active cell-cycle, and this was correlated with loss of reconstitution potential in BMT assays (M. T. Baldrige *et al.*, 2010, K. C. MacNamara *et al.*, 2011a). More recently, TNF was also proposed as a direct mediator of impairment of HSCs function under myelosuppressive conditions (C. J. H. Pronk *et al.*, 2011).

Increased levels of IFN γ and TNF have been detected in the serum and in the BM in patients with BMF syndromes (C. Dufour *et al.*, 2001, C. Dufour *et al.*, 2003, C. Dufour *et al.*, 2004), in experimental models of BMF and in an experimental model of infection (J. L. Johns *et al.*, 2009, A. M. de Bruin *et al.*, 2013, Y. Zhang *et al.*, 2013). These clinical conditions share as a common denominator the emergence of alterations in haematopoietic function mirrored in alterations in haematopoiesis in BM or/and in effector cells in the periphery.

Additionally, in several models of infection it was proposed that the alterations in the proliferative status of HSCs and subsequent functional impairment are directly mediated by IFN γ receptor signal in HSCs (M. T. Baldrige *et al.*, 2010, K. C. MacNamara *et al.*, 2011a, A. M. de Bruin *et al.*, 2013). More recently, a similar role was suggested for TNF during stress-induced haematopoiesis (C. J. H. Pronk *et al.*, 2011). However, our findings obtained in mixed BM chimeric mice disagreed with these previous reports and indicated that alternative mechanisms mediate the loss of quiescent HSCs during chronic VL.

Our findings also strongly suggest that IFN γ and TNF receptor signaling converge to regulate the expansion of BM T cells following infection, since the absence of either IFN γ R or TNFR expression on T cells prevented their accumulation. Additionally, CD4⁺ T cells from TNF-RdKO were impaired in their ability to express IFN γ compared to WT CD4⁺ T cells, arguing in favor for an important indirect role of TNF signaling in controlling T cell-dependent haematopoietic dysfunction. In this context, experiments involving transfer of IFN γ R and TNFR deficient CD4⁺ T cells into RAG2 recipients would be highly informative.

If proven true, the hypothesis that the signal from both IFN γ R and TNFR in CD4⁺ T cells is required to mediate haematopoietic dysfunction during infection, efforts could then focus on determining which molecular mediators are activated non-redundantly by both signaling pathways. This could potentially lead to the isolation of a molecular target that could prevent CD4⁺ T cells from having a deleterious impact on haematopoiesis and simultaneously preserve their capacity to control parasite burden. A possible approach would be the transcriptional characterization of BM CD4⁺ T cells from WT, IFN γ R KO and TNFR KO isolated from

chronically infected mice. From this initial screening, potential targets that are upregulated in WT BM CD4⁺ T cells but unchanged in both BM CD4⁺ T cells IFN γ R KO and BM CD4⁺ T cells TNFR KO could be selected for further examination.

In a preliminary transcriptomic analysis of BM CD4⁺ T cells from naïve and infected mice, we identified 861 differentially expressed (DE) transcripts (Fold change > 4, p < 0.05). The top ten genes upregulated and downregulated in BM CD4⁺ T cells from infected mice are listed in Table 5.1.

As expected transcripts for *Ifng* and *Tnf* were upregulated in BM CD4⁺ T cells, ~11 fold and ~4 fold, respectively in infected compared to naive mice. In infected mice the expression TNFR1b was upregulated (~3 fold), in contrast the expression IFN γ R2 in BM CD4⁺ T cells was downregulated (~8 fold). These findings require confirmation by qPCR and flow cytometric analysis.

The analysis the alterations in BM CD4⁺ T cells transcriptional profile in the context of predefined canonical pathways, using the analysis tool Ingenuity Pathways, showed the highest degree of association with the network associated to “T helper cell differentiation”, i.e. 29 genes out of a total of 71 genes were DE during *L. donovani* infection (Figure 5.2). Interestingly, the expression of T-bet (master regulator of Th1 cells) was found unchanged. In addition, BM CD4⁺ T cells upregulated the expression of IL-21, a cytokine mainly expressed by NKT cells, Th17 and T follicular helper cells, either suggesting that BM CD4⁺ T cells during chronic infection may display an intermediate immunophenotype (V. Lazarevic *et al.*, 2013, R. Spolski and W. J. Leonard, 2014), or may reflect the heterogeneity of BM CD4⁺ T cell populations with potential to express IFN γ following infection, therefore requiring further extensive characterization.

The anaemia and thrombocytopenia associated with human VL have been mainly attributed to the splenomegaly, due to the observation that splenectomy resolves these alteration in patients. Very recently in our laboratory, it was reported that in experimental VL splenectomy prevented the development of thrombocytopenia but not anaemia (O. Preham unpublished data), suggesting discordant regulation of these two processes. However, the onset of significant alterations in the morphology of BM cells, sometimes resembling myelodysplastic syndromes, have been more difficult to address and suggested that alteration in BM haematopoiesis could contribute to haematopoietic dysfunction, which is most likely multifactorial in VL patients (G. E. Cartwright *et al.*, 1948, N. A. M. Aljurayyan *et al.*, 1995, K. K. Dhingra *et al.*, 2010, N. Varma and S. Naseem, 2010).

Many questions remain to be solved regarding the impact of VL on haematopoietic functions, some of which have been discussed above and elsewhere in this thesis. Nonetheless, the findings reported here have helped to shape a platform for future studies addressing the impact of VL in haematopoiesis, and have added to the extensive body of studies addressing the impact of chronic infection/inflammation in haematopoietic function.

This thesis was developed in the context of a neglected tropical disease, and we hope that our findings contribute to future studies devoted to the improvement of therapeutics approach, namely the prevention/treatment of haematopoietic dysfunctions, which aggravate the life conditions of VL patients in areas commonly characterized by socioeconomic fragilities.

5.1 FIGURES

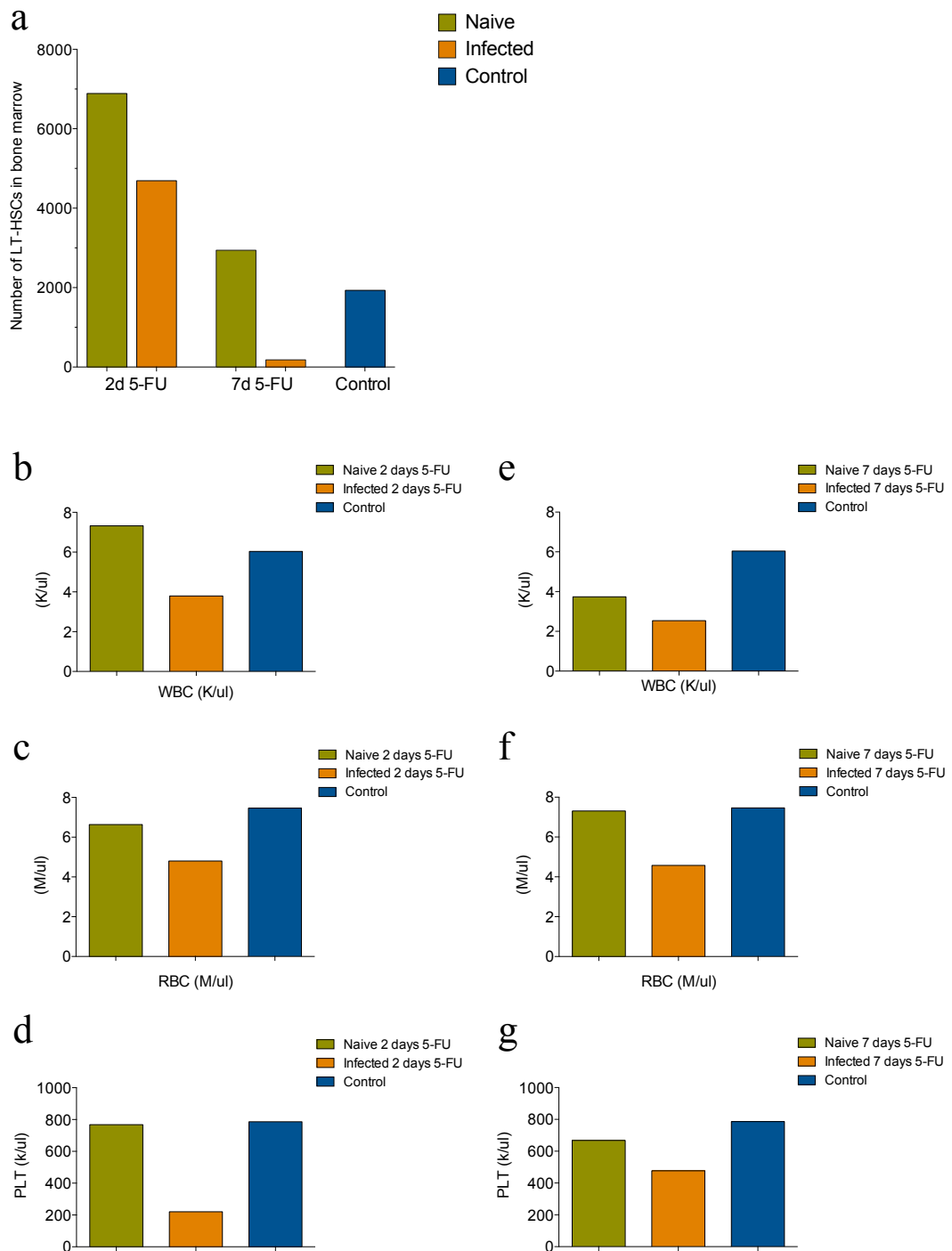


Figure 5.1 - Changes in blood parameters after 5-FU treatment. (a) Number of LSK CD150⁺ CD34⁻ CD48⁻ cells (LT-HSCs) in BM following 5-Fluororacil (5-FU) administration. (b-d) Concentration of white blood cells (WBC; b) red blood cells (RBC; c), and platelets (PLT; d) in PB following two days of 5-FU administration. (e-g) Concentration of WBC (e), RBC (f) and PLT (g) in PB following seven days of 5-FU administration. In each time point, one naive and one mouse infected with *L. donovani* for 38 days were injected intravenously with a single dose of 50 mg/kg of 5-FU, an unmanipulated naive mouse was used as control.

Table 5.1 - Top ten significantly up-/down-regulated genes in BM CD4⁺ T cells from mice infected with *L. donovani* for 28 days (compared to uninfected controls)

Gene name	Description	Fold change infected vs. naive	log ₂ Fold change infected vs. naive	adjusted p value	Regulation
Saa3	Mus musculus serum amyloid A 3 (Saa3), mRNA [NM_011315]	1802	11	0.0016	Up
Gm5486	Mus musculus 2 cells egg cDNA, RIKEN full-length enriched library, clone:B020041A18 product: hypothetical protein, full insert sequence. [AK139943]	200	8	0.0016	Up
Tff1	Mus musculus trefoil factor 1 (Tff1), mRNA [NM_009362]	181	7	0.0011	Up
Amt2	Mus musculus aryl hydrocarbon receptor nuclear translocator 2 (Amt2), mRNA [NM_007488]	178	7	0.0008	Up
Bace2	Mus musculus beta-site APP-cleaving enzyme 2 (Bace2), mRNA [NM_019517]	170	7	0.0049	Up
Rasd2	Mus musculus RASD family, member 2 (Rasd2), mRNA [NM_029182]	168	7	0.0005	Up
Tff1	Mus musculus trefoil factor 1 (Tff1), mRNA [NM_009362]	157	7	0.0014	Up
Il20ra	Mus musculus interleukin 20 receptor, alpha (Il20ra), mRNA [NM_172786]	147	7	0.0001	Up
Synpo2	Mus musculus synaptopodin 2 (Synpo2), mRNA [NM_080451]	144	7	0.0003	Up
Serpina9	Mus musculus serine (or cysteine) peptidase inhibitor, clade A (alpha-1 antitrypsin, antitrypsin), member 9 (Serpina9), mRNA [NM_027997]	137	7	0.0019	Up
Dapl1	Mus musculus death associated protein-like 1 (Dapl1), mRNA [NM_029723]	234	-8	0.0003	Down
Klra15	Mus musculus killer cell lectin-like receptor, subfamily A, member 15 (Klra15), mRNA [NM_013793]	230	-8	0.0013	Down
Gprc5b	Mus musculus G protein-coupled receptor, family C, group 5, member B (Gprc5b), transcript variant 2, mRNA [NM_022420]	185	-8	0.0003	Down
Adh1	Mus musculus alcohol dehydrogenase 1 (class I) (Adh1), mRNA [NM_007409]	147	-7	0.0003	Down
A530021J07 Rik	PREDICTED: Mus musculus Riken cDNA A530021J07 gene (A530021J07Rik), miscRNA [XR_035179]	144	-7	0.0008	Down
Klra16	Mus musculus killer cell lectin-like receptor, subfamily A, member 16 (Klra16), mRNA [NM_013794]	135	-7	0.0003	Down
St8sia6	Mus musculus ST8 alpha-N-acetyl-neuraminide alpha-2,8-sialyltransferase 6 (St8sia6), mRNA [NM_145838]	129	-7	0.0007	Down
Atp1b1	Mus musculus ATPase, Na ⁺ /K ⁺ transporting, beta 1 polypeptide (Atp1b1), mRNA [NM_009721]	126	-7	0.0003	Down
Grm6	Mus musculus glutamate receptor, metabotropic 6 (Grm6), mRNA [NM_173372]	120	-7	0.0002	Down
2610019F03 Rik	Mus musculus RIKEN cDNA 2610019F03 gene (2610019F03Rik), mRNA [NM_173744]	108	-7	0.0012	Down

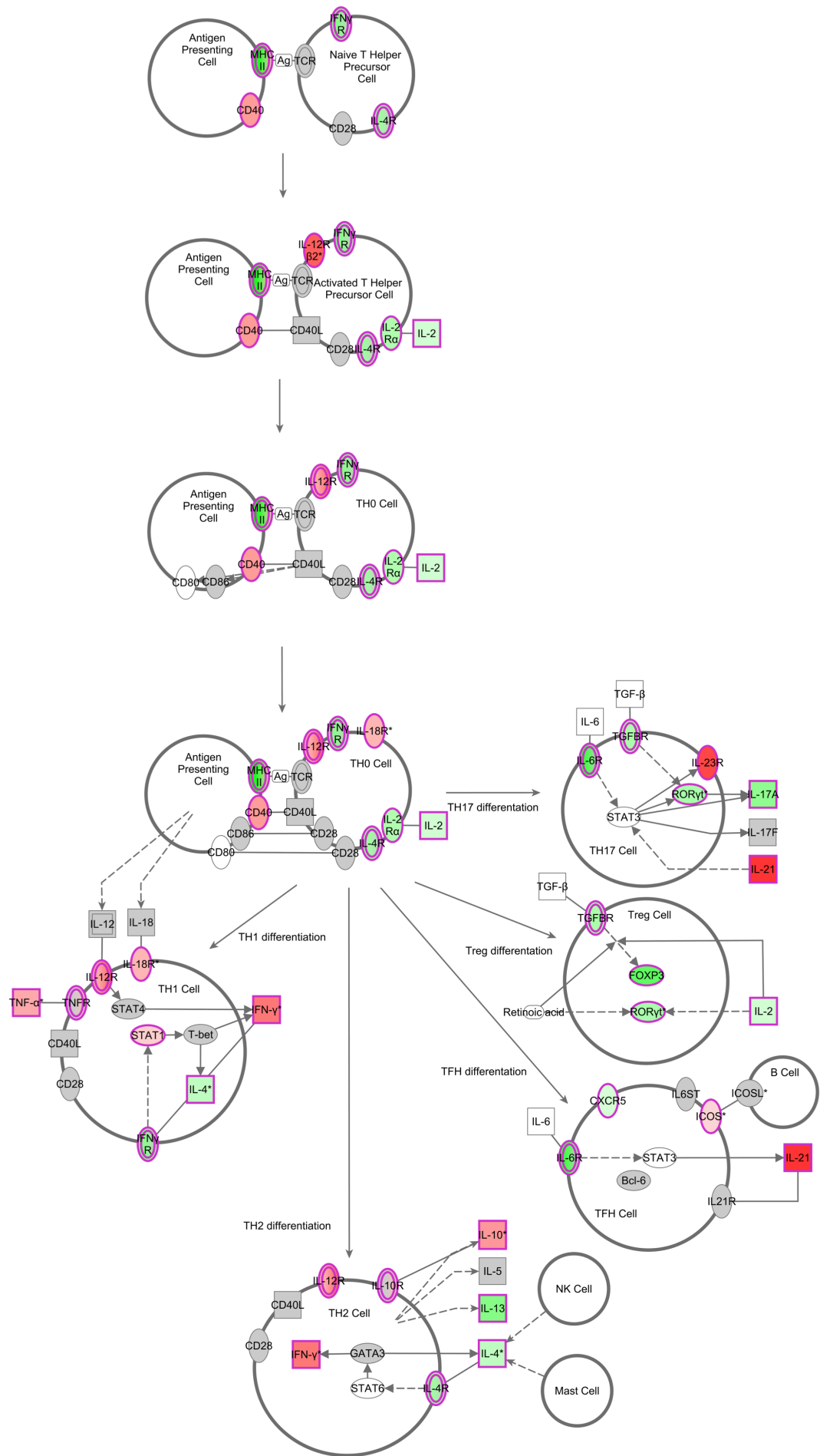


Figure 5.2 - DE genes in BM CD4⁺ T cells of naïve vs. *L. donovani* infection mapped to IPA canonical pathway of Th cell differentiation. The Ingenuity Pathway Analysis tool analyzed nearly 1000 genes significantly regulated in BM CD4⁺ T cells following *L. donovani* infection (Fold change > 3, p < 0.05), with the canonical pathway “ T helper differentiation” identified as having significant enrichment (p= 5.25 x 10⁻¹¹). Red indicates upregulated and green down-regulated genes. Grey indicates unchanged according with the defined cut-off.

ABBREVIATIONS

5-FU	5- Fluorouracil
AA	Aplastic anemia
ACK2	Anti-Mouse CD117 (cKit)
AdCMV-lacZ	Replication-deficient β -galactosidase encoding recombinant adenovirus
ALAS2	5'-Aminolevulinate Synthase 2
Ang	Angiopoietin
AP-1	Activator protein 1 (TF)
APC	Antigen presenting cell
APC	Allophycocyanin (Fluorochrome)
APRIL	A proliferation-inducing ligand, also known as tumor necrosis factor ligand superfamily member 13
aPTT	Activated Partial Thromboplastin Time
ARRIVE	Animal Research: Reporting of In Vivo Experiments (guidelines)
ATF2	Activating Transcription Factor 2
AXIN1	Axis inhibition protein 1
B6	C57BL/6 mice, often referred to as black 6 mice
BA	Basophils
BAFF	B-cell activating factor, also known as tumor necrosis factor ligand superfamily member 13B
BCL2	B-cell lymphoma 2
BCLXL	B-cell lymphoma-extra large
BCP	B-cell progenitor
BFU-E	Burst forming unit–erythrocyte
BM	Bone marrow

Bmi1	Polycomb complex protein B lymphoma Mo-MLV insertion region 1 homolog
BMP-2	Bone morphogenetic protein 2
BMP-6	Bone morphogenetic protein 6
BMSCs	Bone marrow stromal cells
BMT	Bone marrow transfer assay
BrdU	Bromodeoxyuridine
BSA	Bovin serum albumin
BSP	Bone sialoprotein
c-mpl	Myeloproliferative leukemia protein, also known as thrombopoietin receptor
C/EBP α	CCAAT enhancer-binding protein α
CAFC	Cobblestone area-forming cells
CAR	CXCL12-abundant reticular (cells)
CCL2	Chemokine (C-C motif) ligand 2, also known as monocyte chemotactic protein 1
CCL3	Chemokine (C-C motif) ligand 3, also known as macrophage inflammatory protein 1-alpha
CCL8	Chemokine (C-C motif) ligand 8 (CCL8), also known as monocyte chemoattractant protein 2
CCR2	C-C chemokine receptor type 2
CCR7	C-C chemokine receptor type 7
CD	Cluster of differentiation
Cdc42	Cell division cycle 42 (a Rho family GTPase)
cdk	Cyclin-dependent kinase
CDKIs	Cyclin dependent kinase inhibitors
Cdkn	Cyclin-dependent kinase inhibitor
cDNA	Complementary DNA
CEMCs	CXCL12-expressing mesenchymal cells

CFSE	5(6)-carboxyfluorescein diacetate N-succinimidyl ester
CFU	Colony forming units
CFU-C	Colony-Forming Unit Culture
CFU-E	Colony forming unit-erythroid
CFU-F	Colony forming units-fibroblast
CFU-GEMM	Colony-forming unit granulocyte-erythroid-macrophage-megakaryocyte
CFU-OB	Colony-Forming Unit-osteoblast
cKit	Stem cell growth factor receptor, also called Proto-oncogene c-Kit or tyrosine-protein kinase Kit or CD117
CLPs	Common lymphoid progenitors
CML	Chronic myeloid leukaemia
CMPs	Common myeloid progenitors
CMV	Cytomegalovirus
CRA	Competitive repopulation assay, also referred as competitive bone marrow transfer assay
Cre	Cre recombinase
Cre	cAMP-responsive elements
CRs	Cytokine receptor
CXCL10	C-X-C motif chemokine 10, also known as Interferon gamma-induced protein 10
CXCL12	C-X-C motif chemokine ligand 12, also known as stromal cell-derived factor 1
CXCR4	C-X-C chemokine receptor type 4
CYLD	Deubiquitinase cylindromatosis
DAMPs	Damage-associated molecular pattern molecules
DAPI	4',6-Diamidino-2-Phenylindole, Dihydrochloride
DCs	Dendritic cells
DICER1	Double-stranded RNA (dsRNA) endoribonuclease Type III

DKK1	Dickkopf-related protein 1
DMEM	Dulbecco's Modified Eagle medium
DNA	Deoxyribonucleic acid
Dnmt3a	DNA (cytosine-5)-methyltransferase 3A
dsRNA	Double-stranded RNA
DTR	Diphtheria toxin receptor
E	Embryonic day
Ebf-1	Early B-Cell Factor 1
Ebf1	Early B cell factor 1
eGFP	Enhanced green fluorescent protein
EKLF	Erythroid Krueppel-Like Transcription Factor
EO	Eosinophils
EP	Erythroid progenitor
ERK	Extracellular-signal-regulated kinases, also known MAP kinases
Ery	Erythroid
ES	Embryonic stem (cells)
EVI9	Ena/Vasodilator-Stimulated Phosphoprotein-Like 9
FA	Fanconi anemia
FACS	Fluorescence activated cell sorting (technology)
Fas	Fragment, apoptosis stimulating (cell receptor)
FasL	Fas ligand
FcR	Fragment crystallizable region receptor
FCS	Fetal calf serum
FLs	Fetal livers
Flt3	FMS-like tyrosine kinase 3

FOG-1	Friend of GATA protein 1
FOXO	Forkhead box proteins O
Foxp3	Forkhead box protein 3
FZD	Frizzled protein
Fzd	Frizzled (receptor)
G-CSF	Granulocyte colony stimulating factor, also known as colony-stimulating factor 3
GAS	IFN γ -activated site promotor sequences
GATA-1	Erythroid transcription factor, also known as GATA-binding factor 1
GATA-2	GATA binding protein 2
GATA-3	Trans-acting T-cell-specific transcription factor GATA-3
Gfi-1b	Growth Factor Independent 1B Transcription Repressor
GFP	Green fluorescent protein
gIP-10	Interferon gamma-induced protein 10, also known as C-X-C motif chemokine 10
GM-CFCs	Granulocyte-Macrophage colony forming cells
GM-CSF	Granulocyte/macrophage colony-stimulating factor
GMPs	Granulocyte/monocyte progenitors
GSK3 β	Glycogen synthase kinase 3 beta
H2B	Histone Cluster 2
Hb	Hemoglobin
HCT	Hematocrit
hi	High
HLA	Human leukocyte antigen
HME	Human monocytic ehrlichiosis
HOXB4	Homeobox protein Hox-B4
HPC-1	Haematopoietic progenitor cells 1

HPC-2	Haematopoietic progenitor cells 2
HSCs	Haematopoietic ctem cells
HSPCs	Haematopoietic stem and progenitor cells
ICAM1	Intercellular Adhesion Molecule 1
IFNAR	IFN α / β receptor
IFN α / β	Interferon alpha/beta
IFN γ	Interferon-gamma
IFN γ R	Interferon gamma receptor
Ig	Immunoglobulin
IKK	Inhibitor of nuclear factor kappa-B kinase
IL	Interleukin
IL-7R α	Interleukin-7 receptor- α , also referred as CD127
INK4a	Inhibitor of kinase 4a. Also known asp16INK4a.
iNOS	Inducer of nitric oxide synthase
IRF	Interferon regulatory factors
ISG	Interferon Stimulated Genes
ISRE	Interferon-stimulated response elements
IT-HSCs	Intermediate-term Haematopoietic ctem cells
I κ B α	Nuclear factor of kappa light polypeptide gene enhancer in B-cells inhibitor alpha
JAK	Janus kinase (part of JAK-STAT pathway)
JNK	c-Jun N-terminal kinase (a MAPK)
KCs	Kupffer cells
KO	Knockout
KSL	cKit ⁺ Sca1 ⁺ Lineage ⁻ cells (also referred as LSK)
LCMV	Lymphocytic choriomeningitis virus

Ld28	Infection with <i>Leishmania donovani</i> for a period of 28 days
LDU	Leishmania-Donovani units
LEF	Lymphoid enhancer binding factor
lerp	Leptin receptor
LMPPs	Immature lymphoid-biased progenitors/ lymphoid primed multipotent progenitors
lo	Low
LPS	Lipopolysaccharide
LRP5/6	Single-membrane-spanning low-density receptor-related protein 5/6
LSK	Lineage ⁻ Sca1 ⁺ cKit ⁺ cells (also referred as KSL)
LT	Lymphotoxin- α
LT-HSCs	Long-term Haematopoietic stem cells
LTC-IC	Long-term culture-initiating cell
LV9	Ethiopian strain of <i>Leishmania donovani</i>
LY	Lymphocytes
M-CSF	Macrophage colony stimulating factor
mAb	Monoclonal antibody
MAPK	Mitogen-activated protein kinases
MCP-1	Monocyte chemotactic protein , also known as CCL2
MD-2	Origin of abbreviation unknown. Also referred to as lymphocyte antigen LY96.
MDS	Myelodisplastic syndrome
MegE	Megakaryocytes / Erythrocytes cellular lineages
MEKK1	Mitogen-activated protein kinase kinase kinase
MEPs	Megakaryocyte/erythrocyte progenitors
mES	Murine embryonic stem (cells)
MFI	Mean Intensity Fluorescence

MHC I	Major histocompatibility complex class I molecules
MHC II	Major histocompatibility complex class II molecules
MIF	Macrophage migration inhibitory factor, also known as glycosylation-inhibiting factor
MIP-1 α	Macrophage inflammatory protein 1-alpha
miRNA	Micro RNA
MkP	Megakaryocyte progenitor
MO	Monocytes
MPPs	Multipotent progenitor cells
mRNA	Messenger RNA
MSCs	Mesenchymal stem cells
MX1	Myxovirus (Influenza Virus) Resistance 1, Interferon-Inducible Protein P78 (Mouse)
Myc	Avian Myelocytomatosis Viral Oncogene Homolog
MyD88	Myeloid differentiation primary response gene 88 protein
MyRP	Myeloid-restricted progenitor
NE	Neutrophil
NES	Nestin
Nestin	Neuroectodermal stem cell marker
NF κ B	Nuclear factor kappa-light-chain-enhancer of activated B cells
NK	Natural Killer (cells)
NOS2	Nitric oxide synthase (enzyme)
NOTCH	Not an abbreviation but refers to a mutation resulting in a notch in Drosophila wings.
ns	Statistically not significant
OB	Osteoblast
OCN	Osteocalcin

ODN	CpG oligodeoxynucleotides (TLR9 agonist)
p38	P38 mitogen-activated protein kinases
Pam3CSK4	N-Palmitoyl-S-[2,3-bis(palmitoyloxy)-(2RS)-propyl]-[R]-cysteiny1-[S]-sery1-[S]-lysyl-[S]-lysyl-[S]-lysyl-[S]-lysineSynthetic diacylated lipoprotein
PAMPs	Pathogen-associated molecular patterns
PAX5	Paired box protein 5
PB	Peripheral blood
PB	Peripheral blood
PBMCs	Peripheral blood mononuclear cells
PBMNCs	Peripheral blood mononuclear cells
PBS	Phosphate-Buffered Saline
PDGFR	Platelet-derived growth factor receptor
PFA	Paraformaldehyde
PKDL	Post-kala-azar dermal leishmaniasis
PLT	Platelets
PMA	Phorbol 12-myristate 13-acetate
poly I:C	Polyinosinic:polycytidylic acid
PRRs	Pattern recognition receptors
PT	Prothrombin Time
Pten	Phosphatase and tensin homolog
qPCR	Quantitative real-time polymerase chain reaction
RA	Rheumatoid arthritis
Rb	retinoblastoma (protein)
RBCs	Red blood cells
rDCs	Regulatory dendritic cells

rIFN γ	Purified mouse recombinant IFN γ
RIP	Receptor-Interacting Protein 1, also known as Receptor (TNFRSF)-Interacting Serine-Threonine Kinase
RNA	Ribonucleic acid
RNI	Reactive nitrogen intermediates
ROI	Reactive oxygen intermediates
ROS	Reactive oxygen species
RPMI	Roswell Park Memorial Institute medium
RT	Room temperature
RT (reaction)	Reverse transcription reaction
Runx-1	Runt-related transcription factor 1, also known as acute myeloid leukemia 1 protein
Runx2	Runt-related transcription factor 2
Sca1	Stem cell antigen 1
SCF	Stem cell factor, KIT-ligand or steel factor
SCID	Severe combined immunodeficiency
SCL/TAL1	Stem cell leukemia/T-cell acute lymphocytic leukemia protein 1
SD	Standard Deviation
SDF-1	Stromal cell-derived factor 1
SDF-1 α	Stromal-cell derived factor-1 α , also known as CXCL12
SDF1	Stromal cell-derived factor 1, also referred as C-X-C motif chemokine 12 (CXCL12)
SEM	Standard Error Mean
siRNA	Small interfering RNA
SLAM	Signaling lymphocyte activation molecule
SOCS1	Suppressor of cytokine signaling 1
SP	Side population

ST-HSCs	Short-term Haematopoietic stem cells
STAT	Signal transducer and activator of transcription (STAT) protein family
T-bet	T-cell-specific T-box transcription factor T-bet
TCF-1	T-cell factor transcription factor
TCR	T cell receptor
TFs	Transcription Factors
TGF- β	Transforming growth factor beta
Th	T-helper
Th1	T-helper type 1 lymphocytes
Th2	T helper type 2 lymphocytes
TIR	Toll/interleukin-1 receptor
TLRs	Toll-like receptors
TNF	Tumor necrosis factor
TNFR	Tumor necrosis factor receptor
TNFR-dKO	Tumor necrosis factor receptor double KO, also referred as Tnfrsf1-dKO
TNFR α	Tumor necrosis factor receptor 1a or Tnfr-p55
TNFR β	Tumor necrosis factor receptor 1b or Tnfr-p75
TNK	T-cell natural killer cell progenitor
TPA	12-O-Tetradecanoylphorbol-13-acetate, also known phorbol 12-myristate 13-acetate
TPO	Thrombopoietin
TRADD	Tumor necrosis factor receptor type 1-associated DEATH domain protein
TRAF2	Tumor necrosis factor receptor-associated factor 2
TRE	TPA DNA-response elements
Treg	Regulatory T cells
TRIF	TIR-domain-containing adapter-inducing interferon- β

TYK2	Tyrosine-protein kinase 2
VCAM1	Vascular cell adhesion molecule 1
VL	Visceral leishmaniasis
vWF	Willebrand factor
WBC	White blood cells
WNT	Wingless-Int, also known as Wingless-type MMTV integration site family member
WT	Wild-type

REFERENCES

- "World health organization (who). Leishmaniasis: Epidemiology and access to medicines. Geneva, switzerland: Who; 2012. Available at: [http://Www.Who.Int/leishmaniasis/resources/leishmaniasis worldwide epidemiological and drug access update.Pdf](http://Www.Who.Int/leishmaniasis/resources/leishmaniasis_worldwide_epidemiological_and_drug_access_update.Pdf) [accessed 11.12.13].".
- Agrawal, Y., A. Sinha, P. Upadhyaya, S. Kafle, S. Rijal and B. Khanal (2013). "Hematological profile in visceral leishmaniasis." 2013 **2**(2): 6.
- Aird, W. C. (2003). "The hematologic system as a marker of organ dysfunction in sepsis." Mayo Clinic Proceedings **78**(7): 869-881.
- Akashi, K., X. He, J. Chen, H. Iwasaki, C. Niu, B. Steenhard, J. W. Zhang, J. Haug and L. H. Li (2003). "Transcriptional accessibility for genes of multiple tissues and hematopoietic lineages is hierarchically controlled during early hematopoiesis." Blood **101**(2): 383-390.
- Aljurayyan, N. A. M., M. N. Alnasser, I. M. Alfawaz, I. H. Alayed, A. S. Alherbish, A. M. Almazrou and M. O. Alsohaibani (1995). "The hematological manifestations of visceral leishmaniasis in infancy and childhood." Journal of Tropical Pediatrics **41**(3): 143-148.
- Anthony, B. A. and D. C. Link (2014). "Regulation of hematopoietic stem cells by bone marrow stromal cells." Trends in Immunology **35**(1): 32-37.
- Arieta Kuksin, C., G. Gonzalez-Perez and L. M. Minter (2015). "Cxcr4 expression on pathogenic t cells facilitates their bone marrow infiltration in a mouse model of aplastic anemia." Blood **125**(13): 2087-2094.
- Askenasy, N. (2015). "Interferon and tumor necrosis factor as humoral mechanisms coupling hematopoietic activity to inflammation and injury." Blood Reviews **29**(1): 11-15.
- Baena, E., M. Ortiz, C. Martinez-A and I. M. de Alboran (2007). "C-myc is essential for hematopoietic stem cell differentiation and regulates lin(-)sca-1(+)-c-kit(-) cell generation through p21." Experimental Hematology **35**(9): 1333-1343.
- Baldrige, M. T., K. Y. King, N. C. Boles, D. C. Weksberg and M. A. Goodell (2010). "Quiescent haematopoietic stem cells are activated by ifn-gamma in response to chronic infection." Nature **465**(7299): 793-U799.
- Baldrige, M. T., K. Y. King and M. A. Goodell (2011). "Inflammatory signals regulate hematopoietic stem cells." Trends in Immunology **32**(2): 57-65.
- Barreda, D. R., P. C. Hanington and M. Belosevic (2004). "Regulation of myeloid development and function by colony stimulating factors." Developmental and Comparative Immunology **28**(5): 509-554.
- Basu, S., A. Ray and B. N. Dittel (2013). "Differential representation of b cell subsets in mixed bone marrow chimera mice due to expression of allelic variants of cd45 (cd45.1/cd45.2)." Journal of Immunological Methods **396**(1-2): 163-167.
- Becker, A. J., E. A. McCulloch and J. E. Till (2014). "Cytological demonstration of the clonal nature of spleen colonies derived from transplanted mouse marrow cells (reprinted from nature, vol 197, pg 452-454, 1963)." Journal of Immunology **192**(11): 4945-4947.
- Becker, A. J., J. E. Till and E. A. McCulloch (1963). "Cytological demonstration of clonal nature of spleen colonies derived from transplanted mouse marrow cells." Nature **197**(486): 452-&.

- Belyaev, N. N., J. Biro, J. Langhorne and A. J. Potocnik (2013). "Extramedullary myelopoiesis in malaria depends on mobilization of myeloid-restricted progenitors by ifn-gamma induced chemokines." Plos Pathogens **9**(6).
- Belyaev, N. N., D. E. Brown, A.-I. G. Diaz, A. Rae, W. Jarra, J. Thompson, J. Langhorne and A. J. Potocnik (2010). "Induction of an il7-r(+)-c-kit(hi) myelolymphoid progenitor critically dependent on ifn-gamma signaling during acute malaria." Nature Immunology **11**(6): 477-U441.
- Biswas, T., M. Chakraborty, K. Naskar, D. K. Ghosh and J. Ghosal (1992). "Anemia in experimental visceral leishmaniasis in hamsters." Journal of Parasitology **78**(1): 140-142.
- Boettcher, S., R. C. Gerosa, R. Radpour, J. Bauer, F. Ampenberger, M. Heikenwalder, M. Kopf and M. G. Manz (2014). "Endothelial cells translate pathogen signals into g-csf-driven emergency granulopoiesis." Blood **124**(9): 1393-1403.
- Boles, N. C., K. K. Lin, G. L. Lukov, T. V. Bowman, M. T. Baldrige and M. A. Goodell (2011). "Cd48 on hematopoietic progenitors regulates stem cells and suppresses tumor formation." Blood **118**(1): 80-87.
- Bryder, D., V. Ramsfjell, I. Dybedal, K. Theilgaard-Monch, C. M. Hogerkorp, J. Adolfsson, O. J. Borge and S. E. W. Jacobsen (2001). "Self-renewal of multipotent long-term repopulating hematopoietic stem cells is negatively regulated by fas and tumor necrosis factor receptor activation." Journal of Experimental Medicine **194**(7): 941-952.
- Buechler, M. B., T. H. Teal, K. B. Elkon and J. A. Hamerman (2013). "Cutting edge: Type i ifn drives emergency myelopoiesis and peripheral myeloid expansion during chronic thr7 signaling." Journal of Immunology **190**(3): 886-891.
- Bunn, P. T., A. C. Stanley, F. d. I. Rivera, A. Mulherin, M. Sheel, C. E. Alexander, R. J. Faleiro, F. H. Amante, M. M. De Oca, S. E. Best, K. R. James, P. M. Kaye, A. Haque and C. R. Engwerda (2014). "Tissue requirements for establishing long-term cd4(+) t cell-mediated immunity following leishmania donovani infection." Journal of Immunology **192**(8): 3709-3718.
- Cain, C. J. and J. O. Manilay (2013). "Hematopoietic stem cell fate decisions are regulated by wnt antagonists: Comparisons and current controversies." Experimental Hematology **41**(1): 3-16.
- Cartwright, G. E., H. L. Chung and A. Chang (1948). "Studies on the pancytopenia of kala-azar." Blood **3**(3): 249-275.
- Casanova-Acebes, M., C. Pitaval, L. A. Weiss, C. Nombela-Arrieta, R. Chevre, N. A-Gonzalez, Y. Kunisaki, D. Zhang, N. van Rooijen, L. E. Silberstein, C. Weber, T. Nagasawa, P. S. Frenette, A. Castrillo and A. Hidalgo (2013). "Rhythmic modulation of the hematopoietic niche through neutrophil clearance." Cell **153**(5): 1025-1035.
- Challen, G. A., N. Boles, K. K.-Y. Lin and M. A. Goodell (2009). "Mouse hematopoietic stem cell identification and analysis." Cytometry Part A **75A**(1): 14-24.
- Chappuis, F., S. Sundar, A. Hailu, H. Ghalib, S. Rijal, R. W. Peeling, J. Alvar and M. Boelaert (2007). "Visceral leishmaniasis: What are the needs for diagnosis, treatment and control?" Nature Reviews Microbiology **5**(11): 873-882.
- Cheers, C., A. M. Haigh, A. Kelso, D. Metcalf, E. R. Stanley and A. M. Young (1988). "Production of colony-stimulating factors (csfs) during infection - separate determinations of macrophage-csf, granulocyte-csf, granulocyte-macrophage-csf, and multi-csf." Infection and Immunity **56**(1): 247-251.

- Chen, X. and J. J. Oppenheim (2011). "Contrasting effects of tnf and anti-tnf on the activation of effector t cells and regulatory t cells in autoimmunity." Febs Letters **585**(23): 3611-3618.
- Chow, A., M. Huggins, J. Ahmed, D. Hashimoto, D. Lucas, Y. Kunisaki, S. Pinho, M. Leboeuf, C. Noizat, N. van Rooijen, M. Tanaka, Z. J. Zhao, A. Bergman, M. Merad and P. S. Frenette (2013). "Cd169(+) macrophages provide a niche promoting erythropoiesis under homeostasis and stress." Nature Medicine **19**(4): 429-+.
- Chow, A., D. Lucas, A. Hidalgo, S. Mendez-Ferrer, D. Hashimoto, C. Scheiermann, M. Battista, M. Leboeuf, C. Prophete, N. van Rooijen, M. Tanaka, M. Merad and P. S. Frenette (2011). "Bone marrow cd169(+) macrophages promote the retention of hematopoietic stem and progenitor cells in the mesenchymal stem cell niche." Journal of Experimental Medicine **208**(2): 261-271.
- Christopher, M. J., F. Liu, M. J. Hilton, F. Long and D. C. Link (2009). "Suppression of cxcl12 production by bone marrow osteoblasts is a common and critical pathway for cytokine-induced mobilization." Blood **114**(7): 1331-1339.
- Cotterell, S. E. J., C. R. Engwerda and P. M. Kaye (2000a). "Enhanced hematopoietic activity accompanies parasite expansion in the spleen and bone marrow of mice infected with leishmania donovani." Infection and Immunity **68**(4): 1840-1848.
- Cotterell, S. E. J., C. R. Engwerda and P. M. Kaye (2000b). "Leishmania donovani infection of bone marrow stromal macrophages selectively enhances myelopoiesis, by a mechanism involving gm-csf and tnf-alpha." Blood **95**(5): 1642-1651.
- Coulombel, L. (2004). "Identification of hematopoietic stem/progenitor cells: Strength and drawbacks of functional assays." Oncogene **23**(43): 7210-7222.
- Dalton, D. K., S. Pittsmeek, S. Keshav, I. S. Figari, A. Bradley and T. A. Stewart (1993). "Multiple defects of immune cell-function in mice with disrupted interferon-gamma genes." Science **259**(5102): 1739-1742.
- Dalton, J. E., A. Maroof, B. M. J. Owens, P. Narang, K. Johnson, N. Brown, L. Rosenquist, L. Beattie, M. Coles and P. M. Kaye (2010). "Inhibition of receptor tyrosine kinases restores immunocompetence and improves immune-dependent chemotherapy against experimental leishmaniasis in mice." Journal of Clinical Investigation **120**(4): 1204-1216.
- Davies, C. R., P. Kaye, S. L. Croft and S. Sundar (2003). "Leishmaniasis: New approaches to disease control." British Medical Journal **326**(7385): 377-382.
- de Bruin, A. M., O. Demirel, B. Hooibrink, C. H. Brandts and M. A. Nolte (2013). "Interferon-gamma impairs proliferation of hematopoietic stem cells in mice." Blood **121**(18): 3578-3585.
- de Bruin, A. M., S. F. Libregts, M. Valkhof, L. Boon, I. P. Touw and M. A. Nolte (2012). "Ifn gamma induces monopoiesis and inhibits neutrophil development during inflammation." Blood **119**(6): 1543-1554.
- de Bruin, A. M., C. Voermans and M. A. Nolte (2014). "Impact of interferon-gamma on hematopoiesis." Blood **124**(16): 2479-2486.
- de Vasconcelos, G. M., F. Azevedo-Silva, L. C. Dos Santos Thuler, E. T. G. Pina, C. S. F. Souza, K. Calabrese and M. S. Pombo-de-Oliveira (2014). "The concurrent occurrence of leishmania chagasi infection and childhood acute leukemia in brazil." Revista brasileira de hematologia e hemoterapia **36**(5): 356-362.
- Delgado, M. D. and J. Leon (2010). "Myc roles in hematopoiesis and leukemia." Genes & cancer **1**(6): 605-616.

- DeZern, A. E. and E. C. Guinan (2014). "Aplastic anemia in adolescents and young adults." Acta Haematologica **132**(3-4): 331-339.
- Dhingra, K. K., P. Gupta, V. Saroha, N. Setia, N. Khurana and T. Singh (2010). "Morphological findings in bone marrow biopsy and aspirate smears of visceral kala azar: A review." Indian Journal of Pathology and Microbiology **53**(1): 96-100.
- Di Rosa, F. and R. Pabst (2005). "The bone marrow: A nest for migratory memory t cells." Trends in Immunology **26**(7): 360-366.
- Domen, J., A. Wagers and I. L. Weissman (2006). "2. Bone marrow (hematopoietic) stem cells." Regenerative Medicine: 13.
- Doulatov, S., F. Notta, E. Laurenti and J. E. Dick (2012). "Hematopoiesis: A human perspective." Cell Stem Cell **10**(2): 120-136.
- Du, W., O. Erden and Q. Pang (2014). "Tnf-alpha signaling in fanconi anemia." Blood Cells Molecules and Diseases **52**(1): 2-11.
- Dufour, C., M. Capasso, J. Svahn, A. Marrone, R. Haupt, A. Bacigalupo, L. Giordani, D. Longoni, M. Pillon, A. Pistorio, P. Di Michele, A. P. Iori, C. Pongiglione, M. Lanciotti, A. Iolascon, Aieop and S. M. Ospedale (2004). "Homozygosity for (12) ca repeats in the first intron of the human ifn-gamma gene is significantly associated with the risk of aplastic anaemia in caucasian population." British Journal of Haematology **126**(5): 682-685.
- Dufour, C., A. Corcione, J. Svahn, R. Haupt, N. Battilana and V. Pistoia (2001). "Interferon gamma and tumour necrosis factor alpha are overexpressed in bone marrow t lymphocytes from paediatric patients with aplastic anaemia." British Journal of Haematology **115**(4): 1023-1031.
- Dufour, C., A. Corcione, J. Svahn, R. Haupt, V. Poggi, A. N. Beka'ssy, R. Scime, A. Pistorio and V. Pistoia (2003). "Tnf-alpha and ifn-gamma are overexpressed in the bone marrow of fanconi anemia patients and tnf-alpha suppresses erythropoiesis in vitro." Blood **102**(6): 2053-2059.
- Duran-Struuck, R. and R. C. Dyskoz (2009). "Principles of bone marrow transplantation (bmt): Providing optimal veterinary and husbandry care to irradiated mice in bmt studies." Journal of the American Association for Laboratory Animal Science **48**(1): 11-22.
- Dutra, R. A., L. F. Dutra, M. d. O. Reis and R. C. Lambert (2012). "Splenectomy in a patient with treatment-resistant visceral leishmaniasis: A case report." Revista da Sociedade Brasileira de Medicina Tropical **45**(1): 130-131.
- Eaves, C. J. (2015). "Hematopoietic stem cells: Concepts, definitions, and the new reality." Blood **125**(17): 2605-2613.
- Elishmereni, M. and F. Levi-Schaffer (2011). "Cd48: A co-stimulatory receptor of immunity." International Journal of Biochemistry & Cell Biology **43**(1): 25-28.
- Ellerin, T., R. H. Rubin and M. E. Weinblatt (2003). "Infections and anti-tumor necrosis factor alpha therapy." Arthritis and Rheumatism **48**(11): 3013-3022.
- Endele, M., M. Etzrodt and T. Schroeder (2014). "Instruction of hematopoietic lineage choice by cytokine signaling." Experimental Cell Research **329**(2): 207-213.
- Engwerda, C. R., M. Ato and P. M. Kaye (2004a). "Macrophages, pathology and parasite persistence in experimental visceral leishmaniasis." Trends in Parasitology **20**(11): 524-530.

- Engwerda, C. R., M. Ato, S. Stager, C. E. Alexander, A. C. Stanley and P. M. Kaye (2004b). "Distinct roles for lymphotoxin-alpha and tumor necrosis factor in the control of leishmania donovani infection." American Journal of Pathology **165**(6): 2123-2133.
- Essers, M. A. G., S. Offner, W. E. Blanco-Bose, Z. Waibler, U. Kalinke, M. A. Duchosal and A. Trumpp (2009). "Ifn alpha activates dormant haematopoietic stem cells in vivo." Nature **458**(7240): 904-U911.
- Fernandez, K. S. and P. A. de Alarcon (2013). "Development of the hematopoietic system and disorders of hematopoiesis that present during infancy and early childhood." Pediatric Clinics of North America **60**(6): 1273-+.
- Feurerer, M., P. Beckhove, N. Garbi, Y. Mahnke, A. Limmer, M. Hommel, G. J. Hammerling, B. Kyewski, A. Hamann, V. Umansky and V. Schirmacher (2003). "Bone marrow as a priming site for t-cell responses to blood-borne antigen." Nature Medicine **9**(9): 1151-1157.
- Fonseca-Pereira, D., S. Arroz-Madeira, m. Rodrigues-Campos, I. A. M. Barbosa, R. G. Domingues, T. Bento, A. R. M. Almeida, H. Ribeiro, A. J. Potocnik, H. Enomoto and H. Veiga-Fernandes (2014). "The neurotrophic factor receptor ret drives haematopoietic stem cell survival and function." Nature **514**(7520): 98-+.
- Frelin, C., R. Herrington, S. Janmohamed, M. Barbara, G. Tran, C. J. Paige, P. Benveniste, J.-C. Zuniga-Pfluecker, A. Souabni, M. Busslinger and N. N. Iscove (2013). "Gata-3 regulates the self-renewal of long-term hematopoietic stem cells." Nature Immunology **14**(10): 1037-+.
- Frenette, P. S., S. Pinho, D. Lucas and C. Scheiermann (2013). "Mesenchymal stem cell: Keystone of the hematopoietic stem cell niche and a stepping-stone for regenerative medicine." Annual Review of Immunology, Vol 31 **31**: 285-316.
- Gerdes, J., F. Dallenbach, K. Lennert, H. Lemke and H. Stein (1984). "Growth fractions in malignant non-hodgkin's lymphomas (nhl) as determined in situ with the monoclonal antibody ki-67." Hematological oncology **2**(4): 365-371.
- Granick, J. L., S. I. Simon and D. L. Borjesson (2012). "Hematopoietic stem and progenitor cells as effectors in innate immunity." Bone marrow research **2012**: 165107-165107.
- Grumolato, L., G. Liu, P. Mong, R. Mudbhary, R. Biswas, R. Arroyave, S. Vijayakumar, A. N. Economides and S. A. Aaronson (2010). "Canonical and noncanonical wnts use a common mechanism to activate completely unrelated coreceptors." Genes & Development **24**(22): 2517-2530.
- Hamid, G. A. and G. A. Gobah (2009). "Clinical and hematological manifestations of visceral leishmaniasis in yemeni children." Turkish Journal of Hematology **26**(1): 25-28.
- Handman, E. (2000). "Cell biology of leishmania." Advances in Parasitology, Vol 44 **44**: 1-39.
- Hao, Z. Y. and K. Rajewsky (2001). "Homeostasis of peripheral b cells in the absence of b cell influx from the bone marrow." Journal of Experimental Medicine **194**(8): 1151-1163.
- Haring, J. S. and J. T. Harty (2006). "Aberrant contraction of antigen-specific cd4 t cells after infection in the absence of gamma interferon or its receptor." Infection and Immunity **74**(11): 6252-6263.
- Hashimoto, D., A. Chow, C. Noizat, P. Teo, M. B. Beasley, M. Leboeuf, C. D. Becker, P. See, J. Price, D. Lucas, M. Greter, A. Mortha, S. W. Boyer, E. C. Forsberg, M. Tanaka, N. van Rooijen, A. Garcia-Sastre, E. R. Stanley, F. Ginhoux, P. S. Frenette and M. Merad (2013). "Tissue-resident

- macrophages self-maintain locally throughout adult life with minimal contribution from circulating monocytes." *Immunity* **38**(4): 792-804.
- Ho, A. D. and W. Wagner (2007). "The beauty of asymmetry: Asymmetric divisions and self-renewal in the haematopoietic system." *Current Opinion in Hematology* **14**(4): 330-336.
- Hoang, A. T. N., H. Liu, J. Juarez, N. Aziz, P. M. Kaye and M. Svensson (2010). "Stromal cell-derived cxcl12 and ccl8 cooperate to support increased development of regulatory dendritic cells following leishmania infection." *Journal of Immunology* **185**(4): 2360-2371.
- Hu, J. and A. August (2008). "Naive and innate memory phenotype cd4(+) t cells have different requirements for active itk for their development." *Journal of Immunology* **180**(10): 6544-6552.
- Huang, C.-Y., A. L. Bredemeyer, L. M. Walker, C. H. Bassine and B. P. Sleckman (2008). "Dynamic regulation of c-myc proto-oncogene expression during lymphocyte development revealed by a gfp-c-myc knock-in mouse." *European Journal of Immunology* **38**(2): 342-349.
- Ismail, A., A. F. A. Gadir, T. G. Theander, A. Kharazmi and A. M. El Hassan (2006). "Pathology of post-kala-azar dermal leishmaniasis: A light microscopical, immunohistochemical, and ultrastructural study of skin lesions and draining lymph nodes." *Journal of Cutaneous Pathology* **33**(12): 778-787.
- Iwasaki, H., S.-i. Mizuno, Y. Arinobu, H. Ozawa, Y. Mori, H. Shigematsu, K. Takatsu, D. G. Tenen and K. Akashi (2006). "The order of expression of transcription factors directs hierarchical specification of hematopoietic lineages." *Genes & Development* **20**(21): 3010-3021.
- Jain, A. and M. Naniwadekar (2013). "An etiological reappraisal of pancytopenia - largest series reported to date from a single tertiary care teaching hospital." *BMC hematology* **13**(1): 10-10.
- Jiang, Q., W. Q. Li, F. B. Aiello, R. Mazzucchelli, B. Asefa, A. R. Khaled and S. K. Durum (2005). "Cell biology of il-7, a key lymphotrophin." *Cytokine & Growth Factor Reviews* **16**(4-5): 513-533.
- Johns, J. L. and M. M. Christopher (2012). "Extramedullary hematopoiesis: A new look at the underlying stem cell niche, theories of development, and occurrence in animals." *Veterinary Pathology* **49**(3): 508-523.
- Johns, J. L., K. C. MacNamara, N. J. Walker, G. M. Winslow and D. L. Borjesson (2009). "Infection with anaplasma phagocytophilum induces multilineage alterations in hematopoietic progenitor cells and peripheral blood cells." *Infection and Immunity* **77**(9): 4070-4080.
- Jung, T., U. Schauer, C. Heusser, C. Neumann and C. Rieger (1993). "Detection of intracellular cytokines by flow-cytometry." *Journal of Immunological Methods* **159**(1-2): 197-207.
- Junt, T., H. Schulze, Z. Chen, S. Massberg, T. Goerge, A. Krueger, D. D. Wagner, T. Graf, J. E. Italiano, R. A. Shivdasani and U. H. von Andrian (2007). "Dynamic visualization of thrombopoiesis within bone marrow." *Science* **317**(5845): 1767-1770.
- Kafrouni, M. I., G. R. Brown and D. L. Thiele (2003). "The role of tnf-tnfr2 interactions in generation of ctl responses and clearance of hepatic adenovirus infection." *Journal of Leukocyte Biology* **74**(4): 564-571.
- Kaushansky, K. (2006). "Mechanisms of disease: Lineage-specific hematopoietic growth factors." *New England Journal of Medicine* **354**(19): 2034-2045.
- Kawai, T. and S. Akira (2010). "The role of pattern-recognition receptors in innate immunity: Update on toll-like receptors." *Nature Immunology* **11**(5): 373-384.

- Kaye, P. and P. Scott (2011). "Leishmaniasis: Complexity at the host-pathogen interface." Nature Reviews Microbiology **9**(8): 604-615.
- Kaye, P. M., M. Svensson, M. Ato, A. Maroof, R. Polley, S. Stager, S. Zubairi and C. R. Engwerda (2004). "The immunopathology of experimental visceral leishmaniasis." Immunological Reviews **201**: 239-253.
- Kiel, M. J., O. H. Yilmaz, T. Iwashita, O. H. Yilmaz, C. Terhorst and S. J. Morrison (2005). "Slam family receptors distinguish hematopoietic stem and progenitor cells and reveal endothelial niches for stem cells." Cell **121**(7): 1109-1121.
- Kim, C. H. (2010). "Homeostatic and pathogenic extramedullary hematopoiesis." Journal of blood medicine **1**: 13-19.
- Kim, E. Y., J. J. Priatel, S. J. Teh and H. S. Teh (2006). "Tnf receptor type 2 (p75) functions as a costimulator for antigen-driven t cell responses in vivo." Journal of Immunology **176**(2): 1026-1035.
- Kim, S. I. and E. H. Bresnick (2007). "Transcriptional control of erythropoiesis: Emerging mechanisms and principles." Oncogene **26**(47): 6777-6794.
- King, K. Y., M. T. Baldrige, D. C. Weksberg, N. T. Eissa, G. A. Taylor and M. A. Goodell (2010). "Irgm1 is a negative regulator of interferon signaling and autophagy in the hematopoietic stem cell." Experimental Hematology **38**(9): S21-S21.
- King, K. Y. and M. A. Goodell (2011). "Inflammatory modulation of hscs: Viewing the hsc as a foundation for the immune response." Nature Reviews Immunology **11**(10): 685-692.
- Kirstetter, P., K. Anderson, B. T. Porse, S. E. W. Jacobsen and C. Nerlov (2006). "Activation of the canonical wnt pathway leads to loss of hematopoietic stem cell repopulation and multilineage differentiation block." Nature Immunology **7**(10): 1048-1056.
- Kitagawa, M., I. Saito, T. Kuwata, S. Yoshida, S. Yamaguchi, M. Takahashi, T. Tanizawa, R. Kamiyama and K. Hirokawa (1997). "Overexpression of tumor necrosis factor (tnf)-alpha and interferon (ifn)-gamma by bone marrow cells from patients with myelodysplastic syndromes." Leukemia **11**(12): 2049-2054.
- Kondo, M., A. J. Wagers, M. G. Manz, S. S. Prohaska, D. C. Scherer, G. E. Beilhack, J. A. Shizuru and I. L. Weissman (2003a). "Biology of hematopoietic stem cells and progenitors: Implications for clinical application." Annual review of immunology **21**: 759-806.
- Kondo, M., A. J. Wagers, M. G. Manz, S. S. Prohaska, D. C. Scherer, G. F. Beilhack, J. A. Shizuru and I. L. Weissman (2003b). Biology of hematopoietic stem cells and progenitors: Implications for clinical application. Annual review of immunology. Volume 21. W. E. Paul. **Volume 21**: 759-806.
- Kopterides, P., S. Halikias and N. Tsavaris (2003). "Visceral leishmaniasis masquerading as myelodysplasia." American Journal of Hematology **74**(3): 198-199.
- Ku, C.-J., T. Hosoya, I. Maillard and J. D. Engel (2012). "Gata-3 regulates hematopoietic stem cell maintenance and cell-cycle entry." Blood **119**(10): 2242-2251.
- Kuhn, R., F. Schwenk, M. Aguet and K. Rajewsky (1995). "Inducible gene targeting in mice." Science **269**(5229): 1427-1429.

- Kumar, R., N. Singh, S. Gautam, O. P. Singh, K. Gidwani, M. Rai, D. Sacks, S. Sundar and S. Nylen (2014). "Leishmania specific cd4 t cells release ifn gamma that limits parasite replication in patients with visceral leishmaniasis." *Plos Neglected Tropical Diseases* **8**(10).
- Lafuse, W. P., R. Story, J. Mahylis, G. Gupta, S. Varikuti, H. Steinkamp, S. Oghumu and A. R. Satoskar (2013). "Leishmania donovani infection induces anemia in hamsters by differentially altering erythropoiesis in bone marrow and spleen." *Plos One* **8**(3).
- Lazarevic, V., L. H. Glimcher and G. M. Lord (2013). "T-bet: A bridge between innate and adaptive immunity." *Nature Reviews Immunology* **13**(11): 777-789.
- Leclercq, V., M. Lebastard, Y. Belkaid, J. Louis and G. Milon (1996). "The outcome of the parasitic process initiated by leishmania infantum in laboratory mice - a tissue-dependent pattern controlled by the lsh and mhc loci." *Journal of Immunology* **157**(10): 4537-4545.
- Lento, W., K. Congdon, C. Voermans, M. Kritzik and T. Reya (2013). "Wnt signaling in normal and malignant hematopoiesis." *Cold Spring Harbor perspectives in biology* **5**(2).
- Li, X., K. K. McKinstry, S. L. Swain and D. K. Dalton (2007). "Ifn-gamma acts directly on activated cd4(+) t cells during mycobacterial infection to promote apoptosis by inducing components of the intracellular apoptosis machinery and by inducing extracellular proapoptotic signals." *Journal of Immunology* **179**(2): 939-949.
- Lin, F.-c., M. Karwan, B. Saleh, D. L. Hodge, T. Chan, K. C. Boelte, J. R. Keller and H. A. Young (2014). "Ifn-gamma causes aplastic anemia by altering hematopoietic stem/progenitor cell composition and disrupting lineage differentiation." *Blood* **124**(25): 3699-3708.
- Lin, S., R. Zhao, Y. Xiao and P. Li (2015). "Mechanisms determining the fate of hematopoietic stem cells." *Stem Cell Investigation* **2**(5).
- Lipoldova, M. and P. Demant (2006). "Genetic susceptibility to infectious disease: Lessons from mouse models of leishmaniasis." *Nature Reviews Genetics* **7**(4): 294-305.
- Lu, B. F., C. Ebensperger, Z. Dembic, Y. L. Wang, M. Kvatyuk, T. H. Lu, R. L. Coffman, S. Pestka and P. B. Rothman (1998). "Targeted disruption of the interferon-gamma receptor 2 gene results in severe immune defects in mice." *Proceedings of the National Academy of Sciences of the United States of America* **95**(14): 8233-8238.
- Lucas, T., A. Waisman, R. Ranjan, J. Roes, T. Krieg, W. Muller, A. Roers and S. A. Eming (2010). "Differential roles of macrophages in diverse phases of skin repair." *Journal of Immunology* **184**(7): 3964-3977.
- Luis, T. C., M. Ghazvini, B. A. E. Naber, E. F. E. de Haas, J. J. M. van Dongen, R. Fodde and F. J. T. Staal (2010a). "Canonical wnt signaling regulates hematopoiesis in a dosage-dependent fashion." *Experimental Hematology* **38**(9): S95-S95.
- Luis, T. C., B. A. E. Naber, W. E. Fibbe, J. J. M. van Dongen and F. J. T. Staal (2010b). "Wnt3a nonredundantly controls hematopoietic stem cell function and its deficiency results in complete absence of canonical wnt signaling." *Blood* **116**(3): 496-497.
- Luis, T. C., B. A. E. Naber, P. P. C. Roozen, M. H. Brugman, E. F. E. de Haas, M. Ghazvini, W. E. Fibbe, J. J. M. van Dongen, R. Fodde and F. J. T. Staal (2011). "Canonical wnt signaling regulates hematopoiesis in a dosage-dependent fashion." *Cell Stem Cell* **9**(4): 345-356.
- Luis, T. C., F. Weerkamp, B. A. E. Naber, M. R. M. Baert, E. F. E. de Haas, T. Nikolic, S. Heuvelmans, R. R. De Krijger, J. J. M. van Dongen and F. J. T. Staal (2009). "Wnt3a deficiency

- irreversibly impairs hematopoietic stem cell self-renewal and leads to defects in progenitor cell differentiation." Blood **113**(3): 546-554.
- Lyman, S. D. and S. E. W. Jacobsen (1998). "C-kit ligand and flt3 ligand: Stem/progenitor cell factors with overlapping yet distinct activities." Blood **91**(4): 1101-1134.
- MacNamara, K. C., M. Jones, O. Martin and G. M. Winslow (2011a). "Transient activation of hematopoietic stem and progenitor cells by ifn gamma during acute bacterial infection." Plos One **6**(12).
- MacNamara, K. C., K. Oduro, O. Martin, D. D. Jones, M. McLaughlin, K. Choi, D. L. Borjesson and G. M. Winslow (2011b). "Infection-induced myelopoiesis during intracellular bacterial infection is critically dependent upon ifn-gamma signaling." Journal of Immunology **186**(2): 1032-1043.
- MacNamara, K. C., R. Racine, M. Chatterjee, D. Borjesson and G. M. Winslow (2009). "Diminished hematopoietic activity associated with alterations in innate and adaptive immunity in a mouse model of human monocyctic ehrlichiosis." Infection and Immunity **77**(9): 4061-4069.
- Malek, T. R., K. M. Danis and E. K. Codias (1989). "Tumor necrosis factor synergistically acts with ifn-gamma to regulate ly-6a/e expression in lymphocytes-t, thymocytes and bone-marrow cells." Journal of Immunology **142**(6): 1929-1936.
- Maltby, S., N. G. Hansbro, H. L. Tay, J. Stewart, M. Plank, B. Donges, H. F. Rosenberg and P. S. Foster (2014). "Production and differentiation of myeloid cells driven by proinflammatory cytokines in response to acute pneumovirus infection in mice." Journal of Immunology **193**(8): 4072-4082.
- Maroof, A., N. Brown, B. Smith, M. R. Hodgkinson, A. Maxwell, F. O. Losch, U. Fritz, P. Walden, C. N. J. Lacey, D. F. Smith, T. Aebischer and P. M. Kaye (2012). "Therapeutic vaccination with recombinant adenovirus reduces splenic parasite burden in experimental visceral leishmaniasis." Journal of Infectious Diseases **205**(5): 853-863.
- Marwaha, N., R. Sarode, R. K. Gupta, G. Garewal and S. Dash (1991). "Clinicohematological characteristics in patients with kala-azar - a study from north-west india." Tropical and Geographical Medicine **43**(4): 357-362.
- Massberg, S., P. Schaerli, I. Knezevic-Maramica, M. Koellnberger, N. Tubo, E. A. Moseman, I. V. Huff, T. Junt, A. J. Wagers, I. B. Mazo and U. H. von Andrian (2007). "Immunosurveillance by hematopoietic progenitor cells trafficking through blood, lymph, and peripheral tissues." Cell **131**(5): 994-1008.
- Matatall, K. A., C.-C. Shen, G. A. Challen and K. Y. King (2014). "Type ii interferon promotes differentiation of myeloid-biased hematopoietic stem cells." Stem Cells **32**(11): 3023-3030.
- Matsui, K., N. Giri, B. P. Alter and L. A. Pinto (2013). "Cytokine production by bone marrow mononuclear cells in inherited bone marrow failure syndromes." British Journal of Haematology **163**(1): 81-92.
- Megias, J., A. Yanez, S. Moriano, J.-E. O'Connor, D. Gozalbo and M.-L. Gil (2012). "Direct toll-like receptor-mediated stimulation of hematopoietic stem and progenitor cells occurs in vivo and promotes differentiation toward macrophages." Stem Cells **30**(7): 1486-1495.
- Melby, P. C., B. Chandrasekar, W. G. Zhao and J. E. Coe (2001). "The hamster as a model of human visceral leishmaniasis: Progressive disease and impaired generation of nitric oxide in the face of a prominent th1-like cytokine response." Journal of Immunology **166**(3): 1912-1920.

- Mellado, M., L. Martinez-Munoz, G. Cascio, P. Lucas, J. L. Pablos and J. Miguel Rodriguez-Frade (2015). "T cell migration in rheumatoid arthritis." Frontiers in Immunology **6**: 1-12.
- Mendez-Ferrer, S., D. Lucas, M. Battista and P. S. Frenette (2008). "Haematopoietic stem cell release is regulated by circadian oscillations." Nature **452**(7186): 442-U444.
- Mercer, E. M., Y. C. Lin and C. Murre (2011). "Factors and networks that underpin early hematopoiesis." Seminars in Immunology **23**(5): 317-325.
- Mercier, F. E., C. Ragu and D. T. Scadden (2012). "The bone marrow at the crossroads of blood and immunity." Nature Reviews Immunology **12**(1): 49-60.
- Mikkola, H. K. A., J. Klintman, H. D. Yang, H. Hock, T. M. Schlaeger, Y. Fujiwara and S. H. Orkin (2003). "Haematopoietic stem cells retain long-term repopulating activity and multipotency in the absence of stem-cell leukaemia *scl/tal-1* gene." Nature **421**(6922): 547-551.
- Miranda de Araujo, V. E., M. H. Franco Morais, I. A. Reis, A. Rabello and M. Carneiro (2012). "Early clinical manifestations associated with death from visceral leishmaniasis." Plos Neglected Tropical Diseases **6**(2).
- Mirantes, C., E. Ptssegue and E. M. Pietras (2014). "Pro-inflammatory cytokines: Emerging players regulating hsc function in normal and diseased hematopoiesis." Experimental Cell Research **329**(2): 248-254.
- Mirkovich, A. M., A. Galelli, A. C. Allison and F. Z. Modabber (1986). "Increased myelopoiesis during leishmania-major infection in mice - generation of safe targets, a possible way to evade the effector immune mechanism." Clinical and Experimental Immunology **64**(1): 1-7.
- Mizrahi, K. and N. Askenasy (2014). "Physiological functions of *tnf* family receptor/ligand interactions in hematopoiesis and transplantation." Blood **124**(2): 176-183.
- Monteiro, J. P., A. Benjamin, E. S. Costa, M. A. Barcinski and A. Bonomo (2005). "Normal hematopoiesis is maintained by activated bone marrow *cd4*(+) t cells." Blood **105**(4): 1484-1491.
- Monteiro, J. P. and A. Bonomo (2005). "Linking immunity and hematopoiesis by bone marrow t cell activity." Brazilian Journal of Medical and Biological Research **38**(10): 1475-1486.
- Mossadegh-Keller, N., S. Sarrazin, P. K. Kandalla, L. Espinosa, E. R. Stanley, S. L. Nutt, J. Moore and M. H. Sieweke (2013). "M-csf instructs myeloid lineage fate in single haematopoietic stem cells." Nature **497**(7448): 239-+.
- Murphy, M. J., A. Wilson and A. Trumpp (2005). "More than just proliferation: Myc function in stem cells." Trends in cell biology **15**(3): 128-137.
- Murray, H. W., C. M. Lu, S. Mauze, S. Freeman, A. L. Moreira, G. Kaplan and R. L. Coffman (2002). "Interleukin-10 (il-10) in experimental visceral leishmaniasis and il-10 receptor blockade as immunotherapy." Infection and Immunity **70**(11): 6284-6293.
- Nagai, Y., K. P. Garrett, S. Ohta, U. Bahrn, T. Kouro, S. Akira, K. Takatsu and P. W. Kincade (2006a). "Toll-like receptors on hematopoietic progenitor cells stimulate innate immune system replenishment." Immunity **24**(6): 801-812.
- Nagai, Y., K. P. Garrett, S. Ohta, B. Ulen, S. Akira and P. W. Kincade (2006b). "Hematopoietic stem/progenitor cells express functional toll-like receptors that potentially stimulate replenishment of the innate immune system." Journal of Immunology **176**: S309-S309.

- Nakamura-Ishizu, A., H. Takizawa and T. Suda (2014). "The analysis, roles and regulation of quiescence in hematopoietic stem cells." Development **141**(24): 4656-4666.
- Nemeth, M. J. and D. M. Bodine (2007). "Regulation of hematopoiesis and the hematopoietic stem cell niche by wnt signaling pathways." Cell Research **17**(9): 746-758.
- Nguyen Hoang, A. T., H. Liu, J. Juarez, N. Aziz, P. M. Kaye and M. Svensson (2010). "Stromal cell-derived cxcl12 and ccl8 cooperate to support increased development of regulatory dendritic cells following leishmania infection." Journal of immunology (Baltimore, Md. : 1950) **185**(4): 2360-2371.
- Nimmo, R. A., G. E. May and T. Enver (2015). "Primed and ready: Understanding lineage commitment through single cell analysis." Trends in cell biology **25**(8): 459-467.
- Orford, K. W. and D. T. Scadden (2008). "Deconstructing stem cell self-renewal: Genetic insights into cell-cycle regulation." Nature Reviews Genetics **9**(2): 115-128.
- Orkin, S. H. (2000). "Diversification of haematopoietic stem cells to specific lineages." Nature Reviews Genetics **1**(1): 57-64.
- Orkin, S. H. and L. I. Zon (2008). "Hematopoiesis: An evolving paradigm for stem cell biology." Cell **132**(4): 631-644.
- Osawa, M., K. Hanada, H. Hamada and H. Nakauchi (1996). "Long-term lymphohematopoietic reconstitution by a single cd34-low/negative hematopoietic stem cell." Science **273**(5272): 242-245.
- Ouyang, W., S. Rutz, N. K. Crellin, P. A. Valdez and S. G. Hymowitz (2011). Regulation and functions of the il-10 family of cytokines in inflammation and disease. Annual review of immunology, vol 29. W. E. Paul, D. R. Littman and W. M. Yokoyama. **29**: 71-109.
- Owens, B. M. J. and P. M. Kaye (2012). "Stromal cell induction of regulatory dendritic cells." Frontiers in Immunology **3**: 262-262.
- Oyoshi, M. K., R. Barthel and E. N. Tsitsikov (2007). "Traf1 regulates recruitment of lymphocytes and, to a lesser extent, neutrophils, myeloid dendritic cells and monocytes to the lung airways following lipopolysaccharide inhalation." Immunology **120**(3): 303-314.
- Pablo Quintero, J., A. M. Siqueira, A. Tobon, S. Blair, A. Moreno, M. Arevalo-Herrera, M. V. Guimaraes Lacerda and S. Herrera Valencia (2011). "Malaria-related anaemia: A latin american perspective." Memorias Do Instituto Oswaldo Cruz **106**: 91-104.
- Pace, D. (2014). "Leishmaniasis." Journal of Infection **69**: S10-S18.
- Pearl-Yafe, M., K. Mizrahi, J. Stein, E. S. Yolcu, O. Kaplan, H. Shirwan, I. Yaniv and N. Askenasy (2010). "Tumor necrosis factor receptors support murine hematopoietic progenitor function in the early stages of engraftment." Stem Cells **28**(7): 1270-1280.
- Peschon, J. J., D. S. Tarrance, K. L. Stocking, M. B. Glaccum, C. Otten, C. R. Willis, K. Charrier, P. J. Morrissey, C. B. Ware and K. M. Mohler (1998). "Tnf receptor-deficient mice reveal divergent roles for p55 and p75 in several models of inflammation." Journal of Immunology **160**(2): 943-952.
- Peterson, V. M., J. J. Adamovicz, T. B. Elliott, M. M. Moore, G. S. Madonna, W. E. Jackson, G. D. Ledney and W. C. Gause (1994). "Gene-expression of hematoregulatory cytokines is elevated endogenously after sublethal gamma-irradiation and is differentially enhanced by therapeutic administration of biologic response modifiers." Journal of Immunology **153**(5): 2321-2330.

- Pietras, E. M., R. Lakshminarasimhan, J.-M. Techner, S. Fong, J. Flach, M. Binnewies and E. Passegue (2014). "Re-entry into quiescence protects hematopoietic stem cells from the killing effect of chronic exposure to type I interferons." Journal of Experimental Medicine **211**(2): 245-262.
- Pinho, F. A. d. (2015). "A patogênese da pancitopenia na leishamiose visceral canina e murina." Doctoral Thesis, Instituto de Medicina Tropical de São Paulo, University of São Paulo, São Paulo. Retrieved 2016-02-03, from <http://www.teses.usp.br/teses/disponiveis/99/99131/tde-20022015-120914/>.
- Pittet, M. J., M. Nahrendorf and F. K. Swirski (2014). "The journey from stem cell to macrophage." Year in Immunology: Myeloid Cells and Inflammation **1319**: 1-18.
- Prendergast, A. M. and M. A. G. Essers (2014). "Hematopoietic stem cells, infection, and the niche." Bone Marrow Niche, Stem Cells, and Leukemia: Impact of Drugs, Chemicals, and the Environment **1310**: 51-57.
- Price, P. W. and J. Cerny (1999). "Characterization of cd4(+) t cells in mouse bone marrow. I. Increased activated/memory phenotype and altered tcr v beta repertoire." European Journal of Immunology **29**(3): 1051-1056.
- Pronk, C. J. H., O. P. Veiby, D. Bryder and S. E. W. Jacobsen (2011). "Tumor necrosis factor restricts hematopoietic stem cell activity in mice: Involvement of two distinct receptors." Journal of Experimental Medicine **208**(8): 1563-1570.
- Rebel, V. I., S. Hartnett, G. R. Hill, S. B. Lazo-Kallanian, J. L. M. Ferrara and C. A. Sieff (1999). "Essential role for the p53 tumor necrosis factor receptor in regulating hematopoiesis at a stem cell level." Journal of Experimental Medicine **190**(10): 1493-1503.
- Requena, J. M., M. Soto, M. D. Doria and C. Alonso (2000). "Immune and clinical parameters associated with leishmania infantum infection in the golden hamster model." Veterinary Immunology and Immunopathology **76**(3-4): 269-281.
- Reya, T. and H. Clevers (2005). "Wnt signalling in stem cells and cancer." Nature **434**(7035): 843-850.
- Reya, T., A. W. Duncan, L. Ailles, J. Domen, D. C. Scherer, K. Willert, L. Hintz, R. Nusse and I. L. Weissman (2003). "A role for wnt signalling in self-renewal of haematopoietic stem cells." Nature **423**(6938): 409-414.
- Rezzoug, F., Y. Huang, M. K. Tanner, M. Wysoczynski, C. L. Schanie, P. M. Chilton, M. Z. Ratajczak, I. J. Fugier-Vivier and S. T. Ildstad (2008). "Tnf-alpha is critical to facilitate hemopoietic stem cell engraftment and function." Journal of Immunology **180**(1): 49-57.
- Rieger, M. A. and T. Schroeder (2012). "Hematopoiesis." Cold Spring Harbor perspectives in biology **4**(12).
- Robb, L. (2007). "Cytokine receptors and hematopoietic differentiation." Oncogene **26**(47): 6715-6723.
- Rodriguez, S., A. Chora, B. Goumnerov, C. Mumaw, W. S. Goebel, L. Fernandez, H. Baydoun, H. HogenEsch, D. M. Dombkowski, C. A. Karlewicz, S. Rice, L. G. Rahme and N. Carlesso (2009). "Dysfunctional expansion of hematopoietic stem cells and block of myeloid differentiation in lethal sepsis." Blood **114**(19): 4064-4076.
- Rossol, M., K. Schubert, U. Meusch, A. Schulz, B. Biedermann, J. Grosche, M. Pierer, R. Scholz, C. Baerwald, A. Thiel, S. Hagen and U. Wagner (2013). "Tumor necrosis factor receptor type I

- expression of cd4+t cells in rheumatoid arthritis enables them to follow tumor necrosis factor gradients into the rheumatoid synovium." Arthritis and Rheumatism **65**(6): 1468-1476.
- Rusten, L. S., F. W. Jacobsen, W. Lesslauer, H. Loetscher, E. B. Smeland and S. E. W. Jacobsen (1994). "Bifunctional effects of tumor-necrosis-factor-alpha (tnf-alpha) on the growth of mature and primitive human hematopoietic progenitor cells - involvement of p55 and p75 tnf receptors." Blood **83**(11): 3152-3159.
- Santos, M. A., R. C. Marques, C. A. Farias, D. M. Vasconcelos, J. M. Stewart, D. L. Costa and C. H. N. Costa (2002). "Predictors of an unsatisfactory response to pentavalent antimony in the treatment of american visceral leishmaniasis." Revista da Sociedade Brasileira de Medicina Tropical **35**(6): 629-633.
- Sashida, G. and A. Iwama (2012). "Epigenetic regulation of hematopoiesis." International Journal of Hematology **96**(4): 405-412.
- Schaniel, C., D. Sirabella, J. Qiu, X. Niu, I. R. Lemischka and K. A. Moore (2011). "Wnt-inhibitory factor 1 dysregulation of the bone marrow niche exhausts hematopoietic stem cells." Blood **118**(9): 2420-2429.
- Schuerch, C. M., C. Riether and A. F. Ochsenbein (2014). "Cytotoxic cd8(+) t cells stimulate hematopoietic progenitors by promoting cytokine release from bone marrow mesenchymal stromal cells." Cell Stem Cell **14**(4): 460-472.
- Schuettpelz, L. G. and D. C. Link (2013). "Regulation of hematopoietic stem cell activity by inflammation." Frontiers in Immunology **4**.
- Scumpia, P. O., K. M. Kelly-Scumpia, M. J. Delano, J. S. Weinstein, A. G. Cuenca, S. Al-Quran, I. Bovio, S. Akira, Y. Kumagai and L. L. Moldawer (2010). "Cutting edge: Bacterial infection induces hematopoietic stem and progenitor cell expansion in the absence of tlr signaling." Journal of Immunology **184**(5): 2247-2251.
- Selleri, C., T. Sato, S. Anderson, N. S. Young and J. P. Maciejewski (1995). "Interferon-gamma and tumor-necrosis-factor-alpha suppress both early and late stages of hematopoiesis and induce programmed cell-death." Journal of Cellular Physiology **165**(3): 538-546.
- Sercan, O., D. Stoycheva, G. J. Haemmerling, B. Arnold and T. Schueler (2010). "Ifn-gamma receptor signaling regulates memory cd8(+) t cell differentiation." Journal of Immunology **184**(6): 2855-2862.
- Serio, B., C. Selleri and J. P. Maciejewski (2011). "Impact of immunogenetic polymorphisms in bone marrow failure syndromes." Mini-Reviews in Medicinal Chemistry **11**(6): 544-552.
- Shi, C., T. Jia, S. Mendez-Ferrer, T. M. Hohl, N. V. Serbina, L. Lipuma, I. Leiner, M. O. Li, P. S. Frenette and E. G. Pamer (2011). "Bone marrow mesenchymal stem and progenitor cells induce monocyte emigration in response to circulating toll-like receptor ligands." Immunity **34**(4): 590-601.
- Sinclair, A., B. Daly and E. Dzierzak (1996). "The ly-6e.1 (sca-1) gene requires a 3' chromatin-dependent region for high-level gamma-interferon-induced hematopoietic cell expression." Blood **87**(7): 2750-2761.
- Singh, R. K., A. Srivastava and N. Singh (2012). "Toll-like receptor signaling: A perspective to develop vaccine against leishmaniasis." Microbiological Research **167**(8): 445-451.

- Sitnicka, E., D. Bryder, K. Theilgaard-Monch, N. Buza-Vidas, J. Adolfsson and S. E. W. Jacobsen (2002). "Key role of flt3 ligand in regulation of the common lymphoid progenitor but not in maintenance of the hematopoietic stem cell pool." Immunity **17**(4): 463-472.
- Smelt, S. C., S. E. J. Cotterell, C. R. Engwerda and P. M. Kaye (2000). "B cell-deficient mice are highly resistant to leishmania donovani infection, but develop neutrophil-mediated tissue pathology." Journal of Immunology **164**(7): 3681-3688.
- Snoeck, H. W., S. Weekx, A. Moulijn, F. Lardon, M. Lenjou, G. Nys, P. C. F. VanRanst, D. R. VanBockstaele and Z. N. Berneman (1996). "Tumor necrosis factor alpha is a potent synergistic factor for the proliferation of primitive human hematopoietic progenitor cells and induces resistance to transforming growth factor beta but not to interferon gamma." Journal of Experimental Medicine **183**(2): 705-710.
- Spolski, R. and W. J. Leonard (2014). "Interleukin-21: A double-edged sword with therapeutic potential." Nature Reviews Drug Discovery **13**(5): 381-393.
- Staeger, S., T. Joshi and R. Bankoti (2010). "Immune evasive mechanisms contributing to persistent leishmania donovani infection." Immunologic Research **47**(1-3): 14-24.
- Stager, S., A. Maroof, S. Zubairi, S. L. Sanos, M. Kopf and P. M. Kaye (2006). "Distinct roles for il-6 and il-12p40 in mediating protection against leishmania donovani and the expansion of il-10(+) cd4(+) t cells." European Journal of Immunology **36**(7): 1764-1771.
- Stanley, A. C. and C. R. Engwerda (2007). "Balancing immunity and pathology in visceral leishmaniasis." Immunology and Cell Biology **85**(2): 138-147.
- Sugimura, R., X. C. He, A. Venkatraman, F. Arai, A. Box, C. Semerad, J. S. Haug, L. Peng, X.-b. Zhong, T. Suda and L. Li (2012). "Noncanonical wnt signaling maintains hematopoietic stem cells in the niche." Cell **150**(2): 351-365.
- Sugiyama, T., H. Kohara, M. Noda and T. Nagasawa (2006). "Maintenance of the hematopoietic stem cell pool by cxcl12-cxcr4 chemokine signaling in bone marrow stromal cell niches." Immunity **25**(6): 977-988.
- Svensson, M., A. Maroof, M. Ato and P. M. Kaye (2004). "Stromal cells direct local differentiation of regulatory dendritic cells." Immunity **21**(6): 805-816.
- Takizawa, H., S. Boettcher and M. G. Manz (2012). "Demand-adapted regulation of early hematopoiesis in infection and inflammation." Blood **119**(13): 2991-3002.
- Taylor, A. P. and H. W. Murray (1997). "Intracellular antimicrobial activity in the absence of interferon-gamma: Effect of interleukin-12 in experimental visceral leishmaniasis in interferon-gamma gene-disrupted mice." Journal of Experimental Medicine **185**(7): 1231-1239.
- Tesio, M., Y. Tang, K. Muedder, M. Saini, L. von Paleske, E. Macintyre, M. Pasparakis, A. Waisman and A. Trumpp (2015). "Hematopoietic stem cell quiescence and function are controlled by the cyld-traf2-p38mapk pathway." Journal of Experimental Medicine **212**(4): 525-538.
- Thoren, L. A., K. Liuba, D. Bryder, J. M. Nygren, C. T. Jensen, H. Qian, J. Antonchuk and S.-E. W. Jacobsen (2008). "Kit regulates maintenance of quiescent hematopoietic stem cells." Journal of Immunology **180**(4): 2045-2053.
- Tian, T., M. Wang and D. Ma (2014). "Tnf- α , a good or bad factor in hematological diseases?" Stem Cell Investigation **1**(6).

- Tokoyoda, K., A. E. Hauser, T. Nakayama and A. Radbruch (2010). "Organization of immunological memory by bone marrow stroma." Nature Reviews Immunology **10**(3): 193-200.
- Tokoyoda, K., S. Zehentmeier, H.-D. Chang and A. Radbruch (2009a). "Organization and maintenance of immunological memory by stroma niches." European Journal of Immunology **39**(8): 2095-2099.
- Tokoyoda, K., S. Zehentmeier, A. N. Hegazy, I. Albrecht, J. R. Gruen, M. Loehning and A. Radbruch (2009b). "Professional memory cd4(+) t lymphocytes preferentially reside and rest in the bone marrow." Immunity **30**(5): 721-730.
- Trumpp, A., M. Essers and A. Wilson (2010). "Awakening dormant haematopoietic stem cells." Nature Reviews Immunology **10**(3): 201-209.
- Tsapogas, P., S. Zandi, J. Ahsberg, J. Zetterblad, E. Welinder, J. I. Jonsson, R. Mansson, H. Qian and M. Sigvardsson (2011). "Il-7 mediates ebf-1-dependent lineage restriction in early lymphoid progenitors." Blood **118**(5): 1283-1290.
- Van Os, R., L. M. Kamminga, A. Ausema, L. V. Bystrikh, D. P. Draijer, K. Van Pelt, B. Dontje and G. De Haan (2007). "A limited role for p21(cip1/waf1) in maintaining normal hematopoietic stem cell functioning." Stem Cells **25**(4): 836-843.
- Varma, N. and S. Naseem (2010). "Hematologic changes in visceral leishmaniasis/kala azar." Indian Journal of Hematology and Blood Transfusion **26**(3): 78-82.
- Visnjic, D., Z. Kalajzic, D. W. Rowe, V. Katavic, J. Lorenzo and H. L. Aguila (2004). "Hematopoiesis is severely altered in mice with an induced osteoblast deficiency." Blood **103**(9): 3258-3264.
- Vonfreedenjeffry, U., P. Vieira, L. A. Lucian, T. McNeil, S. E. G. Burdach and R. Murray (1995). "Lymphopenia in interleukin (il)-7 gene-deleted mice identifies il-7 as a nonredundant cytokine." Journal of Experimental Medicine **181**(4): 1519-1526.
- Wakkach, A., N. Fournier, V. Brun, J. P. Breittmayer, F. Cottrez and H. Groux (2003). "Characterization of dendritic cells that induce tolerance and t regulatory 1 cell differentiation in vivo." Immunity **18**(5): 605-617.
- Walasek, M. A., R. van Os and G. de Haan (2012). "Hematopoietic stem cell expansion: Challenges and opportunities." Hematopoietic Stem Cells Viii **1266**: 138-150.
- Walter, D., A. Lier, A. Geiselhart, F. B. Thalheimer, S. Huntscha, M. C. Sobotta, B. Moehrle, D. Brocks, I. Bayindir, P. Kaschutnig, K. Muedder, C. Klein, A. Jauch, T. Schroeder, H. Geiger, T. P. Dick, T. Holland-Letz, P. Schmezer, S. W. Lane, M. A. Rieger, M. A. G. Essers, D. A. Williams, A. Trumpp and M. D. Milsom (2015). "Exit from dormancy provokes DNA-damage-induced attrition in haematopoietic stem cells." Nature **520**(7548): 549-+.
- Wang, L. D. and A. J. Wagers (2011). "Dynamic niches in the origination and differentiation of haematopoietic stem cells." Nature Reviews Molecular Cell Biology **12**(10): 643-655.
- Wang, L. D. and A. J. Wagers (2012). "Dynamic niches in the origination and differentiation of haematopoietic stem cells (vol 12, pg 643, 2011)." Nature Reviews Molecular Cell Biology **13**(1).
- Warr, M. R., E. M. Pietras and E. Passegue (2011). "Mechanisms controlling hematopoietic stem cell functions during normal hematopoiesis and hematological malignancies." Wiley Interdisciplinary Reviews-Systems Biology and Medicine **3**(6): 681-701.

- Whitmire, J. K., N. Benning and J. L. Whitton (2005). "Cutting edge: Early ifn-gamma signaling directly enhances primary antiviral cd4(+) t cell responses." Journal of Immunology **175**(9): 5624-5628.
- Wilkins, J. A. and O. J. Sansom (2008). "C-myc is a critical mediator of the phenotypes of apc loss in the intestine." Cancer Research **68**(13): 4963-4966.
- Wilson, A., M. J. Murphy, T. Oskarsson, K. Kaloulis, M. D. Bettess, G. M. Oser, A. C. Pasche, C. Knabenhans, H. R. MacDonald and A. Trumpp (2004). "C-myc controls the balance between hematopoietic stem cell self-renewal and differentiation." Genes & Development **18**(22): 2747-2763.
- Winkler, I. G., V. Barbier, R. Wadley, A. C. W. Zannettino, S. Williams and J.-P. Levesque (2010). "Positioning of bone marrow hematopoietic and stromal cells relative to blood flow in vivo: Serially reconstituting hematopoietic stem cells reside in distinct nonperfused niches." Blood **116**(3): 375-385.
- Yamamoto, R., Y. Morita, J. Oehara, S. Hamanaka, M. Onodera, K. L. Rudolph, H. Ema and H. Nakauchi (2013). "Clonal analysis unveils self-renewing lineage-restricted progenitors generated directly from hematopoietic stem cells." Cell **154**(5): 1112-1126.
- Yarali, N., T. Fisgin, F. Duru and A. Kara (2002). "Myelodysplastic features in visceral leishmaniasis." American Journal of Hematology **71**(3): 191-195.
- Yoshida, T. and K. Georgopoulos (2013). "Gata-3 controls self-renewal in stressed hscs." Nature Immunology **14**(10): 1032-1033.
- Young, N. S., P. Scheinberg and R. T. Calado (2008). "Aplastic anemia." Current Opinion in Hematology **15**(3): 162-168.
- Zganiacz, A., M. Santosuosso, J. Wang, T. Yang, L. H. Chen, M. Anzulovic, S. Alexander, B. Gicquel, Y. H. Wan, J. Bramson, M. Inman and Z. Xing (2004). "Tnf-alpha is a critical negative regulator of type 1 immune activation during intracellular bacterial infection." Journal of Clinical Investigation **113**(3): 401-413.
- Zhan, Y. F., G. J. Lieschke, D. Grail, A. R. Dunn and C. Cheers (1998). "Essential roles for granulocyte-macrophage colony-stimulating factor (gm-csf) and g-csf in the sustained hematopoietic response of listeria monocytogenes - infected mice." Blood **91**(3): 863-869.
- Zhang, X., R. Goncalves and D. M. Mosser (2008). "The isolation and characterization of murine macrophages." Current protocols in immunology / edited by John E. Coligan ... [et al.] **Chapter 14**: Unit 14.11-Unit 14.11.
- Zhang, Y., A. Harada, H. Bluethmann, J. B. Wang, S. Nakao, N. Mukaida and K. Matsushima (1995). "Tumor-necrosis-factor (tnf) is a physiological regulator of hematopoietic progenitor cells - increase of early hematopoietic progenitor cells in tnf receptor p55-deficient mice in-vivo and potent inhibition of progenitor-cell proliferation by tnf-alpha in-vitro." Blood **86**(8): 2930-2937.
- Zhang, Y., M. Jones, A. McCabe, G. M. Winslow, D. Avram and K. C. MacNamara (2013). "Myd88 signaling in cd4 t cells promotes ifn-gamma production and hematopoietic progenitor cell expansion in response to intracellular bacterial infection." Journal of Immunology **190**(9): 4725-4735.
- Zhao, J. L. and D. Baltimore (2015). "Regulation of stress-induced hematopoiesis." Current Opinion in Hematology **22**(4): 286-292.

Zhu, J. and S. G. Emerson (2002). "Hematopoietic cytokines, transcription factors and lineage commitment." Oncogene **21**(21): 3295-3313.